TESIS DE LA UNIVERSIDAD DE ZARAGOZA
2023
61

Alfonso Serrano Del Valle

Estudio de la inmunogenicidad y mecanismos de muerte celular en nuevas terapias antitumorales. Aplicación al mieloma múltiple

Director/es
Naval Iraberri, Javier
Marzo Rubio, María Isabel

ISSN 2254-7606

Prensas de la Universidad
Universidad Zaragoza

ISSN 2254-7606

Universidad Zaragoza
1542

Tesis Doctoral

ESTUDIO DE LA INMUNOGENICIDAD Y MECANISMOS DE MUERTE CELULAR EN NUEVAS TERAPIAS ANTITUMORALES. APLICACIÓN AL MIELOMA MÚLTIPLE

Autor

Alfonso Serrano Del Valle

Director/es

Naval Iraberri, Javier
Marzo Rubio, María Isabel

UNIVERSIDAD DE ZARAGOZA
Escuela de Doctorado

2021

IMMUNOGENICITY AND CELL DEATH MECHANISMS IN CANCER TREATMENT.

APPLICATION TO MULTIPLE MYELOMA.

Alfonso Serrano del Valle

Departamento Bioquímica y
Biología molecular y celular
Facultad de Ciencias
Universidad
de Zaragoza
1542

UNIVERSIDAD DE ZARAGOZA

DEPARTAMENTO DE BIOQUÍMICA Y BIOLOGÍA MOLECULAR Y CELULAR

Facultad de Ciencias

Tesis Doctoral

IMMUNOGENICITY AND CELL DEATH MECHANISMS IN CANCER TREATMENT.

APPLICATION TO MULTIPLE MYELOMA.

Memoria presentada por

Alfonso Serrano del Valle

Septiembre 2020

Dña. ISABEL MARZO RUBIO, Profesora Titular de la Universidad de Zaragoza y D. JAVIER NAVAL IRABERRI, Catedrático de Biología Celular, adscritos al Departamento de Bioquímica y Biología Molecular y Celular de la Universidad de Zaragoza

CERTIFICAN:

Que la memoria de la Tesis Doctoral titulada: ”IMMUNOGENICITY AND CELL DEATH MECHANISMS IN CANCER TREATMENT. APLICATION TO MULTIPLE MYELOMA” (“*Estudio de la inmunogenicidad y mecanismos de muerte celular en nuevas terapias antitumorales. Aplicación al mieloma múltiple”*), presentada por D. Alfonso Serrano del Valle, ha sido realizada en el Departamento de Bioquímica y Biología Molecular y Celular de la Facultad de Ciencias bajo nuestra dirección y que reúne las condiciones requeridas para que su autor pueda optar al Grado de Doctor por la Universidad de Zaragoza.

Zaragoza, 22 de Julio de 2020

Isabel Marzo Rubio Javier Naval Iraberri

Esta tesis doctoral se ha realizado gracias a una beca de formación de personal investigador en formación del Gobierno de Aragón (BOA nº 241, 10 de Diciembre 2014) y a un contrato con cargo a un proyecto de I+D+i en líneas prioritarias de la RIS3 Aragón y de excelencia de carácter multidisciplinar cofinanciado por el Programa Operativo FEDER Aragón 2014-2020 (Referencia LMP98_18).

“Poco basta cada día si cada día logramos ese poco.”
— Santiago Ramón y Cajal

‘A person who never made a mistake never tried anything new’
— Albert Einstein

A mis Padres, a mi Hermano
y a mis Tíos, Jose y Rocío.

RESÚMEN.

En la investigación oncológica, el estudio de los mecanismos moleculares de muerte celular provocados por la quimioterapia es esencial no sólo para llegar a comprender los mecanismos de acción inherentes de estos fármacos, sino también para idear, optimizar y mejorar nuevos enfoques terapéuticos que permitan atajar las tan temidas recaídas. Además, durante los últimos años, la inmunoterapia ha irrumpido en la clínica como un tratamiento que brinda de una cierta esperanza a los pacientes con cáncer. De hecho, cada vez está creciendo con más fuerza la idea de que son realmente las respuestas inmunológicas antitumorales las que están detrás de los efectos a largo plazo provocados por tratamientos quimioterápicos convencionales o dirigidos. Por ello, cuando se está frente a una enfermedad tan compleja, heterogénea y polifacética como es el cáncer, es necesario abordar el problema desde una perspectiva integradora, combinando tanto los aspectos relativos a los mecanismos de muerte como de la respuesta inmunológica asociada a los mismos. Hoy en día, los tratamientos antitumorales utilizados o en desarrollo son capaces de inducir muerte celular mediante distintos mecanismos como la apoptosis, necroptosis, muerte celular inmunogénica (ICD), catástrofe mitótica, entre otras. Nuestro objetivo durante este trabajo ha sido estudiar los diferentes mecanismos de muerte celular inducidos por fármacos antitumorales actuales o de reciente introducción en la clínica, así como explorar la naturaleza inmunogénica subyacente a dichos tipos de muerte celular.

En el presente trabajo hemos comenzado estudiando la contribución de la catástrofe mitótica en la inducción de muerte celular por agentes antimitóticos, así como los mecanismos de muerte accionados cuando dichos fármacos se utilizan en combinación con miméticos de BH3. Tal y como muestran nuestros resultados, el tratamiento individual con agentes antimitóticos provocó manifestaciones típicas de la catástrofe mitótica como la micronucleación o multinucleación, precedidas en la mayoría de los casos por un arresto mitótico prolongado. No obstante, la inhibición de la mitosis por sí sola no provocó una respuesta apoptótica importante. Así mismo, como se puede observar a lo largo de este trabajo y que también fue revelado en el trabajo desarrollado por Gascoigne & Taylor, existe una gran variabilidad inter- e intraindividual existente en los comportamientos y destinos celulares en respuesta a los distintos compuestos antimitóticos. Esto permite enfatizar la complejidad de los mecanismos y respuestas celulares ante dichos tratamientos, dificultando la interpretación y la obtención de conclusiones firmes.

La catástrofe mitótica puede conducir a las células a través de distintas rutas de muerte celular, como por ejemplo, la apoptosis o la necrosis. No obstante generalmente se acepta que en respuesta a fármacos antimitóticos, en la mayoría de ocasiones, la muerte celular muestra características propias de la ruta canónica mitocondrial de la apoptosis. Nuestros resultados también han proporcionado evidencias en esta dirección.

A pesar de esta capacidad citotóxica, el desarrollo de la resistencia a fármacos antimitóticos clásicos como son los inhibidores de microtúbulos es frecuente. Así mismo, el fracaso inicial que han tenido en los ensayos clínicos los nuevos tratamientos antimitóticos más específicos y dirigidos contra proteínas mitóticas, urgen el desarrollo de nuevas aproximaciones terapéuticas que puedan afrontar estos problemas.

En el modelo "competitive network" postulado por Gascoigne & Taylor, indica que el destino de la célula ante una mitosis anómala está determinado por el exquisito balance existente entre la señales de muerte celular y los mecanismos que controlan la salida de la mitosis. Por esta razón, una buena estrategia terapéutica para mejorar la eficacia de estos fármacos antimitóticos pasaría por la inclinación de este balance en favor de las señales de muerte celular, acelerando o intensificando las mismas. A este respecto, la familia de proteínas Bcl-2 desempeña un papel clave en la regulación de las vías apoptóticas de muerte celular y en las decisiones que toma la célula sobre el destino celular ante un bloqueo mitótico prolongado. Por esa razón, los miméticos de BH3 son considerados excelentes candidatos terapéuticos. Así, nuestro objetivo durante esta parte del trabajo ha consistido en estudiar el papel de esta familia de proteínas Bcl-2, tan crítica y al mismo tiempo tan versátil, en la regulación del destino celular tras el arresto mitótico.

Tal y como ilustran nuestros resultados, la combinación de agentes antimitóticos con el mimético de BH3, ABT-737, provocó un efecto citotóxico mayor, especialmente en las líneas celulares A549 y MIA PaCa-2, que las combinaciones con ABT-199, así como los efectos de los fármacos individuales. Otros estudios también apoyan la capacidad del ABT-737 para sensibilizar el tratamiento con taxanos, en múltiples modelos de celulares, así como en modelos tumorales xenotransplantados. Descifrar el papel relativo de los distintos miembros de la familia Bcl-2 en el destino celular ante el bloqueo en mitosis es fundamental desde un punto de vista tanto teórico como terapéutico. Sin embargo, este estudio puede resultar complicado por la superposición funcional que existe entre las diferentes proteínas de esta familia. A pesar del incesante trabajo de varios laboratorios, todavía no se ha logrado alcanzar un consenso general al respecto. En nuestra experiencia experimental, los distintos miembros antiapoptóticos parecen mostrar un efecto protector cooperativo y acumulativo.

En otro orden, aunque nunca ha ganado científicamente una clara unanimidad, se ha propuesto que la duración del arresto mitótico puede influir y dictar el destino celular ante dicho bloqueo. Nuestros resultados en los experimentos de time-lapse también parecen respaldar estas observaciones. Estos experimentos revelaron que las tasas de muerte celular durante la mitosis aumentaron considerablemente con aquellos agentes antimitóticos que provocaban un arresto mitótico más prolongado, como con los MTAs. En estas circunstancias, un bloqueo mitótico prolongado provocaría modificaciones post-traduccionales que reducirían la estabilidad de Mcl-1 y las actividades antiapoptóticas de Bcl-2 y Bcl-X_L por fosforilación. De hecho, nuestros datos muestran que tanto Bcl-2 como Bcl-X_L son fosforiladas en presencia de docetaxel y

vincristina, pero no con barasertib. Así, cuanto más tiempo pase una célula en mitosis, más se permite que se acumulen señales pro-apoptóticas, favoreciendo que las células sucumban durante la mitosis en lugar de escaparse y sufrir un destino celular post-mitótico. En esta misma línea, nuestros datos muestran que la población más propensa a sobrevivir al bloqueo en mitosis, pasó menos tiempo de media en esta fase. Además, nuestros datos sugieren que la administración de ABT-737 con los inhibidores de microtúbulos es capaz de acelerar la muerte celular durante la mitosis. Esta aceleración de la muerte celular inducida por la adición de miméticos de BH3 durante el bloqueo en mitosis provocado por distintos fármacos antimitoticos, también ha sido observada por distintos autores, mientras que otros rebaten estos hallazgos.

En cuanto a la maquinaria molecular que dirige la muerte celular bajo el tratamiento combinado de barasertib y ABT-737, parece seguir una ruta molecular diferente. Curiosamente, tras la inhibición de Aurora B, las células no quedan detenidas demasiado tiempo en mitosis y rápidamente "se saltan" el punto de control del huso-mitótico, saliendo de la mitosis de forma aberrante. De esta forma, las células sobreviven y alcanzan la fase G1 del siguiente ciclo con manifiestas alteraciones morfológicas a nivel nuclear. De hecho, detectamos que las células podían permanecer durante largos períodos de tiempo en este estado sin activarse la muerte celular. Curiosamente, las células A549 y HCT-166 tratadas con el inhibidor de Aurora B, mostraban características propias de un estado senescente, con una mayor actividad β-galactosidasa, así como una morfología celular característica. Cabe destacar que cuando ABT-737 se administró a las células tratadas con barasertib, una vez que estas ya habían desarrollado el fenotipo senescente, el mimético de BH3 sensibilizó de manera muy efectiva las células cancerosas, reconduciéndolas hacia la muerte celular. Esta propiedad senolítica del ABT-737 ha sido previamente demostrada por otros autores en sendos modelos independientes de senescencia *in vivo*. De esta manera, haciendo uso de esta estrategia molecular senolítica podría ayudar a combatir diferentes escenarios como son la eliminación de las células cancerosas senescentes de lesiones pre-malignas, la resistencia por la senescencia o, por ejemplo, las terapias que inducen catástrofe mitótica seguida de la activación de la senescencia celular.

Finalmente, la activación de los mecanismos oncosupresores intrínsecos a las propias células durante la catástrofe mitótica, no es la única forma mediante la cual los agentes antimitóticos pueden eliminar células cancerosas. De hecho, se ha demostrado que las células cancerosas poliploides son intrínsecamente inmunogénicas al activar constitutivamente las vías de estrés del ER, con la consiguiente exposición de señales inmunogénicas como CRT. Estos estudios también mostraron que el tratamiento con alcaloides de la vinca o taxanos también resultó en un aumento de los DAMPs *in vitro* y además de proporcionar protección profiláctica en experimentos de vacunación. Nuestros resultados también apuntan en la misma dirección ya que tanto las células A549 como las células MIA PaCa-2 mostraron un aumento en la expresión de CRT en la membrana con todos los tipos de fármacos antimitóticos y combinaciones probados.

Colectivamente, estos estudios afianzan la existencia de un sistema de inmunovigilancia contra el cáncer que permite seleccionar y eliminar aquellas células que cuentan con un número de cromosomas elevado y que albergan un mayor potencial para transformarse en un fenotipo más maligno y tumorigénico.

Dados los resultados alentadores obtenidos en las combinaciones de estos fármacos en modelos de tumores sólidos decidimos intentar trasladarlo a neoplasias hematológicas como el MM. De hecho, la desregulación del ciclo celular o la interrupción del aparato mitótico son detectados con frecuencia y se cree que juegan un papel importante durante el desarrollo de esta enfermedad. Además, la supervivencia y resistencia del MM también está influenciada de manera decisiva por la familia Bcl-2. Por lo tanto, el uso de miméticos BH3 junto con las terapias dirigidas contra la mitosis, podría considerarse una buena estrategia para mejorar la terapia contra el mieloma. No obstante, de manera general nuestros resultados no mostraron potenciación de la muerte celular cuando los diferentes agentes antimitóticos se combinaron con ABT-737, con la excepción de las células U266 en algunas condiciones. Quizás, otros mecanismos estén encargados de dirigir la muerte de células MM bajo estas condiciones a diferencia de lo observado en tumores sólidos. Estos resultados parece que también se están reproduciendo en la clínica, ya que hasta la fecha, los ensayos que se encuentran investigando los nuevos antimitóticos en combinación con otras terapias sólo han mostrado respuestas parciales o como mucho una estabilización de la enfermedad. Por lo tanto, aunque atacar al aparato mitótico puede ser prometedor, dados estos resultados desalentadores, decidimos proceder con una lógica diferente en nuestra búsqueda para mejorar el manejo de la enfermedad de mieloma.

De esta manera el estrés en el ER, está siendo cada vez más aclamado entre la comunidad científica por tener el potencial de ser una diana terapéutica poderosa contra muchos tumores sólidos y hematológicos. De hecho, el propio proceso de transformación maligna desata un nivel muy considerable de estrés celular que por supuesto, también alcanza y termina afectando a la proteostasis celular. Precisamente en el MM, este microambiente estresante es exacerbado dada la naturaleza intrínseca de las células plasmáticas. La capacidad de las células plasmáticas y de mieloma para fabricar industrialmente ingentes cantidades de inmunoglobulinas hace que estas células sean especialmente dependientes de las señales de supervivencia generadas por la UPR. Sin embargo, aunque las células de mieloma dependen de la UPR para prosperar, al mismo tiempo, esto las hace más adictas y extremadamente vulnerables a la muerte celular asociada al estrés en el ER. Esta peculiaridad adquiere sentido cuando observamos la distinguida eficacia clínica que han tenido los inhibidores del proteasoma en el tratamiento del MM. Aunque el mecanismo de acción del bortezomib se ha caracterizado ampliamente, el mecanismo de acción del carfilzomib no se ha estudiado tan profundamente. De hecho, nuestro grupo ha participado en la caracterización de la muerte celular inducida por carfilzomib en líneas celulares de MM y en modelos murinos xenotransplantados. No obstante, a pesar de la validada eficacia clínica de estos

fármacos, la resistencia a estos sigue siendo recurrente y abarca la mayoría de las recidivas. Esta situación por tanto exige que se diseñen y estudien nuevos esquemas terapéuticos para abordar las recaídas. Dado que el estrés del ER es considerado el 'talón de Aquiles' del MM, en el presente trabajo buscamos explorar estrategias combinatorias basadas PIs que disminuyan notoriamente la supervivencia de las células de mieloma, así como indagar en los “entresijos” de los mecanismos de muerte celular que gobiernan estos procesos moleculares.

En este sentido, la autofagia es otro de los sistemas celulares de reciclaje capaz de eliminar las proteínas celulares no deseadas y que puede ayudar a 'socorrer' al ER cuando las condiciones de estrés son abrumadoras. De hecho, el ER puede dar la voz de alarma y emitir señales que activen la autofagia con el fin de proporcionar asistencia al ER y así restablecer la homeostasis celular. Estudios muestran que en el MM, la autofagia puede actuar como una 'armadura' protectora contra los efectos perjudiciales derivados del estrés del ER durante el proceso de transformación maligna o debidos al fenotipo secretor del MM. Además, la autofagia también podría ser utilizada por las células de mieloma para adquirir resistencia contra los efectos mediados por fármacos. De hecho, el mal pronóstico en pacientes con MM se ha correlacionado con la sobreexpresión de genes relacionados con respuestas antioxidantes, chaperonas y autofagia. Por lo tanto, dirigir la terapia contra el proteasoma y la autofagia de forma conjunta podría considerarse como un prometedor enfoque terapéutico contra esta enfermedad. De hecho, nuestro grupo demostró la capacidad de la cloroquina para potenciar fuertemente la muerte celular inducida por carfilzomib en mieloma tanto en modelos *in vitro* e *in vivo*. Durante este trabajo, se ha logrado observar también una intensificación similar de la muerte celular en las diferentes líneas celulares humanas y murinas analizadas. Además, la mejorada capacidad citotóxica de esta combinación también se ha constatado en una amplia colección de muestras primarias de médula ósea aisladas de pacientes con MM. Aunque el mecanismo molecular aún no se ha aclarado completamente, estos resultados están respaldados por datos de grupos independientes que también mostraron que la inhibición de la autofagia mediante la CLQ u otros inhibidores es capaz de sensibilizar las células cancerosas a los PIs (incluido carfilzomib) y también a otros tipos de quimioterapéuticos. Sin embargo, estas observaciones no están ausentes de polémica ya que algunos autores manifiestan respuestas antagónicas entre el bortezomib y el tratamiento con CLQ. Todo este trabajo preclínico instó a la comunidad científica a lanzar ensayos clínicos que evaluaran este, aparentemente prometedor, régimen quimioterapéutico. Los ensayos clínicos de fase I y pequeños ensayos de fase II mostraron la viabilidad de este enfoque y revelaron una respuesta modesta con resultados contradictorios sobre la eficacia de este enfoque para superar la resistencia a PIs en pacientes refractarios.

De manera similar a lo que ocurre con la CLQ, también hemos observado que el DBeQ, inhibidor de VCP/p97, también aumenta notablemente la muerte celular inducida por carfilzomib tanto en líneas celulares de MM como en células de mieloma

primarias. Cabe destacar que la sensibilización a la muerte celular por DBeQ no fue tan pronunciada como la observada con las combinaciones de CLQ. Aunque no hay información al respecto sobre las combinaciones de carfilzomib y DBeQ, otros autores sí que han manifestado un mayor poder citotóxico con la inhibición dual de p97/VCP y el proteasoma a través de bortezomib.

Descifrar los mecanismos de resistencia que las células cancerosas pueden aprovechar, es fundamental no solo para diseñar nuevos diseños terapéuticos que eviten la recurrencia tumoral, sino también para poder seleccionar aquellos pacientes que pueden beneficiarse de una estrategia terapéutica específica. Hasta el momento, en la toma de decisiones clínicas, todavía no se han llegado a aplicar con éxito biomarcadores de sensibilidad o resistencia a la quimioterapia. Para ampliar aún más nuestra comprensión sobre este tema, nuestro objetivo también ha consistido en tratar de analizar si la respuesta *ex vivo* en células de mieloma primario al carfilzomib, así como las respectivas las combinaciones, son dependientes de diferentes parámetros clínicos u otros criterios de sensibilidad al fármaco. Nuestros datos mostraron que aunque en la mayoría de los individuos, las células de mieloma primario eran sensibles al tratamiento individual con carfilzomib *ex vivo,* algunos pacientes no respondieron a este compuesto. Aunque las diferencias encontradas fueron no significativas, cabe decir que los individuos con anomalías citogenéticas o tratados con un mayor número de líneas de tratamiento tendieron a exhibir una mayor sensibilidad *ex vivo* al carfilzomib. Con respecto a las combinaciones de carfilzomib con CLQ y DBeQ, nuestros datos mostraron que dichos tratamientos generaban respuesta citotóxica *ex vivo* incluso en pacientes con anormalidades citogenéticas, o individuos clasificados como resistentes a PI. Estos resultados abren la posibilidad de poder superar la resistencia a PIs con dichos regímenes combinatorios. Otros autores también han demostrado que la HCLQ o un nuevo inhibidor de VCP/p97 (como DBeQ) sensibilizan las células MM resistentes a PIs. Además, aunque también era solo una tendencia, cuando se segregaron a los pacientes atendiendo a la cantidad de líneas de tratamiento que habían recibido, la respuesta a los compuestos *ex vivo* era mayor con la cantidad de terapias recibidas. Así, los individuos clasificados como "respondedores" a dichas combinaciones mostraron un número medio más alto de líneas totales de tratamiento recibidos.

No obstante, debe recalcarse que muchas de estas tendencias en la relación entre citogenética, líneas de tratamiento y sensibilidad *ex vivo,* se consideraron estadísticamente no significativas y, por lo tanto, el impacto real de estas observaciones debería tomarse con prudencia. Una explicación simple podría consistir en que las respuestas a la terapia *ex vivo* no están relacionadas con el perfil citogenético presentado por los individuos afectados o con la inherente resistencia a los medicamentos que las células de mieloma puedan exhibir. Es más que probable que la respuesta de las células de MM a la terapia dependa de múltiples factores intrínsecos y extrínsecos que pueden impactar en el resultado final. Quizás métodos de estratificación más poderosos como GEP, RNA-seq o tecnologías que permitan un cribado masivo de fármacos, sean capaces

de proporcionar mejores criterios de agrupamiento y estratificación para encontrar una relación más precisa con las respuestas a la terapia.

Durante este trabajo también hemos tratado de caracterizar *in vitro* las vías moleculares de señalización que desencadenan la muerte celular en estas condiciones. Un hecho interesante que también se detectó en trabajos anteriores de nuestro grupo es que la CLQ muestra predilección especial, en términos de potenciación de citotoxicidad, por el carfilzomib en lugar de por el bortezomib. Baranowska y colaboradores obtuvieron también resultados análogos a este respecto. El mecanismo molecular por el cual se materializa esta amplificación aún no se ha podido dilucidar. Algunos estudios parecen apuntar a mecanismos independientes de autofagia en la sensibilización provocada por la CLQ. Para desentrañar este enigma, en este trabajo hemos inspeccionado y analizado a fondo los actores moleculares y las vías involucradas para caracterizar el mecanismo de muerte celular ejercido por estas combinaciones de compuestos.

Hemos observado que las combinaciones de carfilzomib con CLQ o DBeQ no sólo potencian, sino que también aceleran la muerte celular. Este hecho, podría deberse a una mayor acumulación de señales de muerte celular que desencadenan más rápidamente la cascada apoptótica. Consecuentemente, también hemos demostrado que estos tratamientos aumentan la expresión de varios marcadores de la UPR (especialmente XBP1s, BiP, CHOP y, en menor medida, p-eIF2α). No obstante, esta respuesta de estrés en el ER observada, dependía estrechamente del tiempo y variaba sustancialmente entre las distintas líneas celulares de MM. Además, también se observó que el tratamiento con estas combinaciones de fármacos fueron más efectivas a la hora de aumentar los niveles de ROS. Como los datos muestran evidencias de la activación de PERK e IRE1α, también se trató de inspeccionar la participación relativa de estas dos ramas de la UPR en la muerte celular mediante el uso de inhibidores químicos. En este sentido, la inhibición de PERK aumentó la muerte celular inducida por las combinaciones basadas en carfilzomib en la mayoría de las líneas celulares, lo que sugiere que PERK podría tener un papel protector, más que un papel pro-apoptótico. Al mismo tiempo, se observó poco o ningún efecto protector cuando la actividad de RNasa IRE1 era inhibida con 4μ8C, lo que parece indicar que esta rama tiene un papel menor en la muerte celular inducida por estrés en el ER. Las células reaccionan al estrés en el ER generando dos "olas" de activación de la UPR, una de reparación y otra de muerte, separadas en el tiempo. Cómo y por qué la célula activa o cambia de un programa molecular determinado u otro, requiere de una mayor indagación.

Es bien conocida la función fundamental que BiP ejerce para mantener las funciones asociadas del ER y proteger a las células de las agresiones proteotóxicas. Se planteó la hipótesis de que los niveles basales de BiP observados en ciertas líneas podrían estar detrás de la resistencia a los compuestos utilizados. Sin embargo, cuando silenciamos la expresión de BiP mediante siRNAs, aparentemente, la ausencia de BiP no sensibilizó a las células cancerosas a los fármacos quimioterápicos. Nuestros resultados difieren claramente con los manifestados en la literatura en los que el silenciamiento de

BiP mediado por siRNA, sí que sensibilizó a las células cancerosas a diversos tipos de medicamentos (incluido el bortezomib) en distintos modelos de células tumorales. Alternativamente, otras chaperonas como las proteínas Hsp90 o Hsp70, también podrían sobreexpresarse en condiciones de estrés ER y podrían ayudar aliviando el estrés proteotóxico y equilibrando la escasez o ausencia de BiP.

A pesar de la existencia de varios estudios que respaldan la participación de las ramas de PERK e IRE1α en la muerte celular inducida por estrés en el ER, en nuestro modelo experimental, el establecimiento de una conexión entre la UPR y los ejecutores de la muerte celular, probablemente requiera de un estudio más detallado. La señalización mediada tanto por PERK como por IRE1α puede provocar efectos contrapuestos sobre el destino celular, ya sea bien de supervivencia o de muerte celular. Se cree que el resultado final podría estar muy influenciado por el tipo, la intensidad de las señales de estrés y la amplitud de la respuesta a dicho estrés. En nuestro modelo experimental, hemos observado un aumento de la expresión tanto de los marcadores relacionados con PERK como IRE1 que pueden estar asociados tanto a funciones pro-apoptóticas (CHOP) como de supervivencia (BiP o XBP1). Es difícil discernir la contribución individual de estos factores al destino final de la célula. Probablemente, los efectos agudos e irreversibles inducidos por el estrés farmacológico puedan empujar a las células abrupta e inexorablemente hacia la muerte celular. En tal situación, las respuestas de estrés en el ER adaptativas y pro-apoptóticas probablemente coincidirían en el tiempo complicando así su análisis.

Como se ha visto, la familia Bcl-2 ocupa una posición trascendental en las respuestas mediadas por estrés en el ER. Nuestros datos revelaron que mientras los niveles de expresión de algunos miembros permanecieron inalterados (Bcl-2), otros manifestaron una acumulación temprana transitoria que se disipaba con el tiempo (Mcl-1, Bim, PUMA y en menor medida NOXA). Con los datos actuales, no se puede concluir si este patrón de expresión es un efecto secundario de la inhibición del proteasoma o más bien derivado de la señalización de la UPR. Además, aunque abundantes evidencias apuntan a que las proteínas sólo-BH3 pueden ser moduladores importantes de la muerte celular inducida por estrés en el ER, nuestros datos mostraron que la línea celular CRISPR Bim KO solo ofrecía una protección parcial contra la muerte celular inducida por los fármacos utilizados. Por lo tanto, su deficiencia parece ser compensada por otros miembros de BH3 capaces de desencadenar la muerte celular tras el tratamiento farmacológico. Para instigar la muerte celular por la vía canónica, también se requiere la permeabilización de la membrana externa mitocondrial (MOMP) inducida por la oligomerización de Bax/Bak. Sin embargo, nuestros datos han demostrado la capacidad de las terapias basadas en PIs, así como su combinación con CLQ o DBeQ de inducir la muerte celular en células deficientes en Bax/Bak. Esto es importante porque la falta de expresión de estos mediadores pro-apoptóticos está detrás de los mecanismos de resistencia que albergan las células tumorales.

Aunque todavía no se conoce con exactitud el mecanismo molecular responsable de la muerte celular inducida por estrés en el ER, existen pruebas de la participación tanto de la vía de los receptores mortales como de la vía intrínseca de la apoptosis. Nuestros resultados revelaron que la muerte celular inducida por las combinaciones basadas en carfilzomib era dependiente de caspasas en la mayoría de las líneas celulares analizadas. La contribución relativa de cada miembro de la familia de las caspasas variaba con las diferentes líneas celulares MM. Algunas líneas presentaban una mayor dependencia de miembros directamente implicados en la formación del apoptosoma como la caspasa-9, mientras que en otras (U266 y MOPC315.BM), la muerte celular parecía depender más de la caspasa-8, quizás involucrando en menor medida la formación del apoptosoma. Aunque la caspasa-8 sigue la vía extrínseca de los receptores mortales, estudios revelan que el estrés persistente en el ER también podría inducir muerte celular mediada por la caspasa-8. Aunque no está ausente de polémica, diferentes grupos apuntan a diversos mecanismos potenciales por los cuales el estrés persistente en el ER puede inducir la muerte celular mediada por caspasa-8 en ausencia de ligandos mortales. De hecho, una alternativa interesante para la muerte celular independiente de Bax/Bak observada en nuestro modelo, podría apuntar a la caspasa-8 y los receptores DR4/DR5 como elementos clave en este escenario.

También se ha estudiado la implicación de la autofagia en el mecanismo de muerte celular inducido por la combinación carfilzomib-CLQ. Los datos presentados en este trabajo utilizando células deficientes en ATG5 sugieren que la inhibición de la autofagia participa parcialmente, pero no es la única causa de la sensibilización provocada por la CLQ. De hecho, algunos estudios apuntan a que la CLQ potencie la citotoxicidad de los PIs mediante mecanismos independientes de la autofagia. Durante la búsqueda de efectos alternativos mediados por la CLQ, encontramos que algunos autores afirmaban que este compuesto era capaz de restringir la actividad enzimática del proteasoma de una manera no competitiva al unirse reversiblemente al proteasoma cerca del sitio activo. Curiosamente, en este estudio la unión simultánea de un PI y CLQ al proteasoma era estéricamente posible. Nuestros datos también avalan estas observaciones ya que la administración conjunta de CLQ y PIs disminuyó aún más la actividad del proteasoma, que cuando se administraban los PIs individualmente. Curiosamente, el efecto de la CLQ era más potente a la hora de anular la actividad del proteasoma en combinación con carfilzomib que con el tratamiento con bortezomib. En conjunto estos datos, refuerzan idea de que la CLQ pueda funcionar como un modulador alostérico en la terapia basada en PIs.

En los últimos años, los logros alcanzados por la inmunoterapia en la oncología han posicionado claramente a este tipo de terapia como una herramienta fundamental en el tratamiento del cáncer. Además, la idea de que las remisiones duraderas generadas por la quimioterapia clásica o dirigida, son producto de la capacidad de estas para fomentar la inmunovigilancia contra el cáncer, ha transformado la panorámica terapéutica en inmuno-oncología. También, la introducción del concepto de "muerte

celular inmunogénica" ha contribuido indudablemente a este nuevo paradigma. Pero tal vez la primera pregunta que uno debe hacerse cuando se trabaja para desarrollar respuestas inmunes contra el mieloma es: ¿Son las células de mieloma realmente inmunogénicas? Teniendo en cuenta todo el panorama, la inmunogenicidad de la muerte celular y la consiguiente respuesta inmune anticancerígena *in vivo* pueden involucrar los siguientes elementos: Antigenicidad—tipo de tumor; Adjuvanticidad e inflamación—señalización por DAMPs; y factores genéticos y ambientales—hospedador y microambiente.

Comenzando con la **antigenicidad**, existe una enorme diversidad en la carga mutacional que cada uno de los distintos tipos de tumores alberga. Con respecto al MM, aunque este tipo de neoplasias portan una cantidad importante de anomalías citogenéticas, la densidad de neoantígenos suele ser de baja a intermedia. No obstante, los pacientes que exhiben un alto número de mutaciones y de neoantígenos se asociaban con peores tasas de supervivencia cuando eran sometidos a tratamientos convencionales. Aunque existen varios antecedentes que respaldan la existencia de una respuesta inmune anti-mieloma específica de antígeno, hay otros estudios que indican lo contrario manifestando la baja inmunogenicidad de las células mielomatosas. De hecho, nuestros datos también reflejan que a pesar de existir cierto grado de infiltración inmune en el tumor, la protección ofrecida *in vivo* fue escasa o nula. Por ello, aunque se han revelado la existencia de diversos epítopos en el mieloma, los resultados están lejos de ser exitosos, especialmente en cuanto a protocolos de vacunación se refiere. Todavía quedan muchas complejidades técnicas y experimentales que deben abordarse y refinarse para poder desarrollar un protocolo de vacunación exitoso.

En cuanto a la **adyuvancia** conferida por los distintos programas moleculares de muerte celular, la generación de DAMPs en este contexto es de suma importancia. Durante el proceso de muerte celular, se ha visto que diferentes factores, como el tipo de muerte celular, el agente inductor de ICD y la interacción entre varias vías de señalización de estrés celular, influyen en la cantidad y tipo de señales de peligro emitidas. A este respecto, las respuestas al estrés del ER, la UPR (especialmente el brazo mediado por PERK) y la generación de ROS son figuras destacadas en la ICD. Los compuestos utilizados en nuestro trabajo pueden evocar de forma efectiva respuestas de estrés del ER en las células MM y, en particular, aumentar los marcadores asociados con la ICD, como la activación de PERK y la fosforilación de eIF2α. Además, hemos demostrado la capacidad del carfilzomib y sus combinaciones con CLQ y DBeQ para exponer *in vitro* varios DAMPs (chaperonas moleculares como CRT, Hsp70 y BiP). Por lo tanto, en un principio estos regímenes quimioterapéuticos podrían ser buenos candidatos para ser considerados inductores de ICD con la capacidad de potenciar respuestas inmunes protectoras *in vivo*. Aunque la exposición de CRT generalmente se correlaciona con la inmunogenicidad de la muerte celular, aunque necesaria, por sí sola no es suficiente. Para inducir una respuesta inmune antitumoral eficaz, son necesarias también la presencia de otras señales de peligro convencionales como el ATP, HMGB1 e

IFNs tipo I, además quizás de otro conjunto de DAMPs menos convencionales. Una de las consecuencias importantes de esta señalización por DAMPs durante la ICD es la activación funcional de las APCs. Todas estas señales de peligro pueden ser detectadas por las APC, estimular la captación fagocítica de antígenos tumorales, la maduración fenotípica de las APC y su atracción quimiotáctica. Por ejemplo, nuestros datos reflejan que el patrón de DAMPs generado por los compuestos utilizados en nuestro estudio tiene la capacidad de instigar adecuadamente la maduración de las DCs. En esencia, la señalización y las rutas de tráfico celular de DAMPs se consideran procesos flexibles. Probablemente, el tipo y la consecución espacio-temporal de las señales de peligro o estrés generadas, influirán en el nivel de maduración y de la coestimulación proporcionada por las DCs y, por lo tanto, en la respuesta global antitumoral.

Desentrañar los mecanismos moleculares que dotan a las células moribundas o estresadas con características inmunogénicas es primordial para mejorar el potencial terapéutico de las terapias actuales o en desarrollo. El papel del estrés en el ER y la generación de ROS en la ICD ha sido ampliamente contrastado por varios laboratorios independientes. En nuestro trabajo, podemos establecer una asociación entre la respuesta al estrés del ER con la producción de ROS y la emisión de señales de peligro. Sin embargo, no podemos determinar que la generación de DAMPs es una consecuencia directa del estrés producido por los fármacos en el ER ya que no hemos logrado establecer una relación causal a este respecto.

El papel de la autofagia en la señalización de DAMPs también es un tema bajo debate. Particularmente porque se han encontrado discrepancias con respecto a la implicación de la autofagia en la translocación de la CRT dependiendo del tipo de terapia aplicada. Es importante destacar que los diferentes pasos del proceso autofágico pueden desempeñar papeles diferentes en la exposición de CRT. Recientemente, un estudio mostró que cuando se inhibía la autofagia en etapas tempranas, disminuía la translocación de la CRT, mientras que su inhibición en las últimas etapas con CLQ u otros compuestos aumentaba los niveles de ecto-CRT. Nuestros datos también se ven reflejados en este último estudio, ya que el silenciamiento de ATG5, que afecta a las etapas tempranas, también provoca una disminución de la translocación de CRT, mientras que la inhibición de la autofagia con CLQ potencia la exposición a ecto-CRT. También nuestros datos apuntan a que el efecto potenciador de la CLQ en la exposición de CRT sea independiente de la autofagia.

Todos nuestros resultados *in vitro* respaldan por tanto la idea de que los tratamientos farmacológicos utilizados podrían ser capaces de provocar ICD en células de MM. Sin embargo, nuestros resultados *in vivo* revelaron que la vacunación profiláctica con células de MM tratadas *in vitro* con dichos fármacos, no ofrecía una protección inmunitaria importante contra el desarrollo de la enfermedad. Los ratones vacunados con células de MM tratadas con carfilzomib o la combinación de carfilzomib y CLQ, no mostraron mayor supervivencia o retraso en la progresión de la enfermedad. Sólo cuando los ratones fueron vacunados con una formulación que contenía células de

MM tratadas con la combinación de carflizomib-CLQ y el inhibidor de caspasa z-VAD-fmk, se evidenció una pequeña protección contra el desarrollo de la enfermedad. Claramente, nuestros resultados *in vivo* no respaldan los datos observados *in vitro*, lo que indica que puede haber otros factores que influyan en la inmunogenicidad de la muerte celular y la generación de respuestas inmunes antitumorales *in vivo*.

Una cuestión importante en este campo involucra a las funciones desempeñadas por las caspasas en la inmunogenicidad de la muerte celular. Y es que al parecer, las caspasas se han revelado como piezas fundamentales en cómo la muerte celular es percibida por el sistema inmune, modulando e impactando en las señales que emanan de las células moribundas. No obstante, este tema está demostrando ser desafiante y aún no se han podido extraer respuestas completas ni conclusiones sencillas. *In vitro*, nuestros datos muestran que, dependiendo de la línea celular, las caspasas pueden presentar favorecer o dificultar la señalización de este DAMP. Recientemente, se ha demostrado en diferentes contextos, que la anulación de la actividad de las caspasas potenciaba las respuestas inmunes sistémicas por mecanismos que posiblemente impliquen la acumulación de señales inmunogénicas al retrasar el desmantelamiento celular. En esta misma línea, nuestros experimentos de vacunación *in vivo* mostraron que sólo cuando los ratones fueron inmunizados con células tratadas con formulaciones que contenían z-VAD-fmk, la progresión de la enfermedad se retrasó sutilmente. Es posible que por un mecanismo aún desconocido, las caspasas puedan dificultar la translocación ectópica de CRT u otros DAMPs en estas condiciones.

Otros dos elementos importantes que no deben pasarse por alto en el contexto de la ICD son el hospedador y el microambiente tumoral. Los modelos tumorales que surgen espontáneamente están sujetos a procesos de inmunoedición constante por el sistema inmune del huésped, lo que reproduce mejor las dificultades reales encontradas en la enfermedad del cáncer humano. Estas condiciones también podrían ocurrir en el modelo MOPC315.BM utilizado en este trabajo. Aunque hemos encontrado cierto grado de infiltración inmune en los diferentes nichos tumorales, las diferencias fueron débiles y no significativas en la mayoría de los casos. El aumento de la infiltración inmune en los nichos tumorales podría interpretarse como la capacidad de las células inmunes para reconocer el tumor. Sin embargo, aparentemente esta respuesta no fue suficiente para retrasar la progresión de la enfermedad.

A la vista de nuestros datos, la emisión de DAMPs por sí misma podría no ser suficiente para provocar respuestas inmunitarias activas contra el cáncer. De hecho, se considera igualmente decisivo los mecanismos subyacentes involucrados en la recepción, transmisión y respuesta de las células inmunes a estas señales de peligro. Cuando nos enfrentamos a una enfermedad tan compleja y adaptativa como es el cáncer, se deben considerar aspectos adicionales como la propia naturaleza inmunosupresora de esta enfermedad. En particular, el MM se caracteriza por una disfunción inmune generalizada que podría obstaculizar la inmunovigilancia y la eficacia de la inmunoterapias. Aunque estos factores inmunosupresores no se han evaluado *in vivo*, sí que hemos observado la

mayoría de estas características en muestras de pacientes con MM. Además, se ha demostrado que el modelo MOPC315.BM compromete importantes órganos hematopoyéticos como el bazo y la médula ósea que pueden explicar la escasa respuesta inmune observada en los ratones vacunados. Por esa razón, aunque puede existir una respuesta antitumoral inicial, las células MM pueden sabotear los compartimentos hematopoyéticos disponibles una vez que se establece la enfermedad, deprimiendo la inmunovigilancia antitumoral.

Una de las razones detrás de la disfunción inmune en el MM está mediada por la regulación negativa ejercida por las proteínas inhibidoras del punto de control como el eje PD-1/PD-L1. De hecho, observamos que un alto porcentaje de células MOPC315.BM expresaban PD-L1 en condiciones basales. Parece factible que la ausencia de protección inmune evidenciada en los experimentos de vacunación, pueda ser debida a la capacidad de las células MOPC315.BM para eludir la inmunovigilancia a través del eje PD-1/PD-L1. Por ello, este punto de control inmunitario podría considerarse como un buen enfoque terapéutico para provocar una respuesta potente iniciada por la ICD y convertir el microambiente hostil en un lugar inmunológicamente más ameno. Sin embargo, nuestros datos revelaron que el bloqueo del punto de control tanto individualmente como en combinación con formulaciones de vacunación, no extendía significativamente la supervivencia de los ratones. A partir de estos resultados, podríamos inferir que el eje PD-1/PD-L1 puede no estar implicado en la evasión inmune provocada por las células MM, y que puede no ser el responsable de la pequeña protección inmunitaria observada en nuestro estudio. Mientras algunos autores sí que han observado con éxito respuestas *in vivo* con este tipo de inmunoterapia, otros estudios niegan que el bloqueo de PD-1 o CTLA-4 tenga repercusiones sobre la progresión en modelos de mieloma. En humanos, el bloqueo del punto de control en monoterapia también ha producido escasas respuestas clínicamente objetivas. Además de la vía PD-1/PD-L1, existe un amplio abanico de inhibidores del punto de control inmunitario y que también pueden tener funciones importantes en la evasión inmunitaria del mieloma (CTLA-4, LAG-3, TIM-3, GITR, TIGIT) y que podrían incluso compensar el bloqueo del eje PD-1/PD-L1.

El intenso trabajo de investigación básica en la “poyata” ha ayudado a consolidar la señalización de DAMPs y la ICD como actores importantes en las respuestas inmunitarias antitumorales. Sin embargo, algunas preguntas aún permanecen sin resolver, especialmente cuando se intenta proyectar estos conceptos a la 'cama' del paciente, es decir, en la práctica clínica. Por ejemplo: ¿Cuál es la repercusión real de estos procesos moleculares en la clínica? o ¿los regímenes quimioterapéuticos actuales (dosis y pautas) pueden desencadenar ICD en los tumores de pacientes? Más importante aún es que los datos preclínicos suponen que la exposición de DAMPs sólo ocurre como consecuencia de la quimioterapia. Sin embargo, estos no tienen en cuenta la posibilidad de que la exposición de DAMPs también pueda ocurrir en ausencia de terapia, ni sus implicaciones en la transformación maligna o en las respuestas inmunitarias contra el cáncer. De hecho, cada vez más se está consolidando la idea de que los DAMPs y los

procesos moleculares relacionados con la ICD puedan servir como una fuente de biomarcadores pronósticos para ser descubiertos en pacientes con cáncer.

En este trabajo hemos demostrado por primera vez que las células de mieloma en muestras de médula ósea aisladas de pacientes con discrasias de células plasmáticas, muestran niveles elevados de ecto-CRT en su superficie. Además, aunque se observó una gran variabilidad interindividual, nuestros datos sugieren que los niveles de ecto-CRT parecen aumentar con la progresión de la enfermedad. Este hallazgo junto con el hecho de que los pacientes con un perfil citogenético alterado mostraron niveles aumentados de ecto-CRT y que la exposición a la CRT aparentemente no está influenciada por la quimioterapia, conjuntamente pueden apuntar a la transformación maligna como el instigador principal de la expresión ectópica aumentada de este DAMP. Esto también ha sido observado en pacientes con AML o NSCLC, en los cuales se exhibían niveles aumentados de ecto-CRT independientemente de la quimioterapia.

Ya sea inducida por la quimioterapia o, más bien, derivada del proceso de transformación oncológica, determinar la exposición o expresión de CRT podría ser relevante ya que podría tener un valor pronóstico en pacientes con cáncer. La literatura actual muestra que, dependiendo del tipo de tumor este DAMP podría asociarse bien con una mejor vigilancia inmunológica contra el cáncer y, en consecuencia, con un mejor pronóstico clínico o, alternativamente, con un fenotipo más agresivo y una etapa avanzada de la enfermedad. En esta línea, nuestros datos mostraron que los pacientes con niveles elevados de ecto-CRT se asociaban con un microambiente en la médula ósea más disfuncional y patológico. Los datos revelaron que los pacientes con niveles altos de ecto-CRT exhibían un perfil de células T alterado, con ratios bajos de células T $CD4^+/CD8^+$ consecuencia de una menor frecuencia de linfocitos T $CD4^+$ y un mayor número de células T $CD8^+$. Además también presentaban un mayor número de células NK, mDC, pDC y Tregs. También, la cohorte de pacientes CRT^{hi} mostró una mayor actividad en el eje PD-1/PD-L1. Así, nuestros datos sugieren que los pacientes CRT^{hi} poseen rasgos inmunológicos reminiscentes de un microambiente medular óseo asociado a un estado inmunitario debilitado y comprometido y que también podría traducirse en un mal resultado clínico en el contexto de la enfermedad de MM. En concreto, en el análisis de los aspectos clínicos de los pacientes parece indicar que el aumento de la exposición a ecto-CRT se asocia con un mal pronóstico en la enfermedad de MM. Las personas con expresión aumentada de ecto-CRT exhibieron significativamente un menor tiempo medio de progresión, mayores posibilidades de desarrollar plasmacitomas extramedulares, un mayor número de líneas de tratamiento y albergan un perfil citogenético de alto riesgo. Esta relación entre los niveles de CRT y el pronóstico clínico en pacientes con cáncer se ha visto que depende de manera crítica del tipo de tumor específico que se analiza.

Es interesante que los individuos con niveles elevados de ecto-CRT también presenten más alteraciones citogenéticas y esto posteriormente se correlacione con un mayor grado de infiltración de células efectoras inmunes (células NK, $CD8^+$ T y DCs), a

pesar de que su estado funcional pueda no ser completamente operativo. Es posible que estos defectos citogenéticos puedan ocultar un estado genómicamente inestable y que, en consecuencia, tengan un mayor número de mutaciones somáticas y el repertorio de neoantígenos sea mayor. En tumores sólidos altamente mutagénicos, la alta densidad mutacional y, por lo tanto, la mayor cantidad de neoantígenos, se ha correlacionado con una mayor infiltración inmunitaria, una mejor inmunovigilancia y una mayor supervivencia tras el tratamiento con bloqueo del punto de control. Sin embargo, esto no ocurre en el MM. A pesar de que las células MM tienen una densidad mutacional intermedia, este parámetro junto con el repertorio de neoantígenos aumentan con la progresión del mieloma y se correlacionan con un peor desenlace clínico en pacientes con MM. Es posible que en MM, estos factores por sí solos (e incluso con la ayuda de la terapia del bloqueo del punto de control), no sean suficientes para revertir el profundo microambiente inmunosupresor presente en esta enfermedad. Por lo tanto, aunque inicialmente puedan ser educados y entrenados para combatir el mieloma, las respuestas inmunes efectoras eventualmente pueden fallar en su cometido para confrontar la enfermedad. Esto enfatiza la complejidad de las redes inmunosupresoras subyacentes que permiten a las células de mieloma escapen. Por esta razón, la restauración de un estado inmunológico óptimo es de suprema importancia.

CONCLUSIONES.

Los resultados obtenidos durante este trabajo permiten alcanzar las siguientes conlusiones:

1. Aunque los fármacos antimitóticos mostraron individualmente una actividad citotóxica baja o moderada, la capacidad proliferativa de las células tratadas se vió comprometida en gran medida exhibiendo características típicas de la catástrofe mitótica.

2. La combinación del mimético de BH3, ABT-737, con fármacos antimitóticos mostró un potencial citotóxico mayor comparado con los tratamientos individuales en células tumorales adherentes, especialmente en las líneas A549 y MIA PaCa-2. Además, la muerte celular inducida mostró una fuerte dependencia de la acción de las caspasas y de Bax/Bak.

3. Cuando las células A549 y HCT-116 fueron tratadas con el inhibidor de Aurora B, barasertib, estas adquirían un fenotipo senescente que era reconducido hacia la muerte celular dependiente de caspasas con la adición de ABT-737.

4. Cuando las células A549 y MIA PaCa-2 fueron tratatadas con la combinación de fármacos antimitóticos y ABT-737, la subpoblación más proclive a escapar de la mitosis y sobrevivir, pasaba de media menos tiempo en mitosis. Además, la co-administración de ABT-737 con inhibidores de microtúbulos aceleraba la muerte mitótica, mientras que únicamente la combinación de vincristina con ABT-737 precipitaba la muerte celular post-mitótica.

5. La depleción de MAD2, BUB1 y BUBR1 en las células A549 inducida por barasertib correlaciona con su temprana salida de mitosis. Mientras, la acumulación de estas proteínas mitóticas en respuesta al tratamiento con inhibidores de microtúbulos podría indicar una intensa señalización del SAC.

6. Las proteínas antiapoptóticas de la familia Bcl-2 parecen jugar un papel redundante y cooperativo en las decisiones del destino celular ante el bloqueo en mitosis. Así como Bcl-X_L puede tener un papel auxiliar, otros miembros como Bcl-2 y Mcl-1 también pueden contribuir en la modulación de las señales de muerte en líneas celulares adherentes.

7. La adición de cloroquina o DBeQ, pero no CB-5083, potenció eficazmente la citotoxicidad inducida por carfilzomib en líneas celulares de MM, así como en BMMCs $CD38^+$ aisladas de pacientes con MM. Mientras las combinaciones de bortezomib con CLQ o DBeQ resultaron menos eficaces en la inducción de la muerte celular.

8. El papel esencial de las caspasas en la muerte celular inducida por las combinaciones de CLQ o DBeQ con carfilzomib dependía de la línea celular de MM estudiada. Mientras que en las células NCI-H929 la muerte celular no se veía afectada al inhibirse las caspasas, esta si que se veía seriamente comprometida en estas mismas condiciones en las líneas MM.1S, U266 y MOPC315.BM.

9. La necroptosis parece jugar un papel menor en la muerte celular inducida por las combinaciones de CLQ o DBeQ con carfilzomib ya que su inhibición mediante Nec-1 y NSA, en presencia de inhibidores de caspasas no provocó efectos significativos sobre la muerte celular.

10. El tratamiento combinado con carfilzomib junto con CLQ o DBeQ aumentó la expresión de diversas proteínas implicadas en la UPR tanto de la rama dirigida por PERK como IRE1α sugiriendo la activación de una respuesta de estrés en el ER.

11. La reducción de la expresión de BiP mediante siRNAs no aumentó la muerte celular en las líneas MM.1S y U266 ante el tratamiento combinatorio de inhibidores del proteasoma con CLQ o DBeQ, lo que sugiere que BiP no está implicada en la sensibilidad a estos fármacos.

12. El tratamiento con carfilzomib y su combinación con CLQ o DBeQ puede elevar los niveles de ROS como el $O2^{\bullet-}$ en las líneas U266, MM.1S y MOPC315.BM. Mientras el tratamiento con estos fármacos en presencia de inhibidores generales de caspasas impidió la generación de ROS (excepto en las células NCI-H929).

13. El tratamiento individual con carfilzomib o su combinación con CLQ o DBeQ induce una acumulación inicial de proteínas sólo-BH3 (PUMA, Bim y en menor medida NOXA) que puede superar el aumento inicial de Mcl-1 e inducir la muerte celular.

14. Las combinaciones de fármacos basadas en inhibidores de proteasoma utilizadas son capaces de inducir muerte celular en células MM.1S deficientes en Bax y Bak, sugiriendo que mecanismos alternativos de muerte celular pueden verse activados en estas circunstancias.

15. Bim parece mediar parcialmente la muerte celular inducida por las combinaciones de fármacos basadas en Pis utilizadas ya que la depleción de esta proteína en células U266 proporcionaba una protección incompleta sugiriendo que otras proteíans sólo-BH3 podrían estar implicadas y suplir la deficiencia de Bim.

16. La autofagia parece no ser el único mecanismo implicado en la potenciación de la muerte celular provocada por la CLQ en las combinaciones con Pis. La muerte celular se veía aumentada en células deficientes en ATG5 (aunque en menor medida que en las WT) cuando era tratadas con las combinaciones de Pis con CLQ.

17. La combinación con CLQ potencia la inhibición del proteasoma provocada por el carfilzomib de forma mucho más efectiva que cuando se combina con bortezomib lo que permitiría explicar las diferencias observadas en la citotoxicidad mediada por estos tratamientos en células de MM.

18. El tratamiento con carfilzomib-CLQ o DBeQ en células de MM *in vitro* aumentó la exposición de CRT en la superficie externa de la membrana plasmática de distintas chaperonas del ER (CRT, Hsp70, BiP) y aumentó la expresión de marcadores de maduración en DCs derivadas de monocitos lo que sugiere que estos fármacos podrían ser considerados inductores de ICD.

19. El papel de las caspasas en la exposición de CRT bajo el tratamiento con las combinaciones basadas en Pis utilizadas es incierto. Dependiendo de la línea celular,

la inhibición de las caspasas aumentaba la exposición de CRT en células MM.1S y MOPC315.BM, mientras que la reducía en las células NCI-H929.

20. La exposición de CRT es posible que dependa de la fase de la autofagia que se está evaluando. Cuando la autofagia se veía interrumpida en las etapas iniciales a través del silenciamiento de ATG5, esta se veía comprometida parcialmente, mientras que si se inhibía etapas finales de la autofagia con CLQ, la exposición de este DAMP se veía fuertemente potenciada. No obstante, el efecto de la CLQ sobre la potenciación de la exposición de CRT es posible que sea independiente de la autofagia.

21. La vacunación subcutánea con células de MM muertas previamente tratadas *in vitro* con carfilzomib y CLQ no ofreció una protección inmune significativa contra el desarrollo de la enfermedad de mieloma en el modelo ortotópico murino MOPC315.BM.

22. La vacunación subcutánea con células de MM muertas, tratadas con carfilzombi, CLQ y z-VAD-fmk proporcionó ligeramente una mejor tasa de supervivencia y un pequeño retraso en el desarrollo de la enfermedad, posiblemente apuntando a las caspasas como elementos inmunosupresores en la inmunogenicidad de la muerte celular.

23. El análisis de la infiltración de células inmunes en la médula ósea, bazo y tumores extramedulares *ex vivo* podría indicar el inicio de una respuesta inmune anti-mieloma incluso en protocolos de vacunación que no mostraron una protección neta significativa.

24. Aunque las células MOPC315.BM mostraron una elevada expresión de PD-L1 in vitro, la combinación del protocolo de vacunación basado en carfilzomib-CLQ-zVAD, junto con anticuerpos bloqueantes anti-PD1 no mejoró la protección profiláctica proporcionada por la estrategia de vacunación de forma individual.

25. Los pacientes con MM que portaban alteraciones citogenéticas o que exhibían una resistencia ex vivo al tratamiento con carfilzomib podrían también verse beneficiados por la potenciación de la muerte celular inducida por las terapias combinatorias de carfilzomib con CLQ o DBeQ.

26. En pacientes con discrasias de células plasmáticas, las células de mieloma primarias $CD38^{+}$ aisladas de la médula ósea de estos pacientes, mostraron valores elevados de ecto-CRT, independientemente de la quimioterapia y posiblemente asociado con la transformación tumoral.

27. Los pacientes con elevada ecto-CRT mostraban un microambiente en la médula ósea alterado, con ratios en células T CD4/CD8 bajos debido a un mayor número de linfocitos T CD8 y un menor número de células T CD4, una población de células NK aumentada, mayor frecuencia de DCs (pDCs y mDCs), así como de linfocitos Tregs y una mayor expresión del eje PD-1/PD-L1.

28. Los pacientes con niveles elevados de CRT se asociaban a un peor pronóstico ya que estos presentaban con mayor frecuencia plasmacitomas, exhibían un menor tiempo para la progresión, habían sido sometidos a muchas líneas de tratamiento y presentaban un perfil citogenético de alto riesgo.

TABLE OF CONTENTS

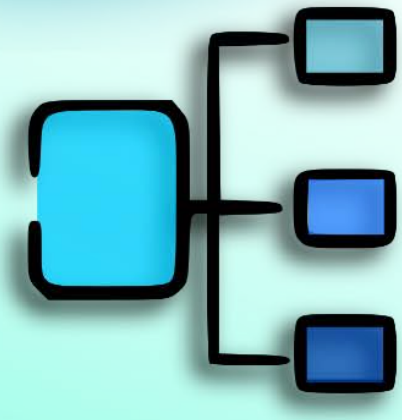

Table of Contents

ABBREVIATIONS & ACRONYMS.

7-AAD: 7-Aminoactinomycine D

ADCC: Antibody-Dependent Cellular Cytotoxicity

ALL: Acute Lymphoblastic Leukemia

Allo-SCT: Allogeneic Stem Cell Transplantation

AML: Acute Myelocitic Leukemia

AnnexV: Annexin-V

APC/C: Anaphase Promoting Complex / Cyclosome

APC: Antigen Presenting Cell

APS: Ammonium Persulphate

ASCT: Autologous Stem Cell Transplantation

ATF6: Activating Transcription Factor 6

BCA: Bicinchoninic acid assay

BH: Bcl-2 homology domain

BiP: Binding Immunoglobulin Protein

BM: Bone Marrow

BMMCs: Bone Marrow Mononuclear Cells

BMPCs: Bone Marrow Plasma Cells

Bortz: Bortezomib

BSA: Bovine Serum Albumin

BUB1: Budding Uninhibited by Benomyl 1

BUBR1: pseudo-kinase BUB1-Related 1

CAR: Chimeric Antigen Receptor

CARD: Caspase-Associated Recruitment Domain

Carfz: Carfilzomib

Cas: CRISPR-associated genes

CDK: Cyclin Dependent Kinase

CLL: Chronic Lymphocytic Leukemia

CLQ: Chloroquine

CML: Chronic Myelocytic Leukemia

CPC: Chromosome Passenger Complex

CRISPR: Clustered Regularly Interspaced Short Palindromic Repeats

crRNA: CRISPR RNAs

CRT: Calreticulin

CTL: Cytotoxic T Lymphocyte

CTLA-4: Cytotoxic T lymphocyte Antigen 4

CYLD: Cyclophilin D

DAMPS: Damage Associated Molecular Patterns.

DC: Dendritic Cell

DD: Death Domain

DED: Death Effector Domain

Dex: Dexamethasone

DISC: Death Inducing Signalling Complex

DR: Death Receptor

DUB: Deubiquitinating enzyme

EMD: Extramedullary Disease

EMTs: Extramedullary Tumours

ER: Endoplasmic Reticulum

FBS: Fetal Bovine Serum

FISH: Fluorescence In Situ Hybridization

GM-CSF: Granulomonocytic Colony Stimulating Factor

GvHD: Graft versus Host Disease

HCLQ: Hydroxychloroquine

HMGB1: High Mobility Group Box 1

HSCT: Haematopoietic Stem Cell Transplantation

HSP: Heat-Shock Protein

HtrA2/Omi: High temperature resistant A2

i.p.: intraperitoneal

i.v.: Intravenous

ICD: Immunogenic Cell Death

IFN: Interferon

IL: Interleukin

IMiDs: Immunomodulatory drugs

IRE1: Inositol-Requiring transmembrane kinase/Endonuclease

JNK: c-Jun N-terminal Kinase

kDA: KiloDaltons

KO: Knock out

LAMP1: Lysosomal-Associated Membrane Protein 1

Len: Lenalidomide

LPS: Lipopolysaccharide

LTR: Long Terminal Repeats

mAbs: monoclonal Antibodies

MAD: Mitotic Arrest Deficient

MAMPS: Microbe-Associated Molecular Pattern

MAPK: Mitogen Activated Protein Kinase

MCC: Mitotic Checkpoint Complex

MDE: Myeloma Defining Event

MDSC: Myeloid-Derived Suppressor Cell

MGUS: Monoclonal Gammopathy of Undetermined Significance

MHC: Major Histocompatibility complex

MILs: Marrow Infiltrating Lymphocytes

MLKL: Mixed Lineage Kinase Domain-like Protein

MM: Multiple Myeloma

MOMP: Mitochondrial Outer Membrane Permeabilization

MPS: Monopolar Spindle Protein 1

mPTP: Mitochondrial Permeability Transition Pore

MRD: Minimal Residual Disease

MTAs: Microtubule Targeting Agents

MTD: Maximun Tolerated Dose

mTOR: Mammalian Target of Rapamycin

Nec-1: Necrostatin-1

NF-κB: Nuclear Factor κB

NGS: Next Generation Sequencing

NK: Natural Killer

NSA: Necrosulphonamide

NSCLC: Non Small Cell Lung Cancer

ORR: Objective Response Rate

OS: Overall Survival

PAM: Protospacer Adjacent Motif

PAMPs: Pattogen-Asssociated Molecular Pattern

PB: Peripheral Blood

PBMC: Peripheral Blood Mononuclear Cells

PBS: Phosphate Buffered Saline

PBST: PBS-Tween

PC: Plasma Cell

PCR: Polymerase Chain Reaction

PD-1: Programmed cell Death protein 1

PD-L1: Programmed Death Ligand 1

PE: Phycoerythrin

PERK: Protein Kinase RNA-activated (PKR)-like ER Kinase

PFA: Paraformaldehyde

PFS: Progression Free Survival

PI: Propidium Iodide

PI: Proteasome Inhibitor

Poma: Pomalidomide

PRRs: Pattogen Recognition Receptors

PS: Phosphatidylserine

PVDF: Polyvinylidene Fluoride

RB: Retinoblastoma

RIPK1: Receptor-interacting serine/threonine-protein kinase 1

ROS: Reactive Oxygen Species

RRMM: Relapsed/Refractory Multiple Myeloma

s.c.: subcutaneous

SAC: Spindle Assembly Checkpoint

SD: Standard Deviation

SDS-PAGE: Sodium Dodecyl Sulphate PolyAcrylamide Gel Elecrophoresis

sgRNA: single-guide RNA

SMAC: Second mitochondria-derived activator of caspase

SMM: Smoldering Multiple Myeloma

TCR: T Cell Receptor

T_H: T helper lymphocyte

TILs: Tumour Infiltrating Lymphocytes

TME: Tumour Microenvironment

TNF: Tumour Necrosis Factor

tracrRNA: trans-activating crRNA

TRAIL: TNF-Related Apoptosis Inducing Ligand

Tregs: T regulatory cells

TTP: Time to Progression

UPR: Unfolded Protein Response

UPS: Ubiquitin-Proteasome System

VCP: Valosin Containing Protein

WT: Wild-type

XBP1: X-box Binding Protein 1

z-VAD-fmk: Benciloxicarbonil-Val-Asp-O-fluoromethylketone

INTRODUCTION

1. INTRODUCTION.

1.1 The History and Nature of Cancer.

Cancer disease has been an old and long-standing contender and probably it has been coexisting with humanity throughout the whole chronicle of human evolution. From the dawn of history, earliest evidences of human carcinomas are dated back to 3000 BC in the ancient Egypt[1]. The practice of human body mummification by this civilization has allowed to conserve fossilized bone tumours in these specimens. Additionally, in what seemed an antique trauma surgery papyrus (the so called Edwin Smith papyrus), medical practitioners described cases of breast ulcers or tumours resected through an archaic cauterization tool[1,2]. However, the origin of the term cancer or carcinoma, came from the greek words 'καρκινος' or 'καρκινομα', meaning 'crab' (because of the finger-like projections that adheres to its surroundings like a crab). This term was coined by the 'Father of Medicine', the Greek physician Hippocrates (460-370 BC)[1,2]. But it was not until the epoch of the Roman physician Celsus (25-50 BC), who described several types of cancers in the book *De Medicina*, when the Latin form cancer, (crab in Latin) started to appear. Later in history, Galen used the term oncos (the Greek word for swelling) to describe tumours[1,2].

Hippocrates early theory of cancer, which hypothesized that this disease accounted for an excess of black bile, prevailed from ancient Greece to Galen and later on during the Middle Age. After this long and obscure period in scientific advances, during the Renaissance, medical science woke up and new theories started to develop as a consequence of autopsy procedures and the study of the human body. In 16th century Paracelsus started to make observations about the environmental contribution to cancer development in mine workers[1,2]. Later on, in the 18th century extended the correlations between cancer and certain chemicals. In 1800s, with the help of the first microscopes and histological techniques, cancer started to be designated as a 'disease of cells' (Virchow, 1860). In the 1900s, work from Ellerman, Bang (1908) and Peyton Rous (1911), discovered the first tumour viruses. Of particular relevance, in this same 20th century, studies with chemical carcinogens radiation and viruses, expanded previous theories and were accepted as etiological factors in cancer disease[1,2]. Additionally, in this same time period, despite being oblivious to DNA and chromosome structure, Theodore Boveri (1914), introduced his theory on cancer[1,3]. In his work *Zur Frage der Entstehung Maligner Tumoren* he wrote that 'tumor growth is based on.....a particular, incorrect chromosome combination which is the cause of the abnormal growth characteristics

passed on to daughter cells'[1,3]. Later, modern molecular biology and the scientific advances in this field could corroborate this ground-braking theory.

Back to the contemporary world, although it may seem so obvious to us now, all cells from our bodies derive and can be traced back to the fertilized oocyte. Therefore, cells are endowed with a great plasticity and autonomy in order to complete whole body morphogenesis and the extraordinary variety of anatomical designs we own[4]. In addition, these features allow for adult tissue maintenance all through the entire human life span. However, this versatility and self-sufficiency, can at the same time give rise to risky situations. Since individual cells carry a complete organismic genome in order to perform these developmental tasks, cells can adopt an improper nature for a normal tissue by gaining access to unauthorised genetic material[4]. Moreover, cell's genome is daily exposed to insults that can introduce aberrations and change the genetic information content. In this way, mutated genes allow cells to take possession of unassigned roles and disobey the principles directing healthy tissue function. As Francis Peyton Rous once neatly portrayed tumours: 'As flesh on his own flesh, cancer cells has been rendered proliferative, rampant, predatory and ungovernable'[4]. To prevent this cellular mutiny, the organism has developed within its armamentarium a broad palette of safeguard mechanisms, both cell-intrinsic and extrinsic, including those performed by our immune system. However, these 'outlaw' tumour cells have found out ways to progress and thrive. Collectively the nature of cancer and the different abilities and traits that a given cell acquire to be transformed are clearly illustrated in the hallmarks of cancer postulated by Hanahan and Weinberg (see **Figure 1.1**)[5].

Despite the intense research work and achievements carried out throughout history, cancer is still an incurable disease. Dealing with such entity demands integration of different therapeutic modalities into more simple approaches. Paraphrasing another Nobel Laureate, as Albert Einstein once said: 'The same level of thinking that created the problem, won't solve the problem'. Recent success of immunotherapeutic protocols unveiled the potential of revitalizing dormant or inactive immunosurveillance in cancer therapy. Moreover, evidences of long-term remissions in patients under conventional chemotherapy and targeted-therapies could be attributed to the engagement of immunological circuitries. It seems then reasonable that future investigations will unite knowledge acquired from both basic mechanistic research of drug action and also from the study of cancer-immune system interactions.

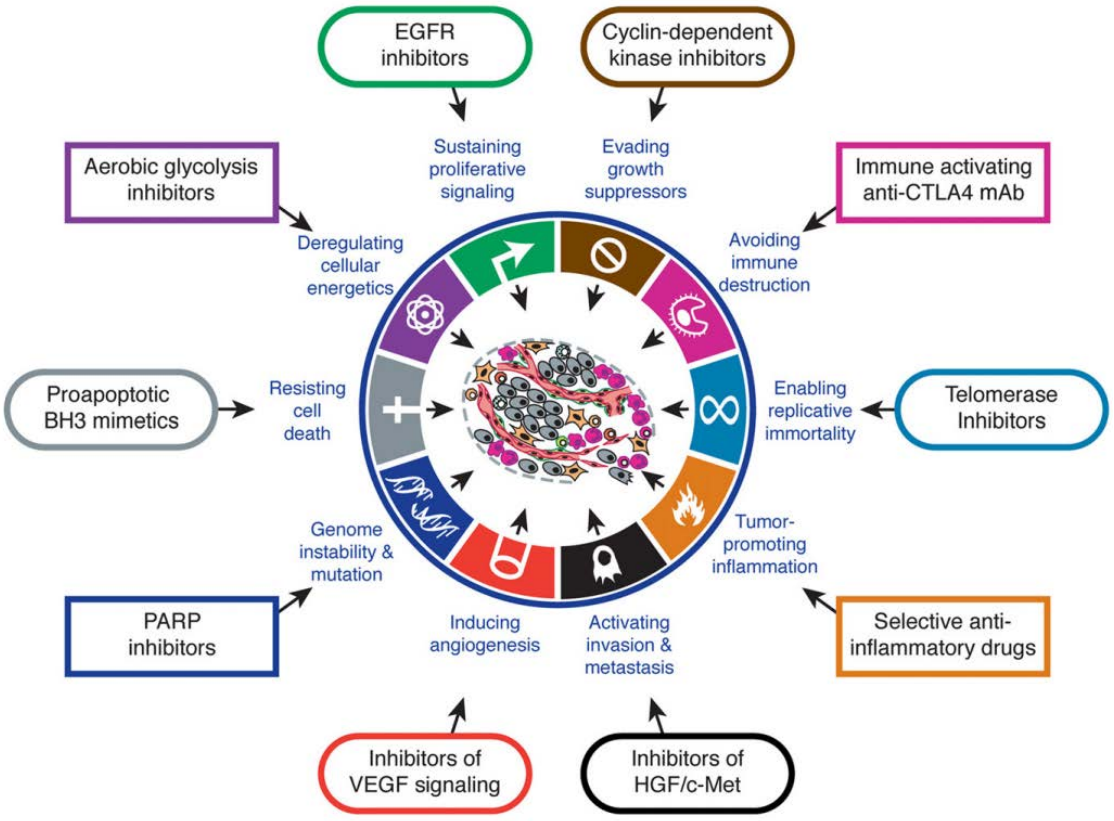

Figure 1.1 | Hallmarks of cancer and therapeutic strategies. Schematic representation of the different biological capabilities endowed by cancer cells and the drugs that disrupt the acquired cancer traits. Adapted from [5].

Although we are facing an era of constant and fascinating research discoveries in the field of cancer biology and oncology, it was only a few decades ago that molecular and cell biology disciplines really took off. Therefore, there is still much to be learnt and basic and clinical research must undoubtedly move forward in order to translate 'bench' discoveries into real 'bed' clinical benefits.

1.2 Cell Death Mechanisms.

1.2.1 Apoptosis.

Apoptosis was first discovered by Kerr and colleagues[6]. This mode of cell death occurs physiologically every day in the human body to ensure an optimal cellular turnover for the correct conservation of whole-body homeostasis. However, dysfunction of this cellular process is behind pathologic situations such as cancer, autoimmune and neurodegenerative diseases[7]. Apoptosis has been classically defined by morphological and biochemical features. Cells undergoing apoptosis are characterized by cell shrinkage, chromatin condensation (pyknosis) and nuclear fragmentation (karyorrhexis). The cell also experiences a blebbing phase that culminates in formation of membrane bound

apoptotic bodies[8]. Biochemically, apoptosis can be identified by the exposure of phosphatidylserine (PS) in the outer leaflet of the plasma membrane, by detecting caspase activation and its cleaved substrates, by assessing cytochrome c release and by observing DNA fragmentation[8].

Apoptosis can be initiated by two different pathways: the **intrinsic** and the **extrinsic pathway**. In both cases this cellular process ends up on the activation of the real executioners of cell death, the **caspase family**. This family of proteases specifically cleaves proteins at aspartic acid residues. Members of this family differ in the recognition of the neighbouring amino acid sequence close to the aspartic residue[9]. Once activated, the cell is unequivocally committed to cell death. To date, 14 caspases have been identified. Depending on their function they can be classified into: **inflammatory** (caspases 1, 4, 5, 11, 12, 13 and 14), involved in cytokine maturation and inflammatory responses; **initiators** (caspases 2, 8 ,9 and 10), which are the first to become activated in response to an apoptotic stimuli and to transduce the signal by activating the effector/executioner caspases; finally, the **effector/executioner** caspases (caspase-3, 6 and 7) are the ones that execute cell death by cleaving key cellular components (DNase inhibitors, cytoskeleton proteins, nuclear laminin proteins, etc)[9–11].

1.2.2 Bcl-2 family of proteins.

The Bcl-2 family plays a critical role in regulating cell fate decisions. They are better known for their roles in apoptosis and regulating mitochondrial outer membrane permeabilization **(MOMP)**[12]. However, they are also implicated in regulating ER-membrane integrity, Ca^{2+} homeostasis at the ER and controlling the initiation of autophagy[13]. Structurally, all the members of this family possess at least one or various BH (Bcl-2 homology) domains. Their members could be functionally divided into pro-apoptotic and anti-apoptotic members (see **Figure 1.2**)[14].

- The **anti-apoptotic proteins** Bcl-2, Bcl-X_L, Mcl-1, among others, have four BH domains (BH1-BH4) and bind and **counteract** the activity of pro-apoptotic members preventing in this way cell demise.

- **Multidomain pro-apoptotic members** Bax, Bak and Bok possess three homology domains (BH1-BH3). Upon apoptotic stimuli, Bax and Bak can **oligomerize** at the outer mitochondrial membrane forming pores that allow the release to the cytosol of different key apoptogenic factors.

- **BH3-only proapoptotic proteins** Bim, Bid, Bad, PUMA or NOXA, among others are characterized by bearing only a BH3 domain in their structure. They are pivotal **initiators** of apoptosis and propagate extrinsic and intrinsic death signals.

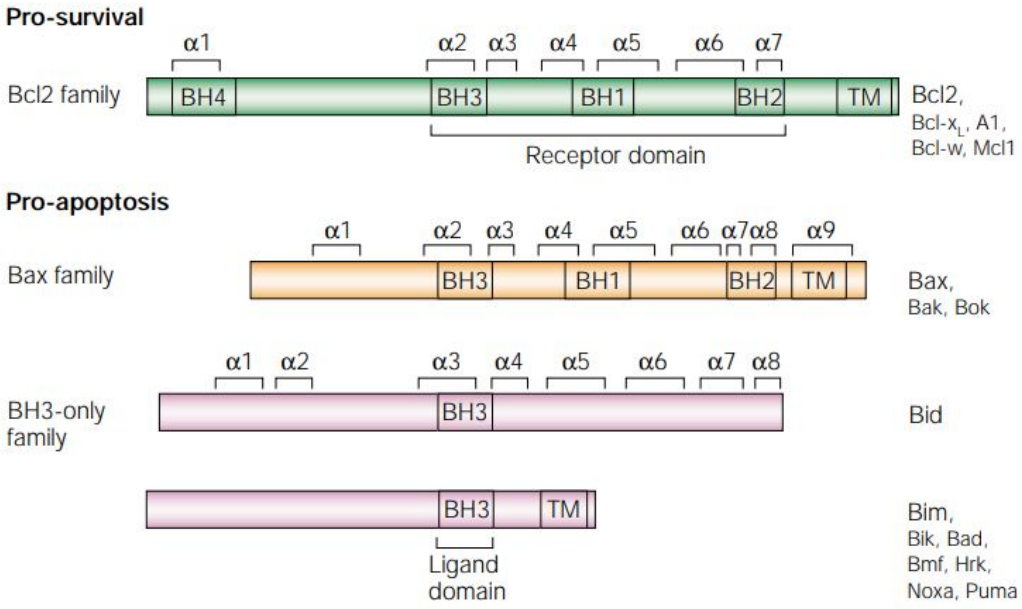

Figure 1.2 | Subfamilies of Bcl-2-related proteins. Schematic representation of the protein structure of Bcl-2 family of proteins indicating different important structural domains such as the BH domains (BH1-BH4) that contain each subgroup, structural secondary structures α-helix (α1-α9) or transmembrane domains (TMs). Adapted from [14].

Different models have been proposed to explain the way Bcl-2 family members control cell death by establishing a complex network of interactions between them (**Figure. 1.3**)[15]:

-*Direct activation model*: This model postulates that BH3-only proteins are divided into activators and sensitizers. **Activator** BH3-only proteins (Bim, tBid, PUMA) directly interact with Bax and Bak inducing conformational changes leading to their activation. Meanwhile, **sensitizer** BH3-only proteins (Bad, NOXA) displace the interaction between anti-apoptotic proteins and BH3-only activators. This way activators are let free to interact and activate Bax and Bak to promote MOMP[16].

-*Displacement model:* In this model, Bax and Bak are constitutively active and therefore, anti-apoptotic proteins sequester Bax and Bak keeping them inactive. Since BH3-only proteins display higher affinity for anti-apoptotic proteins, they would displace this interaction freeing Bax and Bak to induce MOMP. In this scenario, BH3-only members do not directly interact with Bax and Bak[17,18].

-*Embedded together:* This is a unified model in which anti-apoptotic members interact both with BH3-only activators and Bax/Bak. Here, BH3-only sensitizers neutralize anti-apoptotic proteins and displace both types of interaction, allowing activator BH3-only members to activate Bax and Bak. In this model, the membrane is considered an active partner rather than a "passive recipient" that participate in the conformational state of Bcl-2 proteins[15,19].

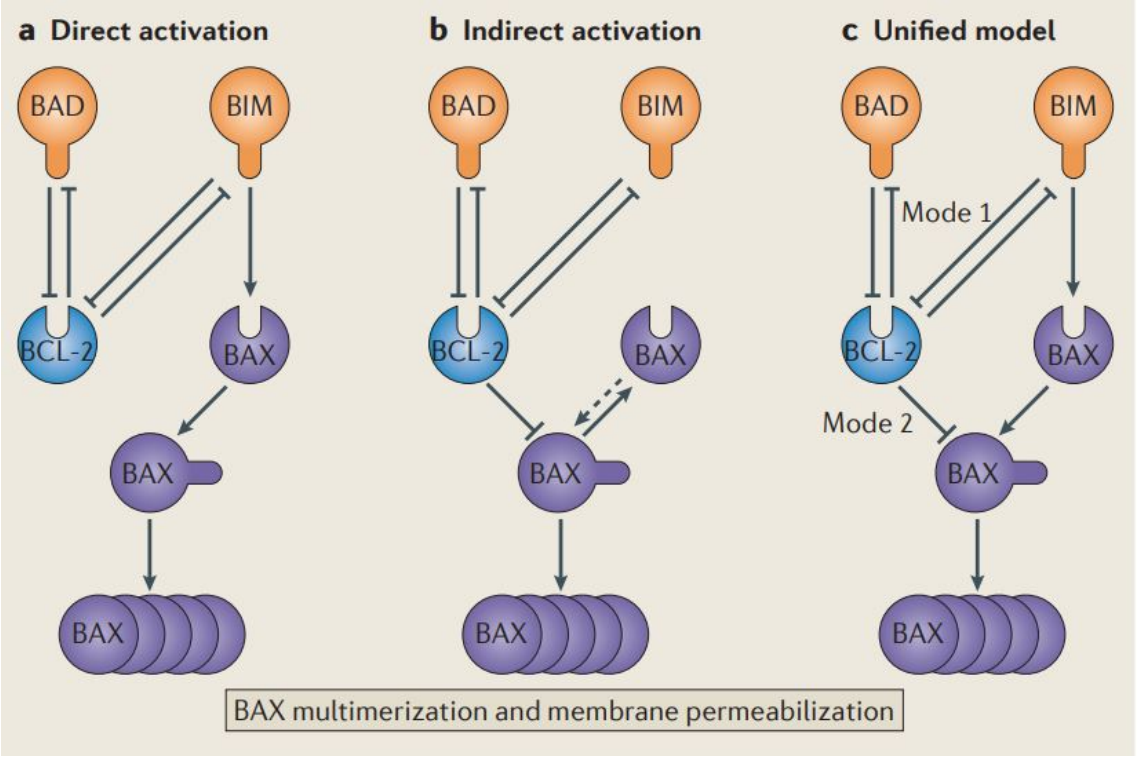

Figure. 1.3 | Models of interaction between Bcl-2 family members that drive apoptotic activation. Schematic representation of the different apoptosis activation models and the interactions between Bcl-2 family members involved in apoptosis triggering. Adapted from [12].

1.2.3 Intrinsic or Mitochondrial Pathway.

This apoptotic pathway is initiated by **intracellular stress** signals (growth factor deprivation, DNA damage, oxidative stress, infection, oncogenic activation) that provoke alterations in the **mitochondria** and eventually induce cell death (see **Figure 1.4**)[20,21]. This pathway is tightly regulated by the Bcl-2 family of proteins that sense these stress signals and skews the balance towards cell death. Upon apoptotic stimuli, **Bax** and **Bak** are activated driving the permeabilization of the outer mitochondrial membrane (**MOMP**) with the ensuing loss of mitochondrial potential and the release of apoptogenic factors (Smac/DIABLO, omi/HtrA2, cytochrome c, AIF, endoG, etc)[22]. These proteins ultimately activate the caspase cascade or other caspase-independent mechanisms

leading to cell death. In particular, cytochrome c binds to and activates **Apaf-1** adaptor protein. **Procaspase-9** molecules are recruited by Apaf-1 leading to the formation of the so called '**apoptosome**'. The close proximity of procaspase-9 molecules in this complex, allows their activation by auto-cleavage. Once, activated this initiator caspase could activate other effector caspases amplifying the caspase cascade. **Smac/DIABLO** and **Omi/HtrA2** are reported to induce apoptosis by inhibiting IAPs (inhibitors of apoptosis proteins), supporting this way caspase activation. **Endonuclease G** and **AIF** induce cell death in a caspase-independent way by translocating to the nucleus and producing DNA fragmentation.

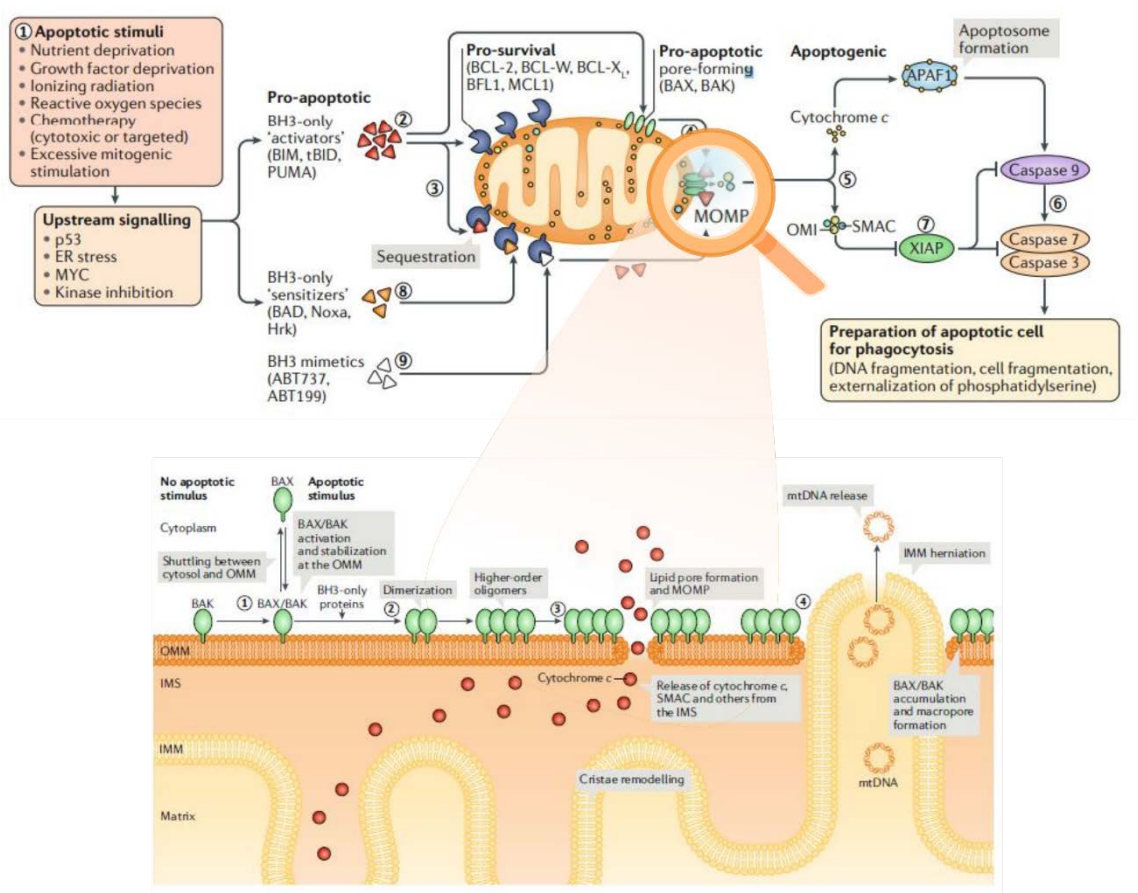

Figure 1.4 | The intrinsic or mitochondrial apoptotic pathway, pore formation and MOMP. The different steps that take place, as well as the different players of the intrinsic apoptotic cascade are represented. Below are depicted the required elements and cellular events that drive mitochondrial outer membrane permeabilization (MOMP) with Bax-Bak mediated pore formation. Adapted from [22,23]

1.2.4 Extrinsic or Death Receptors Signalling Pathway.

This pathway begins with the interaction of extracellular death ligands with its membrane-bound death receptors that transduce the signal into the cell eventually activating the caspase cascade. Death receptors belong to the tumour necrosis factor (**TNF**) superfamily[24]. They share structural similarities and bear a cytoplasmic 'death domain' (DD) that plays a vital role in transducing the death signal into the cell. The most representative members of this family are **Fas/CD95**, **DR4/DR5** and **TNFR1** and their respective death ligands are FasL, Apo2L/TRAIL and TNF-α. Upon ligand binding, usually in the form of trimers, adaptor proteins are recruited to the death domain exhibited by the receptors. In the case of FADD adaptor protein, it binds to Fas or DR4/DR5 receptors whereas TRADD is recruited to TNFR1 receptor upon TNF-α binding. These adaptor molecules bear **DED domains** that interact and recruit initiator **caspases 8 and 10**. In this situation, a high-order molecular complex termed, death-inducing signalling complex (**DISC**) is formed (see **Figure 1.5**)[25]. Is in this complex where procaspase-8 molecules are at close proximity to induce their auto-catalytic cleavage and activation. Once activated, caspase-8 is able to activate effector caspases and trigger apoptosis. Caspase-8 could also engage the intrinsic apoptotic pathway by cleaving Bid[26]. The truncated form of this protein (t-Bid) is capable of activating Bax and Bak, targeting the mitochondria and eliciting cytochrome c release, amplifying this way the death signal.

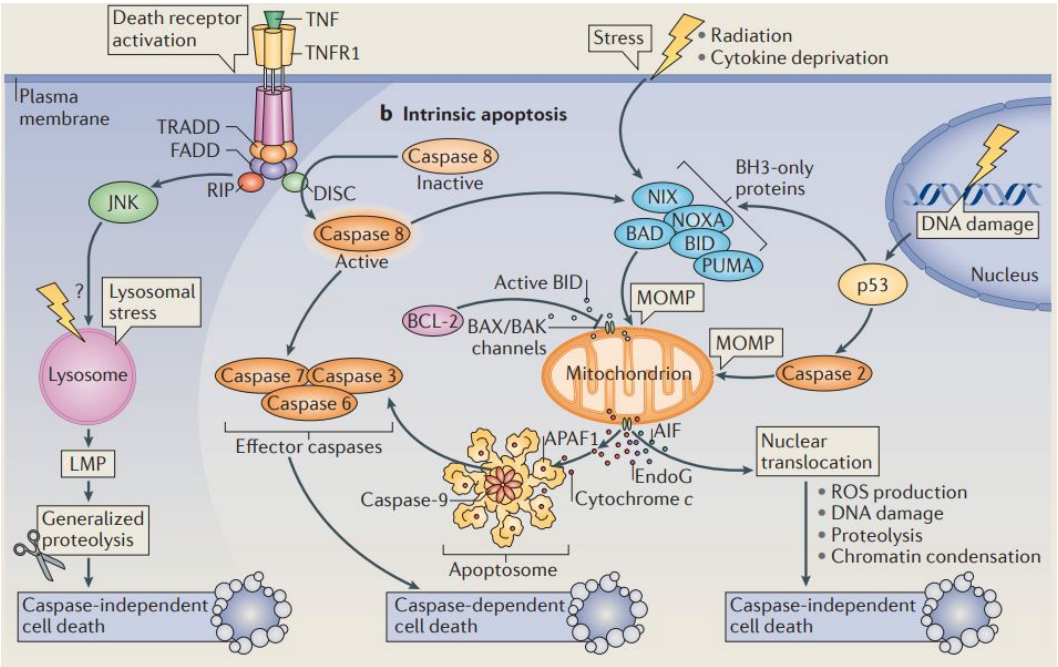

Figure 1.5 | The extrinsic or death receptor apoptotic pathway. The principal actors of cell death receptor pathway are illustrated. In addition, the close connection between extrinsic and intrinsic cell death pathway can also be observed. Adapted from [27]

1.2.5 Necrosis and Necroptosis.

Necrosis has always been considered to be the antithesis of apoptosis. During long time it has been acknowledged as an accidental, unregulated variant of cell demise in response to acute physicochemical insults. Like apoptosis, it has been classically defined by morphological features. It is characterized by cellular swelling, followed by loss of membrane integrity and release of the cellular content to the extracellular milieu[28]. This final event induces a potent **inflammatory** response that alerts and activates the Immune System[29]. However, in the past years a regulated variant of necrosis (**necroptosis**) has been revealed[30]. Hence, necroptosis follows a genetically-encoded and well-regulated programme, which drives the cell to its final demise under necrotic morphological features. In brief, necroptosis can be induced by activation of death receptors (TNFR1, Fas, TRAILR1 and TRAILR2), via activation of PRRs (TLR3, TLR4, etc) or via type I and type II IFNs response[30,31].

The best characterized model is the engagement of TNF-α to TNFR1 receptor (see **Figure 1.6**). This interaction allows the recruitment of TRADD, FADD, RIPK1, cIAP1/ cIAP2 and TRAF2/TRAF5 to the cytosolic domain of TNFR1 forming a short-lived complex termed **complex I**. cIAP1/cIAP2 together with TRAF2/TRAF5 mediate the ubiquination of RIPK1 to form a more stable complex. In these conditions, complex I could initiate alternative signalling pathways involved in cell **survival** (**NF-κB** and **MAPK**-mediated pathways)[32]. When caspase-8 is active, it triggers cell death by apoptosis as previously mentioned. In contrast, when caspase-8 is inhibited (pharmacologically or by $cFLIP_L$), it allows the removal of RIPK1 ubiquitin chain by CYLD. This event leads to RIPK1 activation that forms an alternative complex (**complex II**) by interacting with FADD, TRADD, RIPK3 and caspase-8[32,33]. Once activated, RIPK3 phosphorylates MLKL (mixed lineage kinase domain-like protein) that directly triggers cell death by promoting pore formation at the plasma membrane or by phosphorylating different substrates at mitochondrial or lysosomal organelles.

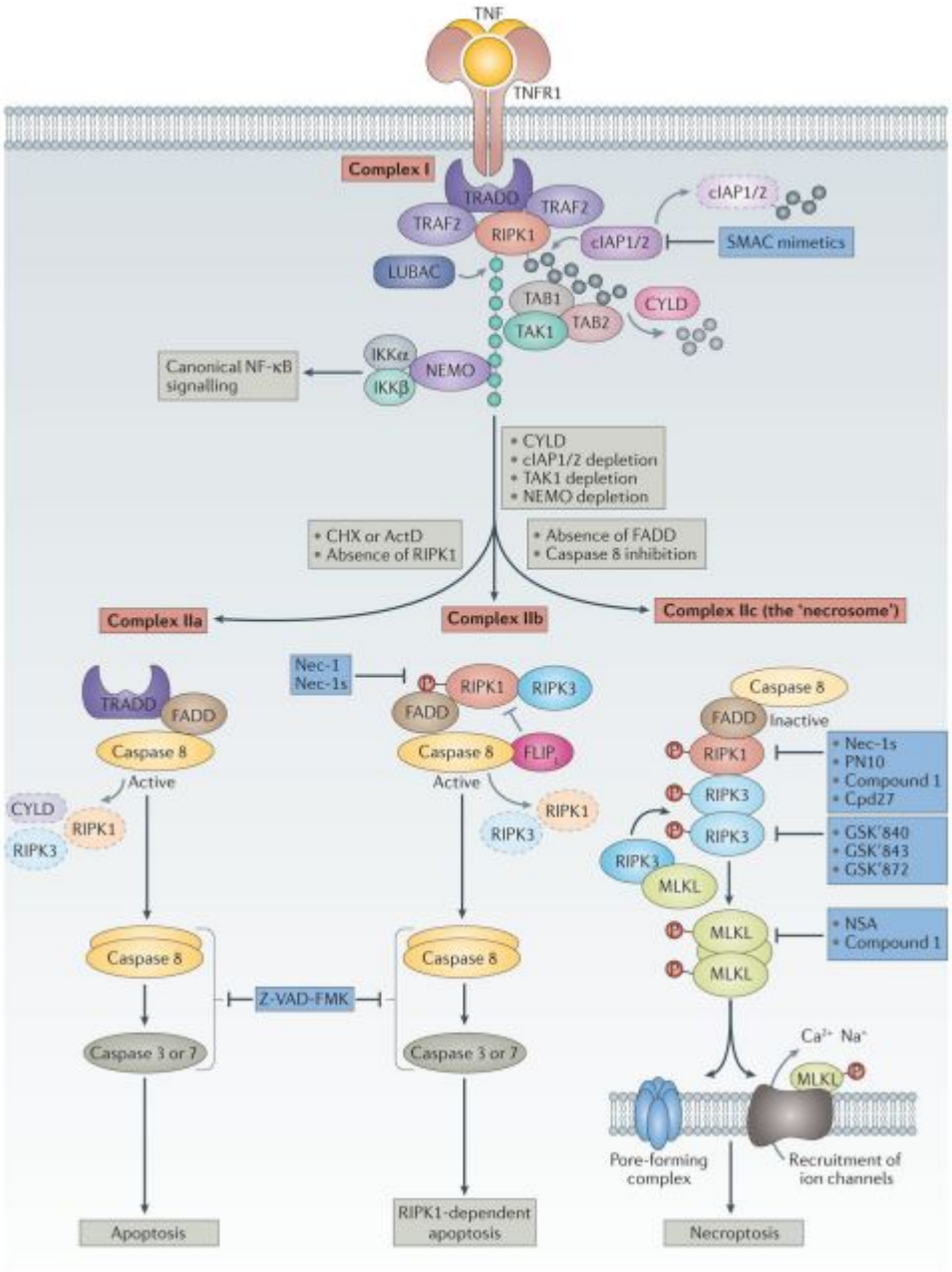

Figure 1.6 | Regulated necrosis or necroptotic signalling pathway. Representation of the elements that participate in necrosome formation and the alternative pathways and complexes that derive in different cellular outcomes. Adapted from [32]

1.3 Cell Cycle, Mitotic Catastrophe and Mitosis-Targeting Therapies.

Cell cycle deregulation is one of the hallmarks of cancer. Moreover, mitosis is probably the most dynamic phase during the cell cycle and it is acknowledged that mitotic cells are in its most vulnerable state[34]. Thus, anti-mitotic therapies are considered a good approach to treat cancer. In fact, microtubule-targeting agents (MTAs) have demonstrated considerable clinical efficacy for years. However, toxicity and resistance to therapy are still major issues of this kind of approach. In the past years, alternative drugs targeting different players of the cell cycle have been developed.

1.3.1 Cell Cycle.

The cell cycle is the cellular process whereby a cell duplicates its genome, grows and eventually divides into two genetically identical daughter cells. It is a finely-tuned cellular process dynamically orchestrated by an exquisitely regulated and coordinated molecular programme[34]. The cell cycle is composed of an interphase and a mitotic phase or M phase. The interphase is divided into the G1, S and G2 phases. During G1 phase, cells grow and prepare for DNA replication that occurs during S phase. After cells have replicated their chromosomes, they enter another growth stage, the G2 phase, in which cells get ready for chromosome segregation and cellular division that takes place during mitosis[35]. After cytokinesis, cells can decide whether entering the cycle or remaining in a resting/quiescent state (G0).

The cell cycle is tightly controlled by the action of two family of proteins: cyclins and their partners the cyclin-dependent kinases (CDKs) (see **Figure 1.7**). The kinase activity of CDKs and therefore, the progression through the cell cycle, is modulated mainly by: cyclins, CDK inhibitors (CKI) and by phosphorylation/dephosphorylation of CDKs[35–37]. In addition, to ensure the accurate transfer of genetic material, cells supervise this process by a series of molecular checkpoints all around the different phases of the cell cycle. Proteins involved in each checkpoint modulate the activity of CDKs arresting the cell cycle, giving time to cells to amend the occurring errors[37,38]. Although there are several checkpoints throughout the cell cycle, the three main ones are: the G1/S or restriction point, the G2/M or DNA replication checkpoint and the mitotic or spindle-assembly checkpoint (SAC)[36,39]. While the interphase checkpoints examine that cells have acquired the appropriate growth, nutrients and factors, as well as the integrity of DNA, in the SAC, cells verify the integrity and the proper segregation of chromosomes[39].

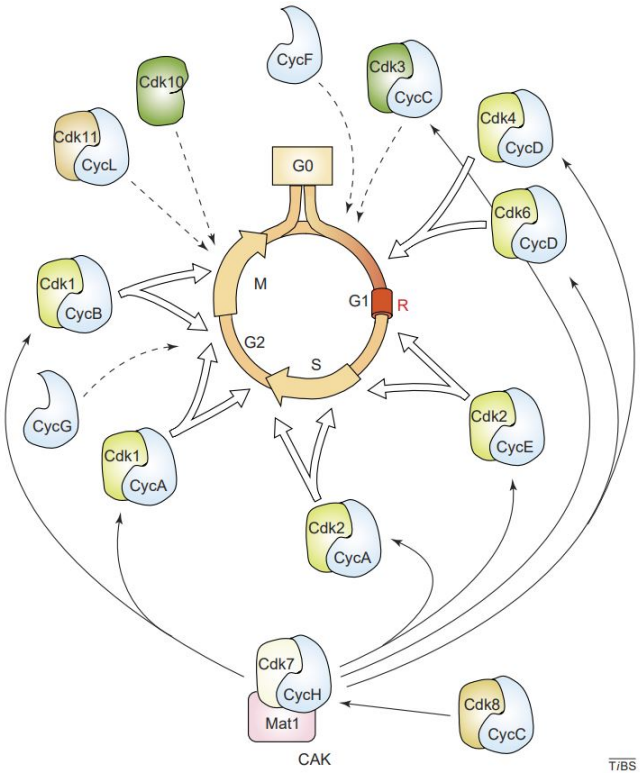

Figure 1.7 | Mammalian cell cycle kinases. Different CDK-Cyclin complexes participate and drive the cell through the different phases of the cell cycle. Adapted from [40]

The cell cycle begins with the assimilation of mitogenic signals, the starters that facilitate the entrance to the cell cycle. These cues promote the formation of CDK4/6-Cyclin D complexes[35,37]. Thereafter, these complexes phosphorylate and inactivate retinoblastoma (Rb) family of proteins. These proteins are major regulators of cell cycle progression during G1/S transition. They regulate the so called 'restriction point', in which in their active form, they prevent transcriptional activation of E2F transcription factors and block promoters of S-phase entry genes[35,37]. Once inactivated, pRb is released from E2F, enabling the transcription of E-type cyclins as well as other genes required in S-phase[36]. Cyclin E forms complex with CDK2 and participates in the phosphorylation of different substrates involved in DNA synthesis, DNA repair, centrosome duplication and maturation[37]. In addition, type-A and type-B cyclins are also upregulated upon pRb inactivation. In this way, once cells have entered S-phase and cyclin-E starts to be rapidly degraded by the proteasome, accumulation of cyclin-A drives the formation of CDK2-Cyclin A complexes. These new complexes phosphorylate important players involved in DNA synthesis, DNA repair, cell cycle checkpoints and other proteins required for completion of S-phase[35,37]. During the last stages of S-phase, cyclin A interacts with CDK1 and together with CDK2-Cyclin B, they phosphorylate multiple proteins that participate in cell cycle regulation and DNA replication required for S/G2 transition[35]. Afterwards,

cyclin A starts to be degraded whereas cyclin B levels become more apparent. Newly formed CDK1-Cyclin B complexes start the regulation of proteins that control G2/M transition and prompt mitosis[35]. CDK1-Cyclin B complexes target numerous substrates that include proteins implicated in centrosome segregation, translation, ubiquitin-mediated degradation, microtubule-binding proteins and other mitotic regulators. Finally, once the cell has all the necessary components, the cell cycle progresses through mitosis and eventually produce two daughter cells with identical genetic material. After cytokinesis, cells may adopt a resting state in G0 or conversely re-enter another round of the cell cycle advancing through G1[37].

1.3.2 Mitosis or M Phase.

Mitosis consists of a complex collection of molecular events, spatially and temporarily choreographed to ensure the accurate segregation of genetic material during the last phase of the cell cycle. It is probably the most dynamic phase during cell division since a substantial amount of events are executed in a relative short period of time. Moreover, during mitosis general protein translation is partially shut down and only certain transcripts (those with IRES motifs or those modulated by cytoplasmic polyadenylation) can be translated[41,42]. In this situation, cells are left defenceless and cannot respond to or adapt against external insults like chemotherapeutic drugs. For these two reasons, cells undergoing mitosis are considered to be in a vulnerable state and makes it an attractive target in cancer.

Mitosis is divided into five stages: prophase, prometaphase, metaphase, anaphase and telophase (see **Figure. 1.8**). As described earlier, CDK1-CyclinB complex regulates the entrance and progression through mitosis. During prophase, loose chromatin starts to condense into individual chromosomes, the nuclear envelope breaks down, and the two centrosomes mature and travel to opposite poles of the cell to form the bipolar spindle[43]. During prometaphase, important protein complexes like Mitotic Checkpoint Complex (MCC), Kinetochore Network (KMN) and Chromosome Passenger Complex (CPC), localize at the centromeric region of chromosomes to drive the proper alignment between chromosomes and the microtubules from the mitotic spindle[44,45]. Once all the microtubules are properly attached to the mitotic spindle, chromosomes start to align in the metaphase plate[46]. The spindle assembly checkpoint (SAC) verifies that all the sister chromatids are correctly bi-oriented and attached to the mitotic spindle. It also drives the degradation of certain proteins that allow for the synchronous segregation of sister chromatids during anaphase. Once each pair of chromatids reach

the opposite poles of the mitotic spindle, DNA starts to decondense, the nuclear envelope starts to be reassembled and the mitotic spindle is dismantled[46]. All these events occur during the last step of mitosis, the telophase. Moreover, during anaphase and telophase, a narrow region of non-kinetochoric microtubules start to form a central spindle in which the CPC plays a central role[47]. The central spindle recruits other proteins that starts to assemble an actinomyosin-based contractile ring that constricts the midzone of the cell that will lead to cytokinesis[47].

1.3.3 Spindle Assembly Checkpoint.

The fidelity of sister chromatids segregation during mitosis is preserved by an evolutionarily conserved mechanism, also known as the spindle assembly checkpoint (SAC)[44,48]. The SAC is composed of several proteins: Ser/Thr kinases like monopolar spindle protein 1 (MPS1) and budding uninhibited by benomyl 1 (BUB1), the pseudo-kinase BUB1-related 1 (BUBR1) and non-kinase components like mitotic arrest deficient 1 (MAD1), MAD2 and BUB3[45,48,49]. It essentially monitors transition from metaphase to anaphase. SAC is activated in the presence of unattached or incorrectly attached chromosomes (including lack of tension between sister kinetochores). Upon detection of these defects, it halts progression through anaphase, thereby inducing mitotic arrest[45,50]. This is accomplished by inhibiting the activity of an E3 ubiquitin ligase, the APC/C (anaphase promoting complex or cyclosome)[34,47,51]. When all chromosomes are properly connected to the mitotic spindle, the SAC is turned off and Cdc20 is then able to activate the APC/C. This active complex (APC/C^{Cdc20}) has two important functions during mitosis, to trigger mitotic exit and to promote sister chromatids segregation[45,50]. These two assignments are fulfilled by ubiquitynating and targeting for proteasomal degradation Cyclin B and securin, the inhibitor of separase, an enzyme which cleaves cohesins, the proteins that maintain sister chromatids held together[45,50]. The mitotic checkpoint complex (MCC), the main effector of the SAC actively sequesters Cdc20 and thereby, inhibits APC/C complex[44,45]. MCC is composed by Cdc20, MAD2, BUBR1 and BUB3. To exert its supervising function correctly, the MCC, other SAC components and important mitotic kinases like Polo like kinase 1 (Plk1) and Aurora B, are recruited to unattached on incorrectly attached kinetochores[45,50]. Thus, kinetochores are positioned at the core of SAC signalling.

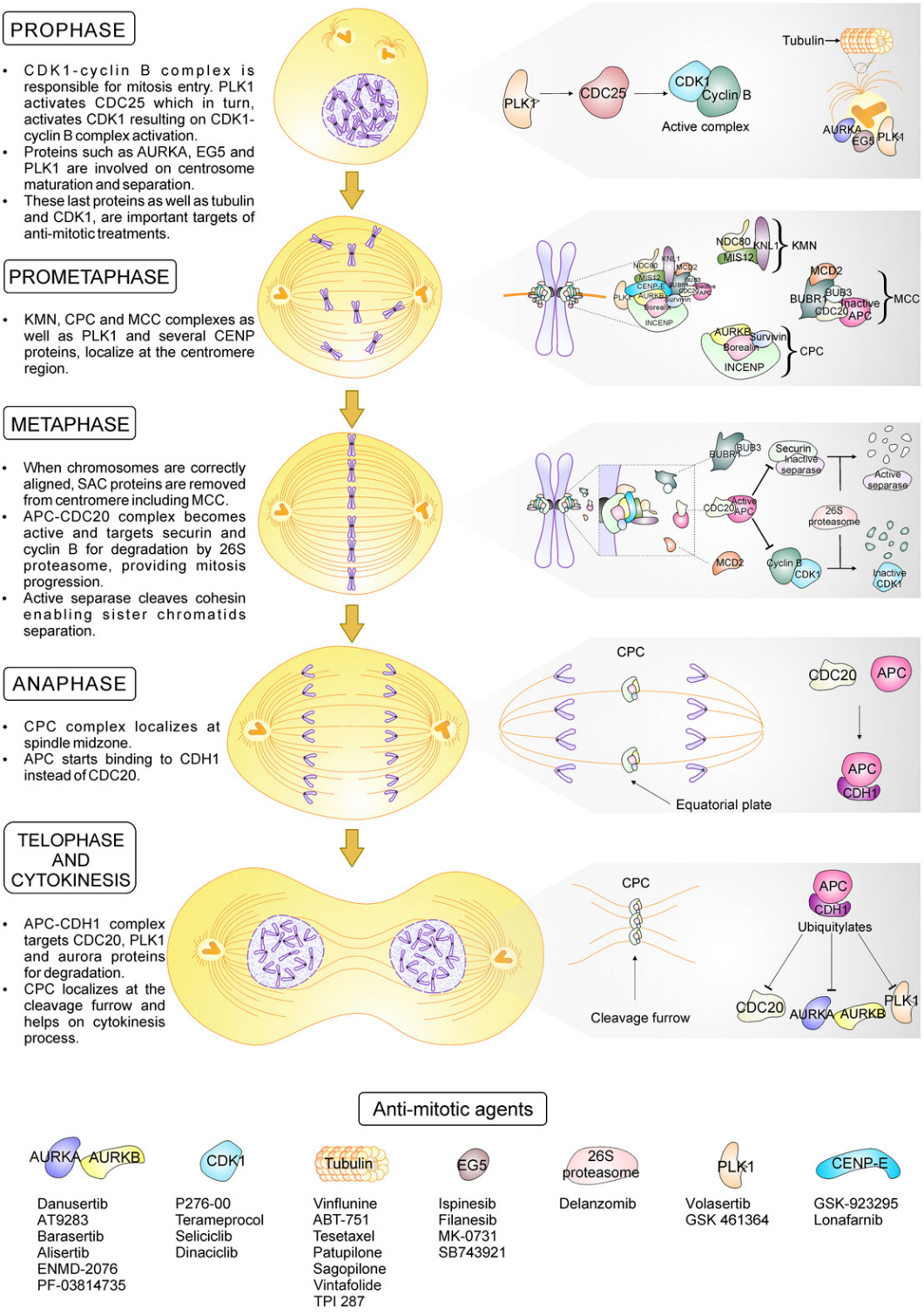

Figure. 1.8 | Mitosis stages and the proteins and complexes involved. The different stages of mitosis, as well as the different mitotic proteins and kinases that drive the cellular and molecular events required to cell division are illustrated. Adapted from [52]

The kinetochore is an important protein assembly of about 100 proteins that connects centromeric DNA to mitotic spindle[44,45]. Central constituents of kinetochore include the constitutive centromere-associated network (CCAN), the KMN network, formed by kinetochore null protein 1 (KNL1), missegregation 12 (MIS12) and nuclear division cycle 80 (NDC80) subcomplexes[45]. In fact, disruption of kinetochore and specially KMN network, hinders SAC recruitment and/or signalling. SAC assembly occurs in a step-wise fashion early in prophase. In particular, MPS1 kinase orchestrates MCC and SAC assembly by phosphorylating KNL1 (an outer kinetochore protein from the KMN network), which allows for subsequent recruitment of BUB1[45] (see **Figure 1.9**). BUB1 is then able to recruit the other SAC and MCC constituents, including BUBR1, BUB3, MAD1 and MAD2[49]. Once all the chromosomes are bi-oriented and sufficient tension is created between sister kinetochores, MCC is disassembled and dissociates from the kinetochores. This process is mediated by the action of phosphatases like PP1 and PP2A-B56, that dephosphorylate key substrates involved in SAC assembly[34].

Another important player in proper chromosome segregation and SAC signalling is Aurora B, a member of the Aurora family of Ser/Thr kinases. In particular, it contributes to kinetochore stabilization, kinetochore-microtubule attachments and hence SAC signalling[53]. Aurora B is thought to be a tension sensor and it is part of the error correction machinery, a mechanism in charge of dynamically stabilizing or destabilizing kinetochore-microtubule connexions[53,54]. Aurora B is part of the multi-protein chromosome passenger complex (CPC) integrated by Aurora B, INCENP, Borealin and Survivin. CPC is divided into a catalytic module, formed by Aurora B and the C-terminal region of INCENP, and a localization module constituted by the N-terminus of INCENP, Survivin and Borealin[53]. The localization module of CPC drives the preferential localization of Aurora B at erroneously attached kinetochores, where tension is low compared to properly bi-oriented kinetochores. In these conditions, Aurora B destabilizes and removes improper microtubule-kinetochore connexions in order to be able to form new and correct bi-oriented attachments[54]. This is partially accomplished by phosphorylating outer kinetochore proteins, like the KMN network, which weakens the affinity of kinetochoric proteins for microtubules[50]. Moreover, Aurora B appears to be upstream in the recruitment of SAC components to the kinetochore. Although the particular mechanism remains unclear, Aurora B is thought to mediate the recruitment of MPS1 to the Ndc80 complex in the outer kintetochore by phosphorylation of the latter[50,53].

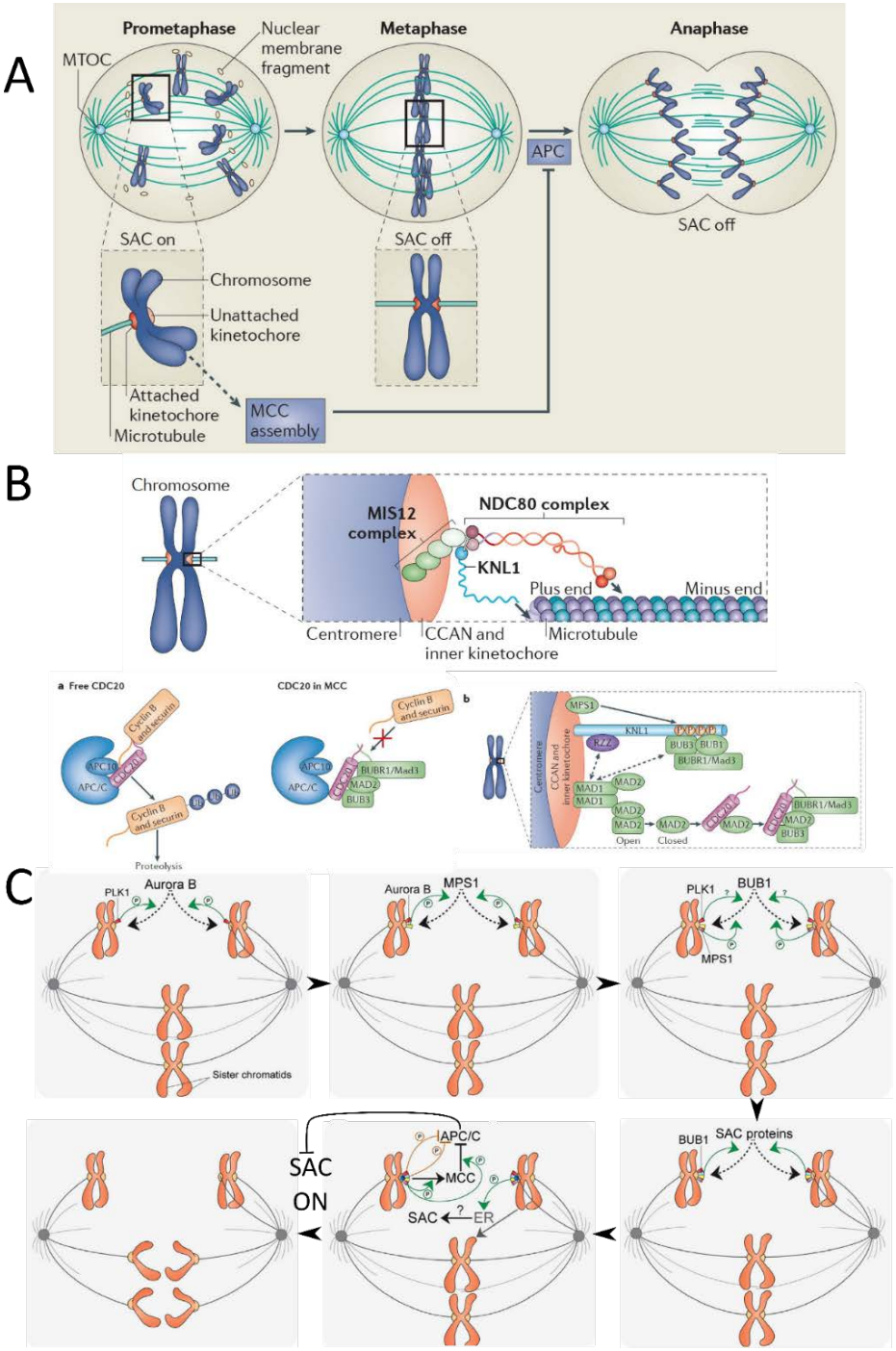

Figure 1.9 | Mitosis stages and the proteins and complexes involved. A. Schematic representation of the role of the Spindle Assembly Checkpoint (SAC) in mitotic progression. **B.** Architectural organization of KMN network (upper side) and the molecular mechanism of kinetochore-based SAC activation (at the bottom). **C.** Recruitment and assembly of SAC and the MCC. Adapted from [45,55,56]

1.3.4 Mitotic Catastrophe and Mitotic Cell Death.

Aneuploidy and genomic instability are common characteristics of tumour cells. These features have the potential to promote carcinogenesis and enable cells to acquire important hallmarks of cancer. Genomic defects like poliploidy or aneuploidy, could arise as a consequence of mitotic errors. Thus, detecting and removing mitotically defective cells is mandatory to prevent cell transformation and tumour formation[47]. Mitotic defects could stem from both, exogenous (such as xenobiotics, drugs, ionizing radiation) and endogenous sources (like DNA replication stress or mitotic stress caused by aberrant ploidy o alterations in factors regulating these mechanisms)[8]. Mitotic defects caused by these elements can bring about alterations in DNA replication, cell cycle checkpoints, chromosome segregation and/or microtubular dynamics. If cells are not competent enough to resolve these and other mitotic defects, different mechanisms in the cellular armamentarium, have evolved to get rid of defective or genomically unstable cells[47]. One of these mechanisms is known as mitotic catastrophe[34] (**Figure 1.10**).

For a long time, this term has been frequently used to designate cases of cell death that occurs during or after an aberrant mitosis[55,57]. However, since not all the mitotic catastrophe modalities result in a form of regulated cell death (RCD) (since it can also drive antiproliferative programmes such cellular senescence), renowned experts have proposed that mitotic catastrophe do not constitute *per se* a *bona fide* cell death mechanism[8]. Instead, mitotic catastrophe has been defined by the Nomenclature Committee of Cell Death as a regulated oncosuppressive mechanism, that operates upstream and exploits antiproliferative measures such as, regulated cell death (apoptosis or necrosis) and senescence[8,55]. Hence, it is considered to be distinct from the aforementioned cell molecular processes.

Faulty or defective mitosis are usually associated with prominent nuclear alterations including multinucleation and macronucleation (that arise from clusters of missegregated chromosomes) and micronucleation (resulting from lagging o acentric chromosomes that are left outside the main nucleus)[55]. These nuclear alterations are the main morphological traits that describe mitotic catastrophe.

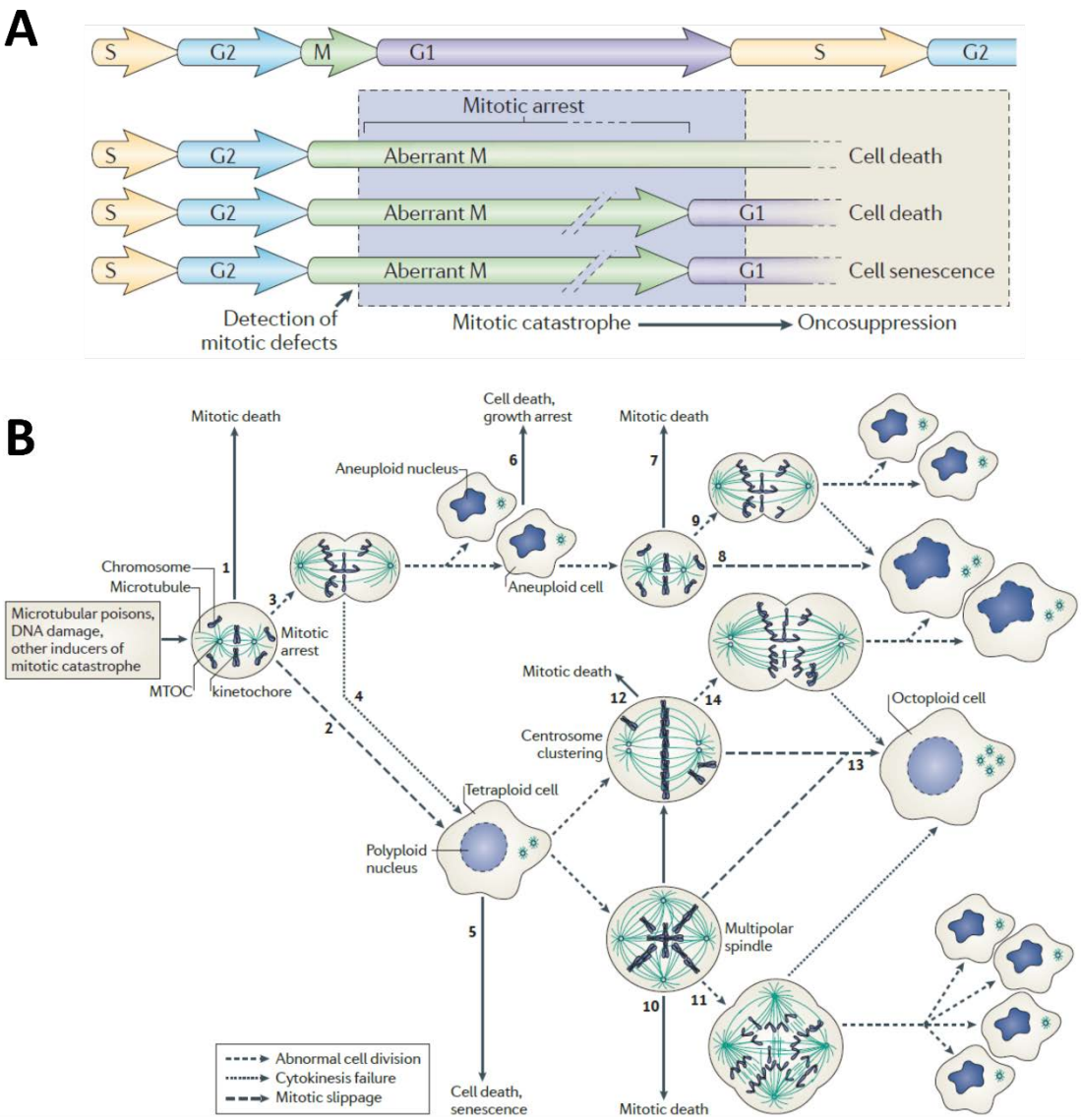

Figure 1.10 | Mitotic catastrophe, definition, types and consequences. A. The different types and cell fates that a cell succumbing to mitotic catastrophe may undergo. Healthy cells progress through the different phases of the cell cycle (G1, S, G2 and M). By contrast, cells that harbour alterations in the mitotic apparatus (oncogenic- or drug-driven), cannot advance through mitosis owing to the activation of mitotic catastrophe. As illustrated, mitotic catastrophe always arise from mitotic perturbations and is always accompanied by some degree of mitotic arrest. Upon the activation of mitotic catastrophe, cells may experience different outcomes: mitotic cell death, reaching the G1 phase of the next cycle dying after slippage and exit mitosis but undergoing senescence. **B.** Consequences of overrunning mitotic catastrophe. When this oncosuppressive mechanism fails, tetraploid and eventually aneuploidy daughter cells may be generated with increased tumorigenic potential. Adapted from [55].

To date, at least three mitotic catastrophe modalities have been defined. In all these different modes, two common denominators stand out: Firstly, mitotic catastrophe always stems from mitotic disturbances and secondly, it is always accompanied by some degree of mitotic arrest. Mitotic cell death occurs when mitotic aberrations engage the cell death machinery in presence of elevated levels of Cyclin B1, that is, when cells have not yet exited mitosis. In presence of mitotic defects, cells could also hijack the surveillance mechanisms and be able to "slip out" from mitosis (referred as mitotic slippage) reaching out the G1 phase of the next cycle. In this situation, cells could undergo cell death in G1 shortly after exiting mitosis, or even years after, as it occurs in delayed radiation-induced cell death[55]. Alternatively, cells undergoing mitotic slippage could exit mitosis and activate an irreversible and anti-proliferative cell cycle arrest state, cell senescence[55]. Therefore, neither situations of mitotic arrest that are followed by resumed proliferation, nor the DNA damage response activated in G2 checkpoint prior to mitosis, are included within this definition[55].

The characterization of the molecular pathways that drive mitotic catastrophe has been a matter of deep investigations in the past years. Moreover, the mechanisms and players that conform and regulate the mitotic apparatus, as well as the molecular pathways involved in cell death and cell senescence programmes, are increasingly gaining more clearness. However, the existing connections between mitotic perturbations and the cell death or anti-proliferative mechanisms they eventually trigger, remain still obscure. Some studies position caspase 2 upstream in the mitotic catastrophe cascade, at least under some experimental conditions. In fact, caspase 2 has frequently been considered a DNA-damaging responsive caspase that acts upstream the mitochondrial apoptotic cascade and its activation usually (but not always), drives the execution of intrinsic apoptosis and MOMP[55,58–60]. Some researches however, simply assign caspase 2 a mere amplification or even null role in the apoptotic process[61]. It has also been proposed that p53 could also be involved in mediating the mechanisms governing mitotic catastrophe[8,55]. In fact, absence of p53 increases polyploidization rate and also facilitates multipolar divisions of tetraploid cells, which eventually causes aneuploidy.

Originally a competing model between two independent cellular networks, the accumulation of death signals and the duration of mitosis, was proposed to explain cell fate after mitotic arrest[62,63] (see **Figure. 1.11**). These two pathways work in opposite directions[63]. One gradually accumulates pro-death signals and the other accounts for the slow and consistent degradation of Cyclin B1, even in presence of a persistent activation of SAC, that ultimately drives mitotic slippage[63,64]. Hence, cell fate is conditioned by which of the two molecular thresholds is trespassed first[47]. If cells rapidly accumulate

death signals and reach sufficient strength to trigger cell death before CDK1-Cyclin B1 activity collapse, cells will die in mitosis. Conversely, if Cyclin B1 levels and thus, CDK1 activity falls below the minimum level required to maintain the mitotic state before death threshold is met, cells exit mitosis and undergo slippage reaching the subsequent G1 phase in a tetraploid state. Several studies provide evidences that support this model. For example, targeting mitotic exit can precipitate cell death in slippage-prone cells[65,66]. Similarly, if cell death is inhibited with pan-caspase inhibitors, an increased proportion of cells are able to slip out of mitosis, (although with the same kinetics), when compared to cell undergoing nocodazole treatment (microtubule inhibitor) alone[67]. This studies also argues in favour of the independence of these competing networks[67,68]. Furthermore, accelerating the timing of mitotic slippage favours survival of mitotic cells[63].

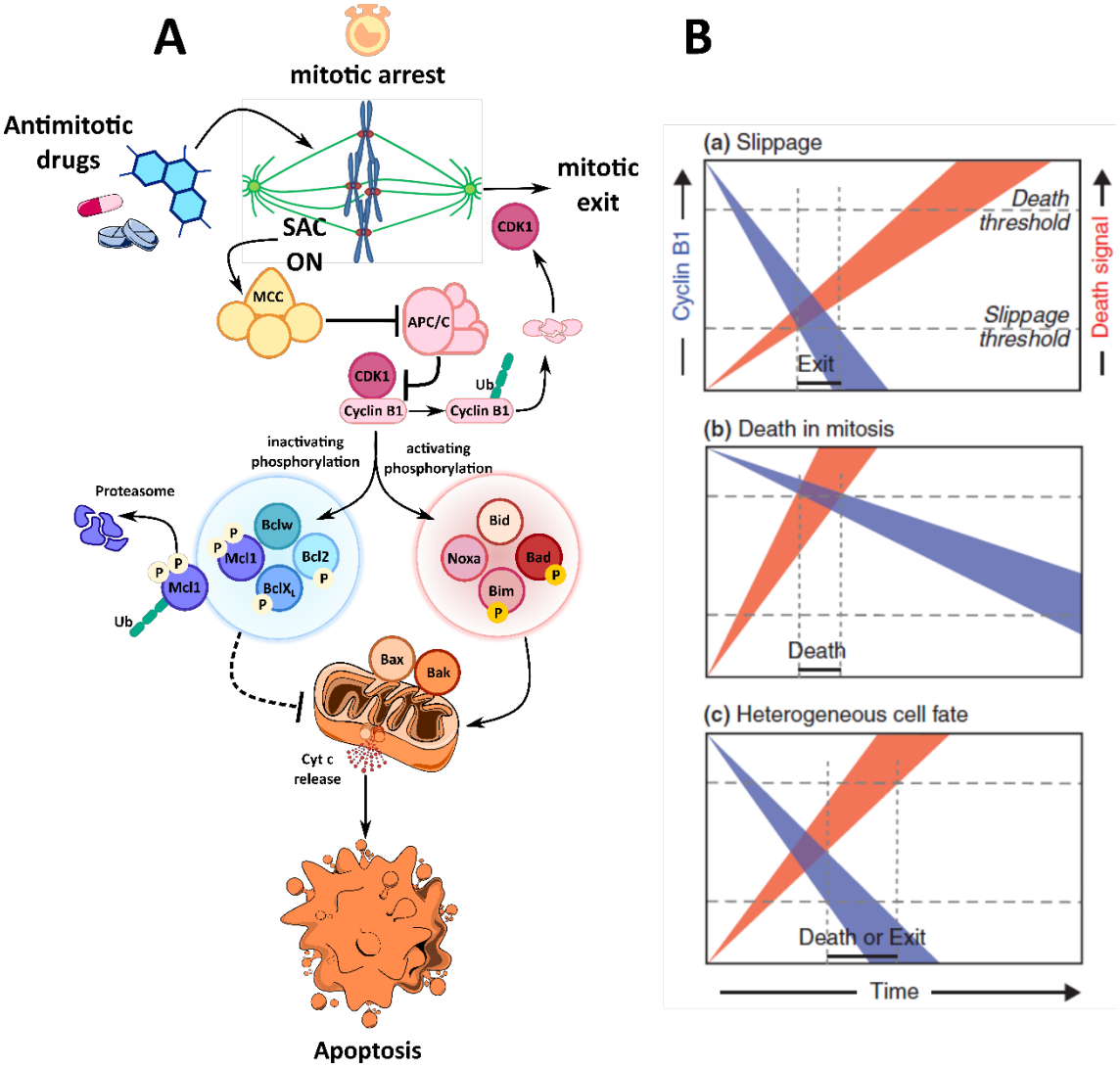

Figure. 1.11 | Overview of competing networks model. A. Description of the molecular pathways and participation of Bcl-2 family of proteins in mitotic cell death during mitotic arrest. Upong antimitotic drug administration, cells may undergo some degree of mitotic arrest that could be followed by mitotic cell death

or mitotic exit (slippage). Bcl-2 family of proteins play a critical role in cell death regulation during mitosis. CDK1-Cyclin B1 could phosphorylate several Bcl-2 family members activating pro-apoptotic proteins and inactivating anti-apoptotic members. This event favours the accumulation and strength of death signals during mitosis which results in Bax/Bak oligomerization and MOMP with Cytocrome c release and eventually apoptosis. Conversely, if cells degrade Cyclin B1 due to residual or unspecific APC/C activity more rapidly than the accumulation of death signals, cells would manage to slip out of mitosis and scape. **B.** Schematic diagram of the competing networks model from Gascoigne & Taylor[63].

As indicated before, death during mitosis occurs through the intrinsic apoptotic pathway. Therefore, it is conceivable to think that Bcl-2 family of proteins could be key determinants of cell fate during mitotic catastrophe. In particular, post-translational regulation of Bcl-2 family has been shown to impact mitotic cell death. In fact, CDK1/Cyclin B1 mediates phosphorylation of anti-apoptotic members (Bcl-2, Bcl-X_L and Mcl-1) during prolonged mitotic arrest[69–71]. Phosphorylated forms of Bcl-2 and Bcl-X_L are considered to have lower affinity for the pro-apoptotic members Bak and Bax, hence promoting its oligomerization and MOMP[72,73]. Regarding Mcl-1, its phosphorylation by CDK1/Cyclin B1 during mitotic arrest fosters its proteolytic degradation via ubiquitination by the SCF/FBW7 or even APC/C^{Cdc20} E3 ubiquitin ligases[63]. Then, when Mcl-1 levels and/or Bcl-2 and Bcl-X_L activity decline, Bax and Bak are free to oligomerize and initiate the mitochondrial apoptotic cascade.

According to this, during a normal mitosis, the transient time that CDK1/Cyclin B1 is active is not sufficient to reduce the levels of anti-apoptotic members and induce cell death. On the contrary, under prolonged mitotic arrest, sustained activation of CDK1/Cyclin B1 (despite its low and continuous decrease), allows for phosphorylation of these anti-apoptotic Bcl-2 members, reducing its activity and triggering apoptotic cell death before mitotic slippage. Furthermore, other members of the Bcl-2 family can also undergo post-translational phosphorylation by CDK1/CyclinB1 complex. In particular, Mac Fhearraigh and Mc Gee, showed that the BH3-only member Bim (specially the Bim_{EL} and Bim_L isoforms), were hyperphosphorylated under sustained mitotic arrest[74]. The final cellular outcome of Bim phosphorylation and its implication in mitotic catastrophe-induced cell death, is still a matter of debate and contradictory results have been reported[47,63]. The phosphorylated forms of Bim could alter its cell death activity, either through increasing the interaction with Bcl-2[75] or through stabilization/destabilization of certain isoforms (Bim_{EL})[76]. Caspase family has also been shown to be a substrate of CDK1, especially caspases 2, 8 and 9. Phosphorylation of these caspases reduces its apoptotic activity, which is thought to be a cytoprotective measure during normal mitosis[47]. This also fits in the competing model, where the amount of inhibited caspases decline with the reduction of CDK1/Cyclin B1 activity levels.

Moreover, although cell death during mitotic catastrophe is mainly mediated by the caspase-dependent apoptotic pathway, there have also been reported cell death scenarios governed by caspase-independent mechanisms[47,63].

1.3.5 Immunogenicity of Mitotic Catastrophe.

Tetraploidization, i.e., the generation of cells that double the normal DNA and chromosomes content of the regular, diploid cells, is thought to be one of the initiating events during carcinogenesis[77,78]. Through a process called the polyploidization/depolyploidization cascade, tetraploid cells could progressively lose chromosomes and DNA content, eventually becoming aneuploid[79]. Many of these cells with an imbalanced chromosome number will succumb to cell death or undergo irreversible growth arrest upon activation of mitotic catastrophe[47,55]. Nonetheless, some of these aneuploid cells will thrive and survive owing an increased genetically unstable and malignant phenotype, which can also provide proliferative advantages compared to their progenitors. This situation causes cellular and specifically, mitotic stress[80]. Chromosome imbalance impacts the composition as well as protein equilibrium and could ultimately overwhelm protein folding capacity of the ER triggering ER stress. Several pieces of evidence connect ER stress with DAMP trafficking. Recently, in line with this, an immunosurveillance mechanism capable of restraining cancer cell ploidy has also been reported[81,82]. For instance, hyperploid cancer cells have been reported to be immunogenic. These cells with increased DNA content, are reported to intrinsically trigger ER stress pathways, that lead to display immunogenic signals such as CRT[81].

Tetraploidy could arise as a result of endoreplication (cells enter subsequent rounds of replication without undergoing mitosis), endomitosis (in which cells with duplicated genome failed to divide) or even due to cell-to-cell fusion (in somatic cells that express fusogenic proteins)[81,82]. In fact, some of these situations could be detonated by mitosis-targeting therapies. Interestingly, in a large screening of approved FDA drugs, some antimitotic agents (vincristine, vinorelbine, docetaxel, paclitaxel, etc), were identified as potential candidates to ICD inducers[83–85]. In fact, vinca alkaloids and taxanes have been shown to increase the surface expression of CRT and release HMGB1 into the extracellular space, but failed in prompting ATP secretion in dying cells[81,86–88]. Nonetheless, despite this deficiency, microtubule poisons were able to vaccinate syngeneic immunocompetent mice against a subsequent rechallenge with live cancer cells[89]. It has been argued, that microtubular inhibitors stimulate active anticancer immune responses through their ability to increment cell ploidy in the tumour cell

population[82]. Similarly, hyperploid cells injected in immunocompetent mice formed tumours less frequently and at a slower pace than their immunodeficient littermates[81]. Moreover, tumours arising from hyperploid clones in immunocompetent mice were immune-selected towards tumour cells with reduced nuclear size and lower overall DNA content[81]. This not only holds to be true in murine models but also occurs in cancer patients. Intriguingly, those cancer patients that responded to anthracycline-based chemotherapy and displayed an increased immune infiltrate, correlated with a reduction in the mean nuclear size of tumour cells[81,82]. Altogether, these studies highlight the existence of an anticancer immunosurveillance system that selects and eliminates cells with increased cell ploidy, which harbour more potential to become malignant and tumorigenic. Importantly, antimitotic agents not only could dispose of cancer cells by deploying oncosuppressive mechanisms upon activation mitotic catastrophe, but also could mobilise and engage this natural immunosurveillance mechanism to eliminate those cells that overcome therapy.

1.3.6 Mitosis-Targeting Therapies.

An important amount of cancer cells possess a tetraploid or aneuploid genome, which intrinsically would eventually lead to more mitotic abnormalities. This situation leaves cancer cells primed to undergo mitotic catastrophe[55]. In addition, mitotic catastrophe inhibition is considered to be one of the gateways to cancer resistance. Moreover, as indicated earlier, cells experiencing mitosis are in a vulnerable state, placing this process as an appealing target in cancer therapy.

Numerous anticancer therapeutics, targeting SAC or DNA damaging pathways, have been shown to induce mitotic catastrophe. Classically, **microtubule targeting agents** (MTAs), also known as spindle poisons, have long been used in the clinic to treat a wide variety of human cancers, in both solid and haematological malignancies[90]. These compounds target microtubule dynamics by binding to tubulin and either promote their stabilization and polymerization, or on the contrary, induce microtubule depolymerisation and disassembly[91]. Among the microtubule hyperpolymerizing agents we can find **epothilones** and **taxanes**, including paclitaxel and docetaxel[52]. These drugs bind to β-tubulin in microtubules and inhibit their depolymerisation stabilizing the structure. In contrast, **vinca alkaloids** (vincristine, vinblastine) and colchicines are catalogued as microtubule destabilizing compounds. Vinca alkaloids bind to β-tubulin close to the α-β-tubulin interphase (the so-called vinca domain), whereas colchicines bind to a different site, the colchicine domain. By altering microtubule arrangement,

kinetochores are not properly attached by the mitotic spindle and therefore, SAC activation and prolonged mitotic arrest take place. Consequently, mitotic catastrophe is eventually triggered with the potential to induce cancer cell death either in mitosis or after mitotic slippage[52,90].

Microtubules also perform important functions in interphase cells. They participate in many other cellular processes like directional trafficking, signalling and motility[90]. Thus, it is though that some of the antitumour effects of MTAs are in part due to impairment of the interphase functions of microtubules, particularly in the case of slow-dividing tumours[90]. However, despite its extended use and contrasted effectiveness in anticancer therapy, off-target toxicities and resistance to therapy are common denominators of this kind of approach[52,92,93]. Novel microtubule targeting agents have been developed and entered clinical trials. Nonetheless, in some of these trials, clinical responses were missing and did not reach the expected standards[52]. Considering these and other obstacles, recent effort has moved to target other mitotic proteins, like mitotic kinases (Plk-1, Aurora A, Aurora B, CDK1, NDC80-NEK2 complex) or mitotic motor proteins (Eg5, CENP-E) (see **Figure. 1.12**). Some of these targets have been found to be upregulated in different types of tumours, placing them as an attractive target in cancer therapy[52].

Aurora kinase inhibitors target the Aurora family of Ser/Thr kinases. In mammals, there are three members of the Aurora family (Aurora A, B and C) and although they share similar substrate specificities, their distinct subcellular location enable them to perform different mitotic specific tasks[53]. **Aurora A** localizes preferentially to the centrosomes and spindle poles and participates in mitotic entry, centrosome maturation, duplication and mitotic spindle formation[90,94]. Aurora A has been found to be overexpressed in several types of human tumours, including breast, ovarian, colon, lung and pancreatic cancer and this amplification correlates with poor clinical outcomes[90,92]. In addition, Aurora A has been shown to downregulate p53 stability via MDM2, further contributing to generate genomic instability and tumour formation. Inhibition of Aurora A provokes aberrant mitotic spindles and chromosome missegregation. Consequently, this leads to a temporary SAC-dependent mitotic arrest which is followed by slippage and induction of apoptosis in the aneuploid daughter population[52,90]. Several Aurora A kinase inhibitors has been developed so far: MLN8237 (alisertib), MLN8054, MK-5108 (VX-689) and ENMD2076). These compounds usually target the ATP binding pocket of the kinase[52]. **Alisertib** has been the Aurora A kinase inhibitor most developed so far. However, despite demonstrating antitumour activity in preclinical models, phase I/II trials have slowed down their clinical development due to lack of efficacy or elevated toxicities[52,90,95]. In the majority of patients with solid tumours,

stable disease was the predominant outcome[52]. Meanwhile, in haematological malignancies (Non-Hodgkin lymphoma, MM or chronic lymphocytic leukemia), slightly better responses were obtained, with up to 27% of patients exhibiting objective responses in the best scenario[52]. Nonetheless, despite this early disappointing results, Alisertib is still under clinical testing in a number of solid and haematological malignancies[95].

As indicated earlier, **Aurora B** is another member of the Aurora family of kinases. It is a subunit of the CPC and localizes at the kinetochores during mitosis. It performs important mitotic functions to ensure the proper segregation of chromosomes. Overexpression of Aurora B has also been detected in multiple human tumours, which has been correlated with poor prognosis as well[90]. Selective inhibition of Aurora B usually overcomes SAC-dependent mitotic arrest and leads to abnormal chromosome alignment and segregation. Moreover, as Aurora B performs important functions in cytokinesis, premature mitotic exit leading to tetraploid and aneuploid offspring is the recurrent outcome[52,92]. Several Aurora B kinase inhibitors have been developed and tested in the clinic (AZD1152 or **barasertib**, and pan-Aurora inhibitors like ABT-348 or ilorasertib, TAK-901, AT9283, etc). Barasertib has demonstrated better efficacy in haematological compared to solid tumours in which cancer cells do not proliferate so rapidly, but still patient's responses were, in the best case, up to 25% in acute myeloid leukemia (AML)[90]. Therefore, these small molecule inhibitors have not been approved yet by regulatory agencies due to this lack of efficacy and also because of its toxicity[90,96].

PLK1 is a mitotic Ser/Thr kinase that plays a vital role in mitotic progression. It participates in centrosome maturation, bipolar spindle assembly, kinetochore-microtubule dynamics, chromosome segregation, cytokinesis and mitosis initiation by activating CDK1/cyclin B1 complex[90,96]. Like other mitotic kinases, PLK1 overexpression is a common feature of several human cancers. Different small molecule **PLK1 inhibitors** have been developed so far, including BI2536, BI6727, GSK461364 among others. They usually target either the kinase domain, inhibiting the catalytic activity, or the polo-box domain in charge of directing PLK1 to its correct substrates[52]. Inhibition of PLK1 activity results in monopolar spindle formation, growth arrest and cell death in preclinical models. BI-2536 was one of the first PLK1 inhibitors developed. Despite apparently rendering good results in phase I trials and manage to reach phase II, disappointing results were obtained in these latter studies[52,97]. BI-2536 was then substituted by an improved BI-6727 formulation tailoring BI-2536 chemical structure. Although the clinical results of BI-6727 were better than its predecessors, still their clinical responses in patients with advanced solid cancer were limited[92,97].

Despite the apparent and initial potential these new generation antimitotic agents showed in preclinical studies, their clinical efficacy has not overcome MTAs clinical success[52]. Ongoing preclinical studies are trying to unravel the causes behind this lack of efficacy. Mitotic slippage could be considered one of these resistance mechanisms to antimitotic agents[52,92]. Therefore, according to the competitive networks model, two strategies aiming to solve mitotic slippage resistance could consist either in targeting mitotic exit to delay slippage or accelerating cell death to engage apoptotic pathways during mitosis[92].

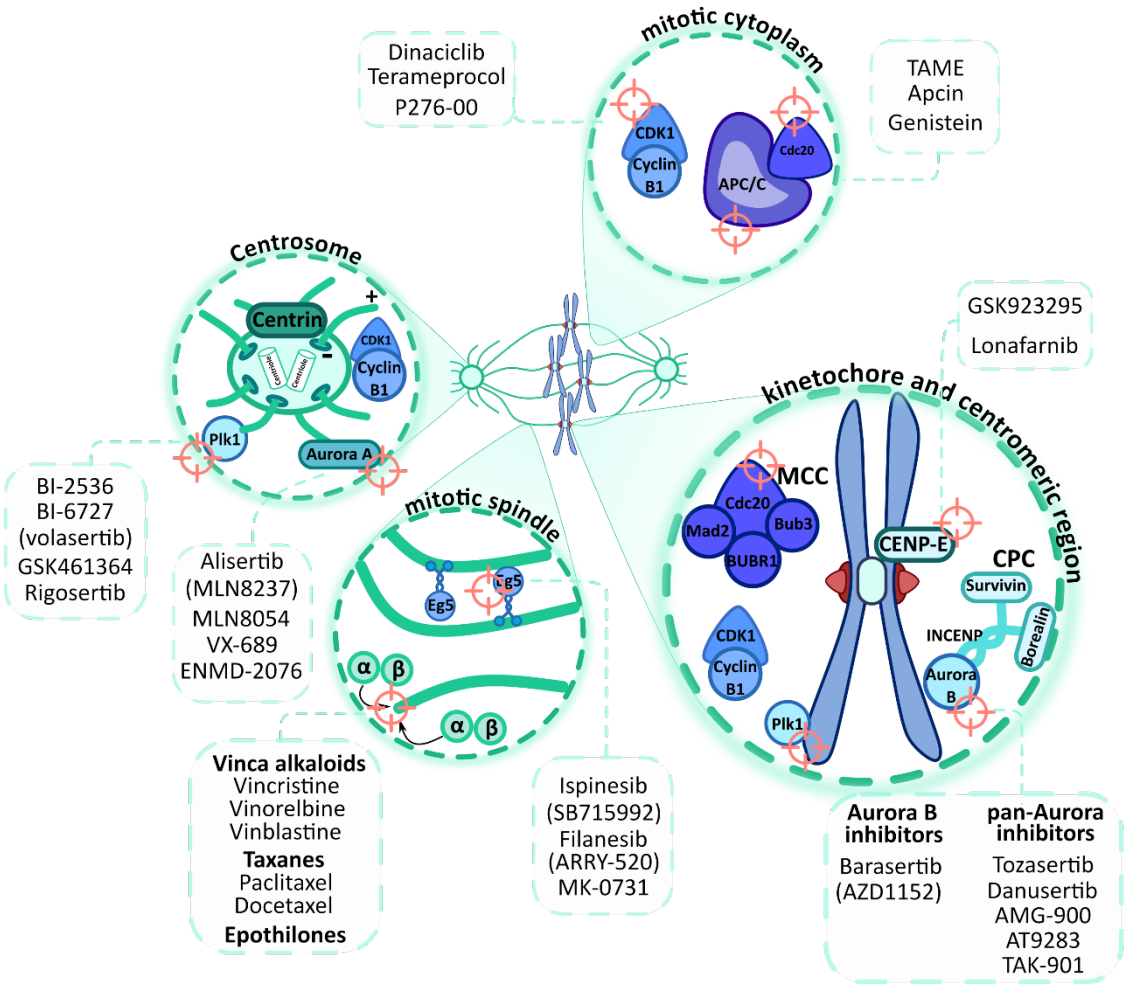

Figure. 1.12 | Overview of current and novel mitosis targeting therapies under development. The different molecular targets and the drugs that target them are illustrated. Some of these chemotherapeutics are already approved and have long been used in the clinic, while others are under preclinical or clinical development.

1.4 ER stress and ER stress-associated cell death.

1.4.1 The ER-associated Degradation and the Ubiquitin-Proteasome Pathways.

The endoplasmic reticulum (ER) is a vital membranous cellular organelle that participates in many functions of cell homeostasis (protein synthesis, calcium storage and regulation, lipid synthesis and storage, glucose metabolism)[98]. It is also the cellular compartment where the secretory pathway begins. The biogenesis and correct folding of one third of newly synthesized proteins (membranous and secretory) takes place in the ER[98]. Protein biogenesis is a complex multi-step process, in which, even with the assistance of different cellular strategies, potentially toxic misfolded/unfolded proteins will be generated. Thus, cells have developed quality control mechanisms to reduce its production and ensure that these harmful species are properly eliminated. The ER-associated degradation **(ERAD**) pathway is part of the ER quality control mechanism developed to sense and target nascent unfolded/misfolded or tightly regulated proteins for degradation via the cytosolic **ubiquitin-proteasome system (UPS**)[99]. The ERAD pathway involves recognition, dislocation or retro-translocation (from the ER to the cytosol) and ubiquitination of proteins to be degraded by the 26S proteasome[99,100]. There are three different ERAD pathways (ERAD-L, ERAD-M and ERAD-C) depending on whether misfolded proteins lay in the lumen, within the membrane or on the cytosolic side of the ER membrane[101]. In a nutshell, these pathways differ in the E3 ubiquitin ligases and in the proteins they form complex with, to be able to discriminate between the different target substrates to be degraded[101]. The following steps esentially describes the ERAD-L and ERAD-M pathways.

The **recognition** step starts when nascent proteins undergo a series of post-translational modifications by N-glycosylation and posterior trimming of the oligosaccharide branches in the lumen of the ER[100]. The process of N-glycosylation consist on the attachment of lipid-linked high-mannose glycans. These pre-assembled oligosaccharides are transferred to the amide side chain of consensus asparagine residues[102]. Multiple enzymes participate in this process: Glucosidase I/II, Glucosyl-transferase, mannosidases as well as lectin-type chaperones like calnexin and calreticulin[99,102]. N-glycosylation is important for the proper folding of glycoproteins as well as, directing correctly folded proteins to ER exit. However, when these glycan structures are trimmed in a specific way, they target misfolded glycoproteins for ERAD and consequently for degradation. Several mannosidases and mannose-specific lectins are involved in this process. The former are in charge of eliminating terminal mannoses whereas the latter recognize these processed proteins and recruit them to

retrotraslocation[99]. A common characteristic of N-glycan trimming process during ERAD recognition is that it occurs at a slow pace[103]. This feature allows proteins to undergo several cycles of folding/refolding by calnexin and calreticulin and also allows to spare intermediate conformational states from premature degradation[103]. Non-glycosylated proteins could also be targeted for ERAD. In this setting, BiP could interact with non-glycosylated proteins and guide them to the retrotranslocation channel[99,103].

To be degraded by the UPS, proteins must be extracted from the ER lumen and be directed to the cytoplasm in a process called **dislocation** or **retrotranslocation**. Since, unfolded/misfolded proteins expose 'sticky' hydrophobic patches that easily aggregate in aqueous environments (like the cytoplasm), the dislocation, ubiquitination and degradation events should be tightly coupled. Similarly to other forms of protein transport in the ER and mitochondria, dislocation occurs through a protein conducting channel[103]. For years, the nature of the export channel in the ER has remained a theme of intense debate. Several candidate proteins have been proposed: Sec61 translocon, multi-spanning membrane protein Derlin-1 or the E3 ligase Hrd1[101,103]. During this process, the ATPase **p97**, also known as valosin-containing protein (**VCP**) plays a central role[103,104]. This enzyme belongs to the AAA+ (ATPases Associated with diverse cellular Activities) family, generally characterized by using the energy from ATP hydrolysis to perform mechanical labors[105,106]. Structurally, VCP/p97 is composed of a N-terminal domain, two ATPase domains (D1 and D2) and an unstructured C-terminal region[104]. Six of these protomers are organized as a two hexameric stacked rings with a central channel formed by D1 and D2 domains. VCP/p97 has particular importance in a wide variety of cellular functions that range from Golgi formation, autophagy, NF-κB activation, DNA replication and repair, cell cycle regulation and chromatin-associated functions, mitochondria-associated degradation and obviously, protein degradation by UPS and ERAD (see **Figure 1.13**)[104]. All these processes share in common the ubiquitination of p97 substrates. This connects VCP/p97 to ubiquitin-dependent processes, in which it generally binds to (directly or indirectly) and extracts ubiquinated proteins from membranes or other cellular structures[105]. To perform this myriad of cellular functions, VCP/p97 relies on a set of at least 30 different cofactors that modulate its function[105].

Back to the retrotranslocation process during ERAD, Hrd1 is also in charge of recruiting the ubiquitin modifying enzymes and polyubiquitinating protein substrates at the cytoplasmic side of the ER membrane[101]. Then heterodimeric cofactor UFD1-NPL4 (ubiquitin fusion degradation protein 1 and nuclear protein localization protein 4), recruits VCP/p97 to ubiquitinated substrates at the ER membrane[103,104]. Another cofactor, Ubx2 also recruits VCP/p97 to the ER membrane and specially promotes the interaction between p97 and Hrd1 (Hmg2 regulated degradation), which is a membrane-

bound ubiquitin ligase that ubiquitinates ERAD-substrates. Once in the membrane, VCP/p97 uses the energy from ATP hydrolysis to pull the substrate out from the channel. After the extraction, VCP/p97 and its substrate are released by the Ubx2 anchor. This event allows diffusion of the complex for VCP/p97 release and trimming of the polyubiquitin chain by cytosolic deubiquitinases (DUBs) prior to entering the proteasome for degradation.

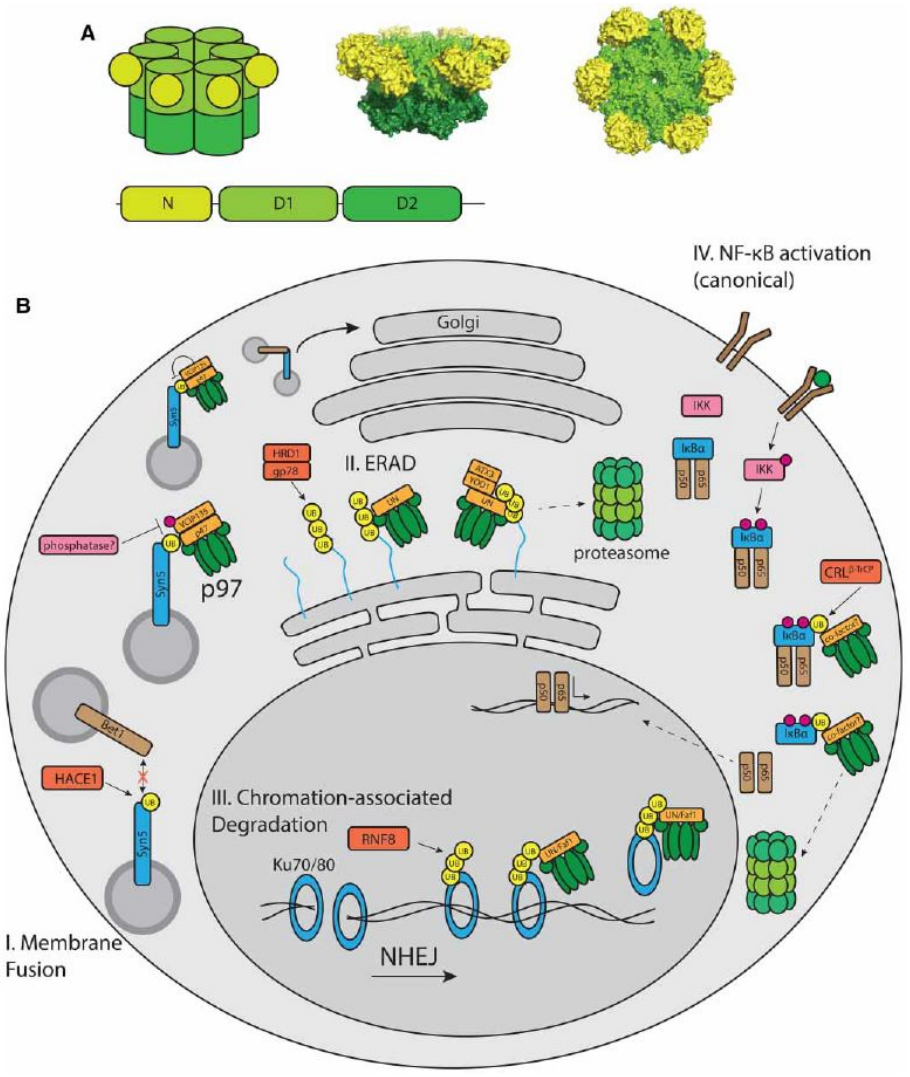

Figure 1.13 | Cellular processed controlled by p97/VCP action. A. The structure of p97/VCP protein with the monomers forming a barrel-like shape is illustrated. **B.** The different cellular processes in which p97/VCP plays a role are depicted. Adapted from [104]

The **ubiquitin-proteasome system** (**UPS**) and autophagy are the two major proteolytic systems in eukaryotic cells. They are responsible for the elimination of 80-90% and 10-20%, respectively of cellular proteins[107]. The last series of events described

above occurring during ERAD, are part of the UPS. Its activity is vital for the proper functioning of important cellular processes (apoptosis, cell survival, cell cycle progression, DNA repair, antigen presentation, etc)[108]. The different steps included in the UPS are: polyubiquitination, deubiquitination and degradation of the target protein by the proteasome[107,108].

Ubiquitination is accomplished by the cooperative work of three enzymes: the ubiquitin activating enzyme (E1), the ubiquitin-conjugating enzyme (E2) and the ubiquitin-ligase (E3). First, ubiquitin must be activated by E1 using ATP to form an ubiquitin adenylate. Then, activated ubiquitin is passed to E2 forming a thioester bond. Finally, E3 catalyses the transfer of ubiquitin from E2 to Lys residues of the substrate[107]. Since the proteasome catalytic active sites are well confined into the core structure, to prevent uncontrolled degradation, proteins undergo a multistep process to enter and finally be degraded after polyubiquitination. Cytosolic chaperones or other shuttling ubiquitin-binding enzymes transport ubiquitinated proteins to the proteasome[109].

The 26S **proteasome** is composed by a core 20S subunit capped at one or both sides by 19S regulatory subunits. Structurally, eukaryotic proteasomes are arranged as four stacked hetero-heptameric rings with a barrel-like shape, following an α_7-β_7-β_7-α_7 0rganization[110,111]. The 20S core particle is where the proteolytic/peptidase activity resides, more specifically at the β-subunit lumen[110]. The 19S regulatory particle is a complex protein assembly that functions as a substrate processing device[111]. It is in charge of receiving ubiquitinated substrates, deubiquitinating, unfolding and translocating them to the core 20S particle[110,111]. Substrate binding to the cap receptors allows a conformational change that aligns the 19S translocating channel with the 20S gate and also activates the opening of the gate[110]. It also promotes ATP hydrolysis conferring the driving force to unfold and propel the substrate through the translocating channel towards the catalytic chamber. An integral deubiquitinase enzyme (DUB) of the 19S complex occupies a well-positioned place just above the translocation channel to remove the entire ubiquitin chain when the protein is committed to degradation[110]. The 20S core contains six active β-sites which hold different substrate specificities[110,111]. The substrate preferences of each catalytic site is determined by the interactions within the substrate binding pocket formed by the catalytic site and the neighbouring β subunits[110]. The β5 catalytic site with chymotrypsin-like activity preferentially cleaves after a hydrophobic residue, meanwhile the β2 or trypsin-like site preferentially cleaves after basic aminoacids and finally the caspase-like or β1 active site preferentially cuts after acidic residues[109,110]. This multicatalytic nature of the proteasome allows for the rapid and productive degradation of target proteins. Additionally, the proteasome also counts on alternative regulatory caps or inducible catalytic β-subunits that highlights the ability

of this cellular machinery to perform specific cellular roles like the immunoproteasome involved in MHC-I ligand generation.

1.4.2 The Unfolded Protein Response.

Tumour cells are constantly coping with aggressive insults and subjected to different types of cellular stress. Some of these extrinsic (hypoxia, nutrient deprivation, acidosis) and intrinsic (oncogenic activation, genetic alterations, exacerbated secretory capacity) factors are common instigators of ER stress[112]. To **cope with ER stress**, cells activate an adaptive and well-conserved mechanism called the UPR. The **UPR** is a finely-tuned process controlled by three membrane-bound ER stress sensors: Protein Kinase RNA-activated (PKR)-like ER Kinase (PERK), Inositol-Requiring transmembrane kinase/Endonuclease (IRE1) and Activating Transcription Factor 6 (ATF6) (see **Figure 1.14**). These sensors remain inactive in basal conditions due to the interaction with Binding Immunoglobulin Protein (**BiP**, also known as GRP78) through their ER luminal domains. Under ER stress conditions, BiP dissociates from the ER stress sensors to help in protein folding[98]. This event allows ER stress sensors to self-activate by homo/oligomerization and trans-auto-phosphorylation in the case of PERK and IRE1, and translocation to the Golgi in the case of ATF6.

First, the UPR tries to restore cell homeostasis, by attenuating protein translation, enhancing degradation of misfolded proteins and increasing levels of ER chaperones and redox enzymes to increase folding capacity[98]. However, if ER stress is not dissipated, the UPR can engage pro-apoptotic programmes governed mainly by the IRE1 and PERK branches. **IRE1** is a Ser/Thr kinase that also has an endoribonuclease domain. When activated, IRE1 drives XBP1 (X-box Binding Protein 1) mRNA splicing, leading to a more stable XBP1s protein that acts as a transcription factor upregulating genes controlling ER homeostasis maintenance[113]. Among the XBP1 targets, it positively regulates the expression of chaperones (BiP among others), foldases, ERAD components as well as other cellular pathways related to cell survival, immunity, cell differentiation and metabolism[113]. Moreover, during the chronic phase of ER stress, IRE1 is also able to degrade many ER-targeted mRNAs through regulated IRE1-dependent mRNA decay (RIDD) process. Activation of **PERK** signalling leads to phosphorylation of eIF2α. Once phosphorylated, eIF2α inhibits eukaryotic translation initiation factor 2B (eIF2B) blocking translation and consequently reducing protein load in order to try to restore ER homeostasis[114,115]. Nonetheless, some transcripts like ATF4 are translated more efficiently during ER stress. ATF4 increases the expression of genes involved in

aminoacid and redox metabolism, ubiquitin ligases, GADD34 phosphatase and the transcription factor CAAT/enhancer-binding protein (C/EBP) homologous protein (CHOP/GADD153). ATF4 and CHOP are also key determinants of ER stress-induced cell death[116]. Finally, **ATF6** is a type II transmembrane ER resident protein that contains a bZIP domain in its cytosolic region with transcription factor like activities[102,112]. Under ER stress conditions, ATF6 is translocated to the Golgi apparatus where it is processed by S1P and S2P proteases releasing the cytosolic fragment of ATF6 (ATF6f), acting as an active transcription factor. ATF6f mainly regulates the expression of chaperones, XBP1 expression and genes involved in the ER-associated degradation (ERAD) pathway[112,117].

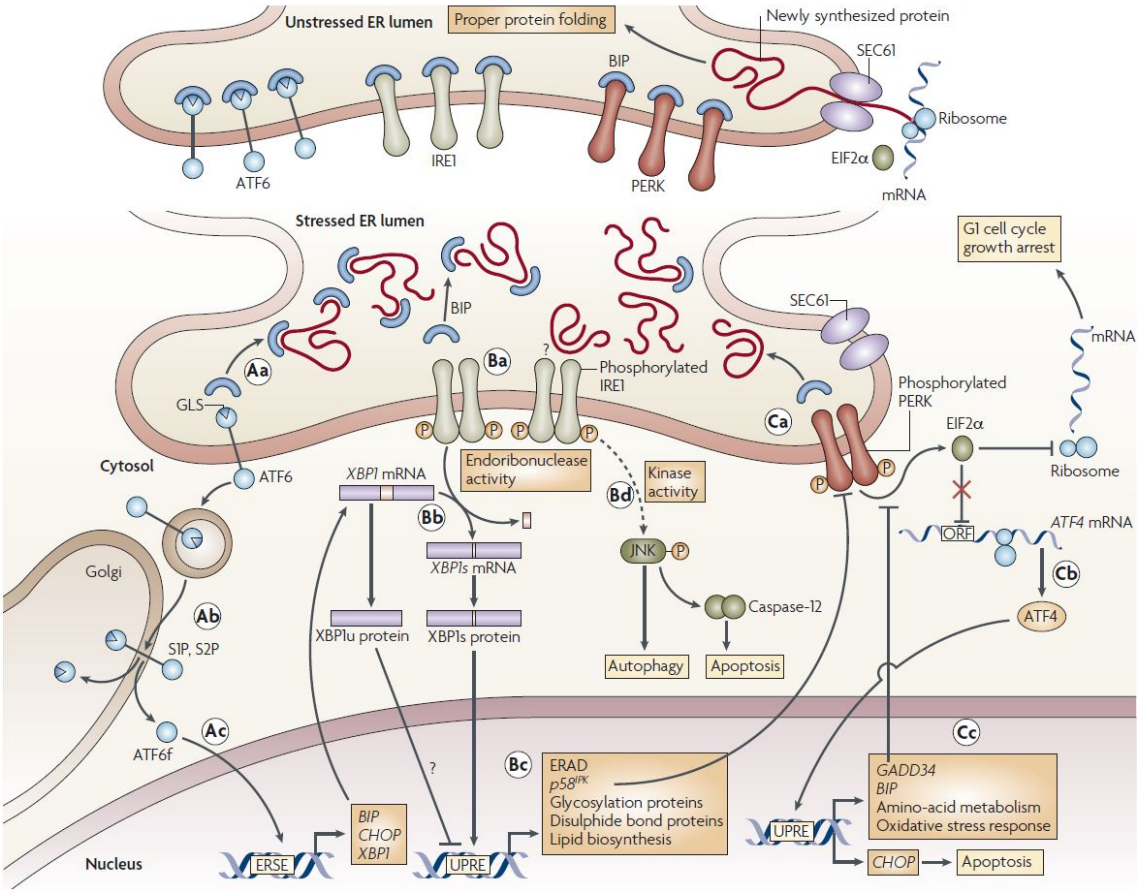

Figure 1.14 | Unfolded Protein Response signalling pathways. The three arms of the UPR commanded by ATF6, PERK and IRE1 ER stress sensors and the molecular events that drive downstream activation of the ER stress response are illustrated. Adapted from[118]

1.4.3 ER Stress-Associated Cell Death.

As it will be reviewed in the following sections, the role of the UPR is not only circumscribed to restore cell balance and promote cell survival. This evolutionary-conserved cell mechanism plays also important roles in cell death, as well as in engaging danger signalling and hence in host's immunity.

As noted, although UPR activation is initially conceived to restore cell homeostasis, it is also able to shift the cellular demise towards cell death. When cells cannot cope with stress insults and ER stress persists, the UPR is able to trigger pro-apoptotic programmes controlled mainly by IRE1 and PERK arms. Although IRE1 signalling is mainly pro-survival, it is also able to trigger cell death. Activated IRE1 can act as a docking platform to recruit other proteins such as the adaptor protein TRAF2, that subsequently tethers ASK1 which causes activation of JNK/p38 MAPK pathway[115,116]. These downstream stress kinases, are reported to promote apoptosis in several ways. JNK is able to phosphorylate and regulate the activity of several Bcl-2 family members. For example, JNK phosphorylation has been shown to inhibit the anti-apoptotic members Bcl-2, Bcl-X_L and Mcl-1, as well as activating pro-apoptotic members Bid and Bim, hence promoting cell death[98,119,120]. As regards to p38 MAPK, it phosphorylates and activates transcription factor CHOP (GADD153) which contributes to apoptosis controlling several Bcl-2 family members[121,122]. In addition, although not completely understood, it has been stated that continuous activation of RIDD can eventually provoke cell death, presumably due to degradation of mRNAs encoding folding proteins required to alleviate ER stress[115,116].

In the case of PERK signalling, the activation of this sensor leads to phosphorylation of eIF2α on serine 51, which results in the inhibition of global protein translation[116]. However, some transcripts like ATF4 and CHOP transcription factors are translated more efficiently during ER stress[98], being considered as key figures in ER stress-induced cell death[116]. ATF4 can drive the expression of transcription factor CHOP/GADD153[112]. Additionally, eIF2α phosphorylation alone can also enhance CHOP translation directly[98]. ATF4 can also induce GADD34 upregulation. Through this mechanism, a negative feedback loop on eIF2α phosphorylation status is activated, hence GADD34 counterbalances phospho-eIF2α mediated block of protein translation and thus protein synthesis is re-initiated[112,123]. This process is thought to restore normal protein synthesis but under severe or prolonged ER stress, this increment in protein load in a yet overwhelmed environment, drives the cell to ER collapse and cell death. CHOP can also increase the transcription of Bim[121] and PUMA[124], two BH3-only proteins

implicated in ER stress-associated cell death. Moreover, it has been reported that NOXA is also upregulated by ATF4 in a CHOP- or IRE1-independent manner[125].

Although CHOP activation has been studied more extensively in the PERK context, this transcription factor has also been found to be activated by ATF6 and IRE1 pathways[116]. Several studies have shown through genetic maneuvers that CHOP expression, either in lack or excess, is important for cell death induction by ER stress. Thus, CHOP overexpression induced apoptosis in a Bcl-2 dependent way and CHOP-deficient mice showed increased resistance to ER stressors such as tunicamycin[126,127]. In clear contrast, while its contribution to cell death in ER stress scenarios cannot be neglected, CHOP has been demonstrated not to be completely required for ER stress-associated cell death, as PERK-deficient and phosphorylation incompetent eIF2α(S51A) mutant cells that fail to induce CHOP expression, yet they are still susceptible to cell death under ER stress conditions[128].

1.4.4 Bcl-2 Family in ER-stress-Associated Cell Death and Beyond.

Although Bcl-2 family members are better known for their roles in controlling mitochondrial permeability and cell death mechanisms, they may also play important roles in regulating calcium ER homeostasis and also in cell death induced by ER stress.

Regarding the regulation of PERK-mediated induced cell death by anti-apoptotic proteins, it was reported that ATF4/CHOP pathway downregulates the expression of Bcl-2 and Mcl-1 contributing in this way to cell death[121,129]. The extrinsic apoptotic pathway could be also upregulated under ER stress conditions. Thus, CHOP and ATF4 have been shown to increase the expression of DR4 and DR5 receptors[130], that oligomerize in Golgi apparatus under ER stress, activating cytosolic caspase-8 engaging Bid-dependent cell death[131]. This way ER stress is able to trigger both extrinsic and intrinsic apoptotic pathways. In fact, bortezomib have been shown to cooperate and potentiate cell death induced by Apo2L/TRAIL in MM cell lines[132]. Bid has also been proposed to be activated by caspase-2 and participate in ER stress-associated cell death[114]. Upon prolonged ER stress conditions, the UPR can also induce apoptosis through p53-mediated upregulation of PUMA and NOXA[133]. That p53 is in some way involved in ER stress-induced cell death is out of doubt, as demonstrated by deletion or knockdown experiments showing an increased protection against ER stress insults[133,134]. However, the connection between ER stress and p53 activation remains to be elucidated. It is possible that NF-κB activation might be implicated in this process[135]. Beyond the studies presented above, the importance of Bcl-2 family in ER stress can also be illustrated by experiments in which

cells lacking BH3-only proteins such as PUMA, Bid and Bim, as well as Bax and Bak double-knock-out cells, are protected from cell death by external ER insults[98,136].

Moreover, Bcl-2 family has also been associated in the regulation of ER permeability and other ER-related functions. In fact, several members of this family have been found to be associated with or localized at the ER (Bcl-2, Bcl-X_L, Bax, Bak, Bik and Bok)[137]. Interestingly, an intense crosstalk exists between mitochondria and ER organelles that even increases during ER stress conditions[138]. Therefore, it seems that this cellular organelle is emerging as an additional and crucial place where cell fate decisions could be taken, with the Bcl-2 family as the mediators and integrators of stress signals. As indicated, the UPR can link ER stress to mitochondrial apoptotic programmes engaging the Bcl-2 family to ultimately drive situations of unresolved ER stress to cell death.

The communication between mitochondria and the ER seems to be bidirectional. For example, Bax and Bak, besides regulating membrane permeability at the mitochondria (MOMP) and the ER (Ca^{2+} flux), they are also capable of modulating IRE1 activity during ER stress. By forming direct physical interactions with the cytosolic domains of IRE1, Bax and Bak regulate the extent of IRE1 signalling at the ER, as demonstrated by the decreased ability of Bax and Bak double knockout cells to display IRE1 downstream signals such as JNK phosphorylation and XBP-1 splicing[139]. Besides Bax and Bak, it is possible that other Bcl-2 members could interact with the UPRosome and regulate IRE1 activity under ER stress. Another anti-apoptotic protein has been reported to interact with and modulate IRE1 activity, Bax inhibitor-1 (BI-1, also known as TMBIM-6), that is thought to displace Bax and Bak from the UPRosome which is required for IRE1 inactivation[13,140]. Moreover, Bcl-2 and Bcl-X_L have been shown to form protein-protein interactions with BI-1[140,141]. Intriguingly, targeting Bak to ER membrane could induce cytochrome c release and mitochondrial apoptosis due to Bim_{EL} and PUMA activity[142].

Moreover, Bax and Bak can also oligomerize at the ER membrane under ER stress conditions and, in a similar way to mitochondria, increase the permeability of its membrane and cause the release of ER resident proteins such as calreticulin, BIP/GRP78, PDI and GRP94[13,140]. This process is triggered by BH3-only members and counteracted by Bcl-2 and Bcl-X_L[143,144]. Although the mechanism by which ER permeabilization leads to cell death is still unknown, it has been speculated that ER permeabilization could bring about release of Ca^{2+} stores and increase Ca^{2+} flux to the mitochondria through mitochondria ER-associated membranes (MAMs) instigating cell death by mitochondrial permeabilization transition pore (mPTP). In addition, ER

leakage of essential ER resident proteins could aggravate ER stress and enhance ROS production due to global redox imbalance and mitochondrial failure[13].

Taken together, the ER is delineated as an important stress sensor and integrator where also cell fate decisions may take place, with Bcl-2 family as the critical circuitry that connect and modulate the mechanisms involved in cell fate (UPR, apoptosis, autophagy and beyond).

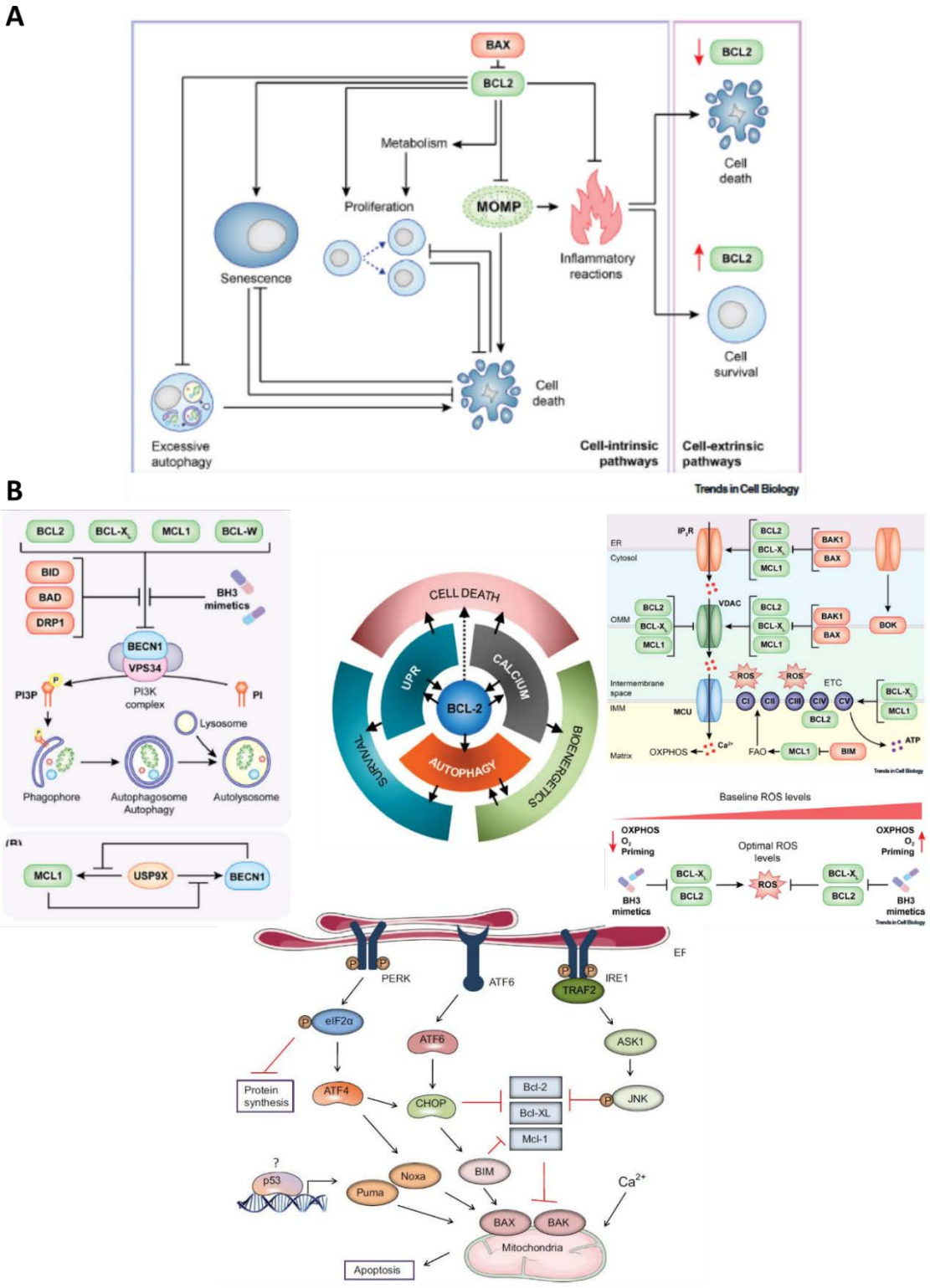

Figure. 1.15 | Bcl-2 at the crossroads of autophagy, ER stress and apoptosis and beyond. **A.** Bcl-2 family members are integral sensors in the cell with the ability to control multiple cellular processes beyond canonical functions like mitochondrial outer membrane permeabilization (MOMP). This family can modulate cellular functions in cell senescence, autophagy, ER stress responses, inflammation, Ca^{2+} and redox metabolism and bioenergetics. **B.** Through this myriad of molecular pathways Bcl-2 family integrate the information and exert an impact on cell's fate. Adapted from [13,116,145,146]

1.5 Autophagy.

1.5.1 Autophagy in Cancer.

Autophagy (literally, "self-eating") is a physiological process used by the cell to actively and specifically dispose of and recycle undesired, superfluous and/or damage proteins and organelles[117,147]. Therefore, basal autophagy is part of cell's maintenance mechanisms to sustain cell homeostasis. Under different stress conditions such as (but not limited to) nutrient deprivation, oxidative, proteotoxic stress, hypoxia or chemical insults, autophagy functions as a protective cellular gateway to promote survival[117,148]. On the other hand, autophagy could also engage cell death pathways. More accurately, some regulated instances of cell death have been shown to be regulated by components of the autophagic machinery[148].

Owing to its important role in preserving intracellular homeostasis, dysfunction of autophagic programmes is associated with different degenerative processes. In the particular case of cancer, autophagy plays a double-edged sword role[147,148]. On one side, autophagy mediates oncosuppressive effects and mutations in essential autophagic genes have been found in different human cancers[147,149]. Similarly, deletion of key autophagy genes (*BECN1*, *ATG5*, *ATG7*) in various murine models, fosters malignant transformation and oncogenesis with the development of spontaneous lung or liver carcinomas and lymphomas[148]. Several mechanisms potentially explain the tumour suppressive functions of autophagy. For example, among other mechanisms, autophagy can prevent accumulation of genetic defects that arise as a consequence of overproduction of ROS by removing dysfunctional mitochondria or aggregates of ubiquitinated proteins with redox activity[150,151]. Moreover, autophagy may hamper the metabolic reprogramming that occurs during malignant transformation also by clearing defective mitochondria[152]. It has also been proposed that autophagy participates in oncogene-induced cell death and oncogene-induced senescence, two important cell-intrinsic tumour-suppressive mechanisms[148]. Autophagy could also suppress carcinogenesis thanks to its capacity to mediate inflammatory responses by clearing inflammasomes and damaged organelles that could release endogenous inflammatory molecules[153].

Autophagy is also implicated at different levels in adaptive, innate immunity and also in releasing immunostimulatory signals in dying cancer cells (described in more detail in following sections). Thus autophagy could also have an impact on anticancer immune responses[154]. On the other hand, autophagy can also support tumour progression. During carcinogenesis, cancer cells adapt to harsh conditions that arises during the oncogenic process. One of this adaptive mechanisms is the upregulation of autophagic responses. In this way, cancer cells alleviate cell-intrinsic and environmental stimuli that in normal conditions would drive cells to death. In line with this notion, advanced human tumours with an invasive phenotype manifest an increased autophagic flux[148,155]. Similarly, in several murine cancer models, genetic interventions that target autophagic components hinder tumour progression, corroborating the driving force that autophagy exerts on cancer development[147,148]. Therefore, the current view on autophagy and cancer is that on early stages autophagy hinders tumour initiation while in more advanced states of the disease, autophagy may promote tumour progression[156].

1.5.2 The Autophagic Pathway.

To date, several autophagic-related processes have been defined such as macroautophagy, microautophagy, endosomal microautophagy and chaperone-mediated autophagy[157]. Moreover, based on the precise composition of the autophagy cargo, specific instances of micro- or macroautophagy can also be defined (mitophagy, nucleophagy, xenophagy, among others)[157]. The best characterized form of autophagy thus far is macroautophagy (referred herein as autophagy). It is defined as the mechanism by which intracellular material is firstly and progressively confined within nascent double-membrane vesicles (phagophores or isolation membranes)[147,148,157]. Different membranous organelles including ER, Golgi apparatus, plasma membrane, mitochondria, ER-Golgi intermediate compartment (ERGIC) and even recycling endosomes, contribute to the nucleation and expansion/elongation of the emerging phagophores[147,148]. Once the phagophore is completely sealed, wrapping around the autophagic cargo, is termed the so-called autophagosome. Afterwards, these double-membraned structures experiment a series of maturation steps that culminate with the fusion of the autophagosome with the lysosome creating an autolysosome. This fusion event promotes the activation of lysosomal hydrolases that digest the autophagic cargo. The products of autolysosomal degradation (sugars, nucleosides/nucleotides, amino acids and fatty acids), can be recycled back to the cytoplasm and be re-incorporated to cellular metabolism.

Autophagy is a well-regulated molecular programme (see **Figure. 1.16**). Up to 30 core ATG genes and conserved autophagic proteins have been identified in yeast and mammals[147,158]. Briefly, the autophagic flux starts with the activation of ULK1 (ATG1) that forms complex with (ULK2, ATG13, FIP200 and ATG101). ULK complex is activated and assembled at ATG9 enriched membranes. Thereafter, this complex activates Beclin 1 (BECN1) that serves a molecular scaffold to form a multiprotein complex composed by BECN1, AMBRA1, ATG14, UVRAG and the class III phosphatidylinositol 3 kinase (PI3K) VPS34 and its regulatory subunit VPS15, that drives the generation and initial nucleation of the phagophore[117,157,159]. Autophagosome membrane expansion requires ATG5-ATG12 complex to interact with ATG16. Further elongation of the phagophore also requires the conversion of the free form of microtubule-associated protein 1 light chain 3 (LC3-I) into the lipid-conjugated and membrane-bound form (LC3-II) that are loaded to the autophagosome membrane[160]. In the LC3 conversion participates ATG4b in association with ATG7 and the ATG5-ATG12 complex[157,159,161]. When incorporated onto forming autophagosomes, LC3-II participates in substrate uptake by binding to several autophagic receptors[157]. The following event in the autophagic process involves the fusion of autophagosomes with lysosomes. In this step, Rab GTPases, HOPS (homotypic fusion and protein sorting-tethering complex) and SNAREs (soluble N-ethylamleimide-sensitive attachment receptors) play a crucial role[157,160]. A master regulator of autophagy is mammalian target of rapamycin (mTOR), a downstream kinase in the PI3K cascade. It prevents the execution of autophagy when nutritional cues are prolific. Thus, under non-stressed conditions mTOR complex 1 (mTORC1) phosphorylates and inactivates ULK1/2, thereby inhibiting autophagy initiation[160]. When nutrients are scarce, ATP levels decline and consequently, AMP accumulates, AMPK is able to sense declining ATP/AMP ratios and become activated. AMPK is then able to inactivate mTORC1 as well as stimulating direct autophagic players like ULK1, VPS34 and Beclin 1 [148].

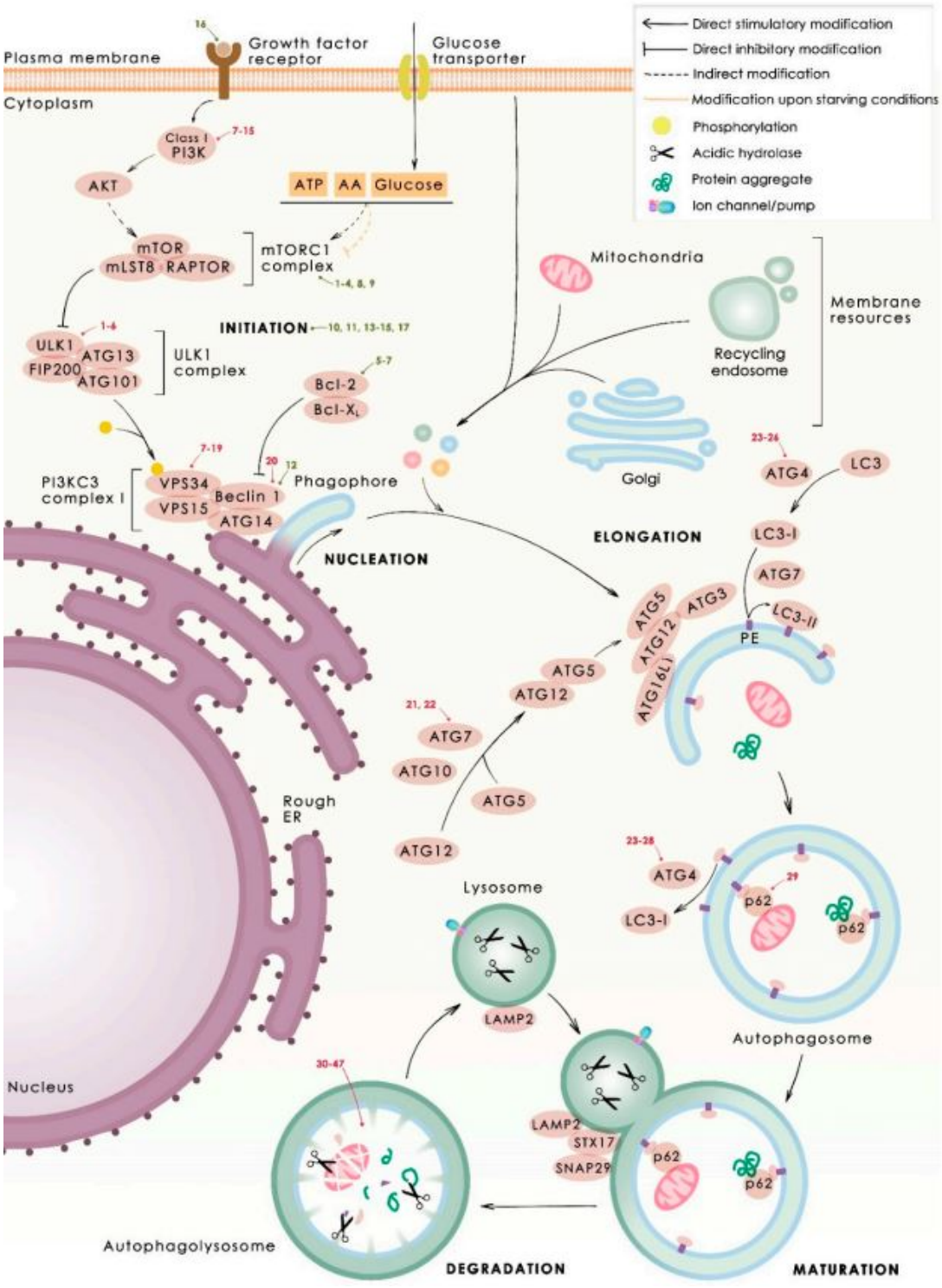

Figure. 1.16 Autophagy the mechanisms. The different phases of autophagic process (nucleation, elongation, maturation and degradation), with the main players of each process are illustrated. Adapted from [162]

1.5.3 The Interplay between ER Stress and Autophagy.

As described in previous sections, proteasomal degradation and autophagy are the two main mechanism at cell's disposal to clear undesired cellular proteins. Under ER stress conditions, when the cytoprotective and restorative capacity of the UPR is overwhelmed, several signals emanate from the ER to trigger autophagy in an attempt to re-establish cellular homeostasis before succumbing to cell demise. Some of these signals originate from IRE1 and PERK and even ATF6 ER stress sensors[117,163]. Activation of IRE1 can lead to the recruitment of TRAF2 and ASK1 that subsequently activate JNK. Thereafter, activated JNK phosphorylates (and inhibits) Bcl-2 and Bcl-X_L which prevents the interaction with BECN1, a key autophagic inducer[164,165]. Moreover, as exposed earlier, PERK activation promotes ATF4 and CHOP expression that in turn upregulates ATG12 and TRB3 respectively, further stimulating autophagic flux[163,165].

ER stress conditions could also drive Ca^{2+} release from the ER that subsequently, could foster autophagy by directly or indirectly stimulating DAPK, PKCθ or AMPK activity[165]. Regarding ATF6 induction of autophagy, depending on the cancer model, several diverse and complex mechanisms have been proposed[166]. On the other side, autophagy can also modulate the extension and duration of ER stress by clearing excessive ER membranes and luminal or embedded proteins to restore ER normal size[117]. Moreover, ER stress-autophagy connection may also have implications on cell demise. As discussed on previous sections, although the first task of the UPR is to restore cellular homeostasis upon ER stress conditions, it can also trigger cell death. Similarly, autophagy is also considered a survival mechanism. However, under certain circumstances it has been shown to promote cell death[167,168]. For that reason, autophagy activation after ER stress could also have cytotoxic consequences. The final outcome of autophagy activation is complex and could depend on the intensity and the type of stimulus and the type of cell and context under consideration[165].

1.5.4 Targeting Autophagy in Cancer.

Given the importance of autophagy in cancer, initial clinical testing of autophagy modulators (in particular chloroquine, CLQ or hydroxychloroquine, HCLQ) in combination with different anticancer approaches (radiotherapy, chemotherapy or targeted therapies) has been conducted in a diverse set of human cancers (skin, brain, blood, among others)[169]. Nonetheless, the clinical benefits of these first collection of trials were quite modest. This could be partially explained by the randomness and little

rationalization behind such combinations[170,171]. Moreover, pharmaceutical industry was unable to replicate the findings on the observed autophagy addiction, especially of Ras-driven cancers[172–174]. These results lead to the partial abandonment of research programmes on small-molecule autophagy-related inhibitors by pharmaceutical companies. However, new data had shed some hope to the matter and showed that only under certain perturbations or conditions, the autophagic dependence of cancer cells become apparent. For example, combination of MAPK inhibitors with autophagy blockers showed synergistic anti-proliferative effects in diverse tumour models[175,176]. Another good example that could be therapeutically relevant is the connection that exists between ER stress and autophagy. A wide collection of ER stress inducers have shown to initiate autophagic responses. For example, tunicamycin and thapsigargin, besides inducing a potent ER stress response, activate autophagy in colon and prostate cancer cells as an adaptive mechanism to alleviate ER stress[177]. Likewise, among the different cellular responses that are triggered under proteasome inhibition, initiation of autophagic response is considered one of them[109]. In fact, it has been proposed that one of the resistance mechanisms to proteasome inhibition in MM could be provided by autophagy activation[156,158]. Autophagy have been shown to play an important role in plasma cell ontogeny and development. Furthermore, in MM cells, autophagy is thought to be essential to MM survival in order to confront the increased immunoglobulin synthesis and high proliferative demands[158]. Therefore, targeting both ER stress and autophagy in MM could be envisaged as an attractive therapeutic strategy that would potentially overcome PI resistance[156].

Interestingly, a notably growing body of evidence supports that the anticancer activity exerted by autophagy is also due to the capacity to modulate tumour microenvironment and immunesurveillance[178]. All these studies have precipitated a resurgent interest in targeting autophagy in cancer in combination with other therapies (as mentioned, ER stress being one of them), in a more rationalized manner. However, a note of caution should be raised. The dual role of autophagy and UPR in cancer, makes it a complex issue that may yield the final outcome to be context dependent. If autophagy activation following ER stress, adopts a prosurvival role, then inducing ER stress and concomitantly blocking autophagy should precipitate cancer cells to their demise. Nonetheless, in some settings, autophagy could also favour ER stress-induced cell death, becoming an auxiliary reinforcement in case cancer cells develop apoptotic resistance mechanisms[165].

Chloroquine (CLQ) is a 4-aminoquinoline drug that has long been used as an antimalarial drug, as well as for the treatment of different illnesses (rheumatoid arthritis, lupus erythematosus, amoebic hepatitis)[179,180]. CLQ and its derivatives are

lysosomotropic agents that inhibit lysosome acidification and block autophagosome-lysosome fusion, thus preventing autophagic cargo degradation[161]. In the unprotonated form, they can easily diffuse across membranes and when they get into an acidic environment like the lysosome, they get protonated and accumulate in these acidic organelles increasing its pH[180]. Currently, all trials testing the therapeutic potential of autophagic inhibitors in cancer therapy are using CLQ or its derivative hydroxychloroquine (HCLQ). These cheap compounds are the only clinically approved drugs that can inhibit autophagy, at least at some extent. In fact, the term autophagic inhibitor could be considered a loose designation. CLQ and HCLQ are not truly specific enough and much of the anticancer effects observed so far could be attributed to other autophagy-independent mechanisms. Many ongoing clinical trials are testing CLQ or HCLQ in combination with radiation, conventional chemotherapy and targeted agents like PIs, HDAC inhibitors, mitotic drugs, kinase inhibitors and others, in multiple neoplasms[174]. In MM, the a phase I and a small phase II clinical trial combining bortezomib with HCLQ have been completed and rendered moderate results[181].

1.6 Targeting ER Stress in Cancer.

Because of the critical role played by the UPR and ERAD in ER and cellular homeostasis, dysfunction of any of these pathways will inevitably have important consequences on human physiology[182]. In fact, ER stress or UPR and ERAD alterations have been linked to diverse pathological conditions such as cancer, metabolic disorders, neurodegenerative diseases and ischemic conditions[112].

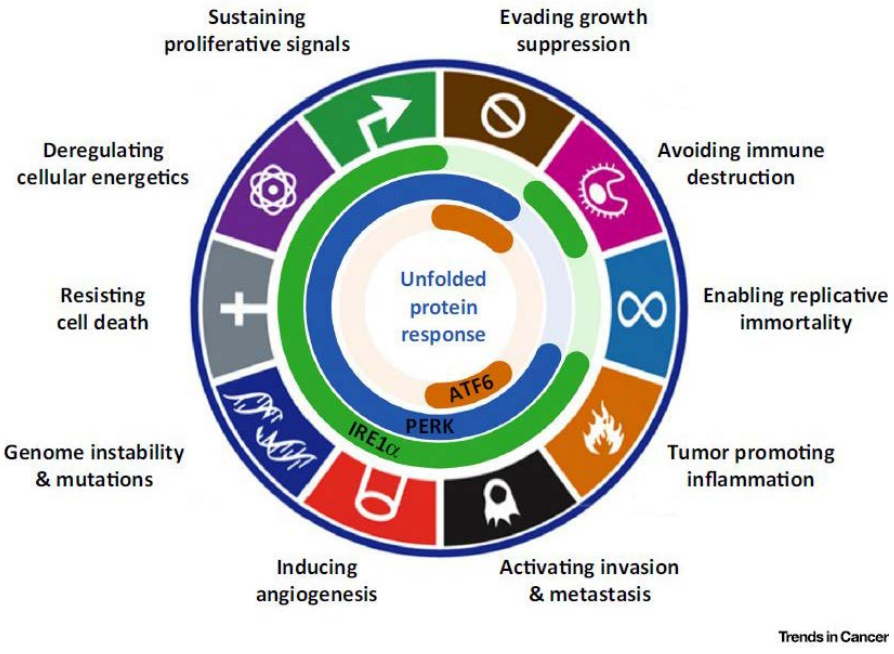

Figure. 1.17 | ER stress & hallmarks of cancer. Here is represented the different hallmarks of cancer in which ER stress and particularly the different UPR arms (ATF6, PERK and IRE1α) participates. Adapted from [112]

During tumour development cancer cells have to cope with harsh conditions that are widely known to trigger ER stress (e.g. nutrient deprivation, hypoxia, acidic pH, genomic instability)[113,117]. Thus, as an survival and adaptation mechanism, UPR activation constitutes an important **hallmark** of numerous human cancers[112,183]. Supporting this notion, solid tumours usually show upregulation of different UPR markers such as PERK, IRE1 or ER chaperones BiP/GRP78 and GRP94 or [112]. Activation of the UPR endows cancer cells with the ability to acquire essential characteristics (invasiveness, dormancy, resistance to therapy, tumour-driven angiogenesis, etc) required for tumour progression[113,117,184] (see **Figure. 1.17**). In addition, ER stress could also negatively influence immunity at different levels, especially in the myeloid compartment, favouring in this way tumour development[185–187].

With all these players around the table, it seems tempting **to target ER stress** and the cellular pathways involved. In fact, ER stress as a therapeutic target, is increasingly getting more adepts in the cancer crusade against many solid and blood neoplasms[188]. In the particular case of **multiple myeloma (MM)**, the elevated production of immunoglobulins leave these cells heavily reliant on the survival arm of the UPR. In fact, the first role of the UPR in the Immune System was discovered in the context of B-cell development[189]. Therefore, as plasma cell development and survival strongly relies on an intact UPR[189,190], it does not seem unusual that UPR activity increases with MM progression[191]. Furthermore, whole genome sequencing studies have revealed that MM patients frequently harbour mutations in genes related to the UPR[192]. Among the UPR mediators, XBP1 has been found to be overexpressed in MM and has also been identified to be mutated in a small subpopulation of patients, suggesting a possible causative function in MM pathogenesis[192–195]. Nevertheless, although myeloma cells count on the UPR to thrive, they are extremely sensitive to ER stress-associated cell death[196–198]. This feature explains why **proteasome inhibitors (PIs),** have shown a prominent clinical efficacy in the treatment of MM[199,200]. Currently, three PIs have been approved for the treatment of MM: bortezomib, carfilzomib and ixazomib. However, resistance to therapy is recurrent and in most of the cases accounts for the lethality of the disease[195,201].

For these reasons, novel ER stress/UPR-targeting therapies have emerged. Apart from the proteasome, another way to inhibit protein clearance and bring about a potent stress response to induce cell death of UPR-dependent tumours is by targeting ERAD[188]. In particular, VCP/p97 inhibitors like eeyarestatin, DBeQ and more recently CB-5083 have yielded promising leads.

DBeQ (N2,N4-dibenzylquinazoline-2,4-diamine) is an ATP-competitive p97/VCP inhibitor that has exhibited *in vitro* promising anti-myeloma effects[202,203]. Moreover, it has shown not only to impair ubiquitin-dependent degradation through ERAD, but also to target autophagy by blocking autophagosome formation[203]. As noted earlier, upon overwhelming ER stress, cancer cells may upregulate autophagy as an alternative clearance pathway to alleviate stress.

CB-5083 is an optimized version of DBeQ with drug-like properties that has been further developed reaching phase I trials. It has effectively shown broad antitumour activity in solid and haematological xenograft cancer models[104,204]. In the particular case of MM, it exhibited robust anti-myeloma activity both in primary cells (even harbouring a PI resistance background) and *in vivo* myeloma models[205].

Given its important role in myeloma pathogenesis, novel drugs targeting the RNAse domain of **IRE1** (4μ8C, MKC-3946, STF083010) have been developed and showed significant tumour growth inhibition in mouse myeloma models[206,207], as well as in primary myeloma plasma cells[207]. The mode of action of **4μ8C**, and other inhibitors of this group, consist on forming a stable imine in the Lys of the catalytic core of the RNAse domain of IRE1 blocking its activity. In addition, new potent and selective first-in-class inhibitors have been developed against **PERK** (GSK2606414 and the optimized form GSK2656157)[208,209], which have shown promising pre-clinical results in a model of pancreatic cancer[209,210]. These compounds bind to the ATP binding site in the kinase domain preventing ATP binding and the ensuing eIF2α phosphorylation[209,211]. Another alternative is targeting chaperon activity and quality control[188]. For that purpose, chaperon inhibitors targeting BiP or Hsp90 have been developed and were shown to induce cell death in different cancer cell models[212,213].

Nonetheless, given the dual role of ER stress and UPR related pathways in cancer, a word of caution needs to be taken when targeting these cellular pathways, as on one side we may be inhibiting the pro-tumorigenic role of UPR mediators but in the other, we may reduce the immunogenicity of cancer cells dampening danger signalling (or vice versa). Therefore, future investigations assessing the *in vivo* repercussion on overall immunity (whether it be MDSCs in the TME or immune cells in ICD) as well as cell-autonomous responses on cancer cells, on immunocompetent mice models are needed in order to truly evaluate the therapeutic relevance of these approaches in cancer.

1.7 Immunogenic Cell Death.

Every day in the human body, billions of cells pass away and are kindly replaced by newborn members leaving no trace behind, allowing in this way conservation of whole-body homeostasis. In order to occur without catastrophic consequences, this process must remain almost completely unnoticed to the Immune System. During this physiological, programmed cell death, mainly in the form of apoptosis, intracellular content is confined within membranous bodies that are rapidly cleared by phagocytes in an immunological 'silent' manner. Hence, apoptosis has long been considered a non-immunogenic or even tolerogenic process, whereas necrosis and necroptosis have been shown to play a key role in inflammation and immune related processes[214,215]. However, the new concept of "immunogenic cell death" (ICD) has challenged this traditional view and has granted apoptosis with immunogenic abilities. Compared with the classical form, this immunostimulatory kind of apoptosis is characterized by the ability of dying cells to elicit robust adaptive immune responses against altered self-antigens/cancer-derived neo-epitopes, in the case of tumour cells, or against pathogen-derived antigens (Ags) during the course of an infection[216].

Besides antigenicity, another vital factor needed to unleash a genuine immune response is adjuvanticity, conferred by microorganism- and/or danger-associated molecular patterns (MAMPs and DAMPs, respectively). These are molecules that are exposed or released by dying cells and let the Immune System know the existence of a menace to the organism[217]. This 'danger' state is sensed in the human body by pattern recognition receptors (PRRs) displayed by innate immune cells such as monocytes, macrophages and dendritic cells (DCs), hence promoting activation and maturation of these cells to engage the adaptive arm of the Immune System[218].

Screening studies have been carried out to unveil the immunogenic potential of myriads of anticancer agents[85]. To date, only a small yet diverse collection of anticancer therapies, whether chemotherapeutic drugs (e.g., anthracyclines, oxaliplatin, bortezomib)[219,220] or physical modalities (e.g., radiotherapy, hypericin-based photodynamic therapy (Hyp-PDT), and high hydrostatic pressure (HHP))[221,222] have been shown to induce *bona fide* ICD. On the basis of drug-induced ICD, neither structural nor functional characteristics from these therapies can be used to predict their immunogenic capacity. As examples we can find oxaliplatin-cisplatin and melphalan-cyclophosphamide paradigms[223,224]. However, a common denominator can be extracted from the action mechanisms of all these approaches: ER stress and ROS generation. Thus, activation of the ER stress pathways also known as the UPR, and specially, the

PERK-mediated arm, is vital for the vast majority, if not all, the scenarios where ICD occurs[225].

During the past decade important changes have been witnessed, particularly in the way the different types of cellular demise are perceived. Necrosis was first conceived as an accidental, pathological and pro-inflammatory form of cell death, whereas apoptosis was recognized to be a non-immunogenic, physiological and regulated way of cell demise[214]. However, these features are no longer so apparent since necroptosis has been shown to be triggered by a genetically-encoded and well-regulated molecular programme that cause the cell to reach their final destiny undergoing necrotic morphological features[28,31,226]. On the other hand, apoptosis is no longer considered to be an immunologically 'silent' process, since some apoptotic cells are able to induce antigen-specific immune responses[219].

In the cancer field, the role of the Immune System has been overlooked for many years, at least in part, due to the way chemotherapy and other anticancer therapies were usually tested. Particularly, the standardized usage of immunodeficient mice models to assess the efficacy of these treatments has had detrimental consequences to gain insight on the precise role of the Immune System in cancer therapy[227]. Nonetheless, with the advent of cancer antigenicity and ICD concepts, together with the Danger Theory, oncological research and clinical focus are increasingly getting skewed towards developing novel and improved immunotherapeutic protocols[228].

1.7.1 ICD, the Anti-Cancer Immune Cycle and ICD Modalities.

The ICD concept has been defined as an unique class of regulated cell death capable of eliciting complete antigen-specific adaptive immune responses through the emission of a spatiotemporally defined set of danger signals[229,230]. These signals or, DAMPs, are endogenous molecules that perform conventional intracellular functions but when extracellularly exposed, gain immunogenic competences. The release or membrane exposure of these molecules, allow their interaction with their cognate receptors (PRRs) displayed by innate immune cells such as monocytes, macrophages and DCs. This is followed by the activation and maturation of these cells that migrate to draining lymph nodes, loaded with cancer-derived antigen-specific cargoes, where cancer material is presented to T cells ($CD4^+$ and $CD8^+$ T lymphocytes) giving rise to a potent anticancer adaptive immune response (see **Figure 1.18**)[231].

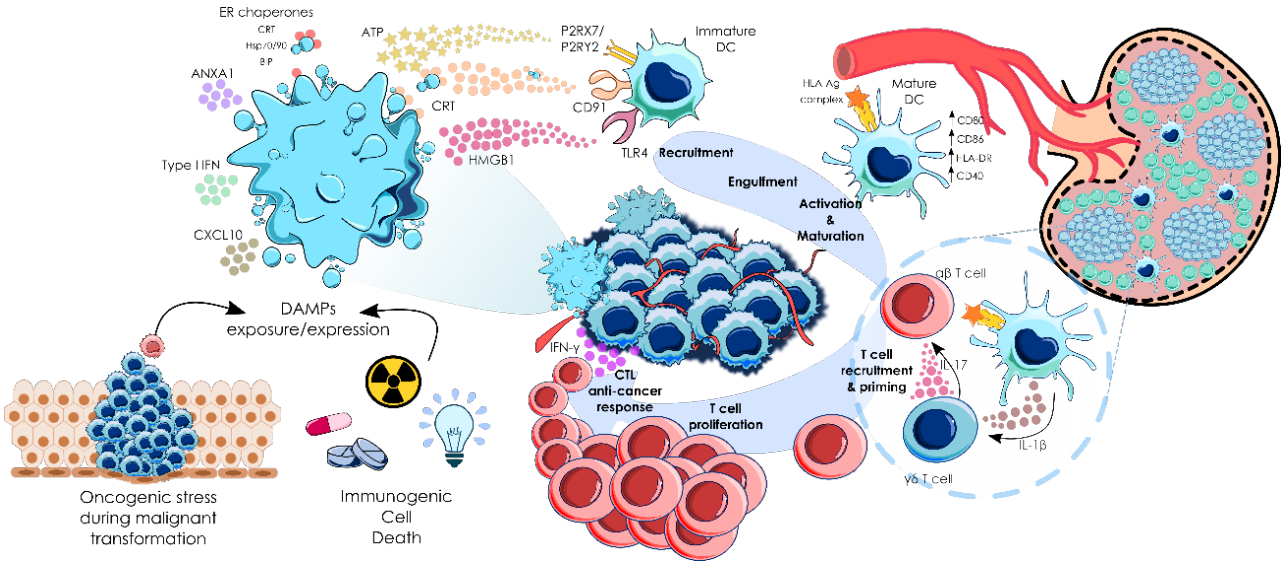

Figure 1.18 | Immunogenic cell death cycle. Cancer cells subjected to some type of chemotherapeutics and other anticancer therapies expose calreticulin (CRT) and other endoplasmic reticulum chaperones, such as Hsp70, Hsp90 on their surface, secrete ATP, initiate type I interferon (IFN) response that is able to trigger the production of CXC-chemokineligand 10 (CXCL10), and release high-mobility group box 1 (HMGB1) and annexin A1 (ANXA1). When secreted or exposed extracellularly, they bind to their cognate receptors on the surface of myeloid or lymphoid cells, which enables the engulfment of cell corpses by antigen-presenting cells, including dendritic cells (DCs). This process in the context of proper immunostimulatory signals, eventually leads to the priming of an adaptive immune response involving both αβ and γδ T cells. This culminates in the establishment of a CTL-mediated anticancer immune response with potential to kill therapy-resistant cancer cells via an IFNγ-dependent mechanism. In the clinical setting cancer cells with higher expression of some DAMPs have been found. Depending on the cancer type, this could be correlated with good or bad prognosis, as well as to markers of an active anti-cancer immune response.

To date, four modes of ICD have been described, each one related to a particular type of inducing stimulus and to the emission of a specific set of danger signals[216] (see **Figure 1.19**).

1) **Pathogen-driven ICD**, as one of the defence mechanisms against invading pathogens.

2) **ICD exhibited by physical cues**, such as Hyp-PDT, irradiation and HHP.

3) **Necroptosis** has also been shown to constitute a distinct variant of ICD, as the regulated form of this type of cell death but not accidental necrosis, was able to vaccinate syngeneic mice against a rechallenge with cells of the same type[232]. Moreover, RIPK3 or MLKL deficiency abrogated the ability of these cells to secrete the required immunogenic signals that lead to an anticancer immune response in mice[233]

4) **ICD evoked by chemotherapeutics**, in which, using different type of interventions (siRNAs, shRNAs, ATP-degrading enzymes, etc) against essential components involved in cell death pathways[87,88,219], it has been demonstrated that a

diverse panel of drugs are able to drive genuine and protective immune responses in mice. Of note, despite some screening studies using large drug libraries have been performed, only a small group of candidates have emerged to be valid ICD inducers[84,85,219,223]. The chemical nature of these agents, is considerably diverse: oxazophorines like cyclophosphamide[234] approved for the treatment of several tumours; Pt-based compounds as oxaliplatin[235], used against colorectal carcinoma; anthracyclines[236] such as idarubicin and doxorubicin, approved for the treatment of a wide variety of cancers; anthracenediones such as mitoxantrone, the most studied member; and dipeptides like bortezomib, currently used in the treatment of MM and mantle cell lymphoma[237]. Similar to bortezomib, carfilzomib another proteasome inhibitor used in the treatment of MM, has also shown to expose CRT in different MM cell lines[238]. Attractive as it may seem, no simple structure-function relationship has been found that could predict the suitability of these compounds to trigger ICD. This is clearly exemplified by the oxaliplatin-cisplatin paradigm, two structurally-related agents that exert its mechanism of action by causing inter- and intra-strand DNA-adducts and yet only the former is capable of prompting anticancer immunity[223,235]. Likewise, although both melphalan and cyclophosphamide function as DNA alkylating drugs, exclusively cell death induced by the latter is immunogenic[224]. Moreover, combinatorial strategies can be exploited to compensate the DAMPs scarcity of some therapeutic agents to restore immunogenicity and hence transform tolerogenic cell death systems into immunogenic modalities[223,239], which most likely will be the future of cancer therapies to achieve clinical success.

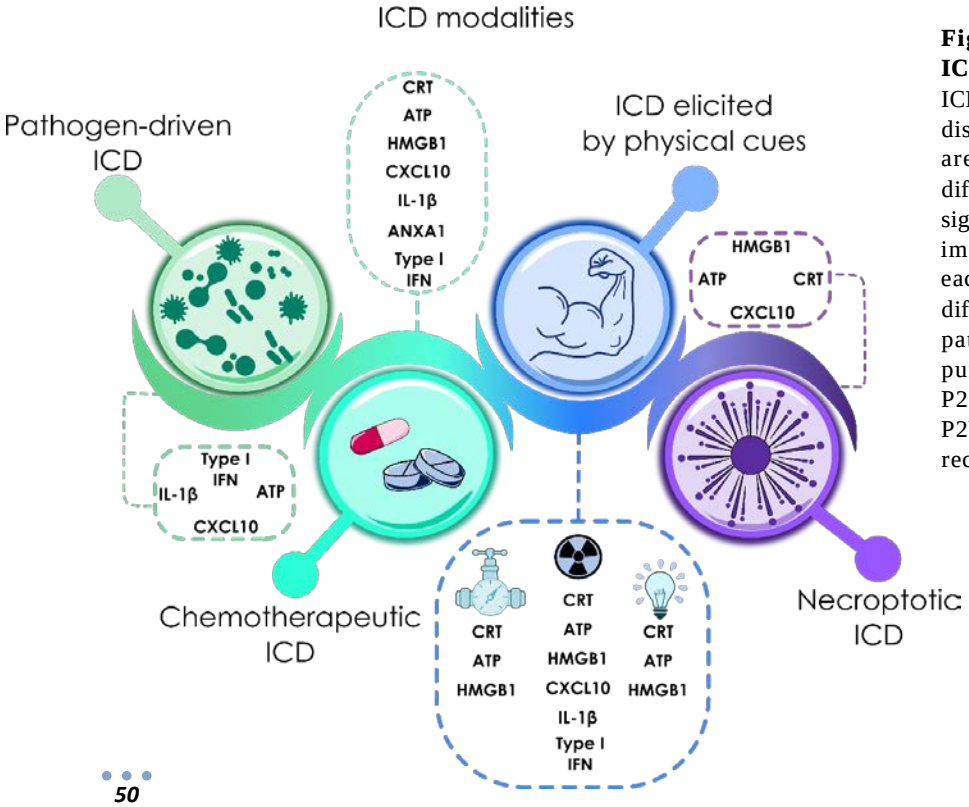

Figure 1.19 | Forms of ICD. Different variants of ICD could be evoked by distinct types of stimuli that are associated with a differential set of danger signals. Even in the form of immunogenic chemotherapy, each drug could instigate differential danger signalling pathways[216]. ; P2RX7, purinergic receptor P2X7; P2RY2, purinergic receptor P2Y2; TLR4, Toll-like receptor 4

1.7.2 ICD-related Danger Signals and Mechanisms of DAMP Trafficking.

Classically, the Immune System has been considered to be designed to confront foreign intruders. For decades, the self/non-self model of immunity has explained immune responses on the basis of self (homeostatic and non-antigenic) and non-self (pathogen-driven and antigenic)[240,241]. However, the capacity of endogenous (self) entities to mount an active immune response under sterile conditions unveiled its limitations. The danger model proposed by Polly Matzinger helped to address these issues[218,242]. In this model, the Immune System preferentially responds to challenges by discriminating between dangerous and safe entities irrespective of their origin (endogenous or foreign)[218]. Thus, besides antigenicity other contextual cues are needed to alert the Immune System that the tissue is damaged. This context is provided by danger signals.

Several factors, such as the type of cell death, the ICD stimuli and the connection between various cellular stress responses, influence the type of danger signals emitted during the course of cell death[241]. Furthermore, not all the DAMPs exposed during cell death are immunostimulatory. In fact, there are some molecules that exhibit immunosuppressive properties and play important roles in cell death tolerance (Prostaglandin E2, adenosine, etc)[216,241]. Among all the members of the DAMP family, the best studied, and the ones which have been shown to be pivotal for ICD are described in the following sections.

1.7.2.1 Calreticulin and Other Molecular Chaperones.

Calreticulin (CRT) is a, highly conserved, soluble, ER-associated chaperone with numerous functions inside and outside the ER (calcium homeostasis, assembly of MHC-I, etc)[243,244]. In stressed or dying cells, CRT is exposed into the outer leaflet of the plasma membrane (ecto-CRT) where it functions as a potent 'eat-me' signal through binding to LRP1 (also known as CD91), and possibly other scavenger receptors, displayed by phagocytic cells. This role in phagocytic clearance of dead cells was first described by Gardai *et al.*[245]. Nonetheless, Obeid *et al.*[219] went a step further and demonstrated that CRT exposure was a key determinant in ICD-driven anticancer immunity. Actually, cancer cells undergoing cell death triggered by certain chemotherapeutics, expose CRT on their surface, which leads to the engulfment by DCs and, more importantly, to tumour antigen presentation and anticancer cytotoxic T lymphocyte (CTL) specific responses[229].

Furthermore, ecto-CRT has been shown to prompt IL-6 and TNF expression on DCs, priming pro-inflammatory T-helper type 17 (Th17) polarization[246].

Likewise, other ER-resident chaperones such as heat-shock protein 70 (Hsp70) and Hsp90, play also an important role in the immunogenicity of dying cancer cells. Thus, ecto-Hsp90 has been reported to enhance DC uptake of bortezomib-treated MM cells, including primary cells isolated from MM patients and induction of anticancer immunity[247]. On the contrary, Dudek-Peric *et al.*[224], using blocking antibodies against Hsp90 in a DC maturation assay, reported that this chaperone was not (or at least partially) involved in the immunogenicity of melanoma cells treated with melphalan. The specific role of Hsp70 in the immunogenicity of cancer cells has not been studied so extensively. However, it has been reported that in shikonin- or gemcitabine-treated cells, Hsp70 was involved in DC-mediated activation of $CD4^+$ and $CD8^+$ T cells [248,249], or in the case of Hyp-PDT treatment, Hsp70 promotes nitric oxide (NO) generation in innate immune cells[250]. In a different context, Hsp70 has shown to efficiently vaccinate mice against murine MM cells using a DNA-based vaccination strategy[251]. BiP/GRP78, the fundamental regulator of ER function and the UPR in ER stress responses, has been described to be secreted and to participate in the cross-presentation of tumour-derived Ags in DCs, inducing Ag-specific CTL immune responses[252]. Indeed, chaperones as efficient protein folding mediators, are often present bound to antigenic peptides. When released, these chaperone-peptides complexes enter APCs by endocytosis via CD91 receptors and are cross-presented on MHC-I and MHC-II molecules to $CD8^+$ and $CD4^+$ T cells[253,254]. Thereby, these molecules not only potentiate immunogenicity of dying cancer cells by acting merely as potent danger signals, but also contribute to boost cancer antigenicity assisting in the cross-presentation process.

With regards to the kinetics and the cellular pathways involved in the exposure of CRT, it has been documented that they may differ depending on both the apoptotic phase under evaluation and the inducing stimulus (see **Figure 1.20**)[227]. For example, there are some instances where ecto-CRT exposure precedes phosphatidylserine (PS) externalization[255,256], is systemically accompanied by ERp57 to the plasma membrane and requires PERK-mediated phosphorylation of eIF2α. This is followed by caspase-8 activation and specific cleavage of BAP31, leading to the subsequent activation of Bax and Bak. CRT relocation also requires anterograde ER-Golgi trafficking and the exocytic pathway in a SNAP23-dependent manner[255]. On the contrary, Hyp-PDT mediated CRT exposure requires PERK, Bax, Bak and the secretory pathway but not eIF2α phosphorylation and caspase-8 activation[257]. However, there are other ways by which CRT can be relocated to the cell surface and that are independent from the aforementioned mechanisms. Other studies claimed that CRT can bind with high-affinity

to phosphatydilserine[258,259] in a Ca^{2+}-dependent manner, and thus during cell death these two molecules are co-translocated at the same time in a caspase-independent fashion[260].

1.7.2.2 ATP.

During the course of ICD, dying cells expel ATP[86,87] to the extracellular milieu where it functions as a powerful short-range 'find me' signal[261]. Once externalized ATP binds to ionotropic (P2X7) and metabotropic (P2Y2) purinergic receptors on APCs[86,261], stimulating their phenotypic maturation and chemotactic attraction respectively[148]. In particular, extracellular ATP can activate the caspase-1 dependent NLRP3 complex (the so called inflammasome) triggering IL-1β secretion[86]. This in turn promotes $CD8^+$ T cell[86], as well as, IL-17 producing-γδ T cell[262] antitumour responses[86]. Correspondingly, mice harbouring deficiencies in any of these components (*Nlrp3*$^{-/-}$, *P2rx7*$^{-/-}$ or *Casp1*$^{-/-}$) appeared to be incapable of promoting adaptive immune responses in drug-induced ICD[86,262]. The molecular mechanisms of ATP secretion during ICD are also dependent on the ICD-inducing stimulus (see **Figure 1.20**). In mitoxantrone- or oxaliplatin-driven early apoptotic ATP secretion, autophagy has been demonstrated to be mandatory, as depletion of important autophagic components (ATG5, ATG7 and BECN1) prevented ATP release[263]. Moreover, other molecules involved in different cellular processes like lysosomal exocytosis (LAMP1, VAMP1), membrane blebbing (ROCK1, myosin II), apoptotic machinery (caspases) and membrane permeabilization (PANX1) have been shown to be essential in ICD-induced ATP externalization[263]. Interestingly, PANX1 activation and surface exposure, as well as, LAMP1 translocation are strongly dependent on caspases rather than on the autophagic machinery[263]. In fact, it is possible that remodelling of autophagic effectors and components of lysosomal function or PANX1 hemichannels by caspases rather than the mere presence of these components *per se*, are the real originators of ATP secretion[263,264]. However, similarly as it occurs in Hyp-PDT induced CRT relocation, ATP secretion mechanisms differ from that described for chemotherapy-induced ICD. In particular, Hyp-PDT mediated ATP is autophagy independent[265], and rather requires the PERK-mediated proximal secretory pathway and PI3K-regulated exocytosis[257].

1.7.2.3 HMGB1.

High mobility group Box 1 (HMGB1) is a non-histone chromatin-binding protein localized in the nucleus, where it interacts with DNA and regulates transcription[266]. In particular, it regulates the activity of NF-κB and p53 among other transcription factors and favours V(D)J recombination[227,267]. Extracellularly, HMGB1 is able to perform cytokine-based functions in monocytes and macrophages under the influence of pro-inflammatory molecules (TNF, LPS, IL-1β)[227,267,268]. When released by dying cells, HMBG1 exerts potent immunostimulatory effects by interacting with distinct PRRs (TLR2, TLR4 and RAGE)[269]. During chemotherapy- or radiotherapy-induced cell death, HMGB1 is released from dying cells and signals through TLR4-MyD88 axis on DCs, facilitating antigen processing and presentation[88,270]. The molecular pathways that participate in the release of this DAMP remain to be elucidated. It has been documented that necrotic cells passively release huge amounts of HMGB1 acting as a potent mediator of inflammation[268]. Similarly, HMGB1 is also released by secondary necrotic cells and the usage of z-VAD-fmk (a broad caspase inhibitor that delays secondary necrosis) impede HMGB1 discharge in cells undergoing ICD[88,271]. The immune related features of HMBG1 are strongly influenced by its redox status[272,273], which may account for the observed contradictory results[274,275]. This redox modulation together with the different behaviours witnessed in various studies have hindered the way to draw out firm conclusions[264].

1.7.2.4Type I IFNs.

Secretion of type I IFNs is a common response upon infection by viral or bacterial entities and are critical in microorganism-defence responses[216]. Neoplastic cells could also engage type I IFNs secretion when succumbing to therapy-driven ICD, probably as a consequence of the release of double-stranded mitochondrial DNA that leaks out to the cytosol when cell death is triggered[276–279]. The immunostimulatory effect of type I IFNs originates from its ability to activate signal transduction pathways that culminate in CXCL10 release, a potent T cell chemotactic signal[280]. Consequently, disruption of IFNAR receptors, with blocking antibodies or through genetic interventions, reduces the efficacy of anthracycline-based chemotherapy or abolished the ability of anthracycline-killed tumour cells to vaccinate mice against a subsequent rechallenge with living cancer cells[280].

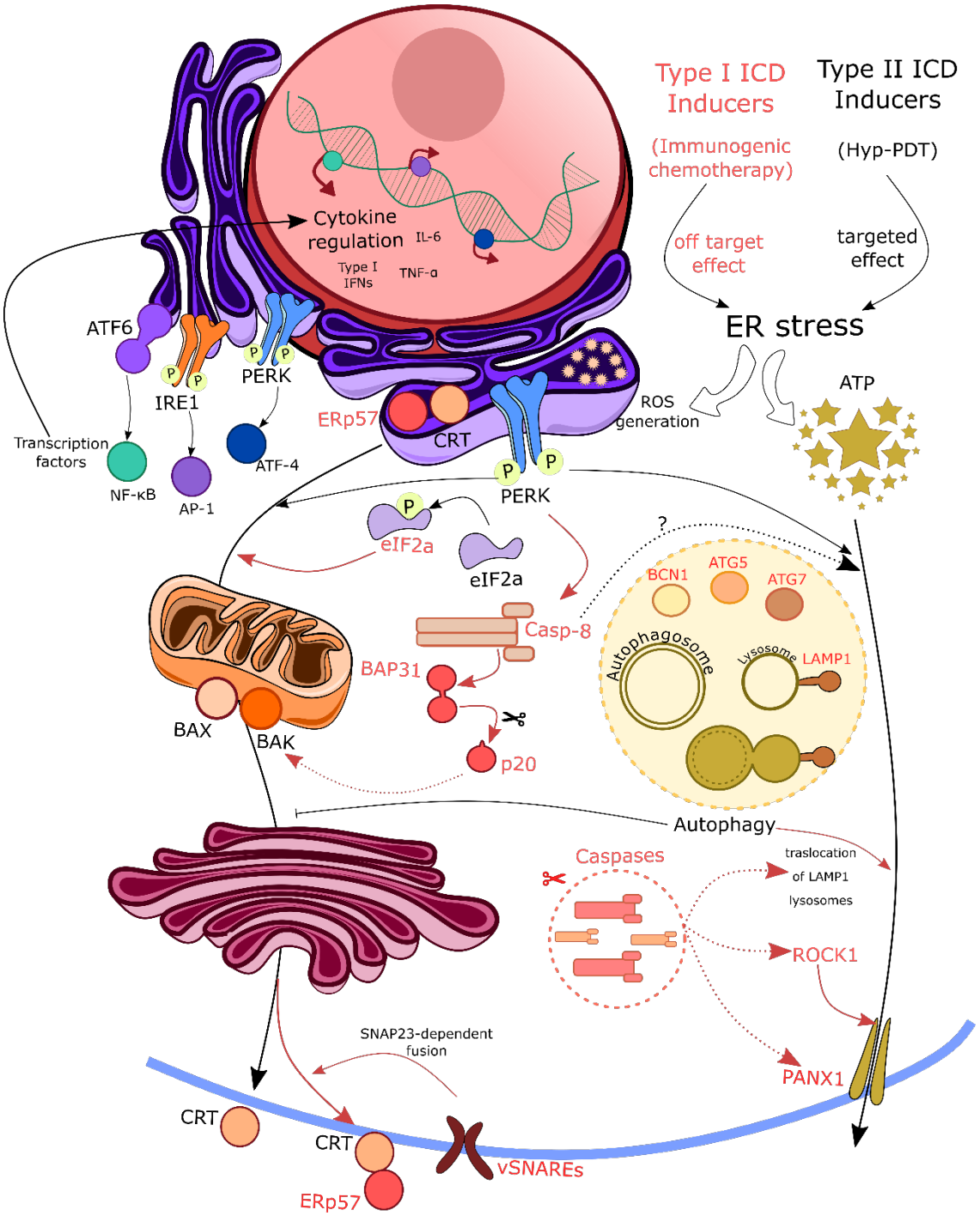

Figure 1.20 | Mechanisms of DAMPs exposure. Differential mobilization pathways can be observed between Type I and Type II ICD inducers, defined by their off-targeted or targeted effect on the ER, respectively. Exposure of CRT in the plasma membrane upon treatment with Type I ICD inducers requires an intrincate pathway with activation of the ER stress–ROS signaling mediated by the activation of the PERK, and the ensuing phosphorylation of eiF2α. This is followed by the required cleavage of B-cell receptor-associated protein 31 (BAP31) by preapoptotic caspase-8. Bax/Bak activation is also mandatory in this process. Finally CRT relocation also requires anterograde ER-Golgi trafficking and the exocytic pathway in a SNAP23-dependent manner[255]. Along all the way from the ER to the plasma membrane, CRT is accompanied by ERp57. Upon treatment with Type II ICD inducers fewer requirements are needed, since this pathway only relies on PERK, Bax, Bak, and the secretory pathway. Regarding ATP secretion upon type II ICD inducers treatment, it follows a pathway quite similar to that of CRT, except for Bax/Bak and involving partially caspase 8. In Type I ICD inducers it is required an independent pathway mediated by autophagy as ATG5, ATG7 and BCN1 are required in ATP release. Moreover, other molecules involved in different cellular processes like lysosomal exocytosis (LAMP1), membrane blebbing (ROCK1), apoptotic machinery (caspases)

and membrane permeabilization (PANX1) have been shown to be essential in type I ICD-induced ATP externalization[263].CRT, calreticulin; eIF2a, eukaryotic initiation factor 2; ER, endoplasmic reticulum; ICD, immunogenic cancer cell death; PANX1, Pannexin 1; PERK, protein kinase R-like ER kinase; PI3K, phosphatidylinositol-4,5-bisphosphate 3-kinase; ROCK1, rho-associated, coiled-coil-containing protein kinase 1; ROS, reactive oxygen species; SNARE, SNAP (soluble N-ethylmaleimide-sensitive factor attachment protein) receptor.

1.7.3 ICD in the Clinical Setting & DAMPs as Prognostic Factors in Cancer Patients.

A growing body of evidence points to a role for the Immune System in human anticancer responses. For instance, loss of function mutations in essential DAMP-signalling components has been correlated with poor prognosis and aggressive disease in cancer patients. For example breast cancer patients bearing mutations in FPR1, TLR3, TLR4 and P2RX7 alleles displayed worse metastasis-free and overall survival rates upon adjuvant chemotherapy[281–283]. Similarly, TLR4 and FPR1 loss-of-function mutations negatively impacted on prognosis of colorectal cancer patients treated with oxaliplatin-based chemotherapy[281,282]. Noteworthy, accumulating clinical evidence is supporting the idea that DAMPs and ICD may serve as important platforms for unveiling prognostic biomarkers in cancer patients (see **Figure. 1.21**)[284]. Recently, a thorough and large-scale retrospective meta-analysis evaluated the eligibility/competence of ICD-associated components to operate as prognostic biomarkers[285].

Many studies investigating the role of CRT in the immunogenicity of cell death, either carried out *in vitro* or using *in vivo* animal models, assume the fact that CRT exposure is a consequence of the therapy itself. However, most of these studies have not considered basal surface expression of CRT on cancer cells and its potential implication on malignant transformation. Current data indicate that CRT expression is augmented in tumours compared to healthy tissue, and that CRT levels may be associated with cancer aggressiveness and disease progression[284]. Furthermore, accumulating clinical evidence is supporting the notion that CRT exposure/expression, and other DAMPs may serve as important indicators of cancer patients prognosis[284].

Different studies have shown that, depending on the cancer cell type, CRT expression could behave as a positive or negative prognostic factor for cancer patients. For example, in several solid and hematologic cancer types, increased expression of CRT correlates with a favourable clinical outcome and occasionally, with increased presence of immune populations reminiscent of an active anti-cancer immune response[284,286–292]. Conversely, in some cancer types higher CRT levels were accompanied with a poor clinical outcome[293–295]. Consistent with these results, a large metagene analysis also

revealed branched/divergent immunotranscriptome profiles that partially matched with unique cancer types, but also overlaped with a general cancer immunoprofile[285]. Additionally, other molecules involved in ICD or ER stress response such as phosphorylation of eIF2α, Hsp70, Hsp90 and BiP/GRP78 have been shown to correlate with CRT expression along with patient prognosis[286,289,296,297].

To date, clinical studies supporting cell death-associated immunogenicity in the context of ICD, are still limited and usually do not offer a clear-cut association[285,298,299]. It has been proposed that these studies are complicated by several variables, including: lack of knowledge regarding the best chemotherapeutic dosing regime and schedules that would induce ICD, complications on supervising disease responses and follow-ups, scarcity of validated biomarkers, variations in cancer types and disease stages, among others[285,298,299]. In 2017, Garg and colleagues reviewed the outcome and efficacy of ICD inducers in the clinical practice also in the context of immunological biomarkers[220]. Also, a large study conducted over 1,798 mammary tumour specimens from breast cancer patients under adjuvant chemotherapy, showed for that expression of parameters associated with ICD (like autophagy or HMGB1) have a positive impact on patient's survival[300]. Furthermore, studies that focused on CRT analysis also revealed a positive correlation between increased CRT expression and patient's response to chemotherapeutics categorized as ICD inducers[290,292]. Less encouraging results in the interplay between chemotherapy, ICD markers and patient's response were reported by other authors. For example, Aoto *et al.*, manifested that although patients under neo-adjuvant therapy displayed an increased CRT and HMGB1 expression, no correlation with patient's survival or response to therapy were found[301]. Studies in NSCLC or AML patients, manifested increased and heterogeneous ecto-CRT levels in basal conditions, that is, in absence of chemotherapy. This situation also correlated with improved immunosurveillance and superior relapse-free and overall survival[284,287,289]. However, as noted this increment in DAMP signalling was chemotherapy-independent. During oncogenic transformation cancer cells are imbued in lots of different types of cellular stress and insults. Consequently, ER stress response could be activated culminating in CRT translocation and danger signalling with the ensuing anticancer immune response. Interestingly, in some cases, cancer patients displaying low CRT expression are resistant to therapy[292]. Conceivably, reduced CRT levels may be due to a defective ER stress response either oncogenic- or chemotherapy-driven. The use of ER stressors that restore ER stress response, would sensitize cancer cells by revitalising danger signalling and prompting cancer immunosurveillance.

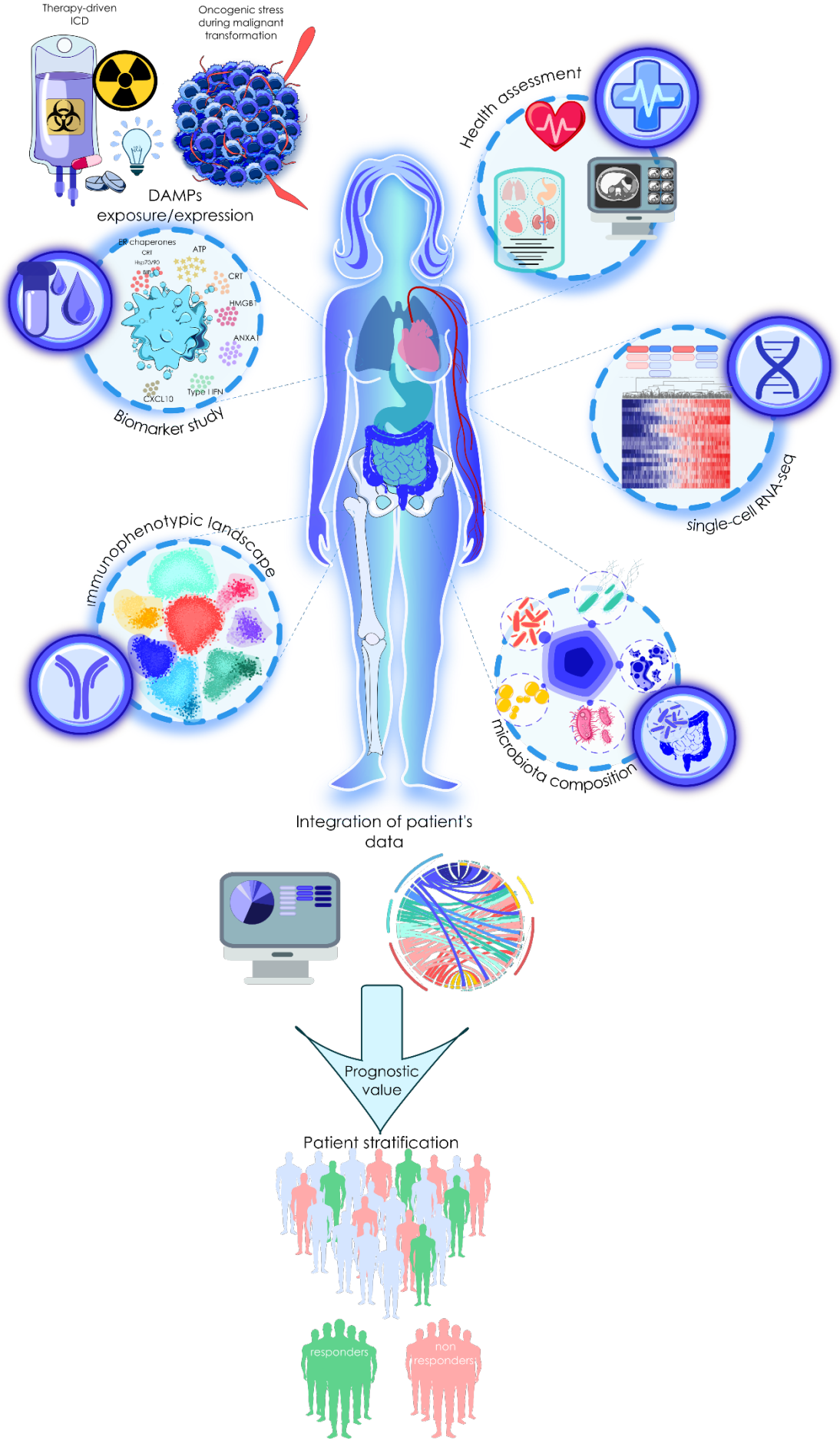
Therapy-driven ICD
Oncogenic stress during malignant transformation
DAMPs exposure/expression
Health assessment
ER chaperones
CRT
Hsp70/90
BiP
ATP
CRT
HMGB1
ANXA1
CXCL10
Type I IFN
Biomarker study
single-cell RNA-seq
immunophenotypic landscape
microbiota composition
Integration of patient's data
Prognostic value
Patient stratification
responders
non responders

Figure. 1.21 | Novel prognostic biomarkers in cancer patients. Integration of different approaches that inform about patient's clinical status, gene expression profiles and mutational panoramics with single-cell RNA-seq, mass cytometry techniques that picture the entire immunophenotypic landscape of tumours or blood, microbiota diversity and composition and biomarkers studies evaluating DAMPs or markers associated with cell-intrinsic pathogen defence responses (ER stress and autophagy), will provide invaluable knowledge about disease monitoring and therapy-response. This will allow to better stratify patients and identify those suitable cancer patients that will benefit from chemo(immuno)therapeutic modalities.

Numerous clinical studies are currently focused on the role of ICD in the clinical response to chemotherapy[220,299]. Some of these are still ongoing trials or have been just completed, but results are still not available. Moreover, many clinical trials are also evaluating combinatory chemo-immunotherapy regimens[299,302] Results arising from these trials are awaited with great expectation to shed more light into this matter and hopefully this knowledge would be finally translated into long-term benefits in cancer patients.

1.7.4 ICD – ER stress connection.

As stated before, numerous studies have been carried out to decipher ICD mechanisms and large screening studies have been performed to unveil the immunogenic potential of myriads of anticancer agents[84,85,223]. All this work has converged towards a common denominator in ICD molecular pathways: ER stress and ROS generation[225,303]. Then, activation of the ER stress pathways also known as the UPR, and specially the arm commanded by PERK, is vital for the vast majority if not all the scenarios where ICD occur[225,255].

ER stress-mediated emission of DAMPs (especially CRT) seems to be an evolutionary conserved process. Similarly to mammalian cells, yeast, some unicellular parasites and even nematodes, are able to relocate the corresponding CRT orthologues into their surface under stress conditions[304,305]. In fact, although the yeast ER stress response entirely relies on IRE1[306], again PERK or in this case the functional orthologue GCN2, appeared to be involved in this process as GCN2 knockout compromised the mobilization of CNE1 (CRT in yeast) upon mitoxantrone treatment[210,304]. This underscores not only the vital role that CRT plays as a way to communicate a danger state to the outside but also emphasize the important role of PERK as a cornerstone in danger signalling.

As mentioned in previous sections, CRT exposure induced by chemotherapeutics requires ROS-based ER stress with a decisive participation of PERK-mediated phosphorylation of eIF2α[255]. Meanwhile, in hypericin-PDT induced ICD, the ER stress module is similarly required with PERK being fundamental (but not eIF2α phosphorylation), possibly through modulating proper secretory pathway functioning, in both ecto-CRT induction and ATP secretion[210,257]. Regardless of these dissimilarities, PERK abrogation through genetic maneuvers, significantly diminished (but not completely abolished) the immunogenicity of stressed cancer cells *in vivo*[255,257]. Altogether, PERK have shown to be a major player in ICD-derived emission of danger signal(s). However, depending on the driven stimulus it could be involved in CRT alone or in both ATP and CRT emission[210,225,307]. Nevertheless, context dependency determines whether PERK contribution comes from its UPR-related function[255] or through its capacity to modulate the proximal secretory pathway[257]. Additionally, other novel PERK cellular functions related to actin cytoskeleton dynamics and formation of ER-plasma membrane contact sites may also sustain DAMP trafficking during ICD[210,225,308,309].

Interestingly, although the three branches of the UPR (PERK, IRE1α and ATF6) were triggered under cardiac glycoside treatment[84], abrogation of IRE1α and ATF6 pathways through genetic interventions did not alter CRT exposure in dying cells under the influence of different types of therapies (mitoxantrone, oxaliplatin, UVC irradiation)[255]. Furthermore, tunicamycin and thapsigargin, two potent chemical ER stressors, have been shown to efficiently restore CRT relocation and/or *in vivo* immunogenicity of cis-platinum or mytomicin C, two reported non-ICD inducers[223]. Of note, it seems that ER stress alone is not sufficient to trigger CRT translocation or *in vivo* immune responses[307]. In line with this, tunicamycin and thapsigargin have been shown to be ineffective (or at least not so effective as other *bona fide* ICD inducers) in prompting ICD[223,307]. Nonetheless, in some settings thapsigargin has reflected the opposite[310].

The importance of ER stress (and not only the process itself but also the inherent kinetics and power) in ICD has been manifested in the way ICD inducers have been classified. Indeed, there are two main groups of ICD inducers: type I and type II (see **Figure. 1.22**)[225,227]. This categorization consider whether the real cause of cell death is a consequence of a direct/primary effect on the ER, or whether the cell death pathway follows a distinct itinerary and ER stress is merely a by-product of the therapy under consideration[227]. For example, some oncolytic viruses (Newcastle disease virus)[311,312], Pt(II) N-heterocyclic carbene complex[313] and hypericin-PDT[257] fall within type II ICD inducer category as they selectively target the ER provoking intense ROS-based ER stress[225,227]. Conversely, anthracyclines (type I ICD inducers) exert its cytotoxic effects

primarily on the nucleus, where they are mainly localized[236] and leave the ER stress as a secondary side-effect. Bortezomib is also considered a type I ICD inducer, because although it affects ER stress homeostasis generating a potent ER stress response[108,197,198,314] and elevation cellular ROS levels[315], its direct cellular target is the inhibition of 26S proteasome[198]. Thus, as the cellular targets of these two types of ICD inducers are different, it is conceivable that the cellular responses triggered (particularly in the ER stress context) are different both in their kinetics and potency. Consequently, this has clear implications in the quality and amount of danger signals emitted. In fact, it has been shown that hypericin-PDT (a type II ICD inducer) has a superior capacity of emitting faster, a higher number and a broader spectrum of DAMPs, compared to type I ICD inducers[225,227,257,316,317].

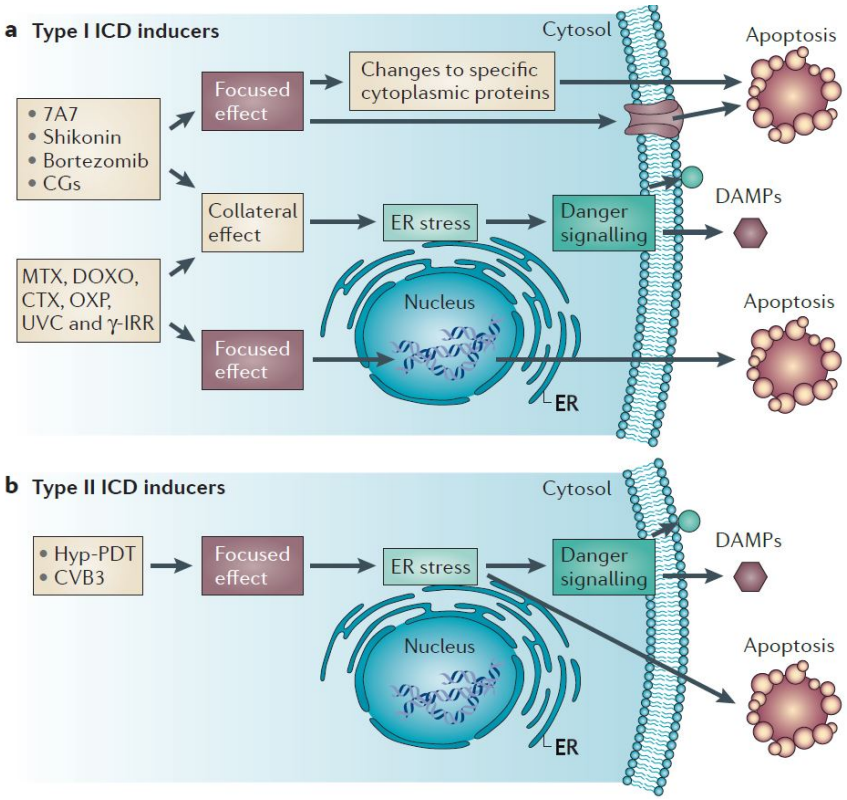

Figure. 1.22 | Classification of ICD inducers. ICD inducers are divided into type I and type II depending which is its primary cellular target. Type I ICD inducers target cellular components different from the ER and as an off-target effect they bring about an ER stress response. In contrast, the primary cellular target of type II ICD inducers is the ER and hence are supposed to instigate deeper ER stress responses and probably DAMP trafficking than type I ICD inducers. Adapted from [227]

It's important to mention that, in some regulated variants of cell demise, ROS-mediated ER stress may be dispensable for triggering ICD and the ensuing *in vivo* immune responses[225,232]. Specially, different to hypericin-PDT based and anthracycline-induced ICD, the necroptotic variant occurred in absence of apparent ER stress or PERK activation[232]. This reveals that there may be alternative mechanisms that may take part in the induction of danger signalling and further reinforces the idea that ICD induction may be stimulus and context-dependent.

ER stress could also instigate immunosuppressive effects in the tumour microenvironment. In particular, transmissible ER stress has been observed in myeloid cells incubated with tumour supernatants obtained under ER stress conditions[185,186,318,319]. Moreover, tumour cells can activate in a paracrine fashion the UPR in tumour-infiltrated myeloid cells (DCs, MDSCs) that adopt an immunosuppressive phenotype, showing an impaired antigen presenting capacity, secretion of pro-inflammatory cytokines (IL-6, TNFα, IL-23, etc), as well as other immune-restraining factors[185,320]. Supporting this notion, mice tumours exposed to thapsigargin displayed exacerbated tumour growth which correlated with an increased number and aggressive phenotype of MDSCs[321]. Collectively, all these data seem to point to the fact that low to moderate ER stress may contribute to create an immunosuppressive environment, whereas high-level ER stress, such as the one occurred in ICD, could bring about immunostimulatory responses[187].

Besides the contributions to ICD stated before, ER stress may further boost DAMP signalling abilities of stressed cancer cells through the induction of autophagy[210,263]. It is known that upon UPR activation, autophagy is activated as a defence mechanism to promote cell survival[117,163,165,322]. Moreover, as mentioned in previous sections, autophagy plays a crucial role in ATP secretion during ICD driven by chemotherapeutics[263]. For these reasons, it may seem feasible that ER stress-induced autophagy triggered by ICD inducers further contributes to the immunogenicity of dying cancer cells. However, whether autophagy is directly induced by these drugs or is just a consequence of ROS-based ER stress in the context of ICD, is a point that needs to be thoroughly explored. Nonetheless, there are at least three facts that question the involvement of ER stress-induced autophagy in ICD: 1) The extensive characterization of molecular pathways involved in autophagy-mediated ATP secretion comprise molecular mechanisms (caspases, LAMP1-dependent trafficking, PANX1 channels lysosomal exocytosis) that seem to be independent of ER stress/UPR pathways[263]. 2) In chemotherapy-induced ICD, autophagy does not regulate the emission of DAMPs which are dependent on ER stress pathways[87,255,263]. 3) Finally, ATP secretion and CRT exposure appear to follow a different time-course, since CRT mobilization has been shown to occur prior phosphatidylserine externalization, whereas ATP is expelled during the blebbing phase of apoptosis. Altogether, these considerations may point to the fact that ER stress and autophagy are two independent constituents of ICD.

Under Hyp-PDT treatment, autophagy has also been shown to be activated and to confer resistance against ROS-mediated cytotoxicity of stressed cancer cells[323,324]. One might argue that as hypericin is a direct ER sensitizer[317] (type II ICD inducer), autophagy

is triggered as a consequence of ER stress induction. Meanwhile type I ICD inducers, as ER stress is not the primary target, could induce autophagy upon interaction with other cellular targets. Furthermore, as mentioned before, the ICD pathways involved in danger signalling are not identical when triggered by type I or type II ICD inducers. Thus, contrary to chemotherapy-induced ATP secretion, in the Hyp-PDT scenario, ATP secretion is not dependent on autophagy machinery[265]. Outstandingly, autophagy was found to attenuate CRT translocation and DCs maturation as well as suppress DC-mediated proliferation of $CD4^+$ and $CD8^+$ T cells[265]. This has been rationalized as the autophagy machinery is able to get rid of oxidized proteins and organelles[265,324], which in turn would alleviate the ER retention system that becomes overwhelmed under ER stress conditions when damaged or unfolded proteins accumulate[243,325]. Hence, during Hyp-PDT treatment, ER stress and ROS production allow oxidized proteins to accumulate leaving the ER retention system saturated[323,324]. Under these conditions, autophagy inhibition increases the amount of oxidized proteins (possibly by augmenting ROS-based ER stress) and favours that ER resident chaperones such as CRT could escape from ER confinement[243,265,310]. Similarly, in a model of melanoma, in wild-type as well as in BRAF-resistant cells (which display a pronounced autophagy flux), concurrent silencing of ATG5 and treatment with a MEK-inhibitor (U0126), amplified the levels of ecto-CRT and ecto-HSP90 to a higher extent compared to those cells in which autophagy was intact[326]. Additionally, emerging mechanisms underpinning the crosstalk between the autophagic flux and the endosomal pathway could contribute to unravel the interplay of autophagy in modulation of ER-stress driven DAMP trafficking[210,327–329].

All the aforementioned has clear implications for cancer therapy. Although UPR activation is initially intended to reinstate cell homeostasis, it can also shift the cellular fate towards cell death. In this way, the UPR-dependency of tumour cells together with the connection of ER-stress and the emission of danger signals (or ER stress-ICD connection), can be harnessed to design novel therapeutic tools. These therapeutic approaches not only would reduce tumour burden (as a consequence of ER-stress associated cell death) but also improve the immunogenic capacity of dying cancer cells to elicit long-term adaptive immune responses.

1.7.5 Immunomodulatory Effects of Chemotherapy on Immune Cells.

Classically, conventional chemotherapy has been thought to reduce tumour burden by directly killing cancer cells. However, it is becoming more apparent that the clinical effect of chemotherapeutics also depends on off-target effects, especially on the Immune System [302] (see **Figure. 1.23**).

The dosing scheme has important repercussions on the final immune effect. In particular, cancer patients are currently treated with chemotherapeutics based on the maximum tolerated dose (**MTD**)[330]. With this strategy, drugs are administered at the highest achievable dose without presenting **intolerable** off-target toxicities. MTD regimen usually provoke myelosuppression, neutropenia, thrombocytopenia and lymphopenia among other side effects[331]. In particular, high dose regimens affect mainly to $CD4^+$ and $CD8^+$ T effector cells, but it can also negatively act on NK, NKT or DCs populations[330]. Hence, in these conditions anticancer immunesurveillance is impaired. That is why cytotoxic dosing schedules are followed by a resting interval of 3-4 weeks to allow hematopoietic compartment to be restored. On the other side, low dose **metronomic** chemotherapy involves a more **frequent** administration maintaining drug serum levels at **lower** concentrations to reduce their toxicity[332]. This type of schedule was originally designed to increase the anti-angiogenic effects of conventional chemotherapy[333]. However, it has been shown that metronomic chemotherapy can have a moderate effect over anticancer immune responses. In fact, several clinical trials have explored the potential of metronomic chemotherapy in combination with immunotherapy[333,334].

Besides the previously described ICD-related immunogenic effects on cancer cells, chemotherapy could also have an impact over the phenotypical and functional characteristics of immune populations in cancer patients. In particular, chemotherapeutic agents can influence the hematopoietic compartment by several ways[335]:

- *Refreshed reconstitution of immune populations after transient lymphodepletion:* The general immune depletion, usually exerted by **high-dose** chemotherapeutics may make room to a more effective reconstitution of the hematopoietic compartment[302]. In this sense, the recovered immune pools could be skewed to anticancer immune clones and enriched in memory T cells[336,337]. In haematological cancers, the evidence of fast immune recovery after chemotherapy, is an indicator of favourable outcome and less relapse frequencies[338–340]. Haematopoietic stem cell transplantation (HSCT) is a powerful

approach to confront oncohematological malignancies like leukemias, lymphomas or MM[341]. After HSCT, which usually requires HDT preconditioning regimens and post-transplant infusion of cyclophosphamide or other chemomobilization protocols, innate immune cells are the first pool to recover[342–344]. In fact, NK cell reconstitution is one of the frontline defences that mediate graft-vs-tumour effect in leukemia[345] and myeloma patients[343,344]. However, the effectiveness of cyclophosphamide in recovering these pools are under debate[346–348]. In fact, current efforts are focused on devising novel post-HSCT maintenance protocols that effectively mobilize NK cell and/or CTL anti-myeloma pools while avoiding special alloreactive cells that cause GvHD[346,347,349,350]. Similarly, in AML, although NK cells is the main population affected at diagnosis, it can be rescued within a few weeks of chemotherapy induction[351]. In solid cancers, like in breast cancer patients, it has also been reported that $CD8^+$ T cells recover at a higher pace than $CD4^+$ T cells after chemotherapy administration[352,353]. Moreover, in advanced ovarian cancer patients, recovery of adequate numbers of T cells was shown to be associated with higher time to progression rates and overall survival[354]. Altogether, high-dose chemotherapeutic regimens could be used as a platform to precondition the Immune System for immunotherapy. The therapeutic effect of immunotherapies like vaccines may be enhanced by skewing the T-cell repertoire towards tumour antigens with this approach[355].

- *Elimination or inhibition of immunosuppressive populations/mechanisms*: MDSCs and Tregs are acknowledged immune subsets with immunosuppressive functions that dampen anticancer immune responses. So far, different drugs have been shown to target these immune cells. Low-dose cyclophosphamide has shown to reduce Treg numbers and their suppressive function[356]. Metronomic cyclophosphamide also achieved a reduction in Tregs in advanced solid tumours[357] and metastatic breast cancer patients[358]. Gemcitabine has also been reported to deplete Tregs in tumor-bearing mice, as well as in cancer patients[359,360]. In the case of MDSCs, gemcitabine and 5-FU can reduce MDSCs *in vivo* in EL4 tumour model. Gemcitabine alone has also shown to reduce MDSCs frequencies in various murine cancer models[302]. Docetaxel and doxorubicin have also been revealed to reduce and shape the phenotype of the remaining MDSCs in 4T1 mammary tumour model[361,362]. Microtubular inhibitors like paclitaxel deplete MDSCs in mouse models and melanoma patients[363]. On the other hand, contrary to these anti-immunosuppressive effects, chemotherapy could also pose negative consequences to the cancer immune environment. In particular, it has also been reported that breast cancer patients display higher levels of circulating MDSCs upon doxorubicin or cyclophosphamide treatment[364]. Similarly, cyclophosphamide treatment could also drive

the expansion of MDSCs that inhibit long-term tumour control in a mouse model of lymphoma[365].

- *Exerting immunostimulatory effects on effector cells*: Chemotherapy could elicit positive direct or indirect effects over innate and adaptive effector cells. Metronomic cyclophosphamide has been shown to enhance NK effector functions in end-stage cancer patients[357]. Combination of 5-Fluorouracil (5-FU) with IFN-α also rendered increased levels of infiltrating NK cells in tumour bearing mice[366]. On the adaptive arm, different studies have underscored the positive influence that chemotherapy has demonstrated on T cell responses[335]. Cisplatin and paclitaxel administered at low doses increased $CD8^+$ T cell activation both in mouse models and cancer patients[367]. Moreover, 5-FU plus cisplatin neoadjuvant chemotherapy augmented the intratumoral infiltration of T cells in patients with esophageal squamous cell carcinoma[368]. Breast cancer patients under anthracycline or taxane-based chemotherapy showed increased amounts of immune effector cells within the tumour and this positively correlated with response and survival rates[302]. Microtubular inhibitors, such as taxanes (docetaxel and paclitaxel), or vinca alkaloids (vinorelbine) have been shown to increase circulating $CD8^+$/Treg ratios in breast and NSCLC cancer patients respectively[369]. Novel targeted therapies such as tirosin kinase inhibitors, BRAF inhibitors and others have also been shown to improve immune effector fitness in different ways[302]. For example, the tyrosin kinase inhibitor imatinib, has also been manifested to increase the frequencies of CTLs and NK cells in gastrointestinal tumours correlating with disease outcome[370]. In MM, *in vitro* or preclinical studies have suggested that lenalidomide[371,372] or bortezomib[373–375] could enhance anti-myeloma NK cell function. However, a recent longitudinal study revealed that NK cells displayed an immature phenotype and poor anti-myeloma *ex vivo* cytotoxicity upon frontline treatment (bortezomib-lenalidomide-dexamethasone). In these conditions, when lenalidomide maintenance was applied no impact on NK activity was observed[376]. Indirectly, T cell effector actions could be enhanced by activation of DCs. Direct stimulation of DCs by chemotherapeutics has also been reported[335]. Some chemotherapy regimens could induce mobilization/differentiation of DC BM precursors, increase DCs maturation signals or upregulate the cross-presentation machinery[335].

Combinatorial regimens of chemo- and immunotherapy have been proposed to proceed through two directions. One in which immunotherapy is harnessed to counterbalance the detrimental immunosuppressive effects of chemotherapy and other in which immunotherapies and chemotherapies work hand in hand to reinforce their immunostimulatory outcomes[302]. Thorough comprehension of all the chemotherapy-

driven effects on immune cells in the context of anti-cancer therapies, may assist in devising more effective combinatory interventions with current and novel immunotherapies[302].

1.7.6 Pathogen Immune-Mimicry by Anticancer Immune Responses?

Classically, the Immune System has been considered to deal with non-self invaders. For decades, immune responses were explained on the basis of **the self** (homeostatic and non-antigenic) and **non-self** (pathogen-driven and antigenic) **model**[240]. When attending this model, an immune response is only triggered when recognition of certain types of entities occurs: foreign non-self (pathogen-derived), missing self (downregulation of physiologically expressed molecules like MHC-I) or altered-self (self-antigens that due to mutations become altered and of sufficient discordance to pass immune tolerance and be recognized as foreign)[241]. However, different studies conducted at the end of the 20th century unveiled some of the limitations this model bears. In particular, the capacity of endogenous (self) entities to mount active immune responses under sterile conditions.

The **danger model** was proposed by Polly Matzinger in the late 1990's to help address these issues[218,242]. In this model, the Immune System is able to discern between threatening and homeostatic elements, whether they are endogenous or external, and mount an appropriate response[218]. Thus, besides the differentiation between the self/non-self dichotomy, other accompaining cues are required to warn the Immune System that the tissue is in danger or damaged. As said, this context is provided by danger signals. The term danger signal has been used as an umbrella term that harbour all types of molecular entities from MAMPs (or PAMPs) to DAMPs. These signals are able to bind to their cognate receptors (PRRs and other immunostimulatory receptors like LRP1, purinergic P2 receptors or formyl peptide receptor FPR1) on immune cells and inform the Immune System about an organismal insult[241].

The vast majority of danger signals bind to PRRs. For instance, the same PRRs that recognize MAMPs can at the same time bind and respond to endogenous DAMPs. For example, the same TLR4 that binds to LPS from invading pathogens, could also be triggered by endogenous HMGB1[377]. This redundancy in sensing danger has prompted some authors to raise a question that remains unresolved and that could unify the models presented above: "Could sterile-dying cells mimic immunologically the behaviour of a

pathogen-infected cell?"[241]. In fact, PRR signalling is not the unique process that infected and non-infected dying cells share in common. UPR pathways and autophagy, two modulators of ICD and DAMP signalling, are vital processes for controlling intracellular viral or bacterial invasions[216]. Defects in the autophagic machinery have shown to be detrimental in controlling viral infections[216]. Viruses and bacteria produce cellular situations that are common instigators of ER stress. Viruses require a high demand of protein synthesis to build virions and bacteria steal cellular nutrient resources and enhance ROS generation. In response, the UPR could fight viral infections by shutting down protein translation by phosphorilating eIF2α. Moreover, besides their roles in ICD, the UPR could also modulate immune responses by regulation of cytokine generation[378]. In particular, the UPR could have an impact at different levels on cytokine regulation:

- *Activation of upstream PRRs*: ER stress could activate multiple PRRs. For example, the NLRP3 inflammasome is activated through a mechanism that involves RIDD activity of IRE1, promoting IL-1β generation[379]. The RNAse activity of IRE1 has also been involved in generating small RNAs that trigger RIG-I PRRs and consequently NF-κB activation. The cytosolic sensor stimulator of interferon gene (STING), could also be activated in a UPR-dependent manner and instigate IFN production[380]. However, the complete mechanisms involved remains still elusive. Finally, the cytosolic NOD1/2 receptors UPR-dependent activation entails the interaction of these receptors with TRAF2 recruited by IRE1.

- *Activation of inflammatory signalling pathways and cytokine regulatory transcription factors*: Cytokine genes are activated by different transcription factors, being NF-kB and AP-1 the most important TFs involved in inflammatory cytokine production. In basal conditions, NF-κB is sequestered at the cytoplasm by IκB. Upon upstream signalling, IκB kinase (IKK) phosphorylates and targets IκB for proteasomal degradation. This allows NF-κB to translocate to the nucleus where it functions as a transcription factor. Once in the nucleus, NF-κB upregulates genes of inflammatory cytokines such as IL-6 and TNF-α[381]. The three UPR branches (PERK, IRE1 and ATF6) have been shown to promote NF-κB or AP-1 activation through different mechanisms[378]. For example, IRE1 activation triggers MAPK signalling cascade with the activation of p38, ERK and JNK stress kinases that promote inflammation via activation of NF-κB or AP-1 [378]. The UPR can also regulate type I IFN production. Interferon regulatory factors (IRF) are an important family of proteins that regulates type I IFN

production during innate immune responses[382]. Upon ER stress, one of its members, IRF3 dimerizes, translocates to the nucleus and modulates IFN generation[378]. Finally, the transcription factors properly activated during the UPR response (CHOP, XBP1s, ATF4) can bind to promoters of inflammatory cytokine genes such as IL-6, IL-23p19 or TNF-α, enhancing their expression[383]

These data place the UPR and ER stress as well-positioned systems to detect danger/damage and transduce these stress signals to build strong immune responses. All the above, has important implications in cancer therapy. By studying the molecular mechanisms involved in cell-intrinsic pathogen defence responses, we can exploit these same tools to increase the immunogenicity of anticancer therapies. Accordingly, anticancer therapies that evoke cell-autonomous molecular pathogen defence responses (like ER stress or autophagy) could stand as good candidates to trigger immune response against altered self-antigens (altered self-mimicry)[241]. For instance, radiotherapy or certain chemotherapies have been shown to generate self-dsRNAs that activate TLR3 or RLRs activating IFN responses enforcing antitumour immunity[241,384]. Moreover, ICD but not other forms of regulated cell death, has been associated with a pathogen response-like chemokine (PARC)-signature[385]. This chemokine signature consists in the concomitant release of CXCL1, CCL2 and CXCL10 chemokines resembling the response of host tissues to microbial infections. This response culminates with the activation of neutrophils, the first responders to foreign incursions, with the ensuing activation of the respiratory burst, killing the residual and possibly therapy-resistant cancer cells[385]. These cell-autonomous responses (ER stress, autophagy, type I IFNs and the PARC signature) are good examples of how anticancer drugs may copy bugs and this may provide novel clues on how cell-intrinsic mechanisms could be harnessed to fight cancer back (see **Figure. 1.23**).

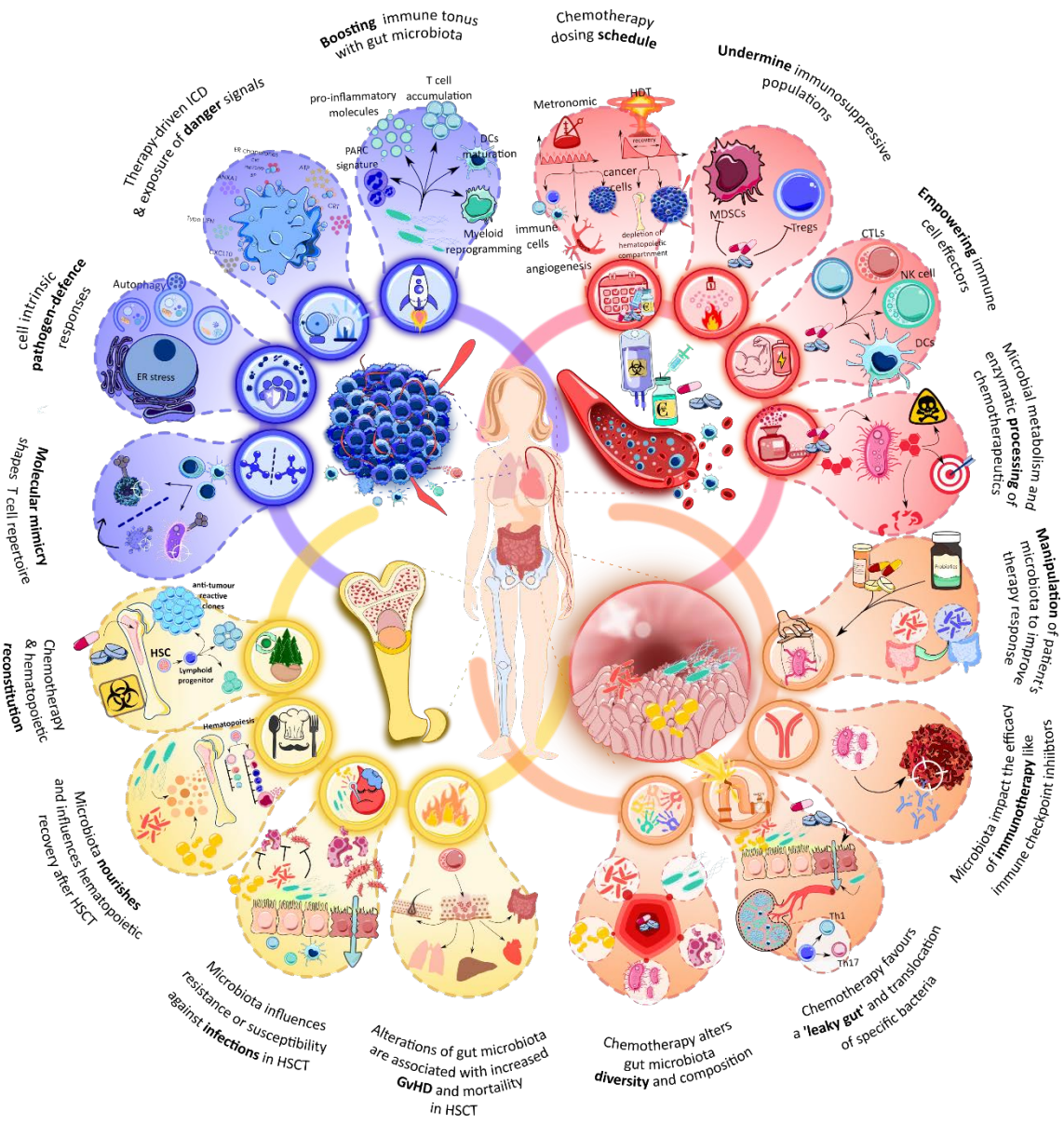

Figure. 1.23 | Integration of the different immunomodulatory modalities. ICD (Upper-left; blue) Tumor microenvironment (TME) and how the microbiota and chemotherapy affect the tumor immune response. Molecular mimicry between microbial antigens and tumor-associated antigens may allow crossreactivity and shape T cell repertoires. Cell-intrinsic pathogen-defense responses such as autophagy and ER stress can potentiate anticancer immune responses. Therapy-driven ICD leads to exposure of DAMPs and alarmins, alerting the immune system and enhancing antitumor immune responses. The gut microbiota also impacts on distant sterile tissues, boosting anticancer immunosurveillance, and can favor the secretion of proinflammatory molecules, T cell accumulation, DC maturation, myeloid reprogramming, and PARC signatures, thus promoting a strong immunoreactive TME. (Upper-right; red) Chemotherapy, microbiota, and the immune system: dosing schedule impacts on anticancer immunity. HDT regimens provoke higher tumor cell toxicity accompanied by depletion of the hematopoietic compartment. Metronomic chemotherapy involves a more frequent but less toxic scheme and may have antiangiogenic, anticancer, and immunostimulatory effects. Chemotherapy can also undermine immunosuppressive populations and empower immune cell effector function. Microbial metabolism of chemotherapeutics may potentiate desirable effects, increase toxicities, or dampen drug effectiveness. (Lower-right; orange) Gut microbiota and its relationship with (immuno)chemotherapeutic approaches. Microbiota composition can be modulated through probiotics, antibiotics, or fecal microbiota transplantation. The microbiota also affects the efficacy of immune checkpoint blockers (PD1/PD-L1 and CTLA-4). Chemotherapy can alter gut

microbiota diversity and composition, favor a leaky gut, and induce translocation of specific bacteria to secondary lymphoid organs for priming of immune cells. (Lower left; yellow) Interplay between effects on the hematopoietic compartment and the outcome of (allogeneic) HSCT. Gut microbiota composition has been associated with mortality rates and GvHD in HSCT; reintroduction of some species could provide protection. Microbiota diversity and composition influence resistance/susceptibility to infections in HSCT patients by maintaining intestinal barrier integrity and preventing eruption of 'pathobiont' and opportunistic infections. Microbiota-derived products or signals also affect hematopoietic recovery after HSCT by nourishing the hematopoietic compartment and by modulating host metabolism. Chemotherapy and HDT regimens (e.g., during HSCT) may allow more effective reconstitution of the hematopoietic compartment and select for a T cell repertoire enriched in antitumor clones. Abbreviations: CRT, calreticulin; CTL, cytotoxic T lymphocyte; DAMP, damage associated molecular pattern; DC, dendritic cell; ER, endoplasmic reticulum; GvHD, graft-versus-host disease; HDT, high-dose chemotherapy; HSC, hematopoietic stem cell; HSCT, HSC transplantation; ICD, immunogenic cell death; IFN, interferon; MDSC, myeloid-derived suppressor cell; NK, natural killer cell; PARC, pathogen response-like chemokine; PD-1/PD-L1, programmed cell death protein 1/programmed cell death protein 1 ligand; Th1/Th17, type 1/17 T helper cell; Treg, regulatory T cell.

1.8 Multiple Myeloma.

1.8.1 Disease Stages: from Asymptomatic to Overt Disease.

Multiple myeloma is a haematological malignancy that arises due to uncontrolled proliferation of abnormal **plasma cells** (PCs) in the bone marrow (BM). It accounts for 10-20% of all haematological neoplasms and 0.9% of all newly diagnosed cancer cases worldwide[386]. Currently, patients that met the following criteria are diagnosed as MM patients: presence of ≥10% of BM plasma cells (BMPC) infiltration or biopsy-proven bony or extramedullary plasmacytoma, presence of one or more signs of the **CRAB criteria** (hypercalcemia, renal insufficiency, anemia and bone lesions) and/or other myeloma-defining events (MDE) such as, serum free light-chain levels of ≥100 or presence of 1 or more focal lesions revealed by MRI[387].

MM is regularly preceded by a premalignant condition termed monoclonal gammopathy of undetermined significance (MGUS). Clinically, **MGUS** is defined based on presence of <3 g/dL of serum M-protein, less than 10% of BMPC infiltration and no manifestation of CRAB or MDE criteria[387]. Approximately, 1% of MGUS patients per year will develop and progress to overt MM. In some patients, an intermediate disease stage between MGUS and MM makes an appearance: **smoldering** multiple myeloma (**SMM**). This stage is characterized by increased levels of serum M-protein of more than 3 g/dL and/or presence of 10%-60% of BMPC infiltration, but asymptomatic for myeloma-related end organ damage. In this case, 10% of SMM patients will progress to MM within the first 5 years after diagnosis[388].

Finally, in the last stages of the disease, when MM cells lose their dependence on BM-derived survival signals, MM could grow extramedullarly and infiltrate other organs developing **extramedullary disease** (EMD) or **PC leukemia** [388]. These end-stage forms of MM are considered high-risk states and have a poor median survival of only 6-12 months from diagnosis[389]. This clinically well-defined range of premalignant phases provide an opportunity to study clonal evolution and malignant transformation of cancer and to unravel the mechanisms of progression to detect high-risk patients. Although the new sequencing technologies are providing a bulk of information, predicting disease progression from MGUS/SMM to overt MM still remains defiance[390].

1.8.2 Genetic Alterations in Multiple Myeloma.

The use of genomic techniques such as fluorescence *in situ* hybridization (FISH), copy number arrays and exome sequencing have shown that MM is not a single disease but rather, comprises a wide spectrum of molecular entities that could eventually have an impact over the clinical outcome[391]. Several genetic alterations have been proposed as driving events in the malignant transformation of myeloma cells (see **Figure. 1.24**).

Chromosomal **translocations** and **aneuploidy** (being hyperploidy the more frequent entity) are thought to be primary events in myelomagenesis[389]. During plasma cell development, class-switch recombinations and rearrangement of V(D)J locus take place. This type of rearrangements could lead to abnormal fusion of the strong *IGH* enhancer to other partner genes that can pose a selective advantage over other clones. Among the most recurrent partner genes in MGUS, SMM and MM we can found *NSD2* (or *MMSET*), *FGFR3* and *CCND1*[391]. Translocation **t(4;14)** occurs approximately in 15% of MM patients and results in *NSD2* and *FGFR3* overexpression. Translocation **t(11;14)** has an incidence of 14% in MM patients and involves overexpression of *CCND1* (Cyclin D1), important for cell cycle progression[391]. Among other less recurrent translocations found in MM patients we can highlight: **t(14;16)** and **t(14;20)** involving the oncogenes *MAF* and *MAFB* respectively found in 3% and 1.5% of the patients, and **t(6;14)** which involves *CCND3* and is found in less than 1% of MM patients[391].

As indicated before, **hyperdiploidy** is the most frequent form of aneuploidy found in MM. Patients with this genetic abnormality are characterized by bearing extra copies (trisomies or tetrasomies) of odd-numbered chromosomes (usually it involves chromosomes 3, 5, 7, 9, 11, 15, 19, 21)[388]. Tipically, patients that present hiperdiploidy are less likely to hold primary *IGH* translocations, although co-occurrence of these two types of abnormalities have been identified[391]. Other **copy number alterations** involving

whole arms or an interstitial short region of amplification or deletion are also prevalent in MM. For example, loss of the short arm of chromosome 1 (del(1p)), gain(1q), del(13q) and del(17p), among others have been observed in MM patients[389].

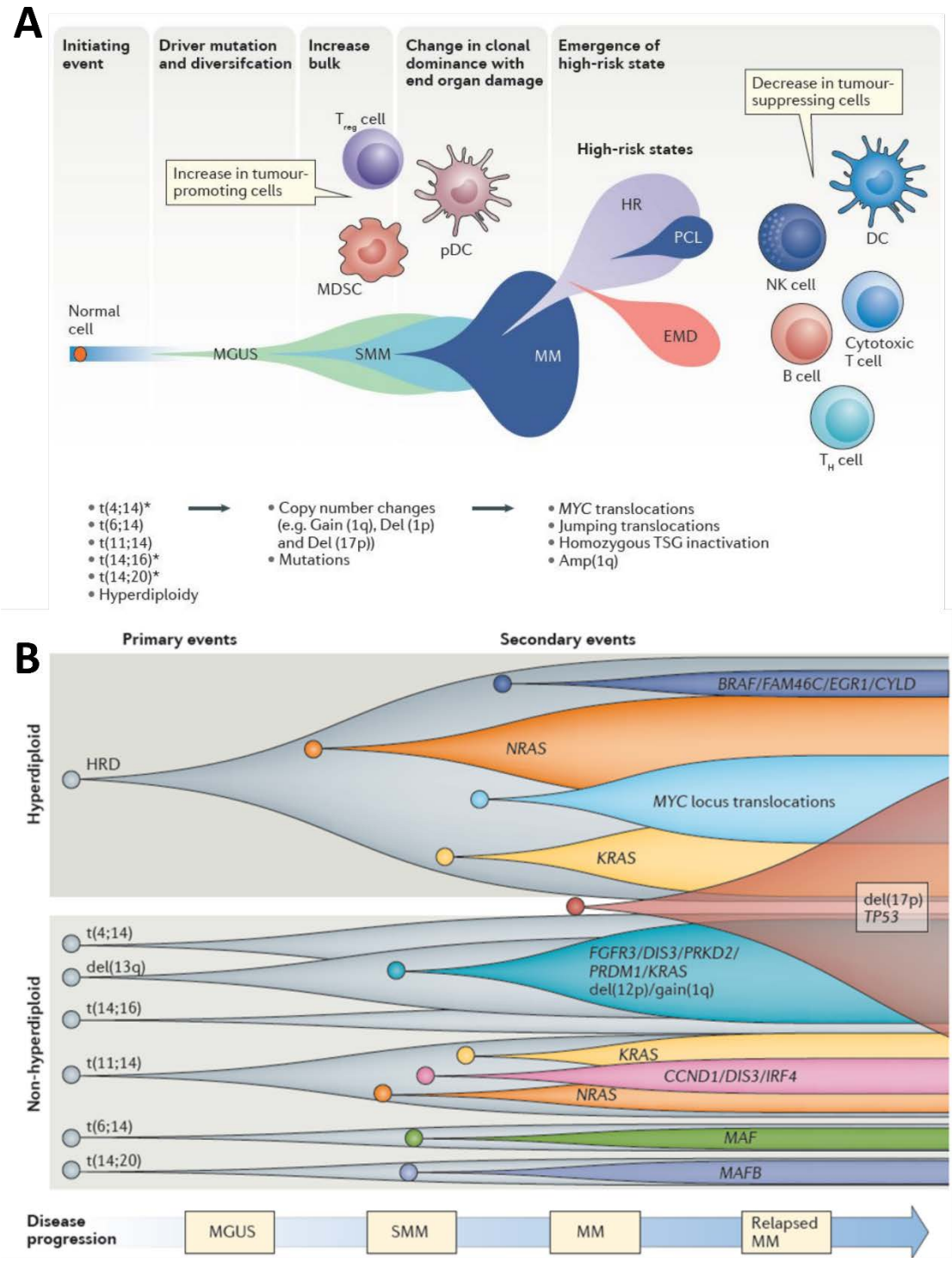

Figure. 1.24 | Stages and mutations in myelomagenesis. A. The path from a normal healthy cell and the clonal evolution through the different stages of MM disease is illustrated. **B.** Detailed description of the

co-occurring genetic alterations that drive the progression through the different disease stages. Adapted from [389,392]

Although next-generation sequencing (NGS) studies have not come up with specific driver mutations in MM, recurrent mutations have been found in subclones of malignant plasma cells. The most important and overlapping mutations found between MM patients involve *KRAS* (21-23% of cases), *NRAS*(20%), *FAM46C* (11%), *DIS3*(11-9%), *BRAF* (7%) and *TP53* (8-3%), which affect several signalling pathways including RAS-ERK, p53, NF-κB and G1/S cell cycle regulation[389,391]. MYC oncogene is an important factor that regulates up to 15% of all genes in the cell. It integrates signals from various cellular pathways and has pleiotropic effects by regulating processes like cell proliferation, apoptosis and cellular metabolism among others[393]. Importantly, MYC has been found to be deregulated in 49-67% of MM patients[391,393]. MYC deregulation in MM is primarily thought to occur through translocations, although gains/amplifications of MYC at 8q24.21 are also present in a considerable subset of newly diagnosed patients[394]. Moreover, RAS activation (mutations in *NRAS* and *KRAS* are two of the most frequently mutated genes in MM) could also increase MYC stabilization[393].

1.8.3 Prognostic Factors and Risk Stratification of Multiple Myeloma.

Several factors are currently used to evaluate the risk of progression (see **Figure. 1.25**). Most of them are based in clinical manifestations, imaging and molecular markers. Although they are still not perfectly precise, these markers help clinicians to assess and manage patient's care making the right therapeutic decisions.

- *Traditional staging systems:* **Durie-Salmon** staging system is one of the first stratification systems for MM. Here, patients are classified into different groups (I low, II intermediate and III high) attending whole-body tumour burden parameters (levels of haemoglobin, M protein, serum calcium, serum creatinine and the lytic lesions observed by x-ray imaging) followed by a subcategorization (A,B) depending on renal function[395,396]. A more simple and accurate method for evaluating MM prognosis is the international staging system (**ISS**). This system only uses serum β2-microglobulin and serum albumin (two disease-independent markers that could be altered by other factors) as MM prognostic biomarkers. In the revised form (**R-ISS**), which has become the gold-standard method to stratify symptomatic MM patients,

LDH serum levels and cytogenetics were introduced as additional prognostic markers[395,397].

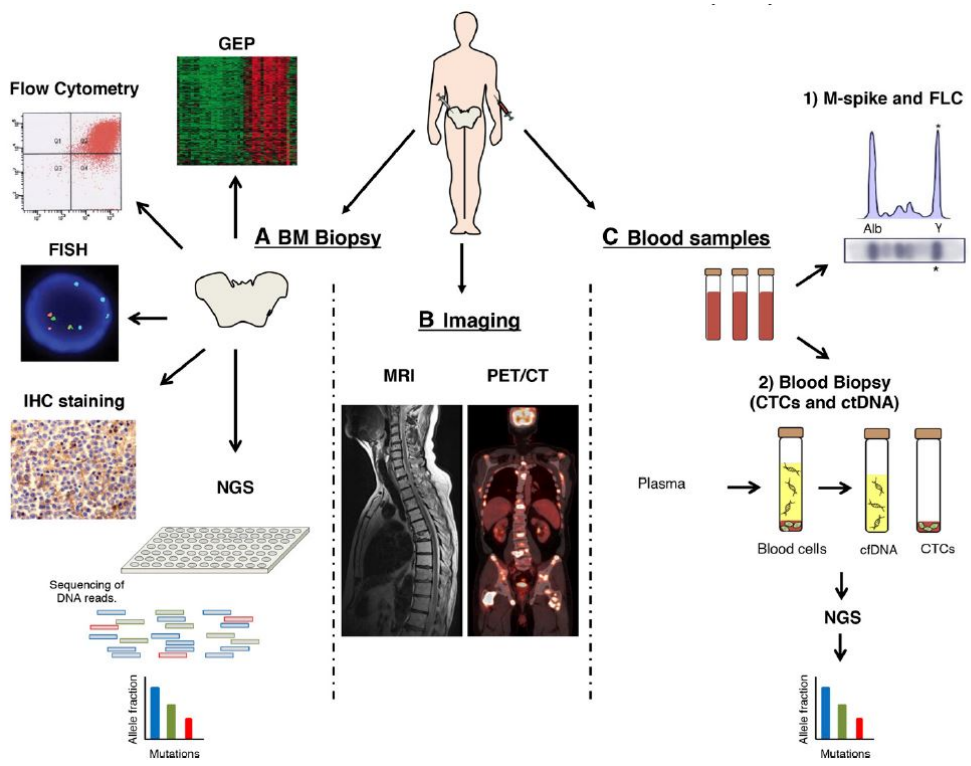

Figure. 1.25 | Landscape of prognostic biomarkers in MM. The current or more novel techniques and biomarkers used to monitor and stratify MM patients are presented. These include A. BM-biopsy derived methods: Gene expression profiling (GEP), flow cytometry, fluorescent in-situ hybrization (FISH), immunohistochemistry (IHC) staining, and next generation sequencing (NGS). B. Imaging methods (MRI and PET/CT scans). C. Blood-derived methods: circulating tumour cells (CTCs) and circulating tumour-DNA (ctDNA), in addition to conventional free-light chain ratio and M-spike in protein electrophoresis. Adapted from [395].

- *Free heavy and light chains*: Serum free light chain (FLC) has been used for years to aid in MM diagnosis and monitoring patient's responses. FLC levels and the **FLC ratio** are currently used to guide treatment regimens and define response rates. For instance, abnormal (involved/uninvolved) FLC ratio is considered one of the MDE for diagnosing MM patients[395]. This biomarker has also been proven to accurately predict high-risk SMM progression[398]. Moreover, abnormal FLC ratio has also been reported to predict survival, treatment response and early progression after ASCT in symptomatic MM patients[395,396].

- *Imaging:* MM staging is mainly dependent on biochemical, molecular, BM sampling or flow cytometry assessment. However, imaging techniques provide also valuable information about the spatial heterogeneity of the disease. Classically, radiographic x-ray findings were used as part of the Durie-Salmon staging system[397]. Novel imaging modalities (CT, **MRI**, **PET/CT** scans) with superior sensitivity, have been included in daily MM clinical practice to detect presence and number of focal lesions[395]. In fact, the number of focal lesions detected by MRI and the metabolic activity in PET/CT scans were associated with poor PFS and OS rates[396,397].

- *Cytogenetic molecular makers.* As described above, genetic alterations such as translocations, copy number alterations including hyperdiploidy and chromosome arm gains or deletions are common hallmarks of MM disease. To that end, interphase FISH has been used over the past years to detect such alterations[395]. Among the different types of aneuploidy observed in MM, patients with hypodiploidy (less than 46 chromosomes) have the worst prognosis, followed by pseudodiploidy (46 chromosomes) and hyperdiploidy (more than 50 chromosomes)[391]. In terms of translocations, t(11;14) and t(6;14) are groups with fewer probability to develop high-risk states, whereas t(4;14), t(14;16) and t(14;20) are reported to develop high-risk states more likely[389]. Sadly, this scenario is not that simple since low-risk states could become more aggressive and vice versa. Therefore, gene-gene interactions are important factors that must be taken into account. For example, isolated hyperdiploidy, which is associated with better prognosis, losses its survival benefit in combination with del(17p). On the contrary, the poor prognosis provided by t(4;14) is revoked when combined with trisomies of chromosomes 3 and 5[391]. Moreover, this cytogenetic-based risk assessment has therapy-specific implications. For instance, there are some poor prognosis alterations such as t(4;14) that can be rescued with therapies like proteasome inhibitors (PIs). Conversely, other poor prognosis translocations such as t(14;16) and t(14;20) are correlated with innate resistance to PIs[395]. Del (17p), which affects *TP53*, is also one of the genetic alterations with the worst prognosis in MM[397].

- *Novel and potential biomarkers.* Development of **NGS** technology has allowed to detect even low frequent mutations generating a mutational landscape of each patient. Moreover this kind of approach has allowed to dive deeper in the sub-clonal heterogeneity of this disease and track down the generation of high-risk states[389]. In particular, mutations in *IRF4* and *EGR1* have been reported to be positive prognostic markers whereas mutations in *TP53*, *ATM* and *ATR* DNA repair genes have been

associated with poor clinical outcome[395]. Importantly, NGS technology also opens the door for precision medicine in MM, providing the tools to identify patients that would benefit from specific therapies[390]. For example, patients with *BRAF* mutations could be treated with specific BRAF inhibitors. Nowadays **minimal residual disease (MRD)** is emerging as a reliable prognostic factor in MM[395]. Several studies have shown the superior capacity of MRD in predicting patient's response and clinical outcome compared to current traditional response criteria[395,397]. MRD negativity correlates with improved PFS and OS rates in MM patients[396]. There are several methods to assess MRD: multiparameter flow cytometry (MFC), allele-specific oligonucleotide quantitative PCR (ASO-qPCR), NGS and PET/CT scans[395,396]. However, each of these techniques has its pros and cons. Because of the patchy nature of myeloma BM infiltration and because BM biopsy is an invasive and painful procedure, **liquid biopsy** could stand as a promising alternative[395]. This approach is able to reliably reproduce the mutational landscape and clonal heterogeneity of malignant plasma cells in the BM. Liquid biopsy includes detection of circulating tumour cells (**CTCs)** or circulating tumour DNA (**ctDNA)**. Although larger studies are necessary, both parameters have proven to be effective in predicting risk of progression, therapy response and OS, as well as the capacity to reproduce the clonal architecture of the disease compared to BM matched samples[399,400].

- *Immunotherapy biomarkers.* In the last years, immunotherapy has revolutionized cancer treatment. In MM several immunotherapeutic approaches are yielding promising results in relapsed/refractory patients. However, there are still patients that do not benefit from current immunotherapeutic protocols. Thus, identifying predictive biomarkers is a challenge that would help to determine the right patients that will respond to immune-based therapy. **Mutational load** have been reported to be associated with increased survival and better response rates to checkpoint blockade therapy in melanoma[401], non-small cell lung cancer (NSCLC)[402] and mismatch repair (MMR) deficient colorectal cancer[403]. Although the mutational burden in MM is not as high as in these tumours, genomic alterations are frequent in this disease. Thus, this biomarker could be potentially informative in predicting immunotherapy responses in MM patients. However, further studies are needed to gain insight in this topic[396]. Similarly, presence of **tumour infiltrating lymphocytes** (**TILs**) has been associated with improved survival in melanoma and NSCLC patients treated with checkpoint inhibitors[404,405]. Data supporting these observations in MM are still lacking or poorly developed, hence future studies are awaited to unravel the predictive potential of TILs in MM. In checkpoint blockade

therapy, **PD-1/PD-L1** expression in immune cells or cancer cells respectively seems to be a pertinent biomarker to assess the clinical benefit. In solid tumours the predictive value of PD-1/PD-L1 expression has yielded better results, particularly in melanoma[406]. In MM, although PD-1 expression is upregulated on NK cells and T cells and myeloma cells express higher levels of PD-L1, checkpoint blockade has not rendered good results as monotherapy[395]. Other checkpoint inhibitors are also gaining relevance in cancer immunotherapy (TIM-3, LAG-3, etc). Interestingly, Huang *et al.* reported that serum levels of soluble PD-L1 were a predictive factor for the duration of response after ASCT[407]. It has been reported that some tumours rely on the expression of one or various checkpoint inhibitors to counteract anticancer immunosurveillance. Future studies are expected with great expectancy to test the predictive capacity of these novel biomarkers.

1.8.4 Bone Marrow Microenvironment & Immune Dysfunction.

The adult BM is the primary site where haematopoiesis occurs, that is, haematopoietic stem cells give rise to different type of blood/haematopoietic lineage cells (erythrocytes, megakaryocytes, platelets, monocytes, granulocytes and lymphocytes)[408]. In physiologic conditions, a wide variety of both cellular and non-cellular components such as extracellular matrix (ECM), cytokines, chemokines and growth factors, comprise the BM niche. The cellular compartment in the BM includes both non-hematopoietic and hematopoietic cells: endothelial cells, osteoclasts, osteoblasts, adipocytes, sympathetic neurons, reticular or BM stromal cells (BMSCs) or their precursor mesenchymal stems cells (MSCs), different immune cells such as B cells, T cells, NK/NKT cells, DCs, macrophages and neutrophils among others[409].

The BM microenvironment plays a vital role in the development and progression of MM (see **Figure. 1.26**). In particular, MM cells find good allies in **BM stromal cells** (BMSCs), which are important players sculpting a permissive BM microenvironment[410]. Through cell-to-cell[411] o exosome-mediated contacts[412] with MM cells, they secrete cytokines that favour the recruitment of immunosupressive populations such as Tregs and MDSCs[413,414]. Moreover, MM-BMSCs contacts also upregulate pathways supporting MM cell growth and survival[415]. This cellular interaction also triggers NF-κB signalling and IL-6 secretion, as well as increase the production of other pro-angiogenic factors by BMSCs, important for MM pathogenesis[415]. The **osteoblastic niche** is also impaired in MM patients, which accounts for the lytic bone lesions characteristic of this disease[409].

Shortly, by diverse cellular mechanisms osteoblasts numbers and activities are disrupted in favour of activated and increased bone-resorbing osteoclasts[409].

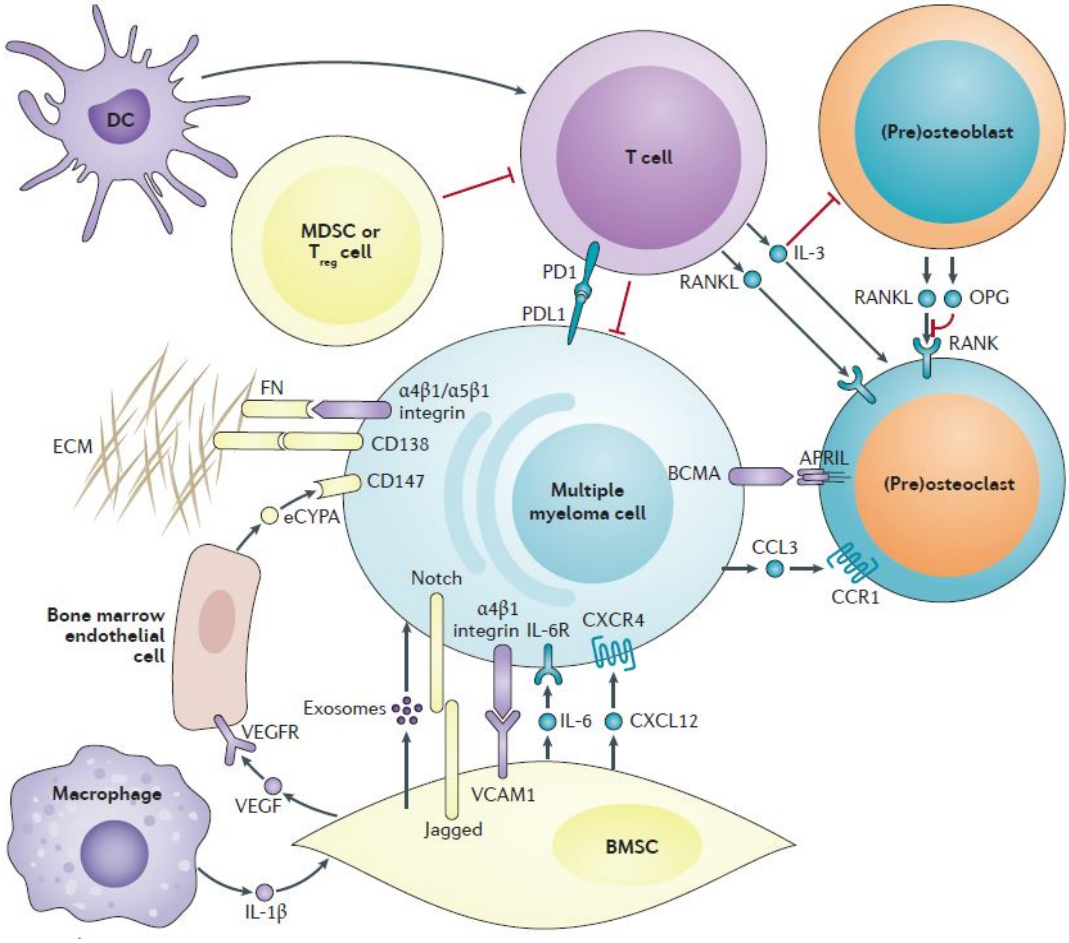

Figure. 1.26 | BM microenvironment in MM. Here are depicted the different cell populations, molecules and cellular elements that participates in the MM-associated BM microenvironment. Adapted from [416].

It is important to point out that MM is a genuine example in which the Immune System is compromised. **Deficits in antibody production** or immunoparesis due to a reduction of BM B-cell progenitors is a common feature in MM[417]. General disruption of **T cell** immune profile has also been observed. In particular, decreased $CD4^+$ T cell frequencies[418–421] and slight or even significant increase in $CD8^+$ T cells have been reported in MM patients[421,422]. Accordingly, MM patients display decreased blood and BM CD4/CD8 ratios[418–421]. For instance, $CD4^+$ lymphopenia has been associated with advanced disease and lower survival[422]. Moreover, polarization towards Th2 phenotype and increased serum levels of IL-4 and IL-10 has also been described. On the contrary, other groups support elevated Th1/Th2 ratios in blood of MM patients[408].

Regulatory T cells (Tregs) are an important type of immunosuppressive T cells with important functions in regulating immune homeostasis and tolerance. They can be identified as $CD4^+$ T cells that express high levels of CD25 and Foxp3 transcription factor, or alternatively as $CD4^+/CD25^+$ T cells with low or no expression of CD127 membrane marker. Treg immunosuppressive abilities rely on their capacity to secrete inhibitory cytokines such as IL-10 and TGF-β or just by direct contact, they counteract T cell, NK cell and APCs function[415]. Conflicting results are still found in the number of Tregs present in MM patients. Some studies reported increased PB Treg cell counts in MM patients which correlated with poor prognosis[423–425]. In contrast, others support that myeloma patients harbour reduced circulating numbers of dysfunctional Tregs[426]. Although data analysing the number of BM Tregs is scarce, studies seemed to detect no differences or even slight increases in Tregs numbers in MM patients compared to healthy volunteers[427,428].

Myeloid-derived suppressor cells (MDSCs) are also a major issue in MM, as expansion of this population usually correlates with disease progression and a negative clinical outcome[414]. They are an heterogeneous population of immunosuppressive cells derived from the myeloid lineage[429]. They can be divided in two different subsets with distinct immunosuppressive abilities: **granulocytic MDSCs** (G-MDSCs) and **monocytic MDSCs** (MO-MDSCs)[429]. MO-MDSCs are reported to suppress NK and T cell function by increasing NO production through iNOS and depleting L-arginine levels by arginase (Arg-1) and also iNOS[430]. NO suppresses T cell activity through various mechanisms (inhibition of MHC-II expression, inhibition of JAK3/STAT5 pathway and induction of T cell apoptosis) whereas L-arginine is required for T cell proliferation[429]. Meanwhile G-MDSCs mainly act by increasing ROS levels which have detrimental and suppressive functions.

Regarding the **NK cell** compartment, it has been found to be increased in peripheral blood and BM of MM patients compared to healthy donors[415]. Unexpectedly, patients with higher numbers of NK cells at diagnosis had worse prognosis[431]. However, regardless of the augmented NK cell circulation and infiltration, these cells seem to be functionally inactive[415]. For instance, reduced expression of NKG2D activation ligand as well as increased PD-1 expression, render NK cell functionally inactive in MM patients[408,415].

DCs are one of the most potent APCs required for initiating and priming adaptive immune responses. Different studies have shown that DCs accumulate at tumour sites, which usually correlates with poor prognosis[432]. They can be classified in two main

subsets: **myeloid** DCs (mDCs) and **plasmacytoid** (lymphoid) DCs (pDCs). Functionally, mDCs are thought to stimulate the differentiation to Th1 lymphocytes and Th17 cells. They are also specialized in cross-presenting exogenous antigens onto MHC-I to prime $CD8^+$ T cell responses[433]. Meanwhile, pDCs are better known for their ability to produce and secrete large amounts of type I IFNs, which influence the activation of $CD8^+$ T cells[434]. Nonetheless, they have also been associated with Th2 differentiation and to play an important role in immune tolerance[433]. In fact, elevated pDCs in the tumour microenvironment has been correlated with poor prognosis in several human cancers[433]. In MM, several studies have documented an impaired DC function, which directly impact on effective priming of T cell-mediated anticancer immune responses[408,415]. However, contradictory results have been reported regarding the alterations in DCs frequencies and phenotypes[435–437]. Nonetheless some studies have highlighted the potential role of pDCs in MM pathogenesis by conferring growth and survival signals as well as resistance to therapy in MM cells[435,438].

Finally, MM is also characterized by augmented expression of programmed cell death ligand 1 (**PD-L1**), one of the immune checkpoint inhibitory ligands that counterbalance T cell activity by binding to PD-1 on activated T cells[439,440].

Despite all the manifested efforts, the composition of the immune microenvironment in MM has yet not been fully deciphered.

1.8.5 Therapeutic Repertoire & Clinical Management of Multiple Myeloma.

Over the past two decades, treatment regimens and survival rates of myeloma patients have witnessed a radical improvement, with ASCT, IMiDs, proteasome inhibitors and monoclonal antibodies as the contributors to this advance. The initial therapy of choice has to take into consideration several factors: required (rapid) control of the disease, cease symptoms and clinical complications, allow collection of stem cells for **ASCT** eligible patients, among others. According to the clinical guidelines from the European Society of Medical Oncology (ESMO), for patients in good clinical conditions (less than 65 years or fit patients with less than 70 years old), ASCT after a previous induction with HDT is the standard **front-line treatment**[441]. Regarding the induction regimen, several combinations have been tested and the response rates have significantly improved. Nowadays, three-drug regimens are the backbone of therapy induction prior ASCT. Some of these schedules are already approved and others are under investigation

and combine bortezomib-low dose dexamethasone with a third agent: thalidomide (VTD), doxorubicin (PAD), lenalidomide (RVD) or cyclophosphamide (VCD). In Europe, VTD and VCD are the most widely used regimens. However, new combinations are currently being tested in clinical trials. After induction therapy, patient's stem cells are collected. This is followed by a preparative regimen of 200 mg/m^2 of melphalan just before ASCT.

In **transplant ineligible** patients, the first treatment options that are approved by the EMA are bortezomib-melphalan/prednisone (**VMP**) or lenalidomide plus low dose dexamethasone (**Rd**). Although not yet approved by the EMA, addition of bortezomib to Rd (**VRd**) has shown significant improvements in response rates and PFS. There are other treatment combinations that are approved by regulatory agencies but that have shown no superior benefits in terms of PFS and OS. These regimens need to be taken into consideration in case other treatment options could not be prescribed (melphalan/predisone/thalidomide (MPT) or VCD).

When this first line of treatment fails and relapse occurs, there are still available therapeutic schemes to keep fighting the disease. In case the first relapse came after an IMiD-based treatment, **PI-based doublets** with carfilzomib-dexamethasone (**Kd**) or **Vd** are indicated**. Triplet combinations** based on bortezomib are also indicated as second-line therapy: daratumumab (DaraVD) or panobinostat (PanoVD) or elotuzumab (EloVD) or VCD. In case the relapse came from a bortezomib-based line of therapy, lenalidomide-dexamethasone (Rd) or triplets with Rd as a backbone are indicated: DaraRd or KRd or IxaRd or EloRd.

As described above, the **current chemotherapeutic palette** in MM include: proteasome inhibitors (bortezomib, carfilzomib, ixazomib), immunomodulatory drugs (IMiDs, such as thalidomide, lenalidomide and pomalidomide), pan-histone deacetylase (HDAC) inhibitors (panobinostat), alkylating agents (melphalan, cyclophosphamide, bendamustine) and corticosteroids (dexamethasone and prednisone)[390].

- ***Alkylating agents and corticosteroids.*** Until the development of proteasome inhibitors and IMiDs, alkylating agents combined with corticosteroids have been the standard therapy in MM[442]. During the 1960s the application of alkylating agents and corticosteroids extended the median survival of MM patients for two years[390,391]. The application of high-dose melphalan followed by ASCT in the late 1990's, further extended the median survival to 5 years compared to HDT alone. Alkylating agents such as melphalan, cyclophosphamide and bendamustine produce DNA inter-strand crosslinking. These covalent adducts deform the DNA helix and interfere with polymerase function producing a genotoxic DNA damage response that eventually

activates apoptotic programmes[390,443]. The demonstration of the deleterious effect that high-dose corticosteroids have on MM cells, was also one of the early improvements in the treatment of MM[391]. Corticosteroids such as prednisone and dexamethasone are able to target lymphoid cells by agonizing glucocorticoid receptors (GRs). Activation of these receptors, triggers downstream signalling cascades (e.g. MAPK) or recruit coregulators that translocate to the nucleus where they modulate gene expression. This eventually could induce intrinsic apoptotic programmes and suppress proliferative and survival pathways, like for example NF-κB[390,444].

- ***IMiDs.*** The so called immunomodulatory drugs comprise different thalidomide analogues that display multiple anti-myeloma effects, including: immunomodulation, anti-angiogenic, anti-inflammatory and anti-proliferative effects. These compounds were initially developed to take advantage of their anti-angiogenic and anti-TNFα (anti-inflammatory) properties, while reducing thalidomide off-target toxicities. Preclinical studies have revealed a plethora of anti-myeloma targeting effects. For example, IMiDs downregulate adhesion molecules (via inhibition of TNFα) required in MM-BMSC contacts in both type of cells[445]. This results in a reduction of pro-survival signals that come from BMSCs. Additionally, although all IMiDs possess anti-angiogenic activities, thalidomide stands out as the one with the greatest activity. This effect is thought to occur through the regulation of chemotactic factors from BMSCs involved in endothelial cell migration (TNFα, VEGF, βFGF)[446].

As its name would suggest, IMiDs have important immune-modulatory functions. In particular, IMiDs have shown to co-stimulate previously activated $CD4^+$ and $CD8^+$ T cells towards a Th1 type response both *in vitro* and *in vivo*[447]. In addition, enhanced functions and proliferative capacity of NK and NKT cells by IMiDs have also been documented[448,449]. Importantly, different studies have shown the capacity of IMiDs to potentiate antibody-dependent cellular cytotoxicity (ADCC) in NK cells[448,449]. Moreover, IMiDs have also been shown to mediate suppression of Tregs *in vitro*[447]. Finally, above all the previous anti-myeloma effects, a unifying mechanism involving Cereblon protein (CRBN) was unravelled. Ito *et al.* identified Cereblon to be a target of thalidomide[450]. CRBN binds to and forms complex with three partners (cullin4, DDB1 and Roc1) and together compose the cullin-4 RING E3 ligase (CRL4) that has E3 ubiquitin ligase activity. Other important players in this mechanism are IKZF1 (Ikaros) and IKZF3 (Aiolos) zinc finger transcription factors.

Ikaros and Aiolos have been shown to be important in B and T cell development[451]. In addition, Aiolos has also been involved in long-lived plasma cell development[451]. IMiDs have shown to bind and stabilize CRBN, enhancing its affinity for Ikaros and Aiolos which results in their ubiquitination and posterior degradation via proteasome[442,451]. Degradation of these factors provoke alterations in gene expression such as downregulation of IRF4 and c-MYC in B cells and upregulation of IL-2 expression in T cells[442].

- ***Proteasome inhibitors***. As noted before, MM cells are extremely dependent on the UPR and the ubiquitin-proteasome system. MM cells use these pathways to cope with the stress produced not only by the altered proteostasis occurred during malignant transformation but also, in this particular case, by the MM highly secretory phenotype.

  As the name stands, PIs target and inhibit the proteasome increasing in this way the proteotoxic stress that results from accumulation of unfolded proteins and/or proteins targeted to degradation. This process eventually triggers apoptosis through activation of the UPR among other mechanisms. To date, bortezomib (Velcade) and more recently carfilzomib (Kyprolis) and ixazomib (NINLARO) have been approved for the treatment of MM. New generation PIs such as oprozomib and marizomib are under development and currently facing clinical trials. Bortezomib was the first PI approved by regulatory agencies in 2003 for the treatment of RRMM patients. However, over the years its overproven clinical efficacy has set bortezomib as a front-line treatment, often in combinatory regimens with IMiDs or corticosteroids, achieving a leading position in the standard of care in MM.

  Bortezomib is a dipeptide boronic acid that reversibly inhibits the chymotrypsin-like activity of the β5 subunit of 26S proteasome. Several anti-myeloma effects of bortezomib have been reported, including: alterations in the NF-κB activity[452], accumulation of cell cycle proteins[453], imbalance between pro- and anti-apoptotic proteins[454,455], ER stress induction[197], inhibition of MM-BMSCs interaction, as well as inhibition of IL-6 secretion by stromal cells[442,456].

  Carfilzomib is a second-generation PI that also selectively inhibits chymotrypsin-like activity of the the β5 subunit of 26S proteasome. Unlike, bortezomib and ixazomib, carfilzomib is an irreversible inhibitor due to its epoxyketone nature. This characteristic provides a more sustained/prolonged

inhibition of the proteasome, which encouraged carfilzomib to enter clinical trials and test if may overcome PI resistance[442]. In fact, carfilzomib has shown clinical efficacy in bortezomib-resistant patients and have a reduced incidence of peripheral neuropathy compared to bortezomib. Moreover, in a large phase III clinical trial which compared bortezomib plus dexamethasone (Vd) against carfilzomib plus dexamethasone (Kd), showed that carfilzomib was superior to bortezomib[457]. However, resistance to therapy is still a concern and importantly, increased cardiac adverse events have been reported in the Kd group[108,457]. Carfilzomib-induced cell death occurred through both intrinsic and extrinsic apoptotic pathways and in a caspase-dependent manner[238,458]. Activation of JNK pathway, probably downstream of the UPR, seems to be implicated in cell death[458]. In addition, Bax and in a lesser extent Bak also become activated in response to carfilzomib[238]. Currently, the possibility to use carfilzomib in other treatment regimens and other patients subgroups (newly diagnosed or after ASCT) is being explored[200].

Finally, **ixazomib** emerged as the first orally bioavailable PI that also reversibly inhibits β5 chymotrypsin-like activity of 26s proteasome. It was developed to overcome bortezomib resistance and side effects ixazomib has shown promising therapeutic activity alone and in combination with Rd. Further studies await to test ixazomib efficacy in a different number of settings.

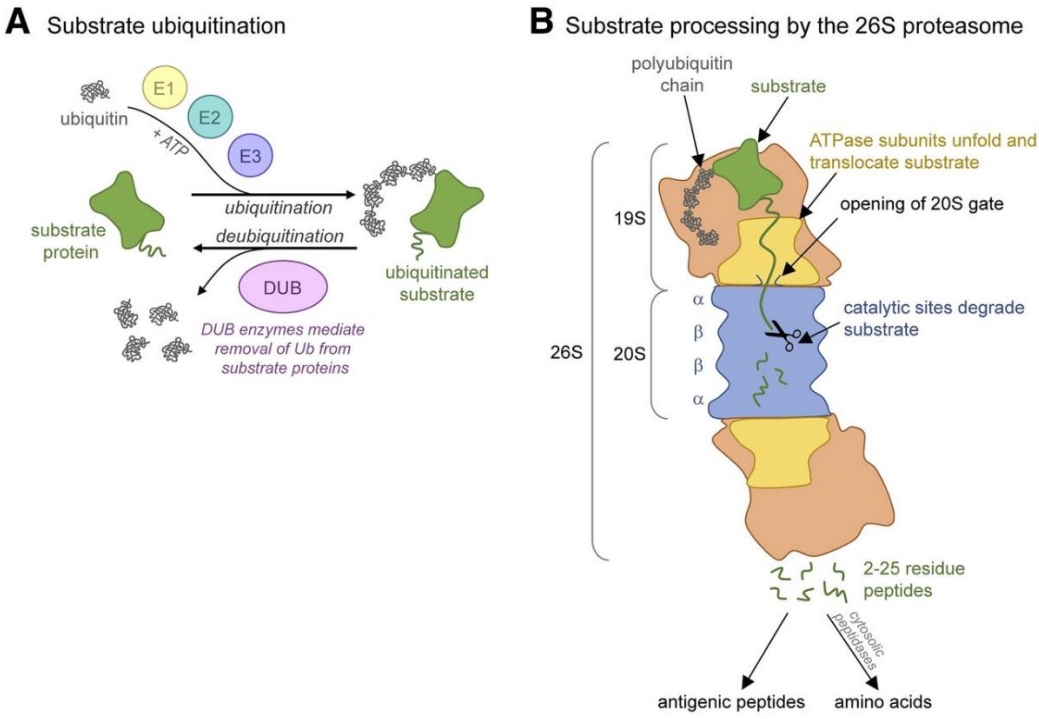

Figure. 1.27 | Structure and primary steps involved in ubiquitinated substrate processing by 26S proteasome. **A.** Schematic representation of the ubiquitination process that drives targeted proteins to proteasomal degradation. **B.** Schematic illustration of the structure of 26S proteasome with some of the most important molecular events that take place to degraded protein substrate. Adapted from [110]

- ***HDAC inhibitors.*** Histone deacetylase proteins are important regulators of gene expression[459]. By post-translationally modifying histone proteins, they regulate the accessibility of the chromatin to other cellular factors required for gene expression[460]. They can also target non-histone proteins inducing a plethora of biological effects[460]. There are a total of 11 types of human HDACs that can be divided in four classes (I, IIa, IIb, and IV), each one with a different specificity, subcellular location and enzymatic activity[459,460]. High expression of several HDACs has been associated with poor survival in MM patients. For that reason, targeting these proteins has been proposed as a good approach for MM treatment. For instance, panobinostat (pan-HDAC inhibitor) has been approved in combination with bortezomib and dexamethasone in RRMM patients[459]. Regarding the *in vitro* action mechanism of HDAC inhibitors in MM, they are thought to act by interfering with aggresomes (unfolded protein aggregates) formation. HDAC6 is a microtubule-associated deacetylase that target unfolded proteins to dynein motors for transportation into aggresomes. Therefore, panobinostat-treated MM cells fail to clear protein aggregates. Moreover, bortezomib and proteasome inhibitors induce accumulation of protein aggregates and aggresome formation, thereby acting synergistically with HDAC inhibitors[460]. This mechanism may account for the effectiveness of this approach observed in myeloma patients.

Nonetheless, although overall survival and patient outcomes have considerably improved, drug resistance is still a major concern and accounts for the fatality of the disease[195,201]. That is why novel and more efficient (immuno)therapeutic approaches may take the relief and overcome tumour recurrence.

1.8.6 Immunotherapy in Multiple Myeloma.

Despite all previous described stones in the immunotherapeutic path (**section 1.8.4**), immune-based interventions have potential to be successful in this disease (see **Figure 1.28**). Graft-vs-myeloma effect was firstly evidenced in patients subjected to ASCT or under donor lymphocyte infusions, indicating the existence of an active immune response against myelomatous cells[461]. In addition, in high-risk SMM patients, which already hold immune defects, a shift towards an activated T cell and NK compartment was observed when subjected to nine cycles of lenalidomide plus low-dose dexamethasone[462]. These data suggests that the 'cold' immunosuppressive environment present in MM could be rescued. By using the right therapeutic interventions, we can shift this 'coldness' towards a 'warmer' atmosphere where active anticancer immune responses effectively fight cancer cells. In fact, although there is still much room for improvement, current immunotherapeutic approaches are rendering positive results in relapsed and refractory patients.

Among the novel and more promising immune-based therapies that are under investigation, we can include: 1) Antibody-based therapies with daratumumab and elotuzumab as the flagships of this kind of approach, 2) Boosting the immune effector line of defence with adoptive cell therapy (ACT), either with expanded tumour-infiltrating lymphocytes (TILs), NK cells or CAR-T cells, 3) Releasing the brakes of immune response with immune-checkpoint blockade, 4) Enhancing general antitumour immunity through vaccination strategies, and finally 5) Combinatorial strategies of the aforementioned immunotherapies themselves or combined with immunogenic chemo- or radiotherapies (see Figure 1.29).

Noteworthy, all of these approaches can theoretically be benefited by ICD. Hence, the immunostimulatory potential of chemotherapeutics or other ICD-related modalities could be exploited to enhance general immunity or at least create an immune-friendly tumour microenvironment. This way, some of the drawbacks occurring in the clinical setting in some therapies could be circumvented to achieve a good immune response in cancer patients[298].

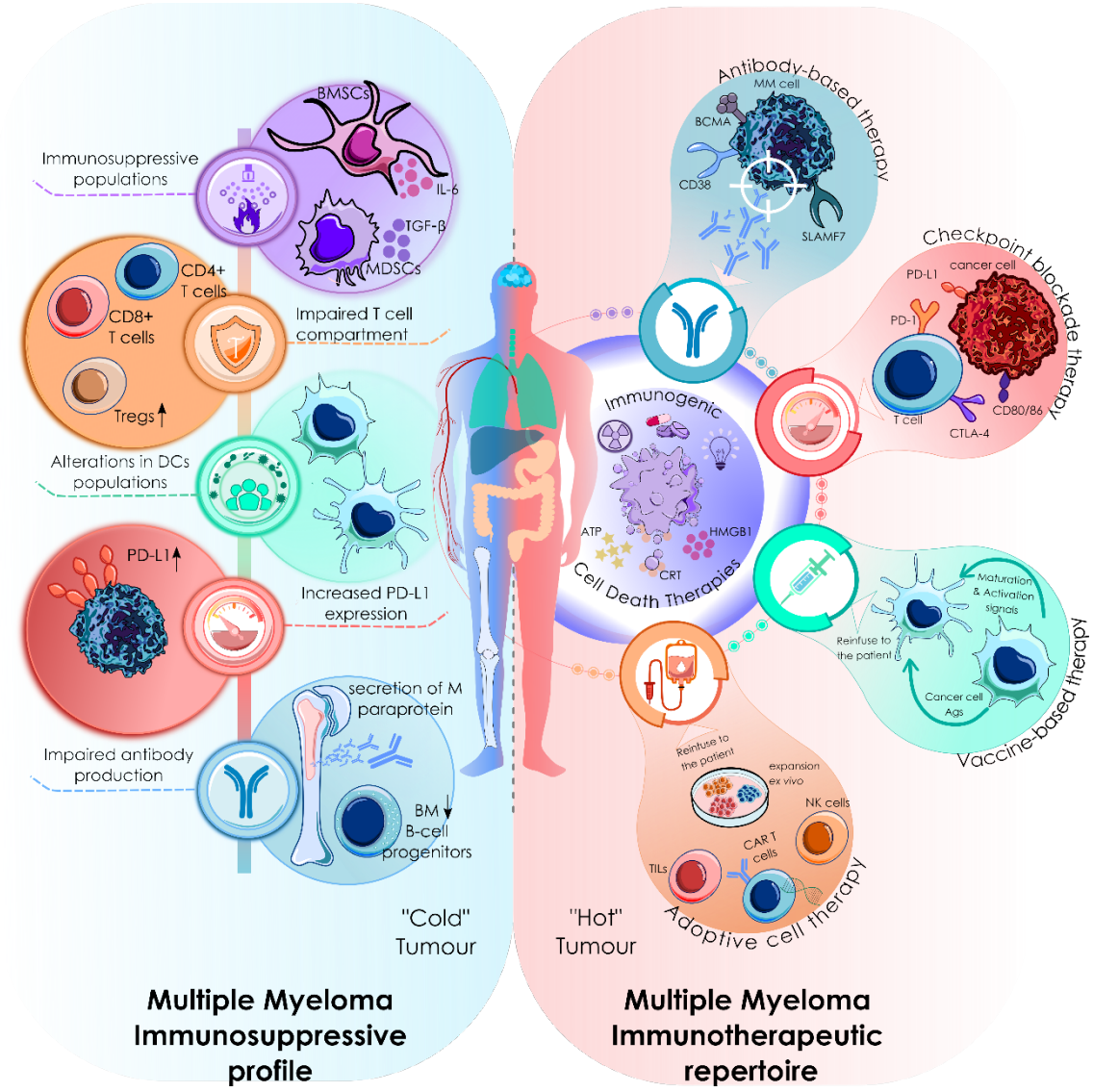

Figure 1.28 | Current clinical immunological scenario in MM. MM is a genuine example in which the Immune System is compromised. It is characterized by: 1) Deficits in antibody production due to a reduction of bone marrow (BM) B-cell progenitors. 2) General disruption of T-cell immune profile, characterized by increased numbers of regulatory T cells (Tregs), aberrant CD4/CD8 ratios and altered CD4+ T cell numbers among others. 3) Increased expression of programmed cell death ligand 1 (PD-L1), one of the immune checkpoint inhibitory ligands that counterbalance T cell activity. 4) MDSCs and BMSCs are also a major issue in MM. They are important players sculpting a permissive BM microenvironment, through cell-to-cell[411] o exosome-mediated contacts with MM cells, they secrete cytokines that favour the recruitment of immunosupressive populations such as Tregs. 5) An impaired DC function and alterations in DCs frequencies and phenotypes have been found in in MM patients. At the right are depicted the current immunotherapeutic repertoire in MM therapy with antibody-based therapies, checkpoint blockade, vaccines and adoptive cell therapies.

1.8.6.1 Antibody-based therapy.

Although monoclonal antibodies (mAbs) have been in the anticancer therapeutic armamentarium for some years, effectively treating some solid and haematological cancers, it was only a few years ago that **daratumumab** was approved for the treatment of MM. Daratumumab is a mAb that selectively targets **CD38**, an antigen highly expressed in aberrant plasma cells and at relatively low levels on normal lymphoid and myeloid cells, including normal PCs. Similarly, other anti-CD38 mAbs are currently under investigation such as isatuximab and MOR22. As single agent, daratumumab showed a promising efficacy, yielding objective response rates (ORRs) of approximately 30%, progression free survival (PFS) of 4 months and overall survival (OS) of 20 months, in relapsed and refractory MM (RRMM) patients heavily treated with at least two prior lines of therapy[463–465]. Daratumumab has been shown to kill MM cells through a plethora of mechanisms ranging from antibody-dependent cellular cytotoxicity (ADCC) mediated by NK cells, complement-mediated cytotoxicity (CDC), antibody-dependent cell phagocytosis (ADCP) mediated by macrophages and even apoptosis via direct cross-linking[466]. NK cell-mediated cytotoxicity seems to be one of the main mechanisms, and since patient NK cell profile may vary, this may account for differences in response rates among patient's cohorts[467].

Nowadays, another mAb, **elotuzumab**, has been approved in MM therapy targeting the SLAMF7 molecule expressed among normal and myeloma PCs, NK and T cells. The mechanism of action of elotuzumab is thought to differ from that of daratumumab. This thought is based on the fact that elotuzumab alone has not reached objective responses in MM patients but when combined with lenalidomide and dexamethasone, in a phase II trial and afterwards in the Eloquent-2 phase III trial, significantly improved ORRs and OS in RRMM patients[463,468].

Combination of chemotherapy with this kind of approach could render synergistic effects and improve patient's outcomes. Interestingly, IMiDs have shown to prime MM cell lines to daratumumab-induced NK cell-mediated cell death[469]. In fact, several clinical trials combining IMiDs and daratumumab have been performed obtaining good results[470]. Similarly, the efficacy of daratumumab alone was even improved with combination regimens of daratumumab plus lenalidomide and dexamethasone or daratumumab with bortezomib plus dexamethasone, significantly extending PFS period with strong and durable responses[463,471]. As carfilzomib has shown better survival curves compared to bortezomib, combinations of daratumumab plus

carfilzomib and dexamethasone are currently under phase I investigation (clinical trial NCT03158688).

Other novel and promising designs of these kind of therapy are the conjugated antibodies and the bi-specific T cell engagers (BiTEs). **Conjugated antibodies** carry in their structure cytotoxic molecules that are guided by the specificity of the antibody part and delivered directly into the target. In particular, an anti-BCMA specific antibody linked to a new class of antimitotic agent, monomethyl auristatin F, has been developed (GSK2857916) and has demonstrated in a phase I trial a 60% response rate and PFS of 7.9 months in RRMM patients with at least three prior lines of therapy including daratumumab, IMiDs and PIs[472]. Other molecules of this type with specificity for BCMA but with other cytotoxic cargoes are under development (HDP-101 and MEDI2228)[473]. Regarding the **BiTEs**, these are bispecific antibodies that hold on one side specificity for the target cancer cell epitope and on the other recognize (generally) CD3 molecules on T cells facilitating the contact between them. This way, some of the problems that arouse in the immunocompromised tumour microenvironment may be partially overcome. There are several BiTEs targeting the BCMA antigen that are currently under development (BI 836909, EM801 and JNJ-64007957) and showed positive results in preclinical models[473]. Some of these have now entered clinical trials (NCT02514239, NCT03145181, NCT03269136 and NCT03269136), we will have to wait to new updates of these and other studies to witness the efficacy of these new formulations.

1.8.6.2 Adoptive cell therapy.

Another way to confront the tumour is by directly using and improving patient's own defences (immune effector cells) to kill cancer cells with **adoptive cell therapy (ACT)**. By expanding, activating and even engineering NK or T cells outside the immunosuppressive tumour microenvironment, some of the immune barriers may be successfully, or at least partially overcome.

As mentioned earlier, graft versus myeloma effect has been observed in patients subjected to autologous stem cell transplantation (ASCT). This effect is thought to be mainly mediated by T cells, therefore this population and more specifically tumour infiltrating lymphocytes (TILs), in the case of myeloma marrow infiltrating lymphocytes (MILs), represents one of the major immune effector cells that could be used to fight MM. Although clinical data in this issue is still scarce, encouraging results have been reported by Noonan *et al.*[474], achieving at least 90% reduction of tumour burden with a

PFS of 25.1 months, hence demonstrating the feasibility and efficacy of this kind of approach.

Genetically engineered T cells stand as a novel and leading therapeutic opportunity in cancer in general and also in MM. Within this group, there are two categories: 1) **Transgenic TCRs**, with specificity towards a tumour antigen in the context of MHC molecule and 2) chimeric antigen receptor **(CAR) T cells**, which express fusion proteins composed of a single-chain variable fragment (scFv) that directs the specificity towards the cancer cell antigen, coupled to intracellular signalling modules (CD3ζ) or costimulatory molecules (CD28 or CD137/4-1BB). These two approaches have different pros and cons. TCR engineered T cells have the advantage to recognize both intracellular and surface antigens, therefore virtually any tumour antigen could be targeted. However, they are restricted to the HLA-I type limiting the patient eligibility criteria. Moreover, potential recombination with TCR α and β chains could lead to off-target toxicities due to generation of unexpected MHC-TCR-peptide complex with homology with the complex formed with tumour peptide[475]. Fatal and sudden toxicities have been observed in two patients from a trial which used transgenic TCR T cells with specificity to MAGE-A3 class I peptide, due to unwanted specificity of transgenic TCR towards the myocardial protein titin[476]. Therefore, caution in selecting the proper Ag must be taken. In myeloma, transgenic TCR T cells for NY-ESO1 peptide and its homolog LAGE are currently under clinical testing[477]. Regarding the use of CAR T cells, one of its limitations is that only surface antigens can be targeted, so the number of available targets is lower with this approach. Therefore, the success of this therapy relies on selecting the appropriate target, to selectively kill the cancer cell limiting off-target and targeted-toxicities on healthy tissue. To date CD19 CAR T cells have shown remarkable results on acute lymphoblastic leukemia, chronic lymphocytic leukemia and non-Hodgkin lymphoma[478,479]. Although there are several antigens in the anti-myeloma CAR T cell repertoire including CD19, CD138, CD38 and SLAMF7, to date BCMA CAR T cell formulation is the one that has been developed in further extent[475]. Several clinical trials have tested or are currently testing BCMA CAR T cells in heavily treated RRMM patients reporting encouraging results. In these studies, overall response rates were close to 80% or even higher and CR were achieved in an important proportion of patients[475,480].

Similarly**, NK cells** also pose as a committed ally in cancer therapy. They belong to the innate arm of the Immune System and hence, they do not rely on MHC restriction or antigen recognition, but rather they are dependent on the balance between activating and inhibitory receptors. In MM, NK cell numbers and functionality are usually altered, therefore restoration of NK cell compartment with ACT could represent a suitable

opportunity to cope with this disease. There are many therapeutic options in this field that are currently under clinical evaluation and that mainly differ in their source (umbilical cord vs. peripheral blood), in their allo-reactivity (autologous vs. allogeneic), and the expansion and stimulation protocols used to prepare and improve these cells[481]. One conclusion may be drawn out from all these studies: the superior capacity of allo-reactive NK cells to bring myeloma down. Regarding the use of **CAR NK cells** in MM, they are still under preclinical studies and have not move yet to clinical investigation.

Here chemotherapy could also improve the effectiveness of these approaches. In particular, lenalidomide has shown to improve the function and persistence of anti-myeloma CS1 CAR T cells *in vivo*[482]. Carfilzomib has also revealed activating and sensitizing activities over NK cells and MM cells respectively[483]. In addition, the combination of expanded and activated allogeneic NK cells (eNK) with therapeutic mAbs directed against tumour antigens (e.g., daratumumab in the case of MM), could give excellent results through ADCC mediated by eNK cells[484,485].

1.8.6.3 Releasing the brakes with checkpoint blockade.

The Immune System holds a complex array of mechanisms to differentiate between self and non-self and to maintain self-tolerance. During the multistep T cell activation process, besides the recognition with the T cell receptor (TCR) of the target antigen in the context of MHC/HLA molecules on APCs, costimulatory signals are required to immune activation to succeed. Engagement of CD28 on T cells with CD80/86 (also known as B7-1 and B7-2) on APCs (along with many other stimulatory interactions harboured in the immune synapse) is crucial in order to proceed with the immune response against the instigating antigen, otherwise the interaction could be perceived as 'non-strange' and develop tolerance. Similarly, returning to the homeostatic state and preventing damage of tissues by exacerbated T cell responses requires negative feedback signals that terminate the immune responses when the foreign menace has been removed from the body. To that end, **checkpoint inhibitors** are the major class of receptors that provide these attenuation signals to cope and limit the T cell response.

Multiple inhibitory checkpoints have been discovered so far: CTLA-4, PD-1, LAG-3, TIM-3, etc. Although, currently both stimulatory and inhibitory checkpoints are under investigation, the checkpoint blocking antibodies which have been clinically developed more extensively are directed against CTLA-4, PD-1 and PD-L1. **CTLA-4** is an inhibitory receptor expressed on activated T cells and binds to B7 costimulatory molecules on APCs

with higher affinity than CD28, blocking and displacing costimulatory interactions and eventually leading to abrogation of T cell activation responses. **Ipilimumab**, a blocking antibody against CTLA-4, was the first of these type of drugs clinically tested, showing important improvements in metastatic melanoma patients[486,487]. Like CTLA-4, **PD-1** is also a checkpoint inhibitory receptor expressed on activated T cells and has two known ligands, PD-L1 and PD-L2. PD-1/PD-L1 (PD-L2) signalling axis interferes with TCR signalling and contributes to T cell exhaustion. As PD-L1 / PD-L2 are widely expressed among different cell types, and their expression is known to increase under IFN-γ exposure, it is thought that this pathway is a late mechanism of protection from T cell activation and represents a physiological pathway to regulate termination of inflammatory reactions[487,488]. **PD-L1** is upregulated in tumour cells acting as a disguise mechanism that allows them to escape from T cell-mediated tumour surveillance. Moreover, PD-L1 expression has been linked with poor prognosis in a variety of human cancers[489,490]. On the other hand, probably due to the immunesuppressive character of the tumour microenvironment, TILs show higher expression of PD-1[491,492].

In MM, PD-L1 expression is upregulated on myeloma cells but not in normal plasma cells from healthy donors[440,493–495]. In fact, higher PD-L1 expression in MM cells was associated with disease progression as shown in the differences of PD-L1 expression between MGUS, MM and relapsed/refractory MM (RRMM) patients[440]. Blocking PD-1 alone with **nivolumab** has not reached good clinical objective responses with half of the patients experiencing only disease stabilization in a phase I study[463,496]. Similarly, on KEYNOTE-013 study, Ribrag and colleagues assessed the clinical efficacy of the anti-PD-1 mAb **pembrolizumab** as single agent in patients with RRMM. None of the 30 enrolled patients in the study experienced any response and the best outcome observed was again disease stabilization[497].

Although checkpoint blockade therapy alone has shown promising results in some cancer patients, this response is not universal and strongly relies on the tumour microenvironment. Thus, checkpoint blockade efficacy may also be refined by induction of more propitious immunogenic conditions in the tumour tissue through ICD. Recent preclinical studies have shown that immunogenic chemotherapy may sensitize cancer cells to checkpoint blockade leading to synergistic responses. In a lung mouse cancer model, an approved chemotherapy regimen (oxaliplatin plus cyclophosphamide) was able to foster $CD8^+$ T cell infiltration and increase $TLR4^+$ DCs in tumour tissue, which led to sensitization of tumours to immune checkpoint therapy[498]. Another study also showed that the CDK inhibitor dinaciclib was able to increase immune infiltration and activation within tumours and combination with anti-PD1 therapy resulted in enhanced anticancer

activity in three different syngeneic mouse cancer models[499]. In the clinical practice, NSCLC patients treated with combined regimens of chemotherapy (platinum-based) with different anti-PD1 agents have demonstrated considerable higher response rates and improved clinical outcome compared to that seen on single-agent modalities[500]. In patients with metastatic renal cell carcinoma, combination of anti-PD1 (nivolumab) plus pazopanib or sunitib also showed promising clinical responses[501].

In MM, preclinical data show that lenalidomide, one of the so-called immunomodulatory drugs (IMiDs), reduces the expression of PD-1 and PD-L1 in MM cells and BM accessory cells isolated from RRMM patients. Moreover, a synergistic effect between lenalidomide and anti-PD-1 or anti-PD-L1 was observed[502]. These results encouraged the rationale of using PD-1/PD-L1 blockade in combination with IMiDs in the treatment of MM. Hence, phase I and phase II clinical trials on RRMM patients who underwent at least three prior lines of therapy have been conducted[503,504]. These studies showed ORRs of 60% with even some cases of complete response. Therefore, development of phase III clinical trials were the following step to test these combination modalities[505]. Pembrolizumab plus Len and Dex (KEYNOTE-185, NTC02579863), Pembrolizumab plus Poma and Dex (KEYNOTE-183, NTC02576977) and another phase III study testing three different combination regimens (Poma and Dex vs. nivolumab, Pom and Dex vs. nivolumab, elotuzumab, Pom and Dex; CheckMate 602, NCT02726581) were developed. However, these studies were discontinued due to the increase of unprecedented deaths in the pembrolizumab group as well as lack of objective responses in the tested groups.

1.8.6.4 DC-based vaccines and its enhancement/upgrade with ICD.

Due to its particular nature, DCs are at the fine-tuned crossroads between innate and adaptive immunity, playing a pivotal role in anticancer host immune responses. Therefore, **DC-based vaccines** seem to be a good option to **re-educate** the host Immune System against myeloma, leading not only to the expansion of antitumour specific T cells, but also to long-term memory generation. In fact, since its first documented clinical use on melanoma patients in 1995[506], DC-based vaccines have gained momentum in anticancer therapy and have usually showed positive survival benefits in a diverse set of human cancers[507–510]. In the particular case of MM, DC-vaccines achieved anticancer immune responses and disease stabilization in the vast majority of patients[511,512]. In fact, in haematological cancers, a complete "resetting" of the

haematological system occurs following ASCT, leaving a huge opening to vaccination strategies to succeed[463]. However, although considerable objective clinical responses have been observed, the overall clinical outcome still has not reached the expected standards[508,513].

As mentioned earlier, due to the hostile microenvironment surrounding MM cells, DC populations are dysfunctional in MM, showing impaired T-cell stimulation capacity[408,514]. Moreover, it is said that the antigens displayed by myeloma cells are presented to DCs in absence of the appropriate costimulatory signals, driving these interactions to inadequate effector immune responses and even creating tolerance against cancer cells[514]. For these reasons, there is a consensus that DC vaccines may need to be optimized and standardized in order to enhance their clinical efficacy. There are several factors that have a direct impact on DC biology and the quality and potency of the ensuing T cell responses: route of administration and frequency of injection, delivery system, use and type of adjuvants, nature of DC vaccine formulations, and nature of tumour cell lysates/antigen cargo[463,513]. Among these, the immunogenicity of dying cancer cells used to load DCs could be easily and notably improved using ICD-inducers.

Numerous studies have proven the potential of ICD-inducers to improve the ability of DCs to stimulate effector cells and enhance anticancer T cell responses *in vivo* in different preclinical models. For example, γ-irradiation, one of the first therapies known to induce ICD, has been shown to effectively induce DCs maturation and stimulate *in vivo* CTL responses[515], as well as efficiently immunized mice against a subsequent rechallenge with live syngeneic cancer cells in various preclinical models[516]. Different ICD-related modalities such as UV light[517], oncolytic viruses[518], HHP[519], heat shock[520] among others have shown to upregulate maturation markers in DCs, as well as to prime antigen specific T-cell responses both *in vitro* and *in vivo*. Hyp-PDT, another prototypic ICD inducer, has demonstrated to trigger high quality ICD with emission of a wider spectrum of DAMPs compared to chemotherapy- or radiotherapy- ICD modalities. This ICD modality is also equally effective in inducing complete tumour regression *in vivo* both in curative and prophylactic vaccination settings[521]. DCs charged with Hyp-PDT treated cells significantly enhanced CTL responses, IFN-γ producing $CD8^+$ T cells and Th1-driven immunity in ectopic murine mammary tumours[522] as well as orthotopic glioma mice models[523].

In the clinical practice, melanoma and high-grade glioma patients have successfully been treated with DC vaccines loaded with γ-irradiated tumour cells[524]. Glioblastoma multiforme patients who underwent conventional treatment plus DC-

based therapy showed increased short-term (1-3 years) survival rates compared to control group receiving conventional therapy[524]. Relapsed Non-Hodgkin's B-cell lymphoma (NHL) patients have also benefited from DC vaccines pulsed with γ-irradiated, heat shock or UV light-treated tumour cells[291]. Accordingly, CRT and HSP90 expression levels on NHL cells positively

In MM, data regarding the use of ICD-dying cells to provide an enhanced immunogenic feed to DCs and the expected *in vivo* anticancer immune responses are still lacking. In particular lenalidomide has shown to impact DCs biology and enhance CD8+ T cell cross-priming by primed DCs[525]. Another study evaluated ICD induced by bortezomib in MM cell lines and MM primary cells, as well as the capacity of bortezomib-treated cells to increase maturation markers in DCs and to induce proliferation and polarization towards IFN-γ producing T cells *in vitro*[247]. There is currently an ongoing phase II clinical trial testing DC/MM fusion vaccines in combination with lenalidomide and GM-CSF (NCT02728102). We will need to wait for further studies to see the clinical advantages of combining this type of approaches.

SCIENTIFIC PREMISES & AIMS OF THE STUDY

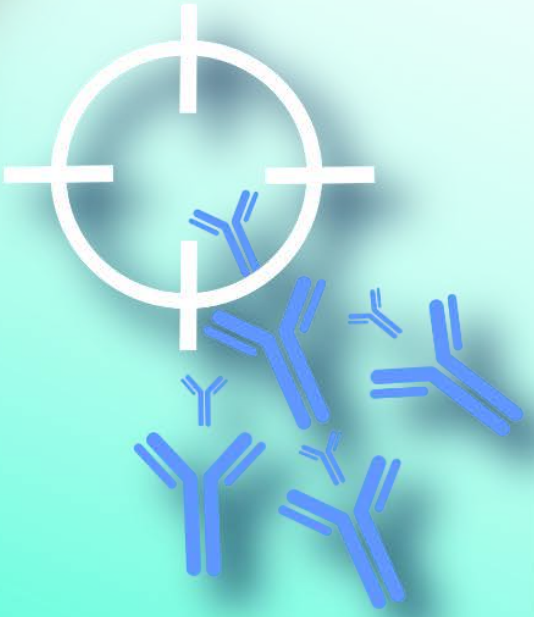

2. SCIENTIFIC PREMISES AND AIMS OF THE STUDY.

In cancer research, the study of the molecular cell death mechanisms triggered by chemotherapeutics is vital not only to understand its inherent mechanisms of action, but also to devise optimized and improved novel therapies and tackle relapse. However, since cancer cells are extremely heterogeneous and hide a reckless evolving nature, targeted-therapies have their limits and probably do not cover the whole cancer cell population. Experience gathered in the past has reflected the need to engage a system that could follow the evolutionary pace of cancer, co-evolve with it, and therefore, confer long-term protection. At this respect, during past years immunotherapy has burst into the clinic providing new hope for cancer patients. Indeed, immunological responses are thought to be behind the long-term effects of conventional or targeted-therapies. Henceforth, dealing with a complex, heterogeneous and multifaceted disease like cancer, a combined and intertwined examination of these two elements is critically required.

Throughout this work two main scientific research lines have been investigated:

- The contribution of mitotic catastrophe and its underlying intrinsic cell death mechanisms to the action of antimitotic drugs and its combination with BH3 mimetics in solid cancer cell lines.

- The immunogenicity and cell death mechanisms exerted by novel anti-myeloma drugs and its combination with potential ER stressors in MM models.

Regarding the first research line of this study, over the past years, several novel antimitotic agents have demonstrated effective antitumoral activities. Antimitotic agents generally trigger mitotic arrest, which may be accompanied by cell death through apoptosis, but also through alternative cell death mechanisms like mitotic catastrophe. However, the molecular mechanisms that connect both processes and dictate cell fate upon mitotic arrest still remain elusive. Some data point to the intrinsic mitochondrial pathway as the main player in cell death upon mitotic arrest. Bcl-2 family of proteins are key regulators of the intrinsic apoptotic pathway and hence may play a potential role in this scenario. Current literature does not shed much clarity into this matter either. For that reasons, in this work we ought to investigate the contribution of mitotic catastrophe and its intrinsic cell death mechanisms in the action of antimitotic drugs and its combination with BH3 mimetics in solid cancer cell lines. Additionally, death induced by some antimitotic agents such as docetaxel, vincristine, paclitaxel, among others have been proposed to be immunogenic. One reported possible mechanism is through the generation of polyploid cells. However, there are few reports about the immunogenicity

of these agents when the final cell fate is cell demise, especially through mitotic catastrophe, rather than polyploidization.

To that end, attending to the aforementioned scientific needs, the following objectives were proposed:

1. Elucidate the cell death mechanism triggered by antimitotic agents.
2. Study the contribution of mitotic catastrophe to the tumoricidal action of antimitotic agents.
3. Study the role of Bcl-2 family of proteins in cell death induced by mitotic catastrophe.
4. Evaluate the combination of antimitotic agents with BH3-mimetics and its anticancer therapeutic effect on tumour cell lines.
5. Examine the immunogenicity of antimitotic agents through the quantification of ICD-associated DAMPs.

As regards to the second and more extensive part of this work, over the last years a large number of both basic and clinical studies, have been devoted to immunotherapy research. The finding that some chemotherapeutic drugs to elicit an active immune response against the tumour, and also to modulate the cancer immune environment, has transformed the therapeutic scenario of oncoimmunology. However, although some patients benefit from immunotherapy and achieve long-term remissions, others fail to do so and eventually relapse. Moreover, some tumour types respond to immunotherapy much better than others. So, it is of paramount importance to readily identify those cancer patients who could benefit from immunotherapy and to develop improved (immuno)therapeutic strategies that may be strengthened by novel tools such as ICD-related processes and immunomodulatory chemotherapy.

For many years, apoptosis has been envisaged as an immune-silent process whereas necrosis or, more recently, necroptosis, has long been recognised to arouse inflammatory reactions and stir up immune-related processes. However, the emerging immunomodulatory abilities of dying/stressed cells have challenged this classical view, turning apoptosis from a tolerogenic to an immunostimulatory type of cell death under certain circumstances. For instance, anticancer immune responses probably account for the sustained remissions observed in cancer patients subjected to conventional or targeted-therapies. However, whether this influence emerges from direct effects on cancer cells through immunogenic cell death (ICD), or rather by modulating the immune-environment, needs further clarification. This paradigm shift offers clear implications in designing novel anticancer therapeutic approaches.

To date, several screening studies have been undergone to uncover the immunogenic capacity of current and novel chemotherapeutics. These studies unveiled the intrinsic potential of a diverse panel of drugs to induce danger signalling upon cell death which was translated into an *in vivo* anticancer immune response. Basic mechanistic research also evidenced that ER stress and ROS production were crucial constituents for ICD induction. Activation of ER stress pathways, and especially, PERK-mediated molecular actions have proven to be a central piece in ICD-based contexts[225]. During carcinogenesis, tumour cells have to handle severe contingencies known to unleash ER stress, constituting an important hallmark of several human cancers[117]. Of note, although primarily devised to reinstate cell homeostasis, unfolded protein response (UPR) activation can also shift cell fate towards cell demise. All these considerations have an obvious relevance in cancer therapy. Tumour cell addiction to the UPR, in conjunction with the existing interplay between ER-stress and the emission of danger signals, can be employed to devise novel and improved therapeutic protocols. From a theoretical point of view, these approaches will be intended not only to shrink tumour load, but could also engage immunostimulatory signalling of dying cancer cells to obtain long-term remissions. Accordingly, ER stress and the UPR have emerged as important targets in anticancer therapy.

Notably, in multiple myeloma (MM), a lethal plasma cell disorder, myeloma cells have an increased manufacturing capacity to generate vast amounts of immunoglobulins. Therefore, the well-being of these cells is determined, at least in part, by the survival arm of the UPR. At the same time, this feature makes myeloma cells extremely vulnerable to ER-stress insults, that can trigger cell death. Consequently, chemotherapeutic drugs such as proteasome inhibitors that target these pathways, are particularly efficient for the treatment of MM disease[200,237]. The mechanism of action of bortezomib has been studied in some detail. Although it was supposed to be similar to bortezomib, the molecular and cellular mechanisms of carfilzomib, a second generation proteasome inhibitor, have been less investigated. Previous investigations conducted by our group characterised cell death mechanisms induced by this drug in sensitive MM cell line models[238]. Nonetheless, despite its clinical usefulness, many MM patients become refractory to PI-based therapy and undergo poor survival outcomes[201]. Thereby, more effort should be devoted to improve and devise novel therapeutic approaches to tackle relapse. On this regard, autophagy is contemplated as one of the major cellular processes that can clear away misfolded cellular proteins. Moreover, under an ER stress-derived scenario, probably as part of the restorative faculties of the ER to re-establish cell homeostasis, several signals arise from the ER to trigger autophagy and help handling the overwhelming and proteotoxic situation. Therefore, co-targeting the proteasome and autophagy is envisaged to be a promising anti-myeloma therapeutic tactic. In particular, our group demonstrated the ability of chloroquine to strongly intensify cell demise upon carfilzomib treatment *in vitro* and *in vivo*[238]. Nonetheless, the detailed molecular mechanism by which this cell death exacerbation actually ensues, requires further elucidation. Since ER stress is considered to be an usual characteristic in MM disease, in

this work we sought to explore new strategies that presumably would enhance PI-induced cell death and the corresponding underlying mechanisms. Therefore, drugs that impact on ER homeostasis and engage ER stress-associated cell death pathways, such as proteasome inhibitors (currently in use in MM therapy), in combination with novel ER stressors (for instance, those targeting ERAD pathways) would be promising candidates as therapeutic agents for MM. In fact its therapeutic potential goes beyond their cytotoxic capacity, because these agents could also generate danger signals and potentially activate the Immune System.

The idea of achieving death of cancer cells with an increased immunogenic ability is of paramount importance in MM since the Immune System is particularly impaired in this haematological malignancy. In addition, despite MM disease shows a great genomic instability, its mutational burden and neoantigen load is only moderate considering main cancer types list. Nonetheless, in MM disease immunotherapeutic interventions have potential to succeed, as exemplified by the graft-vs-myeloma effect observed in ASCT or in donor lymphocyte infusions or the recent high efficacy of of daratumumab[461]. For that reason, given that ER stress holds a leading spot in modulating cell death immunogenicity, examining and testing the capacity of these approaches to trigger ICD and develop genuine protective anti-myeloma immune responses is of utmost relevance[526]. Moreover, checkpoint blockade therapy has recently been approved and has yielded promising results especially in cancer types classified as highly mutagenic, such as melanoma and lung cancer. Unfortunately, the scenario delineated so far in MM is less encouraging. Although MM patients have been shown to display increased levels of PD-L1, among other checkpoint inhibitors, clinical trials assessing checkpoint blockade in monotherapy have been rather disappointing. Combinatory regimens of checkpoint blockade therapy with other therapeutic approaches are starting to be examined in the clinic. For example, checkpoint blockade therapy and IMiDS have reached phase III clinical trials, however, unexpected increased mortality rates in the combinatory arm led to an abrupt termination of the study[505]. That is why rationalization and proper characterization of therapies themselves is critical to the success of and apply correctly these immuno-chemotherapeutic regimens.

Finally, current clinical knowledge and investigations are corroborating the initial idea that DAMP and ICD-related pathways may also provide a powerful infrastructure for revealing informative prognostic biomarkers in affected cancer patients[284,285]. For instance, current evidences manifest that tumour tissue, as opposed to normal healthy tissue, display augmented CRT expression, and that increased CRT levels may be related to development of a more aggressive phenotype and advanced disease state[284]. However, this may depend on the specific cancer cell type. In fact in the particular case of DAMPs exposure, CRT could behave as a positive or negative prognostic indicator for cancer patients. Analysis of DAMP biomaker's significance in cancer patients, will provide us significant information about the prognostic potential of these molecules, in order to better monitor and stratify cancer patients.

In conclusion, according to above-mentioned information, we have been able to formulate the following specific aims:

1. Deepen into the cell death mechanisms triggered by anti-myeloma drugs in the treatment of MM using human and murine cell lines.

2. Explore combinatory approaches to enhance anti-myeloma activity of PIs with potential ER stressors, such as CLQ or DBeQ in MM cell lines and MM primary cells isolated from BM of MM patients.

3. Examine the immunogenicity of these drugs and combinatory modalities.

    a. Determine DAMPs-associated with ICD *in vitro* in MM cell lines.

    b. Study the immunogenicity of the above drugs and combinations *in vivo* using immunocompetent orthotopic MM mouse model.

    c. Combine successful immunogenic chemotherapy-based vaccination approaches with checkpoint blockade therapy *in vivo*.

4. Determine ecto-CRT expression on BMMCs from MM patients and interrogate its relationship with the BM immune landscape and with the clinical outcome of MM patients.

    a. Examine ecto-CRT expression on the different MM disease stages.

    b. Analyse the relationship between ecto-CRT exposure and the BM immune microenvironment.

    c. Investigate the prognostic potential of ecto-CRT in MM patients.

MATERIALS & METHODS

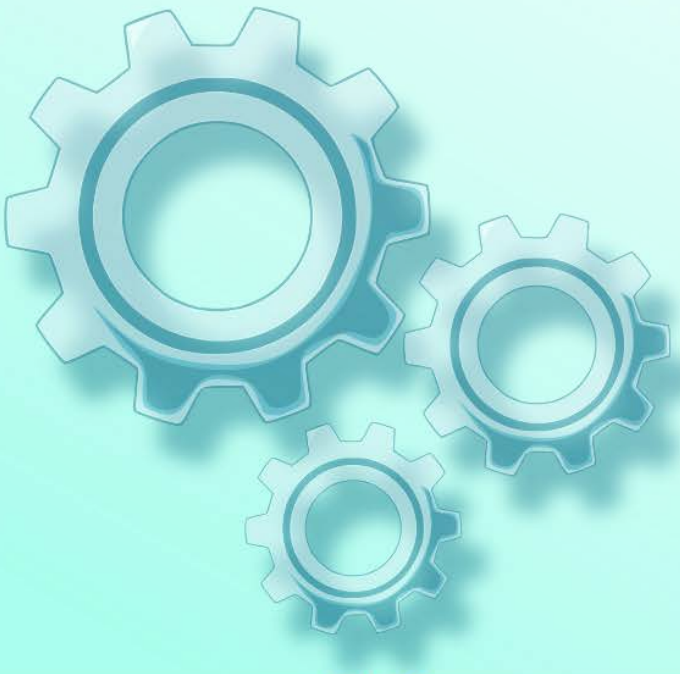

3. MATERIALS AND METHODS.

3.1. Cellular Culture.

3.1.1. Cell lines.

During this work the following cell lines have been used (**Table 3.1.**):

Cell line	Description
293T	Human embryonic kidney cells
A549	Human lung carcinoma
MIA PaCa-2 WT	Human pancreatic ductal adenocarcinoma
MIA PaCa-2 pBABE	MIA PaCa-2 cells transfected with an empty pBABE plasmid
MIA PaCa-2 Bcl-X_L	MIA PaCa-2 cells overexpressing Bcl-X_L
MIA PaCa-2 Bax KO	MIA PaCa-2 cells CRISPR knock-out for Bax
MIA PaCa-2 Bak KO	MIA PaCa-2 cells CRISPR knock-out for Bak
MIA PaCa-2 Bax/Bak DKO	MIA PaCa-2 cells CRISPR double knock-out for Bak and Bax
MIA PaCa-2 H2B-GFP	MIA PaCa-2 cells expressing H2B fused to GFP
A549 H2B-GFP	A549 cells expressing H2B fused to GFP
HCT-116 WT	Human colon carcinoma
HCT-116 Bax/Bak DKO	HCT-116 knock-out for Bax and silenced with shRNAs for Bak
U266 WT	Human MM cell line
U266 CRISPR ϕ	U266 cells transfected with an empty CRISPR control plasmid
U266 Bim KO	U266 cells knock-out for Bim
NCI-H929	Human MM cell line
MM.1S	Human MM cell line
MM.1S CRISPR ϕ	MM.1S cells transduced with an empty CRISPR control plasmid
MM.1S Bax/Bak DKO	MM.1S cells knock-out for Bax and Bak
MM.1S shATG5	MM.1S cells silenced with shRNAs for ATG5
MOPC315.BM	Murine mineral-oil induced plasmacytoma variant that homes to the BM
MOPC315.BM-Luc$^+$	MOPC315.BM cells transduced with ZsGreen-Luc plasmid

Table 3.1.| Cellular lines utilized.

293T cell line was kindly donated by Dr. Atanasio Pandiella (*Centro de Investigación del Cáncer, Salamanca*). **A549** cell line was obtained from ATCC. **MIA PaCa-2** cell line was nicely provided by Dr. Guillermo Velasco (*UCM*). **MIA PaCa-2 pBABE** was obtained previously in our laboratory by Dr. Oscar Gonzalo. **MIA PaCa-2 KO** subcellular lines (MIA PaCa-2 Bax KO; MIA PaCa-2 Bak KO; MIA PaCa-2 Bax/Bak DKO) were designed and obtained during this work using CRISPR-Cas9 technology. **HCT-116 WT** cell line was an acquisition from Dr. Christopher Börner (*Institute of Molecular Medicine and Cell Research, University of Freiburg, Germany*). **HCT-116 Bax/Bak DKO** was obtained by a former member of our laboratory Dr. Vidal Jarauta by shRNA-mediated silencing of Bak on the HCT-116 Bax KO subcellular line also provided by Dr. Christopher Börner. **MIA PaCa-2 H2B-GFP** and **A549 H2B-GFP**

were obtained by two of my mentors, Dr. Oscar Gonzalo and Dr. Isabel Marzo in this laboratory by transfecting pBABE H2B-GFP expressing vector into A549 and MIA PaCa-2 parental cell lines. MM cell lines (U266, NCI-H929 and MM.1S) were acquired from ATCC.**U266 Bim KO** cell line was designed and generated during this work with the collaboration of a younger PhD student from our laboratory (Nelia Jimenez) using CRISPR-Cas9 technology. **U266 CRISPR φ** was obtained by Nelia Jimenez by transducing U266 parental cells with an empty Lentiviral CRISPR-Cas9 empty vector. **MM.1S Bax/Bak DKO** cell line was also designed and generated during this work using CRISPR-Cas9 technology. **MM.1S CRISPR φ** was obtained by a younger PhD student, Manuel Beltrán, by transducing MM.1S parental cells with an empty Lentiviral CRISPR-Cas9 empty vector. **MM.1S shATG5** cell line was obtained by shRNA-mediated silencing of ATG5 in MM.1S parental cells by a former member of our laboratory Dr. Vidal Jarauta. **MOPC315.BM** cell line was kindly donated by Dr. Bjarne Bogen (*Oslo University Hospital, Oslo, Norway*). **MOPC315.BM-Luc**$^{+}$ subcellular line was obtained by transducing a lentiviral pHIV-Luc-ZsGreen expressing vector (Addgene) into MOPC315.BM parental cells.

3.1.2. Cell culture maintenance and culture conditions.

Every cell line used was routinely cultured in filtered-flasks of 25 or 75 cm^2 (TPP). Cells were maintained in a thermostatized incubator (Heraeus Cell) at 37 °C with a saturated humidified atmosphere and 5% of CO_2. When convenient, cell culture passages were performed for proper culture maintenance. At this regard, cell density and viability were determined in an optic microscope (Nikon Eclipse 50i) by using a hemocytometer and Trypan-blue vital stain. Prior to counting and assessing cell viability, adherent cell lines were detached by incubating them with Trypsin/EDTA (PAN™ Biotech) solution for approximately 5 minutes at 37 °C. After checking that adherent cells were detached, trypsin solution was inactivated by adding complete medium (with FBS). Afterwards, cells were centrifuged at 300 xg, supernatant was discarded and cells were suspended in an appropriate complete medium volume to obtain the desired cell density.

The different cell lines were maintained in complete medium. This medium was composed of a base of **DMEM** or **RPMI 1640** mediums, and supplemented with 10% fetal bovine serum (FBS, Sigma), Glutamax™ (stabilized L-glutamine 2mM, Gibco) and antibiotics (penicillin 100U/ml and streptomycin 100 µg/ml, Sigma). MIA PaCa-2, A549 and HCT-116 and each of their subcellular lines were maintained in DMEM complete medium, while MM cell lines were maintained in RPMI complete medium. The murine MM cell lines MOPC315.BM and its variants were maintained in RPMI complete supplemented with non-essential aminoacids (Sigma).

To discard unwanted mycoplasma infections that may intoxicate our results, cells were routinely tested using a PCR-based **mycoplasma detection** kit (Mycoplasma Gel

Detection Kit, Biotools), following manufacturer instructions. Upon mycoplasma detection, affected cell cultures were discarded and a new non-infected vial were thawed, or alternatively proceed to decontamination using BM Cyclin (Roche).

Cell culture manipulations were performed under **sterile conditions** and on laminar flow type II biosafety hoods (Telstar, Terrasa). Plastic and glass material was previously sterilized in an autoclave (Autester Mod 4376, Selecta) at 1.2 atm of pressure during 20-30 minutes. Any solution prepared under non-sterile conditions, was sterilized by passing them through a 0.22 µm filters (Pall).

3.1.3. Freezing and thawing procedures.

Cell lines were frozen and stored in cryovials in liquid nitrogen tanks. Each cryovial (Nunc, Germany) contained, approximately and depending on the cell line, 5-10x10^6 cells. Cells were centrifuged at 340 xg and subsequently resuspended in 1 ml solution containing complete medium or FBS with 10% DMSO (Sigma, Madrid). Vials were frozen immediately at -80 °C during at least 24h and then stored in nitrogen liquid tanks (-196°C) until posterior usage.

The inverse thawing procedure was performed as follows. Cells in cryovials were slowly and gradually thawed by adding small volumes of tempered culture medium. When completely thawed, cells were passed to a centrifuge tube with 10 ml of complete medium and centrifuged at 120 xg for 5 minutes. Supernatant was discarded and cell pellet was resuspended in 10 ml of the corresponding complete medium. Cell density and viability were assessed and after cells recovered and started to grow in exponential phase with an appropriate cell viability, cells were used for downstream applications.

3.1.4. Heat-inactivated Fetal Bovine Serum.

In experiments working with primary blood-borne cells (BM samples and mo-DCs), inactivation of complement by heat was carried out in order to avoid cell lysis by complement system. For that purpose, FBS was heated at 56 °C for 30 minutes in a humidified bath and subsequently was centrifuged at 560 xg during 15 minutes. Supernatant was collected in a new conical tube or alternatively was frozen at -20 ºC for subsequent use.

3.1.5. Isolation of mononuclear cells from peripheral blood or bone marrow samples.

Bone marrow mononuclear cells (**BMMCs**) were isolated from BM samples from patients with plasma cell dyscrasias and from controls were provided by Dr. Luis Palomera, Dr. Gemma Azaceta and Dr. Victoria de Poo (*Hematology service, Hospital Clinico Universitario Lozano Blesa, Zaragoza*) and from Dr. Isabel Izquierdo and Dr. Rosana Diez (*Hospital Universitario Miguel Servet, Zaragoza).* All samples were collected and obtained for research purposes with the informed consent from the subjects and the procedure was approved by CEICA (Comité Ético de Investigación Clínica de Aragón). Peripheral blood mononuclear cells (**PBMCs**) were isolated from buffy coats acquired in the Biobank service from 'Instituto Aragones de Ciencias de la Salud' (IACS, Zaragoza).

The isolation procedure included the following steps. First, 15ml (for BM samples) or 50ml (for buffy coats) conical tubes were previously prepared by adding 6ml and 20ml, respectively, of tempered Ficoll-Paque™ Plus (GE Healthcare). BM samples were diluted with RPMI at 1/3 (BM samples) or 1/2 (blood samples). Diluted samples were then allowed to gently flow down by the side of the tube and let them be installed on Ficoll's front taking special attention that both phases remain unmixed and surface plane is not breached. Samples were then centrifuged for 25 min at 500 xg, with the brakes OFF, since abrupt deceleration may compromise and disrupt density gradient. Upon completion of density gradient centrifugation, the upper plasma layer was removed and mononuclear cells installed at the interphase between plasma and Ficoll phases were collected and transferred to new conical tubes. Afterwards, cells were thoroughly washed 2 times with RPMI medium to eliminate Ficoll traces by centrifuging at 350 xg for 5 minutes and discarding the supernatant each time. Finally, cells were resuspended in 10 ml of RPMI (BM samples) and 50 ml of PBS (buffy coats) and cellular density and viability were assessed as previously described, to continue with downstream applications.

PBMCs were used for the generation of monocyte-derived DCs (section 3.1.7). BMMCs were utilized for studying several parameters. The sensitivity of primary MM cells to different drugs was evaluated. For that purpose, BMMCs were seeded at a cellular density of $1.0x10^6$ cells/ml in RPMI 1640 medium without antibiotics and supplemented with Glutamax™(Gibco), 10% of heat-inactivated FBS and with IL-6 (Peprotech) at 1000 U/ml. After incubating BMMCs with the different drugs for 16h, cells were incubated with anti-CD38-FITC antibodies and with annexin V-DY634 for assessing cell cytotoxicity by flow cytometry, as described in section 3.5.1. In this case, specific MM cell cytotoxicity was analysed by gating on the $CD38^+$ subset and determining the percentage of annexin V^+ cells within this population. Additionally, BM samples were immunophenotyped to evaluate the expression of different proteins on the surface of

MM cells and to characterise the immune microenvironment present in patient's samples by flow cytometry (section 3.4.1.1.2).

3.1.6. Isolation of monocytes derived from PBMCs by MACS.

For the isolation of peripheral blood monocytes in order to differentiate them and generate DCs, Magnetically Activated Cell Sorting (MACS) technique was utilized. With this method, antibody-conjugated MicroBeads are incubated with the heterogeneous population of cells to be sorted. When cell suspension is passed through a column and a magnetic field is applied, those cells that bind the antibody-labelled magnetic MicroBeads will get retained within the column and will not elute. Therefore, depending on the scientific needs, a heterogeneous cell population sample can be sorted through positive or negative selection procedures. Negative selection is applied to deplete a specific cell type. Alternatively, positive selection is the method of choice to sort out a specific cell type from the heterogeneous population.

In this work, a positive selection procedure using CD14-conjugated magnetic MicroBeads (Miltenyi Biotec) has been utilized. CD14 antigen is strongly expressed on most monocytes and macrophages, but also presents a weak expression on neutrophils and some myeloid DCs. Therefore, for the isolation of $CD14^+$ cells from buffy coats, PBMCs were first isolated by Ficoll-Hypaque™ as previously described in section 3.1.5. MACS-mediated separation of monocytes yields a purer and more homogeneous monocyte population compared to adherence method[527,528]. Additionally, monocytes isolated by magnetic separation differentiated better and generated more $CD11c^+$ mo-DCs with higher proliferative capacity, when compared to adherence method[528]. In this case CD14 microbead-based separation does not alter the generation of mo-DCs since CD14 does not have cytoplasmic domain that may signal into the cell when the antibody binds to the targeted molecule, and also because during the cytokine-induced differentiation into immature DCs, CD14 expression is downregulated[527,528].

Cell viability and density from isolated PBMCs were first determined. With this procedure approximately 20% of cells from total PBMCs, all of them $CD14^+$, were recovered. Then, the required amount of cells were collected and centrifuged at 300 xg for 5 minutes. Cell supernatant was discarded and cell pellet was resuspended in 80 µl per 10^7 of MACS buffer (PBS supplemented with 0.5% FBS and 2 mM EDTA). Afterwards, CD14-MicroBeads were added (20 µl/10^7 cells) and cell suspension was incubated for 15 minutes at 4 °C as indicated in manufacturer instructions (Miltenyi Biotec). After the incubation with the magnetic beads, cells were washed with 2 ml per 10^7 cells of MACS buffer and cells were centrifuged at 300 xg for 5 minutes. Once the supernatant was discarded, up to 10^8 cells were resuspended in 500 µl of MACS buffer to proceed through the magnetic separation. Magnetic cell sorting was performed using LS MACS columns (Miltenyi Biotec) and an EasySep MACS separator (STEMCELL Technologies) that generated the magnetic field. The column was installed in the

magnetic field created by the MACS separator and column was pre-conditioned and prepared by rinsing it with 3 ml of MACS buffer. Thereafter, cell suspension was applied onto the column and unlabelled cells run through the column. Three washing steps of 3 ml of MACS buffer each were applied to the column and the total effluent was collected to monitor afterwards the cell separation efficiency by flow cytometry. When the washing steps were completed, MACS column was removed from the magnetic field and placed onto a new conical collection tube. 5 ml of MACS buffer were then pipetted onto the column and with the help of the column plunger, buffer was firmly pushed through the column to allow magnetically-labelled cells to flush out from the column. After that, cell density and viability from isolated $CD14^+$ population were determined. Moreover, cells from total PBMC fraction, the unlabelled effluent fraction and the magnetically-labelled fraction were incubated with CD14-FITC antibodies 20 min at 4 °C for flow cytometry analysis.

3.1.7. Generation of DCs derived from peripheral blood monocytes *in vitro*.

For the *in vitro* DCs maturation assays with MM-treated cells, monocyte-derived DCs were used. These cells share common physiological, morphological and functional features with myeloid DCs[527]. For the generation of monocyte-derived DCs, isolated peripheral blood monocytes (see previous section), were resuspended at $1x10^6$ cells/ml in RPMI 1640 medium supplemented with 10% of heat-inactivated FBS, 2mM Glutamax® and without antibiotics, 250 U/ml of recombinant human IL-4 (Peprotech) and 1000 U/ml of recombinant human GM-CSF. Cells were then cultured with the cytokines in 75 cm^2 culture flasks for a total of 5 to 7 days to allow monocytes to differentiate. Every 48 hours, cells were re-stimulated with the aforementioned cytokine concentrations by changing half of the medium with fresh medium containing both cytokines. After 5-7 days of cytokine-induced differentiation, dendrites were visible under the light of a contrast-phase inverted microscope. At this time point, immature DCs were harvested and counted for downstream applications. To evaluate the efficiency of the process, cells were labelled with CD14-FITC and CD11c-APC antibodies in PBS + 5% FBS for 20 minutes at 4 °C. Immature DCs were positive for CD11c, while undifferentiated macrophages and monocytes were $CD14^+$/CD11c-negative[528].

3.2. Clinical data from patients with plasma cell dyscrasias.

To analyse the implication of CRT exposure in the clinical prognosis of patients with plasma cell dyscrasias, patients were stratified in two groups (CRT^{hi} and CRT^{lo}) based on the median value of CRT exposure in the entire population and different clinical markers were analysed within these populations. Clinical data were provided and collected by Dr. Victoria de Poo from Hospital Clínico Universitario Lozano Blesa and by Dr. Rosana Diez from Hospital Universitario Miguel Servet, after patients were notified and signed the informed consent.

Since BM biopsy is not a trivial procedure, BM control samples corresponded to individuals that may harbour any given (diagnosed or undiagnosed) pathological state that required to be subjected to a BM biopsy to discard any haematological pathology or complication. Alternatively, individuals from lymphoma staging that were monitored for disease development and relapse after treatment, were included within this cohort. In all these individuals, the BM compartment as examined histologically and by flow cytometry by the Hematology and Anatomical Pathology services from Hospital Clínico Universitario Lozano Blesa, was not compromised and consequently were deemed as 'controls'.

3.3. Mice.

For the *in vivo* experiments, as well as the *ex vivo* analysis of murine samples performed in this work, 8 week Balb/cAnNRj male or female mice were used (Janvier Labs). Mice were maintained in specific pathogen-free conditions (SPF) in the animal facility placed at "Centro de Investigación Biomédica de Aragón, (CIBA)". Mice experimentation conducted during this work was carried out according to FELASA instructions and under the approval and supervision of the Ethics Committee for Animal Research from the University of Zaragoza.

3.4. Flow cytometry analysis and determinations.

3.4.1. Protein expression analysis by flow cytometry.

Flow cytometry analysis of protein expression confers several advantages with respect to western blotting techniques. First, it allows for quantitative analysis of protein expression in the native form. Moreover, flow cytometry allows for the identification of both intracellular and external proteins, allows for the simultaneous detection of several proteins and for processing of many samples with almost instant results.

3.4.1.1. Analysis of expression of surface proteins.

Protein expression analysis by flow cytometry was performed by using two different strategies: 1) direct immunostaining using primary antibodies conjugated with different fluorochromes and directed against the target protein, or alternatively 2) by indirect immunostaining in which a primary non-conjugated antibody was incubated first with the sample, and subsequently a secondary fluorochrome-conjugated antibody was utilized for detection of cells attached to primary antibody.

For direct immunostaining, the appropriate number of cells were collected and incubated with primary fluorochrome-conjugated antibodies in PBS+5%FBS for 20-30 minutes at 4 ºC in darkness. Afterwards, cells were centrifuged 300 xg for 5 minutes and washed with PBS+5%FBS. Finally, cells were resuspended in an appropriate volume of PBS (or ABB1x in some instances) and analysed in a BD FACScalibur cytometer.

In case of indirect immunostaining, the appropriate number of cells were collected and incubated with primary antibodies in PBS+5%FBS for 30 minutes at 4 °C. Cells were then centrifuged 300 xg for 5 minutes and washed with PBS + 5% FBS. Afterwards cell pellet were incubated with fluorochrome-conjugated secondary antibody for 30 minutes at 4 °C in darkness. Cells were washed again with PBS + 5% FBS and finally resuspended in the appropriate volume of PBS for flow cytometry analysis.

3.4.1.1.1. Cell surface calreticulin and ER chaperone expression analysis by flow cytometry.

In this work several DAMPs associated with the immunogenicity of cell death have been evaluated. These DAMPs are usually molecules that perform physiological functions inside the cell, but when exposed in the cell surface or released to the extracellular milieu, acquire immunogenic properties. To that end, the translocation and ectopical expression of calreticulin, Hsp70 and BiP in the outer surface of the plasma membrane were evaluated by flow cytometry.

In case of *in vitro* experiments interrogating ICD-associated CRT exposure, $1.5x10^5$ cells were incubated with the corresponding drug treatment and conditions, as indicated for each case, for 24 hours. Afterwards, cells were collected, and washed with PBS + 5% FBS. Subsequently, cells were incubated with 1 µl of anti-calreticulin-Dylight 488 conjugated primary antibody and 1 µl of 7-AAD in 100 µl of PBS + 5% of FBS for 30 minutes at 4 °C in darkness. Cells were then washed with PBS + 5% of FBS and were finally resuspended in a total volume of at least 300 µl of PBS for flow cytometry analysis.

ICD-associated Hsp70 or BiP exposure, a similar protocol was followed like in the ecto-CRT analysis were analysed through indirect immunostaining. Therefore, $1.5x10^5$

cells were incubated with the corresponding drug treatment and conditions, as indicated for each case, for 24 hours. Then, cells were collected and rinsed with PBS + 5% FBS. Subsequently, cells were incubated with 1 µl of anti-Hsp70 or anti-BiP primary antibodies and in 100 µl of PBS + 5% of FBS for 30 minutes at 4 °C. Additionally, one control point was incubated with the corresponding isotype controls for each case incubated in the same conditions than the primary antibody. Cells were then washed with PBS + 5% of FBS and incubated with 0.25 µl of the corresponding secondary antibody conjugated with Alexa488 fluorochrome and 1 µl of 7-AAD for 30 minutes at 4 °C in the dark. Next, cells were washed with PBS + 5% FBS and were finally resuspended in a total volume of at least 300 µl of PBS for flow cytometry analysis.

When evaluating ecto-CRT exposure in BM samples, $4x10^5$ of total primary BMMCs were collected and incubated with 2 µl of anti-calreticulin-Dylight 488 conjugated primary antibody (or the corresponding isotype control), 1 µl of 7-AAD and 8 µl of CD38-APC antibody in 100 µl of PBS + 5% of FBS for 30 minutes at 4 °C in darkness. Cells were then washed with PBS+5% FBS and were finally resuspended in a 600 µl of PBS for flow cytometry analysis.

Quantification of the percentage of ecto-CRT, ecto-Hsp70 or ecto-BiP positive cells was conducted by gating on the 7-AAD negative population in case of tumour cell lines and on $CD38^+$/7-AAD negative population in BMMCs.

3.4.1.1.2. Patients BM immunophenotype.

To examine BM microenvironment and interrogate the connections and the relationship between CRT exposure with different immune markers and immune populations, flow cytometry analysis was performed to immunophenotype BM samples.

After isolating BMMCs as previously described (section 3.1.5), cells were collected and incubated with different fluorochrome-conjugated antibodies for cell surface marker analysis by flow cytometry as described in section 3.4.1.1. Different parameters were analysed. MM cells were immunophenotyped for the expression of different cell markers including CD38, CD138, CD56 and CD45 cell surface markers. For ecto-CRT analysis on $CD38^+$ BMMCs, cells were stained with anti-CRT-Dylight 488 or the corresponding isotype control, 7-AAD and anti-CD38-APC, as indicated in section 3.4.1.1.1. For PD-L1 expression on $CD38^+$ BMMCs, cells were labelled with anti-PD-L1-PE or the corresponding isotype control and anti-CD38-APC antibodies. For the analysis of Treg frequencies, CD4, CD25 and CD127 markers were analysed. In case of NK cell population determination, CD45 and CD56 markers were analysed. For the T cell repertoire, CD4, CD8 and CD3 proteins were determined. Plasmacytoid and myeloid DCs frequencies were determined by analysing lineage markers (CD14, CD19, CD20, CD3, CD56 and CD16) expression as well as CD123, HLA-DR and CD11c markers. PD-1 expression on

specific immune cells was also determined by incubating cells with anti-PD-1-FITC antibody or the corresponding isotype control and gating on the appropriate cell population of interest (NK cells, CD4 or CD8 T cells).

3.4.1.1.3. MM tumour load and immune infiltrate in mice tissues.

After obtaining single-cell suspensions from BM, spleens and EMTs from euthanized mice, as described in section 3.11. MM tumour burden, as well as the degree of infiltration of various immune populations were examined by flow cytometry. $5x10^5$ total cells from each organ were collected and incubated with the proper antibodies to analyse cell surface marker expression. For the analysis of the presence of MM cells in BM, spleen and EMTs, CD138 marker was analysed. In case of MOPC315.BM-Luc$^+$ cells, since these cells were intrinsically fluorescent due to ZsGreen reporter, CD138-APC and ZsGreen expression were analysed. PD-L1 expression was also analysed within MM cell population (Zsgreen$^+$/CD138$^+$). For the analysis of the immune infiltrate, CD4$^+$/CD3$^+$ T cells, CD8$^+$/CD3$^+$ T cells and NK cells (NK.1.1$^+$/CD45$^+$) frequencies were quantified by flow cytometry as previously indicated (section 3.4.1.1).

3.4.1.1.4. mo-DCs maturation assay.

DCs are at the crossroads of adaptive and innate immunity since they can activate adaptive T cells responses, but they can also favour pro-inflammatory innate immune responses through the secretion of a wide range of cytokines (IL-1β, IL-6, IL-12, among others). DCs are specialized and probably the most important antigen-presenting cells of the Immune System. This cell type can be divided into immature and mature DCs based on morphological and functional features. Upon recognition of foreign or neo-antigens in a damaged signalling contexture (sensed by PRRs), DCs are subjected to major morphological and functional changes to start the maturation process. During this process, DCs downregulate receptors involved in antigen capture, while upregulating proteins involved in antigen presentation: MHC-I, MHC-II and costimulatory molecules like CD80, CD86, CD40, CD83. Following maturation, DCs migrate to draining lymph nodes to present the antigen-cargo to T lymphocytes and initiate adaptive immune responses.

Therefore, to interrogate the ability of drug-treated MM cells to stimulate the maturation of immature monocyte-derived DCs, maturation assays were conducted as follows. First, MM cells were treated with different chemotherapeutics for 24 hours. After that time, MM cells were thoroughly washed to eliminate traces of the drugs. Immature mo-DCs generated as previously described (section 3.1.7), were incubated with drug-treated MM cells at different DCs:MMs ratios (1:2, 1:5 and 1:10) for 24 hours in RPMI

medium supplemented with 10% heat-inactivated FBS and 2 mM Glutamax®. Thereafter, cells were collected and stained with different fluorochrome-conjugated antibodies to examine maturation markers HLA-DR, CD80, CD86 and CD83, on $CD11c^+$ population by flow cytometry, as described in 3.4.1.1. As a positive control for DCs maturation, DCs cells were incubated with 100 ng/ml of lipopolysaccharide (LPS) for 24 hours.

3.4.1.2. Analysis of expression of intracellular proteins by flow cytometry.

During this work, the expression of different intracellular proteins was analysed by flow cytometry. For this purpose, target cells were subjected to different experimental conditions as indicated for each case. Next, cells were fixed with PFA 4% for 10 minutes at room temperature. Afterwards cells were washed with PBS and permeabilized with 0.1% saponin in PBS supplemented with 5% FBS for 25 minutes at room temperature. Immediately after, cells were incubated with the appropriate primary antibody (anti-active caspase-3 conjugated with FITC, anti-PUMA or anti-NOXA antibodies) in 100 µl of PBS + 5% FBS. Cells were then washed with PBS+ 5% FBS, centrifuged and resuspended in the appropriate volume of PBS for flow cytometry analysis in case of caspase-3 direct staining. In the case of PUMA and NOXA detection, cells were incubated with 0.25 µl of the respective Alexa-fluor 488 conjugated secondary antibody diluted in 100 µl PBS + 5% FBS for 30 minutes at 4 °C in darkness. After that, cells were thoroughly washed with PBS and resuspended in at least 300 µl of PBS for flow cytometry analysis. The control for unspecific antibody binding was performed by incubating cells with the Alexa-488-conjugated secondary antibody in case of PUMA and NOXA determination.

3.4.1.3. Evaluation of intracellular ATP levels by flow cytometry.

One of the hallmarks of ICD is the secretion by dying/stressed cells of ATP molecules to the extracellular milieu. In the extracellular space ATP molecules act as "find-me" chemotactic signals to attract APCs and stimulate their phenotypic maturation[529,530]. The most appropriate and direct method to examine the presence of ATP on the extracellular space is by an *in vitro* measurement of luciferase-activity. However, the presence of ectonucleotidases that rapidly degrade ATP in the extracellular space may hinder this analysis[531]. Moreover, since luciferin-based assay is highly sensitive, ATP can also be released and detected by mechanical stimulation of cells (washing steps, centrifugation, shear stress, compression, etc)[531]. Therefore as a first approach, a simpler assay measuring intracellular vesicular ATP levels was conducted. This assay is based on the use of quinacrine, a molecule that emits green fluorescence in presence of intracellular ATP, allowing quantifying fluorescent signal by flow cytometry.

In fact this method was utilized by other groups to monitor ATP secretion during ICD[529,530].

To analyse intracellular ATP-containing vesicles, quinacrine staining was performed as follows[529,530]. After incubating cells with the indicated drugs, cells were collected and centrifuged at 120 xg for 5 minutes and supernatant was removed. Thereafter, cells were incubated with 1 µM quinacrine in Krebs-Ringer solution (125 mM NaCl, 5 mM KCl, 1 mM $MgSO_4$, 0.7 mM KH_2PO_4, 2 mM $CaCl_2$, 6 mM glucose and 25 mM HEPES dissolved in milliQ H_2O) at 37 °C for 30 minutes. After incubation in quinacrine solution, cells were stained with 1 µl of 7-AAD in PBS for 10 minutes. Cells were then rinsed with Krebs-Ringer solution and fixed with 1% PFA for 10 minutes at room temperature or analysed immediately after staining by flow cytometry[529,530].

Importantly, ATP depletion by reduction of quinacrine-based staining was quantified on cells with an intact plasma membrane (7-AAD-negative and Quinacrine low cells), in order to rule out ATP depletion due to plasma membrane rupture.

3.4.1.4. ROS quantification by flow cytometry.

ROS are a collection of unstable and highly reactive-oxygen containing molecules. When produced in low levels under physiologic conditions can regulate essential cellular functions but when dysregulated and produced in large amounts can drive pathological situations and even cell demise.

In this work we have measured ROS levels by using two fluorescent probes: dihydroxiethidium (DHE) and 2', 7'- Dichlorofluorescin diacetate (DCFDA). DHE is a fluorescent dye mostly reacts with superoxide radicals, although it can also react with H_2O_2, giving 2-hydroxyethidium (2-OH-Et+) or ethidium (Et+) fluorescent species respectively. DCFDA is a cell permeant reagent that once inside the cell is deacetylated by cellular esterases yielding a non-fluorescent compound that react with intracellular ROS generating the oxidized green-fluorescent product 2',7' dichlorofluorescein (DCF).

For the measurement of intracellular ROS production the following protocol was utilized. Once cells were subjected to the desired experimental conditions were collected and washed with PBS. Then cells were incubated with 5 µM DHE and 20 µM DCFDA fluorescent probes for 30 min at 37 °C in PBS. Cells were then rinsed and resuspended in an appropriate amount of PBS for flow cytometry analysis.

3.5. Cell death and viability assessment.

3.5.1. Determination of phosphatydilserine exposure.

One of the hallmarks of apoptosis is the translocation of PS, which is usually located in the internal layer of the plasma membrane, but when apoptosis is triggered, this lipid is translocated to the outer surface and acts as phagocytosis signal. To determine PS translocation, annexin-V staining was carried out. Annexin-V is a protein that interacts and binds with high-affinity to PS. Depending on the experiment requirements and the rest of flurochrome panel utilized in each experiment, annexin-V FITC or Annexin-V DY634 were utilized. Annexin-V production and the subsequent conjugation with fluorochromes was conducted during this work following the protocol described in [532]. Shortly, Annexin-V protein production and expression was induced and subsequently purified from bacterial extracts. Afterwards, protein was conjugated with the desired fluorochromes as described in[532].

Cells to be stained were collected after subjecting them to the respective experimental conditions. Annexin-V binding to PS is Ca^{2+}-dependent, for that reason cells needed to be incubated with a specific buffer containing Ca^{2+}, that is, Annexin Binding buffer (ABB) which contained: HEPES 10 mM, NaOH 10 mM, $CaCl_2$ 140 mM and NaCl 2.5 mM. Cells were then collected, centrifuged and resuspended in 100 µl of ABB1x containing 4 µl of a 1/100 dilution of fluorochrome-conjugated Annexin V. Cells were incubated with the Annexin-V staining solution for 15-20 minutes at room temperature. Finally, cells were diluted with 200-300 µl of ABB1x and analysed by flow cytometry (BD FACS Calibur). Data were processed using FlowJo software.

In some cases, cells were co-stained with a vital dye, either propidium iodide or 7-AAD (Immunostep), that are usually excluded from cells with an intact plasma membrane. In this way, the integrity of plasma cell membrane can be also evaluated. For this purpose, cells were incubated with 1 µl of 7-AAD or propidium iodide for 10 minutes at room temperature.

3.5.2. Determination of mitochondrial membrane potential.

Another important event that occurs during the apoptotic cascade is the dissipation of the mitochondrial membrane potential due to the permeabilization of the outer mitochondrial membrane. Hence mitochondrial potential is a good indicative of cell's health To evaluate this parameter, the intracellular mitochondrial potential-sensitive probe $DIOC_6(3)$ (3, 3'-Dihexyloxacarbocyanine iodide) was utilized. This compound is a cell-permeant, green fluorescent, cationic lipophilic dye that is capable of staining live cells with an intact mitochondrial potential by accumulating in the mitochondrial matrix. To that end, cells were incubated with the indicated drug

treatments in each experimental conditions. Afterwards, mitochondrial membrane potential was evaluated by incubating cells on complete medium at 37 °C for 20 minutes with $DIOC_6(3)$ at 2 nM. In some cases, cells were co-stained with 1 µl of 7-AAD for 5 minutes to determine the integrity of the plasma membrane. Cells were then analysed by flow cytometry.

3.5.3. Clonogenic assay.

In order to analyse the proliferative and colony-forming capacity of cells, as well as, long-term survival, cells were seeded in 6-well plates. 24 hours later, once cells were properly attached and in growth phase conditions, cells were incubated with the indicated drugs for 48h. After drug incubation time, cells were kindly washed to remove the remaining drugs and death cells and afterwards, surviving cells were cultured for 10 days in complete medium. Thereafter, cells were washed again twice with PBS and fixed with 100% methanol for 30 minutes at room temperature. Cells were then finally stained with crystal violet (1% in 50% ethanol).

3.6. Antibodies.

During this work the following antibodies have been used for flow cytometry analysis.

Antibody	Characteristics	Dilution	Company
PUMA	Rabbit, mAb	1/50	Abcam
NOXA	Mouse, mAb	1/50	Santa Cruz Biotec
BiP/GRP78	Rabbit, mAb	1/100	Cell signalling
Active Caspase-3-FITC	Rabbit, pAb	1/100	BD
CRT-DyLight 488	Mouse, mAb	1/100	Enzo
Hsp70	Mouse, mAb	1/100	Stressgen
Anti-mouse Alexa 488	Goat, pAb	1/250	Thermo Fisher
Anti-rabbit Alexa 488	Goat, pAb	1/250	Thermo Fisher
Human CD138 FITC	Mouse, mAb	20 µl/10^6 cells	BD
Human CD19 PE	Mouse, mAb	20 µl/10^6 cells	BD
Human CD38 FITC	Mouse, mAb	20 µl/10^6 cells	BD
Human CD38 APC	Mouse, mAb	20 µl/10^6 cells	BD
Human CD20 PE-Cy5	Mouse, mAb	20 µl/10^6 cells	BD
Human CD45 PE-Cy5	Mouse, mAb	20 µl/10^6 cells	BD
Human CD56 PE	Mouse, mAb	20 µl/10^6 cells	BD
Human CD4 FITC	Mouse, mAb	20 µl/10^6 cells	BD
Human CD8 PE	Mouse, mAb	5 µl/10^6 cells	Miltenyi Biotec
Human CD3 APC	Mouse, mAb	5 µl/10^6 cells	BD
Human CD25 PE	Mouse, mAb	20 µl/10^6 cells	BD
Human CD127 APC	Mouse, mAb	20 µl/10^6 cells	BD
Human CD56 FITC	Mouse, mAb	20 µl/10^6 cells	BD
Human CD14 FITC	Mouse, mAb	20 µl/10^6 cells	BD
Human CD20 FITC	Mouse, mAb	20 µl/10^6 cells	BD
Human CD3 FITC	Mouse, mAb	20 µl/10^6 cells	BD
Human CD19 FITC	Mouse, mAb	5 µl/10^6 cells	Miltenyi Biotec
Human HLA-DR PerCP-Cy5	Mouse, mAb	5 µl/10^6 cells	BD
Human CD11c APC	Mouse, mAb	20 µl/10^6 cells	BD
Human CD56 APC	Mouse, mAb	5 µl/10^6 cells	Miltenyi Biotec
Anti-PD-1 FITC	Mouse, mAb	1/100	Biolegend
Anti-PD-L1 PE	Mouse, mAb	1/100	Biolegend
Human CD83 PE-Cy5	Mouse, mAb	20 µl/10^6 cells	BD
Human CD86 FITC	Mouse, mAb	20 µl/10^6 cells	BD
Mouse Anti-CD8 APC	Rat, mAb	5 µl/10^6 cells	*
Mouse NK1.1 PE	Rat, mAb	5 µl/10^6 cells	*
Mouse CD3 FITC	Rat, mAb	5 µl/10^6 cells	*
Mouse CD4 PE	Rat, mAb	5 µl/10^6 cells	*
Isotype Control Dylight 488	Mouse, mAb	**	Thermo Fisher
Isotype Control PE	Mouse, mAb	**	Biolegend

Table 3.2.| Antibodies utilized in flow cytometry analysis. * Donated by Julian Pardo's Laboratory;** the concentration of isotype control antibodies utilized was the same as the corresponding target antibody in each case. mAb: monoclonal antibody; pAb: polyclonal antibody;

3.7. Microscopy techniques.

3.7.1. Inverted phase-contrast microscopy.

3.7.1.1. Senescence-associated β-Galactosidase staining.

For the analysis of the senescent features that cancer cells may undergo upon antimitotic treatment, like the enlarged and flattened cellular morphology and the senescence-associated β-Galactosidase (SA-β-Gal) activity, an inverted phase-contrast microscope was utilized to detect these changes.

Cells were seeded in 12-well plates 24 hours before being challenged with the different experimental conditions. Target cells were incubated with barasertib alone or the co-incubation (CI) of barasertib and ABT-737 for 48h, then rinsed. At day 7, ABT-737 was added to barasertib in a delayed fashion (delayed incubation, DI). In case of z-VAD-fmk (50 μM) addition, it was preincubated 1h before the delayed addition of ABT-737. After 24h, on day 8, cell death was analysed by annexin V staining (see section 3.5.1), or alternatively SA-β-Gal staining was carried out.

For SA-β-Gal staining, firstly media was aspirated and cells were gently washed with PBS 2x. Afterwards, cells were fixated with 4% paraformaldehyde (PFA) solution for 10 minutes at 4 °C. Once fixated, cells were rinsed twice, 5 minutes each with PBS. The SA-β-Gal staining solution (40 mM citric acid/Na phosphate buffer, 5mM potassium ferrocyanide, 5mM potassium ferricyanide, 150 mM NaCl, 2mM MgCl2 and 1mg/ml 5-bromo-4-chloro-3-indolyl β D-galactopyranoside (X-gal)) was added to the cells and incubated overnight at 37 °C. After that time, cells were rinsed 2 times with distilled water and observed under phase-contrast microscope.

To quantify the percentage of SA-β-Gal$^+$ cells, positive and negative cells were counted manually using ImageJ software and results were expressed as percentage of SA-β-Gal$^+$ cells from the total population.

3.7.2. Examination of murine histological tissue samples with bright field microscopy.

After collecting and removing femur, tibiae and spleens from euthanized mice, these tissues were prepared for histological examination. Haematoxilin-Eosine staining was performed by the Service of Anatomical Pathology from the Insituto Aragones de Ciencias de la Salud (IACS). Histological specimens were examined with a light microscope (Nikon) using 4x, 20x and even 40x objectives to observe the global architecture of the indicated tissues, as well as to localize MM cells colonizing these tissues. Representative photographs were taken with the digital photograph system equipped in the microscope (DXM 1200F, Nikon).

3.7.3. Fluorescent microscopy.

3.7.3.1. Immunofluorescence.

For the evaluation of the subcellular localization and expression of BUB1 protein in A549 cells, immunofluorescence technique was carried out.

First, samples must be prepared before observing preparations under the fluorescent microscope. To that end, coverslips were placed in 12- or 24-well-plates using tweezers. Although the cell lines used in this experiment were adherent, during mitosis or during cell death, cells may detach from plastic bottom and loose sample during the immunostaining procedure. Thereby, coverslips were covered with poly-L-lysine for 1h at room temperature. Next, coverslips were rinsed with sterile PBS for three times. Afterwards coverslips were sterilized by exposing 15 minutes to UV light. Finally cells were grown in well-plates with coverslips installed inside of them and cells were subjected to the different conditions, as indicated, for 24 hours.

After subjecting cells to the different experimental conditions, cells were immediately fixated with 100% methanol (chilled at -20 °C) at room temperature for 10 minutes or alternatively, with PFA 4% for 10 minutes at room temperature. Next, cells were washed three times with ice-cold PBS. Since the target protein is intracellular, cells must be permeabilized first. In theory, methanol-fixed samples do not require the permeabilization step. In case of PFA-fixated samples, they were permeabilized for 10 minutes with 0.25% Triton X-100 in PBS. Afterwards, cells were washed three times, 5 minutes each. To block unspecific antibody binding, cells were incubated with PBST (PBS + 0.1% Tween 20) supplemented with 10% of goat serum for 1 hour.

Cells were incubated with the primary antibody (anti-BUB1) at 1/400 dilution in blocking buffer (10% goat serum in PBST) in a humidified chamber overnight at 4 °C. After that, cells were washed three times in PBS, 5 minutes each. Subsequently, cells were incubated with the appropriate secondary antibody (goat anti-mouse IgG-PE at 1/200 dilution in blocking buffer for 1 hour at room temperature in the dark. Afterwards, cells were washed three times with PBS for 5 min each in the dark. Additionally, cell's nuclei were counterstained by incubating them with Hoechst 33342 at 2 μg/ml diluted in distilled water for 15 minutes at room temperature. Cells were rinsed with distilled water for three times.

Coverslips were mounted with a drop of mounting medium (Fluoromont-G). Coverslips were then sealed with nail polish to prevent drying and movement of the preparation under the microscope. Preparations were immediately observed with an inverted fluorescent microscope (Olympus IX81) in the service of Imaging and microscopy from 'Instituto Aragones de Ciencias de la Salud' (IACS), or alternatively stored at -20 °C or at 4 °C, until posterior analysis.

3.7.3.2. Time-lapse fluorescent microscopy.

To be able to notice the dynamic changes and processes that occur during mitosis or during the different cell fates that take place upon mitotic catastrophe, endpoint methods like flow cytometry, do not provide information and encompasses the whole cell's 'history'. Thus, these kind of approaches are not suitable enough to examine mitotic catastrophe and its underlying mechanisms[55]. In order to be able to study the contribution of mitotic catastrophe to the tumoricidal action of these drugs, and faithfully piece together the complete 'history' of cell death, novel techniques based on time-lapse fluorescence or high-throughput microscopy have been developed[62,533,534].

To that end, we utilized two genetically modified cell lines A549 H2B-GFP and MIA PaCa-2 H2B-GFP. These cell lines express histone H2B-GFP in order to track down chromatin morphological changes that occur during the cell cycle and specifically during mitosis. Thus, to study the contribution of mitotic catastrophe to the cell death induced by antimitotic drugs, time-lapse microscopy experiments were performed as follows.

A549 H2B-GFP or MIA PaCa-2 H2B-GFP cells were seeded in special glass-bottom 8-well plates (Ibidi) and were cultured in DMEM without antibiotic and without phenol red. Antimitotic agents were added 24h later to the medium at the indicated concentrations. Immediately after, fluorescence images were acquired every 15 min for 48h with a 20x objective in a time-lapse microscope (Leica AF6000 LX), under a controlled CO_2 atmosphere and in a thermostized chamber. At least two fields of view were acquired for each condition to capture enough cells to reach statistical significance. Thereafter, image sequences were analysed and individual cells were tracked down to determine their behaviour. Depending on the condition, between a minimum of 50 and a maximum of 120 cells were analysed using ImageJ software. The time at which each cell experienced a different cell fate or behaviour, as well as the own cell fates itself were recorded and noted down (see **Table 3.3.**).

Data from time-lapse analysis were plotted in such a way that allows for easy comparison between the different conditions, but without dissimulating its inherent complexity[62]. In the different cell fate profiles, each line depicts a single cell. The different cell behaviours a cell may undergo during the 48 h of the experiment, were plotted in different colours for each single line. Finally, the length of each line represents the duration of each cell behaviour represented within each line[62]. In this way fate profiles were generated for all conditions.

Cell fate/behaviour	Description
Interphase	Cells either in G1, G2 or S phase with uncondensed chromatin.
Entrance into mitosis.	Cells enter in mitosis with the characteristic condensation of chromatin.
Cell death in mitosis	When cells died during mitosis
Normal mitotic exit	Cells underwent a normal cell cycle with proper segregation of genetic material during mitosis, characterised by cytokinesis and decondensation of chromatin
Mitosis duration	The time cells spent in mitosis, from the initiation to its end, whether it is normal or aberrant (mitotic cell death or slippage)
Aberrant mitotic exit (slippage)	Cells usually underwent some degree of mitotic arrest and slipped out from mitosis without properly segregating the genetic material.
Cell death after slippage	When cells managed to escape the mitotic checkpoint and exit mitosis (chromatin get uncondensed without cytokinesis) and reach the next G1 stage with gross nuclear alterations (multi- and micronucleation) and succumb shortly after or hours later.
Cell death in interphase	If cells died in interphase without previously entering mitosis.
Survival after slippage	When cells managed to escape from mitotic blockade, slipped and reach the next G1 phase usually presenting morphological attributes of mitotic catastrophe (multi- and micronucleation).

Table 3.3.| Cellular fates and behaviours.

3.8. Induction of MOPC315.BM MM mouse model and disease monitoring.

3.8.1. Intravenous injection and tumour challenge.

The protocol for intravenous injection of MOPC315.BM cells and establishment of the orthotopic MM mouse model has been obtained from Hogaard *et al.*[526]. First, a MOPC315.BM cell culture in the exponential phase of growth, without reaching confluence and taking into consideration the number of cells that will be required for *in vivo* experiments, was previously prepared. Cell cultures were then counted three times to accurately obtain cell culture densities and viabilities. Cellular viability should be superior to 95%. The appropriate number of cells for the experiment were collected and resuspended in RPMI 1640 medium such the dose per mouse would be 200 µl and $5x10^5$ cells.

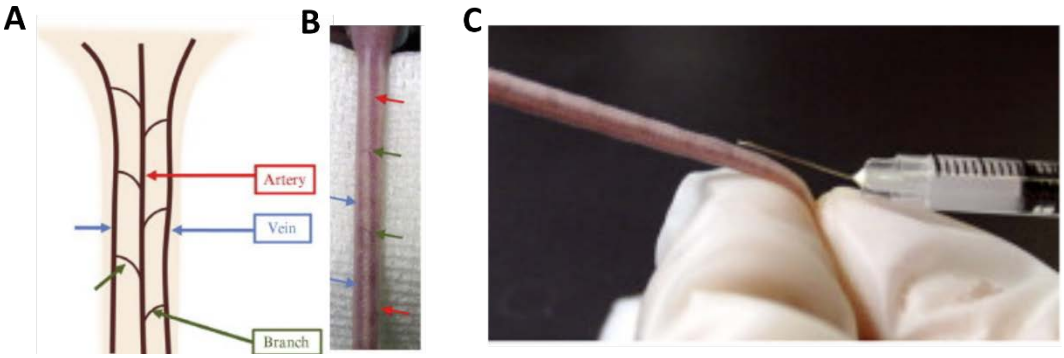

Figure 3.1. | Intravenous injection through the tail vein. A. Schematic diagram of the circulatory system of the tail. The artery occupies a central position and at the sides of the tail two veins can be found. Therefore, the tail must be laterally turned to reach one of the two lateral veins. **B.** Photograph of a natural tail with the different circulatory elements indicated. **C.** Representative photograph of how the intravenous injection should be performed with the needle adopting a parallel position to the tail vein. Adapted from [535].

Prior to intravenous injection, mice were heated with an infrared lamp for 10-20 minutes to allow the tail veins to dilate and facilitate cell injection. Cells were injected using a 27G x 3/4 needle (BD Microlance 3, 27G x ¾ nr. 20, 0.5mm x 19mm). First, the syringe (without the needle) was charged directly with the suspension of cells since the sharp edge of the needle and the shear stress created by the lower needle diameter can damage the cells. Once the syringe is charged, the needle was placed into the syringe and the possible air bubbles that may have formed were pushed away through the needle. Once the needle was prepared, the tail vein dilated and the mice immobilized, the needle was gently and slowly introduced parallel to the tail vein with the bevel of the needle facing upwards. When the needle was inside the vein it easily glided in. Then, the syringe piston was pushed very gently and at a constant pace. If the vein was appropriately cannulated, little or no resistance when injecting the cells should be encountered. Caution must be taken if the vein is not properly cannulated and the hard tissue of the tail vein is hit, since it may clog the needle and also cells may be subjected to unwanted

extra pressure while pushing the piston. Taking and charging one dose at a time avoids damaging the cells for subsequent injections. Cells were kept in ice if the process was delayed for more than 30 minutes.

Mice were observed twice weekly for disease state and humanitarian endpoint signs. Endpoint application was carried out when one of the following signs were observed[526]:

- Development of uni- or bilateral paraplegia.
- Visible extramedullary tumour growth with tumour size greater than 1 cm.
- Presence of distended abdomens, as a consequence of the dramatic splenomegaly or the presence of intraperitoneal extramedullary tumours.
- Weight loss greater than 10%.

When one of these criteria was met, humane endpoint was applied by CO_2 overdose. Afterwards, the required organs were extracted and processed as described in section 3.11.

3.8.2. Blood extraction for M315 paraprotein quantification.

For the quantification of plasma MOPC-315 idiotype-specific IgA M315 paraprotein secretion, blood samples were collected at the indicated time points.

Blood samples were extracted from the submandibular region of the mice by puncturing on the submandibular vein (see **Figure 3.2.**). Mice were restrained with one hand and were punctured with 23G needles at the puncture point, located at the back of the jaw, slightly posterior to the characteristic mole present in the jaw of mice and towards the ear of the animal. When punctured, immediately after, 1.5 ml tubes were grabbed to collect the blood samples. Once the appropriate amount of blood was collected (between 100 to 150 µl), animals were rapidly released in order to allow rapid coagulation of the puncture.

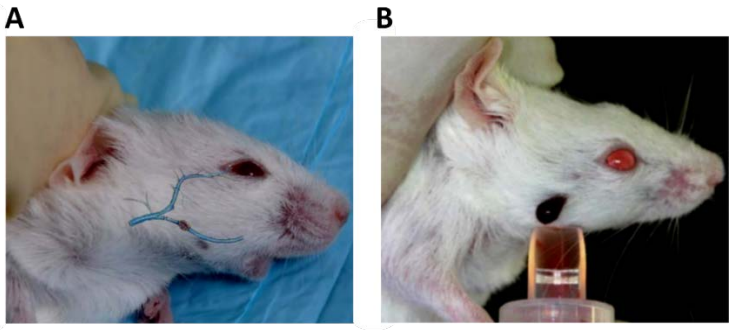

Figure 3.2. | Submandibular blood extraction. A. Schematic representation of the approximate localization of the orbital and submandibular veins. The characteristic mole located at the low mandibular region, together with the eye and the ear of the mouse, draw a putative triangle that more or less represents the localization of the vascular bundle. **B.** Photograph of a puncture performed in mouse submandibular region. Adapted from http://www.medipoint.com/html/animal_lancets.html.

Blood samples were left for 1 hour at room temperature to allow for sedimentation and clotting. Afterwards, samples were centrifuged at 2000 xg for 15 minutes and the serum supernatant was transferred to new marked tubes and stored at -80 °C for later usage.

In some experiments, upon endpoint application, blood was rapidly extracted through intra-thoracic exsanguination or terminal sample collection. For this purpose, a cardiac puncture was performed using a 23G needle by approaching the heart under the sternum. When the heart is punctured, blood will start to pass to the syringe and the piston of the syringe was gently pulled to draw the blood contain.

3.8.3. *In vivo* bioluminiscence imaging.

For disease monitoring, *in vivo* bioluminescence imaging (BLI) was performed at the indicated time points after tumour challenge, as follows. Mice were anesthetized by isofluorane inhalation and were injected intraperitoneally (i.p.) with D-luciferin (150 mg/kg of body weight). After 5-10 minutes to let luciferin distribute thought out the body and be metabolized, dorsal, ventral and lateral views for each mouse were imaged and luciferase activity was recorded and quantitated by using IVIS® Lumina imaging system (PerkinElmer). The threshold of bioluminescence signals was automatically determined using the Living Image software package. Data were then analysed using LivingImage® software (Caliper Life Sciences). Bioluminiscence signals were quantitated using average photons/second/cm^2/steradian for the total area of the mouse.

3.9. *In vivo* prophylactic vaccination with drug-treated cells.

The gold-standard method to identify *bona fide* ICD inducers and to test the ICD-inducing capacity of target drugs is to vaccinate syngeneic immunocompetent mice with cancer cells succumbing *in vitro* to ICD inducers and examine the capacity to elicit protective vaccination responses when rechallenged with living cancer cells of the same type. Therefore, to evaluate the immunogenic capacity of the different anticancer chemotherapeutics used in this study, *in vivo* prophylactic vaccination experiments with MM-treated cells, were carried out. To that end, the following protocol was followed.

MOPC315.BM wt cells were treated, as indicated in each case, with the different drugs for 24 hours. Before injecting into mice, a small aliquot of cells were collected and cell death was analysed for each condition by flow cytometry by Annexin-V / 7-AAD co-staining (section 3.5.1). Cell death was in all cases superior to 95% of the total population. This was critical because injection of cells with a lower cell death rate, rendered overt tumours that grew during the 2-week pre-rechallenge period. This obligated to euthanize

mice due to the growth of tumour from the "apparently death" vaccinated cells, but not because of the intravenous rechallenge, invalidating the results.

When cell death of cancer cell vaccines was ascertained, drug-treated MM cells were thoroughly washed two times with RPMI 1640 to eliminate traces of the chemotherapeutics. Cells were then resuspended in the appropriate volume of RPMI 1640 so that each mouse from each experimental group received 100 µl of cell suspension corresponding to $2.5x10^6$ cells. Balb/c mice were then vaccinated by subcutaneously (s.c.) injecting the cancer cell vaccine into the loose skin installed in the interescapular region. Mice were vaccinated through this procedure once a week for a total of 2 week period. Control mice were injected with the same amount of RPMI 1640. One week later after the second vaccination, mice were rechallenged by intravenously injecting (see section 3.8.1) $5x10^5$ live MOPC315.BM-Luc$^+$ cells for the establishment of the orthotopic MM mouse model.

Disease was monitored by bioluminescence imaging at the indicated time points and by analysing the signs of the disease, as previously described (section 3.8.3). Additionally, blood samples were collected at the indicated time points, in case M315 protein secretion analysis would be required. When mice reached one of the humane endpoints described earlier in section 3.8.1, BM from femurs and tibiae, spleen and extramedullary tumours were collected and processed for further analysis as indicated in section 3.11. In particular, the MM tumour load on the aforementioned organs were evaluated by flow cytometry. Additionally, the immune infiltrate of the BM, spleen and extramedullary tumours were also examined by analysing the frequencies of CD4$^+$ CD3$^+$ T cells, CD8$^+$ CD3$^+$ T cells and NK cells as described in section 3.4.1.1.

3.10. Combination of prophylactic vaccination with drug-treated cells and checkpoint blockade therapy.

Checkpoint blockade immunotherapy has been shown to provide promising clinical benefit in some cancer types. In MM, PD-1/PD-L1 axis has been shown to be a relevant immunosuppressive element with therapeutic potential, although early clinical trials evaluating this checkpoint in monotherapy or in combination with other chemotherapeutics, have not rendered encouraging results. In our mice model, cancer cell vaccine and PD-1 blockade therapy were combined. This was conducted to evaluate whether the lack of immune protection of the vaccination setting was due to the immunosuppressive microenvironment created, at least in part by PD-1/PD-L1 axis, or whether checkpoint therapy may improve anticancer immune responses.

The protocol followed in this experiment, was similar to the vaccination setting with the addition of the administration of blocking antibodies against PD-1. With that purpose, mice were vaccinated with MOPC315.BM wt cells as previously described

(section 3.9). Control groups were inoculated s.c. with the same volume of RPMI 1640. One week after from the 2nd inoculation, female Balb/c mice were rechallenged with live MOPC315.BM-Luc+ cells. On day 5 post-rechallenge, the experimental groups of mice receiving checkpoint blockade therapy (αPD1 control group and carfilzomib+CLQ+zVAD+αPD1 group) were administered i.p. with 100 μg of anti-PD-1 blocking antibody. This procedure was repeated twice a week for a total of 5 administrations. Disease was monitored by BLI, as well as evaluating the major signs of the disease at the indicated time points as previously described in sections 3.8.1 and 3.8.3. When endpoint criteria was met, humane endpoint was applied and the femurs/tibiae, spleen and extramedullary tumours were collected and processed for posterior immunophenotyping. In particular, MM tumour load and the immune infiltrate (NK cells, $CD4^+$ and $CD8^+$ T cells) in these different tissues were examined (section 3.4.1.1).

3.11. Organ preparation and tissue processing for the analysis of tumour load and immune populations infiltration.

To evaluate MM tumour load and the immune infiltration in the different hematopoietic organs where MOPC315.BM cells make niche, organs were collected and processed to obtain single-cell suspension for posterior immunophenotyping by flow cytometry analysis. After humane endpoint was applied (section 3.8.1), the femurs and tibiae from both posterior limbs, the spleen and the extramedullary tumours (when present), were extracted, harvested and processed as follows.

3.11.1. Isolation of whole splenocytes and extramedullary tumours.

The procedure to isolate and obtain single cell suspensions from spleen and extramedullary tumours (EMTs) was the following. Spleens and EMTs from euthanized mice were removed and collected in conical tubes containing RPMI 1640 medium. Under the laminar flow of a biosafety cabinet, spleens and EMTs were deposited in small petri dishes containing RPMI 1640 medium and squeezed with the piston of a sterile syringe. Cell suspension was then passed through a 70 μm cell strainer (BD). Petri dishes were then washed with RPMI medium to recover the rest of the cellular content and the solution was passed again through the cell strainer. Thereafter, isolated whole splenocytes and single cell suspension from EMTs were collected in a conical tube, were centrifuged and erythrocytes were lysed by resuspending in ACK erythrocyte lysing buffer (NH_4CL 154 mM, $KHCO_3$, 10 mM, EDTA 0.1 mM, pH 7.4) by incubating them for 10 minutes at room temperature. Afterwards, 10 ml of RPMI medium was added and cell suspension with lysed erythrocytes was centrifuged for 5 minutes at 300 xg. Supernatant was discarded and cell pellet was resuspended in an appropriate volume of medium. Cells

were then counted and cell viability was determined. Cells were then resuspended into the appropriate volume for flow cytometry immunophenotyping.

3.11.2. Isolation of bone marrow cells.

For the isolation of BM cells, femurs and tibiae from both posterior limbs from euthanized mice were collected and processed to obtain a single-cell suspension. Femur and tibia were removed in undamaged conditions to avoid contamination of the bone marrow. Muscle and connective tissue around the bones were removed and cleaned. Bones were deposited in a petri dish containing RPMI medium. BM from femur and tibia were exposed by cutting on both sides of each bone. With a 25G needle and 1 ml syringe containing RPMI medium, BM was flushed out of the bones. Once the BM cells were dislodged and a single cell suspension was obtained, it was passed through a 70 µm cell strainer to eliminate bone pieces that may remain. Thereafter, extracted BM cells were centrifuged and erythrocytes were lysed by resuspending in ACK erythrocyte lysing buffer (NH_4CL 154 mM, $KHCO_3$, 10 mM, EDTA 0.1 mM, pH 7.4) and incubating them for 10 minutes at room temperature. Afterwards, 10 ml of RPMI medium was added and cell suspension with lysed erythrocytes was centrifuged for 5 minutes at 300 xg. Supernatant was discarded and cell pellet was resuspended in an appropriate volume of medium. Cells were then counted and cell viability was determined. Cells were then resuspended into the appropriate volume for flow cytometry immunophenotyping.

3.12. Molecular biology techniques.

3.12.1. Preparation of media and bacterial cultures.

Manipulations of bacterial cultures and autoclaved material used for this purpose, were performed under the sterile area created by an ethanol burner. For the preparation of Luria-Bertani (LB) medium, 10 g of tryptone (PanReac, AppliChem), 5 g of yeast extract (PanReac) and 5 g of NaCl (Merck) were weighed and dissolved in 1 L of distilled water. This solution was transferred into glass bottles of 500 ml and was sterilized with an autoclave (Autestar Mod. 437-G, Selecta). When bottles were cooled down to room temperature, they were stored at 4 °C until use.

For the preparation of agar-LB, 17.5 g of Plate Count Agar (Sigma) were dissolved in 1 L of distilled water. The solution was transferred into 500 ml glass bottles and were sterilized in the autoclave (Autestar Mod. 437-G, Selecta). Once the bottles were cooled down to room temperature, the antibiotic used for bacterial selection (Ampicillin, Roche) was added at a 100 µg/ml concentration. After homogenization of the mixture, the solution was gently poured over petri dishes to let the agar solidify under the protection

of laminar flow provided by the biosafety cabinets. Once solidified, petri dishes were sealed and conserved at 4 °C.

3.12.2. Generation of competent bacteria and bacterial transformation.

Competent bacteria were obtained from a primary culture of 10 ml of *E.Coli* XL-1 Blue. This culture was expanded by adding 100 ml of sterile LB medium and bacteria were let to grow at 37 °C in an orbital shaker (MaxQ/5000, Barnstead/Labline) until the desired culture density was obtained (A_{600nm}= 0.4). The culture was split into two 50 ml conical tubes that were cooled down at 4 °C. Thereafter, bacterial cultures were centrifuged for 10 min at 4 °C and 2851 xg. Supernatant was discarded and bacterial pellet was suspended in 3 ml of trituration buffer (100 mM $CaCl_2$, Merck; 70 mM $MgCl_2$, Merck; 40 mM $NaCH_3COO$, Panreac). Pellet was homogenized completely and additional 30 ml of trituration buffer were added. Cultures were centrifuged again for 15 minutes at 2851 xg and 4 °C and once again, the supernatant was discarded. Next, the bacterial pellet was suspended this time in 4 ml of conservation buffer (100 mM $CaCl_2$ and 15% glicerol, Panreac). Bacteria were transformed immediately after or alternatively, were conserved at -80 °C in 400 µl aliquots.

Bacterial transformation was conducted by heat-shock method as follows. Aliquots were thawed in ice. Once completely thawed, depending on the target plasmid, 50 to 100 ng of plasmidic DNA was added. Bacterial cells were incubated with the plasmid 20 minutes in ice and subsequently 1.5 minutes at 42 °C. Immediately after, bacteria were transferred to an ice bath for 2 minutes. After that, transformed bacteria were diluted by adding 1 ml of sterile LB and were incubated for at least 15 minutes at 37 °C. Next, bacterial cells were centrifuged 5 minutes at 460 xg. Most of the supernatant was discarded and cell pellet was resuspended in the remaining volume to plate them in agar petri dishes with the corresponding selection antibiotic (Ampicillin 100 µg/ml). Plates were incubated at 37 °C for 24 hours. Once bacterial colonies were grown and became visible, several colonies were selected and each one was transferred to a sterile conical tube with 10 ml of LB supplemented with the selection antibiotic (Ampicillin, 100 µg/ml). This procedure was performed under the updraft of the flame of an ethanol burner and with a sterilized stick. Bacterial suspension was then incubated at 37 °C for 2 to 5 hours in an orbital shaker. After that, bacterial culture was transferred into a greater Erlenmeyer with 50 ml of LB containing the selection antibiotic for culture expansion. The Erlenmeyer was properly sealed with a sterile cotton cap and the bacterial culture was incubated overnight at 37 °C with orbital shaking.

3.12.3. Plasmidic DNA extraction.

To obtain small amounts of target plasmids, the GFX™ Micro Plasmid Prep Kit (GE Healthcare) or Nucleospin Plasmid EasyPure miniprep kit (Macherey Nagel) were utilized following manufacturer instructions**.** The initial bacterial culture volume was approximately between 1.5 and 5 ml and the final elution varied between 20 to 50 µl of Tris/HCl pH 8 or sterile milliQ H_2O, depending on the plasmid. To obtain greater quantities of the target plasmid, 50 to 100 ml of bacterial culture was obtained and the DNA extraction Quantum Prep Plasmid Midiprep Kit (BioRad) was utilized, being the elution this time in 500 µl of sterile MilliQ H_2O.

Plasmidic DNA concentration was measured by taking 2 µl test samples onto the NanoVue spectrophotometer (GE Healthcare, Amersham, UK).

3.12.4. DNA electrophoresis in agarose gels.

DNA electrophoresis in 1% agarose gels was performed for isolation of digestion products or simply to check out the final construct after a cloning procedure. To that end, 0.3 g of agarose (Scharlau) were dissolved and melted in 30 ml of the appropriate buffer. For analytical gels, the TBE buffer (Tris-Borate 45 mM and EDTA 1 mM) was the ideal choice, whereas agarose gels destined to fragment purification, TAE buffer (Tris-Acetic-EDTA, Gibco) was utilized instead. Once the agarose was melted and the solution was tempered, DNA stain SYBR-safe was added at a 1:10000 dilution (Invitrogen). Afterwards the mixture was poured into the electrophoretic beds to let agarose solidify. DNA samples were mixed with loading buffer 10x (Takara). To check and estimate the molecular weight of the target DNA samples, a molecular DNA ladder was also run parallel with the DNA samples. Depending on the size of the samples, either Tracklt 1 kb ladder or Tracklt 100 bp ladder (Biotools), were utilized and mixed with loading buffer 6x (Promega). The electrophoresis was conducted at 90V, 400mA during 30 to 60 minutes. DNA visualization was carried out under UV light in a transilluminator (GelDoc 2000, BioRad) using the software Quantity One.

3.12.5. Purification of DNA fragments.

The purification of DNA fragments was conducted by using either Illustra™ GFX™ PCR DNA or Gel Band Purification kit respectively. When DNA fragments were purified from agarose gels, DNA samples were first run into 1% agarose gel in TAE buffer. When electrophoresis was completed, the band of the desired molecular weight was cut with a sterile scalpel. To avoid the exposure of the desired DNA samples to mutagenic UV light, a small volume of the target DNA sample was loaded into a separated well as a

reporter that together with the DNA molecular ladder, facilitated to determine where exactly perform the cut in the gel and isolate the DNA fragment of interest without inconvenient UV light exposure. Finally, after purification with the kit, DNA concentration were measured in the NanoVue spectrophotometer using 2 µl aliquots.

3.12.6. Generation of knock-out cell lines using CRISPR-Cas9 technology.

Clustered regularly interspaced short palindromic repeats (CRISPR) were first described in 1987 by Japanese researchers as a short direct repeats that were separated by short sequences in *E.coli* genome[536]. CRISPR-Cas system was then found to operate as a microbial adaptive immune system in bacteria and archea that makes use of RNA-guided nucleases to trim foreign and unwanted genetic material[537]. To date, at least three different types of CRISPR systems have been identified. Each functional CRISPR-Cas loci consist on a cluster of CRISPR-associated genes, non-coding RNAs and a characteristic array of repetitive sequences (direct repeats)[538]. These repeats are also interspaced by short and variable sequences that derive from foreign invader DNA targets, also known as protospacers[538]. Altogether these elements conform the CRISPR RNA (crRNA) array. In the DNA target sequence, the protospacer is always accompanied by a protospacer adjacent motif (PAM) that differs from one particular CRISPR system to another. In this work we have utilized the type II CRISPR system derived from *Streptococcus pyogenes* that uses the Cas9 nuclease and the PAM sequence 5'-NGG[538,539]. In this system the crRNA array encodes the guide RNAs and an auxiliary trans-activating crRNA (tracrRNA) that helps to process crRNA array into discrete units.

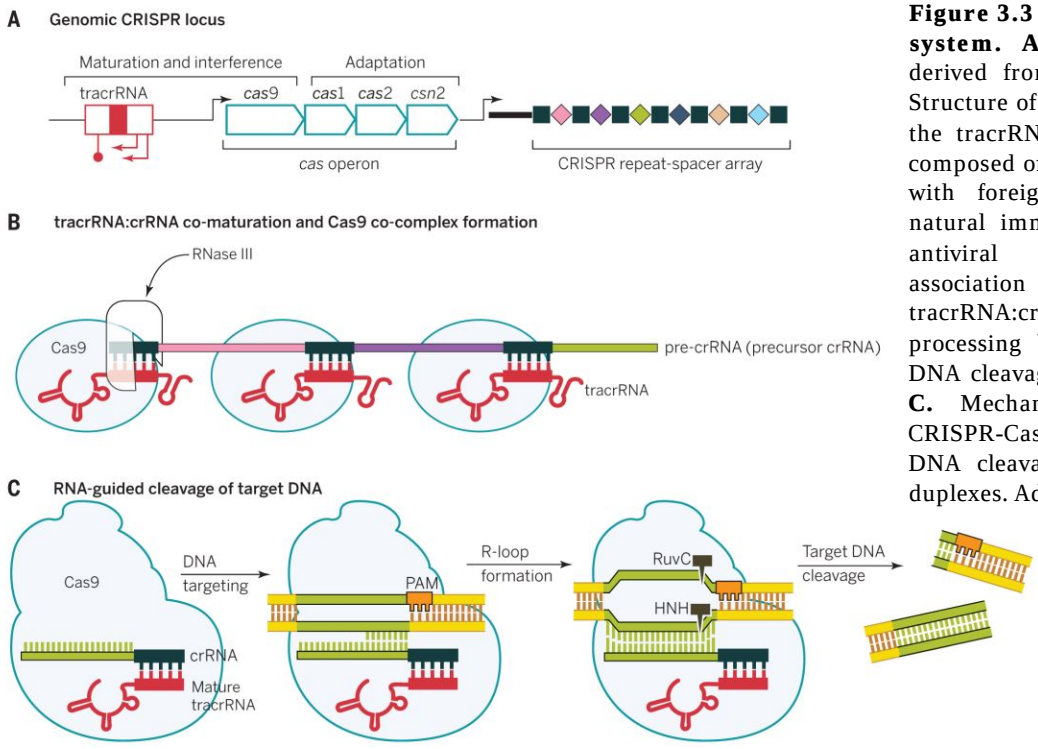

Figure 3.3 | Type II-A CRISPR-Cas system. A. The type II-A system derived from S. pyogenes is shown. Structure of the *Cas* gene operon, with the tracrRNA and the CRISPR array composed of direct repeats interspaced with foreign DNA-targets. **B.** The natural immune adaptive system for antiviral defence requires the association of Cas9 nuclease with tracrRNA:crRNA duplexes, RNA processing by RNAse III and target DNA cleavage among other processes. **C.** Mechanism by which natural CRISPR-Cas system targets the foreign DNA cleavage with tracrRNA:crRNA duplexes. Adapted from[539].

The dual tracrRNA:crRNA duplex was then engineered as a single guide RNA (sgRNA) that contains the two critical factors for the proper functioning of this system: 1) the 20-nt sequence at the 5'end of the sgRNA that drives DNA target specificity by Watson-Crick base pairing; and 2) the double-stranded secondary structure at the 3' end that allow the guide sequence to interact with the Cas9 nuclease[538,539]. In this system the target DNA sequence must immediately precede the PAM sequence 5'-NGG[538,539]. In this way, by modifying the guide sequence, CRISPR-Cas system confers a simple genomic engineering tool that directs Cas9 nuclease to virtually any DNA target sequence, as long as it is adjacent to a PAM sequence[538,539]. Cas9 nuclease then cleaves between 17th and 18th bases (3 bp from 5' of the PAM) of both strands of target DNA which allow the cellular DNA repair machinery to catalyse non-homologous end joining of blunt DNA ends favouring the introduction of insertion and deletions (indels) in target genomic DNA[538,539]. These indels may disrupt the open reading frame of genes driving the silencing or knock out of target genes.

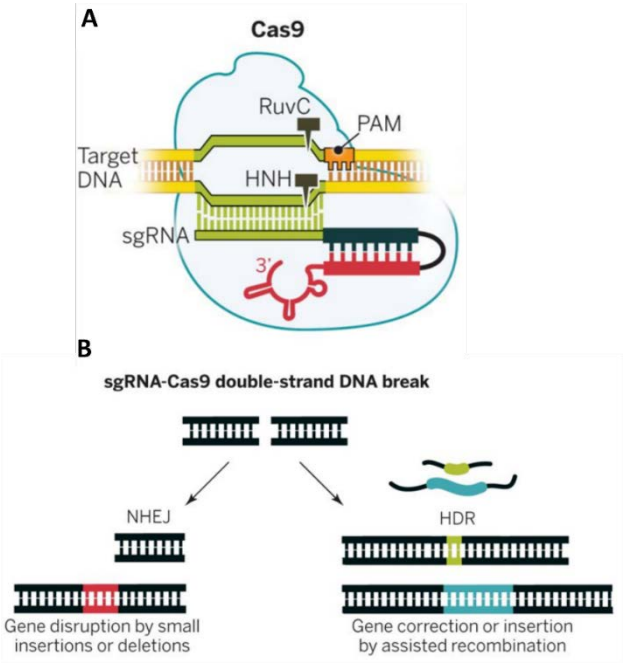

Figure 3.4 | CRISPR-Cas9 as a genome editing tool. A. The sgRNA guiding sequence is engineered so that it contains the 20-nt sequence at the 5' end of the sgRNA that drives DNA target specificity by Watson-Crick base pairing and the double-stranded secondary structure at the 3' end that allow the guide sequence to interact with the Cas9 nuclease **B.** Upon the blunt double-strand brakes generated by Cas9 into genomic DNA, the intrinsic cellular DNA repair mechanisms can proceed through two different directions**.** In absence of a homologous template, non-homologous end joining (NHEJ) occurs and in this process insertion and deletions may occur disrupting gene's open reading frame. In case of a homologous template is provided, directed insertions of corrected or mutated variants could be generated by homology-directed repair (HDR) mechanism. Adapted from [539]

Thereby in this work we made use of this genomic engineering tool to generate KOs cell lines in genes corresponding to different Bcl-2 family members to study their function in our experimental settings. In particular, during this work MIA PaCa-2 Bax KO, MIA PaCa-2 Bak KO, MIA PaCa-2 Bax/Bak DKO, MM.1S Bax/Bak DKO and U266 Bim KO cell lines were generated. For the generation of the MIA PaCa-2 cell line variants, the designing and cloning processes of sgRNAs was taught and supervised by one of my mentors Dr. Oscar Gonzalo. Meanwhile, MM.1S and U266 cell line variants were generated in collaboration with younger PhD students from our laboratory by teaching them this technique. In particular, Manuel Beltrán contributed by helping in the checking process to assure that the target gene was knocked-out by western-blot and in

the generation of the CRISPR control cell line. Nelia Jimenez contributed by performing the transduction of cloned CRISPR-sgRNA expressing lentiviral vectors in U266 Bim KO cells and the corresponding control cell line.

Designing of the sgRNA for the target gene was carried out using the online available CRISPR design tools in http://tools.genome-engineering.org or https://chopchop.cbu.uib.no/. These bioinformatics tools identify suitable target sites based on the presence of a 5'-NGG adjacent PAM sequence and allow for the selection of optimal target sequences based on the minimization of predicted off-target activities[538].

The target sequences of sgRNAs selected for the gene silencing process were the following:

Bak

Bak-sgRNA Fw: 5'- **CACC**GGTCCTCCCAGGCAGGAGTG-3'

Bak-sgRNA Rv: 5'- **AAAC**CACTCCTGCCTGGGAGGACC -3'

Bax

Bax-sgRNA Fw: 5'-**CACC**GGATCGAGCAGGGCGAATGG-3'

Bax-sgRNA Rv: 5'-**AAAC**CCATTCGCCCTGCTCGATCC-3'

Bim

Bim-sgRNA Fw: 5'- **CACC**GCCCAAGAGTTGCGGCGTAT 3'-

Bim-sgRNA Rv: 5'-**AAAC**ATACGCCGCAACTCTTGGGC-3'

Previous to the ligation of the sgRNA to the plasmid backbone, phosphorylation and annealing of sgRNAs were carried out. The quantity of each reagent utilized in this process were the following:

sgRNA top (oligo Fw) 100µM	***1µl***
sgRNA bottom (oligo Rev) 100µM	***1µl***
T4 PNK (10U/µl)	***1µl***
10x Buffer PNK	***1µl***
H_20 MilliQ	***6µl***

The sgRNAs were phosphorylated and annealed in a thermocycler by using the following parameters:

37 °C for 30 min
95 °C for 5 min
Ramp down to 25 °C at 5 °C/min.

In a parallel manner, pSpCas9-BB-2A-Puro and pLentiCRISPRv2 vectors were digested and linearized using BbsI and BsmBI restriction enzymes, respectively as described in section 3.12.7. These enzymes leave the same overhangs in the backbone of each plasmid allowing the utilization of the same sgRNA sequence for both vectors, like in case of sgRNAs for Bax and Bak. Once digested and linearized, vectors were purified as previously described in section 3.12.5. Finally, sgRNAs were ligated with the digested vectors as described in section 3.12.8.

MIA PaCa-2 cells were transfected with pSpCas9-BB-2A-Puro constructs, as described in section 3.13.1. MM.1S and U266 cells were instead transduced with lentiviral particles containing pLentiCRISPRv2 constructs as described in section 3.13.4.

3.12.7. Plasmid digestion.

Digestion of pSpCas9-BB-2A-Puro and pLentiCRISPRv2 vectors were digested and linearized to introduce the corresponding sgRNAs. The digestion mixture comprised the following:

Vector (pSpCas9 /pLentiCRISPRv2)	**1µg**
NEB Buffer 2.1 10x	**5µl**
Restriction enzyme (BbsI or BsmBI; 10 U/µl)	**1µl**
H_20 MilliQ	**40.5µl**

The vector was incubated at 37 °C with the restriction enzyme and the corresponding buffer to create the adequate conditions for the digestion process during 1 hour. As mentioned earlier, the enzymes BbsI and BsmBI although they recognize different target sequences, after the cut of the pSpCas9-BB-2A-Puro and the pLentiCRISPRv2 vectors respectively, they left the same overhangs in both vectors so that the same sgRNA sequences can be cloned in both plasmids.

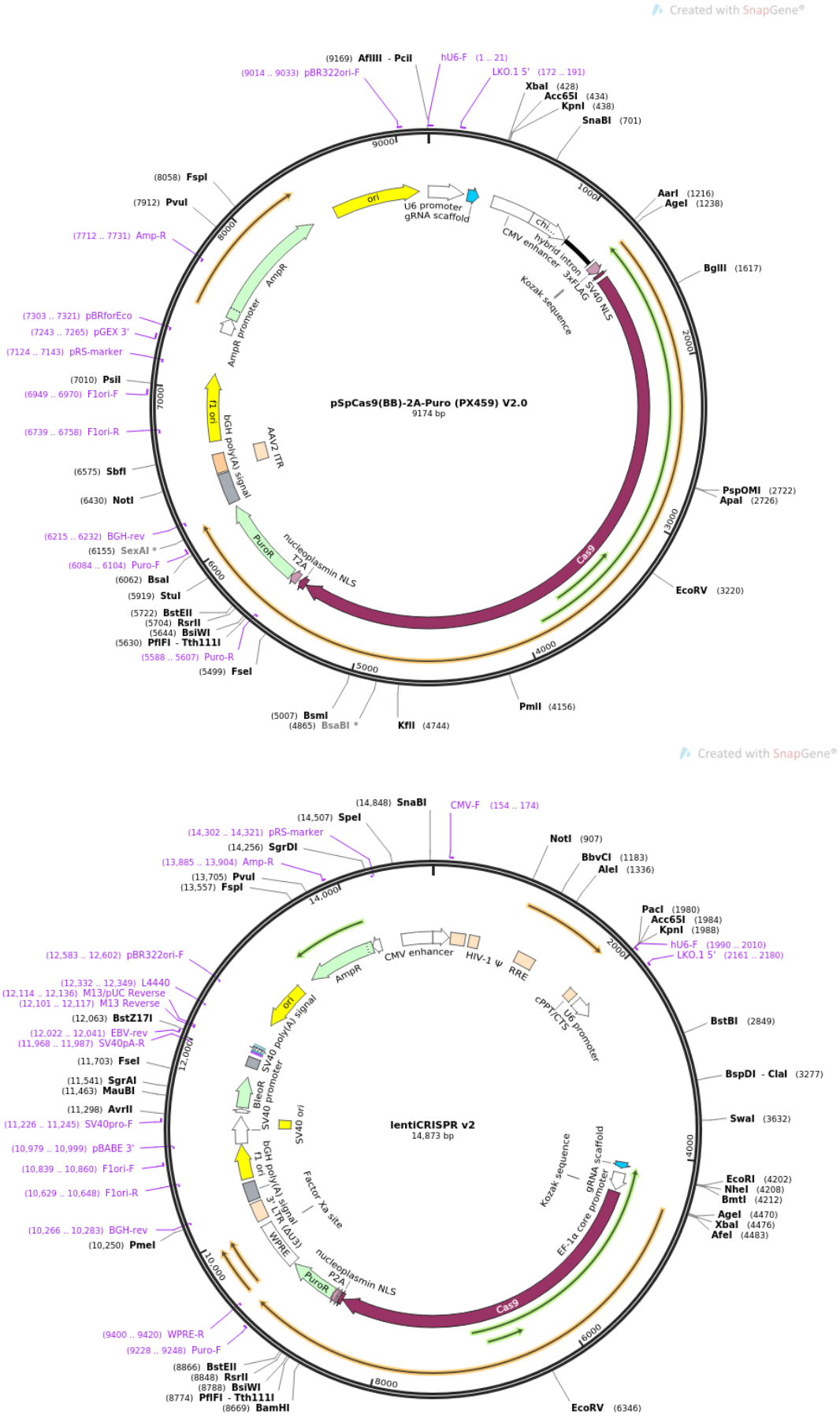

Figure 3.5. | CRISPR-Cas9 associated vectors. A. Genetic map of pSpCas9-BB-2A-Puro vector **B.** Genetic map of pLentiCRISPRv2 vector. (Addgene)

3.12.8. Inserts ligation.

Finally, the last step to obtain the cloned construct of the target sgRNA sequence in the vector backbones (pSpCas9-BB-2A-Puro and pLentiCRISPRv2) a ligation reaction between the target sgRNA and the vector is required. The molar ratio of vector:insert utilized for the ligation process was 1:5. In order to facilitate the analysis of the positive colonies and better monitor the different steps of cloning process, different internal controls were used (see **Table 3.4**). A control for religation was utilized to check and monitor the capacity of the linearized vector to religate without the insert, hence generating false negative colonies. In this case as indicated, the ligation reaction contained all the different components like in the ligation reaction with the exception of the annealed sgRNAs. Additionally, although the linearized vector was previously purified by gel electrophoresis, a digestion control to assess the efficiency of the digestion and purification processes was also utilized. In this case, the solution with which bacterial cells were transformed was composed of similar components to ligation reaction but without the T4 ligase and the annealed sgRNAs. Finally a positive control with undigested vector was utilized to control the efficiency of transformation.

	Ligation	***Φ Religation***	***Φ Digestion***	***+ Transformation***
Linearized vector	*100ng*	*100ng*	*100ng*	*100ng (undigested)*
Annealed sgRNA	*1:5 ratio*	-	-	-
T4 Buffer 10x	*4 µl*	*4 µl*	*4 µl*	*4 µl*
T4 ligase (5 U/µl)	*1 µl*	*1 µl*	-	-
H_20 MilliQ	*Complete to 10 µl*	*Complete to 10 µl*	*Complete to 10 µl*	*Complete to 10 µl*
PEG 4000	*<10% Vf*	*<10% Vf*	*<10% Vf*	*<10% Vf*

Table 3.4 | Conditions and volumes for the ligation reaction. The quantity and relation of the different reagents utilized in the ligation as well as in different internal controls are indicated. Vf= final volume.

The ligation reaction was incubated overnight at room temperature. After that time, the different ligation reactions and corresponding controls were used to transform competent *E.coli* XL1-Blue cells, as described in section 3.12.2. Transformed cells were plated in agar-LB with the selection antibiotic (ampicillin 100µg/ml).

3.12.9. Analysis of positive colonies.

After 24h of plating transformed competent bacteria with the target constructs, various bacterial colonies were selected. Depending on the efficiency of the different molecular processes or reactions and the presence of false positive colonies in the different internal controls, a greater or smaller number of colonies were selected. Each of the selected colonies were picked and expanded in 10 ml of liquid LB with selection antibiotic (ampicillin 100µg/ml) for an additional 24 hour course. Thereafter, plasmidic DNA was extracted with Nucleospin Plasmid Easy Pure Miniprep kit (Macherey Nagel) (section 3.12.3). In this way the generated construct was generated by one single colony and can be utilized for downstream applications. All the cloned constructs were verified by sequencing in the Genomic Sequence Service from CNIO, Instituto Carlos III, Madrid, Spain.

Expanded bacterial colonies, transformed with the different constructs, were stored by keeping 1 ml of the expanded culture and mixing it with 500 µl of glycerol in a previously prepared and sterilized 1.5 ml tube. These vials were stored at -80 °C for downstream applications and to be able to expand a readily available transformed bacteria with the desired vector.

3.12.10. Cell transfection techniques.

3.12.10.1. Transient transfection with Lipofectamine™ 2000.

For the transfection of MIA PaCa-2 cell lines with pSpCas9(BB)-2A-Puro constructs, Lipofectamine™ 2000 Reagent (Invitrogen) was utilized. This transfection method is based on the formation of cationic lipid particles that coat DNA molecules to allow them to enter through cell membranes that usually contain an extracellular negative charge that repels negative DNA molecules. Cells were seeded at $1x10^5$ cells per well in 12-well plates and were allowed to adhere to the well (overnight or during 24 hours) and reach 80% confluency to guarantee an optimal transfection efficiency and also to minimize cytotoxicity. As the manufacturer recommends, transfection medium did not contain antibiotics so that the potential cytotoxicity derived for the increased permeability of these molecules with the cationic particles is reduced. The DNA:Lipofectamine ratio used in transfection experiments was optimized in previous works from our group (Vela 2013 and Gonzalo 2017) and was 1 µg DNA:3 µl Lipofectamine. With that indication, cells were transfected with 300 ng of the CRISPR clone constructs. Vectors and Lipofectamine reagent were diluted in OPTI-MEM Reduced Serum Medium (Invitrogen). After at least 25 minutes of incubation of DNA solution with Lipofectamine solution to allow cationic lipid:DNA complexes to be formed, this mixture was added to cells dropwise. Transfected cells were selected with the antibiotic puromycin, starting 24 to 48 hours after transfection. To that end,

transfected cells were equally distributed in 4-5 wells from 24-well plates and a dose-response curve with increasing puromycin concentrations (from 1 μg/ml to 3 μg/ml) was carried out. In a parallel fashion, the same dose-response curve was conducted in parental cells and the lower dose at which control cells, but not transfected cells succumbed to the selection antibiotic was selected. Cell selection was performed during no more than 72 hours to avoid development of general drug-resistance mechanisms. After that time, cells were rinsed to eliminate the selection agent and after expanding them, they were examined for gene knockout by western blot (section 3.14). Additionally, functional testing by assessing drug cytotoxicity with agents known to trigger intrinsic apoptotic pathway and to be dependent on Bax and Bak-mediated cell death was performed.

3.12.10.2. Transient transfection by electroporation and siRNA-mediated gene silencing.

For the transient knock-down of gene expression in MM cells, siRNA-mediated silencing was carried out by electroporation. This is a physical transfection method that permeabilizes cell membranes by applying electrical pulses that create an electrical field allowing molecules to be transferred into the cell.

The required number of cells to be electroporated ($2x10^6$ cells) were centrifuged at 90 xg for 10 minutes. Supernatant was discarded entirely so that no residual medium covers the cell pellet. Cell pellet was then resuspended in 100 μl of tempered Nucleofector® Solution V (Lonza). The cell suspension was then mixed with the indicated amounts of siRNA. Cells suspensions were not incubated for more than 15 minutes in Nucleofector® solution since cell viability and gene transfer efficiency could be compromised. Each sample was then transferred into an Amaxa certified cuvette paying special attention that no air bubbles were formed. The appropriate Nucleofector® programme was selected for each case (U-001 for U266 cells and S-020 for MM.1S cells). The nucleofection cuvette was then inserted into the cuvette holder and the right programme was applied. Cells were immediately removed from the cuvette to avoid damage to the cells, by first adding 500 μl of pre-warmed complete culture medium with plastic Pasteur pipettes and then transferred to 12-well plates with 1.5 ml of pre-warmed complete culture medium. Cells were incubated 24 hours to allow for gene knock-down.

The concentration of siRNA used in the BiP knock-down experiment and the time selected for functional characterization after gene silencing was determined empirically. A positive control for gene transfection using 2 μg of a fluorescent reporter (TdTomato or pmaxGFP) was also carried out in parallel to evaluate gene transfection efficiency.

3.12.10.3. Generation of lentiviral particles for stable transfection.

Virus are microorganisms with a quite efficient capacity to introduce genetic material into eukaryotic cells. Making use of this feature, this technique is based on the generation of non-replicative lentiviral particles with infective capacity and hence, not only with the ability to introduce foreign DNA into eukaryotic cells but also to integrate it into their genome. Lentivirus, unlike retroviruses, have the ability to infect both replicative and non-replicative cells. Obeying biosafety standards, lentivirus used in research are engineered so that they can insert into the eukaryotic genome the target DNA fragment that is located between the Long-Terminal Repeats (LTR) sequences, but they lack the essential sequences that code for virulence factors. In fact, for more security the different elements required for the assembly of the viral particles are separated across distinct plasmids (3 for 2nd generation systems and 4 for 3rd generation systems) to minimize the probability of generating infective viruses. In this way, once the sequence between LTR sites is integrated into the genome of the target cells, a new lytic cycle cannot be initiated and therefore viruses cannot be propagated and infect new cells.

The packaging cell line utilized was 293T cells. This cell line can be easily transfected and can support the production of high viral titers. In this work we used the 2nd generation lentiviral system. Therefore, 293T cells were co-transfected with 3 plasmids: 1) LentiCRISPRv2 (see **Figure 3.5.**) or pHIV-Luc-Zsgreen (see **Figure 3.6.**) as the transfer plasmids containing the desired transgene or DNA fragment, for the generation of CRISPR-mediated KOs and MOPC315.BM-Luc^{+} cells respectively 2) the packaging plasmid psPAX2 encoding HIV-1 Gag, Pol for the formation of viral capsid Rev, for the reverse transcriptase and Tat required to drive the transcription with LTR promoter, and 3) envelope plasmid pMD2.G which encodes the envelope viral protein VSV-G that endows a wide cellular tropism.

The procedure for lentiviral production was optimized from Addgene and was conducted as follows. 293T cells were seeded at 3.8x10^{6} cells per plate in 10 cm-diameter culture petri dishes with complete DMEM. Cells were then incubated overnight at 37 °C, 5% CO_2 to attain the optimal exponential growth phase conditions prior to transfection. After this time, cells were incubated for 4 hours with DMEM containing 25 µM chloroquine to boost and improve viral production. Meanwhile transfection mixtures were prepared in a final volume of 1 ml of OPTI-MEM (Gibco). First a mixture with transfection plasmids was prepared in 500 µl of OPTI-MEM medium in the following concentration and ratios.

psPAX2	**1.3 pmol**
pMD2.G	**0.72 pmol**
Transfer plasmid	**1.64 pmol**
OPTI-MEM	**500 µl**

Plasmid mixture was then diluted by gently adding 500 µl of OPTI-MEM medium with PEI (polyethylenimine), at a concentration that matches the ratio µg DNA: µg PEI of 1:4. The mixture was incubated for 15-20 minutes at room temperature. Next, the transfection mixture was added gently dropwise to packaging 293T plates and cells were incubated overnight. The next morning, transfection media was removed and replaced with OPTI-MEM supplemented with 10% of FBS. Thereafter, cells were incubated for additional 48 hours for viral production. Several viral harvests were collected to perform two consecutive viral infections on target cells to increase transduction efficiency. The first viral harvest was then conducted at 48 hours post-transfection and the 2nd was performed at 72 hours post-transfection. Viral supernatants were recovered and centrifuged at 500 xg for 5 minutes to pellet any packaging cell and cell debris that may have been generated. Viral supernatants were then filtered through a 0.45 µm PES low-protein binding filters (Acrodisc®). Immediately after, target cells were infected with the harvested lentiviral particles for transduction of the desired DNA material.

Every material utilized for the manipulation of viral particles were autoclaved or sterilized with bleach and disposed off adequately.

Figure 3.6. | pHIV-Luc-ZsGreen plasmid genetic map. Genetic map of pHIV-Luc-ZsGreen plasmid (Addgene) utilized for the generation of MOPC315.BM-Luc+ cells for *in vivo* experiments.

3.12.10.4. Infection of eukaryotic cells with lentiviruses.

As mentioned earlier, to increase the efficiency of infection, target cells were infected two times consecutively with the 48 h and 72 h viral harvests, respectively. The infection procedure was carried out by optimizing the spin-infection method. $5x10^5$ target cells were seeded in 12-well plates resuspending them into 3 ml of viral supernatants. Afterwards polybrene (Sigma) was added to the cells at a final concentration of 10 µg/ml to improve the infection efficiency. Polybrene is a positively charged polycation that reduces the electrostatic repulsion between the negatively-charged target extracellular cell membrane and the lentiviral particle, thereby enhancing receptor-independent adsorption of viral particles. Next, cells were centrifuged for 2.5 hours at 1450 xg. After that time, viral supernatants were removed and cells were resuspended in complete medium and cells were incubated for 48 hours.

To obtain the MM.1S double knockout in Bax and Bak, co-transduction of parental cells with lentiviral particles containing packaged sgRNAs for both Bax and Bak was performed, but this strategy resulted unsuccessful. Instead, first a stable MM.1S Bak KO cell line was generated, and subsequently the double knockout cell line was generated by infecting MM.1S Bak KO cell line with viral particles containing the sgRNA for Bax. Additionally, the empty plasmid (without sgRNA sequence) was utilized to generate the corresponding control cell lines. U266 cells infection with lentiviral particles containing the Bim-sgRNA and the empty LentiCRISPRv2 vector for the control cell line was carried out by Nelia Jiménez. Moreover, in order to monitor the infection and viral production processes, in a parallel manner, viral particles containing a fluorescent reporter transgene were generated and subsequently used to infect target cells.

The LentiCRISPRv2-transfer vectors code for puromycin resistance gene and the selection of positive infected cells was carried out using the mammalian selection antibiotic puromycin in case of CRISPR-mediated KO cell lines. Therefore, only those cells that were correctly infected and that had integrated in their eukaryotic genome the viral DNA will acquire antibiotic resistance. Similar to the described selection procedure in 3.13.1, infected cells were equally distributed in 5 aliquots and seeded in in 24-well plates and a dose-response with puromycin ranging from 0.5 to 3 µg/ml was carried out. In a parallel fashion, parental cells were subjected to the same dose-response curve. The lower dose at which all untransduced cells died, was selected. Cell selection was performed during 72 hours to avoid that selected cells would develop general drug-resistance mechanisms. Cells were rinsed to eliminate the selection agent, expanded and examined for gene knockout by western blot (section 3.14). Additionally functional testing by assessing drug cytotoxicity with agents known to trigger intrinsic apoptotic pathway and to be dependent on Bax and Bak-mediated cell death was performed.

Viral supernatants and every material that may have entered in contact with lentiviral particles were sterilized with bleach and disposed off adequately in biosafety waste containers.

3.12.10.5. Limiting dilution for the generation of stable cell lines.

Lentiviral transduction of eukaryotic cells generates a heterogeneous polyclonal population that differ in the number and site of integration events. Moreover, in this particular case of CRISPR-mediated knockout, transduced population also varies in the Cas9-mediated indels generation, which may affect gene silencing. In order to generate stable cell lines that have a homogeneous genotype, limiting dilution was performed after selection. For that purpose, 30 ml of conditioned complete medium for the required cell lines were prepared by mixing 1/3 of filtered culture medium from the parental cell line in the exponential phase of growth with 2/3 of new complete medium. Conditioned media may contain some factors and/or cytokines secreted by cultured cells that prompt and favour cell proliferation. In this way single-cell cultures will grow in better conditions. Next, a total of 150 cells were resuspended into 30 ml of conditioned media and three 96-well plates were seeded. With this method, there will be some wells which will contain a single cell that will grow and expand to form a homogeneous monoclonal cell line.

After more or less three weeks of cell growth and culture expansion, some of the wells were selected based on the expression of fluorescent reporters (in case of MOPC315.BM cells) or based on the apparent health and size of the forming colony (in case of CRISPR-mediated KOs). These selected clones were further expanded in successive larger wells and flasks. Selected clones were interrogated for gene silencing by Western Blot analysis of the target protein (section 3.13). Moreover functional cell line testing using different BH3 mimetics and other drugs that are supposed to rely on the Bax and Bak dependent intrinsic apoptotic cell death pathway were conducted. These two steps were carried out by Manuel Beltrán (in case of MM.1S Bax/Bak DKO cells) and by Nelia Jiménez (in case of U266 Bim KO cells).

In case of MOPC315.BM-Luc$^+$ cells, luciferase expression was also evaluated. For this purpose, for each selected clone, a curve with decreasing amount of total cells (from $2x10^6$ to $2.5x10^5$ cells) were seeded in a 96-well plate and cells were incubated with D-luciferin potassium salt from firefly at a final concentration of 150 µg/ml. Cells were then imaged and *in vitro* bioluminescence was evaluated using the IVIS imaging system after 10 min of incubation at 37 °C. The clone yielding the highest bioluminescence signal was chosen for downstream *in vivo* experimentation.

3.13. Analysis of protein expression by Western Blot.

3.13.1. Extraction and fractionation of whole cell lysates.

To carry out whole cell lysis and fractionation, cells to be analysed were collected, washed with PBS and suspended in lysis buffer (20 µl/10^6 cells). Lysis buffer was composed of: 1% of Triton-X-100 (Sigma); NaCl 150 mM (Merck); Tris/HCl 50 mM pH 7.6 (Sigma); glycerol 10% (v/v, Scharlau); EDTA 1 mM (Sigma); sodium orthovanadate 1 mM (Sigma); sodium pirophosphate 10 mM (Sigma); leupeptine 10 µg/ml (Sigma); sodium fluoride 10 mM (Sigma); PMSF 1 mM (Sigma). Cell extracts were incubated during 30 minutes in ice and subsequently were centrifuged 30 minutes at 20800 xg at 4 °C. Supernatants were recovered and transferred into a new 1.5 ml tube. Determination of protein concentration was carried out utilizing a BCA kit (Bicinchoninic acid assay, Thermo Fischer Scientific), following manufacturer instructions. Sample readouts were obtained by analysing the absorbance at 550 nm in an ELISA plate reader. Once proteins were quantified, the appropriate volume of loading lysis buffer 3x was added to each cell extract so that the final concentration in the sample was 1x. The loading lysis buffer 3x was composed of the following elements: Tris/HCl 150 mM pH 7,4 (Sigma); 3% sodium dodecylsulphate (SDS, Merck); sodium molibdate 0,3 mM (Sigma); sodium pirophosphate 30 mM (Sigma); sodium fluoride 30 mM (Sigma); glycerol 30% v/v (Scharlau); 2-β-mercaptoethanol 30% v/v (Sigma); bromophenol blue 0,06% w/v. Finally, cell lysates were incubated in a dry bath during 5 minutes at 100 °C just prior to gel loading, or alternatively were conserved at -20 °C until use.

3.13.2. Protein separation. Sodium dodecyl sulphate-Polyacrylamide gel electrophoresis, SDS-PAGE.

Cellular protein separation was carried out in polyacrylamide containing 0.1% SDS. Polyacrylamide percentages varied from 10-15% depending on the mass of the target proteins to be analysed. The composition of stacking and resolving gels are indicated in the following table:

	Stacking (2%)	Resolving 10%	Resolving 12%	Resolving 14%
Acrilamide:Bis (29:1) 40%	0.5 ml	2.5 ml	3 ml	3.5 ml
0.5M Tris-HCl pH 6.8	1.25 ml	-	-	-
1.5M Tris-HCl pH 8.8	-	2.5 ml	2.5 ml	2.5 ml
SDS 10%	50 µl	100 µl	100 µl	100 µl
APS 10%	150 µl	150 µl	150 µl	150 µl
TEMED	15 µl	15 µl	15 µl	15 µl
Distilled water	3 ml	4.7 ml	4.2 ml	3.5 ml

Table 3.5.| SDS-PAGE Gels composition.

As mentioned before, prior to loading the protein samples to the gel, they were heated up to 100 °C and centrifuged during 1 minute at 770 xg. Depending on the gel size, up to 20 µl of protein samples, which corresponded to 50-100 µg of proteins were loaded. Gel electrophoresis was carried out on Hoefer miniVE cubes (GE Healthcare) filled with 1 L "running" electrophoresis buffer (Tris 25 mM, Glycine 180 mM and SDS 0.1% (w/v)). Protein samples run for 2-3h at 180 V and 20 mA per gel. In each gel 5 µl of a molecular weight ladder (Spectra™ Multicolour Broad Range Protein Ladder, Thermo) was also loaded in order to track and assign the different bands to the corresponding molecular weight.

3.13.3. Protein transfer to nitrocellulose or PVDF membranes.

Once the electrophoresis finalized, proteins were transferred to nitrocellulose or PVDF (Polyvinylidene fluoride) membranes (Hybond C-extra, GE Healthcare). PVDF membranes, were pre-activated by incubation on methanol for 30 seconds. Protein transfer was performed in a semi-dry BioRad transfer system. The transfer buffer, in which special sponges were embedded to create the semi-dry conditions, was composed of Tris/HCl 48 mM pH 8,3, glycine 39 mM, SDS 0,037% and HPLC-quality metanol 20% (v/v). Transfer process was carried out at 20 V and 400mA for 75 minutes. Transfer efficacy was checked out by staining the membranes with Ponceau red solution (0.1% w/v ponceau red in HAc 5% v/v).

3.13.4. Protein analysis by immunoblot or western blotting.

Previous to the detection of the immune-complexes, nitrocellulose or PVDF membranes were blocked with skimmed milk 5% (w/v) diluted in PBST buffer (NaCl 0,12 M, Tris/HCl 10 mM pH 8 and 0,5% (w/v) Tween-20 in PBS pH 7,4), during at least 30 minutes to 1 hour. Afterwards, were washed in PBST buffer and membranes were incubated with the specific primary antibodies to detect the target proteins, overnight at 4 °C with gentle shaking. The primary antibodies were diluted at the indicated concentrations in the 'antibody solution' (BSA 5% w/v and sodium azide 0.05% w/v diluted in PBST buffer).

Antibody	Characteristics	Dilution	Company
Bcl-2 (100/D5)	Mouse, mAb	1/250	Abcam
Bcl-X_L	Rabbit, mAb	1/1000	Cell signalling
p-Bcl-2 (ser70)	Rabbit, mAb	1/500	Millipore
p-Bcl-X_L (ser62)	Rabbit, pAb	1/1000	Santa Cruz Biotec
Mcl-1	Mouse, mAb	1/1000	Santa Cruz Biotec
Bim	Rabbit, pAb	1/1000	Millipore
PUMA	Rabbit, mAb	1/500	Abcam
PUMA	Rabbit, mAb	1/500	Novus Biologicals
NOXA	Mouse, mAb	1/250	Santa Cruz Biotec
Bax			
Bak (G-23)	Rabbit, pAb	1/1000	Santa Cruz Biotec
CycB1	Mouse, mAb	1/1000	Santa Cruz Biotec
MAD2	Mouse, mAb		BD
BUB1	Mouse, mAb	1/500	Cell signalling
BUBR1	Mouse, mAb	1/500	BD
p-eIF2α		1/1000	Cell signalling
CHOP/GADD153	Mouse, mAb	1/500	Santa Cruz Biotec
PERK	Rabbit, mAb	1/1000	Cell signalling
XBP1s	Rabbit, mAb	1/1000	Cell signalling
BiP/GRP78	Rabbit, mAb	1/1000	Cell signalling
β-Actin	Mouse, mAb	1/10000	SIGMA
Tubulin	Mouse, mAb	1/10000	SIGMA
Mouse IgG- Alkaline Phosphatase	Mouse, pAb	1/20000	SIGMA
Rabbit IgG- Alkaline Phosphatase	Rabbit, pAb	1/20000	SIGMA
Mouse IgG- Horseradish peroxidase	Mouse, pAb	1/20000	SIGMA
Rabbit IgG- Horseradish peroxidase	Rabbit, pAb	1/20000	SIGMA

Table 3.6.| Antibodies utilized for western blotting. mAb: monoclonal antibody; pAb: polyclonal antibody;

After incubation with the primary antibody, membranes were washed 3x with PBST buffer for 10 min. Thereafter, membranes were incubated with the corresponding secondary antibody conjugated with either horseradish peroxidase (HRP) or alkaline phosphatase (AP), diluted 1/20000 in skimmed milk 2.5% (w/v) in PBST buffer, for 1 hour at room temperature with moderate shaking. Upon completion of secondary antibody incubation, membrane was thoroughly washed with PBST buffer 3x for 10 minute each. Detection of the immuno-complexes were carried out by chemiluminescence, in which the enzyme conjugated to the secondary antibody (HRP or AP) reacts with the substrate and emit chemiluminescent light. Membranes were then incubated with the corresponding substrates (Pierce ECL Western Blotting Substrate, Thermo or PhosphoGLO AP Substrate, KPL) for 90 seconds in case of HRP substrate and

5 minutes in case of AP substrate. Next, the excess of substrate was eliminated and membranes were placed in a transparent plastic case that was laid down onto a radiographic developing cassette. In a dark room specially disposed to photographic developing, a radiographic film (Hyperfilm ECL, GE Healthcare) was placed over the plastic cover that protects the membrane, and the cassette was sealed exposing the film for varying times that depended on the antibodies utilized. Subsequently, photographic film was developed by soaking it in developing solution, then in distilled water and finally in fixation solution (both of them prepared according to manufacturer instructions, Kodak). Once fixated, film was dried and digitalized. Alternatively, detection of chemiluminescent signals was also carried out on an Amersham imager 600.

As internal loading controls to normalize protein expression to that of the housekeeping proteins, membranes were reprobed with either, β-actin or β-tubulin antibodies for 1 hour in a 1/10000 dilution in 2.5% (w/v) skimmed milk in PBST buffer. After that, the subsequent steps of washing, incubation with the conjugated-secondary antibody and immuno-complexes detection, was carried out as explained above.

3.13.5. Protein analysis by ELISA.

MOPC-315 idiotype-specific IgA M315 paraprotein secreted by MOPC315.BM cells was evaluated in serum samples from mice intravenously injected with these cells for disease monitoring. To this end, once blood samples were collected and serum was obtained, M315 quantification was performed by a sandwich-ELISA[526,540].

Costar 96 well EIA/RIA plates were coated with 2 µg/ml of Ab2.1-4 (kindly provided by Dr. Bögen) in 100 µl PBS with 0.02% sodium azide by incubating them overnight at 4 °C. The next day, the coating solution was flicked away from the plate and 200 µl/well of blocking solution (PBS with 1% BSA and 0.02% sodium azide) were added and incubated for 30 minutes at room temperature. Samples and M315 standard were added to the plate and incubated for 2 hours at 37 °C. They were diluted in ELISA sample buffer (PBS with 0.02% sodium azide, 0.1% BSA and 0.1% Tween20). A M315 standard curve was included, starting at 400 ng/ml concentration and decreasing by 2 fold in 10 steps to 0.39 ng/ml. Two different sample dilutions were also included for each sample. For the shorter blood sample collection time points (day 0 and day 10 post-intravenous injection of MOPC315.BM cells), a 1/10 and 1/100 sample dilution were prepared, whereas for the longer blood sample extraction time points (day 20 and day 30), a 1/1000 and 1/10000 dilution were elaborated. After sample incubation, plates were washed three times with 1x ELISA washing buffer. 25x ELISA washing buffer contained the following: 4.48 g NaH2PO4 X H2O, 48.35 g Na2HPO4 x 12H2O, 204.5 g NaCl, 25 ml Tween 20, to make 1 litre with distilled water. After the washing steps, 100 µl of biotin rat-anti-mouse IgA at 1 µg/ml diluted in ELISA sample buffer was added and incubated for 1 hour at 37 ºC. Afterwards, three washing steps with 1x ELISA washing buffer were

followed. Thereafter, 100 µl of streptavidin-alkaline phosphatase diluted 1/3000 in ELISA sample buffer was added and incubated for 1 hour at 37 °C. Another 3x washing steps were followed as previously described. Phosphatase substrate (SIGMA) 1 mg/ml was dissolved in substrate buffer (97 ml diethanolamine (SIGMA), 800 ml distilled water, 101 mg MgCl2 x 6H2O, 200 mg sodium azide, add 10 ml 37% HCL and fill up with distilled water to 1 litre). 100 µl of this solution was added per well. After 30 minute incubation at room temperature, absorbance was read at 405 nm in an ELISA microplate reader (Multiskan 355, Thermo Fischer).

The M315 standard curve was generated and was used to interpolate sample absorbance and to calculate sample M315 concentrations. Each serum sample were duplicated.

3.14. Determination of proteasome activity.

To delve deeper in the mechanism of action of the proteasome inhibitors used in this study and especially in the PI-based drug combinations, the proteasome activity of cells subjected to these experimental conditions was assayed. 20S proteasome activity was quantified using the 20S proteasome assay kit (Merck Millipore), following manufacturer instructions. This test is based on the detection of a fluorescent signal when a proteasome substrate (LLVY) conjugated with a fluorochrome 7-Amino-4-methylcoumarin (AMC) is cleaved and hence free AMC fluorescence is measured using a fluorometer (Biotek). For that purpose, cell lysates and protein extracts were prepared as indicated in section 3.13.1. Proteins were quantified by bicinchoninic method as previously described (section 3.13.1) and 20 µg of protein extract were utilized. Proteasome substrate and the proteasome buffer provided by the manufacturer, were added to cell extracts and were incubated at 37 °C for at least 3 hours. After that time, fluorescent signal was read in a fluorometer (Biotek).

3.15. Statistical analysis.

The statistical analysis of the data presented in this work was performed by using GraphPad Prism 6.0 (GrandPath Software Inc.). As indicated in each case, data were statistically analysed by using the following statistical tests:

- Two-tailed unpaired t-test for the analysis of two groups for independent samples.
- Two-tailed paired t-test for the analysis of two groups with matching or paired samples.
- One-way ANOVA with the Tukey post-test for correction of multiple comparisons, when more than 2 groups were compared.
- Two-way ANOVA with Bonferroni post-test for correction of multiple comparisons was performed to compare tumour growth curves for more than 2 groups.
- Fisher's exact test for comparing the proportions of two nominal variables with small sample sizes.
- Pearson's correlation coefficient in linear regression analysis.
- Mantel-Cox (log-rank) test for survival analysis of Kaplan-Meier curves.

All measurements were expressed as mean ± standard deviation (SD), unless stated otherwise.

RESULTS & DISCUSSION

4. RESULTS & DISCUSSION.

4.1. Study of the Contribution of Mitotic Catastrophe to Cell Death.

Mitotic catastrophe is a *bona fide* oncosuppressive mechanism that can engage cell death programmes and participate in the elimination of cancer cells, especially upon treatment with antimitotic drugs. We first aimed to evaluate the contribution of mitotic catastrophe in the induction of cell death exerted by different antimitotic agents that are either under clinical development or are currently used in the clinic. To have a broader panoramic of how the mechanisms of mitotic catastrophe and cell death are intertwined, and not only have a simplistic view of one particular drug, we decided to use different compounds that target distinct players that hold important functions in the mitotic apparatus. For that purpose, we evaluated the cell death mechanisms induced by an Aurora B kinase inhibitor (barasertib), an Aurora A kinase inhibitor (alisertib) and two commonly used microtubule targeting agents (MTAs), a microtubule stabilizer (docetaxel) and a microtubule depolymerizer (vincristine). We tested these drugs in different cell lines: A549 a model of non-small cell lung carcinoma (NSCLC), MIA PaCa-2 a model of pancreatic ductal adenocarcinoma and HCT-116 a model of colon carcinoma. Firstly, we assessed the sensitivity of these cell lines to the different antimitotic drugs indicated before at doses based on previous work conducted in our group.

Data depicted in **Figure 4.1** indicated that the cytotoxicity of these drugs is relatively low compared to that produced by doxorubicin at indicated doses. Doxorubicin is a well-known DNA-intercalating drug that induces a canonical DNA-damage response that ultimately activates the intrinsic apoptotic pathway. A common feature of these antimitotic agents is that they provoke a reduction in cell viability, as a consequence of either growth arrest or cell death, at relatively low concentrations (data not shown). Moreover, as it usually occurs with antimitotic drugs, cellular responses and *in vitro* pharmacokinetics are delayed in time, since cells must reach the mitotic phase to be affected by these compounds. Consequently, at 24h of treatment, cells do not show apoptotic markers. Cell death started to become apparent after 48h or longer incubation times. As data illustrated, MTAs had a greater cytotoxic activity than Aurora kinase inhibitors, especially in A549 and HCT-116 cells. Perhaps, this could be associated with the fact that microtubules fulfil different cellular functions outside mitosis[96].

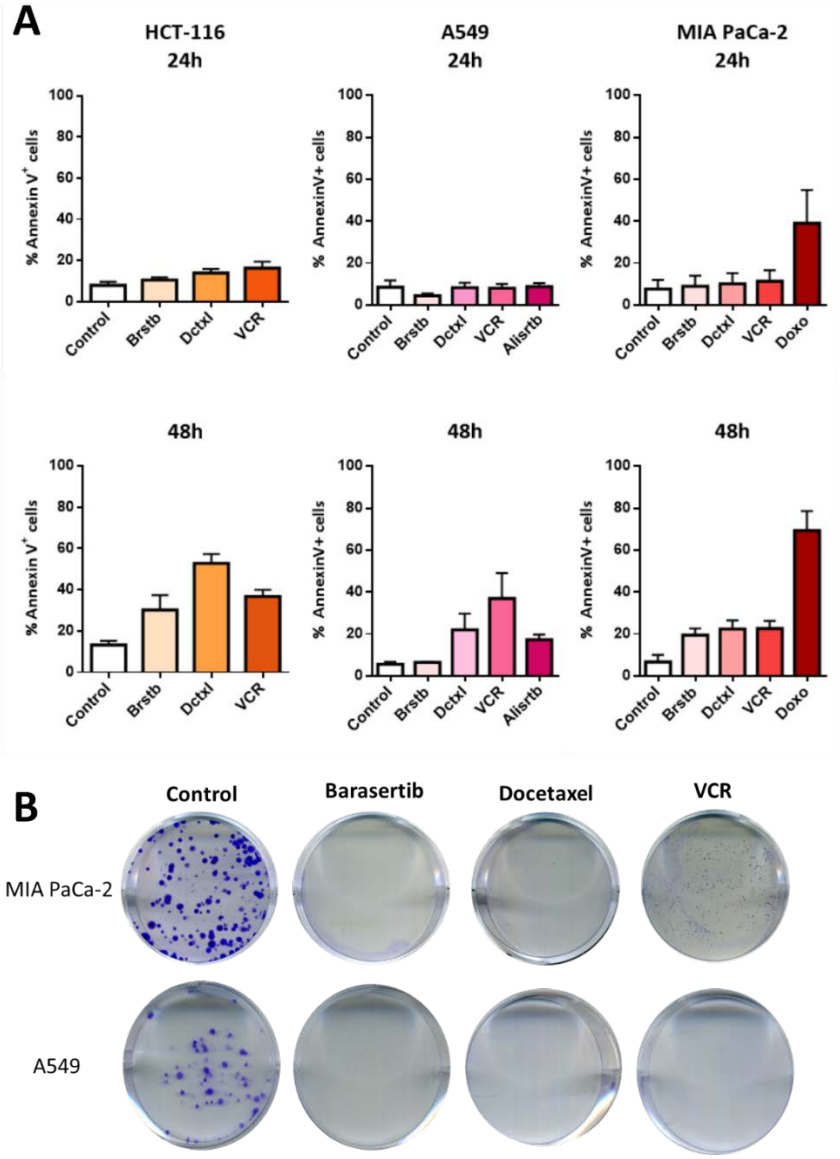

Figure 4.1 | Drug sensitivity of different cancer cell lines to antimitotic agents. A. A549, MIA PaCa-2 and HCT-116 cancer cell lines were exposed to different antimitotic agents for 24 or 48h. Drug doses utilized in each case correspond to barasertib (5 μM), docetaxel (10 μM), vincristine (1 μg/ml), alisertib (5 μM) or doxorubicin (1 μM). Data are presented as mean ± SD from n=3. **B.** Clonogenic assays showing the colony forming capacity of cancer cell lines exposed to different antimitotic drugs at the same concentrations indicated in A during 48h. Representative images from n=2 independent experiments.

It is noteworthy mentioning that drug concentrations assayed, were not intended to kill cancer cells but rather, to prevent mitosis. This approach will allow us to evaluate future possible combinatory strategies to potentiate cancer cell death. Furthermore, although after 48h the majority of the cell population is still viable, they cannot progress through the cell cycle and form new colonies, as shown in the clonogenic assay (**Figure 4.1**). Interestingly, in some cases, as seen in MIA PaCa-2 cells treated with vincristine, small punctae become visible. This situation could account for cells that would have escaped from mitosis and underwent slippage, reaching the G1 phase of the next cell cycle

in a tetraploid state, where they remain arrested by the G1 to S checkpoint without the ability to divide or form new colonies.

It should be noted that the reduced cytotoxic activity observed with the different antimitotic agents, is not probably associated with intrinsic defects in the apoptotic machinery that these cancer cell lines may hide, since doxorubicin administration caused a substantial amount of cell death, at least in MIA PaCa-2 cells. These observations would suggest that an alternative cell death mechanism, different to that elicited by doxorubicin, may be activated upon antimitotic treatment. Alternatively, this resistance to cell death when mitosis is inhibited, could also unmask a potential hidden disruption of the connection between the mitotic apparatus and the apoptotic machinery. More research is needed to clarify this matter.

Microscopical images of the characteristic nuclear morphological alterations that cancer cells experience upon treatment with antimitotic agents were acquired using a bright field, phase-contrast microscope. As illustrated in **Figure 4.2** below, barasertib treatment induced cells to acquire a giant and enlarged phenotype with a flattened shape. Additionally, as observed, within a given cell the appearance of multiple micronuclei are discernible in the different cell lines tested. Upon docetaxel treatment, multinucleation and micronucleation were also clearly apparent. However, in this case cells were not so enlarged and flattened as it occurs in the case of barasertib. It could also be observed that some non-granular rounded cells appeared. Cells with this characteristic morphology have initiated mitosis and, as a consequence of mitotic pause induced by docetaxel, were arrested in this state. Moreover, some detached death cells with granulated morphology typical of the blebbing phase of apoptosis and even cells showing secondary necrosis were also visible. A great proportion of cells treated with vincristine were also arrested in mitosis after 48 hours incubation with this drug. Additionally, dead cells and surviving cells with multiple micronuclei became also discernible. Faulty or defective mitosis is usually associated with prominent nuclear alterations including multinucleation and macronucleation, which generally arise from clusters of missegregated chromosomes, and also micronucleation, which results from lagging o acentric chromosomes that are left outside the main nucleus[55]. These nuclear alterations are the main morphological traits that describe mitotic catastrophe[55,541].

Collectively, our data suggest that the different antimitotic agents at the tested drug concentrations have a reduced or moderate cytotoxic activity on the different cancer cell lines. However, although a substantial proportion of cells did not exhibit apoptotic features at all time points evaluated, its proliferative capacity is blunted upon antimitotic drug treatment. Furthermore, cells treated with antimitotic agents manifest the main nuclear morphological traits typically found in cells undergoing mitotic catastrophe.

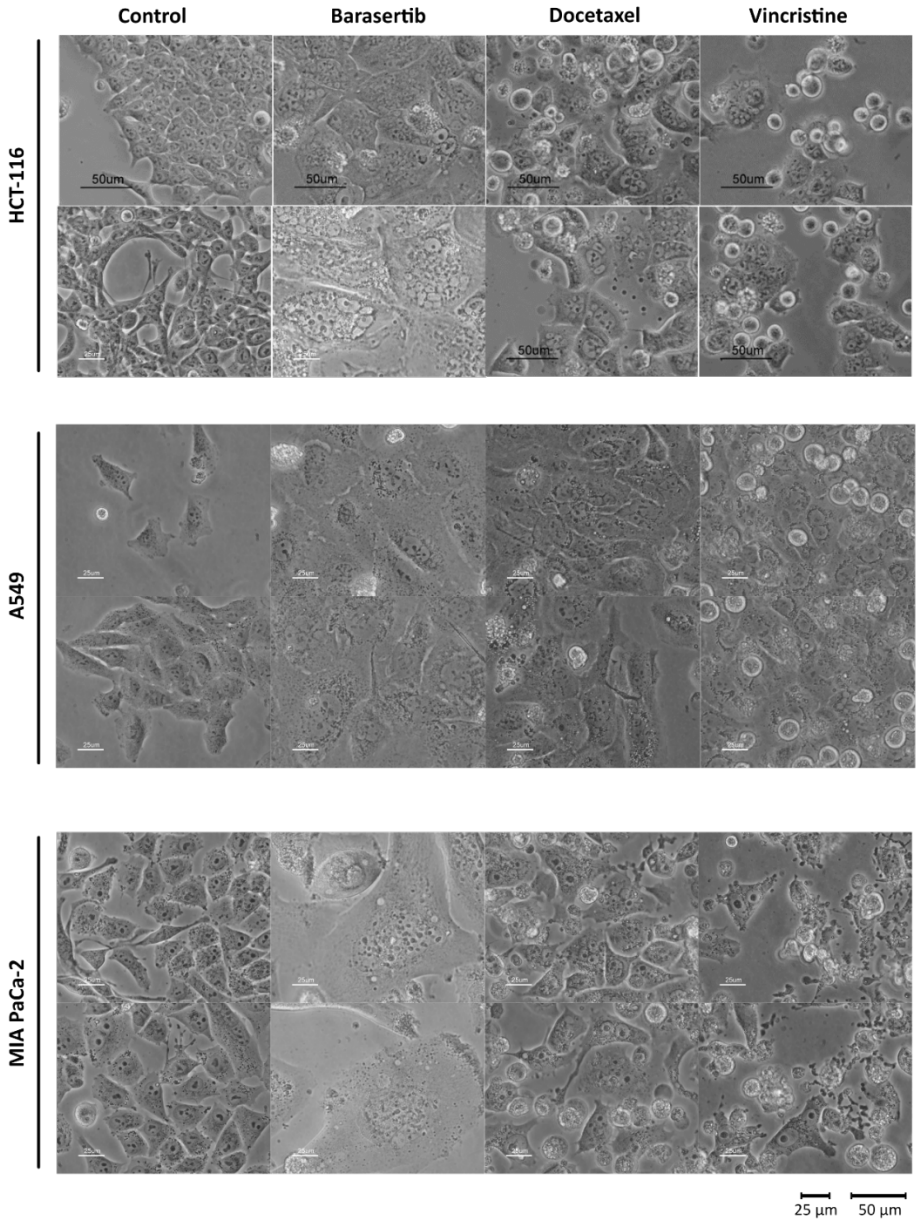

Figure 4.2 | Characteristic morphology of cancer cell lines upon antimitotic drug treatment. A549, MIA PaCa-2 and HCT-116 cancer cell lines were exposed to different antimitotic agents: barasertib 5 µM, docetaxel 10 µM and vincristine 1 µg/ml for 48h. After the corresponding incubation time, cells were imaged with a bright-field phase-contrast microscope by using 20x or 40x objectives. In particular, cells treated with barasertib were imaged with a 20x objective due to its enlarged morphology that these cells presented. Bar, 25 µm or 50 µm as indicated.

4.1.1. Combination of Antimitotic Drugs and BH3-mimetics.

According to the competitive networks model, cell fate in response to aberrant mitosis relies on the finely-tuned balance between cell death signals and the mechanisms that control mitotic exit[62,63]. Moreover, novel antimitotic agents that target mitotic kinases and motor proteins have not rendered good results in clinical trials[96]. Similarly, despite its extended use and proven clinical efficacy, cancer cells develop resistance

mechanisms against MTAs, being mitotic slippage one of them[92]. For these reasons, a good therapeutic strategy to tip the balance in favour of cell death and improve the efficacy of antimitotic drugs, could pass through accelerating or increasing the strength of death signals during mitosis. Furthermore, Bcl-2 family of proteins have been shown to be key determinants of cell fate decisions under prolonged mitotic arrest[73]. BH3 mimetics are small molecule inhibitors that target the canonical groove within the hydrophobic pocket of anti-apoptotic proteins counteracting their pro-survival activity, thereby mimicking the action of BH3-only pro-apoptotic proteins[12,542]. Although several peptide-based and non-peptidic small molecule BH3 mimetics have been developed so far, we focused our attention on ABT-737 and ABT-199. These two inhibitors selectively bind to and neutralise the pro-survival activity of Bcl-X_L, Bcl-2 and Bcl-W in case of ABT-737, whereas ABT-199 selectively blunts Bcl-2 action[12,542].

Consistent with these ideas, in the present study we have combined different antimitotic drugs with BH3 mimetics. We intended to potentiate cell death induced by antimitotic agents and to prevent slippage, as well as to study the underlying mechanisms. We also used these tools as a starting point to dig deeper in the regulatory role that the Bcl-2 family of proteins perform during mitotic catastrophe.

First of all, dose-response curves of ABT-199 and ABT-737 in the different cell lines were generated. After 24h of drug incubation, we evaluated cell death induction by flow cytometry analysis of annexin V binding to phosphatidylserine (PS) (as described in section 3.5.1). HCT-116 cells were the most sensitive from all tested lines, especially upon ABT-737 treatment. Meanwhile, A549 and MIA PaCa-2 cell lines did not show any apparent sensitization at the tested doses (**Figure 4.3**). Based on these and previous results from our laboratory, we selected a sub-lethal drug concentration that enable us to combine these compounds with antimitotic agents, and facilitate the detection of potential drug synergisms. Thus, we decided to use 5 μM of ABT-199 or ABT-737 in MIA PaCa-2 and A549 cell lines and 2.5 μM in HCT-116 for subsequent combination experiments.

Once the appropriate drug doses were selected, we assessed whether BH3 mimetics sensitized cancer cells to the action of antimitotic agents during 24h or 48h incubations.

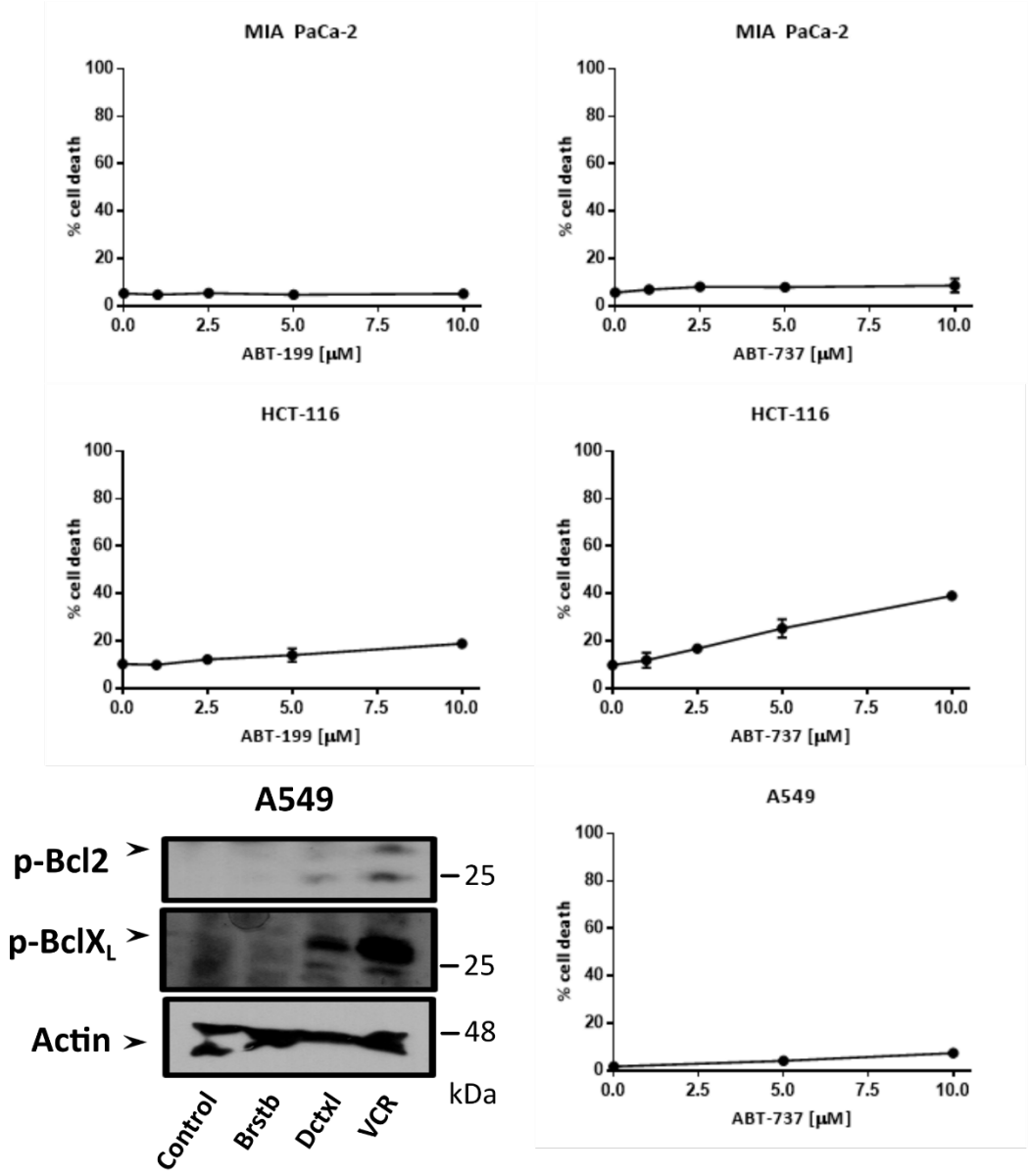

Figure 4.3 | Drug sensitivity of different cancer cell lines to BH3 mimetics. HCT-116, MIA PaCa-2 and A549 cell lines were treated with BH3 mimetics ABT-199 and ABT-737 at different doses for 24h. Cell death was quantitated by flow cytometry analysis determining phosphatidylserine exposure by Annexin V staining. Data are presented as mean ± SD from n=2-3 independent experiments. In addition, a representative western blot illustrating phosphorylation of Bcl-2 and Bcl-X_L when A549 cells were treated with antimitotic agents (barasertib 5 μM, docetaxel 10 μM and vincristine 1 μg/ml) for 24h.

As illustrated in **Figure 4.4** (below), after 24h of drug incubation, cell viability was practically not compromised at all. Small increases in apoptotic levels were seen in the combination of antimitotic agents with ABT-737, particularly in the case of HCT-116 and A549 cell lines. Again, HCT-116 presented the highest amount of apoptosis among the three cell lines studied after short periods of drug exposure. Nevertheless, longer incubation times rendered more promising results. Combinatory regimens of antimitotic drugs and ABT-737 dramatically enhanced apoptosis induction *in vitro* in almost all of cell lines tested. Cell death potentiation was especially striking in the case of A549 cells

and, in a lesser extent, in MIA PaCa-2 cells. Conversely, in HCT-116 cell line, the differences in the amount of apoptosis between drug combinations and individual treatments were moderate and similar to an additive effect (except the combination of barasertib plus ABT-737). Among the different antimitotic agents tested, combination of vincristine with ABT-737 showed the highest apoptotic rate, followed by docetaxel and barasertib combinations in the majority of assessed cell lines. The reason of these sensitivity differences among the different mitotic drug combinations, may arise as a consequence of drug intrinsic mechanisms. In particular, the sensitivity pattern of the drug combinations follows the same configuration observed with the antimitotic drugs alone. By contrast, ABT-199 drug combinations yielded lower potentiation effects than those obtained with ABT-737, reaching at best, an additive effect.

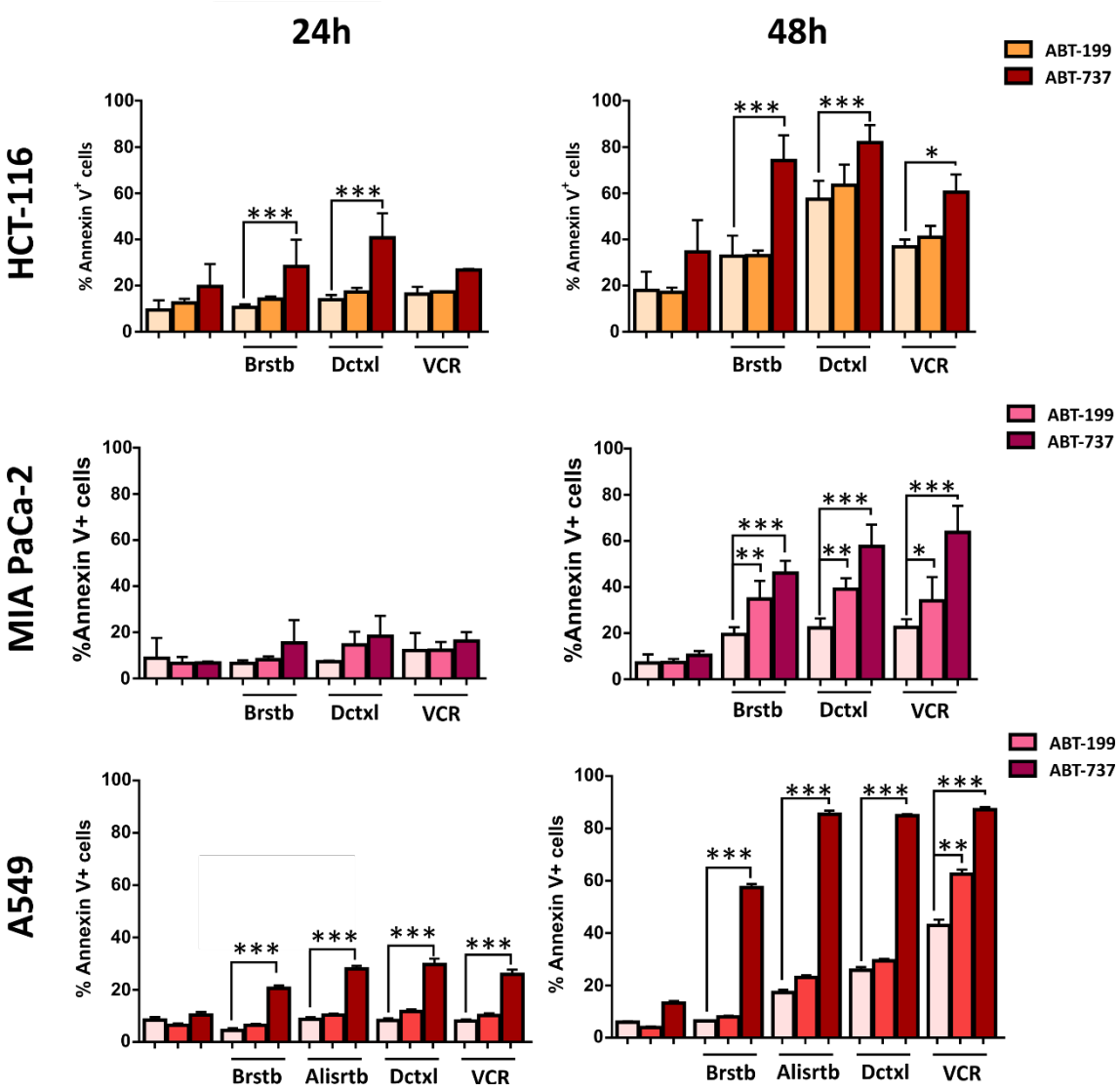

Figure 4.4 | BH3 mimetics potentiates cell death induced by antimitotic drugs. HCT-116, MIA PaCa-2 and A549 cell lines were treated with different antimitotic drugs (barasertib 5 µM, docetaxel 10 µM, vincristine 1 µg/ml and alisertib 5 µM) alone or in combination with BH3 mimetics (ABT-199 and ABT-737; 5 µM) for 24h or 48h. Cell death was quantitated by flow cytometry analysis determining phosphatidylserine exposure by Annexin V staining. Data are presented as mean ± SD from n≥3 independent experiments.

Statistical analysis was performed by using one-way ANOVA with Tukey post-test, where *p<0.05; **p<0.01; ***p<0.001.

The increased antitumour efficacy of ABT-737 combinations compared to that exerted by ABT-199 may be a consequence of the different selective inhibitory properties of these compounds. As described previously, while ABT-737 has a wider selection of targets (Bcl-X_L, Bcl-2 and Bcl-W), ABT-199 can only counteract the pro-survival function of Bcl-2[12,542]. Moreover, although in some cases a particular dependency on one anti-apoptotic protein may develop, generally, cancer cells could compensate this deficiency with other pro-survival members (like Bcl-X_L and Mcl-1). In the particular case of mitotic blockade, it has been reported that a specific addiction to Bcl-X_L may exist[73,543]. In fact, effective sensitization by ABT-737 to taxanes (paclitaxel or docetaxel) has been observed in multiple cancer cell models (breast, prostate, melanoma, hepatoblastoma)[544–547], as well as in xenograft models[548]. Another study demonstrated that specific BH3-mediated inhibition of Bcl-X_L, effectively synergizes with mitotic blockers (taxol and nocodazol), but not with mitotic drivers, such as Aurora kianse B inhibitors or Mps1 inhibitors[543]. These latter compounds do not induce prolonged mitotic arrest and drive cells to aberrant mitosis rapidly overcoming SAC[543]. However, our data partially disagree with this interpretation. We observed an enhancement of cell death induction with combined treatment of Aurora A or B inhibitors with ABT-737, particularly in case of A549 cells in which sensitization was stronger. The authors reasoned that Mcl-1 could be responsible for the lack of sensitization of a specific Bcl-X_L inhibitor and its combination with mitotic drivers[543].

Under prolonged mitotic arrest, members of Bcl-2 family undergo several post-translational modifications that have a critical impact on their pro-survival functions, priming cells to mitotic or post-mitotic cell death[92,547]. As seen in **Figure 4.3**, Bcl-2 and Bcl-X_L become highly phosphorylated in presence of mitotic blockers such as docetaxel and vincristine, but not with barasertib that induce a quite short and transient mitotic arrest (as we will see later in **Figure 4.6**). It is a well-known fact that concomitant to prolonged mitotic blockade, Bcl-2 and Bcl-X_L are phosphorylated by mitotic cyclins (i.e., CDK1)[55,73,547]. It has been postulated that in their phosphorylated form, these anti-apoptotic proteins are less efficient in sequestrating Bax, hence priming cells to death, although this explanation is controversial[549]. This might explain the special vulnerability of cells treated with docetaxel or vincristine to ABT-737 administration. Moreover, this apoptotic priming induced by delayed mitosis in response to MTAs, has been shown to partially rely on the phosphorylation status of Bcl-X_L on Ser62[549]. The pro-survival protein Mcl-1 may also undergo post-translational phosphorylation upon mitotic arrest, but rather, in this case, phosphorylation affects protein stability. When phosphorylated by CDK1, phospho-Mcl-1 is subsequently ubiquitinated and degraded via proteasome[550]. Therefore, as claimed by Bennet and col., mitotic drivers like barasertib, did not induce a potent mitotic arrest and consequently, Mcl-1 levels and Bcl-X_L/Bcl-2 activities remain intact[543]. In this scenario, cells were not primed to die and treatment with antimitotic

agents will not sensitize cancer cells to BH3 mimetics. However, as previously noted, our results differ from these conclusions since barasertib does indeed sensitize cancer cells to ABT-737. For this reason, we focused our attention in trying to unravel the mechanisms of cell death induced by barasertib combined with ABT-737, particularly in A549 and HCT-116 cells. It is noteworthy to mention that the variability of cellular responses to drug combinations in the different cell lines tested, may derive from the particular dependency of a given cell line to anti-apoptotic proteins from Bcl-2 family. Perhaps, this interpretation could explain the reduced cell death potentiation observed in HCT-116 cell line.

Altogether, these results show a significant cell death potentiation when combining antimitotic agents with the BH3-mimetic ABT-737, especially in A549 and MIA PaCa-2 cell lines.

4.1.2. Study of the Mechanism of Cell Death Exerted by Barasertib and ABT-737 Combination.

Aurora B, as part of the CPC, localizes at the kinetochores in early mitosis to regulate chromosome-spindle interactions, sister chromatids cohesion and SAC signalling to ensure the proper segregation of the chromosomes[54]. In addition, during anaphase, CPC is relocated to the mid-zone to regulate cytokinesis[54]. Interestingly, although barasertib drives cells through aberrant mitosis, as it will be shown in **Figure 4.6**, cells do not spend much time restrained in mitosis and rapidly overcome SAC, exiting mitosis thanks to the inhibition of cytokinesis-related functions of Aurora B. Thus, cells reach G1 phase of the next cycle with overt aberrant morphological nuclear alterations (micronucleation, multinucleation and/or macronucleation) (as evidenced in **Figure 4.2**). Moreover, Aurora B inhibition did not promote cell death at the incubation times evaluated so far. For instance, we noticed that cells could persist in this state for long periods of time without triggering cell death. Thereby, we asked whether cell senescence could be activated in response to mitotic catastrophe in these experimental conditions.

Cellular senescence has been defined as a state of long-term and stable cell cycle arrest that is accompanied by the manifestation of a series of stereotyped phenotypic attributes[551]. Hallmarks of cell senescence include, yet not limited to: flattened, extended or enlarged morphology; increased senescence-associated β-galactosidase (SA β-gal) activity; increased levels of p16/INK4A, p53 and p21 levels, all of them important proteins involved in regulating the G1 restriction point; higher levels of DNA damage; the formation of senescence-associated heterochromatin foci; and the secretion of pro-inflammatory molecules and cytokines (such as IL-1, IL-6, IL-8, GM-CSF) that characterize the senescence-associated secretory phenotype (SASP)[552,553]. Accordingly,

we assessed SA β-gal activity in barasertib treated cells following the protocol described in section 3.7.1.1.

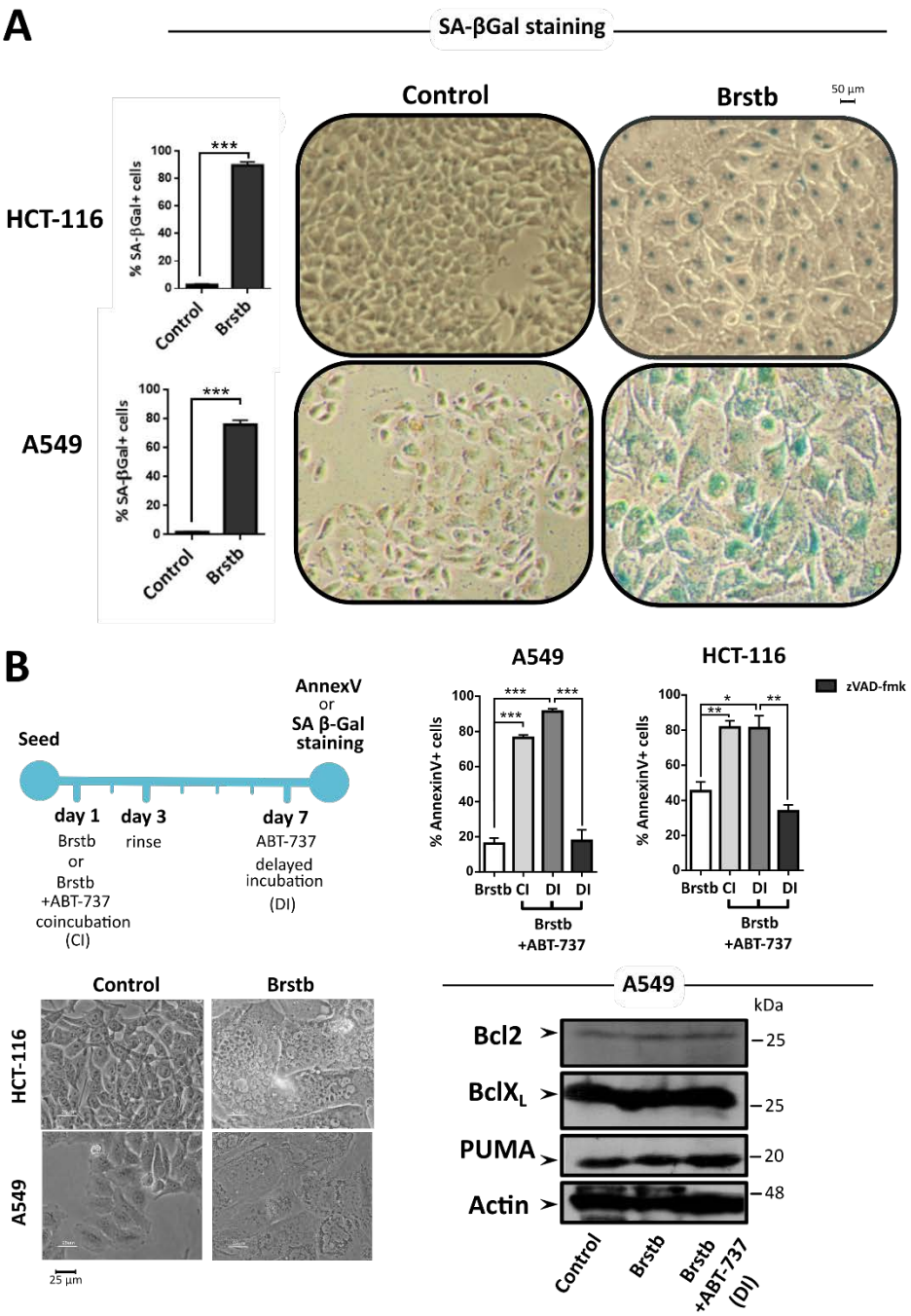

Figure 4.5 | Barasertib induces cell senescence and ABT-737 drives cell death. A. Representative images and quantification of senescence-associated β-Gal staining of HCT-116 and A549 cells subjected to barasertib treatment (5 µM). SA- β-Gal quantification was performed by manually counting the number of stained and unstained cells, expressing the final value in form of percentage from total cells. Statistical analysis was performed by using two-tail unpaired t test, where *p<0.05; **p<0.01; ***p<0.001. **B.** Time-line and protocol followed in SA- β-Gal staining and quantification, as well as in the cell death analysis after a delayed or concurrent incubation of ABT-737 (5µM). As indicated, A549 or HCT-116 cells, were seeded and 24h later, were treated with the indicated drugs (barasertib alone or the co-incubation (CI) of barasertib and ABT-737) for 48h, then rinsed. At day 7, ABT-737 was added to barasertib in a delayed fashion (delayed incubation, DI). In case of z-VAD-fmk (50 µM) addition, it was preincubated 1h before the delayed addition

of ABT-737. After 24h, cell death was analysed by annexin V staining on day 8. Data are presented as mean ± SD from n=3 independent experiments. Statistical analysis was performed by using one-way ANOVA test with Tukey post-test, where *p<0.05; **p<0.01; ***p<0.001. Additionally, immunoblots assessing the expression of Bcl-2, Bcl-X_L and PUMA proteins were generated. Images from control cells and barasertib-treated cells were also acquired before proceeding through SA- β-Gal staining with a phase-contrast microscope. Scale 25 μm or 50 μm as indicated.

First, and prior to staining, cell morphological changes suggestive of senescence were evaluated by light microscopy. As depicted in **Figure 4.5**, barasertib treated cells display a flattened and enlarged morphology, reminiscent of senescent cells. Nuclear morphological traits characteristic of mitotic catastrophe (multinucleation and macronucleation) were also detectable (Figure 4.2 and Figure 4.5). Moreover, increased SA β-gal activity was observed in both HCT-116 and A549 cells treated with the Aurora kinase B inhibitor.

Cellular senescence is considered to be a key intrinsic oncosuppressive mechanism[553], even more important than cell death in terms of tumour suppression[553,554]. However, the senescence-associated inflammatory response is thought to pose both protective and detrimental consequences in carcinogenesis and tumour prevention[555]. In fact, by modulating the tumour microenvironment, many SASP molecules have been shown to promote oncogenic transformation and growth of malignant cells in several cancer models[555,556]. Moreover, senescent cancer cells could entail more hazards than just the pro-inflammatory related ones. For instance, the irreversibility of senescent growth arrest has been questioned. Several studies have shown that senescent cancer cells may have the ability to escape and resume proliferation[556]. In particular, when senescence induction is associated with mitotic defects and polyploidization, cancer cells that subsequently undergo depolyploidization can recover their ability to proliferate[557]. For these reasons, eliminationof senescent cells emerges as a suitable therapeutic strategy in cancer and considerable efforts have been directed to develop senolytic agents for cancer and age-related disorders.

Next, we analysed if the ability of ABT-737 to sensitize cells to barasertib treatment was related to its mitosis targeting effect, or rather to senescence induction. Hence, we evaluated and compared the sensitization ability of ABT-737 when was co-incubated with barasertib to that exerted when both drug incubation and responses were delayed in time. As indicated in **Figure 4.5**, A549 and HCT-116 cells were cultured for 24h and then, were incubated with barasertib alone or the combination of barasertib and ABT-737 (co-incubation, CI). After 48h of drug exposure, cells were rinsed to eliminate the drugs from the media. At day seven, once the senescent phenotype had been developed, some of the cell culture wells treated with barasertib alone on day one, were incubated with ABT-737 during 24h (delayed incubation, DI). Afterwards, apoptosis induction was measured by annexin V binding.

Interestingly, ABT-737 can rescue senescent cells from this irreversible growth arrest and force them to die, whether it is administered concurrently or after an elapsed time interval. Moreover, cell death process executed under these conditions was caspase-dependent, since pre-incubation with z-VAD-fmk prevented cell death. To delve into the mechanisms underlying this molecular addiction, we assessed the levels of several Bcl-2 familly members by Western blot analysis (as described in section 3.13). Our data showed that while the levels of pro-survival Bcl-2 and Bcl-X_L proteins remain roughly constant, there is a slight upregulation of the BH3-only protein PUMA. Senescent cells have indeed increased levels of G1 checkpoint proteins including p21, $p16^{INK4A}$ and $p53^{555}$. Moreover, according to ATCC database, A549 cells express a wild-type p53 gene and one of its main transcriptional targets is PUMA protein. Thus, under these conditions, senescent cells with increased p53 levels, could be primed to death when an apoptotic stimuli, such as ABT-737, is administered. Moreover, the ability of ABT-737 to target and eliminate senescent cells has been previously reported[558,559]. In fact, the senolytic properties of ABT-737 were demonstrated in two independent *in vivo* models of senescence[558,559]. In this way, chemotherapeutic removal of senescent cancer cells from premalignant lesions with senolytic agents, could be beneficial in neoplasias in which the molecular features endowed by cell senescence drive carcinogenesis. Additionally, acquired therapy resistance through senescence in human cancer may also be benefited by this therapeutic strategy.

In conclusion, our data indicate that upon barasertib treatment, cells acquire a senescent phenotype and ABT-737 is able to elicit death in senescent cells in a caspase-dependent manner.

4.1.3. Cell Fate Profiles of Antimitotic Drugs.

Mitosis is a complex and highly dynamic process that if not completed, led to mitotic arrest followed by cell death by mitotic catastrophe or cell survival through alternative paths. Therefore, endpoint methods like flow cytometry analysis of cell death and others, do not provide information about whether the cell follows a particular path after mitotic blockage or exactly when cell death occurs. Thus, these kind of approaches are not appropriate to study mitotic catastrophe and its underlying mechanisms[55]. In order to be able to study the contribution of mitotic catastrophe to the antitumoral action of these drugs, and faithfully rebuild the complete 'history' of cell death, novel techniques based on time-lapse fluorescence or high-throughput microscopy have been developed[62,533,534].

To that end, we have utilized two genetically modified cell lines A549 H2B-GFP and MIA PaCa-2 H2B-GFP, both of which harbour in their genome a version of histone H2B fused to the green fluorescent protein (GFP). In this way, we were able to track the different morphological changes that chromatin experiences during the cell cycle and

specifically during mitosis. Thus, to study the contribution of mitotic catastrophe to the cell death induced by antimitotic drugs, time-lapse microscopy experiments were performed as described in section 3.7.3.2. Briefly, cells were cultured for 24h, and then antimitotic agents were added to the medium and, fluorescence images were acquired every 15 minutes for 48h. Thereafter, image sequences were analysed and individual cells were tracked down to determine their behaviour. Depending on the condition, between a minimum of 50 and a maximum of 120 cells were analysed. Finally, cell fate profiles were generated for all conditions.

Data from time-lapse analysis are presented in **Figure 4.6**. This type of analysis have been depicted in a manner that facilitates comparison between the different conditions but without masking its inherent complexity[62]. In these cell fate profiles, each line represents one cell. The length of each line depicts the duration of each cell behaviour. Finally, the different cell behaviours were plotted in different colours in each single line[62]. In the data presented below, cells may undergo different cell fates and cell behaviours: interphase; normal mitosis; slippage, when cells are arrested and undergo an abnormal mitosis without properly segregating the genetic material; death in interphase, if cell death occurs during interphase before entering mitosis; mitotic cell death, if cells die during mitosis; death after slippage, when cells manage to escape the mitotic checkpoint and reach the next G1 stage and succumb shortly after or a few hours later; and finally survival after slippage where cells manage to escape from mitotic blockade, slipped and reach the next G1 phase usually presenting morphological attributes of mitotic catastrophe, that is multinucleation macronucletation and/or micronucleation. (For more information see **Table 3.3.**)

As highlighted in the pioneering work from Gascoigne & Taylor[62], tumour cells display extensive intra- and inter-line variations in cell fates during prolonged mitotic arrest. We also found these same fluctuations in cell behaviour under the action of different classes of antimitotic drugs, underscoring that the level of complexity is profound. The vast majority of A549 and MIA PaCa-2 control cells, underwent normal mitosis with a normal timing during the course of the experiment. It should be noted that MIA PaCa-2 cells appeared to be more unstable, since some aberrant mitosis and cell death in interphase were observed in these cells in control conditions. It cannot be excluded that MIA PaCa-2 cell were more sensitive to phototoxicity provoked by the laser beam inducing cell death in interphase in a higher proportion of cells.

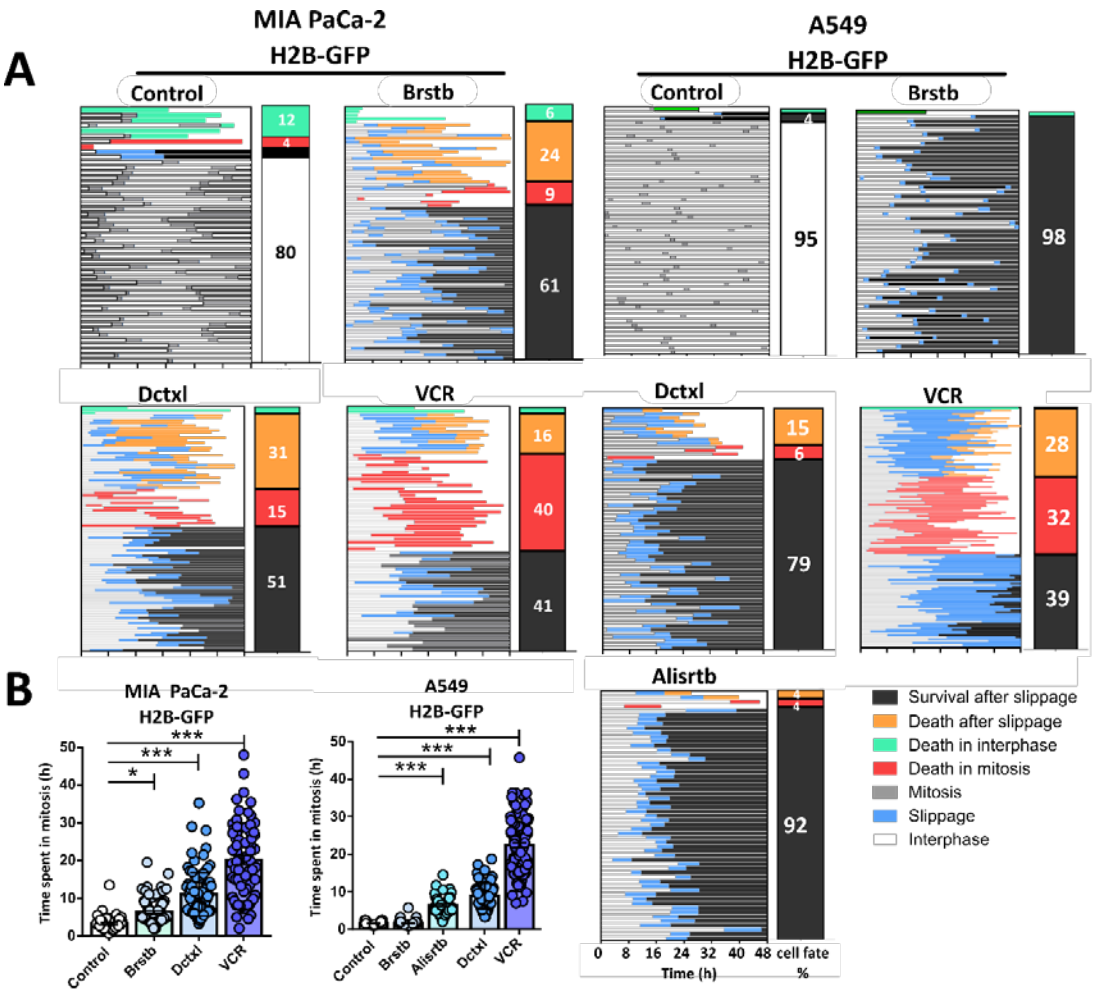

Figure 4.6 | Cell fate profiles of cancer cells exposed to different antimitotic agents. **A.** Cell fate profiles of A549 or MIA PaCa-2 H2B-GFP cells exposed to barasertib (5μM), docetaxel (10μM), vincristine (1μg/ml) or alisertib (5μM) and monitored by time-lapse microscopy during a course of 48 hours. Data for approximately 100 cells were acquired for each condition and presented in the plots. Each horizontal line represents one cell. The length of each line denote the duration of each cell behaviour. Finally, the different colours plotted in a single line illustrate the distinct behaviours each cell may adopt. The percentage of cell experiencing each cell fate during the experiment are plotted in a vertical bar at the right of each cell fate profile. **B.** From the data collected in the fate profiles, the mean time that cells spent in mitosis were analysed in the total population of cells. Time that cells spent since mitotic entry to mitotic exit was measured and plotted in scatter dot plots. Data derived from at least n=2 independent experiments. In B. data are presented as mean ± SD. Statistical analysis was performed by using two-tail unpaired t test, where *p<0.05; **p<0.01; ***p<0.001.

Treatment with the Aurora kinase B inhibitor barasertib in A549 cells, drove these cells through aberrant mitosis that was rapidly discontinued, which lead to abnormal mitotic exit without cytokinesis. In these conditions, nearly 100% of the population survived after slippage during the 48h time period in which cells were tracked. MIA PaCa-2 cells behaved a bit differently in response to barasertib and displayed multiple cell fates. In these cells, although a great percentage (61%) of the population survived after slippage, a considerable proportion of cells died after slippage (24%) and in a lesser extent during mitosis (9%). In both cell lines, cells that managed to

slip out of mitosis acquired the aberrant and obvious nuclear alterations characteristic of mitotic catastrophe (**Figure 4.2**). Additionally, some multinucleated tetraploid cancer cells did not become arrested by p53-dependent G1 checkpoint and were able to re-enter the cell cycle and undergo a successive round of mitosis. The latter occurred in MIA PaCa-2 cell lines that harbour a mutation in p53, but also in A549 p53 wt proficient cells.

Docetaxel treatment provoked more or less the same response that barasertib in A549 cells, with the difference that up to 15% of cells died after slippage and 6% succumbed during mitosis. Again, MIA PaCa-2 cells seemed to be more sensitive to docetaxel than A549 cells, only surviving after slippage 51% of the population. The rest either died in mitosis (15%) or after slippage (31%). Importantly, both in A549 and MIA PaCa-2 cells, docetaxel instigated a longer mitotic arrest than in barasertib or the time of mitosis in control cells. Upon vincristine treatment, both A549 and MIA PaCa-2 cells were especially sensitive to this compound and a significant amount of the population died during mitosis (40% in MIA PaCa-2 and 32% in A549 cells), or after slippage (16% in MIA PaCa-2 and 28% in A549 cells). Noteworthy, the percentage of cells dying in mitosis was significantly higher than in the other treatments. Interestingly, the proportion of cells succumbing during mitosis seemed to positively correlate with the time cells remained arrested during this phase in the different conditions.

As illustrated in **Figure 4.6**, the duration of mitotic arrest was different under each condition. Barasertib induced just a short and transitory mitotic delay, which was rapidly overridden, and that was significantly different to the duration of normal mitosis in MIA PaCa-2, but not in A549 cells. Therefore, at least in A549 barasertib-treated cells rather than experiencing a mitotic arrest, cells were driven through an aberrant mitosis but with an ordinary timing. Barasertib targets Aurora B, a Ser/Thr kinase with crucial functions in chromosome bi-orientation, SAC signalling and cytokinesis[54]. In particular, Aurora B is key to the recruitment of SAC components[53]. It promotes kinetochore localization of Mps1, which is fundamental for initiating SAC cascade and assembly[56]. Thus, when Aurora kinase B is inhibited, SAC and MCC complexes are not assembled and cells are allowed to progress through aberrant mitosis with brief or any mitotic blockade. In addition, thanks to the inhibition of cytokinesis-related functions of Aurora kinase B[54], cells exit mitosis without cytokinesis and reach G1 phase of the next cycle with overt aberrant morphological nuclear alterations (micronucleation, multinucleation and/or macronucleation (**Figure 4.2**).

Alisertib, however induced a longer mitotic arrest than barasertib, but shorter than those induced by MTAs. Alisertib targets Aurora kinase A which has important functions in mitotic entry, centrosome maturation, duplication and mitotic spindle formation[90,94]. Therefore, abrogation of Aurora A activity has been shown to provoke a transient SAC-dependent mitotic arrest which is followed by slippage and induction of apoptosis in the aneuploid daughter population[52,90]. Conversely, MTAs significantly induced extended mitotic arrest than during normal mitosis or under barasertib

treatment. By targeting microtubules, docetaxel and vincristine efficiently activate SAC triggering a potent mitotic blockade. Since cells cannot reorganize microtubules and satisfy the mitotic checkpoint, they remain arrested until one of the cell fates described above ensues. Of both MTAs, vincristine significantly induced the most stringent mitotic arrest. These observations can be explained as follows: Since microtubule destabilizers like vincristine completely depolymerize microtubules, they cannot attach to the kinetochore plate and this provokes a strong SAC signal. On the other hand, since taxanes are microtubule stabilizers, small microtubules may persist and the checkpoint signal is weaker[51].

As anticipated by Gascoigne & Taylor[62], the level of complexity of these kind of studies is deep and data could seem at first overwhelming. The inter- and intra-line variations of cell behaviours observed in this work, although expected, further complicates the molecular scenario of mitotic catastrophe and the ensuing cell fates in response to antimitotic drugs. These fluctuations in response to antimitotic agents could be addressed by the 'competing networks' model proposed by the same authors. Although the genetic background of a particular cell line may influence the rates of mitosis, as well as cell death thresholds, the molecular networks from this model probably occupy broad ranges and may vary from cell to cell[62]. Another simpler and possible alternative is that, although tumour cell lines are inestimable research tools, they may evolve in culture and consequently may not be genetically homogenous[560]. By observing the cell fate profiles, it becomes apparent that these cell fates do not correspond to the observed cell death rates in Figure 4.1. On the other hand, our experimental approach cannot be considered as non-invasive since viral GFP transfection and fluorescence imaging procedures could affect to cellular behaviour. Alternatively, this could also indicate that cells may undergo a cell death mechanism distinct from apoptosis or without producing PS exposure.

Another important observation drawn out from cell fate profiles is that apparently, mitotic cell death increases with treatments that induce a prolonged mitotic arrest. Although this has been contested, the duration of mitotic arrest has been proposed to influence and dictate cell fate[55]. Several independent and compelling pieces of evidence argue in favour for this notion, including the 'competing networks' model at least in the influence that it may have on mitotic cell death and a post-mitotic response[62,543,561,562]. Thus, so far the longer the time cells spend in mitosis, the more pro-apoptotic signals probably accumulate and as a consequence, cells will die during mitosis rather than exit and undergo a post-mitotic cell fate. This issue will further discussed in following sections.

Taken together, these results underscore the complexity of cell fates and cell responses to antimitotic drugs that vary depending on the drug target and highlight the inter- and intra-line variability that these cell responses may entail to the final outcome.

4.1.4. Cell Fate Profiles of Antimitotic and BH3 mimetic Combinations.

According to the 'competing networks' model, cell fate in response to abnormal mitosis is dictated by two competing, yet independent molecular networks: the slow but persistent APC/C-independent Cyclin B1 degradation that occurs even in presence of active SAC, and the accumulation of pro-apoptotic signals[62,63]. Then, it would be feasible to modulate cell fate decisions and improve the effectiveness of antimitotic drugs by accelerating or strengthening the pro-apoptotic signals or by delaying mitotic exit[92]. As clearly demonstrated by our own work and by others, BH3 mimetics are reliable therapeutic tools that can tip the balance in favour of cell death when aberrant mitosis occurred in response to antimitotic agents. Therefore, we then pursued to increase our understanding in the mechanisms that govern cell fate decisions in response to mitotic perturbations. Additionally, we also wanted to delve deeper into the role Bcl-2 family fulfil in this same context of cell fate resolution under mitotic distress. To accomplish these goals, MIA PaCa-2 H2B-GFP and A549 H2B-GFP cells were subjected to antimitotic drugs in combination with the BH3 mimetic ABT-737 and individual cells were tracked down along the 48h course by time-lapse imaging to determine their behaviour. Thereafter, cell fate profiles for all conditions were constructed and analysed. Complete data sets are presented below in **Figure 4.7**.

The mechanism by which ABT-737 enhances apoptosis seems to be different from one type of drug to another. In barasertib-treated cells, as we have seen in the previous section (**Figure 4.6**), an important fraction of cells manage to slip out of mitosis and survive. When ABT-737 was added concurrently with the Aurora kinase B inhibitor, the proportion of cells that died after slippage considerably increased. Conversely, ABT-737 did not accelerated mitotic cell death and the percentage of cells dying during mitotic arrest remained unaffected when compared to barasertib treatment in A549 cells. As regards to A549 cells treated with alisertib and ABT-737, cell fate profiles showed a slightly different pattern. In particular, mitotic cell death was noticeably increased to 16% compared to alisertib treatment alone, whereas death after slippage augmented considerably more (29%). Nonetheless, in MIA PaCa-2 cell line both mitotic cell death and death after slippage augmented in response to combinatory treatment with ABT-737 and barasertib. By contrast, when targeting microtubules with docetaxel and vincristine in combination with ABT-737, the frequency of mitotic cell death was dramatically enhanced in both A549 and MIA PaCa-2 cells. Interestingly, these increments in mitotic cell death rates considerably escalated with those antimitotic agents that provoked a longer mitotic arrest, that is, especially with the MTAs docetaxel and vincristine. Since barasertib prompted minimal, if any, mitotic blockade, especially in A549 cells, the addition of ABT-737 affected post-mitotic death rather than mitotic cell death in this case.

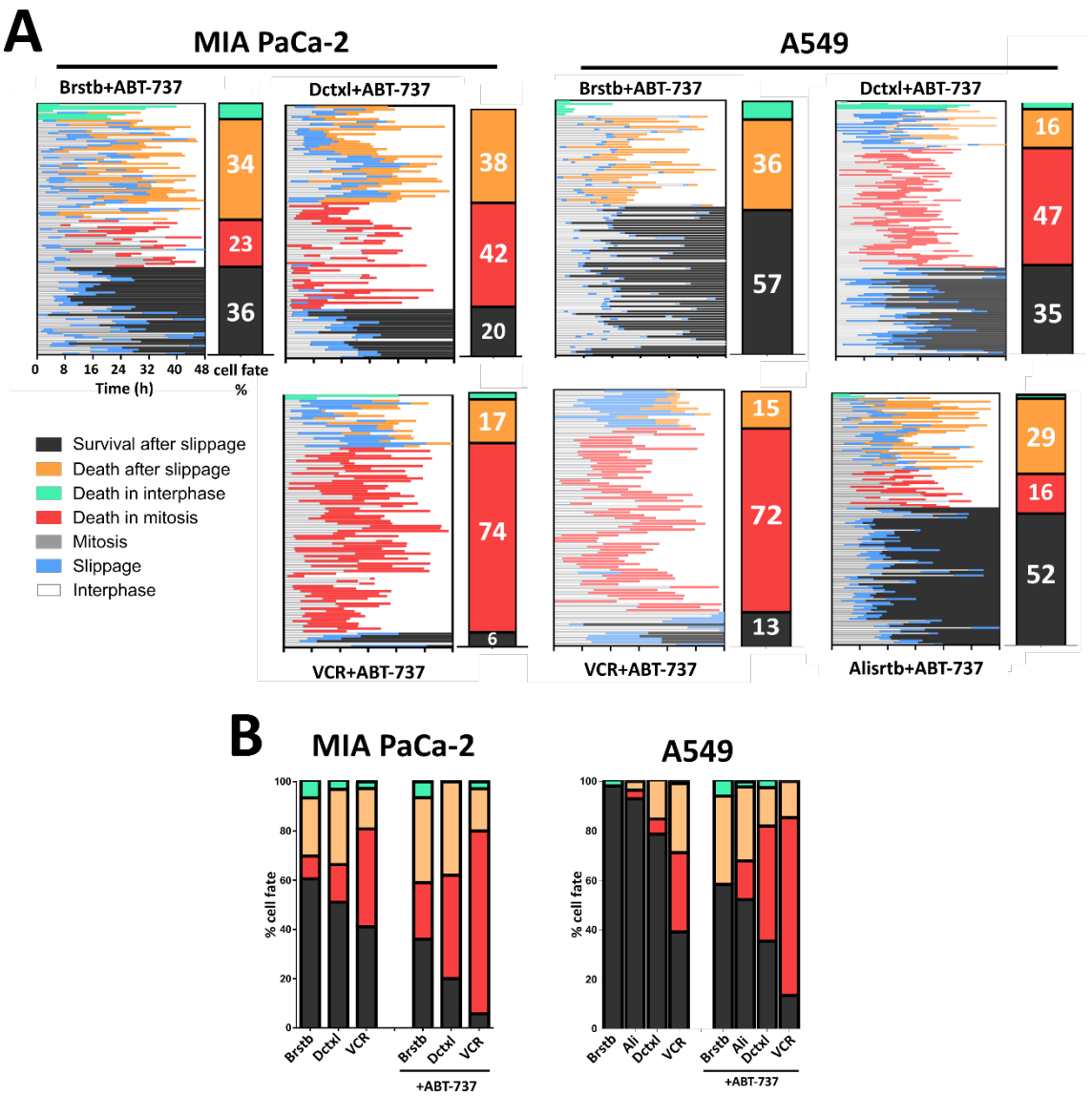

Figure 4.7 | Cell fate profiles of cancer cells exposed to different antimitotic agents combined with the BH3 mimetic ABT-737. A. Cell fate profiles of A549 or MIA PaCa-2 H2B-GFP cells exposed to barasertib (5 µM), docetaxel (10 µM), vincristine (1 µg/ml) or alisertib (5µM), combined with 5 µM of ABT-737, and monitored by time-lapse microscopy during a course of 48 hours. Data from approximately 100 cells were acquired for each condition and presented in the plots. Each horizontal line represents one cell. The length of each line denotes the duration of each cell behaviour. Finally, the different colours plotted in a single line illustrate the distinct cell behaviours. At the right of each cell fate profile, the percentage of cells that experienced each cell fate during each condition are depicted in a vertical bar. **B.** End-point cell fates of cancer cells from the data derived from the cell fate profiles are presented. n=2 independent experiments for each condition.

As discussed earlier, Bcl-2 family are key determinants of cell fate decision upon aberrant mitosis. Although several laboratories have struggled to decipher the particular involvement of each member, no general consensus has been met so far. Some studies point to Mcl-1 as a molecular timer that influences survival during mitosis[563–565]. Mcl-1 levels have been shown to decline under prolonged mitotic arrest induced by MTAs[564]. Genetic manipulation either by overexpressing or depleting Mcl-1 levels, have been

shown to delay mitotic exit or promote mitotic cell death respectively[563]. Others, however, point to other Bcl-2 family members like Bcl-X_L to hold a major role in cell death during mitotic arrest[70,72,543,549,566,567]. For instance, a specific Bcl-X_L inhibitor (WEHI-539), has also been reported to accelerate death in mitosis[543]. By contrast, other studies showed that when Bcl-X_L was depleted or pharmacologically targeted with ABT-737 or its derivative ABT-263, cell fate massively switched from slippage to mitotic cell death in paclitaxel-treated or Cdc20-depleted cells[549,568]. Accordingly, overexpression of Bcl-X_L increased survival and slippage in a breast cancer cell model[549]. Even Bcl-W has been involved in determining the duration of mitotic blockade prior to cell death or slippage[569].

In our experimental settings, we cannot rule out the contribution of any particular Bcl-2 family member. We evidenced in endpoint experiments that targeting Bcl-2 with ABT-199 have a partial or additive effect on cell death induced by antimitotic agents. This potentiation of cell death was considerably enhanced when Bcl-2, Bcl-X_L and Bcl-W were co-targeted by ABT-737. However, our results seem to point out that ABT-737 has an additive or cumulative effect over that produced by ABT-199 combinations, but a dramatic effect over antimitotic drugs alone. This observation suggests a redundant and cumulative effect of Bcl-2, Bcl-X_L and Bcl-W. Cell fate profiles illustrated that ABT-737 accelerated cell death triggered by MTAs and cells preferentially succumbed during mitosis rather than once cells have escaped and faced G1 checkpoint. Therefore, targeting these Bcl-2 family members switched cell fate to mitotic cell death. This enhancement in mitotic cell death escalated with treatments that triggered an extended mitotic arrest like vincristine. One may think that this increased mortality during mitosis, could be explained by the fact that Mcl-1 levels decline during protracted mitosis[564]. Whether this notion is simply due to the fact that cells have more time to accumulate death signals, or rather, owes to alternative effects like Mcl-1 degradation, could not be clarified with the available data.

To sum up, we cannot exclude the contribution of any Bcl-2 member to cell fate decisions, but our data suggest that probably all of these anti-apoptotic proteins may have redundant and cooperative roles in cell fate decisions during aberrant mitosis. These results also suggest that cell fate during aberrant mitosis could be conditioned, among other things, by the time cells spend arrested in mitosis. Therefore, by reinforcing and strengthening death signals, we can accelerate cell death during mitosis and avoid cells to escape and potentially become genetically more unstable and malignant.

4.1.5. Time-based Analysis of Cell Fates. Does Duration of Mitotic Arrest Dictate Cell Fate?

As indicated in the previous section, according to the competing network model, cell fate after an aberrant mitosis depends on the progressive accumulation of death signals or the slow but continuous degradation of Cyclin B1 that drives mitotic exit (see **Figure. 1.11** in section 1.3.4). The molecular threshold that is breached first will determine whether cells die in mitosis or experience a post-mitotic response, either of cell death or survival. Thus, in this dynamic interplay, time stands out as a potential variable influencing cell fate decisions. Although it has never gained general consensus, length of mitotic arrest could indeed affect the final outcome. Several studies support this notion[62,543,561,562]. For instance, by accelerating or strengthening cell death signals or by targeting and delaying mitotic exit, the balance could be shifted towards cell death. Our results shown thus far, also appear to point in that direction. Thereby, we analysed whether the time that cells spent blocked in mitosis determines its cell fate.

We quantitated and analysed the time that cells devoted to mitosis in each of the different types of cell fate that each drug provoked. From **Figure 4.8** presented below it can be inferred that there is a tendency (in some cases statistically significant) in the survival subpopulation (cells that slipped out of mitosis and survived), to manifest reduced mitotic duration times, especially in the combinatory treatments in both A549 and MIA PaCa-2 cells. This could also be appreciated in the analysis of **Figure 4.9**. Here, the mean mitotic duration of cells experiencing mitotic death is represented and was compared to the mean time spent in mitosis by surviving cells from the same population or experimental condition. In this way, all conditions are gathered in a single plot and can be compared collectively, which allows to easily detect the differences between DiM and Survival subpopulations among the different experimental conditions. Altogether, in **Figure 4.8** and **Figure 4.9**, cells that slipped out of mitosis, and especially those who survived, have significantly shorter mitotic arrests than those who died in mitosis in both cancer cell lines, with the exception of vincristine treatment alone. From the data presented in these two figures, we can deduce that cells that manage to survive probably achieve this goal as a consequence of the reduced time that they spent blocked in mitosis. In this way, cells manage to rapidly escape from this phase before accumulation of death signals triggers mitotic cell death.

Moreover, we have previously seen that the different antimitotic drugs used in this work produce varying lengths of the duration of mitotic arrest (**Figure 4.6**). Thus, we decided to analyse the correlation between cell fate percentages in the different experimental conditions and the time that cells, either undergoing DiM or slippage, spent arrested in mitosis. As illustrated in regression analysis from **Figure 4.9**, if we take a closer look into the slippage-prone subpopulation, those conditions (drugs) that provoked a brief mitotic arrest, hence having a low mitotic duration, displayed the highest slippage rates. On the contrary, those treatments that originated a protracted

mitotic blockade and consequently the mitotic duration was elevated within the subpopulation of cells escaping from mitosis, slippage was not so frequently observed. By contrast, within the DiM subpopulation, drugs that triggered low levels of mitotic death also concurred with shorter mitotic arrests, whereas treatments with high DiM rates, coexisted with longer mitotic blockade. In other words, in the slippage-prone subpopulation, cell fate and the duration of mitotic arrest manifested a significant negative correlation, whereas within the DiM population, cell fates and time spent in mitosis significantly revealed a positive correlation. While all the aforementioned was hold true in A549 cells and reached statistical significance, the relationship between these two variables were not so evident in MIA PaCa-2 cells. These results agree with the competing network model proposed by Gascoigne & Taylor[62]. It is consistent to think that cells that manage to survive, spent less time in mitosis and hence escape from dying in mitosis and endure, rather than breach the cell death threshold and succumb to mitotic death. However, our data differs from another study which showed that cells that underwent slippage exhibited longer mitotic arrest times than those that underwent mitotic death. Most likely, these disparities arise due to the fact that authors were assessing the specific influence of MYC transcription factor in cell fate during mitotic arrest, which is completely different to our experimental conditions[562].

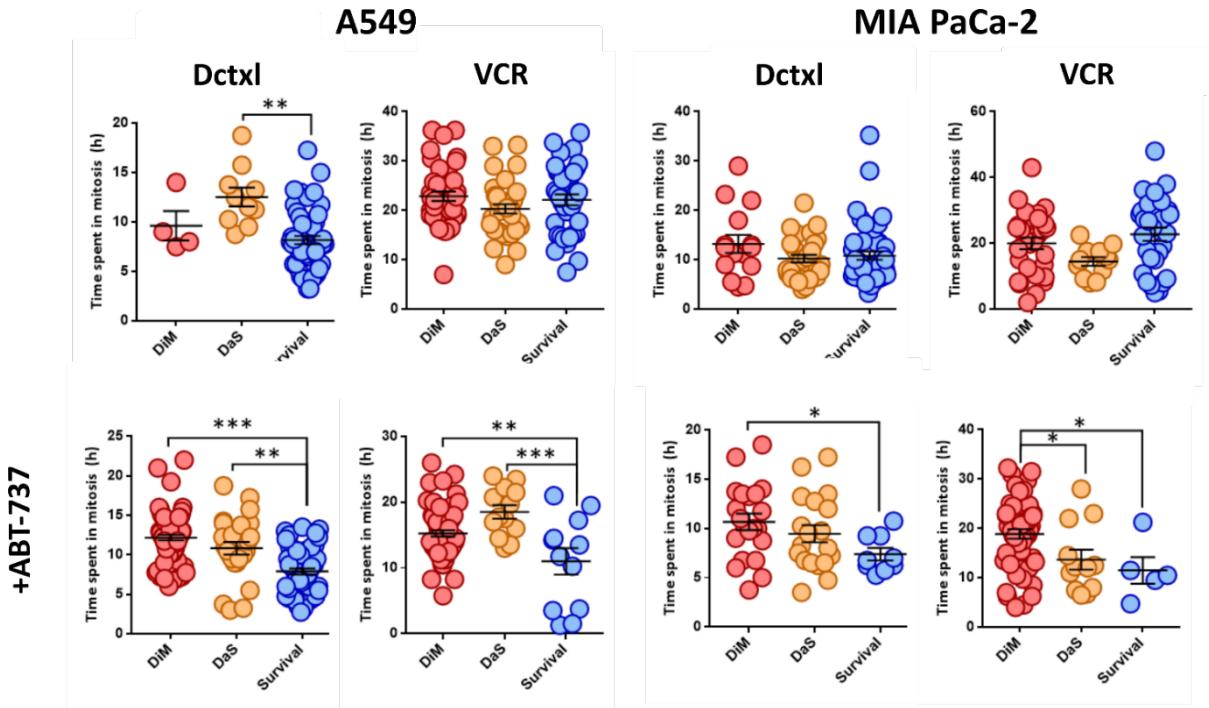

Figure 4.8 | Time-based analysis of mitosis duration in different cell subpopulations. From time-lapse experiments, the duration of mitosis for each cell were collected. For cells undergoing different cell fates: Death in Mitosis (DiM), Death after Slippage (DaS) and Survival after slippage, the time that cells spent in mitosis were measured and are presented in the scatter dot plots. Statistical analysis was performed using one-way ANOVA with Tukey post-test, where *p<0.05; **p<0.01; ***p<0.001. Data are presented as mean ± SD from n=2 independent experiments.

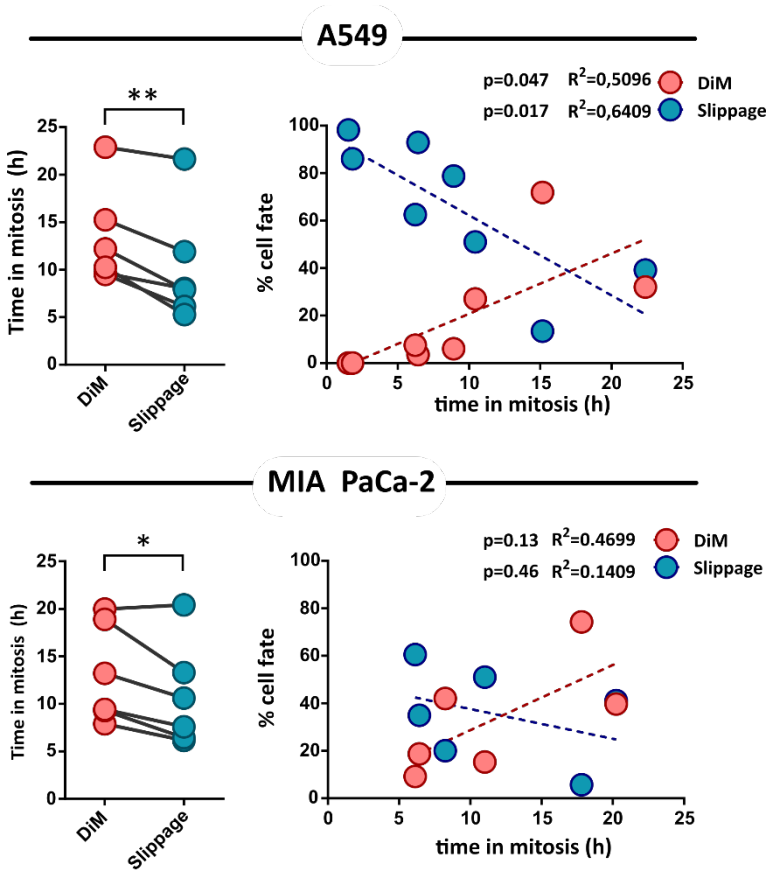

Figure 4.9 | Time in mitosis during DiM and slippage. From time-lapse experiments, the duration of mitosis for each cell were collected and analysed. In the paired analysis on the left is represented the mean time cells were arrested in mitosis with the different treatments and within the indicated subpopulation of cells (either those that underwent slippage or those who died in mitosis (DiM)). Lines connect cell subpopulations from the same experimental condition. In the correlation analysis between time arrested in mitosis and the percentage of cell fate (either DiM or slippage) for a given treatment were plotted. Statistical analysis was performed using two-tail paired t test in the paired analysis, where *p<0.05; **p<0.01; ***p<0.001. In the correlation or linear regression analysis, R square and p values are indicated.

Since the BH3 mimetic ABT-737 targets pro-survival members of the Bcl-2 family, which play a determinant role in cell fate decisions during aberrant mitosis, ABT-737 would enhance the strength or would cooperate in the accumulation of pro-death signals during mitotic arrest. As previously highlighted, in our experimental conditions, ABT-737 increased the rate of cells that die during mitosis, and also, possibly in a lesser extent, after mitotic slippage. Therefore, we next wondered whether ABT-737 not only increases DiM or post-mitotic cell death rates, but also accelerates them. For this purpose, in the mitotic cell death (DiM) subpopulation, we compared the time that cells undertook from entering mitosis to experience cell death, when treated with the antimitotic drugs alone or with its combination with ABT-737. In case of cells overcoming a post-mitotic cell death response, the analysed variable was the time that cells consumed from escaping mitosis until they suffered from cell demise.

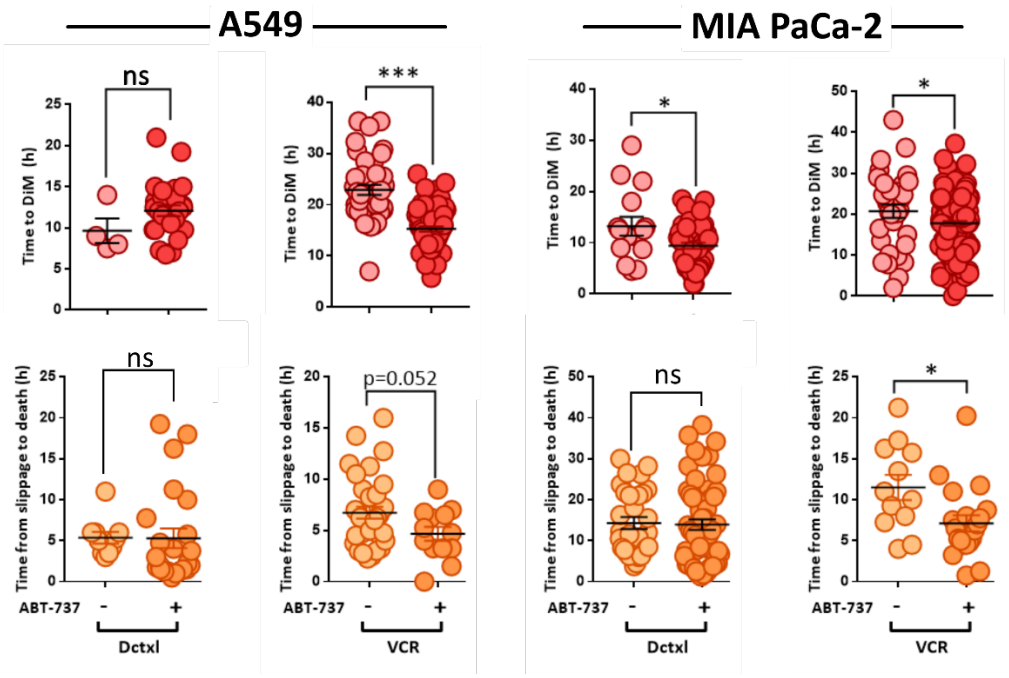

Figure 4.10 | Time to cell demise. From time-lapse experiments, the time cells took to eventually reach to cell demise were calculated and analysed. Scatter dot plots show the kinetics of cell death in the different cell fate subpopulations when ABT-737 were co-administered or not with the corresponding antimitotic drugs. In case cells died during mitosis (DiM), the time cells devoted from mitotic entry till they experienced cell death were represented. In the case of cells that suffered from Death after Slippage (DaS), the time cells took from exiting mitosis to cell death were presented. Statistical analysis was performed by using two-tail unpaired t test, where *p<0.05; **p<0.01; ***p<0.001. Data are presented as mean ± SD from n=2 independent experiments.

As illustrated in **Figure 4.10**, in docetaxel-treated cells, ABT-737 addition did not significantly accelerated the timing of cell death neither during mitosis, nor in the post-slippage G1 phase in A549 cells. Regarding MIA PaCa-2 cells, they significantly exhibited an accelerated mitotic cell death when docetaxel and ABT-737 were administered concurrently, but did not have any effect on the post-mitotic response. In vincristine-treated cells, supplementation with ABT-737 reduced the average time that cells undertook to succumb to their demise either during mitosis or during a post-mitotic response. Our data agree with previous studies which indicated that navitoclax, the orally-available derivative of ABT-737, accelerated apoptosis during mitotic arrest induced by paclitaxel or kinesin-5 inhibitor treatment[568]. Similarly, the specific Bcl-X_L inhibitor WEHI-539 accelerated DiM, and in some cases also post-mitotic death in cells treated with diverse antimitotic agents (taxol, Plk-1 inhibitors, etc)[543]. However, when using nocodazole (another MTA that trigger mitotic arrest), did not manage to accelerate death during mitosis, arguing that there may be additional drug-intrinsic mechanisms that could affect the final outcome[543].

Altogether results from this section denote that survival-prone population spent less time in mitosis, and as a consequence cell death signals cannot accumulate during this vulnerable phase and cells manage to escape and thrive. Additionally, addition of

ABT-737 to MTAs seems to accelerate death in mitosis (excepting docetaxel+ABT-737 in A549 cells), while only vincristine-based combination precipitated post-mitotic cell death.

4.1.6. Analysis of Mitotic Checkpoint Proteins and its Relationship to Cell Death Induced by Antimitotic Agents.

The molecular links between mitotic regulators and cell death executioners have been a matter of intense study over the past years, yet the molecular bridges between these key cellular processes remain elusive[47,55]. In an attempt to dissect the molecular interplay between mitotic checkpoint players and cell death, we assessed the expression and subcellular localization of some of the crucial components of the mitotic apparatus. We evaluated these two characteristics in A549 and MIA PaCa-2 cells subjected to barasertib, docetaxel and vincristine treatment during 24h.

Western-blot analysis of protein expression indicated that in A549 cells, MAD2 levels were markedly decreased in presence of barasertib, whereas treatment with vincristine slightly upregulated MAD2 expression (**Figure 4.11**). In contrast, in MIA PaCa-2 cells, basal levels of MAD2, were elevated when compared to A549 cells. Additionally, barasertib or docetaxel treatment did not produced any apparent change and only with vincristine administration a significant decreased in MAD2 protein levels was observed. Interestingly, BUBR1 seems to follow the same expression pattern of MAD2 in both A549 and MIA PaCa-2 cells. In particular, in A549 cells treated with barasertib downregulated MAD2 expression, whereas BUBR1 levels noticeably increased upon vincristine administration. Similarly, vincristine-treated MIA PaCa-2 cells showed a reduced expression of BUBR1, while protein expression remained unaffected in the other conditions. Noteworthy, in docetaxel and especially in vincristine-treated cells, a mobility shift of BUBR1 could be appreciated. BUBR1 becomes hyperphosphorylated when SAC is active. Therefore, during prolonged mitotic arrest (induced by MTAs), SAC is continuously activated and BUBR1 becomes phosphorylated, accounting for the observed mobility shift. Regarding BUB1 expression, A549 cells show a considerable reduction in BUB1 levels upon barasertib treatment when compared to control cells. Interestingly, BUB1 seemed to accumulate more intensely with MTAs, especially with vincristine, compared to barasertib that hold the lowest protein levels in these cells. Importantly, BUB1 protein accumulation correlates with the time cells spend in mitosis when subjected to the different therapies. In sharp contrast, in MIA PaCa-2 cell line, BUB1 do not suffer significant changes in protein levels. However, as it occurs in A549 cells, a mobility shift of BUB1 towards increased molecular weights can be appreciated in those treatments in which mitotic arrest was more prominent (i.e. vincristine). Similar to BUBR1, BUB1 is also phosphorylated when SAC is activated[570]. The sustained mitotic blockade cells suffer when treated with antimitotic agents could also be appreciated in the increased accumulation of Cyclin B1, especially with vincristine and docetaxel, both

in MIA PaCa-2 and A549 cell lines. As indicated earlier in the introduction, cyclin B1 is the protein that regulates the activity of CDK1 and its expression peaks at late G2/early mitosis driving mitotic entrance. Moreover, Cyclin B1 levels determine that cells remain in mitosis or not. When all chromosomes are properly attached to the spindle and correctly bi-oriented, SAC become inactive which subsequently activates the APC/C^{Cdc20} that target Cyclin B1 (among other proteins) to degradation, driving mitotic exit. Hence, Cyclin B1 levels are a good surrogate marker that indicates whether cells are imbued in mitosis or not.

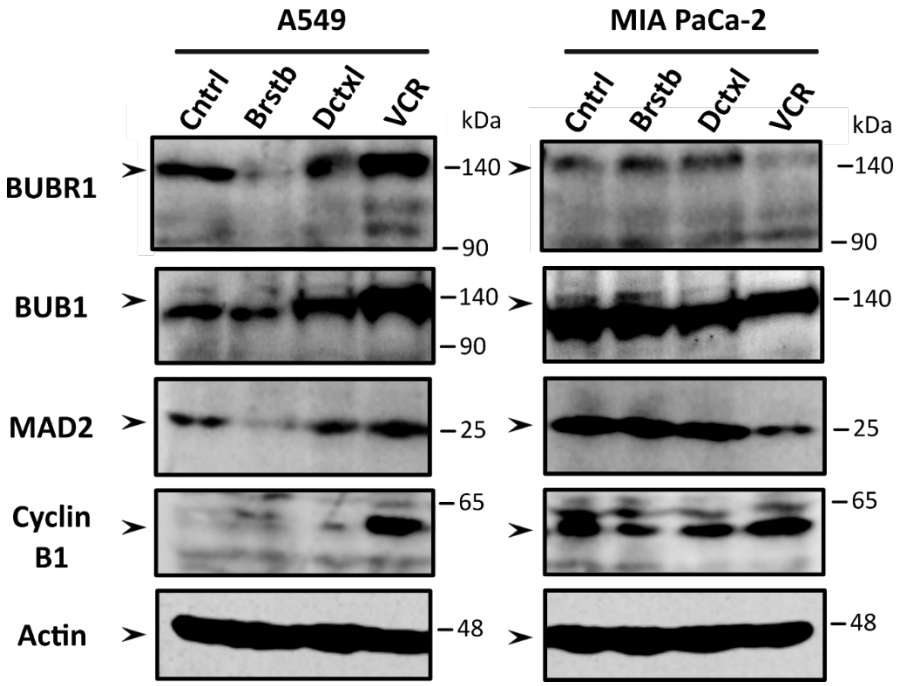

Figure 4.11 | Mitotic proteins expression after antimitotic drug exposure. Analysis of the expression levels by western-blot of different proteins involved in the mitotic apparatus and SAC signalling when exposed to barasertib 5 μM, docetaxel 10 μM or vincristine 1 μg/ml treatment during a course of 24h. Representative images from 2 independent experiments.

MAD2 and BUBR1 are essential components of the SAC and the MCC and hence participate in restraining the activity of APC/C complex by sequestrating its coactivator Cdc20. When the last kinetochore is correctly attached to the mitotic spindle, MCC complex is displaced releasing Cdc20. Thereafter, once the APC/C^{Cdc20} complex is formed, it drives the ubiquitination of Securin and Cyclin B1 among other proteins, to proceed through anaphase. As this model anticipates, loss of MAD2 or BUBR1 expression by genetic manipulation leads to premature mitotic exit giving rise to tetraploid cells with gross nuclear alterations and chromosome instability[571,572]. Moreover, Cyclin B1 was shown to be prematurely degraded in MAD2-depleted cells accounting for the premature exit of these cells[571]. Interestingly, this phenotype is reproduced in A549 cells exposed to barasertib which also exhibited reduced MAD2 and BUBR1 levels. In fact, it has been shown that polyploidy formation is preceded by ubiquitin-dependent degradation of

BUBR1[573]. Furthermore, similar to barasertib-treated cells, MAD2 and BUBR1 silencing promoted a senescence-like phenotype in several models of tumour and non-tumour cells[574–576]. Likewise, p31^{comet}, a spindle checkpoint silencer, has been shown to interact with and disrupt MAD2 function. This eventually led to p21 accumulation and cell senescence[577]. Another study also demonstrated that MAD2-induced senescence is mediated by upregulation of p53-p21 pathway[575,578].

Aurora B function is critical for proper SAC signalling and correct bi-orientation of chromosomes, among other important mitotic-related functions. Aurora B occupies an upstream position in the recruitment of SAC components[53]. It promotes kinetochore localization of Mps1, which is fundamental for initiating SAC cascade. Thereafter, Mps1 prompts kinetochore recruitment of BUB1[56]. In turn, BUB1 in complex with BUB3 mediates recruitment of other SAC proteins to kinetochore[56]. Once BUB1 assembles at the kinetochore, it mediates recruitment of BUBR1 and MAD2 at the kinetochores. Moreover, when Aurora B is inactive, localization of BUBR1 and MAD2 at kinetochores is severely impaired[579]. The same occurs in case of BUB1 depletion. Interestingly, Aurora B reduces the levels of BUB1 at the kinetochores as well, which also agrees with the reduced BUB1 levels observed in A549 cells when treated with barasertib[579]. Therefore, it might be possible that Aurora B-mediated inhibition by barasertib in A549 cells, could account for the mislocalization and posterior depletion in an unknown manner of MAD2, BUBR1 and also BUB1. This in turn would foster cell senescence by upregulating p53-p21 pathway. Furthermore, several studies have reported a direct cross-talk between mitotic kinases (Aurora kinases, Mps1, BUB1, BUBR1 Plk-1) and p53 function and activity[580,581]. In particular, Aurora B has shown to interact with and phosphorylate p53 at multiple residues (Ser 183, Ser-269 y Thr-284) in the DNA-binding domain[581]. Aurora B mediated phosphorylation of p53 has been reported to inhibit p53 transactivation activity or rather promote its degradation[580]. Then in our experimental model, when Aurora B is under the action of small molecule inhibitors, p53 transcriptional activity would become upregulated, promoting the expression of target genes like p21, p14, etc fostering cell senescence. However, this scenario is further complicated by the fact that p53 stability and transcriptional activity is also regulated by other mitotic proteins[581]. For example, BUBR1 has been shown to interact with and promote p53 phosphorylation and stabilization. In addition, in this same work, BUBR1 silencing influenced p53 stability[582]. Whether, cell senescence is a direct consequence of p53 stabilization through Aurora B inhibition, or rather it is a side-effect produced by MAD2 and BUBR1 depletion, which subsequently foster p53-p21 pathway and cell senescence, will require further investigation.

BUBR1 depletion can also be drived by APC/C Cdc20 mediated degradation. When the checkpoint is satisfied, BUBR1 is deacetylated and marked for degradation becoming a substrate of APC/C Cdc20[583]. This acetylation mark converts BUBR1 from being an inhibitor of APC to becoming a substrate of APC-dependent degradation. Thus is possible that upon Aurora B inhibition, SAC components are not recruited to

kinetochores and MCC is not assembled, leading to SAC being inactive and then, BUBR1 and potentially other components (like MAD2) could become substrates of APC/C dependent degradationn. It is possible that the specificity of APC/C for its target proteins eventually becomes deregulated when mislocalization of SAC or MCC components lead to unproper assembly of this complexes. This would lead to degradation of associated proteins like MAD2 or BUBR1 that directly and physically interact with APC. In fact, there are evidences that MAD2 can be ubiquitinated and possibly degraded regulating mitosis[584]. Moreover, since ubiquitinated Cdc20 is still bound to MAD2, the dual complex could be targeted collectively to degradation[585]. For instance, mitotic proteins such as CycB1, Securin, BUB1 and survivin, are degraded in order to exit mitosis[586].

As regards to MTA treatment, as mentioned earlier, probably the accumulation of mitotic proteins (MAD2, BUB1, BUBR1 and CycB1) observed in A549 is indicative of a robust and active SAC signalling. In fact, MAD2, BUB1 and BUBR1 were found to accumulate in mitosis-arrested cells when treated with an experimental compound that drove robust mitotic cell arrest and massive cell death[587]. In addition to the well-known functions in mitotic checkpoint signalling, BUBR1 has also been proposed to sense mitotic damage and engage apoptosis[573]. Several studies support the participation of BUBR1 in cell death and that BUBR1 depletion increase MTAs resistance[573,582,588,589]. It has also been shown that polyploidy formation is preceded by ubiquitin-dependent degradation of BUBR1[589]. Additionally, the crosstalk that exists between p53 and BUBR1 further reaffirm this notion[582]. Then it is possible that BUBR1 accumulation in docetaxel and vincristine treated cells could reflect its increased propensity to die either during or after mitosis, compared to barasertib in which BUBR1 levels are severely diminished. In this scenario, BUBR1 could increase p53 stability by phosphorylation, leaving these cells primed to death[582]. When an additional pro-apoptotic stimuli like BH3 mimetics are supplemented, the rate of cell death dramatically increases. In support of this notion, studies have shown that BUBR1 alone is not sufficient to trigger cell death but rather requires additional pro-apoptotic stimuli to do so[573].

Subcellular localization of mitotic checkpoint protein BUB1 was also evaluated in response to antimitotic agents by using immunofluorescence analysis (**Figure 4.12**). In control conditions, where the majority of cells were in interphase, BUB1 is predominantly cytoplasmic. Apparently, BUB1 preferentially concentrated in the perinuclear region. This same localization pattern is found in barasertib-treated cells, where cells were also in interphase of the next cycle with a tetraploid multinucleated nuclear morphology. Since the vast majority of imaged cells were in interphase in these two conditions, little information can be drawn out. Nonetheless, upon docetaxel and vincristine administration, where cells became arrested in mitosis as a consequence of SAC activation, BUB1 changed its location and also its configuration. In particular, BUB1 seemed to move from a cytoplasmic position to co-localize with nuclear DNA. Moreover, BUB1 in these cells changed from a diffuse/dispersed arrangement in control cells to a more concentrated punctate pattern. Although a co-localization analysis with

kinetochore-specific antibodies has not been performed, this distribution may be evocative of a kinetochore-accumulated disposition of BUB1[590,591].

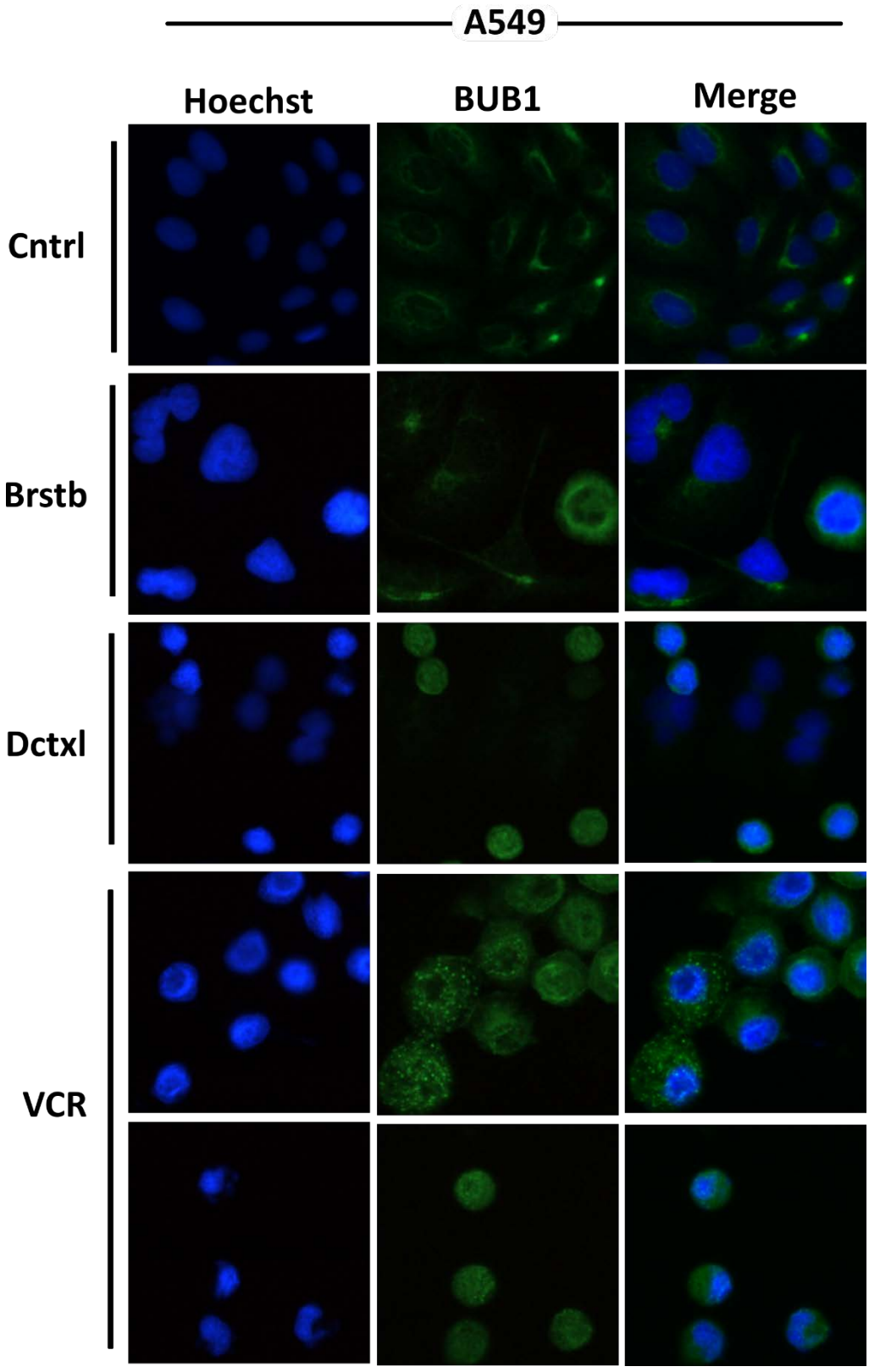

Figure 4.12 | Subcellular localization of BUB1 after antimitotic drug exposure. Representative immunofluorescence images of A549 cells treated with the different antimitotic drugs (barasertib 5 μM,

docetaxel 10 μM or vincristine 1 μg/ml) for 24h. After drug treatment, cells were fixed, permeabilized and co-stained with Hoechst 33342 for nucleus visualization and anti-BUB1 specific antibody for BUB1 subcellular localization. Images were acquired using a fluorescent inverted microscope. Scale: 25 μm.

Collectively, data presented here show that mitotic checkpoint proteins undergo changes in protein levels when challenged with antimitotic agents, which could also be associated with the phenotypic alterations displayed by these cells. In particular, reduction of MAD2, BUB1 and BUBR1 in A549 cells could account for the early mitotic exit that these cells experience when treated with Aurora B inhibitor. Additionally, MAD2 and BUBR1 depletion in these cells may also be responsible for the senescent phenotype sustained in these same conditions. On the other hand, accumulation of mitotic checkpoint proteins could denote an intense SAC signalling and also be responsible for engaging mitotic cell death under MTA treatment.

4.1.7. Role of Bcl-2 Family in the Regulation of Mitotic Catastrophe.

As previously indicated, mitotic catastrophe could engage different cell death programmes (apoptosis or necrosis)[55]. It is generally accepted that, in response to antimitotic drugs, a great majority of instances of cell demise shows hallmarks of apoptosis[63,92]. Bcl-2 family of proteins are key regulators of apoptotic cell death pathways. Moreover, its critical involvement in cell fate decision upon prolonged mitotic arrest has been contrasted long ago. In fact, our results from BH3 mimetics combinatorial experiments reinforce this idea. Therefore, in an attempt to help elucidating and dive deeper in the regulatory interface between mitotic checkpoints and cell death mechanisms during mitotic catastrophe, we aimed to study the role of the Bcl-2 family of proteins in the regulation of cell death induced by different antimitotic drugs, alone or combined with BH3 mimetics.

For that purpose we harnessed different genetically modified cell lines. MIA PaCa-2 Bax KO, MIA PaCa-2 Bak KO and MIA PaCa-2 Bax/Bak DKO were devised and engineered during this work using the CRISPR-Cas9 technology. We also utilized the MIA PaCa-2 Bcl-X_L cell line previously generated in our laboratory that, as the name stands, overexpresses the pro-survival protein Bcl-X_L. Furthermore, the generation of genetically modified cell lines is not a trivial procedure. For that reason, to rule out possible differences that may arise as a consequence of this methodology, in drug sensitivity or in the study of the underlying mechanisms, we used MIA PaCa-2 pBabe cells as a control line for these experiments (readily accessible in our laboratory).

4.1.7.1. Bcl-X_L Overexpression Delays Cell Death Induced by Antimitotic Agents.

In our experimental model, results from combinatorial experiments with BH3 mimetics point to Bcl-2 and Bcl-X_L combined action, but not Bcl-2 alone to be decisive regulators in mitotic catastrophe induced-cell death. In the particular case of MIA PaCa-2 cells, Bcl-X_L basal levels are relatively low (**Figure 4.13A**). In fact, ABT-737 potentiation effect to the action of antimitotic drugs, is moderate compared to other cell lines tested (**Figure 4.4**). To validate these results and shed more light into this matter, we further evaluated the participation of Bcl-X_L by testing whether overexpression of this pro-survival protein impacts on the cytotoxicity exerted by antimitotic agents, as well as in combinatorial regimens with BH3 mimetics.

Results from **Figure 4.13** showed a significant reduction of cell death induced by drug combinations in MIA PaCa-2 Bcl-X_L cells compared to the control MIA PaCa-2 pBABE cell line. However, protection was not complete and after 48h of drugs incubation, cells managed to die even in the presence of high levels of Bcl-X_L. It might be possible that the concentration of ABT-737 used, could overcome protein overexpression and eventually induce cell death. Another potential possibility is that alternative cell death mechanisms independent of the intrinsic pathway may be engaged. Interestingly, compounds that prompt a sustained mitotic arrest (docetaxel and vincristine), were more cytotoxic than those in which mitotic blockade is only momentary and exit from mitosis occur in an accelerated manner (barasertib). On that account, an enduring mitotic delay would instigate Mcl-1 levels to decline and Bcl-2 and Bcl-X_L activities to drop off through phosphorylation. In this situation, adding a BH3 mimetic further contributes to tip the balance to pro-death signals and ultimately induce cell death with more intensity. As a result, these observations may explain the increased cytotoxicity of MTAs than barasertib combined with BH3 mimetics. In addition, at least under these experimental settings, the different anti-apoptotic members seem to hold a cooperative and cumulative protection effect. Actually, inhibition of Bcl-2 with ABT-199 slightly potentiated cell death, but simultaneous inhibition of Bcl-2 and Bcl-X_L (and Bcl-W) with ABT-737, had an additive potentiation effect to that observed by ABT-199. This effect was even greater when presumably Mcl-1 levels are diminished under the action of MTAs.

Further characterization of cell death using different inhibitors, informs us that cell death induced by these drug combinations is manifestly caspase-dependent. As observed in **Figure 4.13**, the pan-caspase inhibitor z-VAD-fmk prevented cell death in all tested drug regimens to almost the basal levels. Moreover, necrostatin-1 (Nec-1) and necrosulfonamide (NSA), two inhibitors of the necroptotic pathway that target RIPK1 and MLKL respectively, did not provoke any apparent effect on cell death. It is important to stand out that generally, necroptosis is triggered when caspases are inactivated (physiologically or with inhibitors). Therefore, treatment with Nec-1 or NSA alone are not expected to bring about any protection, unless the primary cell death mechanism activated in response to these drugs were necroptosis.

Collectively, our results indicate that cell death induced by antimitotic drugs and its combinations with ABT-737 is caspase-dependent and that Bcl-X_L overexpression delays cell demise. Our data also suggest that Bcl-X_L might have a partial or auxiliary role in cell death regulation during mitotic catastrophe in MIA PaCa-2 cells, and that other pro-survival members such as Bcl-2 and Mcl-1 among others, could collaboratively be engaged in cell death modulation by mitotic catastrophe.

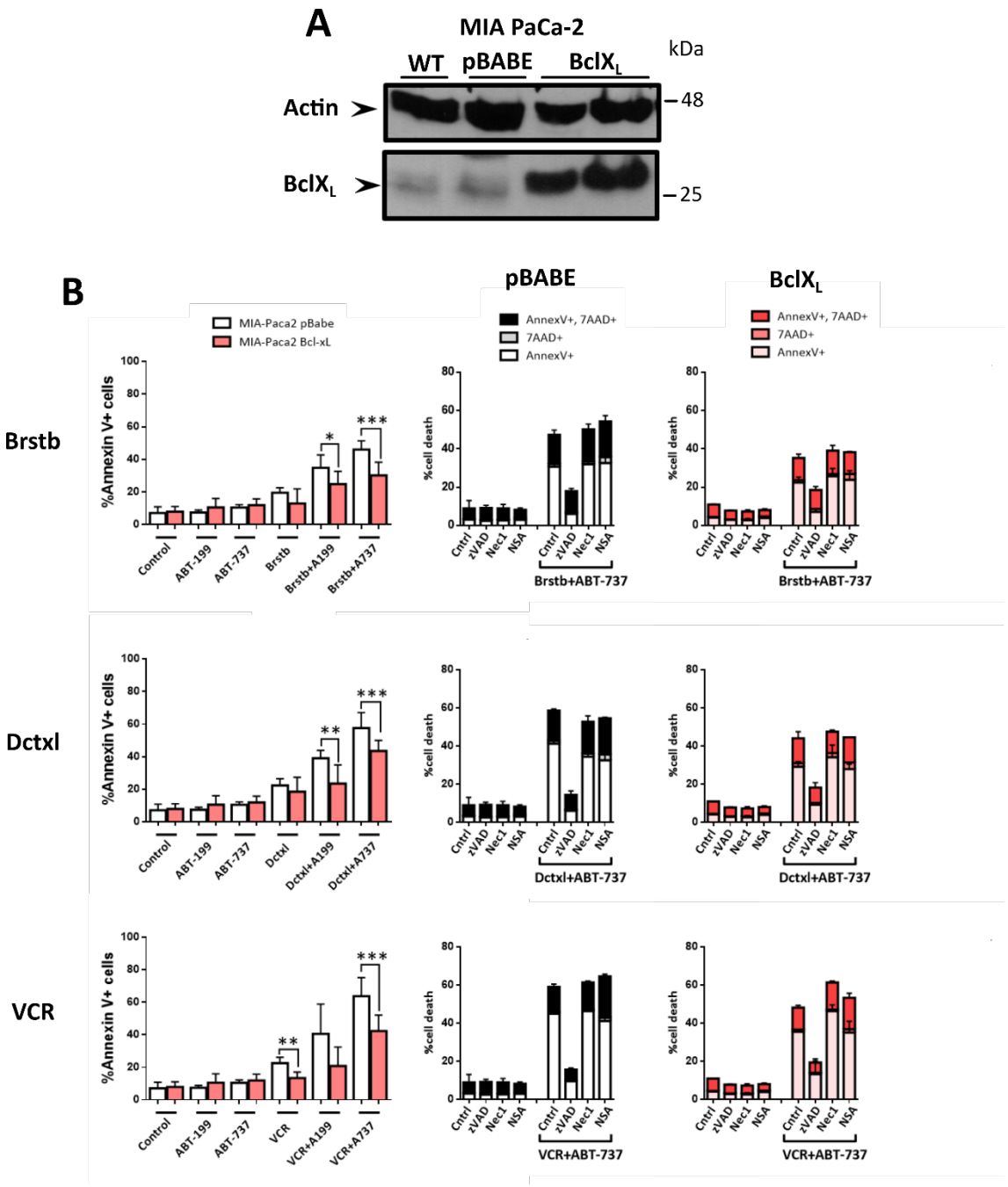

Figure 4.13 | Bcl-X_L overexpression delays cell death induced by antimitotic drugs and BH3 mimetic combinations. A. Western-blot showing the expression of Bcl-X_L in the parental line, the control cell line transfected with an empty vector (pBABE) and two clones from the genetically modified cell line transfected with a BclX_L expressing vector. **B.** Cell death analysis by phosphatidylserine quantification using

Annexin V and 7-AAD co-staining after 48h of drug treatment, at the concentrations previously reported (barasertib 5 μM, docetaxel 10 μM or vincristine 1 μg/ml and ABT-737 5 μM). This study was carried out also in presence of different cell death inhibitors: z-VAD-fmk (50 μM), necrostatin-1 (Nec-1; 30 μM) and necrosulfonamide (NSA; 1 μM) were pre-incubated 1h before the addition of the antimitotic drugs and ABT-737. Data are presented as mean ± SD from n>4 independent experiments. Statistical analysis was performed by using two-tail unpaired t test, where *p<0.05; **p<0.01; ***p<0.001.

4.1.7.2. Participation of Bax and Bak to Cell Death Induced by Antimitotic Agents.

It is generally acknowledged that mitotic catastrophe-induced cell death occurs through the activation of intrinsic apoptotic and caspase-dependent cell death pathway. Results reported in previous sections also point to the same direction. Based on these ideas, we asked whether Bax and Bak are involved in cell death induced by antimitotic drugs alone and in the combined action of antimitotic agents and BH3 mimetics. Using CRISPR-Cas9 technology, we devised and engineered different knockout (KO) cell lines to study the contribution of these proteins to the mechanism of cell death. Western-blot analysis confirmed the absence of expression of the target proteins in the different genetically modified cell lines (**Figure 4.14**).

Our results revealed that Bax and Bak are certainly involved in cell death induced by both antimitotic agents alone and the respective combinations with the BH3 mimetic ABT-737. Absence of Bax or Bak alone, conferred a modest protection when antimitotic agents were administered individually. Statistically significant reductions in cell death were found in barasertib and docetaxel treated MIA PaCa Bak KO cells, whereas a small non-significant tendency was found in cells under vincristine exposure. With regards to Bax conferred resistance, it was slightly smaller than that provided by Bak deficiency. For instance, only barasertib treated cells manifested a significant reduction in cell death while only just a small trend was witnessed after MTAs administration. By contrast, coupled Bax and Bak deficiency had a dramatic and significant impairment on cell death induction. Double knockout cells exhibited a prominent protection reaching the same cell death values presented by untreated cells. Concerning the role of Bak and Bax in the combinatory regimens, similar outcomes could be observed. Lack of Bax or Bak individually, conferred only partial protection, whereas cell death was completely abolished in double knockout cells subjected to the combination of antimitotic agents and ABT-737. Furthermore, these results were reproduced in HCT-116 Bax/Bak DKO cell line. As observed in **Figure 4.14,** in absence of Bax and Bak, HCT-116 cells were significantly protected against the action of antimitotics alone (except for the case of vincristine) and also against the combinatory regimens. These results further strengthen the notion that Bax and Bak are critically involved in cell death induced by these drugs.

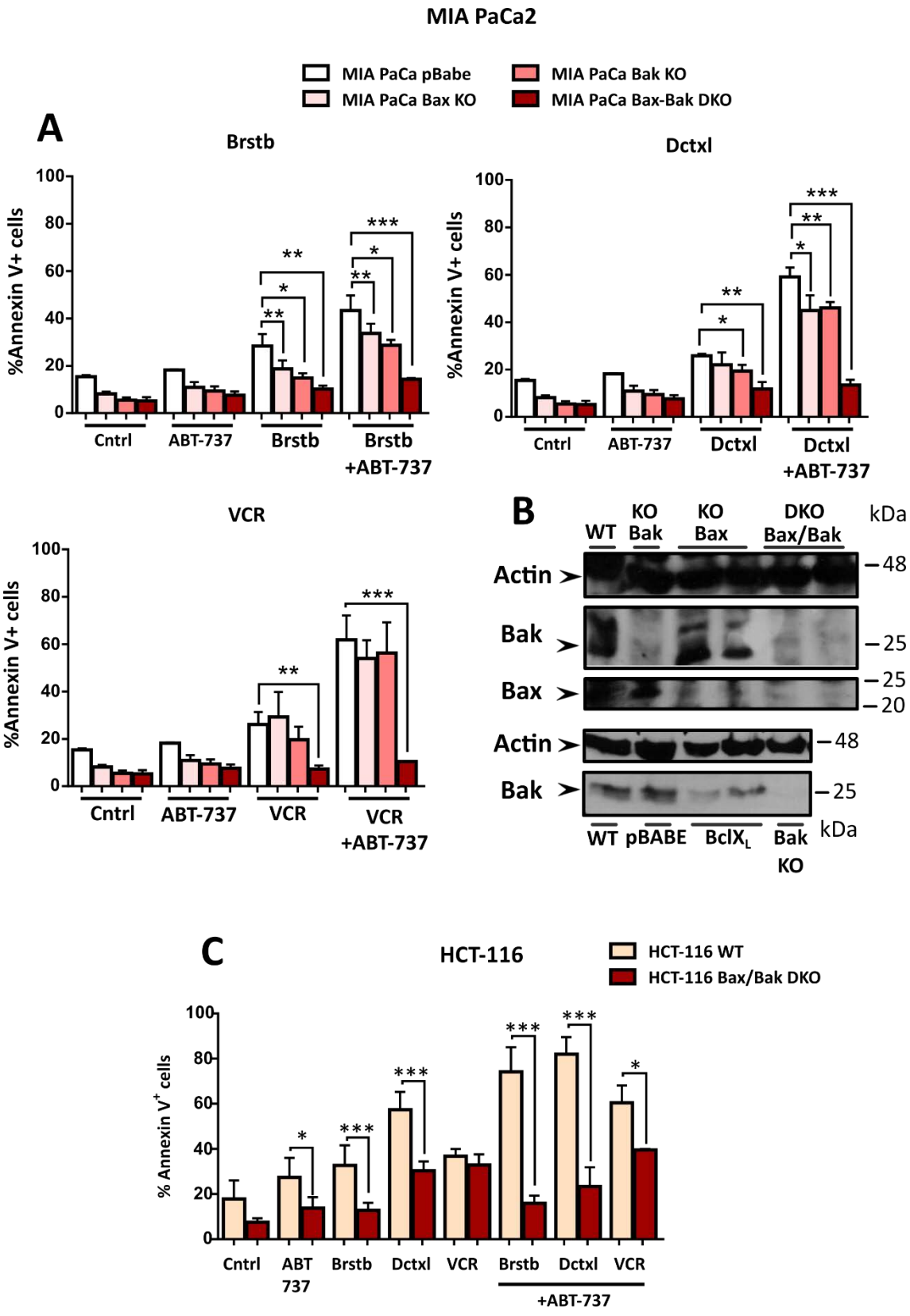

Figure 4.14 | Bax and Bak are involved in cell death induced by antimitotic agents and its combination with ABT-737. A..Cell death analysis by phosphatidylserine quantification using Annexin V staining after 48h of drug treatment, at the concentrations previously reported (barasertib 5 µM, docetaxel 10 µM or vincristine 1 µg/ml and ABT-737 5 µM) in MIA PaCa2 cell lines. Statistical analysis was performed by using one-way ANOVA with Tukey post-test, where *p<0.05; **p<0.01; ***p<0.001 **B.** Western-blot analysis confirming the deficiency in Bax and/or Bak expression in MIA PaCa-2 genetically modified cell

lines. **C.** Cell death analysis by phosphatidylserine quantification using Annexin V staining after 48h of drug treatment, at the concentrations previously reported (barasertib 5 μM, docetaxel 10 μM or vincristine 1 μg/ml and ABT-737 2.5 μM) in HCT-116 cell lines Data are presented as mean ± SD from n>4 independent experiments. Statistical analysis was performed by using two-tail unpaired t test, where *p<0.05; **p<0.01; ***p<0.001.

Our results are consistent with previous reports indicating that cell death induced by mitotic catastrophe, and particularly the one triggered by MTAs or other Aurora inhibitors, is essentially Bax- and Bak-dependent[549,592–595]. Regarding the relative contribution of Bax and Bak to cell death, single knockout cell lines showed that both proteins are functionally redundant. Lack of one of this pro-apoptotic regulators, endows a partial apoptotic resistance that can be compensated by the presence of the other member. Although a slight increase in cell death resistance was observed in Bak compared to Bax deficient cells, these differences were small and non-significant in the majority of our experimental conditions. The relative importance of Bax and Bak in cell death induced by antimitotic agents is a matter of debate and there are several studies supporting and leaning towards one or the other[592,595,596]. Nonetheless, it is worth mentioning that these differences may account for drug-induced intrinsic cell death mechanisms.

Taken together, our results highlight the importance of Bax and Bak as key mediators of apoptosis induced by mitotic catastrophe triggered by antimitotic agents and its combination with ABT-737. Moreover, our data bestow a redundant role on Bax and Bak in cell death triggered by mitotic catastrophe in our experimental settings.

4.1.8. Immunogenicity of Cell Death during Mitotic Catastrophe.

Generally, cancer cell ploidy has been thought to be exclusively controlled through cell-autonomous mechanisms. Recently, an immunosurveillance mechanism capable of restraining cancer cell ploidy has also been reported[81,82]. In particular, hyperploid cancer cells have been shown to be intrinsically immunogenic. These cells with increased chromosome content, are reported to constitutively activate ER stress pathways, that results in the exposure of immunogenic signals such as CRT[81]. Since, mitosis-targeting therapies that drive cells through aberrant cell division, could derive in the generation of tetraploid cancer cells, we tested the ability of the antimitotic agents used in this work to induce DAMP signalling. In particular, we assessed the exposure of CRT in the surface of A549 and MIA PaCa-2 cells treated with different antimitotic agents and its respective combinations with the BH3 mimetic ABT-737.

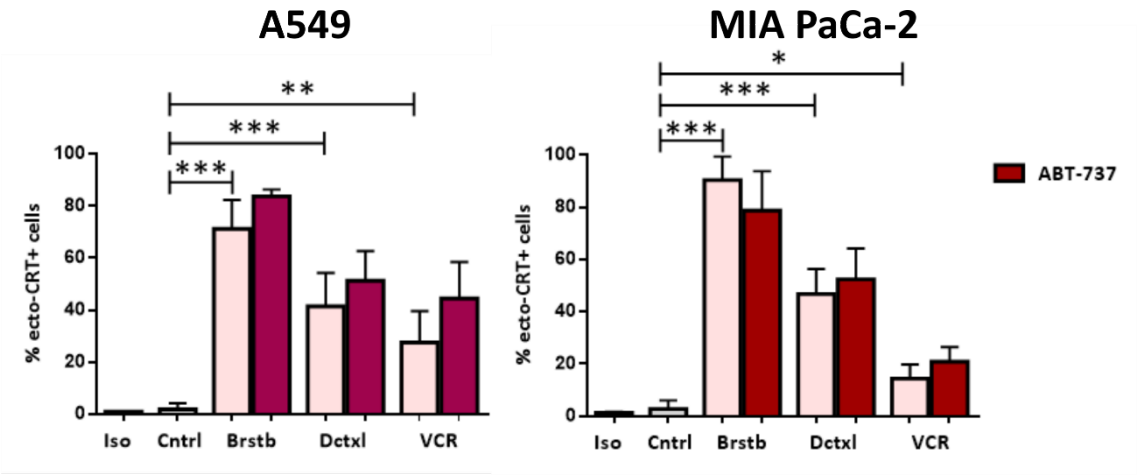

Figure 4.15 | CRT exposure induced by antimitotic agents. Analysis of CRT expression in the outer leaflet of the plasma membrane (ecto-CRT) by flow cytometry. A549 or MIA PaCa-2 cells were treated with the antimitotic agents combined or not with the BH3 mimetic ABT-737 at previously reported doses (barasertib 5 μM, docetaxel 10 μM or vincristine 1 μg/ml and ABT-737 5 μM) for 48h. Cells were then analysed for CRT surface exposure using a specific antibody and selecting only those cells with an uncompromised plasma membrane by gating on the 7-AAD negative population. Data are presented as mean ± SD from n=4 independent experiments. Statistical analysis was performed by using two-tail unpaired t test, where *p<0.05; **p<0.01; ***p<0.001.

Both A549 and MIA PaCa-2 cells exhibited increased surface expression of CRT with all tested drug regimens (**Figure 4.15**). Among the different, antimitotic drugs, barasertib was the treatment that provoked the most potent enhancement in ecto-CRT levels. Intriguingly, as our previous results have shown, although all these antimitotic inhibitors could generate hyperploid cancer cells at some extent, barasertib was particularly efficient in doing so. Therefore, this could explain that the highest ecto-CRT expression levels were triggered by barasertib. On the other hand, when antimitotic agents were co-administered with ABT-737, a general and strong tendency towards increased surface CRT levels compared to antimitotic drugs alone was observed. However, this tendency did not reached statistical significance. This data are in accordance with previous reports, in which treatment with MTAs like vinca alkaloids or taxanes, induced an ER stress signalling response that culminated in the exposure of CRT in the outer leaflet of the plasma membrane[81]. Moreover, it has been reported that when death cancer cells treated with mitotic inhibitors were injected into syngeneic immunocompetent mice, they were able to vaccinate mice against a subsequent rechallenge with live cancer cells of the same type[81,82]. Interestingly, these mitotic inhibitors were inefficient in promoting ATP secretion, necessary to elicit active anticancer immune responses[87]. It has been proposed that their capacity to stimulate antitumour immunity pass through their ability to eliminate hyperploid cancer cells[82].

Altogether, these studies underscore the existence of an anticancer immunosurveillance system that selects and eliminates cells with increased cell ploidy, which harbour more potential to become malignant and tumorigenic. Importantly, antimitotic agents not only could dispose of cancer cells by activating oncosuppressive

mechanisms upon mitotic catastrophe, but also could activate and engage this natural immunosurveillance mechanism to eliminate those cells that slipped out and overcome therapy. However, although *in vitro* CRT exposure have been shown to positively correlate with *in vivo* protective anticancer immune responses, in our experimental settings further experiments should be carried out to categorize these agents as *bona fide* ICD inducers.

4.1.9. Sensitivity of Antimitotic Agents and BH3 mimetic Combinations in Multiple Myeloma.

MM is characterized by holding multiple genetic abnormalities. Many of these genetic aberrations are directly involved in deregulation of Cyclin D genes[597]. Additionally, loss or inactivation of INK4 family of inhibitors have been reported to play a role in myelomagenesis. Therefore, it is conceivable that cell cycle deregulation is a common event featuring MM[597]. Furthermore, chromosomal instability and aneuploidy, which suggests a disruption in the mitotic apparatus, is also a typical hallmark in MM[597]. In fact, several components of SAC and other mitotic proteins have been found to be aberrantly expressed in MM patients, including BUB1, Cdc20, Aurora A, Plk-1, among others. Thus, targeting these cell cycle key factors are a promising strategy to fight against MM disease[597]. Indeed some of these targets are currently under clinical development in MM and also in other hematologic neoplasms. In addition, MM survival is also critically dependent on Bcl-2 family members. In particular, Mcl-1 protein has been found overexpressed in MM patients[598]. Bcl-2 has also been found to be overexpressed in a specific subset of MM patients that hold the translocation t(11;14)[599]. Bcl-X_L has been also implicated in MM survival[598]. BH3 profiling assays have revealed that MM is a highly heterogeneous disease and that its survival dependency on Bcl-2 family of proteins could entail one or various members[598,600]. Therefore combination of BH3 mimetics with mitosis targeting therapies seems a reasonable strategy to enhance myeloma cell death. That is why we considered to investigate the therapeutic efficacy of antimitotic agents and BH3 mimetic combinations in MM cell lines.

As shown in **Figure 4.16,** below, MM cell lines were quite resistant to Aurora A or Aurora B kinase inhibition. Conversely, they were more sensitive to docetaxel or vincristine treatment. In fact, historically vincristine has been used as a standard of care for induction therapy as part of the combinatory regimen of vincristine, adriamycin and dexamethasone[601]. However, other novel therapies like proteasome inhibitors have been shown to be superior in terms of complete response and progression free survival in MM patients[601]. Regarding the sensitivity to BH3 mimetics-based treatment, NCI-H929 were the most resistant cells to ABT-737 action. U266 displayed a moderate sensitivity, while MM.1S cells were especially responsive to ABT-737 induced cell death. Based on these results we choose appropriate doses to be able to see any potentiation effect that may exist between these drugs.

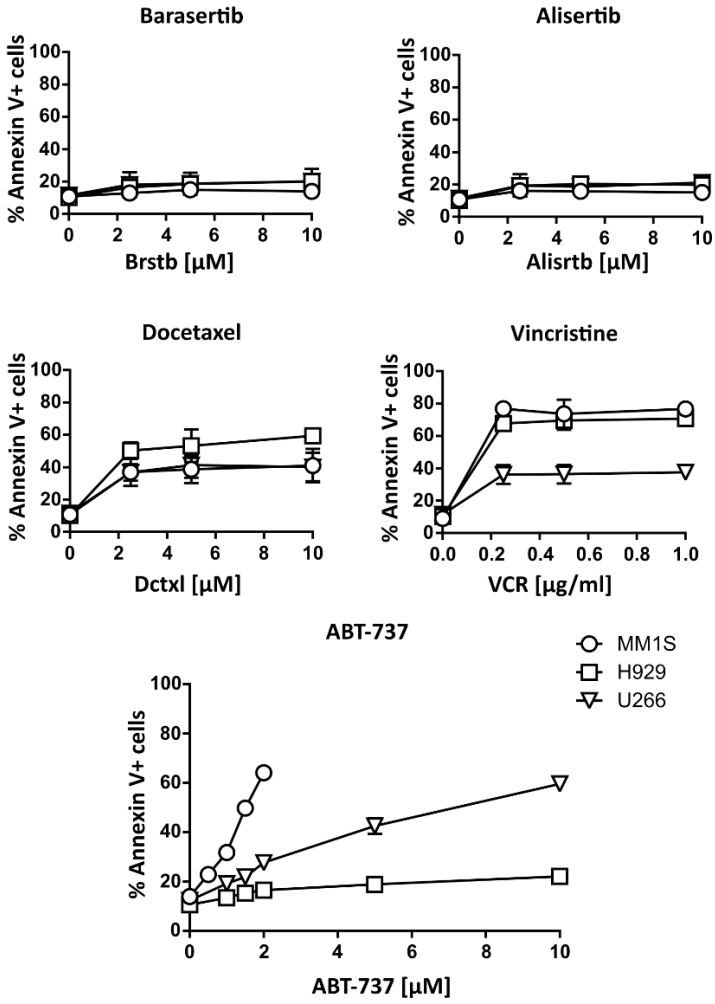

Figure 4.16 | Dose-response curves of antimitotic agents and ABT-737 in MM cell lines. MM.1S, NCI-H929 and U266 cell lines were subjected to different doses of barasertib, docetaxel, vincristine, alisertib and ABT-737. After 24h of drug incubation, cell death was analysed by annexin V staining by flow cytometry. Data are presented as mean ± SD from n=2-3 independent experiments.

As shown in **Figure 4.17**, combination of the different antimitotic agents with ABT-737 did not potentiate cell death at all, except in the case of U266 cells in barasertib and alisertib combinations with ABT-737. In the best of the scenarios, only an additive effect between antimitotic agents and ABT-737 was manifested. This contrasted with the results obtained in the solid cancer cell models. Perhaps, other mechanisms may govern MM cell death and make myeloma cells less addicted to Bcl-2 family upon antimitotic therapy. Further research will be necessary to address all these concerns.

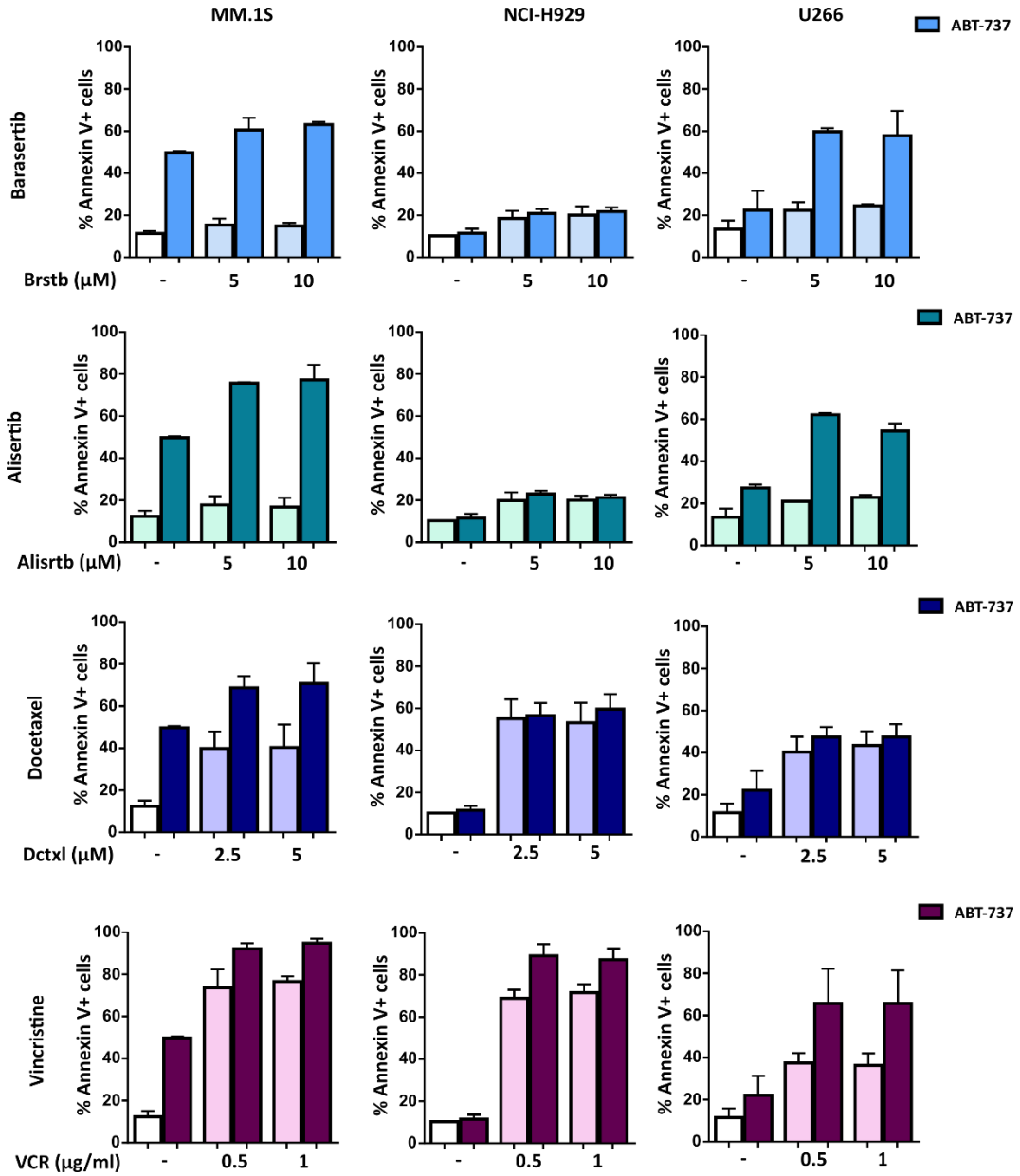

Figure 4.17 | Analysis of cell death exerted by the combination of antimitotic agents and ABT-737. MM.1S, NCI-H929 and U266 cell lines were subjected to two different doses of antimitotic agents (barasertib, docetaxel, vincristine and alisertib) alone and in combination with ABT-737 at given fixed concentration that depended on the cell line. MM.1S were treated with 1.5 µM of ABT-737, while NCI-H929 and U266 cells were subjected to 2 µM of ABT-737. After 24h of drug incubation, cell death was evaluated by annexin V staining by flow cytometry. Data are presented as mean ± SD from n=2-3 independent experiments.

4.2. Immunogenicity and Cell Death Mechanisms in Multiple Myeloma.

Although targeting the mitotic apparatus holds promise in MM, our results have not shown effective potentiation of cell death in combinatory regimens with ABT-737, as opposed to solid cancer cell models. We decided then to follow another strategy to confront MM disease.

ER stress is increasingly being considered as a promising therapeutic target against many solid and haematological cancers[188]. In particular, the elevated production of immunoglobulins in MM, makes these cells heavily reliant on the survival arm of the unfolded protein response (UPR). Nevertheless, since myeloma cells are supported by the UPR to thrive, they are remarkably vulnerable to ER-stress-associated cell death[196–198]. This feature may explain why proteasome inhibitors (PIs), have shown a great clinical efficacy in the treatment of MM[199,200]. Nonetheless, despite its well-proven clinical efficacy, resistance to PI-based therapy arises. Thus, novel therapeutic approaches should be devised to tackle relapse.

At this respect, autophagy is one of the major cellular processes that can dispose of cellular proteins. Under ER stress, when the cytoprotective and restorative capacity of the UPR is exceeded, several signals burst from the ER to trigger autophagy in an attempt to re-establish cellular homeostasis and prevent cell demise. Therefore, simultaneously targeting the proteasome and autophagy simultaneously is conceived to be a suitable therapeutic approach against MM. In this sense, our group previously demonstrated the ability of the autophagy inhibitor, chloroquine, to strongly potentiate cell death induced by carfilzomib *in vitro* and *in vivo*[238]. However, the mechanism by which this cell death facilitation occurs, remains to be determined.

For that reason, in the present work we have studied the mechanisms responsible for this potentiating effect. Since ER stress seems to be considered the 'Achilles heel' of MM, we have also set our sights on devising new combinatorial strategies that would enhance cell death induced by PIs, and delve deeper in their underlying molecular mechanisms. Furthermore, given that ER stress holds a dominant position in the immunogenicity of dead cells, we studied the capacity of these therapeutic approaches, to trigger ICD and to instigate protective anticancer immune responses in a novel orthotopic MM mouse model[526]. Finally, we tested whether the sensitization effect on cell death observed in combinatorial therapies is preserved in $CD38^+$ bone marrow mononuclear cells (BMMCs) isolated from the BM of MM patients. Moreover, available data indicate that depending on the cancer cell type, DAMPs exposure and particularly CRT, could stand as positive or negative prognostic factors for cancer patients. In the present study, we have also assessed the expression of ecto-CRT on the surface of $CD38^+$ BMMCs, and evaluated the possible relationship between this DAMP and different

clinical and biological (immune-) response markers of the BM microenvironment in MM evolution.

4.2.1. Molecular Cell Death Mechanism.

4.2.1.1. Cell Death Potentiation.

As indicated, previous work from our group showed that combination of chloroquine with carfilzomib, but not with bortezomib, strongly potentiated cell death both *in vitro* and using a *in vivo* xenograft mouse model[238]. First, we tried to reproduce these data and to extend the study to a novel orthotopic syngeneic MM mouse model (MOPC315.BM)[526]. We also focused our concern in devising alternative therapeutic combinations that may sensitize and potentially synergize with PIs in the treatment of MM. For this reason, we used the p97/VCP inhibitor DBeQ that targets the ERAD pathway, which is an important molecular pathway involved in ER quality control mechanism that eventually transfer misfolded secretory proteins to the proteasome. Therefore, DBeQ could be an interesting candidate to interfere with ER stress response, and potentiate cell death, when combined with PIs.

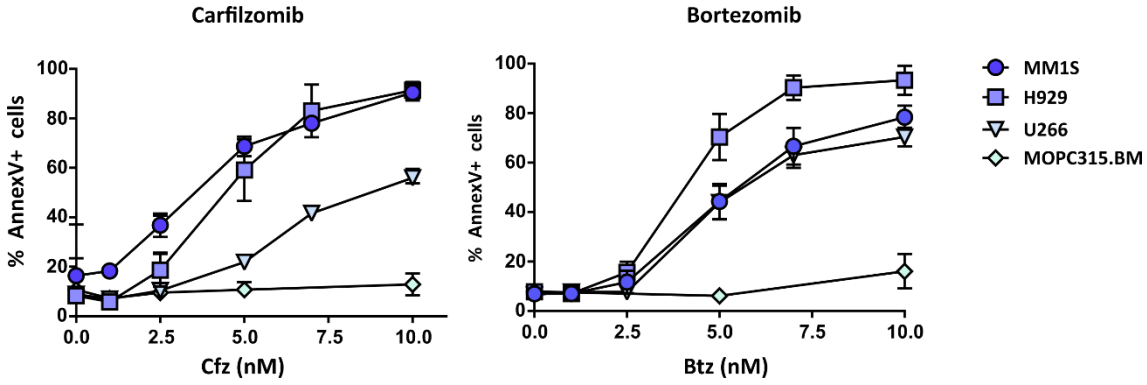

Figure 4.18 | Sensitivity of human and murine MM cell lines to PIs. Analysis of drug sensitivity and cell death through the quantification of phosphatidylserine exposure using Annexin V staining by flow cytometry. Human (MM.1S, NCI-H929 and U266) and murine (MOPC315.BM) MM cell lines were exposed for 24h to PIs (carfilzomib or bortezomib) at different doses. Data are represented as mean ± SD from n=4 independent experiments.

MM cell lines display a differential sensitivity to carfilzomib compared to that observed under bortezomib treatment (**Figure 4.18**). In some cell lines (U266 and NCI-H929) bortezomib, as single agent, seems to be more cytotoxic than carfilzomib, while in other cells such as MM.1S, it seems to occur the contrary, especially at low doses. However, although these differences may exist, they were generally small. MM.1S and NCI-H929 cells were the most sensitive to PI action, whereas murine MOPC315.BM cell line, was more resistant to carfilzomib or bortezomib treatment. In case of U266 cell line,

these cells were more resistant to carfilzomib than MM.1S and NCI-H929, but less than MOPC315.BM cells. In contrast, U266 cells were more sensitive to bortezomib matching cytotoxic levels to that observed in NCI-H929 cells.

When MM cells were co-treated with PIs and the autophagy inhibitor **chloroquine (CLQ)**, cell death was increased compared to that observed when treated with these drugs alone (**Figure 4.19**). In particular, carfilzomib and chloroquine co-administration, strongly potentiated cell death in all the cell lines tested. However, when the first-generation PI, bortezomib was combined with CLQ, the effects observed in cell death were not so conspicuous. Hence, these results confirmed previously reported data from our group, in which the potentiation effect was evident when chloroquine was administered concurrently with carfilzomib, but was less obvious with bortezomib[238].

Analogous results were obtained by Baranowska *et al.*, showing also a preferential hidroxichloroquine potentiation effect on carfilzomib- rather than on bortezomib-induced cell death in MM cell lines[602]. Moreover, cell death enhancement exerted by autophagy inhibitors and PI-based combination or other ER stressors has also been manifested by others. In particular, the autophagy inhibitor 3-methyladendine (3-MA), was shown to synergize with thapsigargin in MM cells[603]. However, another report revealed that concurrent inhibition of autophagy with CLQ and the proteasome with bortezomib rather yielded antagonistic responses[603]. In contrast, addition of bafilomycin A1 or a macrolide antibiotic, two drugs capable of inhibiting autophagy, were able to synergistically sensitize MM cells to bortezomib action[604,605].

Similarly, **DBeQ** markedly increased cell death induced by carfilzomib, but this effect was milder in bortezomib combinations both in human and murine MM cell lines (**Figure 4.19**). Noteworthy, DBeQ cell death sensitization was not so pronounced as that seen with CLQ combinations. Studies from other groups have also reported increased levels of apoptosis upon dual inhibition of p97/VCP and bortezomib[202,606]. No data concerning carfilzomib and p97/VCP inhibitors have been reported so far in the context of MM. For instance, resistance to PI-based therapy has been correlated with incomplete ERAD impairment and the mobilization of alternate clearance pathways such as autophagy or aggresome formation[202]. Besides its role in ubiquitin-dependent ERAD pathway, p97/VCP also plays an important role in autophagy[607,608]. In fact, inhibition of p97/VCP with DBeQ or siRNAs-mediated knock-down, has been reported to impair autophagosome maturation[203,607]. Furthermore, proteasome and p97 molecular pathways, although closely related, they show a considerable degree of non-redundancy, opening the possibility to combinations to overcome PI-based resistance.

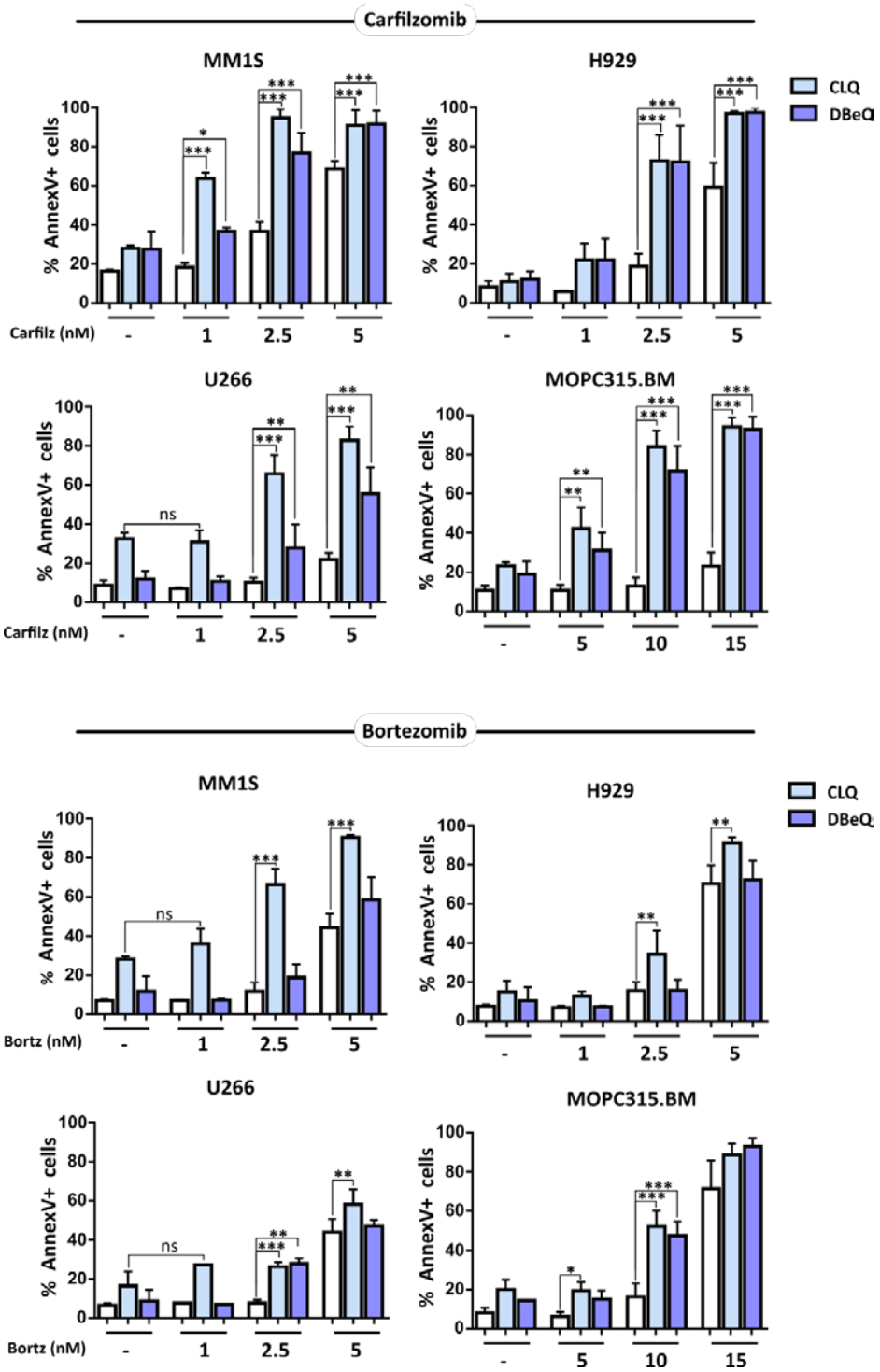

Figure 4.19 | Analysis of the cell death potentiation effect of PI-based drug combinations. Analysis of drug sensitivity and cell death through the quantification of phosphatidylserine exposure using Annexin V staining by flow cytometry. Human (MM.1S, NCI-H929 and U266) and murine (MOPC315.BM) MM cell lines were exposed for 24h to PIs (carfilzomib or bortezomib) at different doses alone or combined with autophagy inhibitor chloroquine (CLQ) and the VCP/p97 inhibitor (DBeQ) at 20 µM and 2,5 µM respectively. Data are represented as mean ± SD from n=4 independent experiments. Statistical analysis was performed by using one-way ANOVA test, with Tukey post-test, where *p<0.05; **p<0.01; ***p<0.001.

In addition, the novel p97/VCP inhibitor **CB-5083** was also tested (**Figure 4.20**). CB-5083 has demonstrated more potency and selectivity than DBeQ and was synthesized and optimized for its ADME-Tox properties making it more suitable for translation into the clinic[104]. In fact, it has already entered phase I trials. However, our results did not show an effective cell death potentiation with carfilzomib and CB-5083 co-treatment. Remarkably, combinations of these two drugs rendered an antagonistic outcome on cell death in U266 cells. It may seem reasonable that the lack of cell's sensitization or priming upon treatment with CB-5083, comes from its improved selectivity and potency. As observed in **Figure 4.20**, small differences in drug concentration provoked great differences in cell death levels when cells were treated with CB-5083 alone, thus neutralising any possible synergistic effect between the drug combinations. As indicated earlier, DBeQ, besides preventing ubiquitin-dependent protein clearance, can also impair autophagosome maturation and hence the autophagic flux, thus mimicking the global effect exerted by CLQ. Therefore, it is possible that the potentiation on cell death observed with DBeQ may be a consequence of targeting autophagy rather than ERAD pathway. With regards to the antagonistic effect observed in U266 cells with CB-5083 and carfilzomib combination, this matter will require further experimental clarification.

Collectively, our results provide a conceptual preclinical framework for simultaneous targeting alternative clearance pathways such as autophagy or in a lesser extent ERAD, together with proteasome inhibition as a potential therapeutic strategy in MM[202]. However, special attention and future investigations are needed to elucidate the differences in the cell death sensitization observed with the different p97/VCP inhibitors.

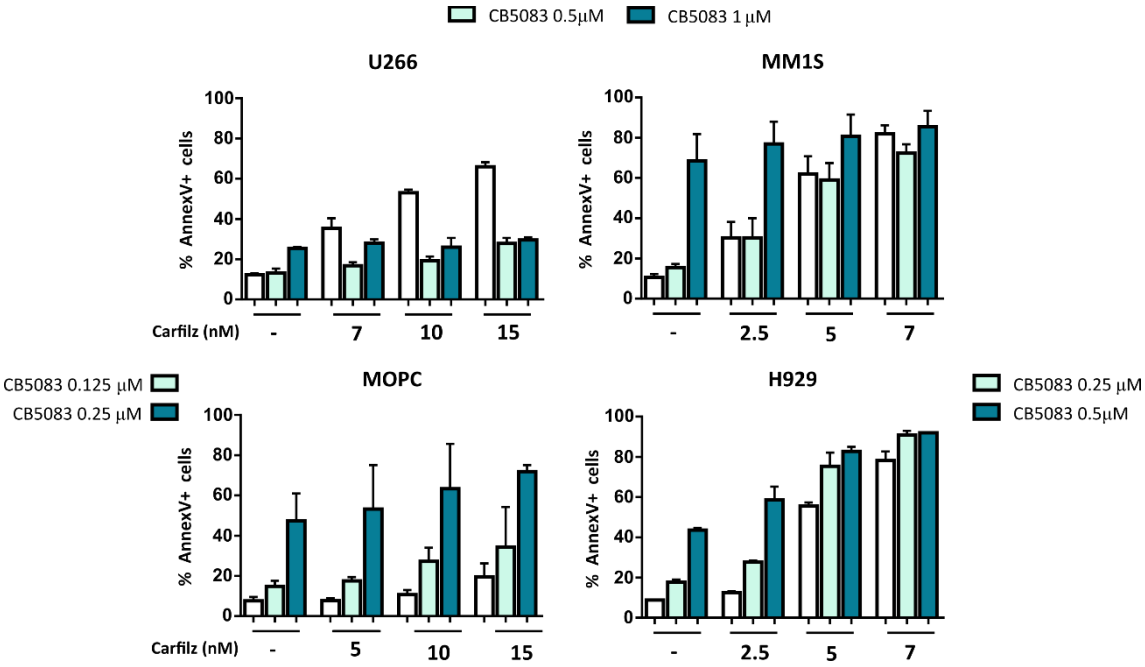

Figure 4.20 | Sensitivity of human and murine MM cell lines to carfilzomib drug combination with novel VCP inhibitor CB-5083. Analysis of drug sensitivity and cell death through the quantification of phosphatidylserine exposure using Annexin V staining protocol by flow cytometry. Human (MM.1S, NCI-

H929 and U266) and murine (MOPC315.BM) MM cell lines were exposed to carfilzomib for 24h at different doses alone or combined with the second-generation VCP inhibitor (CB-5083) at the indicated concentrations. Data are presented as mean ± SD from n=4 independent experiments.

4.2.1.2. Cell Death Kinetics.

To further deepen in the cell death mechanism exerted by combinatory regimens and to unravel the differences in the potentiation of cell death effect observed between carfilzomib and bortezomib, cell death kinetics of the aforementioned treatment modalities were analysed. For that purpose, we performed time-course experiments assessing cell death induced by carfilzomib or bortezomib combined with either CLQ or DBeQ at different time points.

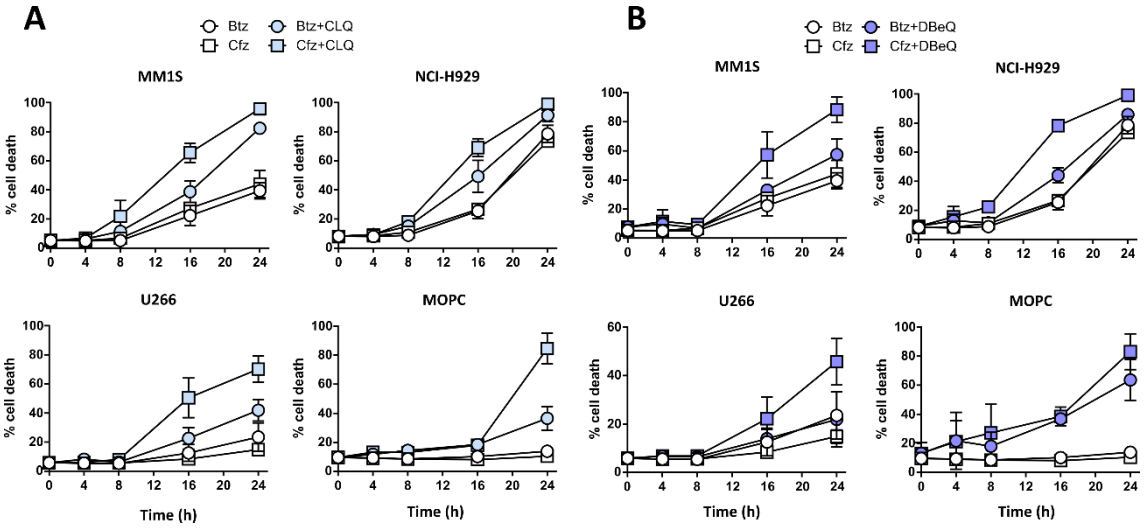

Figure 4.21 | Cell death kinetics. Time-course experiments in which MM cell lines were treated with PIs (carfilzomib or bortezomib) at 5 nM and were combined with **A.** chloroquine (CLQ, 20 μM) or **B.** DBeQ (2.5 μM). Cell death was assessed by analysing phosphatidylserine exposure (determined through Annexin V binding) and membrane permeability (through 7-AAD co-staining). Data are illustrated as total cell death corresponding to the AnnexV$^+$, 7-AAD$^+$ and AnnexV/7-AAD double-positive populations. Data are presented as mean ± SD from n=3 independent experiments.

As illustrated in the **Figure 4.21**, addition of CLQ or DBeQ to carfilzomib treatment accelerated cell death in almost all the cell lines tested. The murine MOPC315.BM cell line showed more resistance, but cell death occurred between 16 and 24h period. Conversely, in the human MM cell lines the apoptotic events started earlier, during 8-16 h interval. U266 cells again showed increased resistance and cell demise seemed to occur at a slower rate. In general, after 16h of drug incubation, cell death levels augmented considerably in the drug combinations compared to the carfilzomib alone. Noteworthy, bortezomib drug combinations were not so efficient in inducing cell demise. Levels of cell death were considerably lower than that observed with carfilzomib combinations after 16h of incubation. In the case of MOPC315.BM cells, owing to its greater resistance, these differences become apparent after 24h of drug treatment.

Thus our results seem to point to the fact that the molecular mechanism behind the cell death potentiation effect may involve in some way, the acceleration of cell death. Whether this escalation in speed cell death dynamics is a consequence of a hastened accumulation of the cell death signals that trigger the apoptotic cascade or any other possible mechanism requires further investigation.

4.2.1.3. Study of Caspases & Cell Death Mechanisms.

Once we determined that drug combinations not only potentiated, but also accelerated cell demise, we next aimed to study the participation of caspases in cell death induced by these drugs. Additionally, we also investigated whether alternative cell death mechanisms, like necroptosis, could also participate in cell death in our experimental settings. Consequently, we first evaluated the activation of the executioner caspase-3 during the cell death pathway activated by these drug combinations.

As illustrated in **Figure 4.22,** below, bortezomib treatment alone activated caspase-3 more efficiently than carfilzomib at the same drug concentration. This is consistent with the higher cytotoxicity observed in cell death assays presented above. Nonetheless, carfilzomib drug combinations provoked a stronger activation of caspase-3 compared to bortezomib drug combinations in all the MM cell lines tested. Therefore, these results agree again with the cytotoxic profiles observed. Moreover, this data suggest that caspase-3 activation is responsible for the cell death induced by these drug combinations.

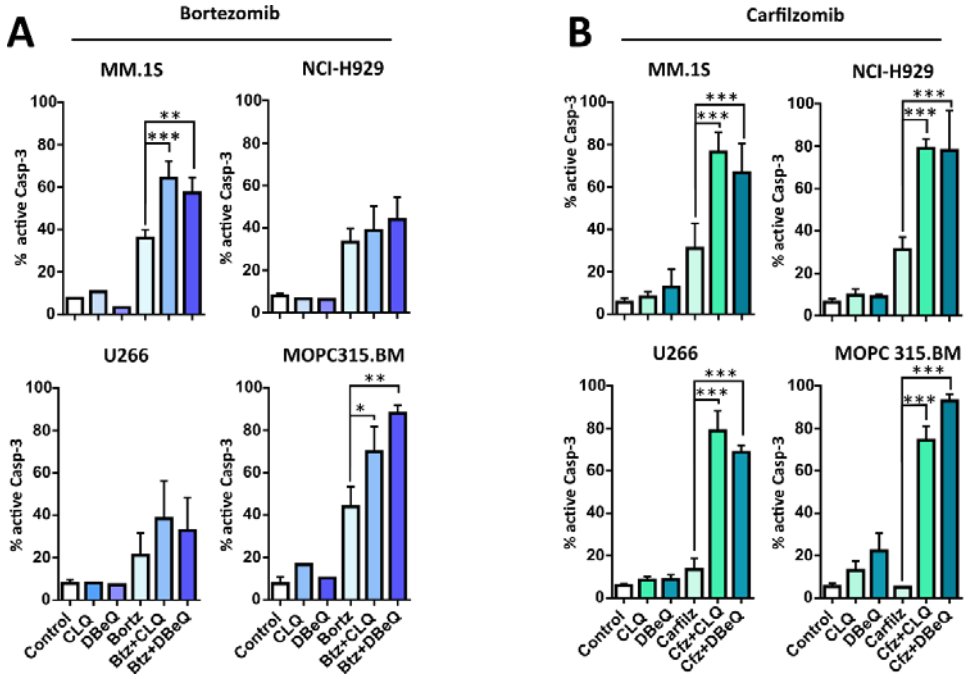

Figure 4.22 | Caspase 3 activation. Analysis of the activation of caspase-3 by flow cytometry. MM cell lines were treated with PIs (carfilzomib and bortezomib) at 5nM in case of MM.1S and NCI-H929 cell lines, 7nM in U266 and 10 nM in MOPC315.BM and combined with chloroquine (CLQ, 20 μM) or DBeQ (2,5 μM)

for 24h. Henceforth, cells were fixed, permeabilized and incubated with anti-active caspase-3-FITC antibody as described in section 3.4.1.2. Data are presented as mean ± SD from n=3 independent experiments. Statistical analysis was performed by using one-way ANOVA with Tukey post-test, where *p<0.05; **p<0.01; ***p<0.001.

To confirm caspase contribution to cell death and dissect the specific role of the different members of the caspase family, we used different caspase inhibitors to this purpose. In particular, the pan-caspase inhibitor z-VAD-fmk, caspase-3 inhibitor z-DEVD-fmk, caspase-9 inhibitor z-LEHD-fmk and caspase-8 inhibitor z-IETD-fmk were utilized. In the majority of cell lines tested, caspases were shown to play an important role in cell death induced by both carfilzomib alone and also in the respective drug combinations with CLQ or DBeQ (**Figure 4.23**). In particular, the presence of the different caspase inhibitors considerably reduced cytotoxicity exerted by these compounds in MM.1S, U266 and MOPC315.BM cells, but not in NCI-H929 cell line. General caspase inhibition with z-VAD-fmk prevented cell death reaching basal levels in all cell lines tested, excepting for NCI-H929 cells.

Regarding the relative contribution of individual caspase members to cell death, the following observations can be drawn out. **Caspase-3** as a critical executioner caspase, was the most important to trigger cell death in our experimental settings, since its inhibition with z-DEVD-fmk reduced cell death to almost the same levels rendered by pan-caspase inhibitor z-VAD-fmk. This correlates with our previous observations on caspase-3 activation flow cytometry analysis.

With respect to the initiator **caspase-9**, it is involved in the apoptosome formation during the intrinsic mitochondrial apoptotic pathway and its activation results in executioner caspase activation[9]. In our experimental system, caspase-9 inhibition with z-LEHD-fmk produced a milder inhibition of cell death compared to the other two caspase inhibitors, (especially in U266 and MOPC315.BM cells), possibly indicating the presence of a bypass that could engage executioner caspases without involving apoptosome formation. Interestingly, within the caspase-dependent cell lines, MOPC315.BM was especially sensitive to z-LEHD-fmk incubation in presence of the different drugs, since addition of this caspase inhibitor increased cell death levels.

Concerning the implication of **caspase-8**, its inhibition with z-IETD-fmk also reduced cell death rates in a moderate fashion. However, its effect was critically dependent on the specific cell line and on the drug treatment under evaluation. Even in the case of the apparently caspase-independent NCI-H929 cells, cell demise was significantly diminished in presence of z-IETD-fmk upon carfilzomib or carfilzomib-CLQ combination. In MM.1S cells addition of z-IETD-fmk reduced cell death levels less than any other caspase inhibitor, indicating that caspase-8 may play a minor role in cell death in these conditions. In U266 cells, z-IETD-fmk mediated protection was comparable to that observed in caspase-9 inhibition or pan-caspase inhibition depending on the drug treatment, as it occurred in case of MOPC315.BM cells.

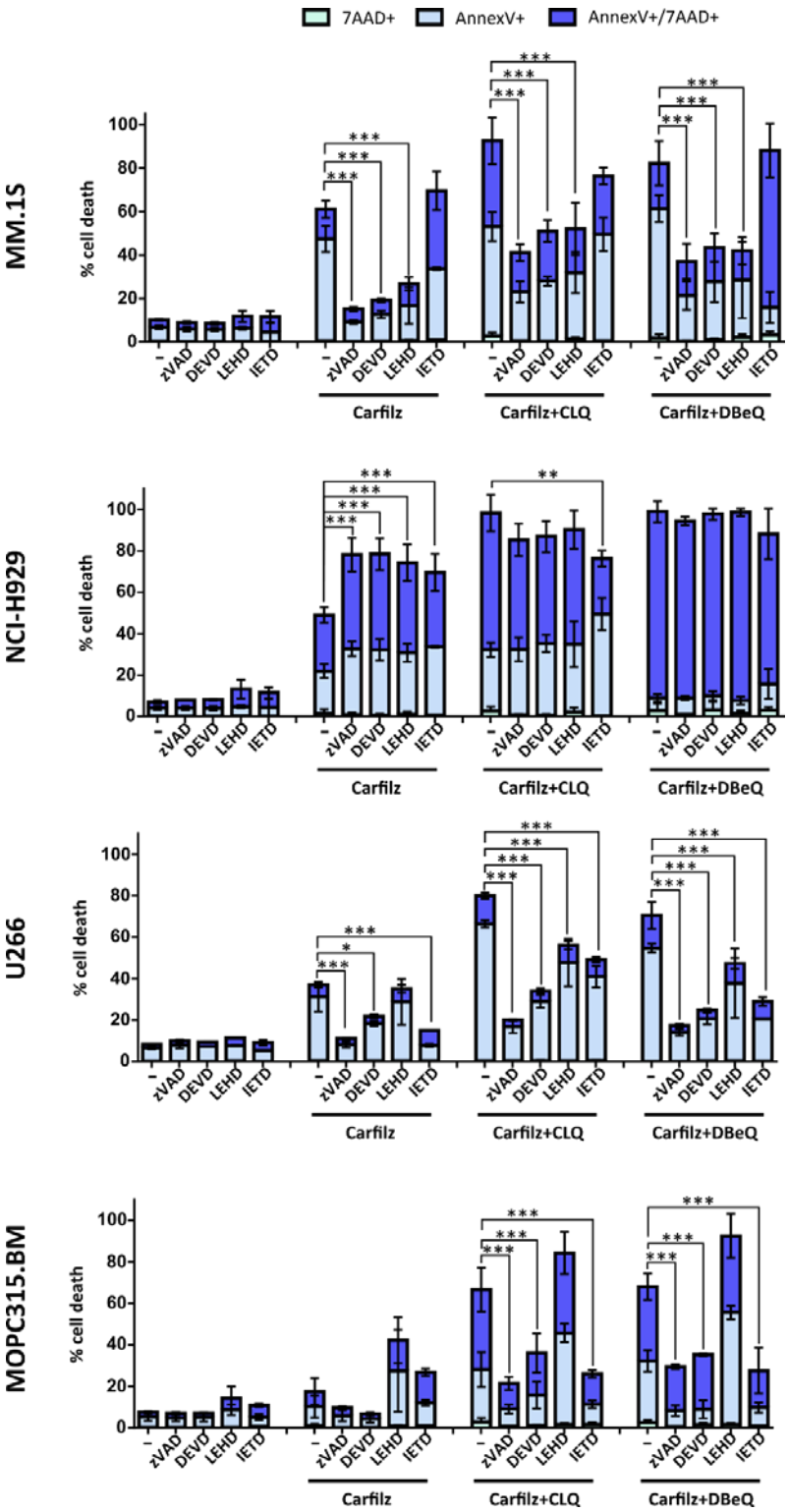

Figure 4.23 | Role of caspases in cell death induced by carfilzomib and its combination with CLQ or DBeQ. MM cell lines were pre-incubated with different caspase inhibitors 1h before administering the indicated drugs. Pan-caspase inhibitor zVAD-fmk, caspase-3 inhibitor z-DEVD-fmk, caspase-9 inhibitor z-LEHD-fmk and caspase-8 inhibitor z-IETD-fmk were incubated at a drug concentration of 30 μM. Thereafter, cells were incubated with carfilzomib at 5 nM in case of MM.1S and NCI-H929 cell lines, 7 nM in U266 and 10 nM in MOPC315.BM and the respective combinations with chloroquine (CLQ, 20 μM) or DBeQ (2,5 μM) for 24h. Cell death was analysed by measuring PS exposure by Annexin V staining and membrane integrity through 7-AAD co-staining. Statistical analysis was performed using one-way ANOVA test with Tukey post-test, where *p<0.05; **p<0.01; ***p<0.001. Data are presented as mean ± SD from n=3 independent experiments.

Although caspase-8 follows the extrinsically activated death receptor pathway, it has been reported that caspase-8 mediated cell death could also be triggered by persistent ER stress[116]. In this scenario, ER stress induced by thapsigargin (a widely known ER stressor) resulted in UPR-dependent upregulation of DR5 receptor and cell death[122,609]. Association of DR4 upregulation and ER stress has also been reported[116]. Different groups have shown that the mechanism by which persistent ER stress induced caspase-8 mediated cell death independently of death receptors, involves the formation of an autophagosome-associated platform[116,610–612]. PIs like bortezomib[613,614] and carfilzomib[615] have also been shown to upregulate or stabilize death receptors (DR4 and/or DR5) and synergize with TRAIL induced apoptosis in several cancer models. However, previous work from our group reported that although bortezomib and Apo2L/TRAIL cooperated in MM apoptosis, this event was not provoked by the upregulation of membrane DR4 and DR5 expression induced by bortezomib[132].

In addition, we also wondered whether other cell death modalities, like **necroptosis**, could contribute to the cell death induced by these compounds. To that end, we utilized the inhibitor of RIPK1 (necrostatin-1, Nec-1) and the inhibitor of MLKL (necrosulfonamide, NSA). These inhibitors were added to cells 1h prior to the addition of carfilzomib and the respective combinations with CLQ or DBeQ. Note that MOPC315.BM cell line was not incubated with MLKL inhibitor since NSA is not operative in murine cell lines. The reason behind this is that the cysteine at residue 86 in human MLKL and targeted by NSA is replaced by a tryptophan residue in murine MLKL[616].

The study of necroptosis participation in cell death induced by these compounds lead to the following results (**Figure 4.24**). Individual inhibition of RIPK1 or MLKL with Nec-1 and NSA respectively in absence of caspase inhibition, did not provoke any significant effect on cell death in all MM cell lines. These results are reasonable given that caspases are still active and that cell death induced by these drugs is mainly apoptotic. According to the accepted model, necroptosis is only triggered when caspases are inactivated. In case of MM.1S and U266 cells, combination of z-VAD-fmk with Nec-1 or NSA inhibition offered a slight, but non-significant additional protection compared to that presented by caspase inhibition alone. Conversely, in NCI-H929 and MOPC315.BM cells concurrent inhibition of apoptotic and necroptotic pathways did not granted additional protection. This was especially intriguing in NCI-H929 cells in which caspases seem not play a major role in cell death. Moreover, these cells presented a significant proportion of cells within the Annexin V/7-AAD double positive population, particularly under carfilzomib plus DBeQ combination suggesting a necrotic-like kind or advanced state of cell death.

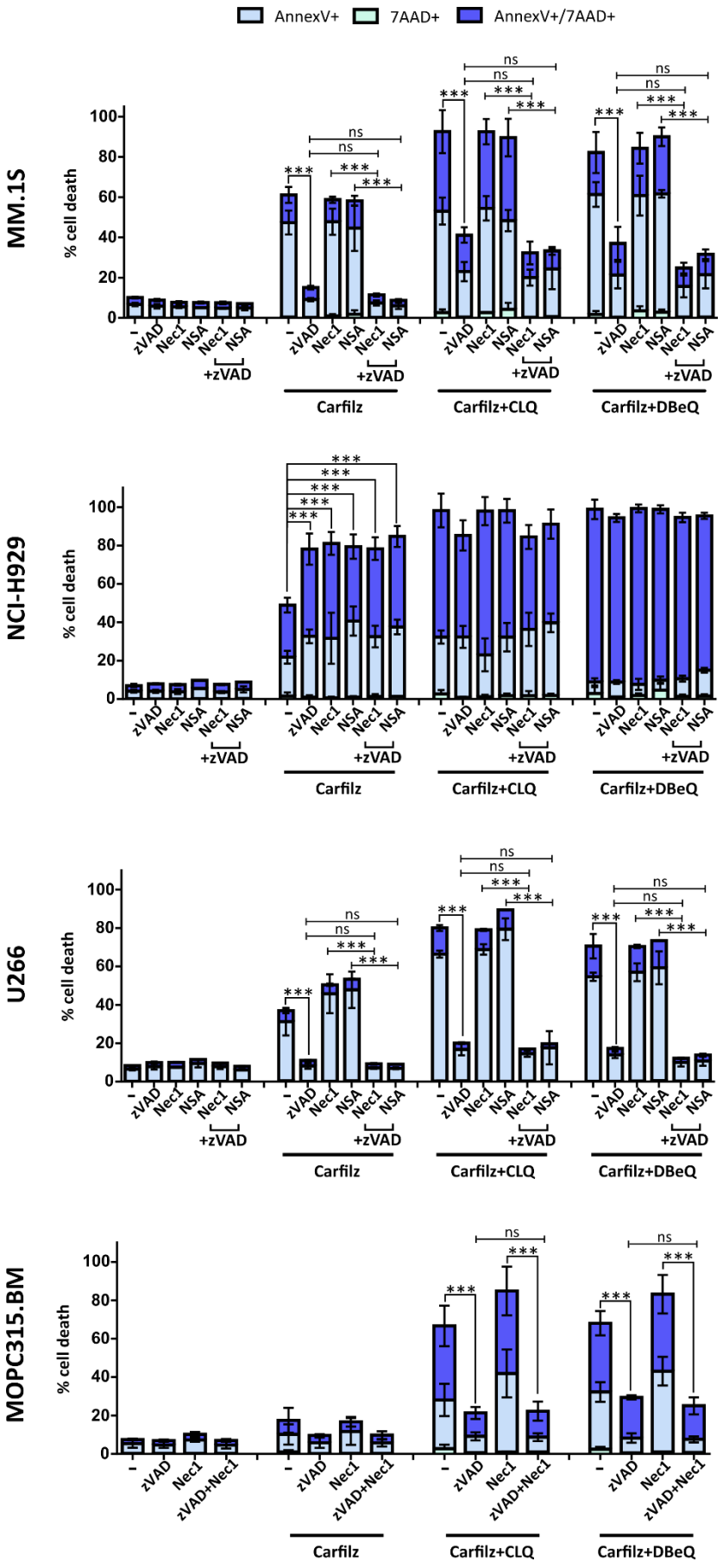

Figure 4.24 | Role of the necrosome in cell death induced by carfilzomib and its combination with CLQ or DBeQ. MM cell lines were pre-incubated with different necroptotic or caspase inhibitors 1h before administering the indicated drugs. Pan-caspase inhibitor zVAD-fmk and RIPK1 inhibitor necrostatin-1 (Nec-1) were incubated at 30 μM, whereas the MLKL inhibitor necrosulfonamide (NSA) was incubated at 1 μM. Hereafter, cells were incubated with carfilzomib at 5 nM in case of MM.1S and NCI-H929 cell lines, 7 nM in U266 and 10 nM in MOPC315.BM and the respective combinations with chloroquine (CLQ, 20 μM) or DBeQ (2,5 μM) for 24h. Cell death was analysed by measuring PS exposure through Annexin V binding and membrane integrity by 7-AAD co-staining. Statistical analysis was performed using one-way ANOVA test with Tukey post-test, where *p<0.05; **p<0.01; ***p<0.001. Data are presented as mean ± SD from n=3 independent experiments.

PIs in general and carfilzomib in particular have been shown to preferentially induce cell death through the mitochondrial intrinsic apoptotic pathway in a caspase dependent manner[108,198,200,238]. Some pieces of evidence such as production of mitochondrial ROS and the ability of carfilzomib to induce extrinsic apoptosis, raise the possibility that PIs like carfilzomib may also trigger necroptosis. However, a recent study reported that when caspases are inhibited carfilzomib was ineffective in unleashing necroptosis even in cells sensitive to this type of cell death[617]. Similarly, our results only showed a quite small, yet non-significant, additional protection (in some cell lines) when necroptotic inhibitors were added concomitantly to pan-caspase inhibitor, even in conditions in which carfilzomib was combined with CLQ or DBeQ that would exacerbate cell death. These results may imply a minor contribution of necroptosis to cell death in our experimental model.

4.2.2. ER Stress-Associated Cell Death.

4.2.2.1. Analysis of the UPR and ER Stress Response.

The UPS plays a key role in cellular protein quality control system, which is in charge of disposing off roughly 80-90% of cellular proteins[109]. Therefore, targeting the proteasome would eventually lead to protein accumulation and ER stress, especially in cells with a highly secretory phenotype such as MM cells. Moreover, CLQ or DBeQ target accessory pathways that contribute to normal proteostasis and can be activated under ER stress conditions and may contribute to ameliorate this situation.

As working hypothesis, we speculated whether CLQ and DBeQ may further enhance and/or accelerate ER stress signals started by carfilzomib treatment and consequently, this would be translated into the increased cell death observed so far. To attend this scientific interrogation and delve deeper in the role of ER stress in the mechanism of carfilzomib-induced cell death, as well as the mechanism governing combinatory drug regimens with CLQ or DBeQ, we studied the expression levels of several proteins involved in the UPR and ER stress response at different time points. Since PERK and IRE1-mediated arms of the UPR are the main signalling pathways involved in ER stress-associated cell death, we focused in these two UPR branches (sections 1.4.2 and 1.4.3). As a positive control of ER stress, cells were treated with the ER stressor drug thapsigargin, a chemical inhibitor of SERCA (ER calcium pump), that provokes a potent Ca^{2+} imbalance and ER stress[618]. Protein expression levels were assessed after 8, 10 and 14 hours of drug incubation (**Figure 4.25** and **Figure 4.26**). We selected these time-points based on preliminary experiments using thapsigargin, evaluating mainly the generation of the spliced form of XBP1 as an ER stress marker.

Starting with the master regulator of the UPR, **BiP** (also called GRP78) levels showed two distinct expression patterns in the different MM cell lines tested. U266 and MOPC315.BM cells displayed high BiP expression under basal conditions. In these cells,

treatment with carfilzomib and CLQ or DBeQ combination, hardly increased BiP expression relative to basal levels (**Figure 4.25** and **Figure 4.26**). Interestingly, these two cell lines displayed more resistance towards the drugs used in this study, suggesting that increased BiP levels would be associated to this drug resistance. With more BiP molecules, cells would have an increased capacity to cope with ER stress, possibly increasing the threshold required to shift from the adaptive UPR signalling to the pro-death UPR pathway. In fact, BIP has been found to be overexpressed in several types of human cancers and to participate in several aspects of cancer development[619,620]. Moreover, increased BiP expression has been reported to confer chemoresistance in different tumour models including those of PI-based therapy[213,621–624]. By contrast, MM.1S and NCI-H929 cells manifested low levels of BiP in basal conditions. Treatment with either carfilzomib or its combinations with CLQ or DBeQ dramatically increased BiP expression. This response is thought to be as part of the UPR adaptive mechanism to deal with ER stress and restore cellular homeostasis[114,115]. For instance, ATF6 has been shown to upregulate BiP levels, among other chaperones in response to ER stress[183]. Moreover, an alternative mechanism in which BiP mRNA was stabilized, rather than degraded by IRE1's RNAse activity, eventually increasing BiP protein levels, has also been reported in fission yeasts[625].

Some of the proteins involved within PERK-mediated arm of the UPR were also studied. In particular, phosphorylation of eIF2α, CHOP/GADD153 and PERK expression were examined. In relation to **PERK** levels, they followed a distinct pattern depending on the cell line under evaluation. In U266 cells, thapsigargin as well as treatment with carfilzomib and its combination with CLQ or DBeQ increased PERK expression at 8h of drug incubation. At longer incubation times, expression seemed to normalize. In MM.1S and MOPC315.BM cells, thapsigargin treatment did not induce an upregulation of PERK levels. However, similar to U266 cells at 8h of treatment, carfilzomib and its combination with CLQ or DBeQ enhanced PERK expression that faded with time. NCI-H929 cells presented elevated levels of PERK in basal conditions. Treatment with thapsigargin apparently reduced PERK expression at shorter incubation times. Moreover, although there are some differences in PERK expression levels between the drug combinations of carfilzomib with either CLQ or DBeQ, a common conclusion can be drawn out. It is possible that as an adaptation mechanism, cells react by upregulating PERK levels to deal with ER stress mediated effects of drug exposure and promote survival[626].

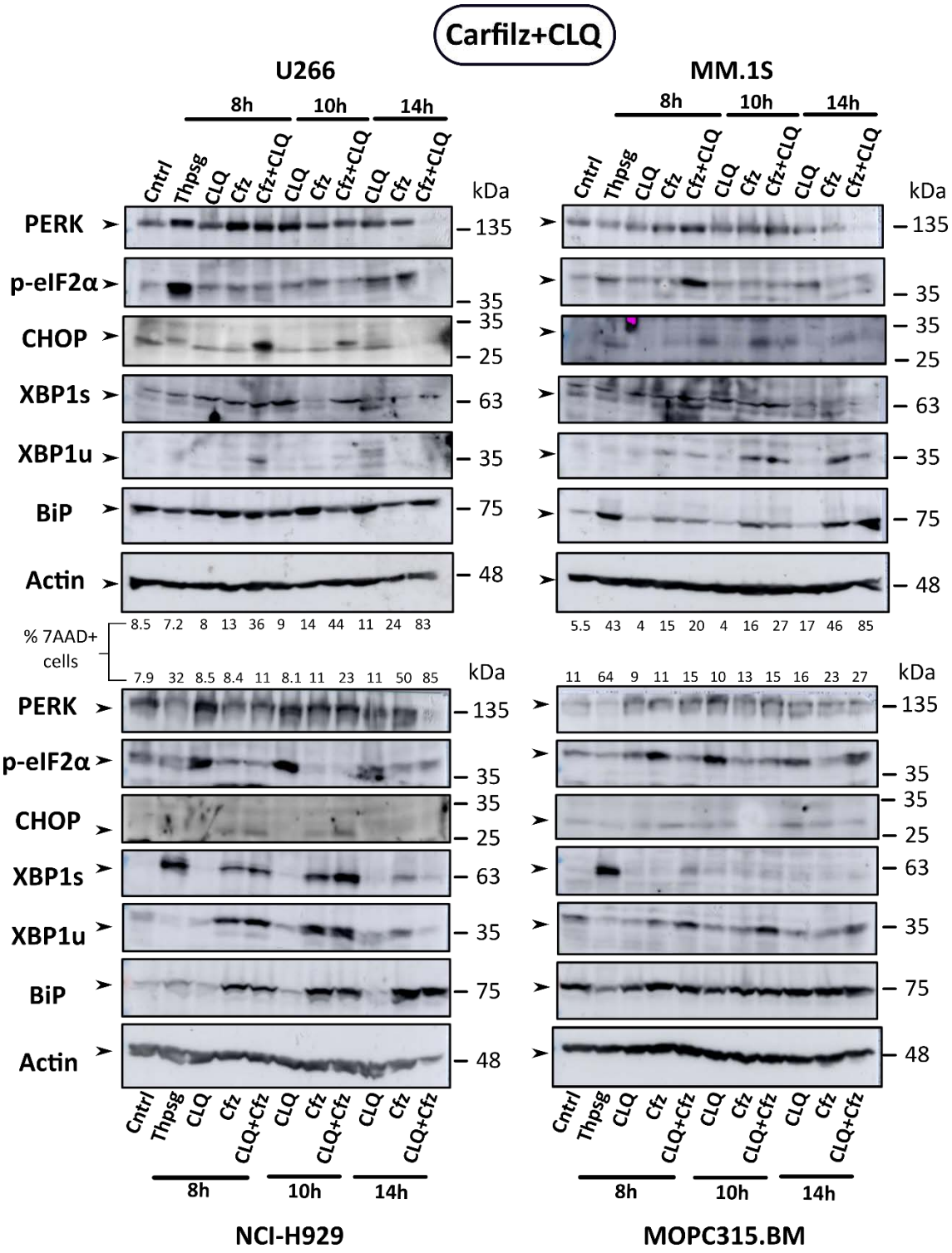

Figure 4.25 | Protein expression levels of different UPR and ER stress response markers in MM cell lines. MM cell lines were incubated at different time points with carfilzomib and/or CLQ. MM.1S and NCI-H929 cell lines were treated with 5 nM of carfilzomib (Cfz), U266 cells with 7 nM of carfilzomib and MOPC.315.BM with 10 nM carfilzomib. CLQ concentration was in all cases 20 μM. In parallel, cell death was assayed evaluating the incorporation of 7-AAD to monitor cytotoxicity in each condition. A representative immunoblot is presented from n=4 independent experiments.

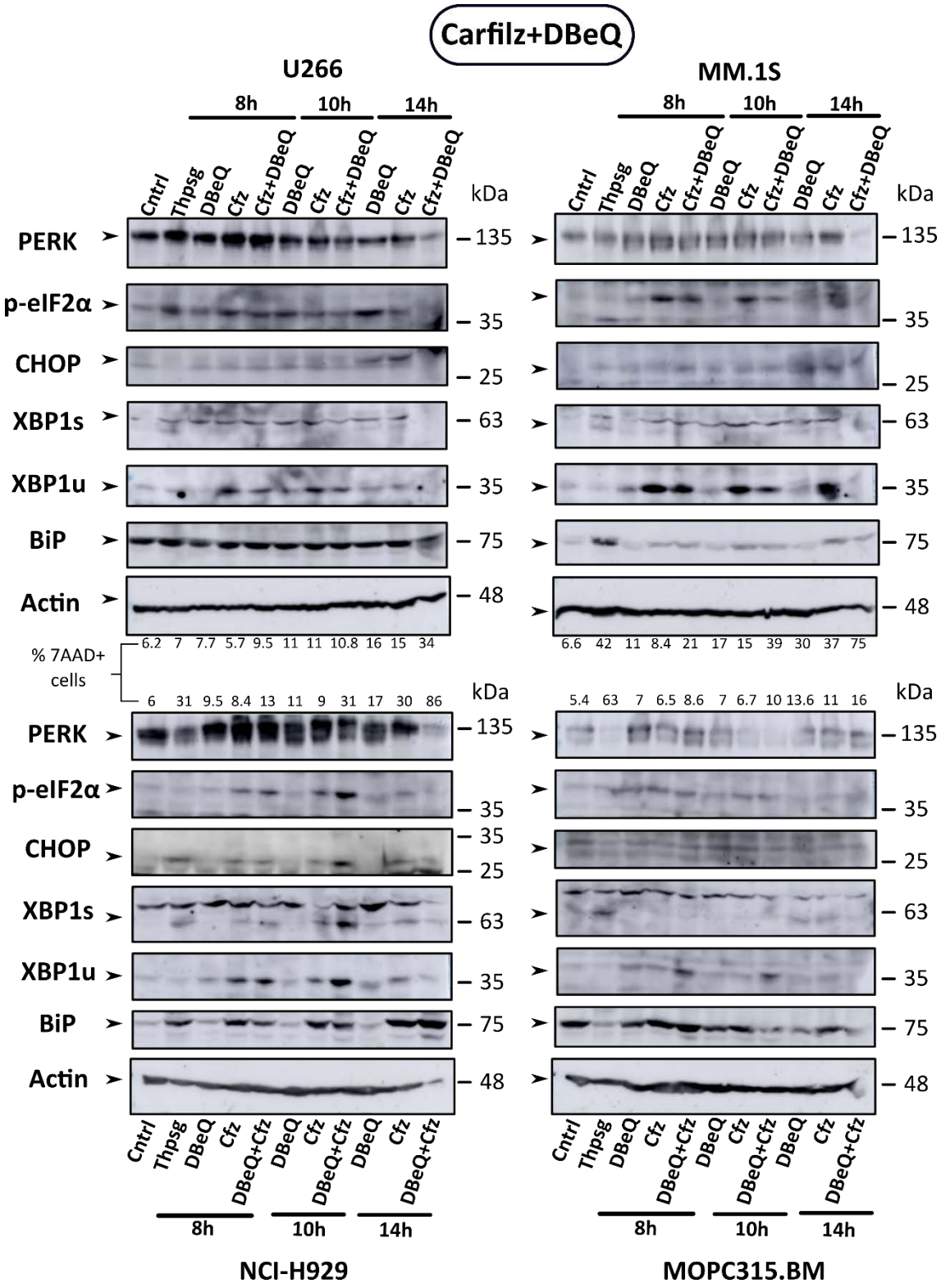

Figure 4.26 | Protein expression levels of different UPR and ER stress response markers. MM cell lines were incubated at different time points with carfilzomib and/or DBeQ. MM.1S and NCI-H929 cell lines were treated with 5 nM of carfilzomib (Cfz), U266 cells with 7 nM of carfilzomib and MOPC.315.BM with 10 nM carfilzomib. DBeQ concentration was in all cases 2.5μM. In parallel, cell death was assayed evaluating the incorporation of 7-AAD to monitor cytotoxicity in each condition. A representative immunoblot is presented from n=2 independent experiments.

After PERK activation, this ER stress sensor mediates phosphorylation and inactivation of the eukaryotic translation initiation factor 2 subunit 1 (eIF2α) to shut down protein translation. In our experimental settings, levels of **p-eIF2α** closely paralleled PERK expression pattern in the different MM cell lines, but sometimes following a different time pattern. In U266 cells, thapsigargin treatment produced a marked increase in p-eIF2α levels. However, at shorter incubation times (8-10h), combined treatments (Cfz+CLQ or Cfz+DBeQ) as well as each of the individual drugs alone (Cfz, CLQ or DBeQ), only augmented eIF2α phosphorylation in a slightly weaker fashion. After 14h of drug incubation, DBeQ, CLQ and carfilzomib, but not the combinations, further increased p-eIF2α levels. The apparent lack of signal in drug combinations could be due to the loss of cellular material (as revealed by the reduced protein levels of β-actin) at later time points because of the high cell death rate observed. MM.1S cells showed elevated levels of p-eIF2α after treatment with carfilzomib alone and the combined treatments with carfilzomib with either CLQ or DBeQ. In the case of MOPC315.BM cells, although p-eIF2α levels augmented with the different drugs, it followed an irregular time-dependent pattern. In **Figure 4.25**, it can be observed that after 8h of drug incubation, eIF2α became phosphorylated after single carfilzomib treatment, but not when combined. Two hours later, CLQ treatment alone produced a marked increase in p-eIF2α levels. Only at longer incubation times, the combinatory regimen of carfilzomib and CLQ, showed augmented p-eIF2α expression. However, in **Figure 4.26**, carfilzomib and DBeQ either single or in combination, only produced a slight increase in p-eIF2α levels. Finally, since NCI-H929 cells displayed a quick cell death kinetics, phosphorylation of eIF2α occurred at earlier time points. In **Figure 4.26**, treatment with carfilzomib and DBeQ produced a slight increase in eIF2α phosphorylation, especially after 10h of drugs incubation.

During acute ER stress conditions, phosphorylation of eIF2α mediates active repression of protein synthesis as a protective mechanism to restore protein homeostasis. PIs have been reported to induce robust PERK signalling and consequently eIF2α phosphorylation[627]. However, persistent ER stress exposure engages long-term adaptation mechanisms that aim to restore protein translation. In particular, the PERK-mediated arm is able to increase the expression of GADD34 that in conjunction with PP1 phosphatase dephosphorylates eIF2α and reinstate protein translation[628]. It is tempting to speculate that the fluctuating and decaying levels of p-eIF2α observed in our experimental system are a consequence of GADD34 activity. In fact, releasing translational inhibition through eIF2α dephosphorylation is a key factor in ER stress-induced cell death[135]. It has been proposed that once the adaptive phase of the UPR have failed to restore homeostasis, GADD34 serves as a negative feedback loop to recover protein translation and engage programmed activation of stress-induced genes that drive the apoptotic phase[629].

Although cap-dependent translation is shut down under sustained PERK signalling and eIF2α phosphorylation, some mRNAs can be translated[627]. This leads us

to the next UPR marker we have evaluated, the **CHOP/GADD153** transcription factor. In all MM cell lines tested, combined treatment of carfilzomib with CLQ or DBeQ upregulated CHOP expression at some extent, although, in the case of carfilzomib + DBeQ, CHOP induction was less evident in some cases. Noteworthy, congruently with p-eIF2α expression pattern, CHOP expression eventually faded with time. Moreover, combination of carfilzomib plus CLQ accelerated CHOP induction in MM.1S and U266 cells. Our results agree with previous reports indicating that bortezomib treatment, activates PERK signalling with the ensuing phosphorylation of eIF2α and CHOP induction[197]. In fact, one of the main mechanisms of ER stress-induced cell death is thought to be mediated by PERK/p-eIF2α/ATF4/CHOP axis[114,630,631].

Although the mechanism by which CHOP triggers apoptosis is not fully elucidated, CHOP has been shown to regulate the expression of several Bcl-2 family members[115,632,633]. In particular, it has been reported that CHOP downregulates the expression of anti-apoptotic Bcl-2[126] and Mcl-1[129] proteins, while enhancing those of pro-apoptotic proteins like Bim and PUMA[98,121]. However, although CHOP is involved in ER stress-induced cell death, its overexpression has been shown not to be sufficient on its own to trigger cell demise[116,126,634]. On the other hand, although PERK and CHOP are key components of ER stress-induced cell death, cells could also undergo cell death in absence of these proteins, reflecting the existence of alternative pathways that could drive cell demise in these conditions[632]. Additionally, CHOP may also contribute to cell death by increasing ROS levels. The endoplasmic reticulum oxidoreductin 1 (ERO1α) is one of the transcriptional targets of CHOP and it participates in creating an hyperoxidizing environment in the ER[116]. Interestingly, CHOP induction is not only restricted to PERK activation, XBP1s and even ATF6 have also been reported to be involved in transcriptional regulation of CHOP[116,631]. This suggest the existence of an intertwined crosstalk between the different UPR branches that controls adaptation and cell fate in response to ER stress[631].

Probably, the most conserved arm of the UPR is the one commanded by the ER stress sensor IRE1α[115]. Under ER stress conditions, IRE1α gets activated and with its RNAse activity, mediates the splicing of XBP1 mRNA, generating **XBP1s** protein (s stands for spliced). As illustrated in **Figure 4.25** and **Figure 4.26**, XBP1s levels were increased in most of the MM cell lines when treated with carfilzomib or its combination with CLQ or DBeQ. However, it must be noted that in some MM cell lines, XBP1s induction after carfilzomib and DBeQ or CLQ treatment was less apparent. For instance, it has been proposed that, as a ER stress adaptation mechanism, MM cells can display an IRE1/XBP1s low signature that could also be correlated with PIs-based therapy resistance[196,635,636]. NCI-H929 cells, one of the most PI-sensitive cell lines analysed, clearly showed the evolution of XBP1s levels under the ER stress response generated by the drugs under study. There is an escalating phase in which XBP1s levels increased peaking at about 10h of drug incubation, and decrease thereafter. In fact, IRE1α signalling has been reported to turn off and to decay with time when ER stress is

sustained[114,637]. Especially, IRE1α-mediated XBP1 splicing is thought to be transient and occur only during the acute phase of the ER stress response, being attenuated upon prolonged stimulation later[115,131]. For instance, a specific mechanism emanating from PERK has been reported to be responsible for IRE1α signalling attenuation[638]. Interestingly, the combination of carfilzomib and CLQ or DBeQ was more effective than carfilzomib alone in augmenting XBP1s levels. This is particularly evident in NCI-H929 cells. These data also agree with the previous potential assumption that combined regimens accelerated and were more effective in delivering death signals.

In UPR signalling, XBP1s acts as an important transcription factor that modulates gene transcription of genes involved in ERAD, protein folding, secretion and lipid synthesis which generates a cellular response that try to restore protein homeostasis and promote cytoprotection[113,115]. Thus, although IRE1α-XBP1 axis is mainly pro-survival, IRE1α can also engage apoptotic pathways[98]. As noted before, XBP1s can also drive CHOP induction and hence contribute to cell death. However, probably the strongest connection between IRE1α pathway and cell death could be attributed to its ability to engage and activate stress kinases JNK and p38MAPK pathways that subsequently targets Bcl-2 family of proteins[98,116]. In particular, JNK has been connected with Bcl-2 and Bcl-X_L phosphorylation[119], decreasing its anti-apoptotic activity and it has been also shown to phosphorylate Bim and Bid, increasing its pro-apoptotic activity[120,121]. In addition, the RNAse activity of IRE1α can also process and degrade many ER-targeted mRNAs by a mechanism termed "regulated IRE1-dependent decay" (RIDD) which depletes protein-folding components further aggravating ER stress[114,115]. Additionally, RIDD process can further amplify cell death signals by degrading mRNAs from anti-apoptotic proteins shifting the balance towards cell death[116]. However, in conjunction with other studies that support a general anti-apoptotic role of IRE1 signalling pathway, RIDD process can also promote survival through mRNA degradation of pro-apoptotic proteins[609]. Therefore, during ER stress, IRE1α downstream signalling can mediate opposing effects on cell fate (either survival or cell death). The final cellular outcome is thought to be greatly influenced by the intensity of stress signals, as well as the duration of the ER stress response[113].

Finally, under basal conditions when IRE1 is deactivated, XBP1 mRNA do not undergo the splicing process and hence **XBP1u** protein is generated (u stands for unspliced). As observed in **Figure 4.25** and **Figure 4.26**, the unspliced form of XBP1 accumulated in the different MM cell lines mimicking at some extent XBP1s levels. XBP1u is a highly unstable protein and usually it is rapidly degraded by the 26S proteasome[115]. In our experimental model, since the proteasome is inhibited, XBP1u protein accumulated. For instance, stabilization of XBP1u levels has also been reported by others in other tumours under PI-based therapy. Interestingly, the unspliced form has been shown to act as a dominant-negative molecule suppressing IRE1α signalling and impairing the generation of active XBP1 spliced species[636,639]. Since IRE1/XBP1 axis is

quite moderately activated in some of our MM cell lines, it is possible that the PI-driven accumulation of XBP1u species could also be behind this lack of XBP1 splicing.

Recent studies proposed that the timing and the amplitude of signalling responses evoked by UPR sensors differ between particular ER stress insults[114]. This consequently, has direct repercussions on cell fate decisions. Moreover, specific ER stress stimuli can preferentially activate one UPR branch or another[114]. For example, IRE1 and PERK arms have been found to be activated before ATF6, in response to calcium imbalance like the one produced by thapsigargin treatment, whereas IRE1 is thought to respond more rapidly to reducing agents[114,640]. In our experimental model we have observed upregulation of markers related to both PERK and IRE1 arms, but we don't attempt to indentify whether the activation of one determined UPR branch precedes the other. This would probably have required an exhaustive time-based analysis, given the dynamic nature of the UPR. Moreover, in our analysis we have observed upregulation of both pro-apoptotic (CHOP) and pro-survival (BiP or XBP1s) markers. It is difficult to unravel the contribution of individual factors to the final cell fate and also to observe the switch from adaptive to pro-death responses that occurs during ER stress response. Probably, the chronic and irreversible nature of drug-based ER stress may precipitate and drive cells inevitably to apoptosis allowing that adaptive factors are co-expressed with pro-apoptotic ones. In such conditions, the inherent distinction between the adaptive and pro-apoptotic ER stress responses would be masked[114].

Collectively, we have shown that treatment with carfilzomib and its combination with CLQ or DBeQ increased the expression of several UPR markers indicating the activation of an ER stress response. In particular, we have found evidences of the activation of both PERK and IRE1 arms of the UPR. Although, there are several previous studies in the literature supporting the involvement of both UPR arms in ER stress-induced cell death, the implication of these pathways in our experimental model requires further clarification. Nonetheless, we have found the pro-apoptotic transcription factor CHOP, to be upregulated especially upon carfilzomib plus CLQ treatment and in a lesser extent with carfilzomib and DBeQ combination or the PI alone. Moreover, combinatory regimens were more effective in triggering the ER stress response, displaying an increased accumulation of all or some of the UPR markers analysed.

4.2.2.2. *Implication of BiP in ER stress-associated Cell Death.*

BiP/GRP78 plays an important role in the cellular stress generated during cancer development[620,630]. For instance, this protein has been found to be overexpressed in several human tumours[620,622]. BiP/GRP78 facilitates tumour proliferation, survival, metastasis and resistance to therapy[620,622]. We also observed that those MM cell lines endowed with increased basal BiP expression, were the ones that better resisted PI-based therapies. Therefore, we sought to investigate the role of BiP in ER stress-induced cell death in our experimental model.

For that purpose, we targeted BiP expression by siRNA-mediated knockdown in U266 and in MM.1S, as described in section 3.12.10.2, and monitored cell death upon carfilzomib treatment and the respective combinatory treatments with CLQ and DBeQ. We conducted these experiments on two cell lines presenting different characteristics as regards to BIP expression. On one side, we selected a cell line that has high basal expression of BiP (U266), and on the other side, we selected a cell line in which BiP expression was lower in basal conditions, but was susceptible to BiP induction when challenged with ER stressors (MM.1S). In this way we will be able to dissect whether BiP expression (basal or induced), can improve cell survival when treated with the aforementioned drugs. First, we determined the optimal conditions to knockdown BiP levels (siRNA concentration and time). As illustrated in **Figure 4.27**, at 0.5 and 1 μM of siRNA, BiP levels were severely diminished after 24h and 48h of performing the electroporation of BiP-targeted siRNAs. Based on these and previous results, we decided to perform the subsequent cell death assays after 24h of siRNA transfection.

We first tried to test the impact of knocking down BiP expression with 1 μM of BiP siRNA over cell death induced by drug treatment. However, we observed no effect in cell demise when BiP was targeted at this concentration (results not shown). Since we previously saw that BiP levels raised after ER stress conditions, we decided to increase the BiP siRNA concentration to 2 μM and even 5 μM, to counteract the possible increment in BiP levels under these challenging conditions. Nonetheless, even targeting BiP at these higher concentrations of siRNA, did not have any significant effect over cell death rates exerted by the chemotherapeutics tested, neither in U266 nor in MM.1S cell lines (**Figure 4.27**). In U266 cells, a slight non-significant tendency towards lower cell death levels was observed upon BiP knockdown, particularly upon carfilzomib-DBeQ treatment. This would mean that by targeting BiP, cells would become more resistant to drugs that induce ER stress, which *a priori* could be interpreted as counterintuitive. However, as noted these changes were barely recognizable in most of the conditions. MM.1S cells that were targeted with BiP siRNA, tended to be marginally more sensitive than their siRNAΦ-targeted counterparts. Again, these differences were quite small and not significant enough to support these observations.

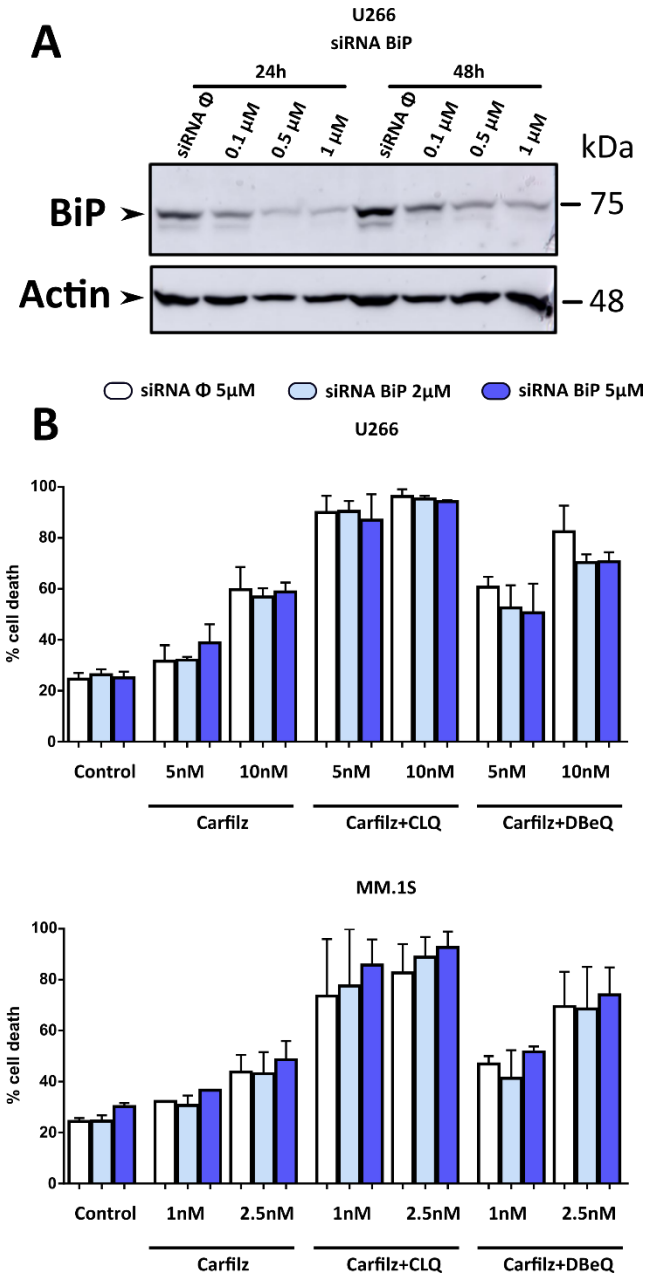

Figure 4.27 | Implication of BiP in ER-stress induced cell death. Determination of the involvement of BiP in ER-stress induced cell death exerted by carfilzomib and the respective combinations with CLQ or DBeQ. **A.** U266 cell line was first knocked-down for BiP expression by transfecting control- or BiP-targeted siRNAs through electroporation. Different siRNA concentrations and post-transfection incubation times were evaluated to assess the efficiency of gene silencing and BiP levels were quantified by western blot. **B.** For functional analysis, BiP expression was silenced in MM.1S and U266 by electroporating the chosen concentration in A of the control or BiP-targeted siRNA. Cells were incubated for 24 hours for gene silencing. After that time, cells were incubated with the different drugs at the indicated concentrations for additional 24 hours. Finally, cell death was assessed by annexinV and 7-AAD co-staining. Statistical analysis was performed by using one-way ANOVA with Bonferroni post-test, where *p<0.05; **p<0.01; ***p<0.001. Data is presented as mean ± SD from n=2 independent experiments

As mentioned earlier, BIP/GRP78 induction is necessary to alleviate ER stress, maintain ER-associated functions and protect cells from the toxic insults that accumulation of unfolded/misfolded proteins may generate[137]. Apart from functioning as the master regulator of the UPR, BiP/GRP78 has been shown to confer protection against ROS accumulation and also to stabilize mitochondrial function[137]. Our results contrast to that reported by others in which targeting BiP by siRNA-mediated knockdown, sensitized cancer cells to a diverse set of chemotherapeutics in different cancer cell models[620,641–644]. Particularly interesting is one study in which by silencing BiP expression, diffuse large B-cell lymphoma cells become more sensitive to bortezomib treatment[641].

In MM, studies have shown that cells were able adapt to stress insults and also to drive therapy resistance, including to PIs, by upregulating BiP levels[645]. In fact, it was proposed that BiP favours aggresome (proteotoxic protein aggregates) delivery to autophagosomes[645]. In this way, BiP mitigates ER stress and assists in the clearance of these toxic species in alternative clearance pathways[645]. Moreover, genetic ablation of BiP followed by bortezomib treatment, enhanced the cytotoxic effect of bortezomib[645]. In this case, gene-mediated suppression of BiP expression was performed with short-hairpin RNAs. Moreover, a detailed analysis of this study suggested that the reported differences on cell death after BiP targeting, were not so abrupt. Furthermore, cell death monitoring was conducted by assessing caspase-3 activation by immunoblot, a semiquantitative method, which could not render the same and more precise quantitative results as flow cytometry does. Additionally, although BiP is the master regulator of the UPR, alternative chaperones like Hsp90 or Hsp70 related proteins, could be induced under ER stress conditions and could help by mitigating proteotoxic stress conditions and compensate BiP scarcity.

To conclude, we have shown that apparently, BiP did not confer protection against cell death mediated by the drugs used in our model and therefore, gene-targeted silencing with siRNAs, did not sensitize cancer cells to chemotherapeutic drugs. This is thought to be the case in situations where basal BiP levels are increased and also after ER stress-mediated induction of BiP, as shown in U266 and MM.1S cell lines.

4.2.2.3. Inhibition of PERK & IRE1 Pathways.

As shown above, the drugs used in our experimental system are able to unleash an ER stress response. However, although some of the UPR markers upregulated in our model, have strongly been associated with ER stress-induced cell death, we have not yet established a clear-cut connection. To further deepen our knowledge and characterize the molecular pathways that instigate cell death signalling and unravel the relative participation of different UPR branches in cell demise, we used chemical inhibitors against PERK and IRE1α ER stress sensors. In particular, we used GSK2606414 and 4μ8C drugs that inhibit PERK and IRE1 respectively. GSK2606414 is a potent and selective first-in-class ATP competitive inhibitor of PERK[208,646]. On the other hand, 4μ8C is a small molecule selective inhibitor that targets a critical lysine in the active site of the IRE1 endoribonuclease (RNAse) domain, forming a stable imine that blocks substrate access, hence suppressing XBP1 splicing and mRNA dependent degradation (RIDD)[188,647].

These inhibitors were pre-incubated 1 hour before the addition of the other drugs (carfilzomib, CLQ and/or DBeQ) and thereafter, cell death was monitored to evaluate the effect of these inhibitors on cell demise (**Figure 4.28** and **Figure 4.29**). Upon PERK inhibition, the cytotoxicity exerted by the different drugs (carfilzomib alone and the

combinations with CLQ or DBeQ) was dramatically enhanced in most of the cell lines tested. Probably, U266 cells were the ones that only showed a mild increase in cell death upon PERK inhibition, especially in carfilzomib treated cells. When 4μ8C was added to the medium, cell death experienced minor or no changes at all in most of the cases.

When both PERK and IRE1 inhibitors were administered concurrently (**Figure 4.29**) and before the addition of the rest of the drugs, in some cases, cell death mimicked the behaviour observed upon PERK inhibition. However, under some conditions, double inhibition of PERK and IRE1 reduced cell death levels provoked by PI-based therapy and its respective combinations, relative to PERK inhibition. In some circumstances, this reduction in cell death even surpassed the levels presented when no PERK or IRE1 inhibitor was added to the medium, that is, when cells were only treated with the conventional drugs. This particularly occurred in U266 cells when subjected to the combination of carfilzomib with CLQ or DBeQ, although it did not reach statistical significance. Under co-inhibition of PERK and IRE1, a significant reduction in cell death levels was also appreciated in NCI-H929 cells treated with carfilzomib and in MOPC315.BM cells treated with carfilzomib and DBeQ, but in this case only when compared to the cytotoxicity produced in presence of PERK inhibitor. Similar results were also obtained when cell death was evaluated by co-staining with $DIOC_6(3)$ and 7-AAD (**Figure 4.28**).

PERK inhibitors have demonstrated anticancer activity and to effectively block *in vivo* tumour growth[102,209,646]. Our data suggest that PERK might have a pro-survival rather than pro-apoptotic role in the cell death induced by the chemotherapeutics used so far. As explained earlier, under ER stress conditions, the cellular responses and cell fate, strongly depend on the integration of different ER stress inputs like the intensity and the duration of the stress signals. It is widely considered that cells respond to ER stress insults with two distinct temporally segregated UPR waves[114]. How the cell engages a given molecular programme or switches from one to another, still requires further comprehension. In a first attempt, cells activate adaptive and repair mechanisms to try to re-establish ER homeostasis and promote survival. At this respect, the three UPR branches (PERK, IRE1 and ATF6) contribute to this end by shutting down protein translation and enforcing partially overlapping transcriptional programmes that target genes involved in protein folding, ERAD, autophagy, redox metabolism, etc[115]. In particular, PERK activation leads to eIF2α phosphorylation, which halts general cap-dependent protein translation reducing ER protein influx and overload. On the other, hand p-eIF2α allows selective translation of ATF4, among other genes. ATF4 controls the expression of pro-survival genes that participate in aminoacid metabolism, redox balance, protein folding and autophagy[114].

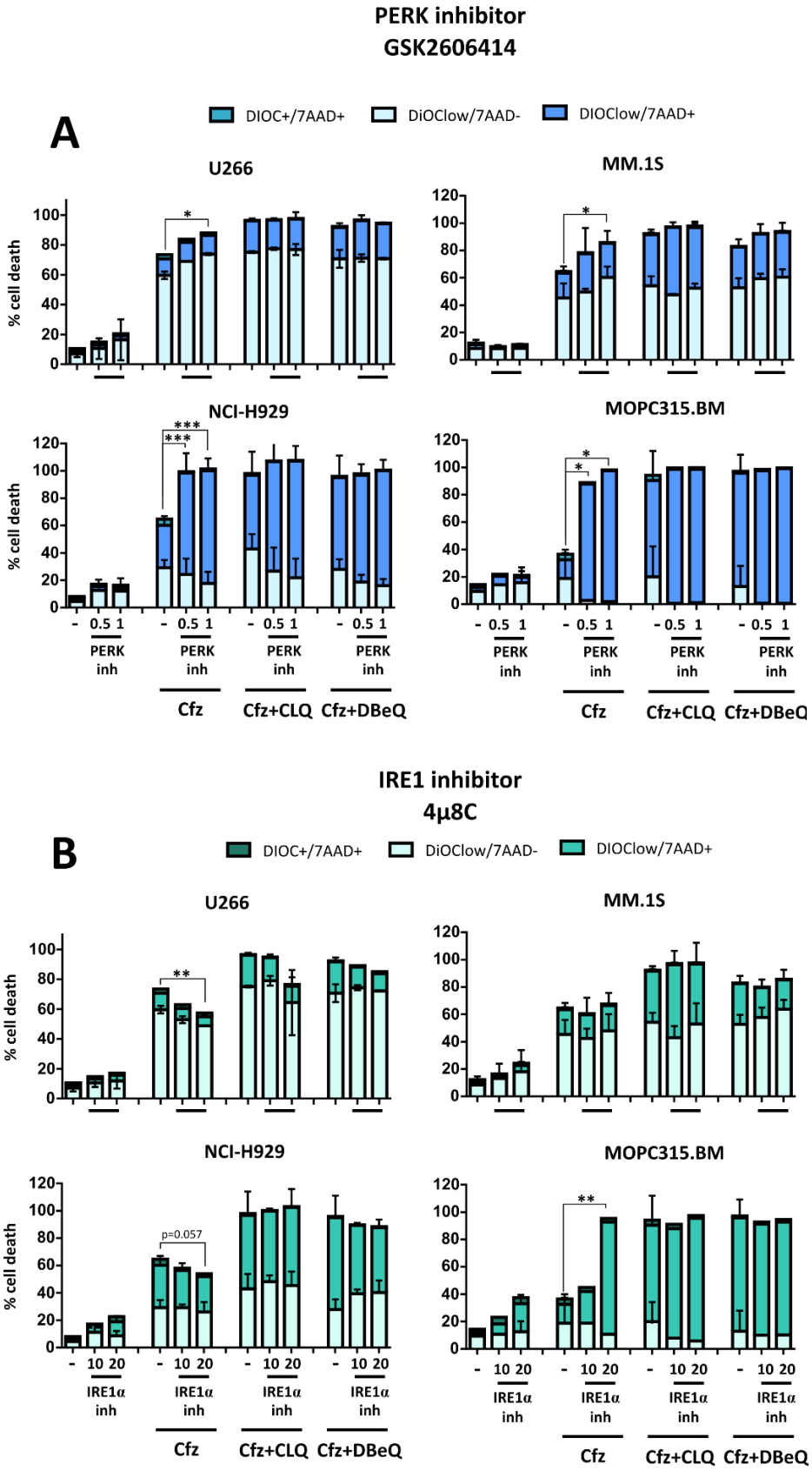

Figure 4.28 | Chemical inhibition of IRE1α and PERK pathways. The implication of IRE1 and PERK pathways to ER-stress induced cell death exerted by carfilzomib and the respective combinations were assessed using small molecule inhibitors of PERK and IRE1α ER stress sensors. Human and murine MM cells were pre-incubated for 1 hour with IRE1α inhibitor (4μ8C) or/and PERK inhibitor (GSK2606414) at the indicated drug concentrations. Afterward cells were incubated with carfilzomib, CLQ and DBeQ as indicated. MM.1S and NCI-H929 and U266 were treated with 5 nM carfilzomib, while MOPC315.BM were treated with 20 nM carfilzomib. All cell lines were incubated with 20 μM CLQ and 2.5 μM DBeQ. Cell death was assessed by determining mitochondrial membrane potential dissipation and plasma membrane permeabilization by co-staining with DIOC and 7-AAD. Statistical analysis was performed by using one-way ANOVA with Bonferroni post-test, where *p<0.05; **p<0.01; ***p<0.001. Data is presented as mean ± SD from n=3 independent experiments

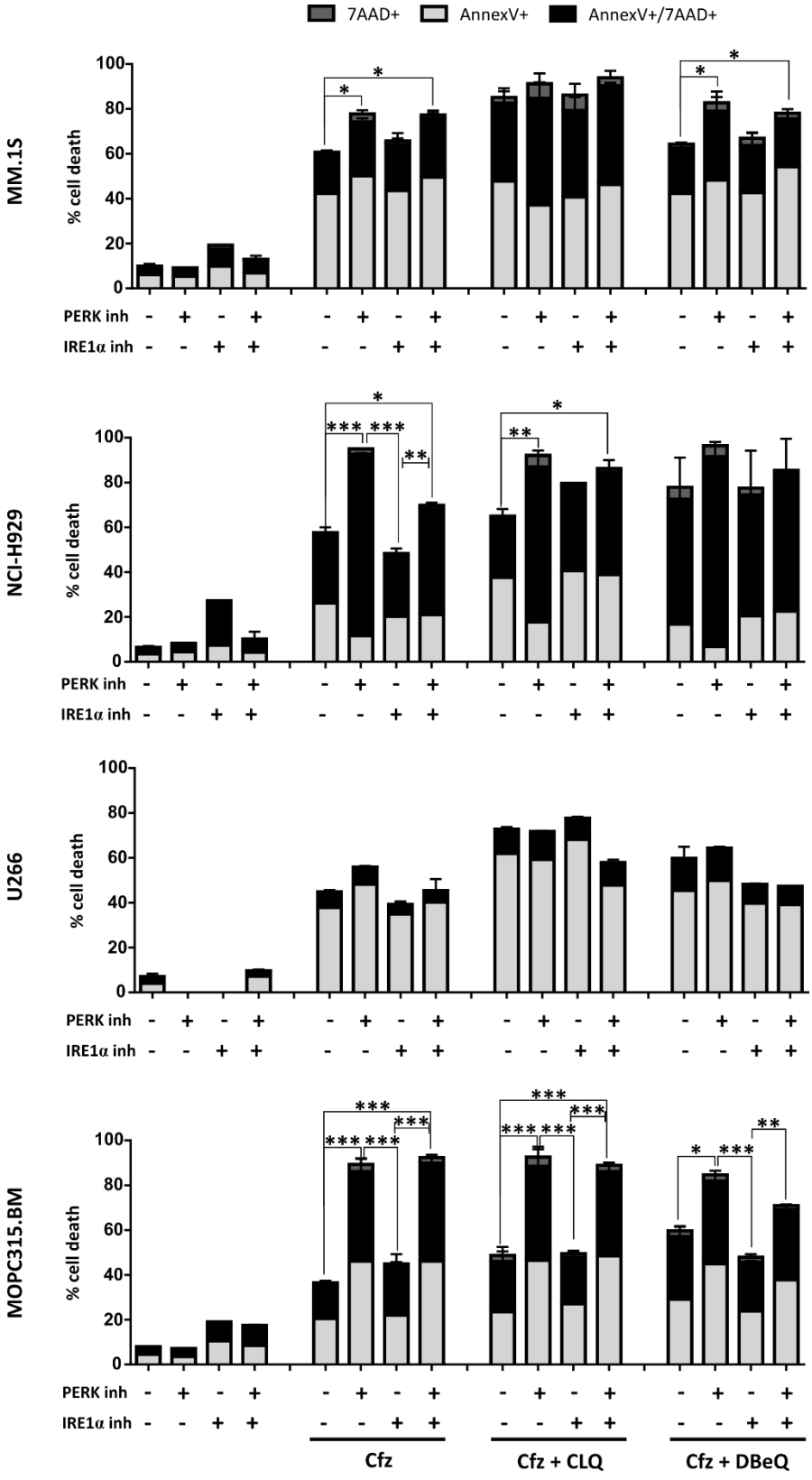

Figure 4.29 | Chemical inhibition of IRE1α and PERK pathways. The implication of IRE1 and PERK pathways to ER-stress induced cell death exerted by carfilzomib and the respective combinations were assessed using small molecule inhibitors of PERK and IRE1α ER stress sensors. Human and murine MM cells were pre-incubated for 1 hour with IRE1α inhibitor (4μ8C) or/and PERK inhibitor (GSK2606414) as indicated at 20 μM and 1 μM respectively. Afterward cells were incubated with carfilzomib, CLQ and DBeQ as indicated. MM.1S and NCI-H929 and U266 were treated with 5 nM carfilzomib when administered alone, while MOPC315.BM were treated with 20 nM carfilzomib. In carfilzomib-based combinations, carfilzomib concentration used was 2.5 nM in MM.1S and NCI-H929 and U266 and 10 nM in MOPC315.BM cells. In drug combinations, all cell lines were incubated with 10 μM CLQ and 2 μM DBeQ. Cell death was assessed by determining PS exposure and plasma membrane permeabilization by co-staining with AnnexinV and 7AAD. Statistical analysis was performed by using one-way ANOVA with Bonferroni post-test, where *p<0.05; **p<0.01; ***p<0.001. Data is presented as mean ± SD from n=3 independent experiments.

Considering all these observations, by inhibiting PERK under ER stress conditions we may also be blocking the initial adaptive and pro-survival response. As a consequence, ER stress overload and proteotoxic stress would dramatically be intensified precipitating cell demise. Another possible explanation can also rationalize the enhanced cell death observed with PERK inhibitors. Among the cellular targets activated by PERK, Nrf2 is a crucial regulator of genes involved in antioxidant responses and redox homeostasis[98,130].

Nrf2 overexpression has been observed in different cancer types conferring protection against oxidative stress, hence, facilitating chemo-resistance[648,649]. Interestingly, bortezomib treatment has been shown to increase intracellular ROS levels, playing a critical role in bortezomib-induced ER stress and apoptosis[650]. Moreover, Nrf2 inhibition was shown to enhanced bortezomib-induced cell death by intensifying ROS levels and ER stress[650]. As it will be covered in the following section, although our results suggest that mitochondrial ROS could be the main source of these species in our model, Nrf2 has been shown to regulate both mitochondrial and cytosolic ROS production[651]. In fact, Nrf2 has been shown to regulate mitochondrial function in several ways. Nrf2-KO cells were shown to display increased spontaneous apoptosis and were especially sensitive to chemically-induced mitochondrial damage, whereas cellular responses that led to Nrf2 activation protected cells against mitochondrial damage[652]. Therefore, in our model it is possible that by inhibiting PERK, we may also blunt downstream Nrf2 antioxidant responses, thereby intensifying ROS levels induced by carfilzomib and the drug combinations, eventually enhancing cell death. Additionally, one study showed that cell death induced by the known ER stressor thapsigargin was not compromised in PERK deficient cells[653].

Regarding IRE1 inhibition, 4μ8C targets the ribonuclease domain, leaving intact the kinase activity of IRE1. The pro-apoptotic signalling instigated by IRE1 probably mainly relies on its kinase activity rather than the ribonuclease domain. When IRE1 is activated it serves as a molecular scaffold that recruits and activates TRAF2/ASK1/JNK cascade to engage cell death signalling[131]. However, RIDD process (dependent on RNase domain) has also been suggested to contribute to cell death by degrading important mRNAs required to cell survival[131]. Therefore, one would assume that by targeting the RNase domain of IRE1, leaving the pro-apoptotic signalling intact, cells would be sensitized to ER stress insults. In fact, MKC-3946, an IRE1 inhibitor that shares the mechanism of action of 4μ8C, it effectively blunted tumour formation in xenograft MM model *in vivo*[654]. Furthermore, MKC-3946 significantly sensitized MM cells to bortezomib[654]. However, this has not been the observed outcome in our experimental settings when using 4μ8C inhibitor. Congruent with our results, Cross and colleagues reported that 4μ8C inhibitor did not sensitize cells to acute ER stress driven by tunicamycin or thapsigargin treatment[647]. The lack of anticancer effect exhibited by 4μ8C has been attributed to the fact that IRE1 is not involved in acute ER stress protection and therefore, XBP1 splicing and also the RIDD process are only responsible for building ER

capacity, but not in preserving ER integrity of stressed cells[647]. Similarly to PERK deficient cells, knock out of IRE1, JNK or other components of IRE1 pathway, did not protect cells from succumbing to ER stress-induced cell death[653].

Although chemical inhibitors are valuable experimental tools, they should be used as a primary approximation and conclusions should be extracted with caution. Although they usually claim to be selective enough, the reality is that they may have uncontrolled off-target effects. In fact, PERK inhibitors have been found to target and inhibit RIPK1 with even more potency that Nec-1[655]. Thus, these drugs were reported to confer resistance to TNF-mediated RIPK1 cell death independently of PERK inhibition[655]. Therefore, caution must be taken when analysing the phenotypes observed under PERK inhibition with these compounds underpinning the risk for misinterpretations.

Collectively our results show that PERK inhibition enhance cell death exerted by carfilzomib and its respective drug combinations in most of the cell lines, while no or quite little protective effect are observed when IRE1 RNase activity is inhibited with 4μ8C. Thereby, these results suggest that PERK might have a protective role against acute ER stress induction, while a minor or no role is played by IRE1 in ER stress-induced cell death.

4.2.2.4. ER stress & ROS generation.

Oxidative stress and ROS production are probably, at least at some degree, behind the anticancer activity of radiotherapy, as well as many chemotherapeutic agents[656]. Moreover, ER stress conditions can also promote ROS generation. For that reason, we aimed to study ROS production by carfilzomib and the respective drug combinations and seek the possible source for these species to further puzzle out the cell death mechanism exerted by these drugs. Different types of ROS can be generated within the cell: superoxide radical, $O_2^{\bullet -}$; hydroxyl radical $OH^{\bullet}$; hydrogen peroxide, H_2O_2 and peroxynitrite, $ONOO^{\bullet -}$). Each ROS type can stimulate different signalling pathways that lead to different cellular outcomes[657]. We have utilized two different probes for detecting ROS accumulation: dihydroethidium (DHE) and 2',7'-dicholorofluorescein diacetate (DCFDA). While DHE detects cellular and mitochondrial superoxide $O_2^{\bullet -}$ production, DCFDA measures mostly intracellular H_2O_2. These molecules react with cellular ROS and generate fluorescent products that can be quantified with flow cytometry.

As illustrated in **Figure 4.30**, carfilzomib treatment alone elevated the rate of DHE-derived fluorescent cells in a dose dependent manner in all MM cell lines. In MOPC315.BM cells, carfilzomib treatment only provoked slight increments in $O_2^{\bullet -}$ levels. This observation correlates with the fact that these cells were also quite resistant to PI-based treatment. Several studies have reported that PI-based therapy, including

bortezomib and carfilzomib, stimulates ROS generation in different cancer cell models[650,658,659]. Moreover, ROS overproduction is thought to be behind bortezomib-induced apoptosis in MM cells[660]. Interestingly, when carfilzomib was combined with CLQ or DBeQ, the fraction of cells that stained positive for the reaction products of DHE, were increased compared to carfilzomib alone. Autophagy and ERAD are alternative pathways that can clear misfolded/unfolded proteins, thus alleviating ER stress and ROS production. By targeting these pathways with CLQ and DBeQ, ER stress initiated by carfilzomib is exacerbated leading to a massive production of ROS. A similar observation was drawn out by Li and colleagues in which combination of bortezomib with the autophagy inhibitor CLQ, markedly increased ROS generation and apoptosis in a pancreatic cancer cell model[650].

On the contrary, distinct and heterogeneous results were obtained when analysing H_2O_2 levels with DCFDA/DCFHDA staining (results not shown). Intringuily in the majority of cell lines (excepting U266 cells), DCFDA staining was reduced upon combinatorial treatments when compared to control conditions. It is possible that since the UPR response upregulates pathways involved in redox homeostasis, H_2O_2 molecules are effectively purged from the cell explaining the low H_2O_2 levels in those treatments that should display a stronger UPR response. However, other studies reported that ER stress inducers like tunicamycin or thapsigargin, despite instigating ER stress responses, did not altered ER redox state and hence possibly, did not favoured ER-based ROS generation[661,662]. All these disagreements may derive from differences in the intensity and/or kinetics of ER stress as well as, from differences in the experimental protocols[662]. As we cannot confirm or rule out the validity of these results neither assure its reliability, for simplicity these results were not presented in this work.

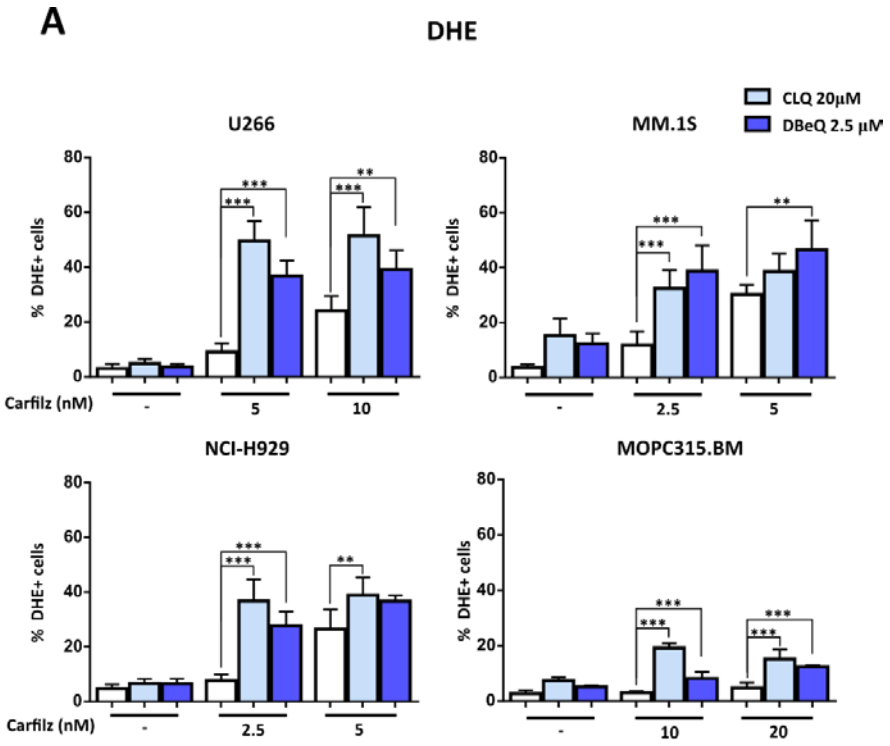

Figure 4.30 |Determination of ROS levels upon drug treatment. MM cell lines were incubated with the different drugs and combinations at the indicated concentrations for 24 hours. ROS levels were then quantified by staining with DHE probes. The percentage of positive cells for DHE staining were plotted. Statistical analysis was performed by using one-way ANOVA with Tukey post-test, where *p<0.05; **p<0.01; ***p<0.001. Data are presented as mean ± SD from n=3 independent experiments.

Once we witnessed that the aforementioned treatments were able to increase ROS production, at least some forms of them, we sought to determine their origin. Many important cellular functions require the generation of ROS in a tightly controlled manner. They can be produced in the cytosol as well as other organelles like the ER and the mitochondria[662]. When these systems malfunction in some way, ROS are generated in an uncontrolled manner causing oxidative stress.

The ER is an organelle imbued in an oxidative environment to guarantee proper protein folding[662]. Many ER proteins like protein-disulfide isomerase (PDI), endoplasmic reticulum oxidoreductin (ERO1α), glutathione ratios, among others, control the redox state within the ER[663]. During the protein folding process, disulphide bond formation requires two electrons to be transferred from the substrate to the active site of the oxidoreductase PDI enzyme[662,663]. Subsequently, ERO1 accepts the electrons from PDI and transfer them to O_2 molecules producing H_2O_2. In fact, this type of ROS is thought to be the major ROS molecule produced in the ER[662]. Under increased ER workload, these systems become less efficient and even malfunction, contributing to ROS generation. Thus, ER stress could be an important source of cellular ROS that could even engage signalling pathways leading to cell death. These observations could give us a hint of the potential origin of ROS in our experimental system. As indicated earlier, although in some cases H_2O_2 levels increased, the general response was a decline in H_2O_2 levels, especially under combinatory treatments. Therefore, collectively these results may suggest that the ER would not be the main generator of ROS, at least at the time point analysed. It is also reasonable to think that after 24h of drug treatment, the global process, from ER stress to ROS generation and apoptosis, would be quite advanced. Moreover, given the short half-life and high reactivity of these molecules, cellular ROS generated in the ER could have already been mitigated by UPR response or reacted with other substrates instead with DCFDA probes, or even be masked by other and later sources of cellular ROS. Thus, it would be advisable to thoroughly scrutinize ROS production at earlier and different time points to shed more light into this matter.

Another potential source of ROS is the mitochondria. Mitochondrial respiration is tightly coupled to electron transfer and hence ROS production, mainly in the form of $O_2^{\bullet-}$ [662,664]. This observation give us another hint about the origin of cellular ROS in our model. Since carfilzomib and the combinations drastically increased $O_2^{\bullet-}$ levels, these results point to the mitochondria as the main source of ROS under our experimental conditions. During ER stress, calcium ER stores are depleted as a massive release of Ca^{2+} towards the mitochondria[665]. This situation initiates a positive-feedback loop that increments cellular ROS levels and oxidative stress. Consequently, increased mitochondrial calcium levels lead to alteration of mitochondrial metabolism, which eventually drives ROS production by mitochondrial machinery[662,663,665]. This enhancement in oxidative phosphorylation and ROS generation, prompts the mitochondria to work at higher pace consuming more oxygen. Under these circumstances of high mitochondrial ROS levels and increased oxygen consumption,

calcium levels also stimulate nitric oxide synthase and inhibit complex IV, further skyrocketing ROS generation[662,663]. Hence upon ER stress, Ca^{2+} release provokes a vicious cycle of mitochondrial ROS generation that eventually drives apoptosis.

Alternatively, during the apoptotic cascade, caspases can also target members of the OXPHOS electron transfer chain also leading to mitochondrial malfunction and ROS generation. In particular, cytochrome c functions as an electron shuttle between complexes III and IV in the electron transfer chain, so cytochrome c release during apoptosis will cause electron leakage and ROS generation[666]. Additionally, caspases can cleave p75 subunit of complex I, disrupting the electron transfer chain and generating ROS mainly in the form of $O_2^{\bullet -}$[666]. To test whether ROS production is the trigger of mitochondrial apoptosis or rather it is downstream of caspase family activation, we evaluated ROS generation upon caspase inhibition with the general caspase inhibitor z-VAD-fmk. Results from **Figure 4.31** showed that in those cells in which cell death was previously demonstrated to be caspase-dependent (U266, MM.1S and MOPC315.BM), $O_2^{\bullet -}$ levels drastically dropped in presence of z-VAD-fmk. These data suggest that in these cells, $O_2^{\bullet -}$ overproduction is probably a consequence of caspase-dependent cleavage of subunits of the electron transfer chain in the mitochondria, driving electron leakage and hence ROS generation. Noteworthy, in NCI-H929 cells which displayed no caspase-cell death dependency, $O_2^{\bullet -}$ levels significantly increased upon caspase inhibition with z-VAD-fmk, especially upon carfilzomib alone or carfilzomib-CLQ combination.

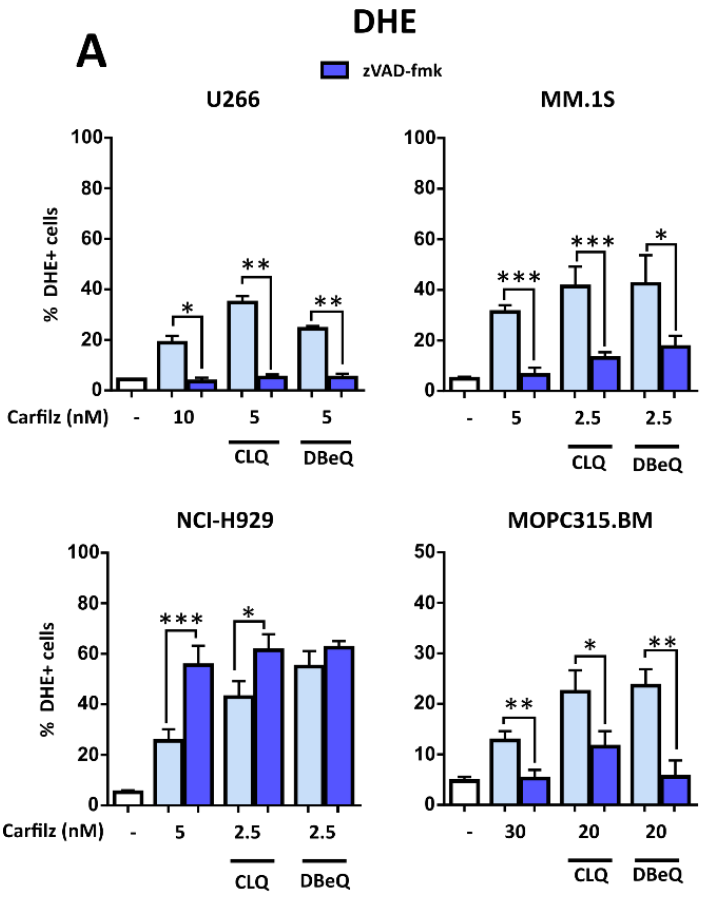

Figure 4.31 | Implication of caspases on ROS production upon drug treatment. MM cell lines were pre-incubated with pan-caspase inhibitor z-VAD-fmk (50 μM) for 1 hour. Afterwards, cells were incubated with the different drugs and combinations at the indicated concentrations for 24 hours. ROS levels were then quantified by staining with DHE and DCFDA probes. The percentage of positive cells for DHE staining were plotted. Data are presented as mean ± SD from n=3 independent experiments. Statistical analysis was performed using two-tail unpaired t test, where *p<0.05; **p<0.01; ***p<0.001.

These results contrasted with previous reports in which z-VAD-fmk did not prevented bortezomib-induced ROS generation in mantle cell lymphoma cells, indicating that ROS production is upstream of caspase activation[659]. Although DCFDA and DHE have been widely used by the research community for monitoring ROS formation in cells, these probes may have some limitations. For example, DCFDA tends to diffuse out of the cells and therefore loss signal[667]. Moreover, auto-oxidation, photo-oxidation, photo-bleaching, photo-conversion and non-specificity are some of the limitations that may hamper the detection of these molecular probes[667]. Furthermore, while some authors claim the specificity of DCFDA and DHE to selectively detect H_2O_2 and $O_2^{\bullet -}$ respectively, others argue against this notion[657,667]. Therefore, results and conclusions drawn out from these kind of assessments should be treated with caution.

Collectively, our data suggest that treatment with carfilzomib and the combinations with CLQ and DBeQ could increase $O_2^{\bullet -}$ levels in most of the MM cell lines tested, while more confounding results were found in H_2O_2 evaluation. These results also point to the mitochondria and especially to the caspase-dependent cleavage of electron transfer chain subunits, as the major source of ROS in our experimental settings.

4.2.2.5. Bcl-2 Family in ER stress-induced Cell Death.

4.2.2.5.1. Bcl-2 Family Expression Levels

Bcl-2 family of proteins are critical regulators of cell death decisions under ER stress conditions. In fact, its implication goes far beyond the mere regulation of intrinsic apoptosis, since Bcl-2 family members are imbued in an intricate bidirectional crosstalk with other molecular programmes like the UPR, autophagy and others[140,314]. Therefore, to further characterize the cell death mechanism of carfilzomib-based drug combinations, we aimed to study the expression of several Bcl-2 family members on MM cells. Because we have previously seen that ER stress response is dynamic, we analysed protein expression by western-blot at different time points (**Figure 4.32**).

Starting with the protein that holds the name for the family, **Bcl-2** levels did not show gross alterations. It is worth noting that the reduction of Bcl-2 expression observed at later time points, especially in U266, MM.1S and NCI-H929 cells, could be a consequence of a massive loss of protein load given the advanced apoptotic stage at that time point, as reflected by the decrease in tubulin levels. Therefore, although Bcl-2 levels could at first be slightly enhanced, it is possible that at later time points they remain unchanged. Our results contrasted with that reported by others in which Bcl-2 levels are downregulated by CHOP-mediated repression[121]. Besides regulation of gene transcription Bcl-2 function can also be modulated by post-translational modifications under ER stress. IRE1α can operate as a molecular scaffold recruiting TRAF2 adaptor molecules that subsequently gather ASK1 to activate JNK stress kinases to initiate apoptosis activation signals[115]. For instance, Bcl-2 and Bcl-X_L can be phosphorylated and

hence see reduced its anti-apoptotic function by JNK[98]. In MM cells, some studies point to other family members such as Mcl-1, rather than Bcl-2, to occupy a distinguished role in cell death induction. In fact, reports indicate that Bcl-2 levels remain unaltered regardless of the apoptotic stimuli utilized[668,669]. One study also corroborated our results and revealed that Bcl-2 levels were not downregulated upon thapsigargin treatment[653].

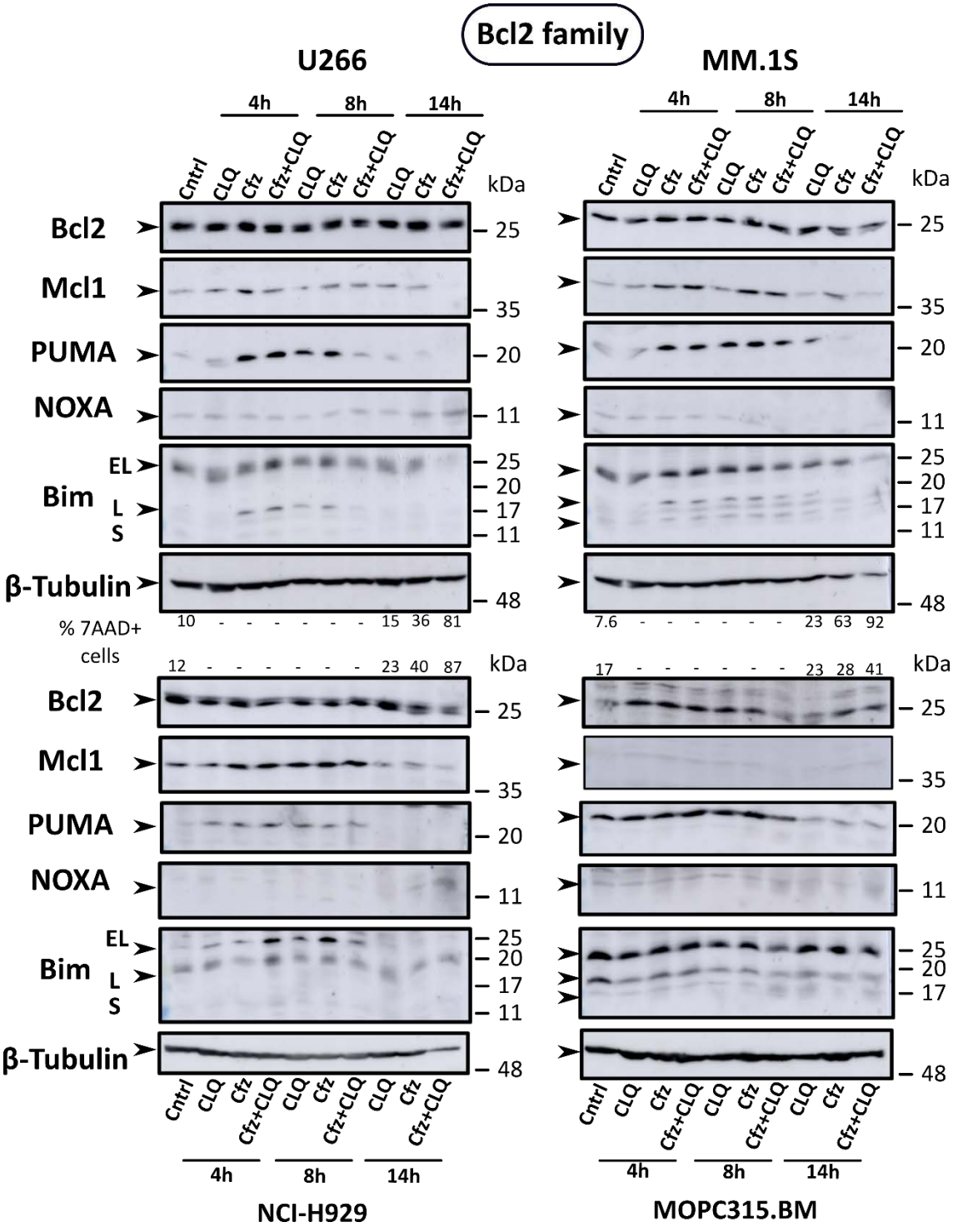

Figure 4.32 | Protein expression levels of different Bcl-2 family proteins upon drug treatment. MM cell lines were treated with the different drugs for the indicated incubation times. In case of MM.1S and NCI-H929 cells were treated with 5 nM of carfilzomib, U266 cells were administered 7 nM of carfilzomib and finally MOPC315.BM cells were treated with 20 nM carfilzomib. All the cell lines were incubated with 20 μM CLQ. Protein expression levels for Bcl-2, Mcl-1, PUMA, NOXA and Bim were analysed by western-blotting. Figure shows a representative immunoblot from n=2 independent experiments.

As regards to **Mcl-1** protein, MM cells showed a low basal expression of this protein. When challenged with the different drugs, MM cells showed a transient accumulation at early time points (4-8h) that faded with time. This was reproduced in the different MM cell lines. Note that probably in MOPC315.BM cells, the anti-Mcl-1 antibody used was only tested for human origin and probably this explains the absence of signal in the immunoblot from the murine cell line. Mcl-1 is characterized by having a short half-life and hence is a protein strictly regulated at the level of protein stability[670,671]. Mcl-1 degradation is usually, but not always, required for initiation of apoptosis, although MM cells are particularly sensitive to Mcl-1 downregulation[672]. Furthermore, Mcl-1 can also be degraded in a caspase-dependent manner. Studies have revealed a caspase-mediated trimming of Mcl-1 during the induction of apoptosis in various cancer cells[454,673]. Possibly, a combination of various of these mechanisms determines Mcl-1 levels in cells: synthesis blockade, proteasomal degradation and caspase-mediated cleavage[454]. These post-translational regulatory mechanisms may explain the initial accumulation and posterior Mcl-1 dissipation upon PI-based therapy. Some studies indicate that Mcl-1 levels increase after proteasome inhibition by bortezomib or carfilzomib[659,674–676], which partially matches our initial Mcl-1 response. Others, however, argue in favour for Mcl-1 degradation upon PI-based therapy in MM cells[454]. Since many of these studies analysed protein expression at fixed time points, it is possible that an initial accumulation of Mcl-1 as a consequence of proteasome inhibition takes place and once the apoptotic cascade is unleashed, Mcl-1 levels are trimmed by the action of caspases. In fact, in some immunoblots, the corresponding band of Mcl-1 is teared apart into two lighter bands (results not shown). Moreover, these cleaved forms of Mcl-1 harbour a pro-apoptotic role that can contribute to MM cell death[677]. Interestingly, Mcl-1 levels have also been shown to decrease as a consequence of PERK-mediated shut down of protein translation in response to ER stress insults[678].

PUMA also showed the same expression pattern in the different MM cell lines. First, it experienced a transient accumulation at 4-8h of drug incubation and faded at later time points. PUMA has been reported to be a caspase substrate[679] and hence, it can experience a caspase-mediated degradation when apoptosis is unleashed. This may explain the reduction of PUMA levels at longer incubation times. Additionally, PUMA can also be degraded via proteasome[680]. Therefore, upon carfilzomib treatment, we cannot ascertain whether the initial PUMA accumulation is mediated by the activation of the ER stress response or via passive prevention of its degradation via proteasome. Analysing **NOXA** levels was more challenging. NOXA expression was hardly noticed in most of the cell lines evaluated. In U266 cells, NOXA expression manifested a gradual

accumulation that peaked after 14h of drug treatment, especially in the drug combination. NCI-H929 cells apparently also showed an increased expression in carfilzomib+CLQ treated cells after 14h of drug incubation. In MM.1S cells no apparent increase in NOXA levels was revealed. In contrast, its expression faded at later time points. Finally, in MOPC315.BM cells, NOXA expression dissipated with time.

Although the exact mechanisms are yet not fully understood, BH3-only proteins have been delineated as critical players in the induction of apoptosis under chronic or irreversible ER stress conditions[98,140]. Among the BH3-only proteins, PUMA and NOXA have been reported to undergo transcriptional upregulation under ER stress[140]. For example, increased PUMA expression has been observed in neuroblastoma cells after tunicamycin treatment[681]. Moreover, PUMA deficient cells displayed reduced cell death rates in response to ER stressors[681]. Likewise, siRNA-mediated silencing of PUMA expression, rendered similar results in ER-stress induced cell death in a melanoma model[682]. CHOP has also been reported to upregulate PUMA expression[124]. Regarding NOXA expression, a study revealed that this protein could be upregulated in an ATF-4 dependent manner[125]. Furthermore, PUMA and NOXA can be upregulated by p53 during ER stress conditions[133,683], although the exact mechanism has not yet been fully elucidated[140]. Bortezomib and carfilzomib-mediated proteasome inhibition have also been shown by us and others to upregulate PUMA and NOXA levels in MM cells[238,454,659].

Related to another protein of BH3-only subgroup, **Bim** levels although depend on the specific isoform and the cell line, also experienced a transitory increment at shorter incubation times, that vanished after longer periods of drug treatment. Nonetheless, differences among specific isoforms and cell lines could be noticed. As presented in **Figure 4.32**, Bim_{EL} isoform was present in most of the cell lines in basal conditions. At shorter incubation times, Bim_{EL} isoform underwent an initial accumulation followed by a gradual declining over time. This occurred in U266, MM.1S and NCI-H929 cells, but not in MOPC315.BM cells in which BIM_{EL} remained unchanged. Regarding Bim_L isoform, it followed the same pattern as its larger relative. Note that BIM_{EL} and BIM_L isoforms increased first upon treatment with combinatory Cfz+CLQ treatment, peaking at 4h of incubation and thereafter experienced a gradual dissolution. Carfilzomib treatment alone followed the same pattern but with a lower kinetic. This was even more pronounced when cells were subjected to single CLQ treatment. This was especially discernible in U266 and NCI-H929 cell lines. These results correlate with our previous observations that suggested that addition of CLQ to carfilzomib treatment increased the kinetics of cellular responses and hence, cell death induced by these drugs. Finally, given its highly apoptotic activity, Bim_S isoform was not present in basal conditions. Moreover its expression in the immunoblot was difficult to be noticed and in some cell lines, its induction was barely appreciated. In U266 and NCI-H929 cells, a faint shadow appeared at 4h of carfilzomib or Cfz+CLQ combination that could correspond to Bim_S isoform. In MM.1S and MOPC315.BM cells, Bim_S expression was more apparent.

In MM.1S cell line it followed the same expression pattern as the other isoforms. In MOPC315.BM cells Bim_S levels seemed to slightly increase at longer incubation times.

Bim holds a distinguished position in the BH3-only subgroup of Bcl-2 family of proteins, due to its highly pro-apoptotic potential[684]. Alternative mRNA splicing yield three major isoforms (although a total of 19 isoforms have been reported) with different apoptotic activity[684,685]. Bim_{EL} and Bim_L are usually found sequestered in microtubules by dynein through interaction with dynein light chains (DLCs)[684]. For apoptosis to be induced, the liberation of Bim from these complexes is critically required. In fact, phosphorylation of Bim by JNK, a stress kinase activated by IRE1-mediated arm of the UPR, has been shown to release Bim molecules from dynein motor complexes and induce Bax-dependent cell death[120]. Regarding the shorter isoform, as mentioned before, Bim_S holds the greatest apoptotic potential among the different Bim isoforms and is usually transiently expressed under apoptotic conditions[120,684]. In contrast to the other larger isoforms, Bim_S do not bear the short peptide motif that mediates DLC-binding[686]. In fact, absence of the dynein binding motif together with its ability to directly bind Bax, may account for its outstanding apoptotic capacity[120,685]. At the transcriptional level, Bim expression can be directly induced by CHOP upon UPR activation[121]. Bim levels can also accumulate due to PP2A-mediated dephosphorylation thereby preventing its ubiquitination and proteasomal degradation[121]. Additionally, the latter is also accomplished upon proteasome inhibition. For instance, bortezomib treatment has been shown to stabilize Bim levels favouring its accumulation by preventing its degradation[687]. Likewise, our group previously reported increased Bim expression upon carfilzomib treatment[238]. The role of Bim and its regulation under ER stress conditions will be further discussed in following sections.

Taken all these results together, it seems that all Bcl-2 family members that have a short half-life and are susceptible to be degraded by the proteasome, experienced the same expression pattern. Whether elevated levels of these proteins were a consequence of the direct inhibition of proteasomal degradation, induction of transcription and active translation, or a combination of the above, remains to be elucidated.

To conclude, we have seen an early accumulation of different Bcl-2 family members, with both pro- and anti-apoptotic functions. Since, Mcl-1 has been shown to be the main player in the anti-apoptotic side, BH3-only member like PUMA or Bim, may counteract and surpassed Mcl-1 activity hence inducing cell death. At later stages, disappearance of the different Bcl-2 family members correlates and may account for the apoptotic cascade activation and cell death induction, since many of these proteins can be degraded by caspase action.

4.2.2.5.2. PUMA & NOXA Flow Cytometry Analysis.

PUMA and NOXA intracellular levels were also analysed by flow cytometry (**Figure 4.33** and **Figure 4.34**). In this case we also detected a time-dependent variation of PUMA and NOXA expression, although with little fluctuations in some cell lines. In MM.1S and MOPC315.BM cells, little to no variation of mean peak fluorescence was observed at 8h of drug incubation. A slight shift towards higher intensities was observed under carfilzomib treatment alone in both cell lines. In the case of MOPC315.BM cells, degradation of PUMA started earlier rendering an additional wider peak with lower intensity. Conversely, a greater increase of PUMA levels were manifested at 8h of drug incubation in U266 and NCI-H929 cells, especially in the drug combinations. NOXA expression also followed a similar pattern at early time-points (8h). In this case, differences in peak intensities were even smaller. NCI-H929 cell line were probably the only one that showed an apparent shift in peak intensities of NOXA with the different drug treatments.

At later time points (16h), a different outcome was obtained. PUMA levels were completely degraded in almost every case. Only in U266 cells, which have manifested a particular resistance towards these therapies, a partial degradation was observed under carfilzomib treatment alone or in the combination with DBeQ. Note that in these conditions, the peak was drastically shifted towards higher intensities. NOXA expression again followed the same pattern manifested by PUMA. A clear degradation was observed in the majority of cell lines, with only U266 cells displaying a partial degradation in carfilzomib treatment alone or under the combination of carfilzomib with DBeQ. In these cases, NOXA fluorescence peak was displaced towards higher intensities. Given that in our experimental settings we are under strong proteasome inhibition, since PUMA is a recognized proteasome, as well as caspase-substrate, its degradation in this case is thought to be mediated via caspases[679,688]. Therefore, when z-VAD-fmk was incorporated, PUMA degradation was abolished and peak fluorescence was recovered. Moreover, under the protection conferred by caspase inhibition, PUMA levels were increased when compared to control cells, as revealed by the higher mean fluorescence intensities displayed in the histograms. The same occurred with NOXA. Levels of this protein were recovered, and even increased when z-VAD-fmk was present. MOPC315.BM cells were probably the only cell line that showed no increased expression upon caspase-inhibition.

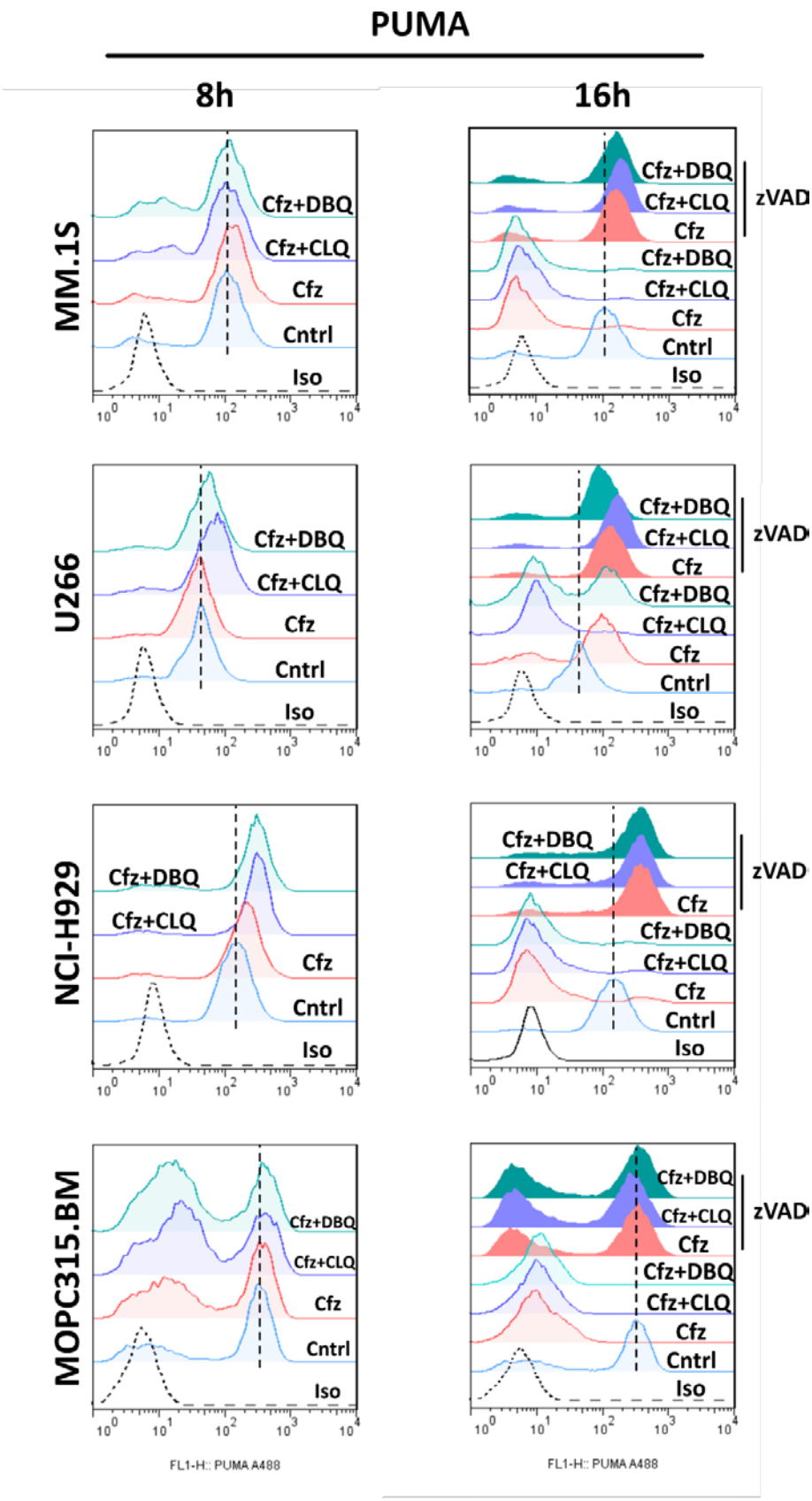

Figure 4.33 | Determination of PUMA protein expression levels by flow cytometry. MM cell lines were treated with the different drugs for the indicated incubation times. In case of MM.1S and NCI-H929 cells were treated with 5 nM of carfilzomib, U266 cells were administered 7 nM of carfilzomib and finally MOPC315.BM cells were treated with 20 nM carfilzomib. All the cell lines were incubated with 20 μM CLQ or 2.5 μM DBeQ when indicated. Cells were also pre-incubated for 1 hour with pancaspase inhibitor zVAD-fmk (30 μM), when indicated. Cells were then fixed, permeabilized and incubated with primary anti-Puma antibody and afterwards with the appropriate alexa-fluor-488 conjugated antibody for determination of Puma expression levels by flow cytometry. Representative histograms from n=3 independent experiments.

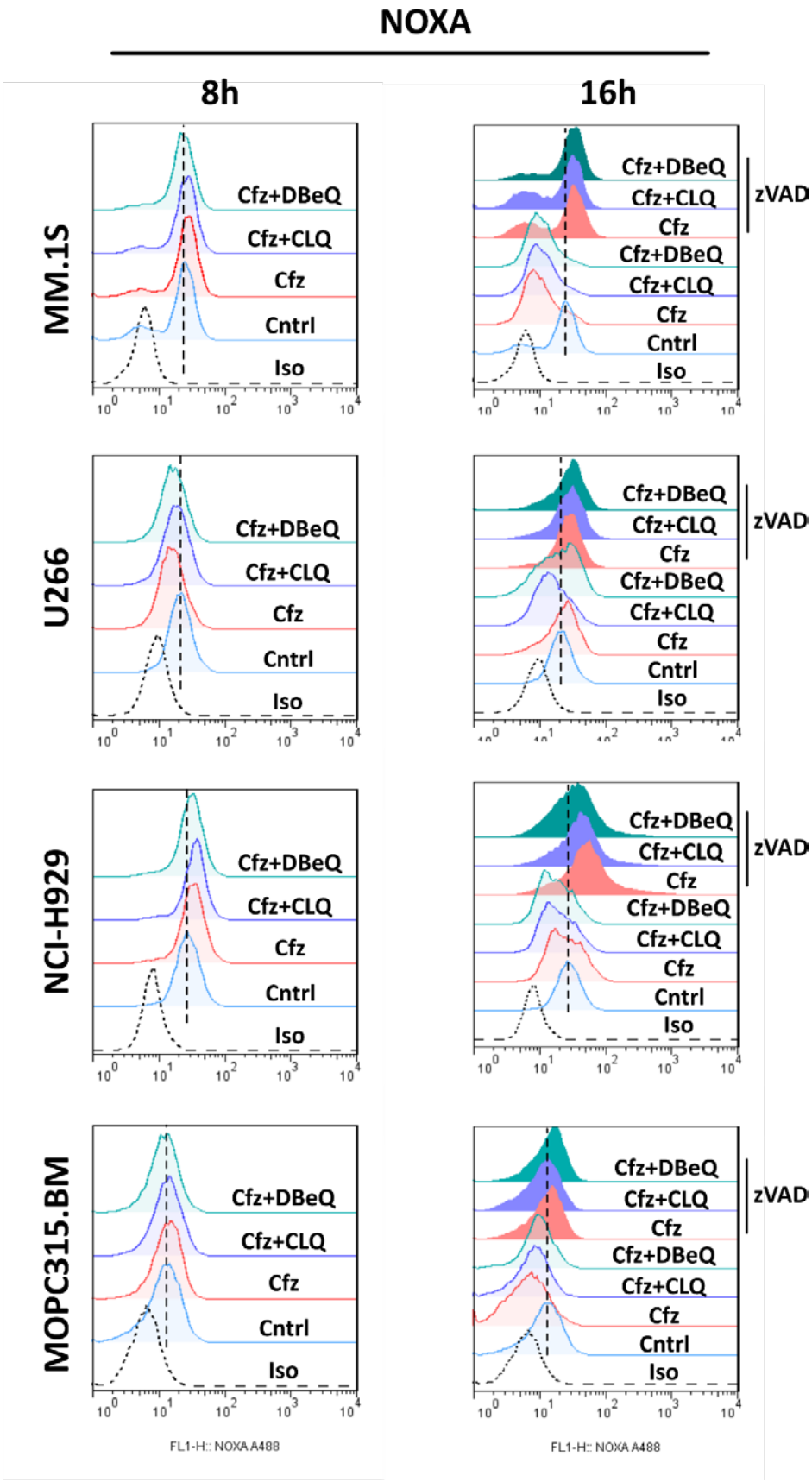

Figure 4.34 | Determination of NOXA protein expression levels by flow cytometry. MM cell lines were treated with the different drugs for the indicated incubation times. In case of MM.1S and NCI-H929 cells were treated with 5 nM of carfilzomib, U266 cells were administered 7 nM of carfilzomib and finally MOPC315.BM cells were treated with 20 nM carfilzomib. All the cell lines were incubated with 20 μM CLQ or 2.5 μM DBeQ when indicated. Cells were also pre-incubated for 1 hour with pancaspase inhibitor zVAD-fmk (30 μM), when indicated. Cells were then fixed, permeabilized and incubated with primary anti-Noxa antibody and afterwards with the appropriate alexa-fluor-488 conjugated antibody for determination of Noxa expression levels by flow cytometry. Representative histograms from n=3 independent experiments.

Perhaps, although the timing of PUMA and NOXA expression differed to that seen in the Western-blot time course, flow cytometry analysis also showed an initial accumulation and posterior degradation of these BH3-only proteins. As mentioned earlier, PUMA and NOXA are thought to be critical contributors to proteasome inhibition-based and as well as to general ER stress-induced cell death[659,689]. Initial accumulation of these proteins could be a consequence of direct proteasome inhibition, transcriptional upregulation, or combination of both mechanisms. Transcriptional upregulation of these BH3-only members have been discussed in the previous section. PUMA degradation has been shown to be mediated both by proteasome- and caspase-based cleavage[679,688]. In our experimental conditions, although proteasome activity is blocked, PUMA protein is rapidly cleared by caspases when apoptosis is induced. As our data show, only when z-VAD-fmk was present, PUMA levels were recovered and the increased expression of this protein compared to control cells became also evident.

Despite NOXA does not have a formal PEST sequence, it has been reported to be degraded by the proteasome in an ubiquitination-dependent[690] and independent manner[691,692]. It is not clear whether the ubiquitin-independent mechanism involves Mcl-1 direct physical interaction or not. Since NOXA is found complexed with Mcl-1 in normal conditions, Mcl-1 targeted degradation via ubiquitination could also drag NOXA to the proteasome[692]. NOXA is a short-lived protein with an estimated half-life of 1-2h[690]. Therefore, unless this short time framework can be captured either by western-blot or flow cytometry, NOXA upregulation cannot be detected. Probably, in the flow cytometry analysis, NOXA upregulation occurred just before the completion of the 8h of drug incubation, and the protein levels detected correspond to the degradation phase. Interestingly, NOXA was stabilized in presence of pan-caspase inhibitor z-VAD-fmk, which suggests that caspases are involved in some way in NOXA degradation. When caspase-mediated processing is prevented, NOXA levels then appeared to be upregulated under the different drug treatments. To our knowledge, unlike PUMA, there are no reports in the literature supporting NOXA processing by caspases[679].

Collectively, data presented above suggest that drug treatment is able to induce an initial accumulation of BH3-only proteins PUMA and NOXA. Given its pro-apoptotic potential, these proteins could trigger cell death upon drug treatment. Afterwards, when apoptosis is unleashed, PUMA and NOXA are rapidly degraded in a caspase-dependent manner. Whether the initial accumulation is a consequence of proteasome inhibition or a direct transcriptional upregulation remains to be elucidated.

4.2.2.5.3. *Role of Bax and Bak in ER Stress-induced Cell Death.*

In the previous section we have witnessed that the expression of Bcl-2 family is modulated under the ER stress conditions evoked by carfilzomib and its drug combinations. The balance between pro-apoptotic and anti-apoptotic members will determine the final cell fate. As we have seen, upregulation of BH3-only members like PUMA, NOXA and Bim, and possibly downregulation of anti-apoptotic proteins (Mcl-1), can shift the balance towards pro-death signalling. The interaction between pro- and anti-apoptotic proteins converges in Bax/Bak activation. In general, ER stress-induced cell death is thought to primarily occur in a caspase-dependent intrinsic mitochondrial apoptotic manner[116]. This requires, mitochondrial outer membrane permeabilization (MOMP) instigated by Bax/Bak oligomerization. Thus, to further increase our mechanistic insight about the cell death pathways activated in these conditions, we studied the role of Bax and Bak in cell death elicited by these drugs. To achieve this goal, MM.1S Bax/Bak deficient cell line and the corresponding control cell line were devised and generated during this work using CRIPSR-Cas9 technology (section 3.12.6). The absence of Bax and Bak by Western-blot was verified and cell death functional testing with a panel of drugs was also carried out.

To our surprise, abrogation of Bax and Bak expression did not have any apparent effect on cell death elicited by carfilzomib, nor bortezomib action alone (**Figure 4.35**). Likewise, cell death rates of bortezomib+CLQ, carfilzomib+CLQ or DBeQ drug combinations remained unchanged in Bax/Bak deficient cells when compared to control cells. In some cases, it seems that depletion of Bax and Bak even conferred a slight increased sensitivity to drug action. These results clearly contrast the data obtained in the functional testing of MM.1S Bax/Bak DKO cell line. In this functional validation, a panel of different drugs, composed of distinct BH3 mimetics and a CDK inhibitor (dinaciclib), were used to test the expected increased resistance of MM.1S Bax/Bak DKO cell line to cell death. Indeed, MM.1S Bax/Bak deficient cells displayed reduced sensitivity to all of these drugs (data not shown).

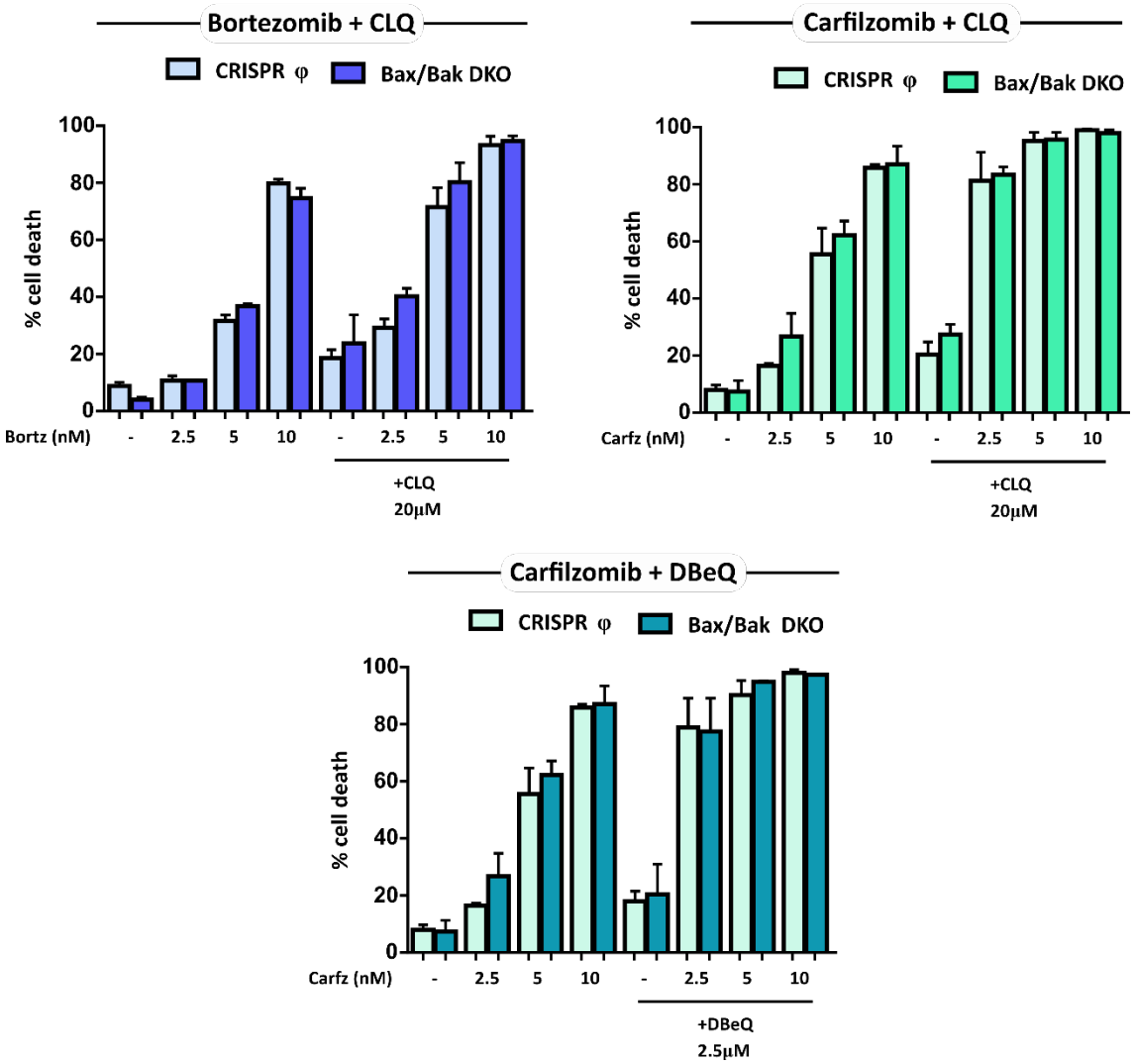

Figure 4.35 |Implication of Bax and Bak in cell death induced by proteasome inhibitors and PI-based combinatory drug regimens. MM.1S CRISPR control and MM.1S Bax/Bak DKO cell lines were incubated with the different drugs at the indicated concentrations for 24 hours. Cell death was analysed by determining PS exposure and membrane integrity by AnnexinV and 7-AAD co-staining. Cell death represents AnnexinV$^+$, 7-AAD$^+$ and AnnexinV/7-AAD double positive populations. Data are presented as mean ± SD from n=3 independent experiments. Statistical analysis was performed using two-tail unpaired t test, where *p<0.05; **p<0.01; ***p<0.001.

Our previous results seem to indicate that cell death upon treatment with the drugs used in our study may follow a caspase-dependent intrinsic apoptotic pathway. Cell death markers in the cell death assays, the study of caspase-3 activation, the different cell death inhibitors used to test cell death mechanisms, the increase in UPR response markers, as well as the modulation of Bcl-2 family expression, all these data pointed to mitochondrial apoptotic cell death pathway as the main mechanism of cell death induced under these experimental conditions. Based on all these observations, we expected that concurrent Bax/Bak depletion would have conferred protection against the action of the drugs used in our study. Bax and Bak activation and oligomerization and hence,

induction of mitochondrial permeability, is a critical step in the apoptotic cascade. Furthermore, the action of these proteins is not only circumscribed to regulation of mitochondrial membrane permeability. In fact, Bcl-2 family and in particular, Bax and Bak can also regulate ER membrane integrity and permeability. Bcl-2, Bcl-X_L Bax, Bak and Bik have been shown to be directly associated with the ER[693–695]. In fact, Bax/Bak overexpression was shown to provoke ER Ca^{2+} efflux, which is incorporated into the mitochondria with the ensuing cytochrome c release, probably through mPTP[13,696,697]. Altogether Bax and Bak functions were expected to play important roles in the cell death induced in our experimental conditions.

Although the way ER-stress engages cell death pathways and eventually triggers cell demise is under debate. Several studies argue in favour for the contribution of Bax and Bak in ER stress-induced cell death[116]. Bax/Bak deficient cells were more resistant to a variety of ER stress insults[137,698–701]. In sharp contrast, other studies revealed alternative Bax/Bak-independent mechanisms by which cells can succumb to ER stressors. For example, one study showed that Bax/Bak deficient cells were equally affected by thapsigargin treatment as their wild-type counterparts[653]. In this scenario, thapsigargin treatment resulted in a caspase-independent necrotic-like cell death, with calcium overload and mitochondrial permeability transition pore (mPTP) formation[653]. These results were also reproduced in colon and prostate cancer cell models[653]. Another independent work showed that Bax/Bak deficient cells also succumbed to cell demise and adopted necrotic-like cell death features upon prolonged ER stress[702]. Alternatively, another study reported that proteasome inhibition can also drive cell death in Bax/Bak deficient cells. In this study, authors argued that participation of several BH3-only proteins, p53, as well as mitochondria deterioration, overridden the need of Bax/Bak in cell death induction[703]. Additionally, another study also manifested cell death and cytochrome c release in Bax/Bak DKO cells[704].

All these studies converge in the existence of alternative Bax/Bak cell death independent mechanisms, which probably involves mPTP and calcium overload as key contributors to cell demise. Nonetheless, the precise mechanism by which cell death is ultimately unleashed is yet to be fully delineated. Is then possible that in a similar fashion, PI-based therapies and its combinations, could instigate cell death following the mechanisms of ER Ca^{2+} release and overload, mPTP and necrotic-like mechanisms described above when Bax and Bak levels are depleted. Furthermore, of clinical relevance, lack of expression of pro-apoptotic mediators such as Bax and Bak are behind the resistance mechanisms harboured by tumour cells[618]. Therefore, the ability of the approaches used in this study to overcome cell death resistance displayed by Bax/Bak deficient cells, highlights the promising potential that these strategies may have in heavily treated patients with acquired chemotherapeutic resistance to apoptotic cell death. Further experiments unravelling the cell death mechanisms activated in Bax/Bak depleted cells, will provide valuable information to develop better and more effective anticancer approaches.

One interesting and alternative explanation for the Bax/Bak-independent cell death that occurs upon chemotherapeutic-induction in our experimental settings, may point to caspase-8 and DR5 as critical enactors in this scenery. The exact molecular mechanism behind ER stress-induced cell death is still a matter of intense scientific debate. There are ample pieces of evidence supporting both the participation of the cell death receptor and the intrinsic mitochondrial apoptotic pathways[705]. A recent study suggested that an important mediator of ER stress-induced cell death was encompassed by the upregulation of DR5 receptor by CHOP[609,638].

DR5 is a pro-apoptotic member of the TNFR superfamily of receptors that engages and transmits extracellular cues to the inside of the cell[706]. As indicated in section 1.2.4, the canonical pathway of activation of these type of receptors, entails binding of homotrimeric extracellular TRAIL molecules to DR5, which favours the assembly of higher-order oligomers[707]. Inside the cell, this event in turn fosters the scaffolding of the intracellular cytosolic death domains which allows recruitment of adaptor proteins (FADD) and pro-caspase 8 into DISC. The close proximity of pro-caspase molecules within these clusters allows a regulated auto-proteolysis generating active caspase-8[708], that ensuingly engages with the intrinsic apoptotic pathway through Bid[709]. The consecution of these molecular events triggers cell's self-destruction programmes in response to external cues. However, during ER stress-induced cell death, cells seem to respond to signals emanating inside the cell.

The exact mechanism of how ER stress triggers cell death involving cell death receptors independently of death ligands (TRAIL) remains a mistery[130]. Recently, Lam and co-workers dissected the intracellular mechanism of activation of DR5 upon ER stress conditions[710]. It was revealed that DR5 molecules promiscuously bind to hydrophobic unfolded/misfolded proteins that accumulate during ER stress conditions, favouring intracellular clustering of DR5 receptors at the ERGIC, thus triggering cell death[710]. However, the participation of DR5 and caspase-8 to ER stress-induced cell death is not out of polemic. Recent reports from an independent group (Glab and co-wokers) showed that DR5 and caspase-8 were dispensable for apoptosis induction upon ER stress conditions[705]. Nonetheless, Lam and colleagues trying to support their scientific findings provided more independent clues to the participation of DR5 and caspase-8 in ER stress-dependent instances of cell death. They make use of the DR5 and caspase-8 CRISPR KO cell lines developed by Glab *et al.* and refuted their findings by proving the contribution of this cell death axis to cell demise upon treatment with ER stressors like thapsigargin[711]. In our experimental scenario, it is tempting to speculate that the Bax/Bak-independent cell death induction observed upon PI-based treatment could be explained by DR5 and caspase-8 contribution to cell demise. For instance, as shown in **Figure 4.23**, inhibition of caspase-8 activity with caspase-8 specific inhibitor z-IETD-fmk, significantly protected cells from succumbing to drug action, especially in U266, NCI-H929 and MOPC315.BM cells. In the specific case of MM.1S cells, caspase-8 inhibition did not reveal any significant protection at this regard, probably suggesting

that DR5/caspase-8 cell death axis may play a minor role in these circumstances. However, we cannot exclude the possibility that when Bax and Bak were present the intrinsic mitochondrial apoptotic pathway may govern in MM.1S cells, whereas upon Bax and Bak depletion, other cell death mechanisms, like the one explained above, may take the relieve and trigger cell demise under these conditions. Perhaps, novel generation of PhD students will shed more light into this conundrum.

In conclusion, our data demonstrate the capacity of PI-based therapies, as well as its combination with CLQ or DBeQ to instigate cell death upon Bax/Bak deficiency. Hence, these approaches may overcome drug resistance displayed by tumour cells deficient in Bax and Bak, underpinning the therapeutic potential of these therapies against multi-drug resistant tumours.

4.2.2.5.4. Role of Bim in ER Stress-induced Cell Death.

Ample pieces of evidence have addressed the role of BH3-only proteins as important modulators of ER stress-induced cell death[13,140]. In particular, Bim has previously been shown to be modulated, both transcriptionally and post-transcriptionally, upon ER stress conditions[13,140]. Therefore, we decided to inspect the role of Bim in cell death induced by carfilzomib and its drug combinations with CLQ and DBeQ on MM cells. For this purpose, U266 Bim KO cell line was devised and generated using CRISPR-Cas9 technology, as described in section 3.12.6. Once the stable cell line was generated and the absence of Bim confirmed by Western-blot, cytotoxic assays were performed to compare the cell death sensitivity to the different chemotherapeutic drugs.

As our data illustrate, Bim depletion caused a mild protection to cell death induced by PIs alone (**Figure 4.36**). Although U266 Bim KO cells displayed a strong tendency towards reduced cell death rates when treated with PIs alone, this difference was statistically non-significant. When challenged with PI-CLQ combinations, U266 Bim KO cells showed a significant, yet partial, reduction in cell death rates when compared with the control cell line. In carfilzomib-DBeQ drug combination, a similar partial cell death protection was observed. Of note, absence of Bim offered a better barrier against cell death induced by bortezomib-based combinations than in carfilzomib-mediated drug regimens. This probably may underpin differences in the mechanism of action of bortezomib and carfilzomib despite being two drugs directed against the same cellular target.

As delineated in the previous section, we and others have shown that Bim levels are transcriptionally upregulated under ER stress conditions[121,238]. In fact, CHOP has been pointed to be responsible for Bim upregulation upon UPR activation[121]. The importance of Bim induction upon ER stress and the concomitant cell death has been nicely delineated in *Bim*$^{-/-}$mice, which showed less TUNEL-positive cells compared to

their wt littermates[121]. Furthermore, thymocytes from Bim deficient mice were less sensitive to thapsigargin or tunicamycin than their wt counterparts[121]. Bim expression regulation and stability is complex and can occur at different levels (transcriptionally, post-transcriptionally, post-translationally, etc)[684]. At the post-translational level, Bim function can be regulated by phosphorylation[712]. Confronting results have been obtained on whether Bim phosphorylation enhances or diminishes its apoptotic activity. Furthermore, Bim has been reported to be phosphorylated by different MAPK members (ERK, JNK, p38) at different sites provoking distinct outcomes on its apoptotic activity[712]. Phosphorylation at some residues by ERK favours Bim ubiquitination and proteasome-dependent degradation[712,713]. Additionally, PP2A-mediated dephosphorylation of Bim has been shown to prevent its degradation under ER stress conditions[121]. Interestingly, proteasome inhibitors would also promote Bim stabilization, resulting in its accumulation[238,687]. On the contrary, other studies report that rather than affecting protein stability, Bim phosphorylation by JNK, provokes its release from dynein and myosin motor proteins unleashing its pro-apoptotic pontential[120].

In sharp contrast, other authors have shown that Bim may be dispensable for cell death upon UPR activation in several cellular systems[116,714]. These findings are more in accordance with our results that manifest that Bim may play a partial redundant role, in which other BH3-only members could also participate in cell death triggered by these drugs. Perhaps, as previous data illustrate, the upregulation of PUMA, and possibly NOXA, could also drive cell death under these conditions when Bim is depleted. In fact, it has been shown that only when Bim, PUMA and Bid were concurrently depleted, these triple-KO cells reproduced the phenotype observed in Bax/Bak KO cells[136]. Other authors also point to caspase-8 and NOXA as the cell death initiators in ER stress-induced cell death conditions[714–716].

To conclude, our data show that Bim contributes in some extent to cell death instigated by PI-CLQ based, as well as, carfilzomib-DBeQ combinations. Nonetheless, its deficiency only offers a partial cell death protection and seems to be redundantly covered by additional BH3-only members that may also become upregulated under these conditions.

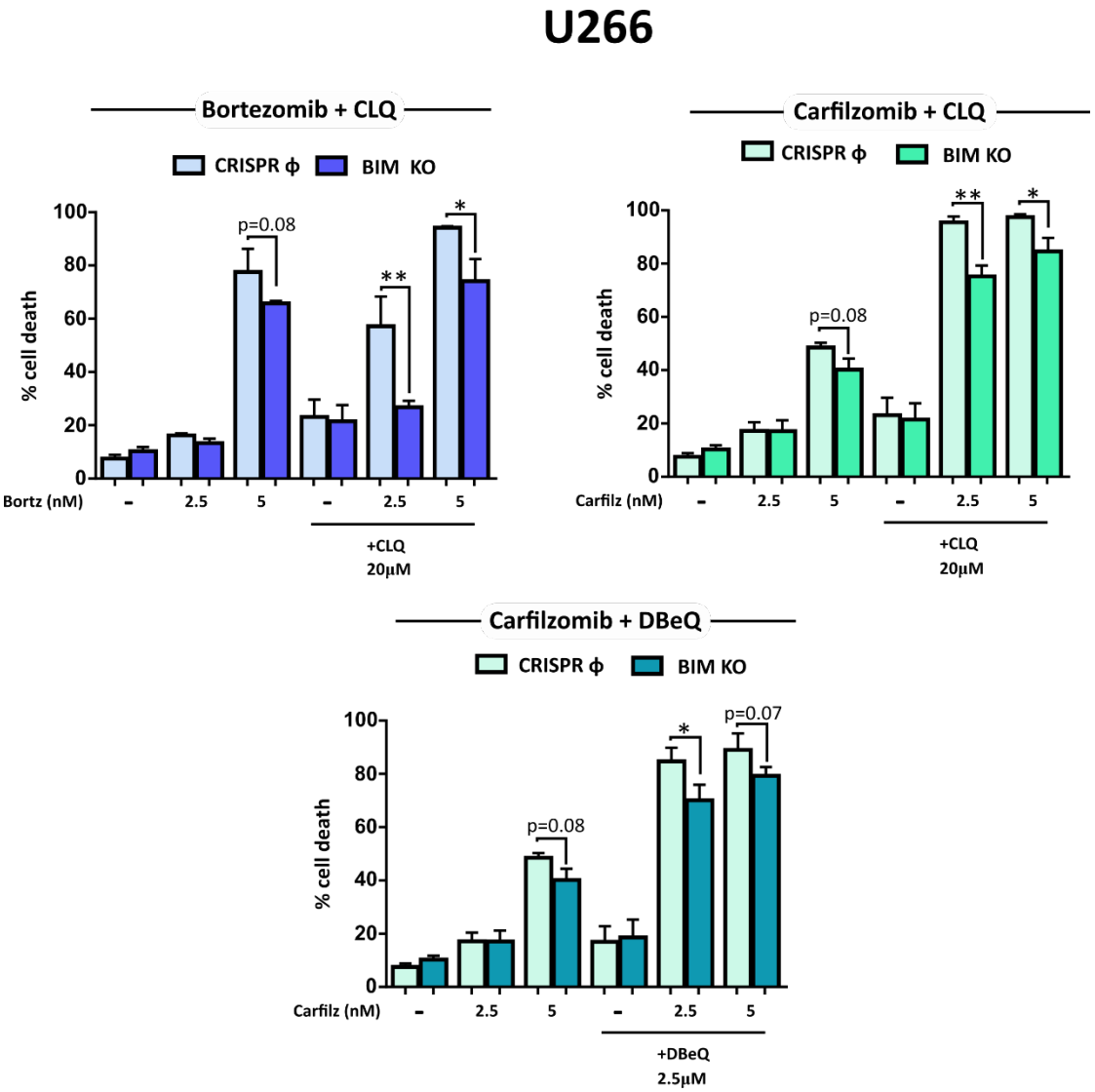

Figure 4.36 |Implication of Bim in cell death induced by proteasome inhibitors and PI-based combinatory drug regimens. U266 CRISPR control and U266 Bim KO cell lines were incubated with the different drugs at the indicated concentrations for 24 hours. Cell death was analysed by determining PS exposure and membrane integrity by AnnexinV and 7-AAD co-staining. Cell death percentage corresponds to AnnexinV$^+$, 7-AAD$^+$ and AnnexinV/7-AAD double positive subpopulations. Data are presented as mean ± SD from n=3 independent experiments. Statistical analysis was performed using two-tail unpaired t test, where *p<0.05; **p<0.01; ***p<0.001.

4.2.3. Role of Autophagy in the Cell Death Mechanism of PI-based Drug Combinations.

In situations of ER stress, autophagy could be activated as an auxiliary mechanism to alleviate and deal with the excess of unfolded proteins[165,166]. Previous work from our group showed that carfilzomib treatment induced autophagy in MM cells in some extent[238]. The observed autophagic flux was not complete since intermediate autophagic markers failed to be fully degraded or accumulate in MM cell lines[238]. On the other hand, it was shown that cell death induced by carfilzomib in ATG5-deficient cell lines was similar to that wild-type cells (Jarauta, 2015). To futher explore the possibility that potentiation of carfilzomib-induced cell death exerted by CLQ co-treatment was independent from the autophagy machinery, we assessed cell death induction in MM.1S WT cells and in autophagy-deficient MM.1S shATG5 cells (**Figure 4.37**).

In cells treated with bortezomib, death levels augmented in a similar manner in both WT and ATG5-deficient cells, suggesting that autophagy is not involved in the increase of cell death observed by combination with CLQ. This agrees with a report indicating that ATG5 knockout, reduced the autophagosome formation induced by bortezomib and decreased MM cells sensitivity to bortezomib action[717]. ATG5 silencing in MM.1S cells did not potentiate but decrease the toxicity induced by carfilzomib. Nonetheless, CLQ addition to carfilzomib further enhanced cell death relative to carfilzomib in ATG5-deficient cells.

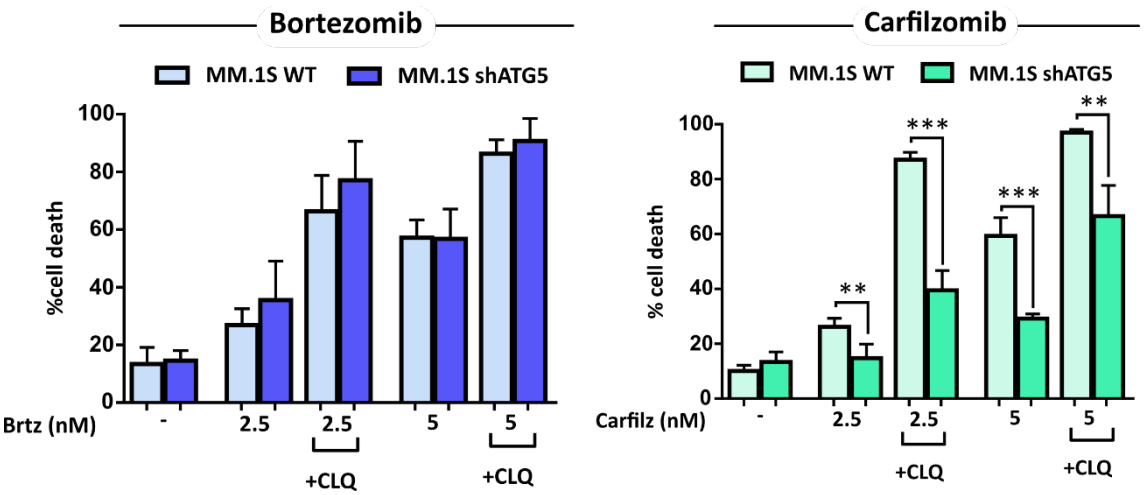

Figure 4.37 |Implication of autophagy in cell death induced by proteasome inhibitors and PI-based combinatory drug regimens. MM.1S WT and MM.1S shATG5 cell lines were incubated with the different drugs at the indicated concentrations for 24 hours. Cell death was analysed by determining PS exposure and membrane integrity by AnnexinV and 7-AAD co-staining. Cell death percentage corresponds to AnnexinV$^+$, 7-AAD$^+$ and AnnexinV/7-AAD double positive subpopulations. Data are presented as mean ± SD from n=3 independent experiments. Statistical analysis was performed using two-tail unpaired t test, where *p<0.05; **p<0.01; ***p<0.001.

If autophagy inhibition mediated by CLQ really was the main mechanism responsible for the enhanced cell death observed in drug combinations, we would expect to find a similar effect in ATG5 KO cells upon PI single treatment. However, as shown, this was not case and when ATG5-deficient cells were treated with carfilzomib and CLQ, since cell demise was still potentiated. Therefore, these results, taken together, suggest that inhibition of autophagy has a minor role, if any, in the mechanism behind the potentiation effect exerted by CLQ. Although the differences in the sensitivity to carfilzomib alone between the parental and the shATG5-deficient cell line could be attributed, in part, to the process of viral transduction and selection, the expectable effect on cell death, if autophagy was the responsible would be the opposite. Nevertheless, a MM.1S-derived cell line transfected with a scrambled version of shATG5 RNA must be usead as a *bona fide* control. Therefore, the comparison of results found in the parental and the shATG5-modified cell line should be taken with caution.

In MM, autophagy has been reported to be a prosurvival mechanism that could provide protection against the high Ig production rate and resistance against drug-mediated effects, including PIs[158]. In fact, expression levels of antioxidant, chaperone and autophagy genes were reported to be inversely correlated with MM patients survival[718]. Moreover, several studies support the idea that ER stress response drives an increase in the autophagic flux in MM and also in other models[109,603,719]. UPR activation can trigger autophagy through PERK/ATF4 and IRE1/TRAF2/JKN related pathways[115]. Proteasome inhibition, has also been revealed to trigger autophagy in different cancer cell models, including MM[603,720–723]. As mentioned before, previous data reported by our group indicated that carfilzomib treatment increased autophagic flux, but this response did not reached completion[238]. Perhaps, this lack of autophagy consummation could be explained by the fact that the processing of some autophagic components requires an intact proteasome to occur[724]. Moreover, studies investigating the direct effect of proteasome inhibition on autophagic markers showed that these effects on autophagosome maturation were ambiguous and depended on the specific drug under study[724]. Nonetheless, this increment in autophagic response was first thought to be cytoprotective since co-treatment with the autophagy inhibitor CLQ potentiated cell death. However, previous results from our group and data presented above in ATG5 deficient cells suggest that autophagy inhibition is not the cause for the sensitization that CLQ bring about. CLQ have successfully been reported to sensitize cancer cells to PIs and also other types of chemotherapeutics[725–727]. Some of these studies reported autophagy-independent mechanisms for CLQ sensitization, as it apparently occurs in our model[173,180,728].

To conclude, our experiments conducted in autophagy defective cells suggest that autophagy inhibition is seemingly not uniquely responsible for the sensitization effect observed in PI-CLQ combinations. Further research will be required to unravel the mechanism behind the cell death potentiation effect of CLQ.

4.2.4. Study of the Proteasome Activity in the Mechanism of Action of PI-based Drug Combinations.

Although it would require further experimental confirmation, as mentioned earlier, autophagy inhibition does not seem to be the major or unique mechanism by which CLQ exert its sensitization effect on carfilzomib-induced cell death. On our search for alternative and/or off-target influences of CLQ, we found that this autophagy inhibitor could also modulate at some degree the activity of the proteasome. Consequently, the activity of the proteasome under the influence of the different PIs alone and in combination with CLQ was evaluated, as described in section 3.14.

Data presented below showed how low doses of bortezomib and carfilzomib alone effectively blocked proteasome activity in the different MM cell lines (**Figure 4.38**). Moreover, proteasome activity blockade seemed to be stronger with carfilzomib than with bortezomib in most of the cell lines evaluated. Probably, this occurs because of carfilzomib is an irreversible proteasome inhibitor while bortezomib and ixazomib are reversible PIs[200,729]. In fact, carfilzomib has been shown to be a more potent and selective PI compared to bortezomib, making it superior at this regard[729]. More importantly, when CLQ was added in combination with PI-based therapy, proteasome activity was further diminished. Interestingly, CLQ was much more effective in reducing the proteasome activity with carfilzomib treatment than under bortezomib-based therapy. As shown in the **Figure 4.38**, proteasome activity was almost completely blunted in carfilzomib-CLQ combinations. With regards to the action of CLQ treatment alone in MM cells, the CLQ dose-response revealed that this compound had the ability to strongly inhibit proteasome activity in MOPC.315.BM cells. In human MM cell lines this inhibitory effect was not so evident as appreciated by the fluctuating levels of proteasome activity. This probably would indicate the reversibility and the instability of the proteasome inhibitory properties of CLQ in these cell lines. Nonetheless, it seems that the concurrent administration of CLQ and PIs, especially carfilzomib, enhances proteasome inhibition. These results argue in favour with a potential mechanism by which these two compounds may cooperate somehow to restrain proteasome activity.

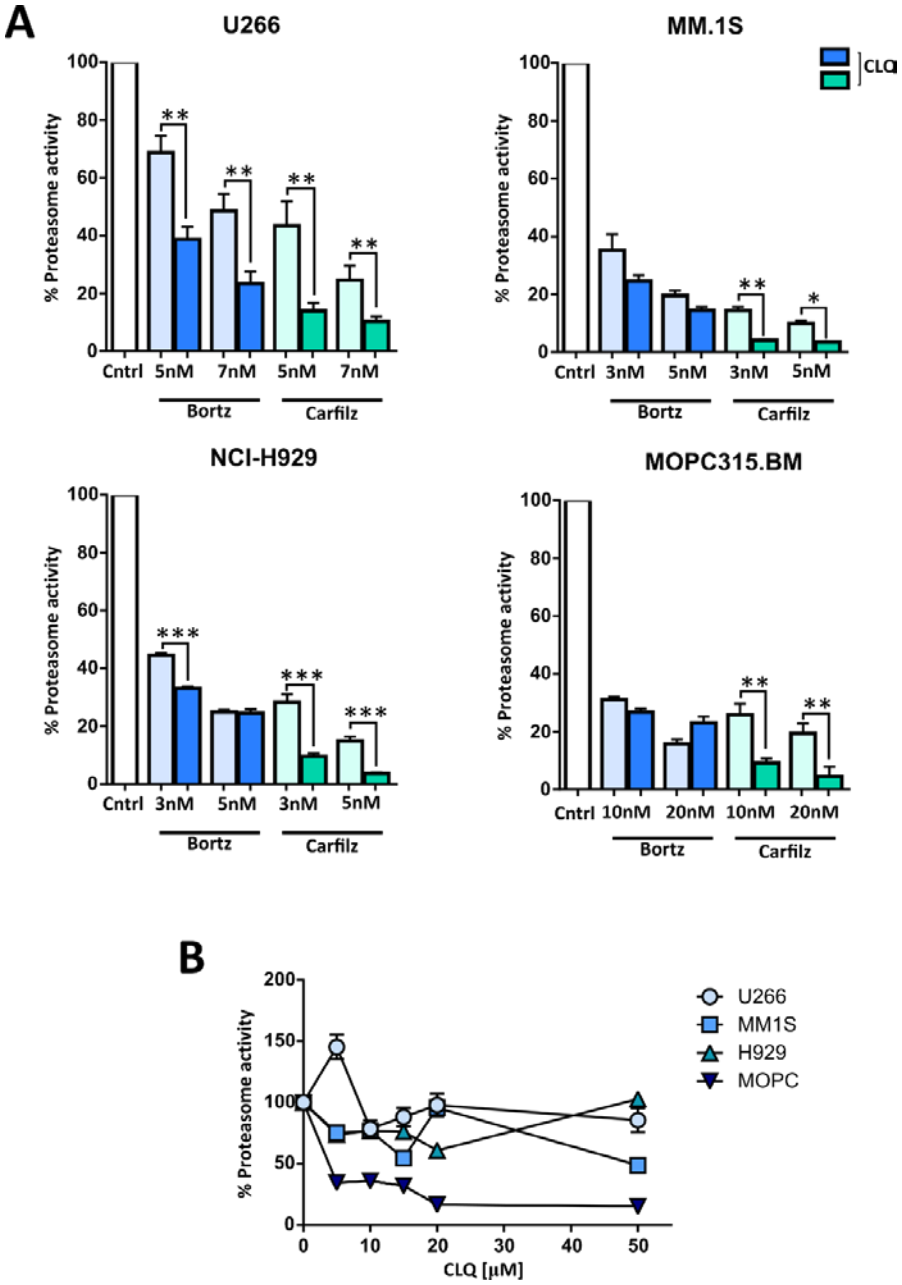

Figure 4.38 | Determination of proteasome activity. A. Quantification of the proteasome activity of MM cells when subjected to proteasome inhibitors or PI-based combinations with CLQ were evaluated. MM.1S, U266, NCI-H929 and MOPC315.BM cell lines were incubated with the different drugs at the indicated concentrations for 16 hours. Protein extracts were prepared and 20S proteasome activity was measured by fluorometric analysis with 20S proteasome activity assay kit following manufacturer instructions. Data are presented as the mean percentage of proteasome activity relative to control cells ± SD from n=2 independent experiments. Statistical analysis was performed using two-tail unpaired t test, where *p<0.05; **p<0.01; ***p<0.001. **B.** Quantification of proteasome activity of MM cells upon treatment with different doses of CLQ. Data are presented as the mean percentage of proteasome activity relative to control cells ± SD from n=2 independent experiments.

CLQ has long been used as an anti-malarial drug and as an autophagy inhibitor. However, Spranger *et al.* showed that this chemical compound was also able to block the enzymatic activity of the proteasome in eukaryotic cell extracts or purified 20S archaeal proteasomes[729,730]. Furthermore, through nuclear magnetic resonance (NMR) spectroscopy assessment, was found that CLQ reversibly bind to the outside of proteasome, yet at close proximity to the active site, between the α and β subunits of the barrel-like core particle[729,730]. These results, in conjunction with a thorough enzymatic kinetic study, dictated that CLQ inhibited the proteasome in a non-competitive manner[729,730]. However, what clearly brought our attention is that MG-132 (a PI that binds to the proteasome active site) and CLQ, were able to simultaneously bind to the proteasome[729,730]. These observations along with data presented here, further reinforce the idea of CLQ acting as an allosteric regulator upon PI-based therapy[729,730]. It is possible that through a mechanism yet to be determined, CLQ modulates the configuration of the active site in such a way that favours the accessibility of carfilzomib to the catalytic site. It is possible that the chemical nature and the irreversibility of carfilzomib plays an important role in this matter. This would enable a more potent inhibition of the proteasome of carfilzomib compared to when reversible PIs such as bortezomib or ixazomib are concurrently used along with CLQ.

Altogether, our data point to the notion that CLQ, possibly through its ability to bind and mildly inhibit the proteasome, facilitates the access or the inhibition exerted by carfilzomib more efficiently than when bortezomib simultaneously binds to the proteasome. Consequently, this increased efficacy in proteasome inhibition would lead to the increased observed cell death rates.

4.3. Immunogenicity of Cell Death & Molecular Mechanism.

Over the last years, the use of immunotherapy has gained momentum in cancer research and clinical oncology. The ability of chemotherapeutics and immune-based anticancer interventions to foster anticancer immunosurveillance, has reinvigorated the therapeutic panoramic in oncoimmunology. Additionally, the advent of "immunogenic cell death" (ICD) concept has contributed to this new conception. ICD can elicit potent adaptive immune responses against tumour-associated antigens in the case of neoplastic cells[216,230,731]. Involved in conferring the immunogenic attributes to cell death, damage-associated molecular patterns DAMPs are critically required. When released or exposed by stressed or dying cells, they bind to their cognate receptors (PRRs) expressed by innate immune cells, such as monocytes, macrophages and DCs[218]. Intensive and thorough mechanistic studies have positioned ER stress and ROS generation at the epicentre of ICD. Thereafter, activation of the ER stress responses or the UPR, and particularly, the PERK-mediated arm appeared to be vital factors for ICD-based

scenarios[225]. As illustrated earlier, the drugs used in our work can effectively evoke ER stress responses in MM cells, being good candidates to be considered as ICD inducers.

In the present section we sought to investigate whether the treatments utilized so far not only can induce cell death but also trigger *bona-fide* ICD with the potential to empower prophylactic anticancer immune responses in a novel orthotopic MM mouse model.

4.3.1. *In vitro* DAMP Exposure.

First, we decided to assess the ability of carfilzomib and the respective drug combinations with CLQ and DBeQ to expose DAMPs *in vitro*. In particular, we evaluated the exposure of different ER chaperones that have been shown to acquire immunomodulatory properties once expressed ectopically in the outer leaflet of the plasma membrane[230]. MM cells were then treated with the corresponding drugs for 24h and the ectopic expression of the different molecular chaperones was quantified by flow cytometry. To properly assess the exposure of these danger signals, ER chaperon expression must be performed on cells with an intact cell membrane, which is easily determined by co-staining with a vital-dye. In this case, we selected and gated on the 7-AAD-negative population and ER chaperone levels were examined.

Results presented in the **Figure 4.39** below, revealed that single treatment with carfilzomib increased the levels of ecto-CRT in carfilzomib-sensitive MM cell lines, that is, MM.1S and NCI-H929 cells. Probably, in U266 and MOPC315.BM cells carfilzomib concentration used was insufficient to elicit a proper amount of cell death (see **Figure 4.18** and **Figure 4.19**) and hence the corresponding exposure of CRT was minuscule. When CLQ or DBeQ were co-administered with carfilzomib, these drug combinations were not only capable of potentiating cell death, as seen in previous sections, but also to strongly enhance the exposure of CRT. In the case of carfilzomib-CLQ combinations, this was already reported by a previous study from our lab[238]. During the work presented here, we further confirmed these results and extended the finding to another ER stressor with carfilzomib-DBeQ combinations.

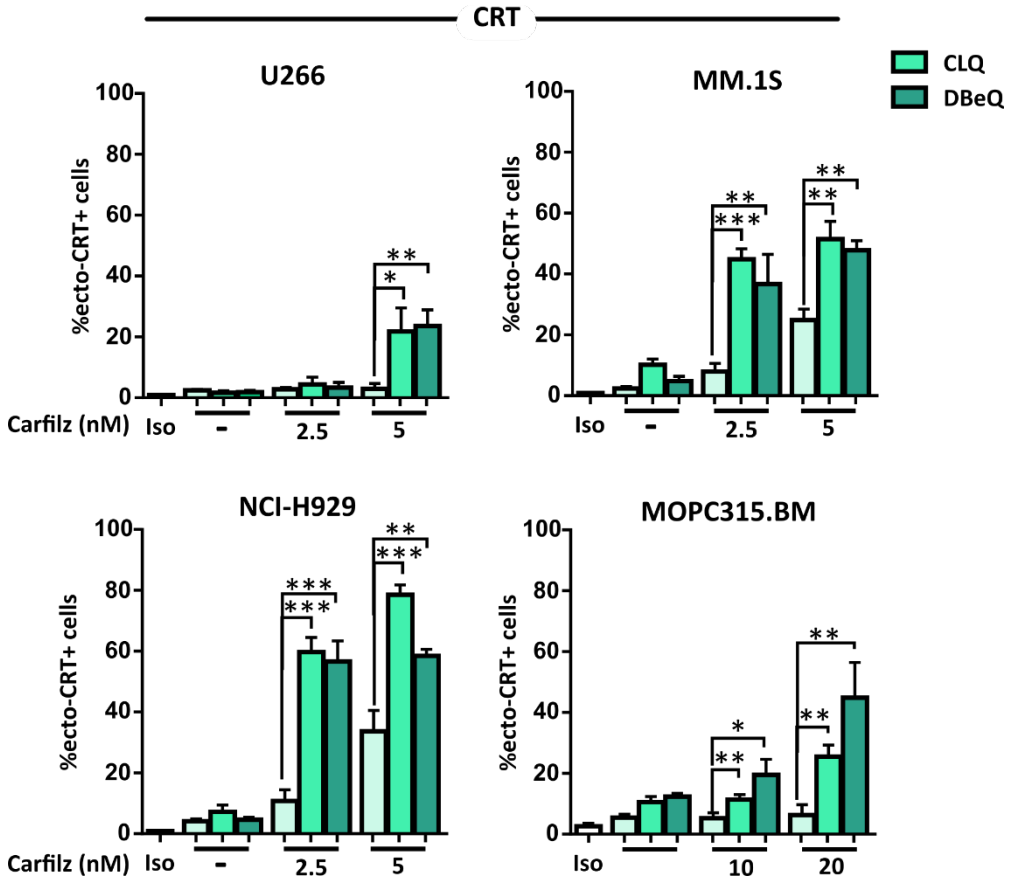

Figure 4.39 | Drug-induced ecto-CRT exposure in MM cells. The ability of different chemotherapeutic drugs to induce the translocation of CRT to cell surface (ecto-CRT) of MM cells was evaluated**.** MM cell lines were incubated with the different drugs at the indicated concentrations for 24 hours (CLQ 20μM and DBeQ 2.5μM). CRT exposure was assessed by flow cytometry using a specific fluorochrome-conjugated antibody as describe in section 3.4.1.1.1. Only cells with an intact plasma cell membrane (7-AAD-negative cells) were considered for ecto-CRT analysis. Data are presented as mean ± SD from 3 independent experiments. Statistical analysis was performed using one-way ANOVA with Tukey post-test, where *p<0.05; **p<0.01; ***p<0.001.

Calreticulin is a highly conserved, soluble, calcium-binding ER-associated chaperone with numerous functions inside the ER (calcium homeostasis, assembly of MHC-I, etc)[243,244]. Nonetheless, CRT has been shown to perform unexpected functions one could ever think of, that a conserved ER chaperone would perform. Gardai *et al.* were the first to describe the role of CRT in phagocytic clearance of dead cells[245]. In apoptotic cells, CRT is externalized to the outer leaflet of the plasma membrane (ecto-CRT) where it functions as a potent 'eat-me' signal. CRT along with other phagocytic signals like phosphatidylserine (PS), mediate the engulfment and removal of apoptotic cells in a process also known as 'efferocytosis' in a tolerant manner[732]. CRT binds to LRP1 (also known as CD91), and possibly other scavenger receptors, displayed by phagocytic cells. Obeid *et al.*[219] further extended the functions of CRT by demonstrating that CRT exposure by dying/stressed cells was a key determinant in ICD-driven anticancer immunity. Since then, several studies have reported the ability of certain chemotherapeutics as well as anticancer therapies to expose CRT on their surface[229].

Among them, we can find the PIs bortezomib and also its descendant carfilzomib[238]. The externalization of CRT instigates the cancer material to be engulfed by DCs. Consequently, uptake of cancer-derive antigens would lead to tumour antigen presentation and anticancer cytotoxic T lymphocyte (CTL) specific responses[229]. Although several laboratories have found that *bona-fide* ICD must rely on the emission of different danger signals to properly elicit complete anticancer immune responses, CRT is regarded by some authors as one of the most potent DAMPs[733].

Despite these and many other studies argue in favour of a immunostimulatory role of CRT in anticancer immune responses, quite recently, it has been reported that CRT can also harbour immunosuppressive functions[734]. In this study, researchers monitored CRT trafficking *in vitro* and *in vivo* in a mouse model that harbours a mutation in exon 9 of *CALR* gene[734]. Mutations in *CALR* are found approximately in 30% of myeloproliferative neoplasms (MPNs)[735,736]. Mutations in this region affect to the KDEL ER retention signal, causing CRT protein to be released[737,738]. Interestingly, when the truncated form of CRT escaped ER retention system and was released to the extracellular medium, it inhibited the phagocytosis of dying cancer cells by DCs[734]. This in turn suppressed anticancer immune responses instigated by chemotherapeutics and even PD-1 blockade[734]. Importantly, these type of mutations in *CALR* gene are not only circumscribed to MPNs, but can also be frequently found in solid tumours as annotated in COSMIC and cBioPortal databases[734]. When tumours bearing these mutated forms were implanted into mice, they underwent a weak response towards immunogenic chemotherapeutics compared to control tumours. Collectively, data from this study point to an immunosuppressive role of extracellular CRT. Other laboratories have also reported that soluble CRT can bring about both pro-inflammatory and anti-inflammatory responses on phagocytes and affect the activation and polarization state on these cells[256,739].

These presumed conflicting roles of CRT in immune-related scenarios may be attributed to different factors: the different molecular partners with which CRT can interact with, the regions of the protein involved in the interactions, CRT mutations and polymorphisms, the subcellular localization of CRT and also the different and varied post-translational modifications that CRT can be subjected to[739]. All these factors have been shown to influence and impact CRT-receptor interactions, the downstream signalling pathways stimulated and the evoked cellular outcomes[739]. Further studies will be necessary to decipher how and when CRT externalization is perceived as immunogenic or rather immunosuppressive to determine the balance between tolerance and immunogenicity.

Similar to CRT, other ER or cytosolic chaperones such as heat-shock protein 70 (Hsp70), Hsp90 and even BiP, have also been found to contribute to the immunogenicity of dying cancer cells in a partially redundant, yet not identical manner[740]. For instance, CRT, Hsp70 and Hsp90 has been reported to bind to the same CD91 receptor displayed by APCs[219,247,741]. We therefore tested whether our experimental conditions could also

mobilize other ER chaperones such as Hsp-70 (**Figure 4.40**) or BiP (**Figure 4.41**) to the plasma membrane.

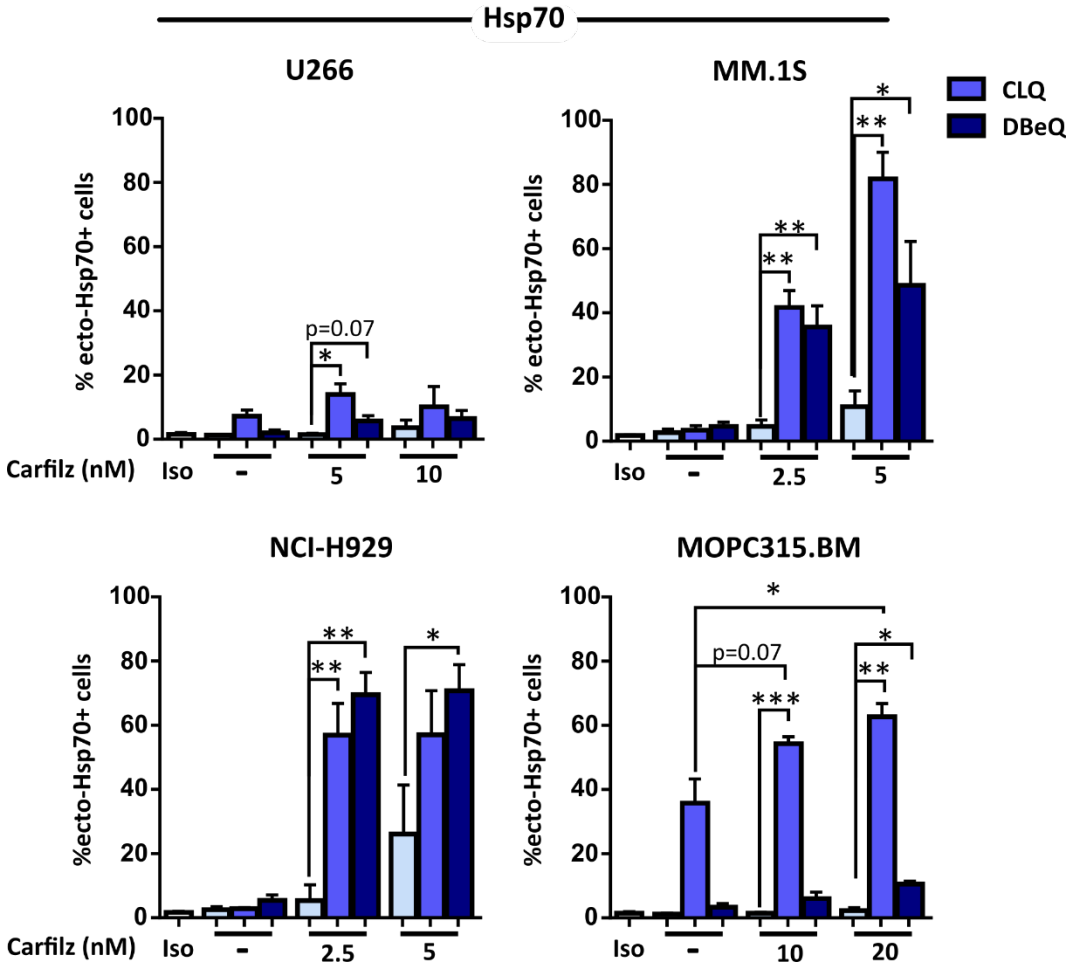

Figure 4.40 | Drug-induced ecto-Hsp70 exposure in MM cells. The ability of different chemotherapeutic drugs to induce the translocation of Hsp70 to the cell surface (ecto-Hsp70) of MM cells was evaluated**.** MM cell lines were incubated with the different drugs at the indicated concentrations for 24 hours (CLQ 20μM and DBeQ 2.5μM). Hsp70 exposure was assessed by flow cytometry using a specific fluorochrome-conjugated antibody as describe in section 3.4.1.1.1. Only cells with an intact plasma cell membrane (7-AAD-negative cells) were considered for ecto-Hsp70 analysis. Data are presented as mean ± SD from 3 independent experiments. Statistical analysis was performed using one-way ANOVA with Tukey post-test, where *p<0.05; **p<0.01; ***p<0.001.

Our data indicate that carfilzomib alone was not as efficient to provoke ecto-Hsp70 exposure as it did with CRT. Only in NCI-H929 cells a noticeable increment in Hsp70 plasma membrane-levels was observed for the higher concentration. In the rest of the cell lines, despite using carfilzomib concentrations that trigger cell death, especially in MM.1S and U266, Hsp70 was not significantly externalized. Noteworthy, when carfilzomib was combined with CLQ or DBeQ, Hsp70 exposure was drastically enhanced in the majority of MM cell lines. Here, DBeQ-carfilzomib combination evoked a weaker response in terms of Hsp70 mobilization compared with CLQ drug

combinations in almost every cell line, with the exception of NCI-H929 cells. Although it managed to reach statistical significance or at least a strong tendency, respectively, MOPC315.BM and U266 cells manifested the lower Hsp70 levels upon carfilzomib and DBeQ combination. It should be mentioned that CLQ treatment alone brought forth a strong mobilization of Hsp70 to the plasma membrane in the case of MOPC315.BM cells. However, combined treatment with carfilzomib significantly further increased ecto-Hsp70 levels in these cells.

The specific role of Hsp70 in chemotherapeutic-induced immunogenicity of cancer cells has probably not been studied so extensively as CRT. However, it has been reported that in shikonin- or gemcitabine-treated cells, Hsp70 was involved in DC-mediated activation of $CD4^+$ and $CD8^+$ T cells [248,249]. Likewise, platinum-based drugs induced translocation of CRT and Hsp70 among other danger signals and effectively enhanced phenotypic maturation of myeloid and plasmacytoid DCs[742]. In the case of Hyp-PDT treatment, Hsp70 promotes nitric oxide (NO) generation in innate immune cells[250]. In a different context, Hsp70 has shown to efficiently vaccinate mice against murine MM cells using a DNA-based vaccination strategy[251]. Hsp70 was also shown to boost NK cytotoxic functions and NK cell cytokine production[743,744]. Supporting their role in anticancer mediated immunity, when extracellularly released, Hsp70 and other chaperones can operate as cytokines or 'chaperokines' and exert immunoregulatory effects by binding to TLR and other receptors on immune cells[745–748].

As regards to the evaluation of plasma membrane levels of BiP in MM-treated cells, results showed that this ER chaperone can also be translocated upon drug treatment (**Figure 4.41**). Carfilzomib treatment alone was able to increase ecto-BiP levels in a weaker fashion (except in the case of NCI-H929 cells) compared to the other DAMPs assessed so far. However, similar to the other chaperones, drug combinations, especially carfilzomib-CLQ combination, significantly increased BiP exposure on MM cells. Here, no major differences were found between CLQ and DBeQ combinations, excepting the case of MOPC315.BM cells in which carfilzomib-CLQ provoked a stronger mobilization of BiP molecules, while combination of carfilzomib and DBeQ faintly succeeded in that task. From the different MM cell lines, NCI-H929 cells were the most sensitive to chaperone exposure, while U266, MM.1S and probably MOPC315.BM cells (under some conditions) were less responsive to translocation of this type of DAMP. Perhaps, this could also be correlated with the increased resistance displayed by these cells (U266 and MOPC315.BM) to drug treatment.

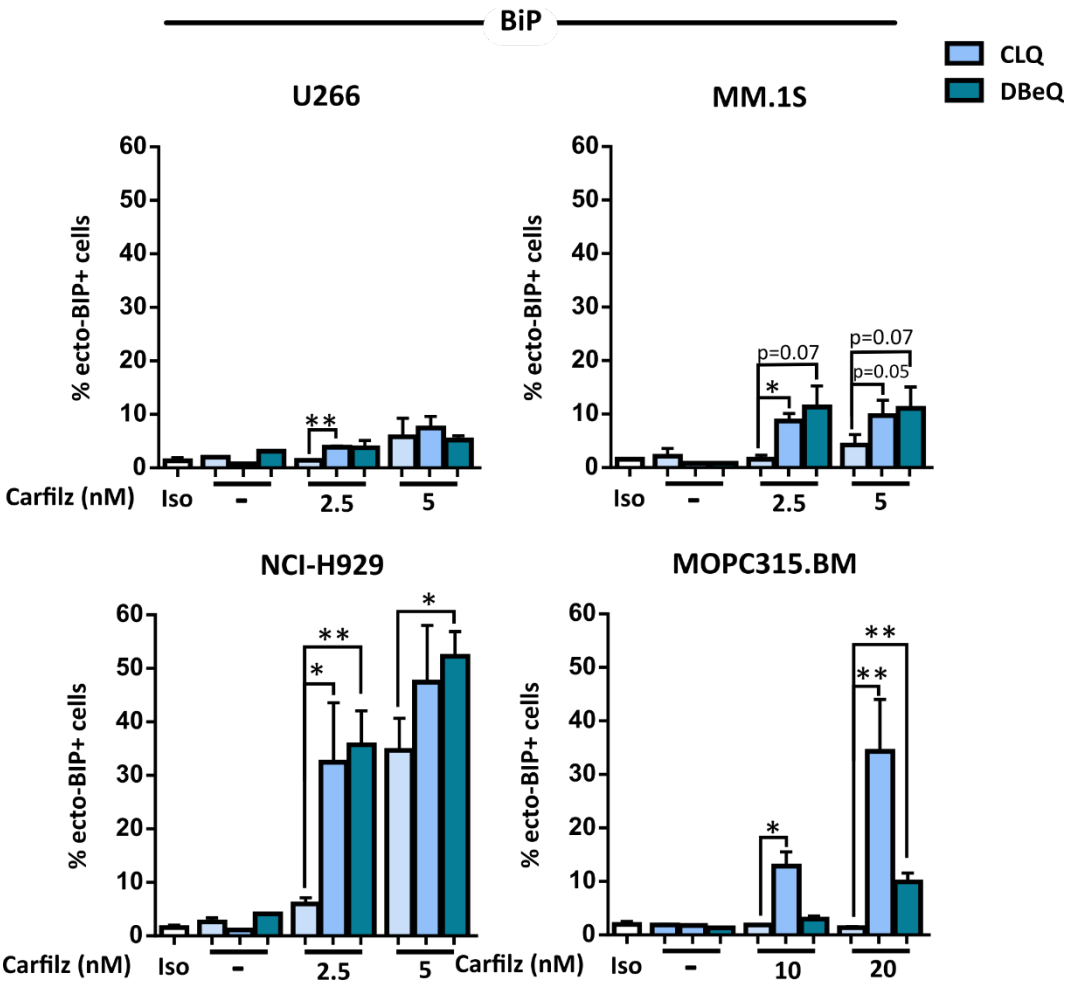

Figure 4.41 | Drug-induced ecto-BiP exposure in MM cells. The ability of different chemotherapeutic drugs to induce the translocation of BiP to the cell surface (ecto-BiP) of MM cells was evaluated**.** MM cell lines were incubated with the different drugs at the indicated concentrations for 24 hours (CLQ 20μM and DBeQ 2.5μM). BiP exposure was assessed by flow cytometry using a specific fluorochrome-conjugated antibody as describe in section 3.4.1.1.1. To ecto-BiP analysis only 7-AAD-negative population was considered. Data are presented as mean ± SD from 3 independent experiments. Statistical analysis was performed using one-way ANOVA with Tukey post-test, where *p<0.05; **p<0.01; ***p<0.001.

While the role of BIP as a fundamental regulator of ER function and the UPR, it is widely documented, emerging functions of how cell-surface or secreted BiP regulates cell signalling and even immunity are just starting to emerge[749]. Recently, it has been reported that a pool of BiP molecules can localize at the outer leaflet of the plasma membrane[750,751]. Moreover, under ER stress conditions, BiP molecules have been shown to be actively relocated to the cell surface[752]. Regarding its immunogenic role as a danger signal, BiP has been described to be secreted and participate in the cross-presentation of tumour-derived Ags in DCs, inducing Ag-specific CTL immune responses[252].

Recapitulating, besides their roles in protein folding, calcium binding and sensing stress signals, chaperones can also acquire novel immunomodulatory properties when exposed in the cell surface or release to the extracellular milieu. Some chaperones can function as ‘eat-me signals’ stimulating the uptake of dead-cells and its derived antigens

by APCs, favouring their activation and maturation[739]. When released extracellularly, they can also operate as cytokines stimulating secretion of pro-inflammatory (or even anti-inflammatory mediators) affecting polarization of phagocytic cells[753]. This cytokine-like or 'chaperokine' function has been reported for a great variety of cellular chaperones including HSP27, HSP60, HSP70, GRP94, HSP90 and others[753,754]. These chaperones specifically bind to TLRs, as well as many other receptors, and exert immunoregulatory effects such as upregulation of adhesion, co-stimulatory molecules on APCs[746,747,753,754]. Moreover, chaperones as efficient protein folding mediators, are often present bound to antigenic peptides. When released, these chaperone-peptides complexes enter APCs by endocytosis via CD91 receptors and are cross-presented on MHC-I and MHC-II molecules to $CD8^+$ and $CD4^+$ T cells[253,254]. Thus, these molecules not only would intensify the immunogenicity of dying cancer cells by merely acting as powerful danger signals, but also may contribute by boosting cancer antigenicity facilitating the cross-presentation process. In fact, these characteristics have prompted their use as vaccines, especially in the oncological setting[753].

To conclude, we have shown that different ER and/or cytosolic chaperones (CRT, Hsp70 and BiP) are exposed in the cell surface of MM-treated cells. As indicated this observation could entail important consequences on the immunogenicity of cancer cell death.

4.3.2. Measurement of Intracelullar ATP Levels.

Apart from CRT or ER chaperon exposure, ICD is a multifactorial and spatiotemporally defined multistep process that deeply depends on other danger signals to effectively drive antitumour immune responses. Among these, release of extracellular nucleotides like ATP has been shown to play a pivotal role in attracting the attention of APCs necessary to stir up antitumor immunosurveillance. We then pursued to analyse ATP release upon drug-treatment in our experimental conditions. ICD-associated secretion of ATP can be evaluated by two complementary methods[755]. Usually, ATP levels can be assayed by detection of luminescent signals emanated from the activity of luciferase oxidizing luciferin molecules in an ATP-dependent manner[755]. Alternatively, an indirect approach based on monitoring intracellular ATP levels can also be used. ATP stability in the extracellular space is quite elusive, mainly due to the presence of ectonucleotidases that rapidly degrade ATP. Additionally, the luciferin-based assay could entail other technical problems such as reproducibility issues, among others. For these reasons, we decided to initially test intracellular ATP with quinacrine which is a more cost-effective approach. In particular, quinacrine is able to detect intracellular ATP-containing vesicles[530]. Quinacrine is a fluorophore that emits green fluorescence in presence of ATP and therefore, this signal can be easily quantified by flow cytometry (as done in this work) or fluorescent microscopy to assess concurrent morphological

features[530]. Thus, we analysed the loss of quinacrine-associated fluorescent signal in MM cells treated with the different drugs used so far, but that remain with an intact plasma membrane (**Figure 4.42**). In this way, loss of intracellular ATP as a consequence of plasma membrane breakdown could be discarded.

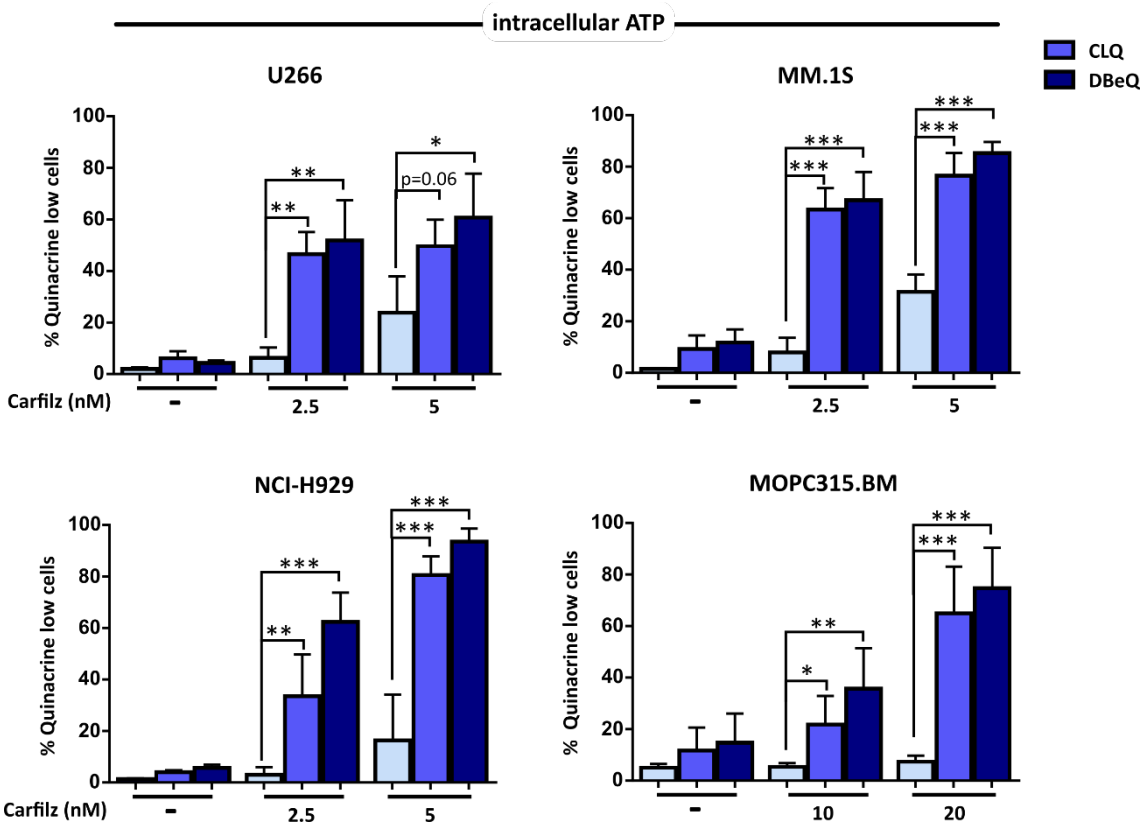

Figure 4.42 | Study of drug-induced ATP depletion. To indirectly assess ATP secretion during ICD, intracellular levels of ATP after drug treatment were assessed. MM cell lines were incubated with different drugs at the indicated concentrations for 24 hours (CLQ 20μM and DBeQ 2.5μM). Thereafter, cells were stained with quinacrine to measure intracellular ATP levels by flow cytometry as described in section 3.4.1.3. In this analysis, percentage of quinacrine low cells were assessed in cells with an intact plasma membrane (7-AAD-negative population). Data are presented as mean ± SD from n= 3 independent experiments. Statistical analysis was performed using one-way ANOVA with Tukey post-test, where *p<0.05; **p<0.01; ***p<0.001.

MM cells treated with carfilzomib as single agent displayed different responses in terms of reducing intracellular ATP levels. MM.1S and U266 cells noticeably increased the percentage of quinacrine-low population at higher doses. A much lower increased was observed in NCI-H929 cells despite using a concentration that effectively triggers cell death in a considerable amount of cells. MOPC315.BM cells practically did not reduce intracellular ATP levels at carfilzomib tested doses. It should be noted that probably in this case, the concentrations of carfilzomib treatment alone used, were not sufficiently higher to induce cell death and/or expel ATP-containing vesicles. A much stronger response was obtained with the combined regimens with CLQ or DBeQ. Under these

conditions an effective reduction of intracellular ATP levels was shown, or in other words, the proportion of cells with quinacrine-low based fluorecence was significantly and strongly enhanced.

During the course of ICD, dying cells expel ATP[86,87] to the extracellular milieu where it functions as a powerful short-range 'find me' signal[261]. Once secreted, ATP binds to ionotropic (P2X7) and metabotropic (P2Y2) purinergic receptors on APCs[86,261], stimulating their phenotypic maturation and chemotactic attraction respectively[148]. Some studies have reported that extracellular ATP can activate the caspase-1 dependent NLRP3 complex (the so called inflammasome) triggering IL-1β secretion[86]. As a consequence, $CD8^+$ T cell[86], as well as, IL-17 producing-γδ T cell[262] antitumor responses are invoked. According to this, mice devoid of any of these components ($Nlrp3^{-/-}$, $P2rx7^{-/-}$ or $Casp1^{-/-}$) seem to be incapable of inciting adaptive immune responses during drug-induced ICD[86,262].

The molecular mechanisms of ATP secretion during ICD is thought to be determined by the specific ICD-inducing stimulus. For example, in anthracyclin- or oxaliplatin-driven early apoptotic ATP secretion, autophagy has been demonstrated to be mandatory[263]. Depletion of important autophagy components (ATG5, ATG7 and BCN1) prevented ATP release[263]. Moreover, this molecular pathway make use of molecules involved in other cellular processes such as lysosomal exocytosis (LAMP1, VAMP1), membrane blebbing (ROCK1, myosin II), apoptotic machinery (caspases) and membrane permeabilization (pannexin 1, PANX1). All these miscellany of molecules have been shown to participate and be indispensable for ICD-induced ATP release[263]. Interestingly, caspases but not the autophagic machinery, were deemed critical contributors to PANX1 activation and surface exposure, as well as, LAMP1 translocation[263]. In fact, it is possible that remodelling of autophagic effectors, lysosomal effectors or PANX1 hemichannels by caspases, rather than the mere presence of these components *per se*, are the real instigators of ATP secretion[263,264]. On the other hand, in other therapy-induced models of ICD, ATP secretion mechanisms may differ from those described for chemotherapy-induced ICD. In particular, Hyp-PDT-mediated ATP has been shown to be autophagy-independent[265], and required the PERK-mediated proximal secretory pathway and PI3K-regulated exocytosis[257].

In our experimental settings, especially in the carfilzomib-CLQ combination, autophagy is presumably being inhibited by CLQ. Therefore, attending the mechanism exerted by chemotherapeutic drugs described above, one would expect that upon autophagy inhibition or deficiency, intracellular ATP levels would not diminish as a consequence of ATP secretion. Our results clearly contrast these observations. Probably, the simplest explanation could be that carfilzomib and its combinations, could provoke an intense ER stress response, and behave more like type II ICD inducers (like Hyp-HDT) and hence follow the autophagy-independent mechanism of ATP secretion exerted by Hyp-PDT[257,264]. Although the ER is not the primary target of carfilzomib, CLQ or DBeQ, targeted pathways are closely related to the ER. Hence, the ER stress response

generated could possibly resemble that of Hyp-PDT and eventually follow danger signalling-associated mechanisms[257]. Alternatively, another possible explanation is that CLQ inhibits the final steps of the autophagic process, while studies on ATP secretion were conducted using models in which autophagy is blunted in early phases[263]. Therefore, upon CLQ inhibition, although acidification of lysosomes and completion of autophagy is inhibited, autophagic intermediaries are still intact and hence could participate in ATP-containing vesicles mobilization and its secretion to the extracellular space. Moreover, we cannot neglect the possibility that depletion of intracellular ATP levels could also be envisaged as a consequence of apoptotic-related mitochondrial impairment as well as a deterioration of mitochondrial metabolism and ATP production in dying or stressed cells. Since the approach we used gives us an indirect readout of ATP secretion, we cannot ascertain that ATP is actually being ejected. Further confirmation experiments by directly quantifying ATP molecules in cell supernatants will provide more clues into this matter.

4.3.3. Mechanism of DAMP Exposure.

4.3.3.1. Caspases & CRT Exposure.

Caspases have been reported to be critical contenders on how cell death is perceived immunologically[731]. These cellular proteases have been involved in some distinct ICD-related scenarios[756]. However, there are no easy answers, and caspases have been involved both in the enhancement and silencing of cell death immunogenicity[731]. Therefore, to deepen our knowledge in the mechanisms behind danger signal emission incited by the drugs used in our study, we studied the contribution of caspases to CRT exposure. For that purpose, we evaluated ecto-CRT levels in presence of pan-caspase inhibitor z-VAD-fmk or the caspase-8 inhibitor z-IETD-fmk, and compare them with caspase proficient cells. Since previous data indicated that cell death induced by these drugs strongly relies on caspases (in most of the cell lines tested), we sought to equilibrate cell death levels in conditions under caspase-inhibition to rule out the possibility that CRT exposure could be affected by this factor. We then utilized higher drug concentrations when cells were incubated with z-VAD-fmk or z-IETD-fmk to normalize cell death levels, excepting the case of NCI-H929 cells which were shown to be caspase-independent.

Results depicted in the **Figure 4.43** revealed two different behaviours that depended on the cell line under consideration. For example, in NCI-H929 cells, ecto-CRT levels were significantly reduced in all treatments in presence of caspase inhibitors z-VAD-fmk and in a lower extent with z-IETD-fmk. Similarly in U266 cells, although it did not reach statistical significance, there was a small tendency towards lower levels of surface CRT when caspases were inhibited. Conversely, MM.1S and MOPC315.BM cells exhibited increased exposure of CRT in the cell surface when cells were pre-incubated

with the caspase inhibitors. Here, z-VAD-fmk apparently manifested more potency in terms of potentiating CRT exposure, than z-IETD-fmk, especially in the case of MOPC315.BM cells, although differences were objectively small. On the contrary, MM.1S cells treated with carfilzomib and DBeQ and under the influence of z-IETD-fmk inhibitor, showed augmented ecto-CRT levels compared to z-VAD-fmk.

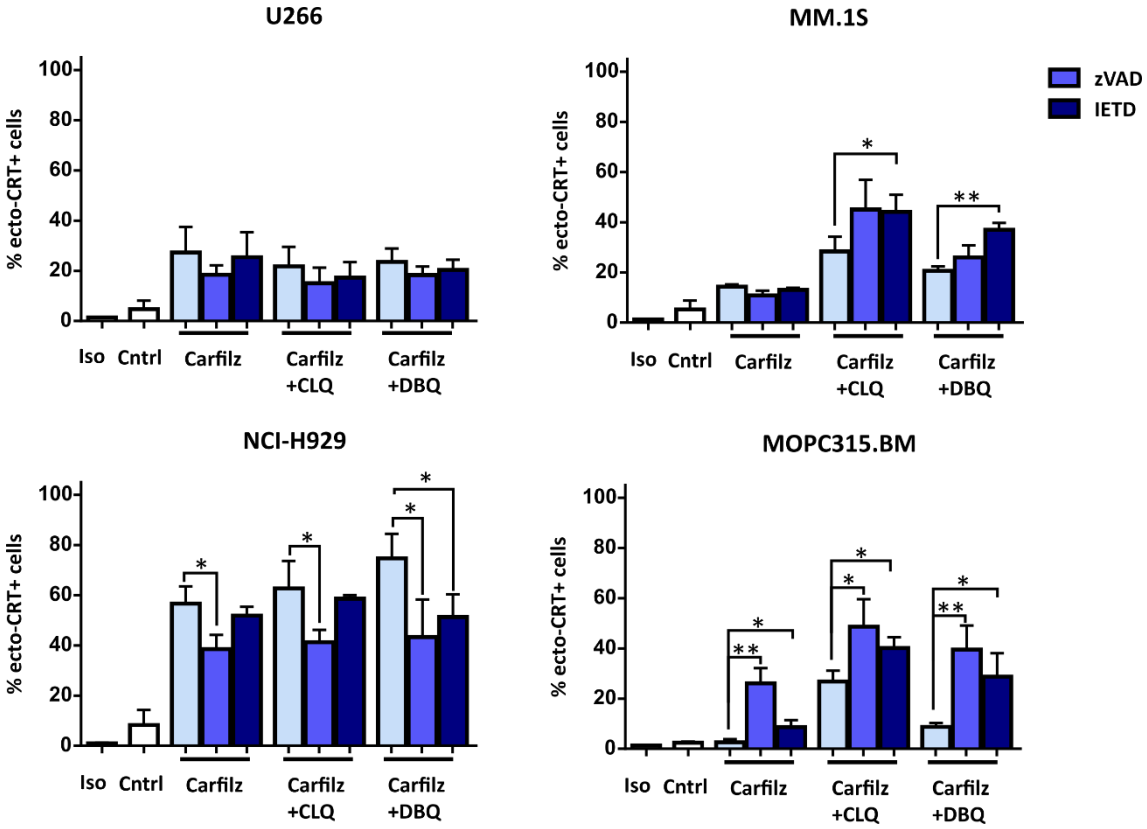

Figure 4.43 | Involvement of caspases on drug-induced ecto-CRT exposure in MM cells. The implication of caspases in the translocation of CRT to cell surface (ecto-CRT) upon drug exposure in MM cells was evaluated**.** MM cell lines were first preincubated with pancaspase inhibitor zVAD-fmk (30 μM) or caspase-8 inhibitor z-IETD-fmk (30 μM) for 1 hour. Afterwards cells were incubated with the different chemotherapeutic agents at the indicated concentrations for 24 hours. MM.1S and U266 were treated with carfilzomib 2.5 and 5nM respectively when no caspase inhibitors were utilized and with carfilzomib 10 nM in conditions in which caspases were abrogated. Similarly, MOPC315.BM cells were incubated with carfilzomib 10nM when caspases were active and carfilzomib 25 nM when caspases were inhibited. CLQ and DBeQ concentrations utilized were always 20 μM and 2.5 μM respectively. CRT exposure was assessed by flow cytometry using a specific fluorochrome-conjugated antibody as describe in section 3.4.1.1.1. Only cells with an intact plasma cell membrane (7-AAD-negative cells) were considered for ecto-CRT analysis. Data are presented as mean ± SD from 3 independent experiments.

Interestingly, in NCI-H929 cells, a cell line in which cell death did not exhibited caspase-dependency, and therefore, ecto-CRT levels were not supposed to be altered due to cell death rates, showed a significant reduction in CRT exposure upon caspase inhibition. Furthermore, as presented in previous sections (**Figure 4.31**), ROS generation was augmented when NCI-H929 cells were treated concurrently with the

anti-myeloma drugs and z-VAD-fmk. According to previous mechanistic studies, ROS production is an essential part in ICD-mediated DAMP emission[255]. Thereby, in this case, our data suggest that ROS generation and CRT translocation follow inverse behaviours under these conditions. Conversely, in MM.1S and MOPC315.BM cell lines, caspase inhibitors effectively protected these cells from drug-induced cell death. In these cells, despite exhibiting reduced cell death rates when caspases were inhibited (a complete normalization of cell death was not achieved), ecto-CRT levels were markedly increased. Interestingly, ROS levels were also blunted under caspase inhibitor influence in MM.1S and MOPC315.BM cells (**Figure 4.31**). Again, despite ROS generation is thought to be required in ICD-related DAMP signalling, ecto-CRT levels were even increased under these conditions.

First and probably the simplest explanation is that as our data point to, the source of measured ROS in our model, is not the same as the one present in anthracycline-induced ICD. Therefore as noted earlier, measured ROS are probably originated at later stages due to mitochondrial dysfunction during cell death execution rather than originating upstream of the cell death cascade. However, we cannot rule out that an early source of ROS could be generated at earlier time periods as a consequence of ER stress and could have contributed to danger signalling. An alternative and yet more complex rationalization is that a different mechanism of DAMP trafficking is being activated. In fact, in some regulated variants of cell demise, ROS-mediated ER stress may be dispensable for triggering ICD and the ensuing *in vivo* immune responses[225,232]. Specially, necroptosis has been shown to occur in absence of apparent ER stress or PERK activation[232]. This reveals that there may be alternative mechanisms that may take part in the induction of danger signalling and further reinforce the idea that ICD induction may be stimulus and context-dependent.

Why in caspase-dependent cells (MM.1S or MOPC315.BM), CRT is more efficiently relocated to the cell surface, while in caspase-independent cells (NCI-H929), CRT exposure is reduced when caspases are inhibited? In caspase-dependent cells, apoptosis is probably the main cell death mechanism activated under drug treatment. In this case, when caspase are inhibited, alternative cell death mechanisms like necroptosis could be triggered. However, although a quite succinct reduction of cell death rates could be appreciated when both caspases and necroptotic pathway were concurrently inhibited compared to caspase inhibition alone (**Figure 4.24**), these differences were fairly small and non-significant. This would suggest that in these cells, when caspases are inhibited, necroptotic pathway is probably not a major cell death mechanism that participates under these conditions. Necroptotic cells have been shown to follow different mechanisms and even has been reported to be at least as immunogenic as their apoptotic counterparts[232]. Moreover, in agreement with some of our results, instances of caspase-independent CRT exposure have also been declared. For example, caspase-8 activation has been shown to be dispensable in Hyp-PDT mediated ICD. Also, in a recent study, it was shown that ICD can be triggered in melanoma cells in presence of z-VAD-fmk[757].

Additionally, we cannot rule out the possibility that CRT exposure in our model could be generated at a later-phase during advanced apoptosis. Time-course experiments performed by a former TFG student, indicated that CRT exposure occurred at later time-points corresponding with cell death timing (results not shown). At this latter phases, intracellular membranes mostly from the ER are recruited to the surface giving rise to a general alteration of the glycocalix, as well as non-specific recruitment of ER membrane proteins such as calnexin to the cell surface[756]. Early apoptotic CRT exposure described for anthracycline-based therapies follow a complete different mechanism[756]. In cells treated with anthracyclins, ecto-CRT exposure precedes phosphatidylserine externalization and is always accompanied by ERp57 to the plasma membrane[255,256]. In this mechanism, caspase-8 activation and specific cleavage of BAP31, leading to the subsequent activation of Bax and Bak is also required[255]. However, there are other ways by which CRT can be relocated to the cell surface and that are independent from the aforementioned mechanisms. Some studies claimed that CRT can bind with high-affinity to phosphatydilserine[258,259] in a Ca^{2+}-dependent manner, and thus during cell death these two molecules could be co-translocated at the same time in a caspase-independent fashion[260]. Although PS exposure is thought to be primarily caspase-dependent, instances of PS translocation in caspase-independent manner has also been reported[758].

To conclude, our data showed that caspases can pose both positive and negative influences on DAMP signalling. Reconciling this dichotomous behaviour will undoubtedly require further examination and integration of the different actors of cell death and immunogenic reactions[731]. What it is clear is that, each cell demise is immunologically different, no matter which cell death modality is being considered[731].

4.3.3.2. Role of Autophagy in CRT Exposure.

Another controversial point in the mechanism of CRT exposure is whether autophagy is actually involved in the CRT translocation process or not. During this work and also in previous reports, we have shown that inhibition of autophagy at late stages with CLQ, enhances the exposure of CRT induced by carfilzomib[238]. However, many studies analysing the role of autophagy in DAMP signalling targeted early or intermediary mediators of autophagy. Nonetheless it is possible that the different stages of the autophagic flux may play different roles in CRT exposure. To shed more light into this topic, we evaluated CRT levels on autophagy-deficient MM cells (MM.1S shATG5) upon treatment with carfilzomib and its respective drug combinations and performed a parallel comparison with the parental cell line. In this case, assessing ecto-CRT levels was a little bit more complicated and some modifications in the conventional protocol were performed. MM.1S shATG5 cells, due to the vector used for lentiviral infection, are inherently fluorescent in the green FL1 channel. Moreover, this fluorescence bleeds out and reaches FL2 and even FL3, leaving unspoiled only FL4 channel. This makes co-staining with the vital dyes like 7-AAD or propidium iodide unpracticable. We then used

SYTOX blue dead cell stain which is excited with the violet 405nm laser and that its emission spectra lies before green fluorophores spectra. CRT readouts were acquired in the FL4 channel using an Alexa-647 fluorophore.

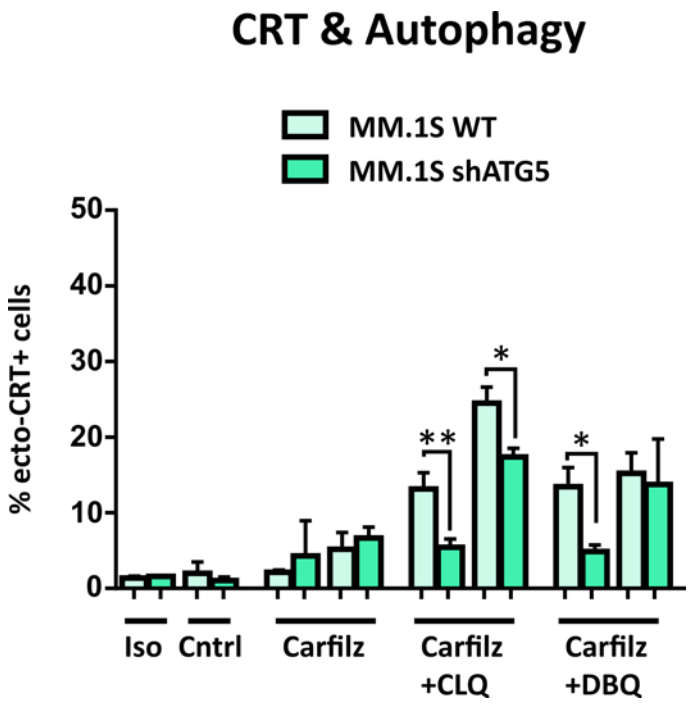

Figure 4.44 | Involvement of autophagy on drug-induced ecto-CRT exposure in MM cells. The implication of autophagy to the immunogenicity of cell death was interrogated, in particular its role in the translocation of CRT to cell surface (ecto-CRT) upon drug exposure**.** MM.1S WT and MM.1S shATG5 cells cell lines were incubated with the different chemotherapeutic agents at two different concentrations for 24 hours: carfilzomib (2.5 nM and 5 nM), CLQ 10 μM and DBeQ 2.5μM. CRT exposure was assessed by flow cytometry using a specific fluorochrome-conjugated antibody as describe in section 3.4.1.1.1. Only cells with an intact plasma cell membrane (Sytox blue negative cells) were considered for ecto-CRT analysis. Data are presented as mean ± SD from 3 independent experiments.

As **Figure 4.44** illustrates, MM.1S shATG5 cells were less efficient in mobilizing CRT to the cell surface when challenged with the same drug concentrations of the aforementioned treatments as the parental cell line. Interestingly, even when autophagy was disrupted in ATG5-deficient cells, CLQ was able to enhance CRT exposure when combined with carfilzomib, especially at higher concentrations. It is also important to mention that the parental cell line probably is not the best control line in this experiment. In theory, generation of a stable cell line transfected with an scrambled RNA-cloned vector should not have any apparent effect on cell behaviour, and should function as the parental cell line. Nonetheless, to rule out any potential off-target effect a proper control cell line should be assessed in parallel to draw out rigorous conclusions.

Conflicting results have been reported regarding the involvement of autophagy in the translocation of CRT during ICD. In some contexts, autophagy seems to suppress the

induction of ecto-CRT. Under Hyp-PDT treatment, autophagy has been shown to be activated and to confer resistance against ROS-mediated cytotoxicity of stressed cancer cells[323,324]. Outstandingly, autophagy was found to attenuate CRT translocation and DCs maturation as well as suppress DC-mediated proliferation of $CD4^+$ and $CD8^+$ T cells[265]. In other words, in autophagy-deficient cells, CRT exposure was intensified[265]. This has been rationalized as the autophagy machinery is able to clear oxidized proteins and organelles[265,324], which in turn would alleviate the ER retention system that becomes overwhelmed under ER stress conditions[243,325]. Hence, during Hyp-PDT treatment, ER stress and ROS production allow oxidized proteins to accumulate leaving the ER retention system saturated[323,324]. Under these conditions, autophagy inhibition would increase the amount of oxidized proteins (possibly by augmenting ROS-based ER stress) and would favour that ER resident chaperones such as CRT could escape from ER confinement [243,265,310]. Similarly, in a model of melanoma, in wild-type as well as in BRAF-resistant cells, concurrent silencing of ATG5 and treatment with a MEK-inhibitor (U0126), amplified the levels of ecto-CRT and ecto-HSP90 compared to those cells in which autophagy was intact[326]. In contrast, in chemotherapy-induced CRT (oxaliplatin and mitoxantrone), autophagy-deficient and autophagy-competent cells were equally effective in exposing CRT in the cell surface[759]. Moreover, ICD induced by oncolytic Newcastle disease virus, and specifically CRT translocation, was inhibited upon depletion of key autophagic genes[311].

Recently, another study showed that inhibition of autophagy at early stages provoked an attenuation of CRT translocation, whereas inhibition of autophagy at later stages with CLQ and other drugs like bafilomycin A1 augmented ecto-CRT levels[760]. These results are in line with our data, since inhibition of autophagy with CLQ potentiated ecto-CRT exposure when combined with carfilzomib, whereas depletion of ATG5, which participates in earlier autophagy phases, reduced or at least did not affect CRT translocation. Moreover, since CRT mobilization is enhanced upon combination of carfilzomib and CLQ, even when autophagy was disrupted in ATG5-deficient cells, this observation may suggest that the potentiation effect of CLQ on CRT translocation is not uniquely mediated by autophagy. These results are in accordance with the hypothesis that the cytotoxicity potentiation effect mediated by CLQ may be autophagy-independent.

Taken together, although we cannot discard the possibility that CRT exposure may rely on the targeted autophagic phase, CLQ may favour CRT trafficking by mechanisms that may not entirely involve autophagy.

4.3.4. DCs Maturation.

Induction of an effective antitumour immune response requires a proper activation of the adaptive Immune System by APCs. DCs stand out as one of the most potent activators of the adaptive immune system due to its capacity to instigate T cell responses[761]. One of the abilities of cells undergoing ICD is their competence to induce functional activation of DCs. This activation process is associated with a phenotypic maturation that entails a wide variety of cellular changes: dendrites development, diminished antigen capture, increased expression of antigen-presenting molecules (MHC class I and class II molecules), upregulation of costimulatory molecules and chemokine receptors and the production and secretion of cytokines and chemokines that regulate T cell differentiation and recruitment[298].

To confirm if the DAMP signature evoked during cell death induced by the drugs used in our study, harbours immunogenic potential, we assessed the ability of MM-treated cells to induce maturation of DCs *in vitro*. First of all, we generated DCs from human peripheral blood monocytes (mo-DCs) *in vitro* as described in section 3.1.7. After a week of differentiation with the proper cytokine cocktail, immature DCs expressed the characteristic marker CD11c and were ready to use. MM cells were then treated for 24h with the usual doses of drugs to induce ICD. Thereafter, cells were thoroughly washed to eliminate residual drugs and were co-incubated with immature DCs for additional 24h. We then analysed markers associated with DCs maturation by gating on $CD11c^+$ cells. In particular, we analysed the expression of co-stimulatory molecule CD86, HLA-DR for proper antigen presentation and the well-stablished marker of mature DCs, with a yet not clearly understood role, CD83. As positive control for DCs maturation we used lipopolysaccharide (LPS). In these experiments, we focused on MM.1S and NCI-H929 human cell lines given their contrasted ability to induce DAMP exposure.

As depicted in **Figure 4.45** the widely known PAMP, LPS, induced a strong phenotypic maturation of DCs as expected. Furthermore, both MM.1S and NCI-H929 treated cells prompted significant phenotypic maturation of DCs, as indicated by the elevated expression of maturation markers on DCs. Interestingly, although the drug combinations were significantly stronger in instigating DAMPs emission (**Figure 4.39**, **Figure 4.40** and **Figure 4.41**), the different drug treatments, including carfilzomib alone, were equally effective in promoting DCs phenotypic maturation. Excepting for the case of HLA-DR expression, LPS was considerably more potent in upregulating the expression of DCs maturation markers than chemotherapeutic drugs. Although expression of the co-stimulatory molecule CD86 was significantly enhanced upon incubation with MM-treated cells, its upregulation was quite modest when compared to LPS. As shown in the **Figure 4.45**, two different DCs:MM ratios were tested. Little to no difference was appreciated on the ability to improve DC maturation when increasing DC:MM ratios. This would suggest that increasing the density of MM-treated cells does

not necessarily correspond to enhanced immunogenic signalling that would translate into improved DC phenotypic maturation at least under these *in vitro* conditions.

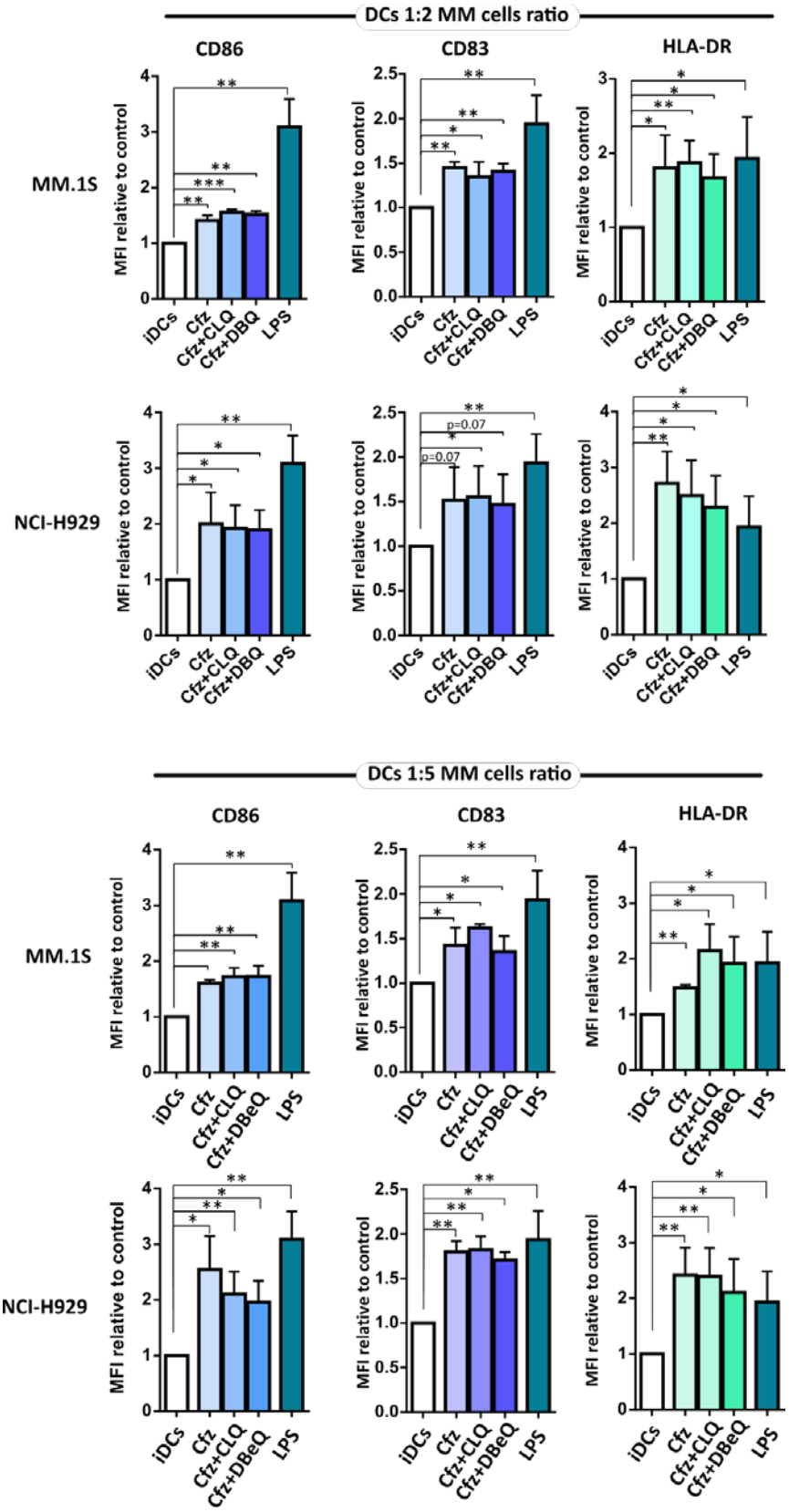

Figure 4.45 | DCs maturation assay with MM-treated cells. The capacity of drug-treated MM-death cancer cells to induce the maturation of monocyte-derived DCs was interrogated. DCs were differentiated for 1 week from monocytes isolated from human buffy coats as described in section 3.1.7. MM cells treated with the indicated chemotherapeutic drugs were washed and then incubated with immature DCs (iDCs) for additional 24 hours. The expression of CD86, CD83 and HLA-DR in the surface of $CD11c^+$ MM cell lines were analysed by flow cytometry and MFI values relative to control iDCs were plotted. Data are presented as mean ± SD from 3 independent experiments.

ICD-induced DAMP signalling can bring about immunostimulatory effects on immature DCs. CRT is able to bind to several receptors on DCs surface, including thrombospondin, complement component, C1q receptors, mannose-binding lectin and CD91/LRP1), favouring this way the phagocytic uptake of apoptotic cells[298]. Blocking this interaction or downregulation of CD91 receptors have been shown to reduce the immunogenicity of anthracycline and Hyp-HDT -based therapies *in vitro* and *in vivo*[219,317]. Likewise, soluble and membrane-bound Hsp70 and Hsp90 chaperones participate in DCs phenotypical maturation by binding to CD91 as well as to TLR2, TLR4 and lectin-type oxidized LDL receptor 1 (LOX-1)[227,317,747,754]. Moreover, ICD induced CRT, Hsp70 and Hsp90 exposure has been shown to increase CD80, CD86, CD83 and MHC-II maturation markers on DCs[247,257].

Furthermore, although we have not directly measured the presence of ATP in the extracellular space, but rather, assessed its intracellular decay, ATP secretion acts as a potent 'find me' signal prompting the chemotactic attraction of myeloid cells including DCs. Probably this mechanism may seem insignificant on an *in vitro* setting, but it is of utmost importance to effectively attract APCs into the intra- and peri-tumoral areas[298]. In fact, inhibition of ATP secretion blunted *in vivo* anticancer immune responses[263]. ATP binding to P2Y2 and P2X7 purinergic receptors results in the activation of NLRP3 inflammasome and the ensuing pro-inflammatory cytokine production, which is crucial for generation of IL-17 producing γδ T cells and production of INF-γ by CTLs[262,283].

Noteworthy, DCs maturation is modulated by the type and spatiotemporal demarcation of danger/stress signals. Thereby, the confluency of all of these signals will delineate the quality and quantity of costimulation provided by DCs and thus have the authority to define the outcome of T cell immunity and the subsequent anticancer immune responses. These reasons may explain the differences between LPS and the danger signals emanated from MM-treated cells.

Taken together, we have shown the capacity of carfilzomib and its drug combinations with CLQ or DBeQ not only to instigate danger signalling, but also to promote upregulation of maturation markers on DCs *in vitro*.

4.4. Immunogenicity of Cell Death *In Vivo.*

4.4.1. Establishment of the MOPC315.BM Orthotopic MM Mouse Model.

For many years the role of the Immune System in cancer prevention and treatment has probably not received all the awareness it should deserve. This situation has been encouraged by the massive usage of immunodeficient mice to test the efficacy of new treatments which has precluded from exploring the impact of these therapies over anticancer immune responses[227]. Thereby, to properly assess therapy-driven anticancer immune responses, immunocompetent mouse cancer models are mandatory[762].

Different syngeneic or spontaneously occurring MM mouse models have been developed so far. They have provided valuable data in the preclinical assessment of (immuno)therapies in the context of MM disease[763]. Recently, various **genetically engineered mouse models** (GEMMs) have been generated. These models are based in the transgenic expression of different mutated MM relevant oncogenes or tumour suppressor genes in the B-cell lineage[764]. Among these models we can highlight Myc/$BclX_{L,}$ vk-Myc, Eμ-Xbp1 and Eμ-MAF transgenic mice. These models usually develop BM plasma cell tumours, although tumour growth could also be restricted to other haematopoietic organs (liver and spleen in mice), paraprotein secretion and osteolytic lesions[765,766]. Usually, double transgenic mouse models, offer a more representative MM-like disease and an earlier tumour onset compared to single-transgenic mice, which usually develop plasmacytomas and lymphomas[765]. Utilization of these tools entails some difficulties and are considered expensive, labour-intensive and time-consuming, limiting their use thus far[764,766].

The **5TMM-related models** have been widely used. These models are derived from cells isolated from aged C57BL/KaLwRij mice, in which a small population of mice, spontaneously develop a disease that bears resemblance to MM[767]. 5T2MM and 5T33MM isolated cell lines, do not grow *in vitro*, but can be propagated *in vivo* by transplanting them into younger healthy recipients[763,767,768]. 5T2MM model could be considered an early-disease model due to its slow progression rate[766,769]. 5T33MM model is a more aggressive one and is more representative of advance/relapse stages of the disease[766]. Additionally, an *in vitro* variant (5T33MMvt) has been generated in this model[770]. Unlike, the 5T2MM model which produces a pronounced bone disease, 5T33MM is characterised by generating more diffused lesions harder to be measured. Additionally, the 5TGM1 subclone (derived also from 5T33MM cell line), has been also adapted for *in vitro* maintenance and intravenous injection of these cells can give rise to a pronounced osteolytic MM disease compared to its predecessor[771,772]. 5TGM1 offers a good alternative in terms of cost-effectiveness to 5T2MM and 5T33MM models[766,768]. In general, these models closely reproduce MM disease based on the ability of myeloma cells to localized in the BM, osteolytic lesions and secretion M-protein[767]. 5TMM-series models have been extensively used for studying pathophysiological aspects of MM disease, the interaction

MM-BM microenvironment interaction, homing mechanisms and for testing *in vivo* effectiveness of anti-myeloma agents[766,768,769]. One of the major drawbacks of these models is the dependency on the use of the exclusive C57BL/KaLwRij mouse strain, of limited availability and with a particular genetic background that may limit the human targets for specific compounds[526,773].

Induced models of MM can be generated by injection of mineral oil derivatives (like pristine), adjuvants and alkanes in the peritoneal cavity of Balb/c mice[774]. These **mineral-oil induced plasmacytomas** (MOPC) can be serially transplanted into other mice pre-conditioned with pristine[768]. MOPC315 and cell lines with similar characteristics (J558, HOPC, etc) were isolated from these plasmacytoma-like tumours. One of the main limitations of these models is that cancer cells grow quite localized at the subcutaneous and peritoneal region and only rarely at late disease stages, mobilize to the BM[775,776]. Additionally, MM is characterized by the production and secretion of unique clone-specific immunoglobulin, referred as the 'idiotype'[777]. This model differs from human MM cells in that they mostly secrete IgA rather than class-G Igs[765]. Considering the constraints presented above, MOPC-derived models do not faithfully replicate human disease and hence, are not contemplated as good MM models[765,768]. Nonetheless, this model has been used in studies of the role of IL-6 in MM pathogenesis, gene expression profile of PCs during tumour progression and in the study of oncogenic rearrangements of *c-myc*. Furthermore, several experimental therapies tested in this model have proven to be effective in evaluating tumour growth rejection and to predict human therapeutic success[765,768]. Additionally, given the immune competence of this model, cancer-immune system interactions can also be studied[763,765].

Recently, the restricted anatomical localization and reduced BM dissemination of these MM MOPC-derived tumours has been fruitfully circumvented by Hofgaard *et al.*[526]. In this study, authors selected a novel stable *in vivo* variant, MOPC315.BM. This cell line has the ability to grow *in vitro*, secrete M315 paraprotein, display tropism for the BM, as well as for other murine haematopoietic organs (spleen, and rarely in the liver) and produce measurable osteolytic lesions[526] when injected intravenously (i.v.)[526]. This was accomplished by serial i.v. injections of MOPC315.4 derived cell line into Balb/c mice. After the i.v. injection tumour cells were flushed from the BM and were recovered from femurs of those mice that developed paraplegia[526]. A total of 9 passages were repeated serially to obtain MOPC315.BM cell line[526]. When MOPC315.BM cells were challenged in parallel with the parental cell lines (MOPC315.4 and MOPC315), the BM-selected variant demonstrated to be far more aggressive and tumorigenic[526]. MOPC315.BM cells displayed faster augmentation of M315 myeloma protein serum levels and increased frequencies and rapid development of paraplegia than its predecessors[526]. Like the 5TGM1 MM model, MOPC315.BM cells can be cultivated *in vitro* and cause MM-like disease upon i.v. injection[526]. One of the advantages of this new model is its ability to reproducibly develop MM-like disease in the common Balb/c murine strain compared with the less frequent C57BL/KaLwRij of 5TGM1 model[526].

For these reasons, we decided to use this novel orthotopic MM mouse model in our study to test the ability of anti-myeloma drugs and its combinations to induce *bona-fide* ICD in prophylactic vaccination experiments. First of all, we characterized and reproduced the model described by Hofgaard and colleagues[526] to set up the conditions, timing, as well as the signs and symptoms to properly monitor disease evolution in posterior experiments. As previously described and as the following illustration manifests, the protocol for establishment of MOPC315.BM MM mouse model is indicated as follows (**Figure 4.46**).

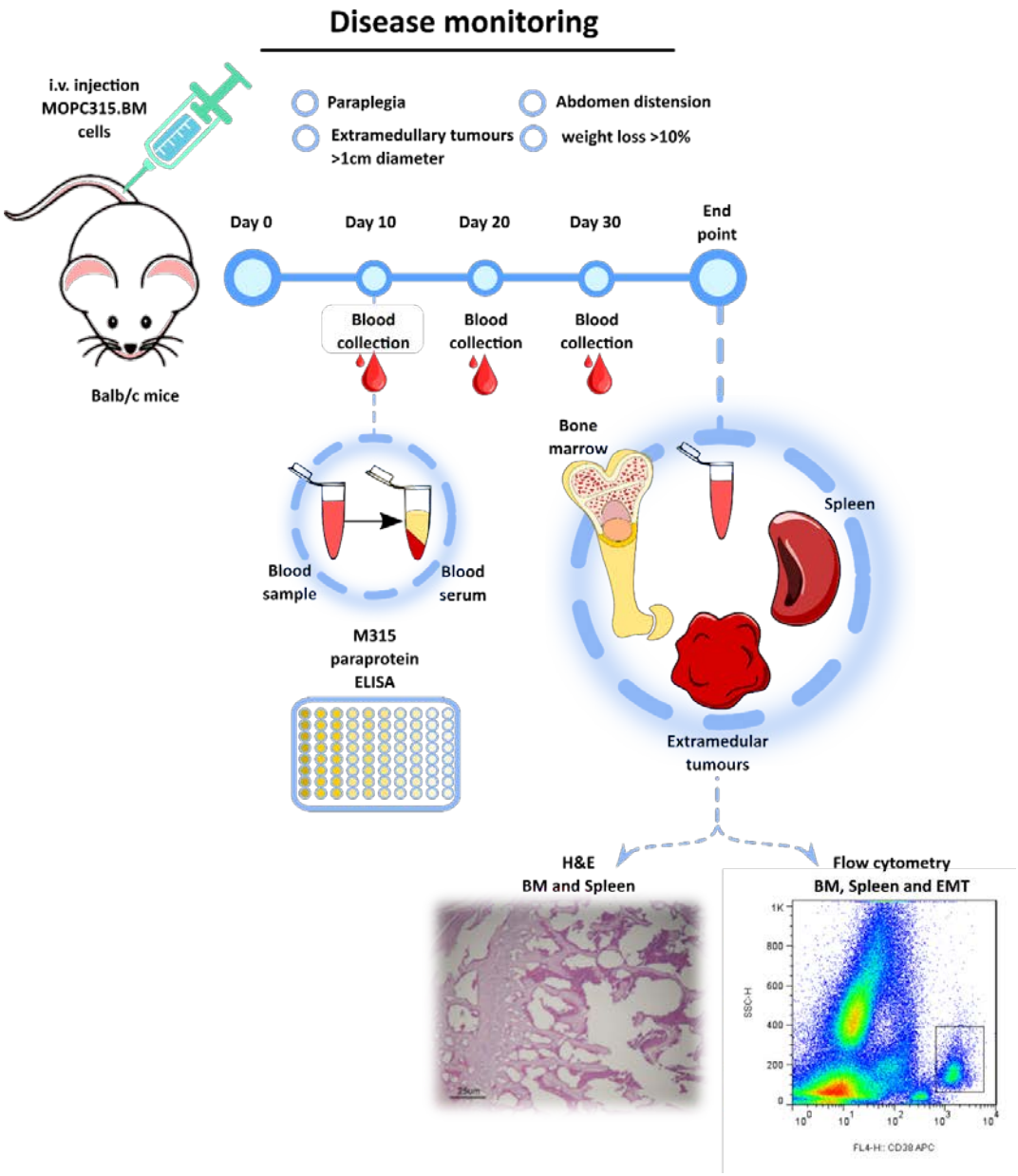

Figure 4.46 | Establishment of orthotopic MM mouse model and disease monitoring. Balb/c mice were intravenously (i.v.) injected with $5x10^5$ MOPC315.BM wt cells and MM disease was monitored by analysing several parameters. Every 2 to 3 days major or endpoint signs of the disease were analysed (paraplegia, abdominal distension, weight loss >10% and extramedullary tumour >1cm). To evaluate M315 protein secretion, blood samples were collected as described in section 3.8.2. Upon humane endpoint

application, femur/tibiae from posterior limbs, the spleen and if present extramedullary tumours were collected for further processing. In femur/tibiae and spleens part of the sample were utilize for histological examination and the other part for analysing MM infiltration in these organs by flow cytometry.

Balb/c male and female mice were i.v. injected with $5x10^5$ MOPC315.BM cells and disease evolution was monitored. Every 2-3 days, mice status was evaluated for endpoint signs: 1) paraplegia, 2) visible extramedullary growth >1cm in diameter, 3) distended abdomens, or 4) weight loss >10%[526]. As **Figure 4.47** shows, no significant changes in total weight were appreciated between control and inoculated mice along the duration of the experiment. Additionally, every 10 days, blood samples were collected from maxillary vein for assessment of M315 secretion as described in section 3.8.2[526]. Results showed that M315 levels progressively and rapidly increased over time. After 10 days of cell's inoculation, M315 serum levels augmented by 10-fold and reached the µg/ml range after 30 days of disease evolution. When endpoint was reached, mice were euthanized and tibiae/femur, spleen and extramedullary tumours (EMT), if present, were prepared and processed for flow cytometry analysis or alternatively, for histological examination as described in section 3.11.

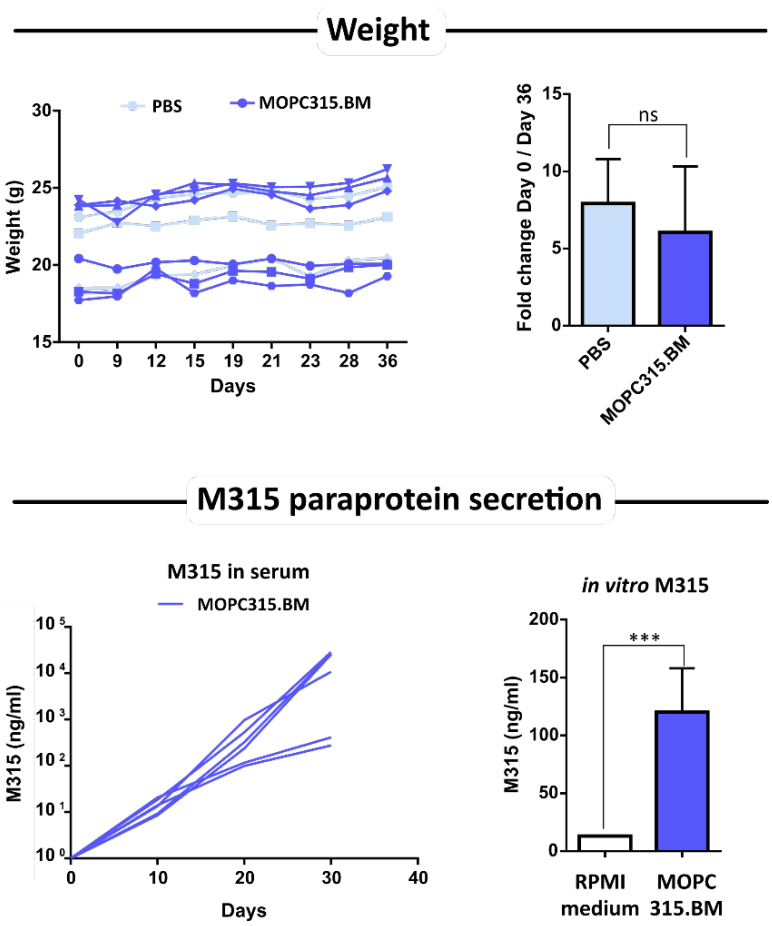

Figure 4.47 Weight analysis and secretion of M315 protein in MOPC315.BM MM mouse model. A. Mice were weighted every 3 to 5 days to monitor weight loss. Individual values of mouse weights are plotted. Lastly, the mean weight fold change between day 0 and day 36 (when humane endpoint was started to be applied) were compared between control group and mice injected with MOPC315.BM cells. **B.** M315 paraprotein was measured by ELISA in blood serum from mice injected with MOPC315.BM cells. *In vitro* production of M315 protein was also analysed by culturing *in vitro* MOPC315.BM cells at 10^7 cells/ml for 4h and measuring M315 protein by ELISA in cell supernatant. Statistical analysis was performed by using two-tail t test, where *p<0.05, **p<0.01, ***p<0.001, ns, non-significant.

As depicted in the histological examinations presented above, H&E sections showed a reduced cellular density in the proximal epiphysis of the femur from MOPC315.BM inoculated mice with increased acellular space between bone trabeculae. These observations reproduce the bone remodelling and osteolytic lesions that occurred during bone disease[778]. Nonetheless, despite the fact that it has been previously described that MOPC315.BM tumours could penetrate cortical bone[526], it was difficult to detect presence of MOPC315.BM cells within BM in H&E examinations of paraplegic mice. Fortunately, we could measure the presence of MOPC315.BM wt cells in BM by flow cytometry analysis using a CD138 specific antibody. As previously described, MOPC315.BM cells also showed tropism for the spleen[526]. In fact, MOPC315.BM mice usually developed splenomegaly as a consequence. Spleen histological sections revealed that tissue architecture was completely compromised. The characteristic nodular structure of the white pulp was clearly disrupted. Additionally, white pulp area was severely diminished and red pulp area was noticeably augmented. Although the red pulp functions as a blood filter removing foreign material and damaged/aged erythrocytes, in rodents it is also a place where extramedullary haematopoiesis occurs[779]. This fact may coincide with the observation of the increased red pulp present in MOPC315.BM mice. Furthermore, MOPC315.BM cells clearly invaded and were easily detected in spleen of injected mice as illustrated with arrowheads in **Figure 4.48**.

At the present moment, there is no perfect or ideal model that can recapitulate all aspects of human MM disease. Each model poses different advantages and drawbacks that should be balanced to choose the adequate model that addresses the specific research needs[763].

GEMMs are good models because they usually reproduce anatomic location and hold specific mutations and oncogenic drivers harboured in human disease[762,780]. However, they are technically difficult to handle, require a high number of mice colonies, bear long latency periods to develop overt disease and usually display low mutational burden and reduced genetic mosaicism, making GEMMs costly and time-consuming[526,780]. Moreover, when studying immunological responses in GEMMs, an important consideration has to be taken into account. Since all tissue-specific cells express the transgene and hence, all cells are simultaneously affected by the same mutation(s), GEMMs may saturate the Immune System given the number of genetically-identical transformations that take place with a relatively reduced mutational pressure (compared with carcinogen-induced oncogenesis)[762]. In fact, Erbb2-induced breast cancer model did not reveal apparent anticancer immunological responses in response to chemotherapy[781].

In contrast, mouse models based on the subcutaneous or orthotopic implantation of syngeneic tumour cell lines, they usually develop the disease at an increased rate, are easily reproducible and can be assayed for high-throughput[780]. The most recent variants of 5TMM and MOPC315-based models (5TGM1 and MOPC315.BM, respectively), share common features that make them suitable candidates for our purposes to study therapy-

MM-immune system interactions. Both models can be propagated *in vitro*, have short latency periods, secrete MM paraprotein, have tropism for the BM (and other murine hematopoietic organs), cause bone disease with measurable osteolytic lesions and both can be utilized in immunocompetent mice to study the role of the Immune System in anticancer therapies.

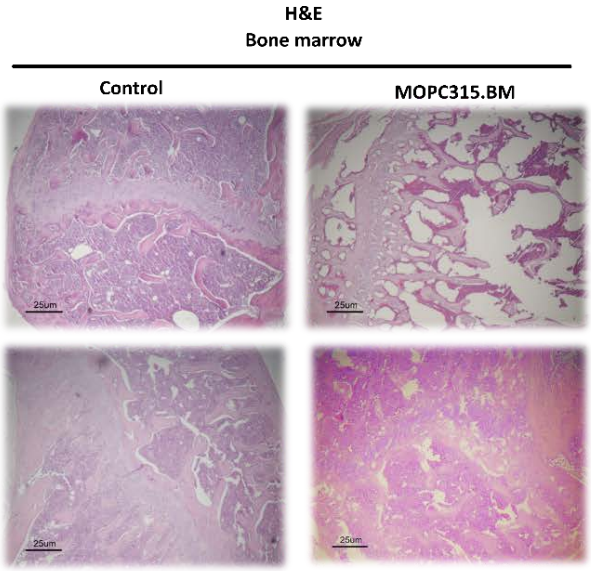

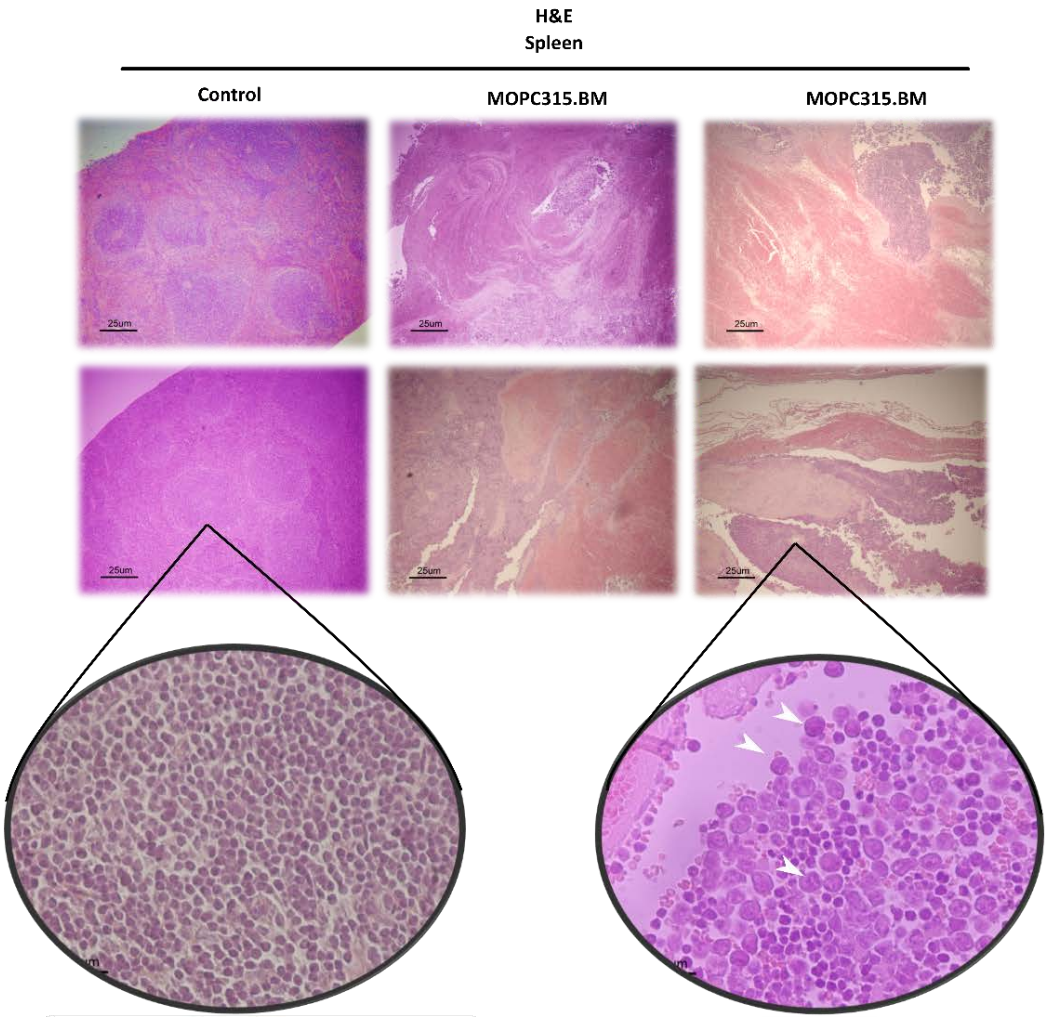

Figure 4.48 | Histological examination of BM and spleen. BM and spleen from control and MOPC315.BM-injected mice were processed for Hematoxylin-Eosin staining and examined under light of an optic microscope. Images were acquired using 4x objectives to see the global architecture of the different histological specimens. To determine the infiltration of MOPC315.BM cells, 40x objectives were utilized. Arrowheads point to MM cells within the affected tissues. Scale= 25 μm.

Nonetheless, although these models are derived and emerged from spontaneous evolution or carcinogen-induced cancers, for proper stabilization and reproducibility of research, single-clonal murine cell lines were generated[526,766]. Thereby, the genetic heterogeneity characteristic of spontaneous or chemically-induced tumours, which is also representative in human MM, is probably lost at some extent. The main differences that may arise between these two models are essentially the isotype of Ig (class type) they secrete (IgA in MOPC315.BM vs IgG2aκ in 5TGM1) and the mouse strain[526,766]. Probably, the C57BL/KaLwRij less common mouse strain makes it less suitable than the more routine and ready to use Balb/c mice. Furthermore, the white fur of Balb/c strain allow to reach greater sensitivities during *in vivo* imaging compared to other strains with darker fur like C57BL/KaLwRij mice[526]. Thereby, given the novelty of MOPC315.BM mouse model and all the aforementioned characteristics we decided to use it to fulfil our scientific demands.

Collectively, with these results we have shown that MOPC315.BM MM mouse model could be easily reproduced and faithfully recapitulate MM-like disease with secretion of M315 paraprotein and with affectation of BM and spleen of involved mice. Moreover, we believe that this model may meet the requirements demanded and suit our research needs.

4.4.2. MOPC315.BM-Luc and BLI Imaging.

To improve our ability to monitor disease progression we next decided to generate a luciferase expressing MOPC315.BM cell line variant. Although serum M315 levels provide indirect information about the tumour burden, do not inform about tumour localization and dissemination patterns. Furthermore, endpoint histological examination and flow cytometry analysis could provide vast amounts of information regarding the phenotype, population frequencies, localization, as well as global architecture and tissue morphology. However, these tools lack the dynamicity of real-time *in vivo* imaging and can only procure data at a given time point. For these reasons we generated MOPC315.BM-Zsgreen-Luc2P$^+$ cell line (MOPC315.BM-Luc$^+$ for now on), by transducing Zsgreen-Luc2P expressing lentiviral vector, into MOPC315.BM wt cells, as described in section 3.12.10.3. This allowed us to perform non-invasive *in vivo* imaging of affected mice and obtain real-time readouts of localization and tumour burden over time.

We then tested the ability of these cells to form tumours and reproduce MM-like disease as the parental cells. As illustrated in **Figure 4.49**, the protocol followed was equivalent to the one used in the previous section with the addition of bioluminescent imaging (BLI) acquisitions with an IVIS lumina imaging system every 10 days.

Bioluminescent imaging (BLI) benefits from improved sensitivity due to high signal-to-noise ratios given its practical lack of unspecific background signal[782]. Then, MOPC315.BM-Luc$^+$ cells were injected i.v. into Balb/c recipients. As shown in **Figure 4.49**, after 10 days of injection, MM foci were discrete but readily visible in spleen and in limbs of some animals. At day 20, light-emitting foci already present at day 10 were expanded with little or no additional dissemination observed. After 30 days of cell inoculation, disease was more spread and novel tumour foci appeared. Most frequently, the localization of the disease seemed to correlate with the anatomical position of spleen, femur, skull, vertebrae, sternum and other parts of the skeleton. At day 40, disease was clearly disseminated and tumour burden was considerably high in most of the animals. This data shows that homing preferences of these cells cover the different niches of the hematopoietic compartment as previously described[778]

Altogether these results show the suitability of MOPC315.BM-Luc$^+$ tumour model for facilitating non-invasive *in vivo* disease monitoring, making possible the assessment of tumour burden and localization in an easy and semi-quantitative manner. Furthermore, since mice start with a complete and unmanipulated Immune System, this model will be useful to gain insight in the role of the Immune System in the therapy response in MM disease. Additionally, this model could also be used to test the immunogenic capacity of chemotherapeutics in prophylactic vaccination experiments.

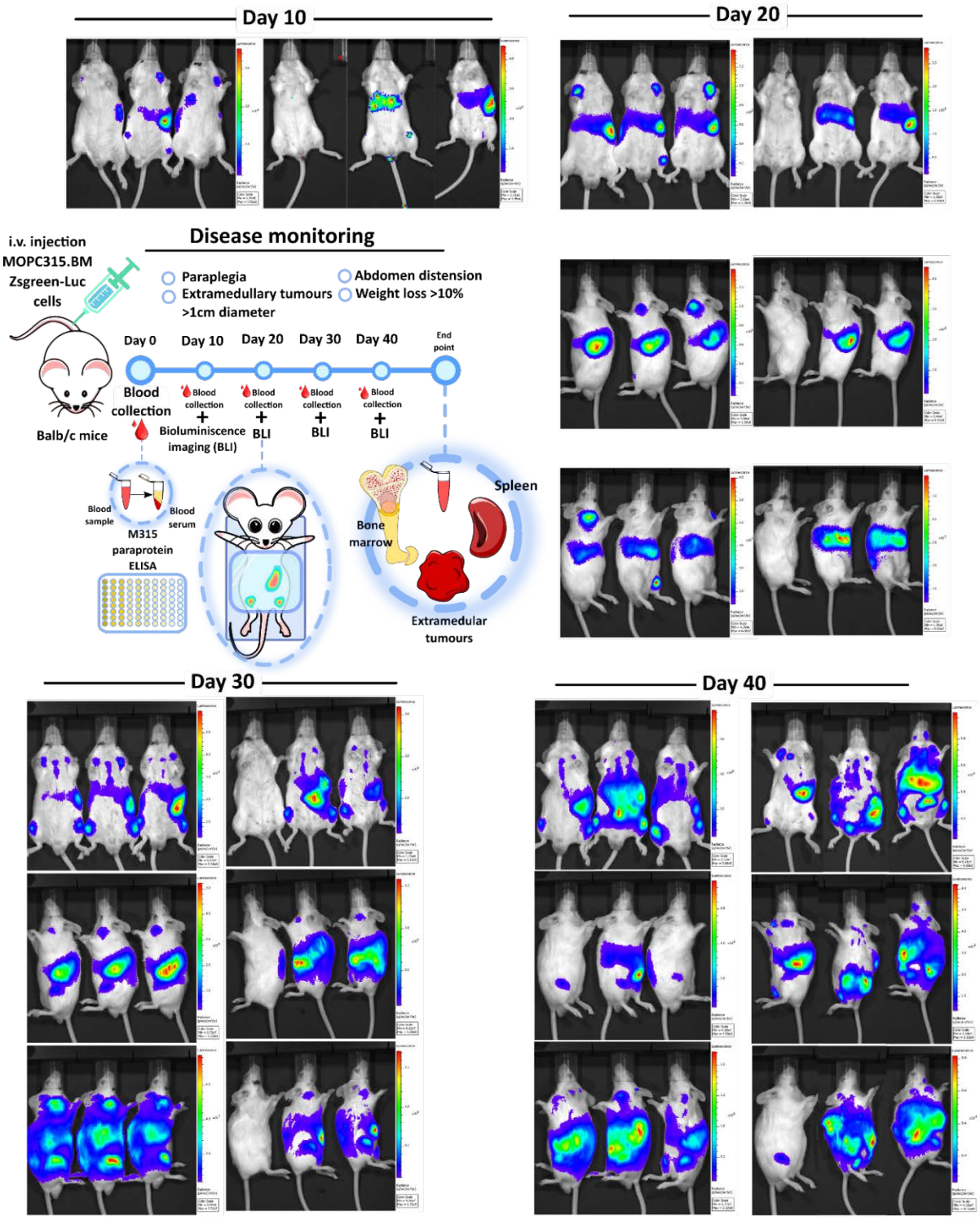

Figure 4.49 | Disease monitoring with bioluminescence imaging (BLI). MOPC315.BM-Luc^{+} cells were generated by transducing lentiviral plasmid encoding Zsgreen-Luc2P construct into MOPC315.BM WT cells as described in section 3.12.10.3. To determine the feasibility of disease monitoring using BLI and to check that no major changes have been produced in the MOPC315.BM mouse model, Balb/c mice were intravenously (i.v.) injected with 5x10^{5} MOPC315.BM-Luc^{+} cells and MM disease was monitored by analysing several parameters. Every 2 to 3 days major or endpoint signs of the disease were analysed (paraplegia, abdominal distension, weight loss >10% and extramedullary tumour >1cm). To evaluate M315 protein secretion, blood samples were collected as described in section 3.8.2. Additionally, every ten days, *in vivo* luciferase activity was analysed with IVIS lumina imaging system as described in section 3.8.3. Upon humane endpoint application, femur/tibiae from posterior limbs, the spleen and if present extramedullary

tumours were collected for further processing. In femur/tibiae and spleens part of the sample were utilize for histological examination and the other part for analysing MM infiltration in these organs by flow cytometry.

4.4.3. Prophylactic Vaccination with Drug-treated Myeloma Cells.

Classically, conventional chemotherapy has been thought to reduce tumour burden by directly killing cancer cells. However, it is becoming more apparent that the clinical effect of chemotherapeutics also depends on off-target effects, especially on the Immune System and its ability to reinstate cancer immunesurveillance[302]. In this work, we have previously shown the ability of carfilzomib and combinatory regimens to induce important hallmarks of ICD *in vitro*, like the ectopic exposure of CRT, Hsp70 and other ER chaperones, as well as intracellular depletion of vesicular ATP, probably indicating the secretion of this molecule to the extracellular space. Furthermore, we have also revealed the ability of MM-treated cells to increase the expression of maturation markers on DCs *in vitro*. All these results point towards the fact that PI-based combinatory treatments could induce ICD in MM cells. However, to validate these results, the gold-standard approach to measure ICD induction *in vivo* relies on the vaccination rechallenge[783]. This procedure requires *in vitro* treatment of cancer cells with the putative ICD inducers that are then injected subcutaneously (s.c.) into immunocompetent mice. After 1 week to let the Immune System develop an adequate response, mice are rechallenged with living cancer cells of the same type in the opposite flank of vaccinated mice. Then, absence of tumour growth is considered a sign of an active immune response against the tumour[783].

In MM disease, myeloma cells are imbued in the enriched BM microenvironment, which plays a vital role in disease development and progression[784]. The interplay between MM cells and the hematopoietic compartment is critical to facilitate MM cells to thrive. For this reason, rather than validating the ICD inducing capacity following the gold-standard approach, we decided to go a step further and evaluate immunogenicity of MM cell death probably in a more challenging, yet more realistic scenario. Instead of vaccinating mice and subsequently injecting live cancer cells subcutaneously and grow ectopically in a 'non-natural' microenvironment, we aimed to evaluate prophylactic vaccination in the orthotopic MM mouse model. This way, although MM cells can also grow extramedullary in human disease, the tumour microenvironment that murine MM and immune cells face in the experimental conditions is closer to the real situation. We followed then the protocol depicted in **Figure 4.50** and further explained in section 3.9. First Balb/c mice, were vaccinated once a week for a total of 2 week period with MM-treated cells with the indicated drug treatments s.c., in the interescapular region, into the loose skin located in caudal position to the neck. The decision of immunizing mice twice was based in the work performed by Paula Jaime-Sanchez and co-workers[785]. Vaccinations were performed with MOPC315.BM wt cells instead of MOPC315.BM-Luc$^+$

cells. We deemed this important since luciferase has been reported to be immunogenic in several immunocompetent mouse models, and hence has the potential to evoke host immune responses against syngeneic cells[786]. Therefore, this potentially would mitigate its value on immunological studies[787]. Nonetheless, the real repercussions and utility on tumour immunology and whether luciferase expression affects tumour cell growth *in vivo* is still questionable[787,788].

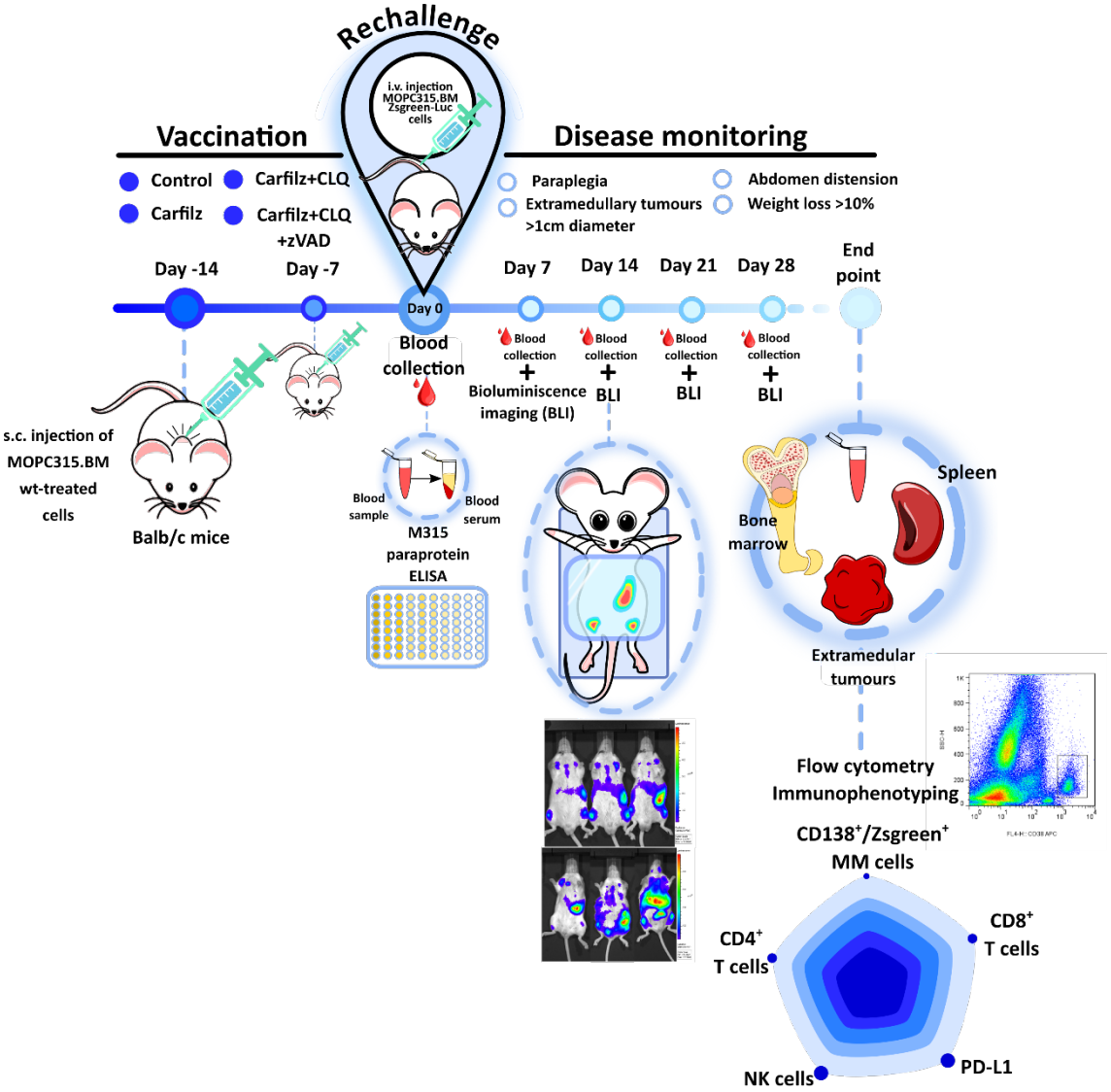

Figure 4.50 | Protocol for prophylactic vaccination of mice with drug-treated MM cells. To test the immunogenicity of cell death exerted by chemotherapeutic drugs, mice were vaccinated with *in vitro* drug-treated MOPC315.BM wt cells. MOPC315.BM wt cells were treated for 24 hours with carfilzomib at 100 nM when administered alone or with carfilzomib 50 nM + CLQ 25 μM in the drug combination. When utilized, pancaspase inhibitor z-VAD-fmk was incubated at 30 μM, 1 hour before of the addition of the aforementioned drugs. Cells were collected, thoroughly washed with PBS and resuspended in RPMI to be prepared for administration. Female Balb/c mice were subcutaneously (s.c.) vaccinated with $2.5x10^6$ drug-treated MOPC315.BM wt cells resuspended in 200 μl of RPMI medium, for 2 times with an elapse time of 1 week between inoculations. Control mice were inoculated s.c. with the same amount of RPMI 1640 medium. After 7 days from the second vaccination, mice were rechallenged by intravenously (i.v.) injecting $5x10^5$ live

MOPC315.BM-Luc$^+$ cells on the different experimental groups of mice. MM disease was monitored by analysing several parameters. Every 2 to 3 days major or endpoint signs of the disease were analysed (paraplegia, abdominal distension, weight loss >10% and extramedullary tumour >1cm). To evaluate M315 protein secretion, blood samples were collected as described in section 3.8.2. MM tumour load was also examined by bioluminescent imaging (BLI) as described in section 3.8.3. Upon humane endpoint application, femur/tibiae from posterior limbs, the spleen and if present extramedullary tumours (EMTs) were collected for further processing. BM, spleens and EMTs were immunophenotyped to analyse infiltration and PD-L1 expression of MOPC315.BM cells in the different affected organs and also to evaluate the frequencies of CD4$^+$ T cells, CD8$^+$ T cells and NK cells as described in section 3.4.1.1.3.

In the MOPC315.BM model, Hofgaard *et al.* reported that the luciferase-expressing cells were considerably slower than wt cells in inducing disease development. Although we have not assessed tumorigenicity of wt and Luc$^+$ in parallel, we did notice that MOPC315.BM-Luc$^+$ model developed a bit slower. Nonetheless, no major tumour growth alterations in MOPC315.BM-Luc$^+$ cells were observed, and probably the low level of immunogenicity harboured by luciferase, resulted in slower tumour growth but was not sufficient to completely eliminate reporter-expressing cancer cells[526]. We opted finally to use wt cells in the vaccination setting, preventing this way any potential alteration or confounding elements that can interfere with the immunogenic capacity of drug treatment. After 7 days of the second immunization, mice were rechallenged by injecting i.v. MOPC315.BM-Luc$^+$ cells into vaccinated mice. Control (non-vaccinated) mice were inoculated with the same amount of RPMI medium. Thereafter, disease monitoring and tumour burden were assessed mainly by BLI and the endpoint signs, as previously indicated. When mice reached endpoint, BM, spleen and EMTs, if present, were collected and processed for further analysis (as described in section 3.11). In particular, we immunophenotyped these organs and determined the frequencies of different immune populations (CD4$^+$/CD8$^+$ T cells and NK cells), tumour burden and presence of MM cells (CD138$^+$/Zsgreen$^+$ cells) and the expression of immunosuppressive markers such as PD-L1 in the surface of MM cells by flow cytometry analysis.

Results from vaccination experiments showed low immune protection in the best case-scenario **(Figure 4.51)**. Survival curves of carfilzomib and carfilzomib+CLQ groups ran almost in parallel with the control group. Noteworthy, vaccination with carfilzomib treated cells, did manifest a small protection at early disease stages, but finally all mice were euthanized at the same time point as the control group. Only the group in which mice were vaccinated with MM cells treated with carfilzomib, CLQ and z-VAD-fmk, showed a low protection against a rechallenge with living MM cells, which almost reached statistical significance. BLI quantification rendered the same results. Carfilzomib and control group followed the same growth pattern, whereas carfilzomib+CLQ manifested even a slightly increased signal than control mice. However, although carfilzomib+CLQ+zVAD group showed an obvious tendency towards delayed tumour growth, differences were not deemed statistically significant.

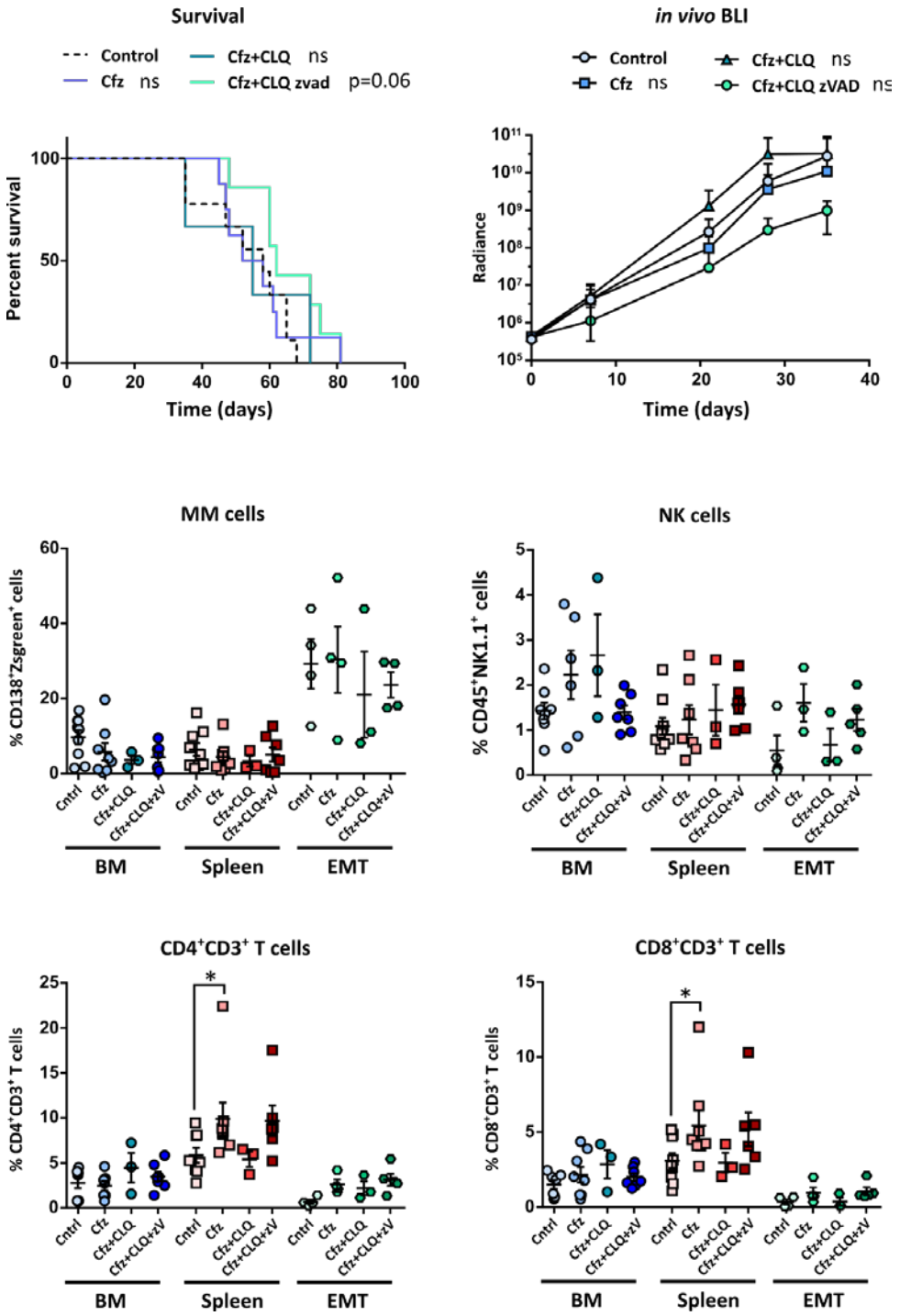

Figure 4.51 | Prophylactic vaccination of mice with drug-treated MM cells. The capacity of drug-treated MM cells to prophylactically vaccinated mice against a subsequent rechallenge with live cancer cells of the same type was examined. Female Balb/c mice were subcutaneously (s.c.) vaccinated with MM drug-treated formulations as indicated in Figure 4.50. MM disease was monitored by analysing several parameters. Every 2 to 3 days major or endpoint signs of the disease were analysed (paraplegia, abdominal distension, weight loss >10% and extramedullary tumour >1cm). Survival curves from the different experimental group of mice were generated. Statistical analysis was performed by comparing each of the experimental groups with control group using Mantel-Cox (Log-rank) test, where *p<0.05. **p<0.01, ***p<0.001, ns, non-significant. MM tumour load was also examined by bioluminescent imaging (BLI) as described in section 3.8.3. Graph corresponding to BLI imaging represents the mean radiance of each

experimental group of mice along the course of the disease. Statistical analysis was performed by comparing each of the experimental groups with control group using two-way ANOVA with Bonferroni correction for multiple comparison, where *p<0.05, **p<0.01, ***p<0.001, ns, non-significant. Upon humane endpoint application, femur/tibiae from posterior limbs, the spleen and if present extramedullary tumours (EMTs) were collected for further processing. BM, spleens and EMTs were immunophenotyped to analyse MOPC315.BM infiltration and immune cell frequencies of $CD4^+$ T cells, $CD8^+$ T cells and NK cells as described in section 3.4.1.1.3. Graph represents the percentage of cells expressing the indicated cell markers from the total population of cells. Statistical analysis was performed by comparing each of the experimental groups with control group using one-way ANOVA with Tukey post-test, where *p<0.05, **p<0.01, ***p<0.001, ns, non-significant. Experimental groups were composed of control mice (n=10), carfilzomib (n=8), carfilzomib+CLQ (n=3), carfilzomib+CLQ+zVAD (n=7) from 2 independent experiments.

Regarding the tumour load present in the different organs in which myeloma cells mainly make niche, the EMTs, as expected, were the ones that showed increased infiltration of MM cells compared to the BM and the spleen. Frequencies of MM infiltrated cells in spleen showed no differences between the different vaccination formulations. In BM and EMTs, there was a tendency of vaccinated groups to display a reduced infiltration of MM cells. Interestingly, the experimental groups in which mice were vaccinated with combinatory regimens (carfilzomib+CLQ and carfilzomib+CLQ+zVAD) manifested the lower tumour load in these two organs. However, all these differences did not reach statistical significance. Results from flow cytometry analysis of MM tumour burden, correlated with the delayed tumour growth observed with BLI imaging and the increased survival rates in carfilzomib+CLQ+zVAD group. However this was not the case in the combinatory regimens in which z-VAD-fmk was not utilized.

T cell and NK cell infiltration in BM, spleen and EMTs, were also inspected. Frequencies of $CD4^+$ and $CD8^+$ T cells in BM of vaccinated mice were barely enhanced compared to control mice, especially in the carfilzomib+CLQ+zVAD group. In the spleen and EMTs of mice vaccinated with carfilzomib- or carfilzomib+CLQ+zVAD-MM treated cells, infiltration of $CD4^+$ and $CD8^+$ T cells was also augmented. T cell expansion was not discernible in carfilzomib+CLQ group of mice. With regards to NK cell frequencies in the different MM homing compartments, BM NK cell population was increased in carfilzomib and carfilzomib+CLQ groups. However, we did not observed such NK cell expansion in carfilzomib+CLQ+zVAD vaccinated mice. Conversely, the spleen NK cell population only showed minor increments in the different vaccinated groups of mice. Finally, NK cell infiltration in EMTs was found to be enlarged only in mice vaccinated with carfilzomib- or carfilzomib+CLQ+zVAD-MM treated cells. As illustrated in the **Figure 4.51**, most of these differences in immune cell populations were in some cases fairly small and remained just as tendencies and did not reached statistical significance, perhaps as a consequence of the high dispersion of the data.

Altogether our data reveal that prophylactic vaccination with MM-treated cells do not offer important immune protection against a subsequent rechallenge with living MM cells of the same type.

As results illustrate, only in the group of mice vaccinated with MM cells treated with carfilzomib+CLQ+zVAD, a small protection and delayed tumour growth became apparent. Several explanations may fit these results. On one side, upon caspase inhibition alternative mechanisms of cell death could be induced. For example, necroptosis can be activated under apoptotic cell death instances when caspases are inhibited. Additionally, necroptosis but not accidental necrosis, has been shown to retain the immunostimulatory properties required in vaccination protocols[232,233]. Whether necroptosis is more immunostimulatory than immunogenic apoptosis is still a matter of debate. Nonetheless, it should be noted that our data revealed that when using necroptosis inhibitors in drug-induced cell death in MOPC315.BM cells *in vitro*, necroptosis did not showed up as a major cell death mechanism once caspase action was abrogated, at least at the time points evaluated (**Figure 4.24**).

Another possible explanation could be formulated as follows. By delaying cell death with caspase inhibitors, the integrity of cells and the intracellular DAMPs they emit, may be better preserved. Moreover, this way we are favouring and allowing cells to die *in vivo* rather than *in vitro*, where secondary necrosis may occur. Secondary necrosis would compromise cell's membrane expelling all the intracellular content to the culture medium, hence losing all or at least part of the immunostimulatory signals when cell pellet is rinsed before being injected into mice. Thereby, under these circumstances most of the immunogenic signals would be lost and hence the immunogenic potential of the vaccine would vanish.

Usually, in vaccination experiments with dying cancer cells, vaccination is performed when at least 50-70% (and sometimes even less) of cells are death[87,88]. In that situation, an important fraction of tumour cells will die *in vivo* and and stressed or dying cells will release and expose all the immunostimulatory signals inside the mice. In the particular case of the MOPC315.BM model, it has demonstrated to be quite aggressive, adaptive and therapy-resistant. For instance, we counted with a quite reduced margin to reproduce this *in vivo* cell death conditions. In fact, during the optimization of this protocol, we observed that despite we managed to induce high level of cell death on MOPC315.BM cells (>90%), there was a small population of cells that resisted and thrived. When these drug-treated cells were injected into mice, this small population that resisted therapy, managed to progress and even develop overt tumours. In fact, vaccinated mice needed to be euthanized, before they actually reached any of the endpoints associated with the intravenous administration of live cells in the orthotopic disease model, because subcutaneous tumours developed faster. We then had to increase the chemotherapeutic dose to reach more than 97% of cell death, but without increasing the time of drug-incubation to prevent secondary necrosis to occur massively. Thereby, probably in these conditions, myeloma cells are not allowed to die *in vivo* and probably immunostimulatory signals are lost during the washing procedure.

Leaving behind the technical and/or experimental difficulties that may explain the weakness or absence of immune protection in our vaccination protocol, biological

and molecular considerations must also be taken into account for the success of immunotherapeutic approaches. To effectively mobilize and mount an active adaptive immune response, *bona fide* ICD should entail three essential elements: antigenicity, adjuvanticity and inflammation.

As regards to the **antigenicity** level, the mutational burden in cancer is far from being homogeneous. Each one of the different tumour types are characterized to have a determined mutational load[789,790]. In MM, although this type of neoplasm harbour an important degree of cytogenetic abnormalities, it is not considered to be between the top list of cancer types with high mutational burden[789]. Nonetheless, despite its low to intermediate neoantigen load, MM patients displaying an elevated mutational and neoantigen burden were associated with worse PFS rates after being treated with current standards of care[789]. Despite these negative connotations, one study showed the feasibility of neoantigen targeting immunotherapy in MM using primary MM samples[791]. In fact, various trials evaluating neoantigen vaccines are currently under development[792]. Moreover, different studies also manifested the existence of myeloma-specific T cells and the possibility to isolate them from BM of MM patients, even being able to be identify these cells in early disease stages[474,777,793]. Graft versus myeloma effect after allo-HSCT and responses to donor lymphocyte infusions could also be considered examples of the existence of a myeloma-specific, and hence antigen-directed immune response[463].

In murine models, the adoptive transfer of idiotype-specific T cells has been shown to be effective in 5TGM1 myeloma model[794]. Additionally, Bogen's laboratory also reported anti-myeloma immunity using transgenic T cells that recognize idiotype-derived from MOPC315 MM model[540]. In the vaccination setting, this type of approach has also been explored in human MM disease and murine models. For instance, MOPC315 model was the first to be utilized in the context of myeloma vaccination[795,796]. As described earlier, this model secretes M315 paraprotein (IgA). Prophylactic vaccination with this protein, provided immune protection against MOPC315 challenge[763,795]. Shortly after, discovery of a specific idiotype-derived peptide of M315 protein that was presented in the context of MHC class II molecules was reported[797]. Additionally, a specific transgenic mice expressing a TCR that recognized this Id-peptide was also generated[798]. In this transgenic mouse strain, rejection of MOPC315 tumours strictly relied on the expression of the paraprotein by injected myeloma cells[799].

Importantly, in MOPC315 model, central and peripheral tolerance towards M-protein have been reported to be induced when tumour burden, and hence M315 protein levels, exceeded a specific threshold[800,801]. This T cell exhaustion/anergy towards Id-protein upon overt disease, has also been noticed by others[763,802]. Although we did not used Id-protein vaccines but rather, used whole-tumour cell formulations, this response could have also occurred under our experimental conditions. In fact, mice were vaccinated twice with a relative high amount of MM-treated cells ($2.5x10^6$ cells/mice). It is possible then that by using this amount of cells, rather than incrementing the immunogenic potential of the vaccine, we rather favoured immune tolerance against

myeloma cells. Alternatively, MOPC315.BM model developed quite rapidly and could reach easily the myeloma tumour burden and T cell exhaustion threshold before immune protection could succeed and be detected.

Several studies have reported that vaccination with dying cancer cells increased the infiltration of T/NK cells in the tumour microenvironment, an indicative fact that an active anticancer immune response has been developed[87,803,804]. In line with this, one interesting point annotated by Ciampricotti *et al.* is that we don't know yet whether conventional chemotherapy foster anticancer immunosurveillance by activating a novel T cell repertoire, or just by refreshing a dormant pool of pre-existing memory T cells previously primed during carcinogenesis[781]. In the latter scenario, only when a pre-existing anticancer immune response would have developed, possibly indicated by the presence of infiltrating T cells on the tumour bed, chemotherapy could have the potential to reactivate it and had a real impact over disease control[781]. As shown, our data also manifested weak increments, in the majority of the cases, in the frequencies of T and NK cell populations in the different tumour niches. However, as noted, in some conditions like in carfilzomib and even carfilzomib+CLQ groups, increased T or NK cell infiltration did not correlate with the global effect on tumour growth. It is then possible that anti-myeloma immune response shifted from immunogenic to tolerant explaining both the weak T cell infiltration and the lack of anticancer immune protection.

In the clinical setting several vaccination strategies have been tried out, such as DC vaccines, vaccination with MM cells and adjuvants, vaccination with myeloma-derived proteins. Still, results are far from being successful. So far, current trials have demonstrated the feasibility and safety of these kind of approaches and patient's therapy responses were, in the best-case scenario, disease stabilization[463,777,805]. There are still many technical or experimental difficulties that should be optimized when developing an effective vaccination protocol[763].

When reviewing the **adjuvanticity** of anticancer immune responses, DAMP generation during regulated cell death programmes is critically required[731]. Several factors, such as the type of cell death, the ICD stimuli and the crosstalk between various cellular stress responses, impact on the type of danger signals produced during the course of cell death[241]. We have previously demonstrated the ability of carfilzomib and the respective drug combinations to induce the exposure of CRT and other molecular chaperones like Hsp70 and BiP, in the surface of MM cells, including those from the murine model. However, although it has been shown that CRT exposure usually correlates with the immunogenicity of cancer cell death, the emission of this DAMP alone is not sufficient to elicit anti-cancer immune responses[286].

Several independent studies have shown that at least, two or three additional danger signals are also required to mount active immune responses *in vivo*. These are ATP, HMGB1 and type I IFNs. Depletion or abrogation of the molecular pathways associated with the production/exposure of any of these different signals, prevented (*a*

priori) the immunogenicity of cell death and *in vivo* immune protection[216,806]. Emission of HMGB1 or the type I IFN response have not been evaluated in this study. Regarding ATP secretion, we have just indirectly assessed intracellular ATP depletion upon drug treatment. Despite these results, we cannot confirm that all the necessary DAMPs are exposed in response to treatment. Besides these classical danger signals, additional important DAMPs, like Annexin A1, and others, have been shown to participate in the context of ICD[216]. These supplementary danger signals could also be necessary to provoke a genuine anticancer immune response.

In DAMP classification, another distinction has recently been proposed: the existence of constitutive and inducible DAMPs (cDAMPs and iDAMPs respectively)[731]. Then, cDAMPs would be endogenous molecules present in healthy cells (ATP, HMGB1) that can be released upon (accidental) membrane rupture, for example under accidental necrosis[731]. However, this form of cell death has not been demonstrated to elicit *in vivo* immune responses[232,233]. Thereby, other type of stimuli should be provided to encompass an authentic form of immunogenic cell death[731]. In contrast, iDAMPs include a wide panel of molecules that are not present in healthy cells but are induced upon cell death conditions[731]. Among them we can highlight: type I IFNs, IL-6, IL-1, TNF-α[731]. Accordingly, these molecules have also been shown to be required to effectively stimulate innate and adaptive immune system[731,807]. Furthermore, it should be noted that not all the DAMPs exposed during cell death are immunostimulatory. In fact, there are some molecules that exhibit immunosuppressive properties and play important roles in cell death tolerance (Prostaglandin E2, adenosine, etc)[216,241]. This is something that is frequently overlooked, but could negatively contribute to immunoregulation. As noted, DAMP signalling and trafficking are deemed plastic in nature and therefore, the different signals emanated and the mechanisms involved, are stimulus and context dependent. Therefore, every ICD inducer, cancer model and experimental setting, should be defined attending at the whole picture[264].

Inflammation has been described as another important element for the success of ICD[731]. In fact, some DAMPs described to be exposed or emitted during ICD are classically considered to be pro-inflammatory molecules (type I IFNs, IL-6, IL-1, TNF-α). Many of these cytokines are part of the molecular response derived by NF-κB activation[731]. Noteworthy, the mechanism of action of proteasome inhibitors like bortezomib has been shown to hamper canonical NF-κB activity[660]. In contrast, other reports point to the opposite direction arguing in favour for a possible NF-κB induction upon bortezomib treatment[452]. This topic will require further enlightment to unveil the role of NF-κB in PI-based therapy response. In addition, activation of UPR pathways can also modulate immune response by impacting at several levels on cytokine production[378]. As previously reported during this work, carfilzomib is capable of bringing forth UPR signalling. Hence, it is tempting to speculate that by activating ER stress response, cytokine production pathways could also be engaged and would contribute to the immunogenicity of cell death.

To sum up, depending on the quality and interplay of the key triad of parameters governing ICD (antigenicity, adjuvanticity and inflammation), the prosperous dialog between these entities and the final immunogenic outcome will be determined[731].

At this point, another interesting question that deserves to be discussed is the role played by caspases in the immunogenicity of cell death. When talking about cell death, caspases are deemed not to be principal enactors of cell demise[731]. Rather, caspases can precipitate apoptosis occurrence by accelerating cellular dismantling, but are not strictly required for cell death to ultimately reach fruition[808]. These considerations may derive from the intricate dialogue that exists between the different cell death pathways, implying that abrogation of one specific pathway, does not offer complete protection, since complementary mechanisms could be activated[808808]. However, the idea that caspases are crucial for the way cell death is perceived by the Immune System is building up vigorously[731,808].

An increasing number of studies is revealing the ability of caspases to modulate signals originating from dying cells, thus influencing the subsequent immune responses[809]. However, this subject is still posing a lot of challenges and plenty of questions remain unanswered yet[731]. Early studies on CRT trafficking showed that caspases were required for anthracycline-driven immunogenicity[230,255]. However, independent mechanistic studies later manifested the intrinsic plasticity harboured by DAMP signalling pathways and in the immunological responses that follow. In particular, alternative pathways in which caspases were not essential for the immunogenicity of cancer cell death were also demonstrated[257].

Quite recently, using immunocompetent syngeneic murine models, it has been shown that *Casp3*$^{-/-}$ TSA tumours were more sensitive to radiotherapy than their caspase-proficient littermates[276]. Indeed, caspase-3-deficient cells treated *in vivo* with the combination of radiotherapy and a checkpoint blocker, were shown to be superior at generating systemic immune responses, responsible for controlling distant non-irradiated lesions (abscopal effect)[276,808]. Inhibition of caspase-3 activity genetically or by chemical inhibition using z-VAD-fmk, was shown to improve type I IFN secretion under these conditions[276]. This effect emanated from the delayed cellular break-down experienced by caspase-deficient cells, allowing for the accumulation of cytosolic DNA, hence promoting type I IFN response[276]. For instance, it has been shown that, double-stranded mitochondrial DNA, leaks out accumulating at the cytosol, when MOMP is triggered[277–279]. In turn, the nucleic acid sensor GMP-AMP synthase (cGAS) recognizes these molecules instigating type I IFN response[277,278]. In fact, activation of caspases has been shown to prevent these responses following MOMP[277,278]. These results would indicate that apoptotic caspases have an immunosuppressive role, and targeting them might have immunostimulatory consequences, boosting anticancer immunity, at least under these experimental conditions[279]. Additional immunosuppressive functions of caspases have also been reported. For example, caspase-3 has been shown to stimulate the secretion of prostaglandin E2 and lysophosphatidycholine, two immunosuppressive

molecules that dampen immune effector cell function and recruit phagocytes to remove cell debris in absence of inflammation, respectively[810,811]. In B16 melanoma model, z-VAD-fmk was found to improve anticancer immunosurveillance and to reduce tumour growth, when co-administered with different types of therapies[757]. This anticancer immune response was achieved by inducing necroptosis in melanoma cells, and was dependent on MyD88-signalling and on $CD8^+$ T cells[757].

We have previously shown that general caspase inhibition with z-VAD-fmk or caspase-8 inhibition with z-IETD-fmk, increased CRT exposure *in vitro* in MOPC315.BM cells. Moreover, when mice were vaccinated with cells treated with z-VAD-fmk, carfilzomib and CLQ, disease progression was weakly delayed. It is possible that by a yet unknown mechanism, caspases may hamper CRT exposure under these conditions. It seems possible, that by delaying cell disassembly, z-VAD-fmk, could favour in this way the accumulation of immunostimulatory signals, enhancing its immunogenic potential, as it occurred in the work of Rodriguiez-Ruiz *et al.*[276].The exact mechanism by which this ephemeral effect was brought about will require further investigation.

Finally, another important point that regards attention when studying the immunogenicity of cell death responses *in vivo*, is the host and the (micro)environmental cues in which the Immune System has to operate. In fact, emission of DAMPs from cancer cells might not be enough to evoke proper anticancer immune responses. Indeed, of such importance are also the underlying mechanisms involved in reception, transmission and response by immune cells to these danger signals.

Clearly, we cannot only circumscribe to ICD-related mechanisms. Leading with a disease with the level of complexity and adaptability such as cancer, additional aspects should be considered, such as the immunosuppressive nature of cancer. In the particular case of MM disease it can be distinguished by the presence of a general immune dysfunction that could disrupt immunosurveillance and the efficacy of immunotherapeutic approaches. In fact, several immune-escape mechanisms have been described in MM: Disruption of the T-cell and NK cell compartments, impaired DC function, production of pro-inflammatory cytokines that suppress immune activation and proliferation, increased expression of checkpoint inhibitory ligands that drives T-cell anergy and exhaustion and the recruitment of immunosuppressive populations that sculpt a permissive BM microenvironment[463,763,812].

Although we have not evaluated the majority of these parameters *in vivo*, during the course of MM disease, MOPC315.BM model has been shown to affect major hematopoietic organs. Compromised spleen red and white pulp and disruption of global spleen architecture may account for the reduced immune response observed in vaccinated mice. In the spleen as an important lymphoid organ, is one of the places where the systemic circulation is massively screened for antigens and pathogens, thus playing a vital role in antigen presentation[779]. In fact this is one of the places in the body where tissue-resident DCs migrate or alternatively, splenic macrophages and DCs capture

blood-borne antigens, to present them to circulating naïve or memory lymphocytes. Thereby, affectation of this important hematopoietic organ during the course of the disease, would probably impair anticancer immunosurveillance and therapy response. The BM, as in human MM disease, is also another niche colonized by MOPC315.BM cells. The BM, besides being a primary lymphoid organ and where haematopoiesis occurs, can also function as a secondary lymphoid organ and undergo extensive migration from blood of mature $CD4^+$ and $CD8^+$ T cells[813]. It is also a preferential hibernating/resting reservoir for maintenance of memory T cells[813–815]. In fact, after initial priming, T cells receive important signals from the tissue microenvironment that can influence critical immune response characteristics, including effector functions, recruitment and expansion in posterior antigen rechallenges[815]. Is for that reason that, although it may exist an initial anti-tumour response at early disease stages, MM cells will sabotage the available hematopoietic compartments once disease is established.

Besides the microenvironment cancer and immune cells may encounter during disease, within a broader integrative perspective, the host in which anticancer immunological reactions take place is also of particular importance. Despite all the invaluable contributions to the cancer-immune interface knowledge, a note of caution should be raised in the study of ICD inducers and the effect of chemotherapy on the immunogenicity of *in vivo* cancer models. Most studies have explored the immunogenicity of cell death *in vivo*, relying on transplanted syngeneic murine cancer cell lines. Under these experimental conditions, the genetic profile of transplanted cell lines cannot be considered equivalent to those of endogenously arising tumours models, and hence their antigenic landscape differs[816]. For instance, different results have been reported as regards to the implication of ICD and the adaptive immune response in the efficient tumour rejection driven by chemotherapy in spontaneously arising *in vivo* tumour models[781,816]. In particular, it has been reported that the adaptive immune system do not participate in the response brought forth by commonly documented ICD inducers in several independent spontaneous breast cancer models[781].

One possible underlying reason for this difference, could be attributed the constant immunoediting that spontaneously arising tumours are subdued[817,818]. This situation better reproduces the real difficulties encountered in human cancer disease with the co-evolving interplay between the tumour and the host Immune System. Similar conditions may arise in the novel MM mouse model we have utilized in this work[526]. As described earlier, this model have been obtained through subsequent rounds of intravenous injections of MOPC315.4 cells that have preferentially migrated, homed to the bone marrow and thrived[526]. Up to nine cycles of cell injections and posterior BM isolation were performed to obtain the MOPC315.BM cell line[526]. Thus, these cells are presumably thought to have undergone a considerable number of immunoediting cycles. Although we have found some degree of immune infiltration in the different tumour niches, differences were deemed statistically non-significant in the majority of the cases. The increased presence of immune cells in tumour niches could be interpreted as the

ability of immune cells to recognize the tumour. However, neither the infiltration nor the global immune protection was stronger enough to delay disease progression. Perhaps, during the selection of BM homing myeloma cells, it seems probable that a selection towards immune-evasive cells had also occurred. MOPC315.BM cells could have also acquired important tools to evade anticancer immunesurveillance. It would be useful to test a *bona fide* positive control that has the ability to elicit active immune responses against myeloma cells in this novel model.

Pioneering work from De Beck and colleagues, clearly showed evidences of the occurrence of ICD *in vivo* in the context of MM, in particular in the 5T33MM model[819]. In this work, authors showed the feasibility of eliciting protective anti-myeloma immune responses by vaccinating mice with immunogenic corpses from MM cells treated with different chemotherapeutics, including bortezomib, melphalan, mitoxantrone and HDAC inhibitors, among others[819]. However, this study also stresses the difficulties in achieving efficient immunizations in MM models, since the vaccination setting did not conferred 100% protection, but rather a delayed tumour growth[819]. This clearly contrasts with results observed in solid tumours such as the CT26 colon cancer model[219]. These differences in vaccination efficiency have been attributed by the authors to the presence of tolerogenic signals, like CD47 that would counteract CRT exposure, hence limiting its immunogenic capacity[819]. It seems feasible that such tolerogenic mechanisms may also be present in our model and may account for the reduced prophylactic protection observed so far.

Collectively, anticancer immune responses are complex in nature, besides the wide and varied range of participants that could make their appearance in this cellular process, the dynamic and evolving character of cancer cells further complicates and add more variables to predict the final outcome.

4.4.4. Role of PD-1/PD-L1 Axis on MM Anticancer Immune Responses.

In our search to achieve a successful induction of ICD and transform the 'cold' MM microenvironment into a 'warmer' place, knowing the cause of lack of immune activation in our MM model is decisive. A strategy that depends only on the instigation of ICD, would be insufficient to activate the Immune System if the tumour microenvironment is not permissive enough. The concept of ICD has usually been developed in tumour models in which adjuvanticity is solely dictated by DAMPS. This is a quite considerable simplified version of the phenomenon itself[216]. As mentioned earlier, MM disease endows an important impairment of immune function. One of the reasons behind this dysfunction is mediated by the upregulation of inhibitory checkpoint proteins like PD-1 by immune cells and PD-L1 by cancer cells. Given the importance of this mechanism for MM pathogenesis, we ought to elucidate whether the lack of immune protection after the prophylactic vaccination setup we observed in MOPC315.BM murine

model, was due to the immune impairment and evasion exerted by PD-1/PD-L1 immune checkpoint axis.

4.4.4.1. In Vitro and Ex Vivo PD-L1 Expression.

First, we evaluated *in vitro* expression levels of PD-L1 in MOPC315.BM cells. As illustrated in **Figure 4.52** MOPC315.BM wt and MOPC315.BM-Luc^{+} cells expressed PD-L1 *in vitro*. Moreover, in the vaccination assay, MM cells isolated especially from the BM or EMTs of mice vaccinated with carfilzomib+CLQ+zVAD MM-treated cells, displayed increased PD-L1 expression when assessed *ex vivo*. Similarly, MM cells from EMT in mice immunized with carfilzomib-treated cells, also exhibited enhanced PD-L1 expression. Differences in PD-L1 expression in MM cells from spleen were much lower and remained unchanged among the different experimental groups. It is worthy to mention that none of the above differences were deemed statistically significant, probably due to the high dispersion of some data.

We also questioned whether chemotherapy may have any effect over the expression levels of PD-L1. With that in mind, we evaluated *in vitro* surface expression of this ligand in the different human and murine MM cell lines available upon sub-lethal drug exposure by flow cytometry. Data revealed that MOPC315.BM and MM.1S cells increased the expression of the inhibitory checkpoint ligand when subjected to even low doses of the chemotherapeutics used so far. Carfilzomib treatment alone had only a minor effect over PD-L1 expression at the higher drug concentration in MOPC315.BM, whereas it did not provoke any apparent effect on ligand expression in MM.1S cell at the tested doses. The combination of carfilzomib and CLQ yielded a significant upregulation of PD-L1 surface levels when compared with carfilzomib alone at each corresponding concentration in MOPC315.BM cells. Similar results were displayed by MM.1S cells in which only a significant increase in PD-L1 were revealed when exposed to the higher drug concentrations. When attending at the results rendered by the combination of carfilzomib and DBeQ, data revealed a minor upregulation in MOPC315.BM cells, but a significant one in MM.1S cell line. Finally, regarding the results obtained in NCI-H929 and U266 cell lines, no major changes in PD-L1 expression were observed when these cells were subjected to the aforementioned drugs. These results would suggest that combination of these chemotherapeutics with checkpoint blockade therapy may have potential to succeed in MM.1S and MOPC315.BM cell lines.

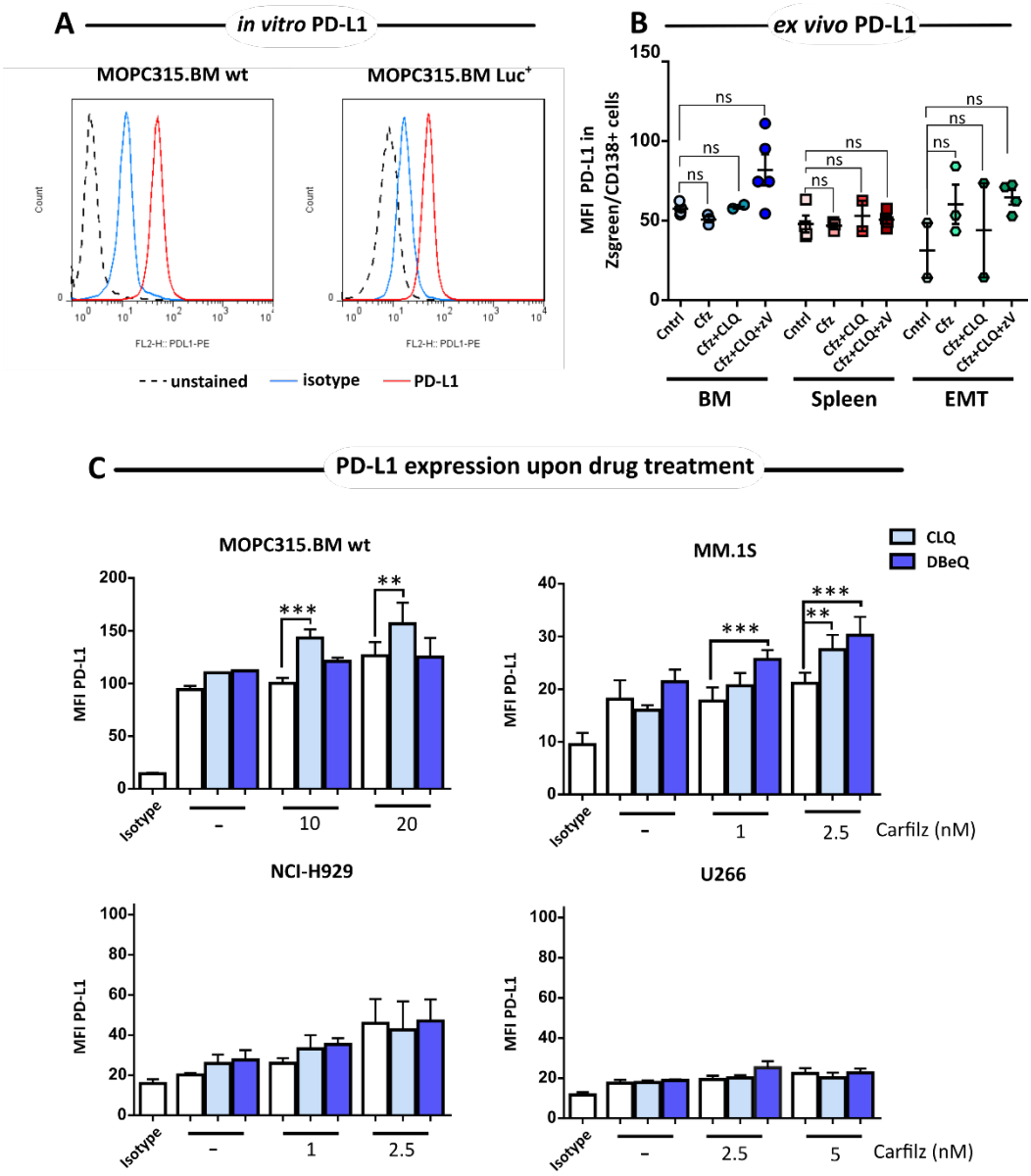

Figure 4.52 | PD-L1 basal expression *in vitro*, *ex vivo* and upon drug treatment. A. Basal PD-L1 expression analysis on MOPC315.BM wt and Luc$^+$ cells. Graph shows histograms from unstained cells or cells stained with isotype control or PD-L1 antibodies. **B.** Analysis of PD-L1 expression of MOPC315.BM-Luc$^+$ cells *ex vivo* in BM, spleen and EMT mouse samples. Graph represents mean fluorescence intensity (MFI) of PD-L1-derived fluorescence in CD138$^+$/ Zsgreen$^+$ cells. **C.** PD-L1 expression in different MM cell lines upon drug treatment. MM cell lines were subjected to the indicated drug treatments for 24 hours (CLQ 20μM and DBeQ 2.5 μM). After that time PD-L1 expression was analysed using a fluorochrome-conjugated specific antibody. Graph represents mean fluorescence intensity (MFI) of PD-L1-derived fluorescence from each cell population. Data represent the mean ± SD from n=3 independent experiments. Statistical analysis was performed by using one-way ANOVA with Tukey post-test, where *p<0.05, **p<0.01, ***p<0.001, ns, non-significant.

As indicated earlier, PD-1/PD-L1 axis is thought to play a vital role in MM pathogenesis[820]. PD-L1-expressing myeloma cells bind to PD-1-expressing tumour-infiltrating T cells and NK cells to dampen immune cell activation and function[440]. This immune checkpoint is then considered an adaptive immune repression mechanism that tumour cells exploit to escape the Immune System. It is noteworthy to point out that usually, PD-L1 and/or PD-1 expression takes place once an immune response has

previously been developed[440]. In MM patients, PD-L1 has been found to be upregulated when compared to plasma cells from healthy volunteers[463,812,820]. PD-L1 can also be overexpressed by DCs and macrophages from MM patients, further complicating the global scenario[812,821]. As regards to PD-1 expression, NK and T cells from MM patients have been shown to be upregulated being a sign of immune exhaustion[463,812,820]. The role of PD-1/PD-L1 axis in MM patients will be further discussed later in the text. Furthermore, this immune checkpoint has also been shown to mediate tumour-derived immunosuppression *in vivo* in several murine MM mouse models[822–824]. For example, in 5T33MM model, myeloma cells have also been reported to overexpress PD-L1, whereas PD-1 was also found to be upregulated on T cells in this model[822,825,826]. To our knowledge, no data regarding PD-L1 expression or checkpoint blockade therapy have been tested in MOPC315-derived models so far. Collectively, immune checkpoint blockade therapy might still represent a good therapeutic opportunity to reactivate the Immune System and fight myeloma disease.

We then conclude that MOPC315.BM cells express high amounts of PD-L1 at basal levels. In fact, *ex vivo* PD-L1 assessment indicated that ligand levels tended to be higher especially at those conditions in which immunization were more effective. Thereby, immune checkpoint inhibitors could stand as a potential mechanism these cells may use for immune evasion. Moreover, sub-lethal doses of carfilzomib-based drug combinations elevated PD-L1 expression on MOPC315.BM and MM.1S cells, opening the possibility for the combination of chemo- and immunotherapeutic modalities.

4.4.4.2. *Combination of Prophylactic Vaccination with Checkpoint Blockade Therapy.*

Based on previously presented data, we hypothesized whether the weak or lack of immune protection observed in the immunizations with MM cell death bodies, generated with apparently 'immunogenic' chemotherapy, is a consequence of the ability of MM cells to evade immunesurveillance, especially through PD-1/PD-L1 axis. Thereby, we selected the only condition that apparently evoked a partial anti-myeloma immune response, that is, immunization with MM cells treated with carfilzomib, CLQ and z-VAD-fmk, and combined it with checkpoint blockade therapy using an anti-PD-1 antibody. We followed a similar protocol used for the previous immunizations (described in section 3.10) (**Figure 4.53**). Given the usually long-lasting half-life of antibodies in the bloodstream (IgGs have a mean half life of 23 days in circulation), this time, blood samples were not collected to avoid potential extraction of anti-PD-1 antibody from mice bloodstream.

Control mice (control and αPD-1 groups) were s.c. injected with RPMI medium, whereas carfilzomib+CLQ+zVAD group and the homologous group that received αPD-1 therapy, were immunized by injecting s.c. MOPC315.BM wt cells treated with the aforementioned chemotherapeutics. A total of two immunizations separated by one

week-lag period were performed before the rechallenge with living MOPC315.B-Luc$^+$ cells. Groups of mice receiving αPD-1 therapy were injected intraperitoneally (i.p.) 100 μg of anti-PD-1 antibody per mice, twice a week, for a total of 5 administrations starting at day 5 post-rechallenge. Disease progression was monitored by BLI and evaluating major signs of the disease as described previously.

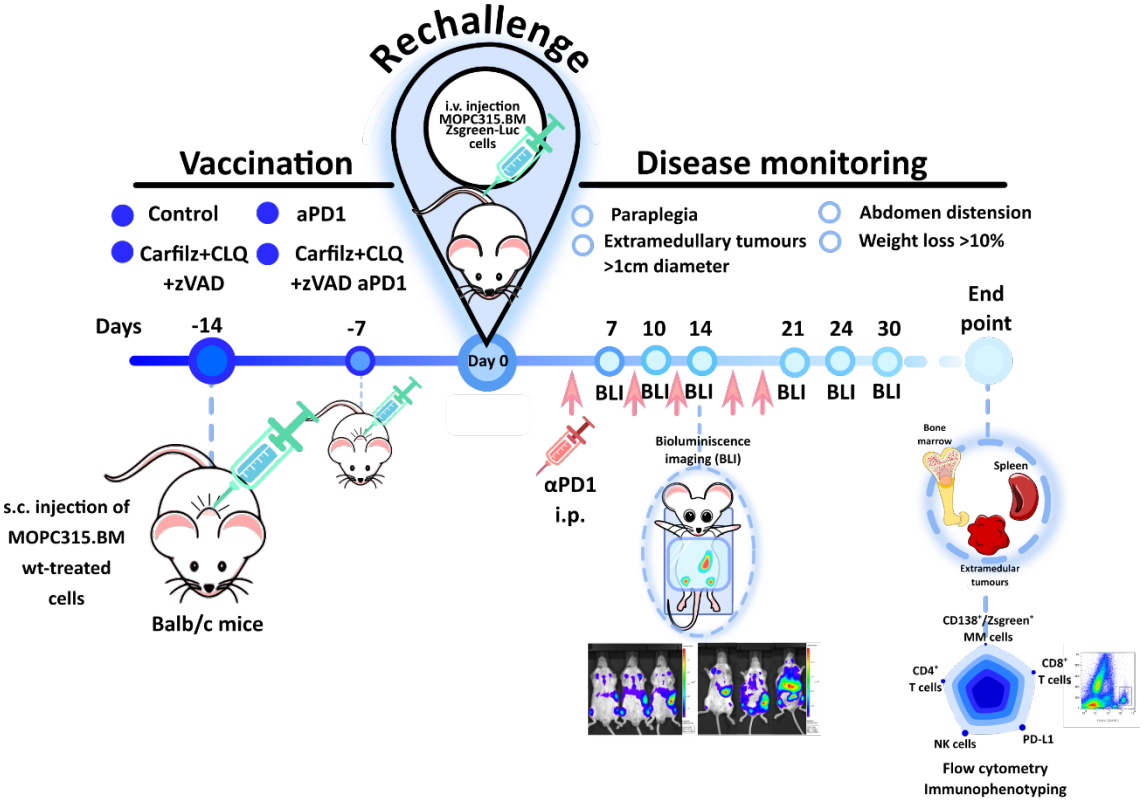

Figure 4.53 | Protocol for combination of checkpoint blockade therapy with prophylactic vaccination with drug-treated MM cells. The role of PD-1/PD-L1 axis in anticancer vaccines was examined. In particular, the potentiation capacity of combinatorial regimens composed of checkpoint blockade therapy and vaccination with death cancer cells was interrogated. The protocol followed for the vaccination was the same as the one exposed in Figure 4.50, with the exception that αPD1 and Cfz+CLQ+zVAD+αPD1 groups of mice were administered 100 μg/mice of blocking antibodies against PD-1, starting at day 5 post-rechallenge and . MM disease was monitored by analysing several parameters. Every 2 to 3 days major or endpoint signs of the disease were analysed (paraplegia, abdominal distension, weight loss >10% and extramedullary tumour >1cm). MM tumour load was also examined by bioluminescent imaging (BLI) at the indicated time points, as described in section 3.8.3. Upon humane endpoint application, femur/tibiae from posterior limbs, the spleen and if present extramedullary tumours (EMTs) were collected for further processing. BM, spleens and EMTs were immunophenotyped to analyse infiltration and PD-L1 expression of MOPC315.BM cells in the different affected organs and also to evaluate the frequencies of CD4$^+$ T cells, CD8$^+$ T cells and NK cells as described in section 3.4.1.1.3.

Data presented in **Figure 4.54** revealed that checkpoint blockade therapy alone did not significantly prolong mice survival to the slightest degree. When mice were immunized with MM cells treated with the indicated drugs, disease progression was significantly delayed, as survival curves illustrate, reproducing our previous results (**Figure 4.51**). However, when mice immunized under these same conditions were treated with anti-PD-1 antibody, no differences in survival rates between both groups emerged. Similar conclusions can be drawn out from BLI assessment. Anti-PD-1 therapy alone did not provoke any reduction in tumour burden as compared with control group. Additionally, anti-PD-1 therapy did not further improved the immune protection exerted by immunized mice, since no differences in tumour load were found when carfilz+CLQ+zVAD and carfilz+CLQ+zVAD αPD-1 groups were compared. Nonetheless, as shown before, mice vaccinated with MM cells treated with the chemotherapeutic formulations displayed reduced tumour burden when compared with their respective control groups. Our data suggest that PD-1/PD-L1 axis is not involved in the immune evasion elicited by MM cells, and that probably is not responsible for the weak immune protection conferred by vaccine formulations in our model. Furthermore we can infer from these experiments that anti-PD-1 checkpoint blockade therapy may not be sufficient to revert the immunosuppressive nature of MM and improve therapeutic response to prophylactic vaccination setups.

Immunophenotypic flow cytometry analysis of tumour tissues showed that MM infiltration in the BM and the spleen were lower in the two groups of mice vaccinated with MM-treated cells than in the respective control groups. This was not the case in the EMTs, where control groups showed reduced tumour burden. However, it must be noted that only one data point was available since only one EMT was recovered in the vaccinated groups of mice. Regarding the level of infiltration by the different immune populations in the tumour niches, NK cell frequencies were increased in the spleen of the two different groups of mice vaccinated with MM-treated cells. In the BM, those groups that were treated with anti-PD-1 antibody, displayed increased NK cell numbers compared to those groups who did not receive checkpoint blockade therapy. However, no differences were found in NK cell infiltration, when comparing vaccinated groups with their respective non-vaccinated controls. In the EMTs, only mice who underwent vaccination with MM cells treated with the chemotherapeutic formulation and also received checkpoint blockade therapy, displayed increased NK cell numbers. However, again only one EMT could be recovered from this group of mice. With regards to the T cell compartment, similar results were noticed. In the BM, $CD4^+$ and $CD8^+$ T cell frequencies were increased upon checkpoint inhibition. However, this time, no differences were found between vaccinated and non-vaccinated groups of mice. A quite different picture could be observed regarding T cell infiltration in the spleen of the different groups of mice. Here, increased T cell frequencies were found in the vaccinated groups of mice compared with their respective non-vaccinated littermates, reproducing results obtained in the previous experiment. However, none of this cited changes were deemed statistically significant probably due to the high dispersion of the data and the

low population size. In EMTs, no major differences in T cell frequencies were observed among the different groups of mice.

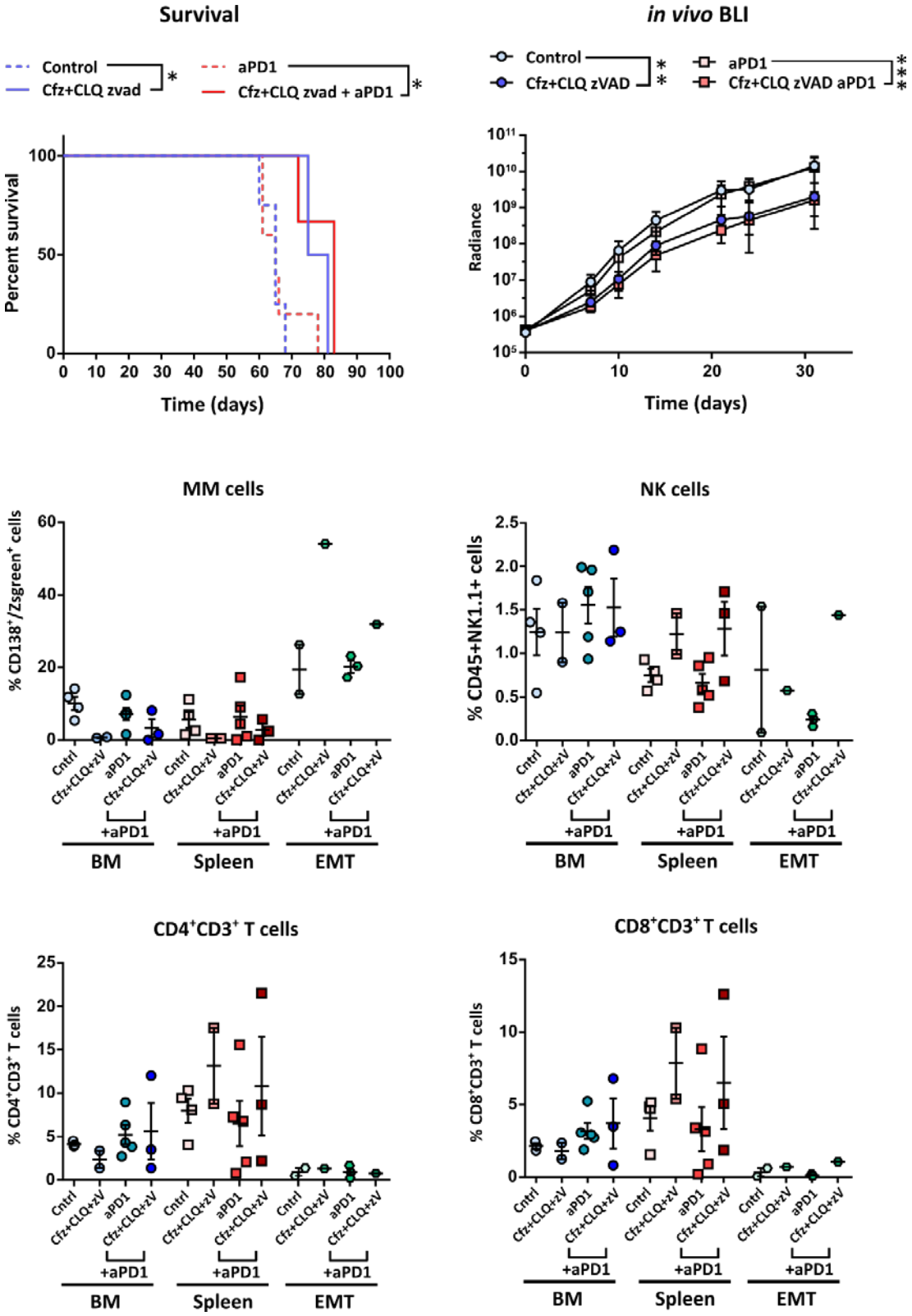

Figure 4.54 | Combination of checkpoint blockade therapy with prophylactic vaccination with drug-treated MM cells. The role of PD-1/PD-L1 axis in anticancer vaccines was examined. The potentiation capacity of combinatorial regimens composed of checkpoint blockade therapy and vaccination with death cancer cells was interrogated. The protocol followed for the prophylactic vaccination, the checkpoint blockade therapy administration schedule, as well as the parameters analysed for disease monitoring is exposed in Figure 4.51. Survival curves from the different experimental group of mice were generated. Statistical analysis was performed by comparing each of the experimental groups with control group using Mantel-Cox (Log-rank) test, where *p<0.05. **p<0.01, ***p<0.001, ns, non-significant. MM tumour load examined by bioluminescent imaging (BLI) (as described in section 3.8.3) was also represented. In this graph the mean radiance of each experimental group of mice along the course of the disease was plotted. Statistical analysis was performed by comparing each of the experimental groups with control group using two-way ANOVA with Bonferroni correction for multiple comparison, where *p<0.05, **p<0.01, ***p<0.001, ns, non-significant. Upon humane endpoint application, femur/tibiae from posterior limbs, the spleen and, if present, extramedullary tumours (EMTs) were collected for further processing. BM, spleens and EMTs were immunophenotyped to analyse MOPC315.BM cell infiltration and immune cell frequencies of $CD4^+$ T cells, $CD8^+$ T cells and NK cells as described in section 3.4.1.1.3. Graph represents the percentage of cells expressing the indicated cell markers from total population of cells. Statistical analysis was performed by comparing each of the experimental groups with control group using one-way ANOVA with Tukey correction for multiple comparison, where *p<0.05, **p<0.01, ***p<0.001, ns, non-significant. Experimental groups were composed of control mice (n=4), aPD1 (n=5) carfilzomib+CLQ+zVAD (n=2), carfilzomib+CLQ+zVAD+αPD1 (n=3), from 1 independent experiment.

It should be noted that the population shortage of this experiment was a consequence of a serious complication we came across. In this experiment during the rechallenge, more than half of the animals rapidly succumbed to the intravenous administration of living MM cells. The most probable cause is that a severe thromboembolic event may had developed in all these passed animals. We still don't know exactly how that could happen, given that the conditions (quantity of inoculated cells, viability, etc) were similar to previous occasions. Further experiments will be necessary to enlarge population size and confirm the results shown here.

Our data contrast with that reported by others in several ways. For example, some studies have shown that PD-L1 blockade in monotherapy was able to delay tumour growth but not completely blunt it in J558L murine MM model[824]. Similarly, PD-1 blockade also yielded prolonged survival rates in myeloma-bearing mice[440,824]. Moreover, targeting PD-1/PD-L1 pathway in combination with other anti-myeloma therapies has been shown to improve the therapeutic response of the latter. In particular, combination of autologous-HSCT with a cell-based vaccine and PD-L1 blockade notably improved survival of myeloma-bearing mice[825]. Radiation-based therapies have also benefited from anti PD-L1 blockade combination[822]. Preclinical work also showed effective combinations between lenalidomide and PD-1/PD-L1 blockade[502]. Likewise, targeting PD-1 with pidilizumab has been shown to enhance T cell responses elicited by DC-myeloma fusion vaccines *ex vivo*[827].

Our negative results indicate that blocking PD-1/PD-L1 pathway do not improve the therapeutic response elicited by vaccination strategies. Thereby, it might seem feasible that this pathway is not behind the reduced or lack of immune protection against

the myeloma disease brought about by the vaccination approach. Supporting our data, similar results were obtained in Vk*MYC MM mouse model, in which blocking PD-1 or CTLA-4 had no repercussions over myeloma disease progression[828]. However, when immune checkpoint blockade was administered in a post-transplant setting, it managed to improve disease control in Vk*MYC MM mouse model[829]. The timing of the immune checkpoint blockade administration is probably a key element to explain the success of these approaches. In line with this, it is important to point out that PD-1 is upregulated, not only in exhausted T cells, but also this mechanism operates as a physiological backup pathway to dampen effector T cells after activation of the TCR. For this reason, the immune repression time period that follows ASCT, may represent an important therapeutic window to apply checkpoint blockade therapy to reinvigorate myeloma-specific T cell clones[823]. Therefore, selecting the right timing for administration of this kind of approaches may be critical for their therapeutic success[830].

Given the lack of response observed in our experiments, another simple explanation that may be considered is that the dosage and schedule of anti-PD-1 blocking antibody administration, was insufficient to bring about overt responses. The available literature provides a plethora of possible “effective” checkpoint blockade therapeutic schemes, that differ in the administration dosages, frequencies and total number of inoculations. We cannot rule out the possibility that administration of such treatment following a different scheme, may have had potent anti-myeloma activity. Future experiments will be needed to verify the efficiency/effectivity of the administration protocol.

Furthermore, the molecule that we have directly assessed and that has been found to be overexpressed is PD-L1 and not PD-1. It is rather tempting to speculate that given the ligand-receptor relationship between these two molecules, and since both proteins participate in the same molecular pathway, that blocking any of them may produce the same global outcome. However, since blocking PD-1 has had no anti-myeloma effect, nor potentiation of other immunotherapeutic approaches, it is possible that PD-1 is expressed at low levels by immune cells, at least at early stages of the disease. Since Balb/c mice are completely immunocompetent *a priori*, one would expect that immune effector phenotypes were indeed functionally active and did not bear exhausted features. It will be quite informative to evaluate PD-1 expression on BM or splenic immune effectors to clarify this conundrum.

Despite the negative results obtained in the preclinical model used in this work, it should be noted that in human disease, checkpoint blockade therapy as monotherapy also failed to yield clinically objective responses in MM patients[463,830]. One possible reason is that, besides PD-1/PD-L1 pathway, a wide panel of immune checkpoint inhibitors exists and may have potential roles in myeloma immune evasion. The great and versatile variety of co-signalling molecules held by T cells, APCs or tumour cells is thought to depend on the specific context and its functions may be partially coincidental and redundant. Moreover, as it has been reported in other cancer types, it is possible that

when PD-1 blocking antibodies are dispensed, compensatory mechanisms could also develop and upregulate alternative immune checkpoints[497].

Although less studied, alternative immune checkpoint inhibitory receptors such as CTLA-4, LAG-3, TIM-3, GITR, TIGIT could also contribute to the immunosuppressive phenotype of MM[831–833]. For example, although TIGIT has yet to be explored in the clinical setting, preliminary studies have already reported expression of TIGIT in $CD8^+$ T cells of MM patients[834–836]. Additionally, different preclinical studies have already showed the effectiveness of targeting this immune checkpoint inhibitor alone or in combination with SCT[829,836]. Similarly, it has been demonstrated that early after ASCTs, T cells from MM patients expressed CTLA-4, TIM-3 and LAG-3 inhibitory molecules[832]. Moreover, a preclinical study also reported increased expression of LAG-3, TIM-3 and other inhibitory molecules on T cells of myeloma-bearing mice, and that concurrent administration of anti-PD-1 and blocking antibodies against LAG-3, TIM-3 or CTLA-4 following sub-lethal whole body irradiation, improved mice survival rates from 30% to 80% in the best scenario[826]. In fact, combinatory regimens of immune checkpoint inhibitors are currently being investigated in MM patients[497].

In line with this notion, work by de Beck and colleagues also showed that besides PD-L1, another molecule was important to the effectiveness of the immune response in the context of vaccination strategies using chemotherapy-treated MM corpses[819]. In particular, they showed that CD47 was also highly expressed in MM cells in basal conditions and chemotherapy reduced the expression of this molecule correlating with the increased immune response observed[819]. This study illustrated that CD47 could also foster immune evasion and account for the immunosuppressive phenotype in myeloma cells.

Dysfunctional T cells are classified into three categories: anergic, exhausted or senescent. Each of these different phenotypes are characterized by increased levels of several inhibitory molecules, impaired effector function like disrupted cytokine production or cytotoxicity, loss of proliferative potential among others[837]. **Anergy** is defined as an induced hypo-responsive state due to insufficient co-stimulation via CD28 or due to elevated co-inhibitory signalling[838,839]. **T cell exhaustion** usually occurs upon chronic antigen exposure and/or stimulation and is characterized by a deterioration of effector T cell functions and the augmentation of inhibitory checkpoint receptors (PD-1, CTLA-4, TIM-3, LAG-3, among others)[839,840] . Lastly, **senescent T cells** are characterized by loss CD28, cell cycle arrest and could undergo telomere attrition[839].

To be successful, it is usually thought that checkpoint blockade therapy requires T cell phenotype to be able to be reversed in order to become activated and fight myeloma. For that purpose, T cells must present an exhausted rather than senescent or even anergic phenotype[841]. Recent work has shown that MM T cells may bear immunosenescent phenotypes, rather than being exhausted, which may explain failure of checkpoint blockade therapy[497,838]. However, evidences for both exhausted and

senescent T cell phenotypes have been reported in MM, and therefore, no consensus has yet been met into this topic[832,837,838,842,843]. Recently, it has also been questioned whether chronically exhausted T cells can be reactivated and respond to checkpoint blockade or rather they are too 'fatigued' to strike back[844]. It has been reported that in this exhausted state, T cells may hold a stable and 'unmalleable' epigenetic and transcriptional landscape that may limit the durability of T cell reactivation[845,846].

Altogether, our results showed that anti-PD-1 antibodies did not improve anticancer immune responses originated by vaccination formulations in MOPC315.BM model, in our experimental conditions. Although checkpoint blockade therapy has emerged as a 'lifeboat' for heavily-treated cancer patients in which no more therapeutic options remained, not all patients and not all cancer types benefit from this kind of approach. Further research will be necessary to decipher these open questions to be able to offer the right therapeutic approaches to the right patients or convert non-responders into individuals that could take advantage from these therapies.

4.5. MM Patients.

Over the last years, MM patients have benefited by a radical improvement in disease prognosis and clinical outcome due to an upgraded therapeutic armamentarium, which has been traduced in better therapeutic responses and longer survival rates. In particular, PI-based therapy has been one of the contributors to this advance. However, despite current efforts, MM is still an incurable neoplasm. Virtually the vast majority of myeloma patients eventually relapse and those who have received at least three prior lines of therapy hold a very poor prognosis[847]. Thereby, there is still plenty of room for therapeutic improvement. In this last section of the work, based on our previous results, we wanted to translate the success of carfilzomib-based combinations with CLQ and DBeQ in established MM cell lines to isolated primary MM samples *ex vivo*. Furthermore, we sought to investigate the relationship between cell surface CRT expression and the BM microenvironment held by MM patients as well as try to correlate the interplay between these two factors with clinical prognostic markers and patient's clinical outcome (see **Figure 4.55**). Globally, a total number of 91 patient's derived BM samples have been processed and studied during this work.

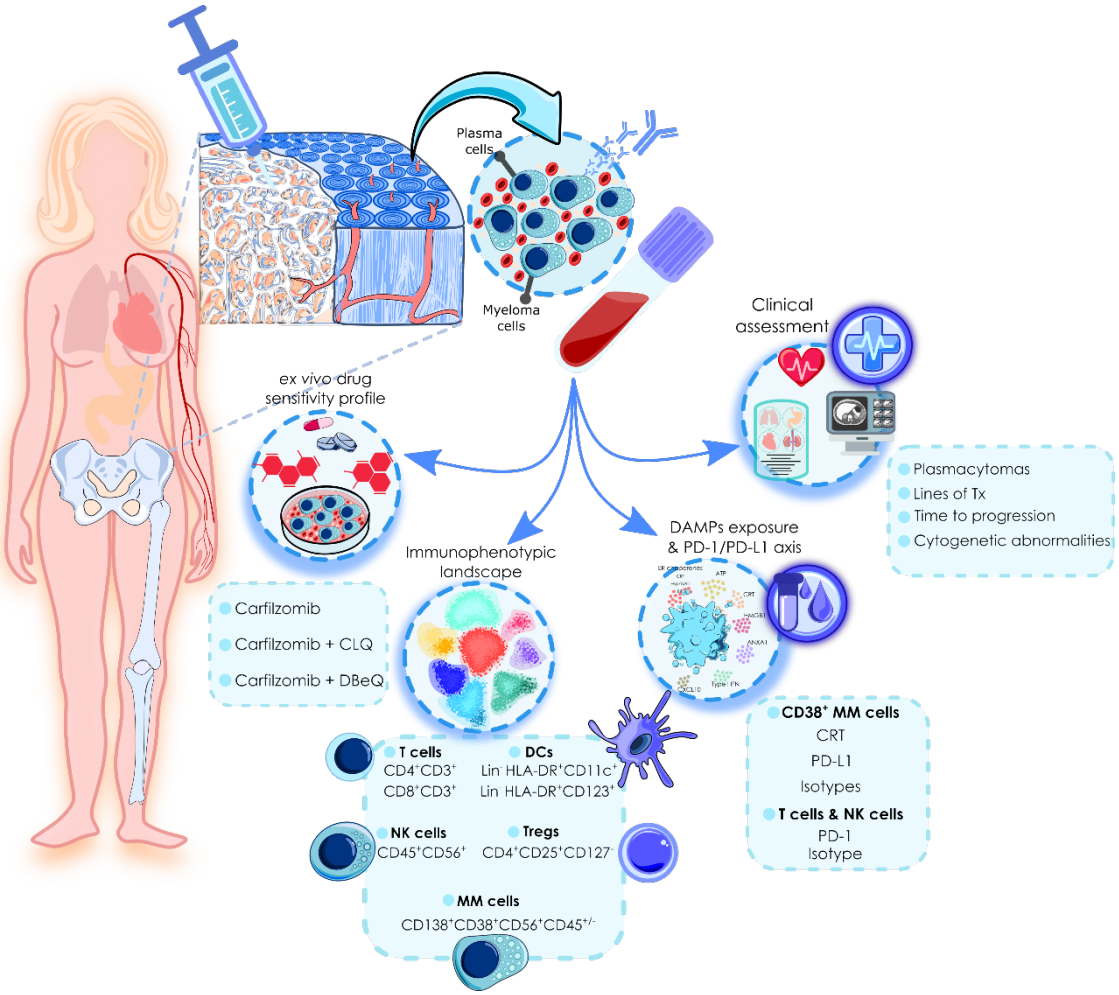

Figure 4.55 |Workflow with BM samples from patients with plasma cell dyscrasias. BM samples were acquired by the Hematology Services at Hospital Clinico Universitario Lozano Blesa and at Hospital Universitario Miguel Servet. BMMCs were then purified by Ficoll-Hypaque density gradient centrifugation, and cells were subsequently used for downstream applications: 1) *ex vivo* drug sensitivity profiling with different drug combinations. 2) Assessment of BM immune compartment. 3) Evaluation of DAMP exposure and PD-1/PD-L1 axis. 4) Data from the BM immunophenotyping were analysed with different clinical markers to investigate the prognostic value of CRT

4.5.1. Carfilzomib Sensitivity of MM Primary Cells *Ex Vivo*.

First, sensitivity to the individual treatment with carfilzomib was analysed. To that purpose drug sensitivity was assessed by quantifying annexin V binding to PS in $CD38^+$ bone-marrow mononuclear cells (BMMCs) after 16h of drug incubation. As presented in **Figure 4.56**, MM primary cells were less sensitive than human MM established cell lines to carfilzomib action. Cell death rates progressively increased with drug dose, reaching a mean value of almost 60% of annexin V^+ cells at the higher drug concentration. As expected, there was a high variability from one patient to another in terms of response to carfilzomib-based treatment.

To date no biomarkers of sensitivity or resistance to PI-based therapy with the ability to prospectively select patients that could be benefited by this type of approach, have been clinically validated or implemented into daily clinical practice so far[848]. To further deepen our knowledge into this matter, we sought to elucidate whether the *ex vivo* drug response elicited by carfilzomib in primary myeloma cells was dependent on the cytogenetic profile harboured by myeloma patients. To this end, we segregated MM patients into two groups (altered or normal), based on the presence or not of different routinely tested cytogenetic abnormalities in the clinical practice.

Results displayed in **Figure 4.56** showed that myeloma patients with an altered cytogenetic profile, tended to be more sensitive to carfilzomib therapy. Differences were especially more noticeable at low doses, but were less evident with increasing drug concentrations. At first, one would expect that patients holding cytogenetic abnormalities would have an increased resistance to chemotherapeutic drugs giving its augmented malignant phenotype. However, this observation could be interpreted the other way around. Myeloma cells with an altered cytogenetic profile, and likely with a more malignant phenotype, would exploit more frantically cellular signalling pathways that ultimately require the UPS to function properly[390]. Therefore, these cells would become addicted to the UPS and hence would explain the increased sensitivity displayed by cytogenetic aberrant myeloma cells to carflizomib. In fact, it has been reported that clinical efficacy, as well as the additive and cumulative benefit of PI-based therapies when combined with other therapeutic approaches, seem to be especially discernible in high-risk MM patients[848]. Moreover, Majumder *et al.* reported that patients harbouring the t(4;14) translocation, one of the high-risk cytogenetic abnormalities routinely tested in our study, displayed increased sensitivity to bortezomib, IMiDs and other targeted drugs[849]. This is also supported by clinical trials showing that patients bearing the traditionally high-risk t(4;14) alteration, displayed overall survival (OS) rates that are in the same range of standard-risk MM patients when treated with bortezomib-based regimens[850,851]. Nonetheless, it should be noted that these tendencies were deemed non-significant, hence the real repercussion of these observations should be taken with caution.

Individual analysis of patient's response to carfilzomib treatment revealed that some patient's responded to this type of drug, while others were intrinsically more resistant. Previous results have not rendered conclusive interpretations on the factors that affect carfilzomib sensitivity. We then segregated patients on PI-resistant and PI-sensitive (PI-R and PI-S, respectively), based on the *ex vivo* carfilzomib drug response. In particular, we deemed as PI-R individuals, those who laid under the lower quartile of cell death values from the totality of cell death rates displayed by all tested samples. As illustrated in **Figure 4.56C**, PI-S cohort showed a clear response to *ex vivo* carfilzomib treatment alone as indicated by the progressive enhancement of cell death rates elicited by this agent. Conversely, PI-R patients certainly showed a poorer drug-response curve, only displaying a hint of responsiveness to carfilzomib treatment at the higher tested

drug concentration. Again, no significant differences were found between PI-R and PI-S subgroups in the proportion of patients that have a normal, or rather, an altered cytogenetic profile. Similarly, the total number of lines of therapies that myeloma patients received prior to the reception of the BM sample were compared between PI-R and PI-S subgroups. It can be noticed that PI-S cohort displayed a higher number of lines of therapy that patients previously received. However, no statistically significant differences were found at this respect. These latter results are in consonance with data from Majumder study, in which patients clustered under the most drug-sensitive group were the ones that had the poorest clinical prognosis[849].

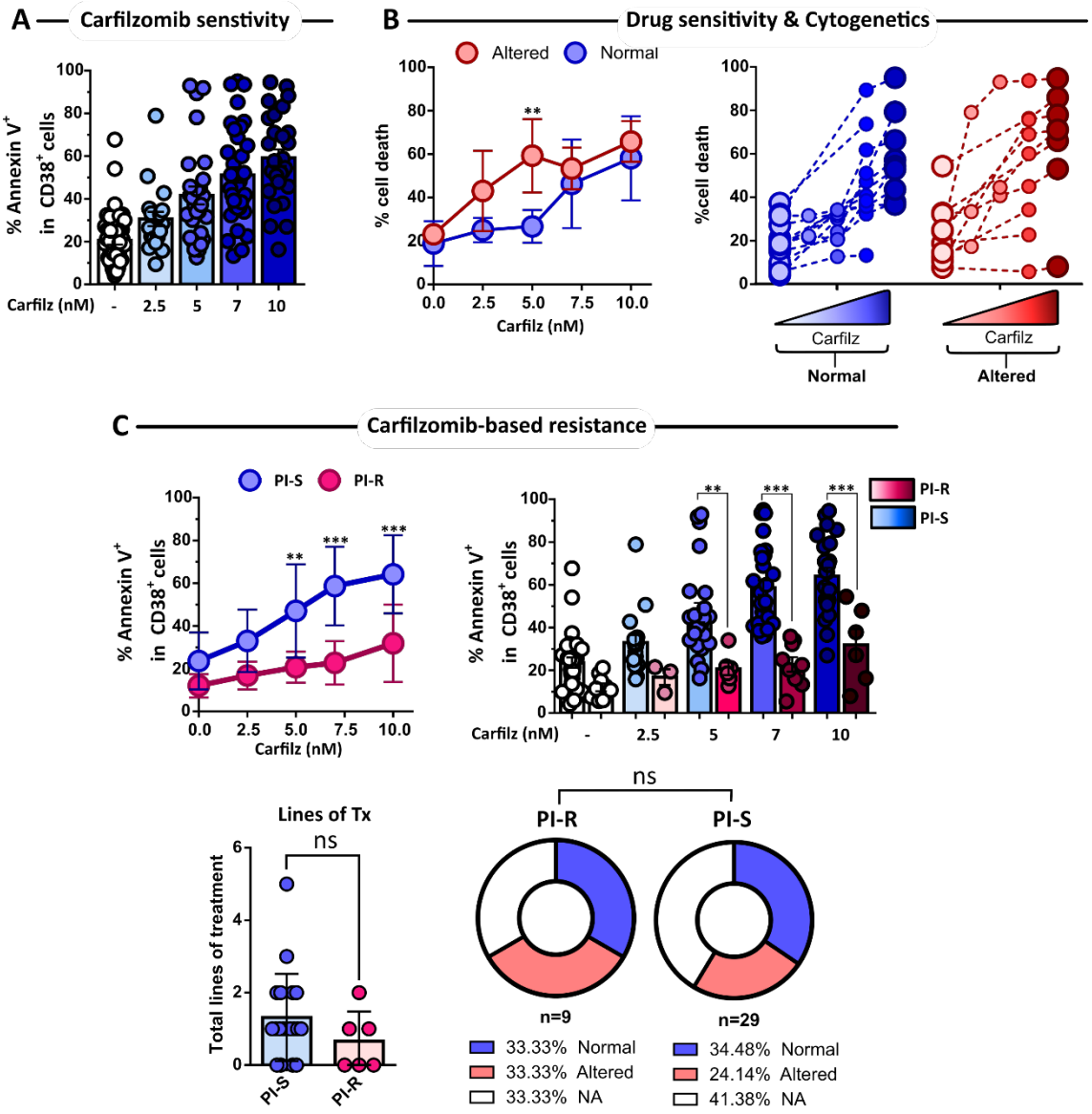

Figure 4.56 | Carfilzomib sensitivity in MM primary cells *ex vivo*. A. The sensitivity of $CD38^+$ BMMCs isolated from MM patients to carfilzomib treatment was evaluated. BMMCs were isolated by density-gradient centrifugation as described in section 3.1.5. BMMCs were then incubated at $1x10^6$ cells/ml with the different drugs at the indicated concentrations for 16 hours. Cells were stained with anti-CD38 fluorochrome conjugated specific antibody and annexin V for determining PS exposure. Specific cell death

in CD38$^+$ population was analysed by flow cytometry. **B.** MM patients were stratified depending on whether their cytogenetic profile normal or altered and differences in carfilzomib sensitivity was analysed. Statistical analysis was performed by comparing each of the experimental groups with control group using two-tail unpaired t test, where *p<0.05, **p<0.01, ***p<0.001, ns, non-significant. **C.** Patients tested for *ex vivo* carfilzomib sensitivity were stratified in PI-resistant (PI-R) and PI-sensitive (PI-S) groups for further analysis. Individuals that fall on the lower quartile of cell death rates upon *ex vivo* carfilzomib treatment, were deemed PI-resistant while the rest were considered PI-sensitive. The relationship between *ex vivo* PI-sensitivity and different clinical markers was then analysed to determine the clinical outcome predicting potential. The mean number of total lines of treatment patients received was analysed between PI-R and PI-S groups. Additionally, the percentage or the number of patients that hold a normal or altered cytogenetic profile were compared between PI-R and PI-S groups. Statistical analysis was performed by using two-tail unpaired t, in dose-response carfilzomib curves and when analysing the lines of therapy between PI-R and PI-S groups. Fisher's exact test was utilized for analysing differences in the frequencies of patients with cytogenetic alterations in PI-R and PI-S groups, where *p<0.05, **p<0.01, ***p<0.001, ns, non-significant. Data are presented as mean ± SD in the different datasets.

An increasing body of knowledge is being deployed to help unravelling the different resistance mechanisms cancer cells may exploit. However, little of these studies have successfully been implemented in clinical decision making. Molecular profiling of MM patients is routinely performed to help in classifying cases and inform about the risk and prognosis to affected individuals[390]. Currently, metaphase G-band karyotyping and FISH profiling methods are able to quantify MM-associated cytogenetic aberrations and provide risk-based stratification of MM patients, but have generally shown little power in predicting drug-specific efficacy[390]. Only a few cases have been reported, including trisomies that predict response to lenalidomide[852], t(4;14) for bortezomib-based and IMiDs-based therapy[849,851] and t(11;14) to venetoclax[853], among others.

It should be noted that conventional cytogenetic methods like metaphase karyotyping have limited detection capacity since it requires proliferating cells to be performed[854]. For this reason, given the low mitotic index and the reduced number of plasma cells in BM compared to other cell types, detection of cytogenetic abnormalities through this approach may not be sensitive enough. Moreover, the prognostic impact that may derive from detection of these aberrations may not be due to the alteration *per se,* but rather it could just reflect a more malignant phenotype[851]. FISH analysis is also subjected to the relatively few numbers of plasma cells in comparison with other cell types in the BM, and PC-enrichment procedures are imperative for proper testing[854].

Perhaps, novel profiling methods will provide better clustering and stratification criteria, would hold more power and will probably find better correlations with therapy responses. For example, a recent study identifying gene expression profiling (GEP) signatures of *in vitro* tested myeloma cell lines, were able to predict clinical treatment response to PI-based therapy in MM patients[855]. Similarly, RNA-seq signatures of newly diagnosed MM patients have been shown to predict treatment outcome in lenalidomide- and bortezomib-based regimens[856]. Future research is needed to direct transcriptomic-based approaches and predict therapy responses in order to be able to define patients clusters that may benefit from a given therapeutic modality from the whole therapeutic

palette, further rationalizing clinical decision making[390]. In addition, other stratification modalities based on high-throughput *ex vivo* drug-sensitivity testing can also provide valuable information to help in this matter and select the right therapeutic strategy to be followed[849]. In this line, research is further improving the *ex vivo* conditions to better define and resemble the physiological microenvironment that cancer cells may encounter in chemo-sensitivity preclinical assays[857].

To conclude, here we have shown that primary CD38$^+$ BMMCs are sensitive to *ex vivo* carfilzomib treatment alone. Although this is the mean global response, some patients failed to respond to *ex vivo* carfilzomib treatment. No major differences were found in the cytogenetic abnormalities presented by myeloma patients, nor in the line of therapies patients received, that may prospectively explain carfilzomib-based drug-resistance or-sensitivity. Nonetheless, data suggest an elevated sensitivity in individuals bearing cytogenetic abnormalities, which may be corroborated by extending the sample size.

4.5.2. Sensitivity of Primary MM Cells to Carfilzomib-based Combinations.

The *ex vivo* response to carfilzomib-based combinations with CLQ and DBeQ were also evaluated. Since MM primary samples were less sensitive to carfilzomib than established cell lines, we used several drug concentrations from both combined compounds, in order to be able to find effective cytotoxic potentiation responses. As illustrated in **Figure 4.57**, concurrent treatment with carfilzomib and CLQ further increased CD38$^+$ BMMCs mortality with respect to single treatment with carfilzomib. Differences in cell death rates between carfilzomib and the respective combinations, were greater especially at lower PI concentrations. However, these differences, although statistically significant, were less pronounced that those obtained in human MM established cell lines. Similar observations could be inferred out from carfilzomib and DBeQ combinations (**Figure 4.58**).

Like in the drug response elicited by carfilzomib treatment alone, while the majority of the patients responded to these drug combinations, a few of them failed to do so. We then segregated them in two groups attending a similar criteria followed in carfilzomib analysis, but in these case, the increment in cell death between carfilzomib and the respective combination, was considered to discriminate the data. As illustrated in **Figure 4.57** and **Figure 4.58**, responders displayed a similar profile to that observed in the global response. Conversely, in non-responders addition of CLQ or DBeQ did not augment at all cell death compared to carfilzomib treatment alone. Since in some instances, basal cell death is a little bit elevated, to more clarity, we normalized cell death exerted by each condition to that observed in control cells to show the specific cell death. Again data showed the cell death potentiation effect provoked by the addition of CLQ or DBeQ over carfilzomib-based regimen. Additionally, in these figures, the sum of the

individual cell death values corresponding to each combination was represented with arrowheads in each combinatory condition. As depicted, drug combinations surpass in almost every concentration the cell death rates that would correspond to an additive effect. These results would potentially indicate that the combinatory drug response is closer to a synergistic rather than an additive effect.

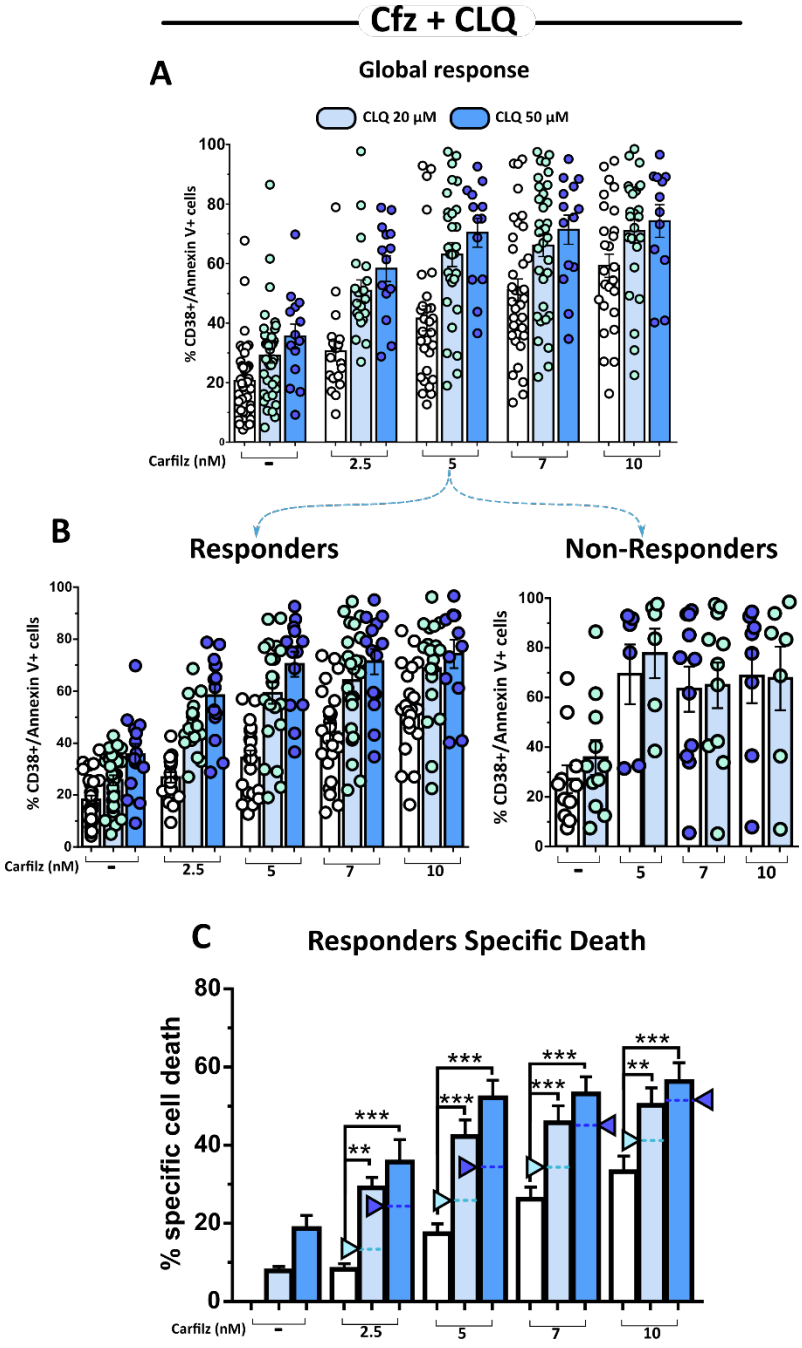

Figure 4.57 | Sensitivity to carfilzomib-CLQ drug combination in MM primary cells *ex vivo*. The sensitivity of $CD38^+$ BMMCs isolated from MM patients to carfilzomib and CLQ treatment was evaluated. BMMCs were isolated by density-gradient centrifugation as described in section 3.1.5. BMMCs were then incubated at $1x10^6$ cells/ml with the different drugs at the indicated drug concentrations for 16 hours. Cells were stained with anti-CD38-fluorochrome conjugated specific antibody and annexin V for determining PS exposure. Cell death in $CD38^+$ population was analysed by flow cytometry. **A.** Global response illustrated by cell death rates of the different carfilzomib-CLQ combinations corresponding to all tested patients were plotted. Statistical analysis was performed using one-way ANOVA test with Tukey post-test, where *p<0.05, **p<0.01, ***p<0.001, ns, non-significant. **B.** Patients tested for *ex vivo* carfilzomib-CLQ combination sensitivity were stratified in responders (R) or non-responders (NR) for further analysis. Individuals that fall on the lower quartile of cell death increments upon *ex vivo* CLQ addition (Cell Death with drug combination – Cell Death in carfilzomib alone), were deemed NR, while the rest were considered as R. The capacity of CLQ addition to enhance cell death in R and NR upon carfilzomib-based therapy is illustrated. Statistical analysis was performed using one-way ANOVA test with Tukey post-test, where *p<0.05, **p<0.01, ***p<0.001, ns, non-significant. **C.** Cell death rates obtained for each condition was normalized to the corresponding values obtained in control cells and the specific cell death in the responders cohort was analysed. Arrow heads indicate the cell death value that corresponds to an additive effect, that is, the sum of individual cell death rates for each combination. Statistical analysis was performed using one-way ANOVA test with Tukey post-test, where *p<0.05, **p<0.01, ***p<0.001, ns, non-significant.

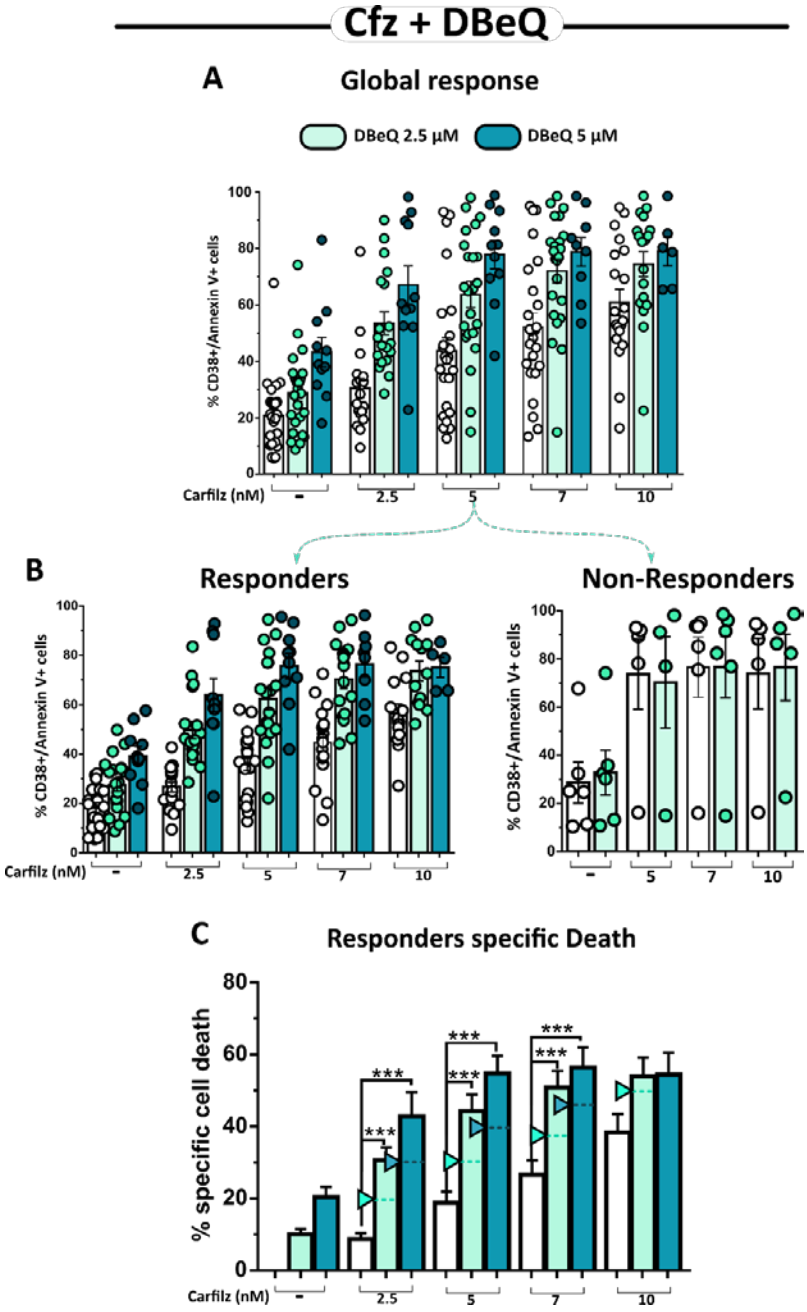

Figure 4.58 | Sensitivity to carfilzomib-DBeQ drug combination in MM primary cells *ex vivo*. The sensitivity of CD38$^+$ BMMCs isolated from MM patients to carfilzomib and DBeQ drug treatment was evaluated. The protocol followed for the isolation, processing and drug treatment of BMMCs is described in Figure 4.57. **A.** Global response illustrated by cell death rates of the different carfilzomib-DBeQ combinations corresponding to all tested patients were plotted. Statistical analysis was performed using one-way ANOVA test with Tukey post-test, where *p<0.05, **p<0.01, ***p<0.001, ns, non-significant. **B.** Patients tested for *ex vivo* carfilzomib-DBeQ combination sensitivity were stratified in responders (R) or non-responders (NR) for further analysis. Individuals that fall on the lower quartile of cell death increments upon *ex vivo* DBeQ addition (Cell Death with drug combination – Cell Death in carfilzomib alone), were deemed NR, while the rest were considered as R. The capacity of DBeQ addition to enhance cell death in R and NR upon carfilzomib-based therapy is illustrated. Statistical analysis was performed using one-way ANOVA test with Tukey post-test, where *p<0.05, **p<0.01, ***p<0.001, ns, non-significant. **C.** Cell death rates obtained for each condition was normalized to the corresponding values obtained in control cells and the specific cell death in the responders cohort was analysed. Arrow heads indicate the cell death value that corresponds to an additive effect, that is, the sum of individual cell death rates for each combination. Statistical analysis was performed using one-way ANOVA test with Tukey post-test, where *p<0.05, **p<0.01, ***p<0.001, ns, non-significant.

To further extend the study of the drug response elicited by combination of carfilzomib with CLQ or DBeQ, and be able to better profile and select the right patients that could be benefited from such drug regimens, drug responses were analysed in different clusters of patients. Therefore, we segregated MM patients attending different clinical or drug-response criteria: presence/absence of cytogenetic alterations, PI-based *ex vivo* resistance, stratification according to the total number of lines of treatment they received and finally drug-responsiveness to carfilzomib-based combinations (**Figure 4.59** and **Figure 4.60**). Detailed analysis of drug responses, revealed the following observations.

No major differences were found in the response to carfilzomib-CLQ combinations between patients with normal or altered cytogenetics. In both patient cohorts, addition of CLQ to carfilzomib increased cell death levels with respect to carfilzomib treatment alone as indicated in the paired analysis. A similar conclusion could be drawn out when comparing the cell death increments upon addition of CLQ in patients bearing normal or altered cytogenetics (right plot in (**Figure 4.59)**. When analysing the data concerning carfilzomib and DBeQ drug combinations, comparable results and interpretations could be obtained (**Figure 4.60**). Our data suggest that patient's cytogenetic signature does not influence the potentiation effect exerted by neither CLQ nor DBeQ, on carfilzomib-based treatment.

We also wanted to inspect whether the intrinsic resistance to *ex vivo* PI-based therapy found in the previous analysis, could also influence CLQ or DBeQ potentiation effect. As shown in **Figure 4.59** and **Figure 4.60**, although drug resistance to carfilzomib treatment alone could be appreciated, addition of CLQ or DBeQ were able to potentiate cell death both in PI-R and PI-S subgroups. Additionally, no statistically significant differences were found when comparing the increments of cell death upon addition of CLQ or DBeQ between PI-R and PI-S cohorts, illustrating that in both groups of patients, addition of CLQ or DBeQ equally intensified cell death exerted by carfilzomib. These results indicate that cell death potentiation effect of CLQ or DBeQ, is not influenced by the inherent PI-based drug resistance observed *ex vivo* in MM primary cells.

When clustering MM patients attending at the number of lines of therapy individuals have previously received, it can be noticed that differences in cell death rates between carfilzomib and combinatory treatments, escalated with the number of therapies received. This tendency towards a greater *ex vivo* sensitivity in heavily-treated patients could also be appreciated by observing the increments in cell death rates. An elevated number of lines of therapy a given patient receives along the course of the disease is a clinical indication of poor prognosis. As discussed earlier, these results are in consonance with data from Majumder *et al.* study, in which patients categorized under the most drug-sensitive group were the ones that had the poorest survival rates[849]. It seems appealing to theorise that those patients would hold a quite malignant phenotype, and therefore would bear an increased oncogenic signalling that relies on an intact ERAD and UPS system to thrive. Hence as mentioned earlier, these cells would probably become addicted to these cellular pathways, and thereby would be more sensitive to drugs targeting these molecular processes. However, it should be stressed out that, in our study, these differences were deemed statistically non-significant.

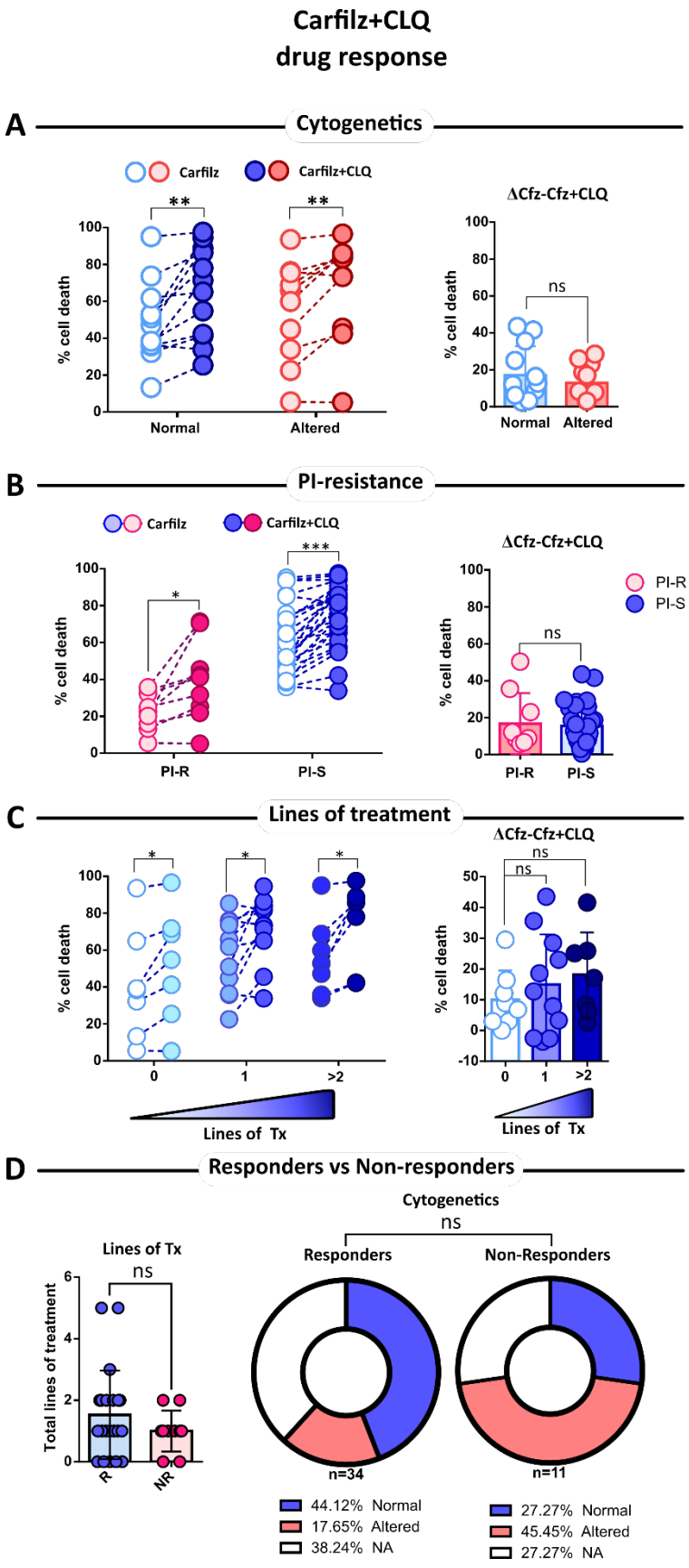

Figure 4.59 | Sensitivity to carfilzomib-CLQ drug combination in MM primary cells *ex vivo*. The sensitivity of CD38^{+} BMMCs isolated from MM patients to carfilzomib-CLQ treatment was evaluated. The protocol followed for the isolation, processing and drug treatment of BMMCs is described in Figure 4.57. **A.** MM patients were stratified depending on their cytogenetic profile (normal or altered) and the differences in the sensitivity to carfilzomib-CLQ combination were analysed. Statistical analysis was performed using two-tailed paired t test for the left plot and two-tailed unpaired t test for the plot in the right, where *p<0.05, **p<0.01, ***p<0.001, ns, non-significant. **B.** Patients tested for *ex vivo* carfilzomib sensitivity were stratified in PI-resistant (PI-R) and PI-sensitive (PI-S) groups for further analysis. Individuals that fall on the lower quartile of cell death rates upon *ex vivo* carfilzomib treatment, were deemed PI-resistant while the rest were considered PI-sensitive. The capacity of CLQ addition to enhance cell death upon carfilzomib therapy in PI-R and PI-S was analysed. Statistical analysis was performed using two-tailed paired t test for the left plot and two-tailed unpaired t test for the plot in the right, where *p<0.05, **p<0.01, ***p<0.001, ns, non-significant. **C.** Cell death potentiation upon CLQ addition in carfilzomib-based treatment was analysed in patients subjected to increasing lines of therapy. Statistical analysis was performed using a two-tailed paired t test for the left plot and two-tailed unpaired t test for the plot in the right, where *p<0.05, **p<0.01, ***p<0.001, ns, non-significant. **D.** The relationship between the sensitivity to *ex vivo* carfilzomib-CLQ combination and different clinical markers was then analysed to determine the predicting potential to therapy response to such combination regimen. Patients were stratified in responders (R) or non-responders (NR) attending at the increment in cell death rates between carfilzomib treatment alone and upon CLQ addition. Individuals that fall on the lower quartile were deemed as NR, while the rest were considered as responders to carfilzomib-CLQ combination. The mean number of total lines of treatment patients received was analysed between R and NR groups. Additionally, the percentage or the number of patients that hold a normal or altered cytogenetic profile was compared between NR and R groups. Statistical analysis was performed by using two-tailed t test when analysing the lines of therapy between R and NR groups and Fisher's exact test for analysing frequencies of patients with cytogenetic alterations between R and NR groups, where *p<0.05, **p<0.01, ***p<0.001, ns, non-significant.

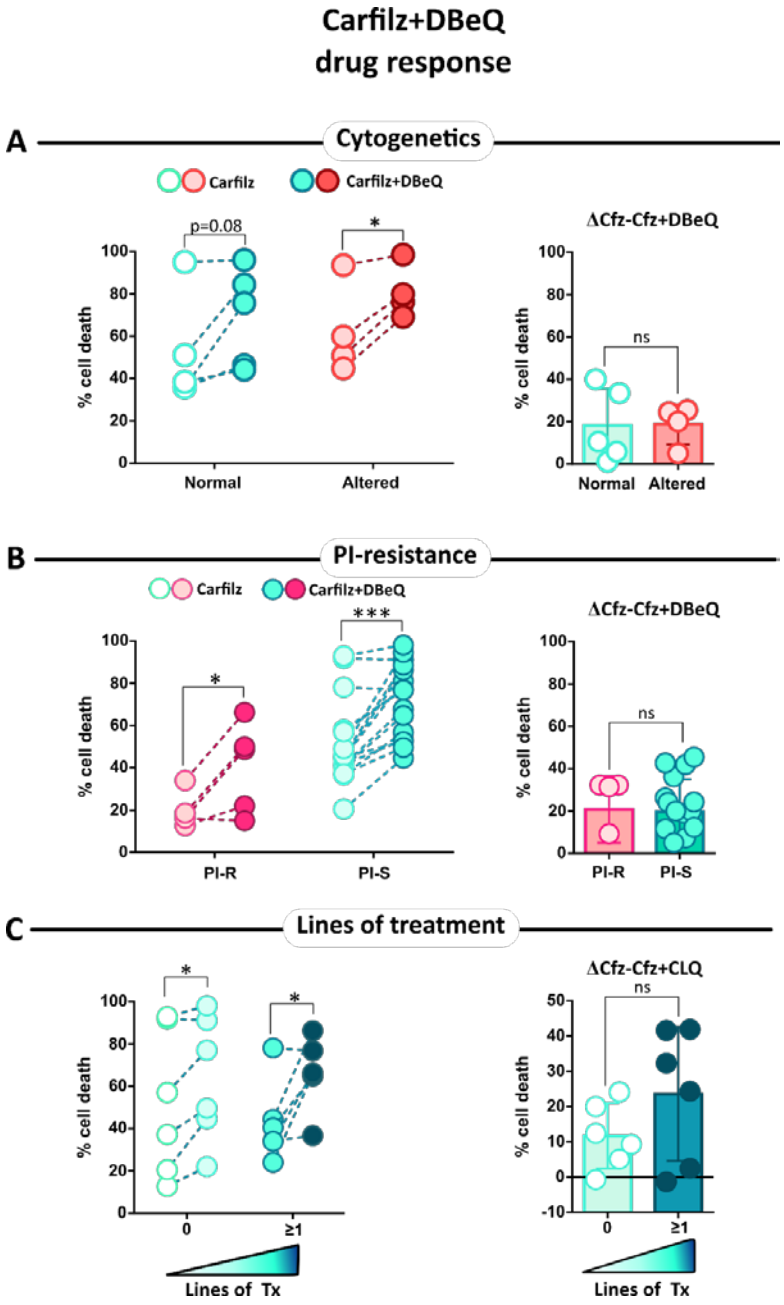

Figure 4.60 | Sensitivity to carfilzomib-DBeQ drug combination in MM primary cells *ex vivo*. The sensitivity of CD38^{+} BMMCs isolated from MM patients to carfilzomib-DBeQ treatment was evaluated. The protocol followed for the isolation, processing and drug treatment of BMMCs is described in Figure 4.57. **A.** MM patients were stratified depending on their cytogenetic profile (normal or altered) and the differences in the sensitivity to carfilzomib-DBeQ combination was analysed. Statistical analysis was performed using a two-tailed paired t test for the left plot and two-tailed unpaired t test for the plot in the right, where *p<0.05, **p<0.01, ***p<0.001, ns, non-significant. **B.** Patients tested for *ex vivo* carfilzomib sensitivity were stratified in PI-resistant (PI-R) and PI-sensitive (PI-S) groups for further analysis. Individuals that fall on the lower quartile of cell death rates upon *ex vivo* carfilzomib treatment, were deemed PI-resistant while the rest were considered PI-sensitive. The capacity of DBeQ administration to enhance cell death upon carfilzomib therapy in PI-R and PI-S was analysed. Statistical analysis was performed using a two-tailed paired t test for the left plot and two-tailed unpaired t test for the plot in the right, where *p<0.05, **p<0.01, ***p<0.001, ns, non-significant. **C.** Cell death potentiation upon DBeQ addition in carfilzomib-based treatment was analysed in patients subjected to increasing lines of therapy. Statistical analysis was performed using a two-tailed paired t test for the left plot and two-tailed unpaired t test for the plot in the right, where *p<0.05, **p<0.01, ***p<0.001, ns, non-significant.

Finally, rather than analysing global drug response and search for differences in the different groups of patients, we formulated the hypothesis the other way around and evaluated whether patients clustered attending our criteria of *ex vivo* response to drug combinations (responders vs. non-responders), have an increased proportion of patients with altered cytogenetics or have received an increased number of lines of therapy or not. In the latter scenario, although responders have a slightly higher mean of total lines of therapies received, these differences did not reach statistical significance. These results corroborate previous observations in which increments in cell death between carfilzomib and its respective combination, escalated with the number of lines of therapy patients

received. Moreover these results also resemble those from carfilzomib response analysis, in which cells from heavily treated patients were deemed sensitive to carfilzomib *ex vivo*.

Regarding the main cytogenetic signature owned by responders and non-responders group, responders tended to have a higher proportion of patients with a normal cytogenetic signature, whereas non-responders cohort was enriched in individuals bearing cytogenetic abnormalities. Since at first myeloma patients bearing cytogenetic abnormalities would have worse prognosis, this observation contrasts with the previous discussed idea that individuals with a malignant phenotype are more sensitive to this kind of therapy. It should be noted that the cytogenetic abnormalities routinely tested in clinical practice in both collaborator hospitals ("Hospital Clínico Universitario Lozano Blesa", HCULB and "Hospital Universitario Miguel Servet", HUMS) have varying degrees of clinical risk, so these results do not completely rule out the former discussed idea. Nonetheless, again all these differences did not reach statistical significance, and conclusions and the real repercussion derived from them should be taken with care. This analysis could only be performed in carfilzomib and CLQ combination. Although carfilzomib and DBeQ drug response was assessed in a substantial amount of samples, when segregating patients in responders and non-responders, no sufficient clinical data were available to drawn out proper conclusions.

As mentioned earlier, cells have two main protein disposal mechanisms: the UPS and autophagy. Although they follow apparently distinct cellular pathways, the proteasome, the UPR and autophagic responses are closely intertwined and can compensate for deficiencies present in each of the other processes[858]. In fact, under ER stress conditions, when the cytoprotective and restorative capacity of the UPR is surpassed, several signals stem from the ER to trigger autophagy and try to re-establish cellular homeostasis. Hence, autophagy could operate as a backup mechanism to alleviate and deal with staggering ER stress conditions[165,166]. In the particular case of MM, autophagy has been reported to be a prosurvival mechanism that could endow myeloma cells with protection against the MM highly secretory phenotype and proffer with resistance against drug-mediated effects, including PIs[158]. In fact, higher expression of genes involved in antioxidant-, chaperone- and autophagy-related processes have been reported to be associated with poor prognosis in MM patients[718]. In addition, several studies reinforce the notion that ER stress response (including the one evoked by PIs) fosters autophagic flux in MM and also in other cancer models[109,603,719–723]. Therefore, simultaneously co-targeting the proteasome and autophagy, could be conceived as a competent therapeutic approach against MM. For instance, during this work and also in previous studies from our group, it has been demonstrated the ability of chloroquine to strongly potentiate cell death induced by carfilzomib *in vitro* and also *in vivo*, using mouse xenograft models[238]. Here, we further extended these findings, confirming the potentiation capacity of CLQ (and also DBeQ) to the anti-myeloma activity elicited by carfilzomib in *ex vivo* human MM primary samples.

Although the full molecular mechanism is yet to be elucidated, CLQ have successfully been reported to sensitize cancer cells to PIs and also other types of chemotherapeutics[725–727]. Some of these studies reported autophagy-independent mechanisms for CLQ sensitization, as apparently occurs in our model[173,180,728] (see section 4.2.1.6). In a similar study, Baranowska and colleagues also demonstrated the ability of hidroxichloroquine (HCLQ) to potentiate carfilzomib-induced apoptosis in isolated primary $CD138^+$ plasma cells[602]. However, the number of patients in this study was considerably low, since only 5 samples were tested. Here, we have evaluated cytotoxic activity of carfilzomib-based combination in an ample collection of patient's-derived BM samples. Furthermore, this augmented sample size has allowed us to identify patients that may not be benefited by such drug combinations. In an attempt to clarify this conundrum, we have also profiled MM patients attending different clinical and drug-sensitivity criteria, yet no clear conclusions emerged from these analysis. One simple and possible explanation is that therapy-responses evaluated so far were independent to the cytogenetic profile held by affected individuals, or the intrinsic drug-resistance that myeloma cells may have developed. Most probably, patient's therapy responses is a multifactorial-dependent variable, in which several intrinsic and extrinsic elements can contribute. Nonetheless, carfilzomib and CLQ or DBeQ combinations exhibited cytotoxic activity even in MM samples which have shown poor *ex vivo* responses to carfilzomib treatment alone. These results would indicate that PI-resistance may be overcome by such combinatory approaches. In line with this, HCLQ has been shown to re-sensitize previously adapted carfilzomib-resistant MM cells[602]. Similarly, a novel VCP/p97 inhibitor (like DBeQ) has been shown to exert potent cytotoxic activity on bortezomib-resistant myeloma cells and also on primary cells[606].

In the clinical setting, a phase I clinical trial evaluated the therapeutic potential of combining HCLQ with bortezomib in RRMM patients[181]. This chemotherapy regimen was well tolerated. From the 22 enrolled patients, 13.6% displayed a very good partial response (VGPR), 13.6% manifested a minimal response and 45.5% had a stable disease[181]. It is noteworthy to point out that all patients who benefited from VGPRs had not previously been treated with bortezomib[181,858]. Furthermore, from the 27% of patients that have a progressive disease, 66% from those had previously relapsed upon bortezomib therapy[181,858]. Therefore, in this case clinical data suggest that CLQ or HCLQ addition may not be sufficient to overcome PI-resistance. Next, a small phase II trial was carried out assessing CLQ combination with bortezomib and cyclophosphamide in RRMM patients. Only 11 patients were enrolled in this trial. From those, 8 patients completed the 2 cycles and were referred to clinical response evaluation. Partial responses were reported in 3 out of 8 patients, while one of them achieved stable disease and the rest (4/8) suffered progressive disease with a clinical benefit of 40%. Results from this study may indicate that complementation with CLQ to bortezomib and cyclophosphamide regimens show at least some degree of efficacy in overcoming PI-resistance in a significant fraction of heavily pretreated patients[859].

To summarise, our data showed that CLQ or DBeQ potentiated cell death elicited by carfilzomib-based treatment *ex vivo*. Moreover, although it would probably require extending sample size to improve statistical significance, patients bearing cytogenetic abnormalities, or individuals classified as PI-R, could also be benefited by CLQ and DBeQ, carfilzomib-based combination regimens.

4.5.3. CRT as Potential Prognostic Factor in MM Disease.

An increasing body of knowledge is reinforcing the notion that danger signals or DAMPs and ICD-related molecular processes, may operate as potential molecular frameworks to uncover prognostic biomarkers in cancer patients[284]. Several studies have reported that CRT expression is upregulated in tumour tissue and that CRT overexpression could be associated with cancer evolution and aggressiveness[284]. Moreover, according to the ICD paradigm, many studies assumed the idea that CRT exposure may be a consequence of the chemotherapeutic treatment. However, most of them do not fully take into account the possibility that CRT plasma membrane exposure could also take place in basal conditions, neither its implication in malignant transformation or in anticancer immune responses[284]. Depending on the cancer type, DAMPs exposure and especially CRT, could stand as positive or negative prognostic factors in cancer patients. To our knowledge, no data related to CRT exposure in MM has been reported so far. Therefore, in the present study we sought to evaluate CRT expression on the plasma membrane of $CD38^+$ BMMCs isolated from patients with varying degrees of MM disease. Furthermore, we examined the possible relationship between this DAMP and the BM immune microenvironment, as well as its connection with different clinical markers in MM patients.

4.5.3.1. CRT in MM Disease.

Since we first noticed that MM patients heterogeneously expressed ecto-CRT at basal conditions, we questioned whether CRT exposure may vary with the different stages of MM disease. Thereby, we compared ecto-CRT expression in $CD38^+$ plasma cells isolated from control BM, MGUS, SMM and MM BM biopsies. It should be noted that samples from control BM, were not exactly from 'healthy' subjects. They corresponded to individuals that may have an underlying (sometimes even undiagnosed) pathological state and that required a BM aspiration to discard any haematological pathology that may drive their symptoms. Nonetheless, these individuals did not harbour any pathological alteration of the BM determined either by histological or by flow cytometry examination. Thus, under these circumstances, the different parameters analysed in the BM from these subjects should be deemed as 'normal' or non-altered.

Data from **Figure 4.60** illustrate a great interindividual variability on CRT surface levels in BM samples. However, it can be shown CRT exposure increased with disease progression. MM patients significantly displayed elevated CRT expression in the outer surface of the plasma membrane compared to MGUS, smoldering or control samples. Although, slightly increased, no differences in CRT exposure between MGUS or SMM with control samples could be evidenced. These results started to point in the direction that ecto-CRT may be associated with malignant transformation.

To shed more light into this idea, once we observed that ectopical expression of this DAMP correlated with disease stages, we interrogated whether a linkage between the expression of this DAMP and the presence (or absence) of cytogenetic abnormalities could also exist. As depicted, patients with an altered cytogenetic signature, significantly revealed augmented ecto-CRT levels compared with patients that do not harbour any cytogenetic abnormality. As noted earlier, routinely tested cytogenetic alterations in MM patients during clinical practice span from standard- to high-risk prognostic behaviours. A detailed segregation of the different cytogenetic alterations and its relationship with CRT exposure and risk profiling will be covered in the following sections. Nonetheless, whether they were accompanied by a poor prognosis or not, appearance of these alterations may result as a consequence of the oncological transformation process. Hence, this further reinforces the idea that expression of this DAMP, could be related somehow to carcinogenesis. Additionally, to puzzle-out the value of ICD-driven DAMP exposure in the clinical setting, we hypothesized whether chemotherapeutic treatment could have any impact over CRT expression on the plasma membrane of myeloma cells. It should be noted that for this purpose, matched or paired samples, prior and post-treatment would be ideal to determine the effect of chemotherapy on CRT exposure. Alternatively, we could compare levels of plasma membrane CRT in newly diagnosed patients or individuals that had not received any prior chemotherapeutic regimen, with those who had been subjected to any preceding anti-myeloma therapy. As **Figure 4.60** denotes, chemotherapy had no significant effect over CRT surface levels in MM samples.

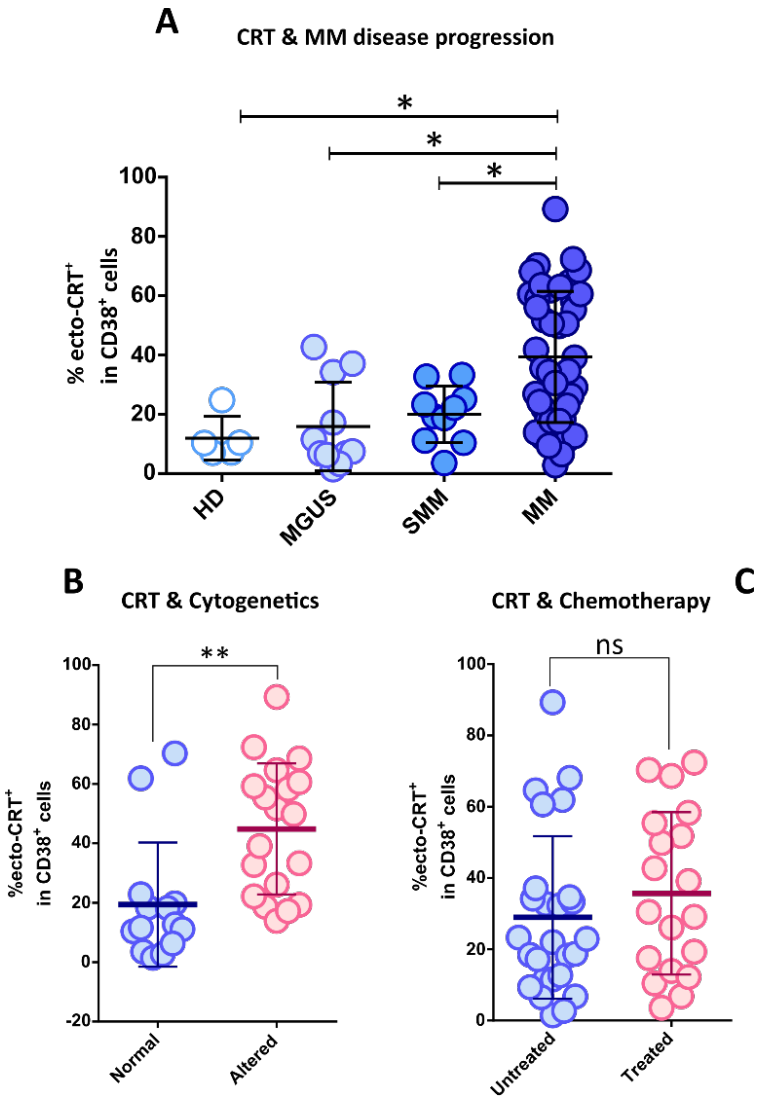

Figure 4.61 | Analysis of CRT exposure in patients with plasma cell dyscrasias. Cell surface exposure of CRT (ecto-CRT) was analysed in patients with plasma cell dyscrasias. In addition, the relationship between CRT and individual's cytogenetic profile, and the possible effect of chemotherapy on CRT exposure were also interrogated. **A**. Ecto-CRT levels were determined in $CD38^+$ BMMCs isolated from clinically diagnosed patients with varying degrees of MM disease (HD, MGUS, SMM, MM). Control BM (HD) was obtained from individual's with other pathologies that held an uncompromised BM evidenced by histological or flow cytometry examination. Statistical analysis was performed using one-way ANOVA test with Tukey post-test, where *$p<0.05$, **$p<0.01$, ***$p<0.001$, ns, non-significant. **B**. Individuals were stratified depending on whether their cytogenetic profile were normal or altered and ecto-CRT levels were compared between these two groups. Statistical analysis was performed using two-way t test, where *$p<0.05$, **$p<0.01$, ***$p<0.001$, ns, non-significant. **C**. The effect of chemotherapy treatment on affected individuals over CRT exposure was examined. Patients were stratified in two groups (treated and untreated) depending on whether they have previously received any chemotherapeutic regimen or not at the moment when BM sample was collected. Ecto-CRT levels were compared between these two groups. Statistical analysis was performed using two-way t test, where *$p<0.05$, **$p<0.01$, ***$p<0.001$, ns, non-significant.

Most research carried out on ICD has centred their attention on mouse models or rather in human established tumour cell lines *in vitro*. Hence, to really unveil the prognostic impact of ICD-related DAMP exposure, as well as its relationship with immunosurveillance and clinical outcome in cancer patients, more studies assessing these and other elements in patient's samples are mandatory. Some studies have shown that neoplastic tissue exhibited increased expression of CRT compared to normal tissue, both in haematological (AML, ALL, CML and NHL) and solid malignancies (glioblastoma, bladder, ovarian, breast, prostate, pancreatic, gastric, colorectal, melanoma and esophageal squamous cell carcinoma, among others)[293,295,860–867].

Although CRT is better known for its functions as an important ER molecular chaperone and a Ca^{2+}-signalling protein, since its discovery in 1974, the knowledge of CRT biological functions and cellular localizations has been growing over the years[243,325]. Although the ER is the most common place where CRT can be found, this protein has also been reported to reside or be localized at different intracellular or even extracellular compartments, including: cytoplasm, nucleus, within cytotoxic granules of T cells, in the cell surface and even in the extracellular space[244,868–870]. Accordingly, CRT has been reported to regulate and perform important and quite diverse non-ER functions, spanning from antigen processing and presentation[871–874], phagocytosis[739], cell adhesion and migration[875–877], cell proliferation[878,879], thrombospondin 1 (TSP1)-mediated focal adhesion disassembly required for cell migration[875,876], resistance to anoikis[880] and even nuclear export of proteins[881,882] and transcriptional activities[244,868,883].

Probably as a reflection of its role in these diverse biological activities, when dysregulated, CRT has also been proposed to hold oncogenic properties and to play a role in tumorigenesis and cancer progression[733,868,884]. Several pieces of evidence point to CRT to promote proliferative, invasive and migratory capacity of cancer cells[868,885]. Moreover, many studies have revealed that depending on the cancer cell type, augmented CRT expression could be associated with a poor clinical outcome, enhanced invasive capacity and cancer aggressiveness[868,886–888]. The impact of CRT exposure or expression on clinical cancer prognosis will be further covered in following sections.

During malignant transformation increased CRT expression and even exposure of this molecule, may be an unwanted consequence of cellular stress. For instance, similar to our data in MM, it has been shown that AML[289,889] and NSCLC[286] patients exposed increased levels of CRT in the surface of cancer cells irrespective of the chemotherapeutic regimen administered. Thereby, it has been proposed that cancer cells may experience chemotherapy-independent cellular stress that drives DAMP signalling and trafficking. Most probably, the source of this cellular stress is a consequence of the malignant transformation process, which already impinges a prominent burden in many cellular processes, including proteostasis[289]. In fact, a robust correlation was found between CRT and expression of other genes related to ER stress responses[289]. This was also corroborated in other cancer types in which increased expression of ER stress response factors, were associated with better clinical outcome, implying that enhanced

ER stress markers like eIF2α phosphorylation, BiP, among others, were associated with increased DAMP signalling and improved immunosurveillance[284]. However, in other cancer types, increased expression of ER stress response markers were associated with worse clinical outcomes. This would indicate the existence of differences in the relationship between ER stress response related processes with the tumour microenvironment and patient's prognosis[284]. Similarly, CRT and ER chaperones have also been found to be released in other autoimmune and stress-related illnesses. For example, extracellular CRT is increased in the synovial fluid in affected joints from patients with rheumatoid arthritis[890]. As a result, patients with autoimmune diseases generate autoantibodies against these molecules[891,892]. Interestingly, it is known that patients that have developed autoimmune diseases harbour a higher risk of suffering from certain types of tumours[893,894]. It is possible that generation of autoantibodies may operate as a mechanism to suppress the immunogenic capacity and the ensuing immune responses of released chaperones, but could also pose a negative side-effect by neutralizing these same immunogenic features that may help tackle cancerous disease[325].

Initially, the presence of an ER-resident and apparently 'sessile' protein like CRT in other cellular localizations was a concept hard to accept. It seems perplexing that CRT can engage all these different biological functions being the ER its primary cellular compartment. Indeed, the mechanisms of cellular relocalization of CRT have been a matter of intense research. But why and how CRT is translocated to the plasma membrane during the malignant transformation process? Is the underlying mechanism of CRT trafficking the same as the one operating during therapy driven-ICD? These and other questions still remain unresolved.

Mechanisms of active CRT translocation to the plasma membrane or to the extracellular space include: the previously discussed ERp57-dependent anthracycline-induced mechanism[255], the ERp57-independent Hyp-HDT-based CRT exposure mechanism[257], and even the Ca^{2+}-dependent binding of cytosolic CRT to PS and subsequent co-translocation during apoptosis[260] (section 4.2.2.3). Most likely, these mechanisms, may explain and have been reported in the context of therapy-driven DAMP trafficking. Although we cannot rule out the possibility that the anthracycline- or the Hyp-HDT-induced mechanisms of CRT translocation could also operate under oncogenic stress conditions, another possible mechanism can also take place. Luminal ER resident proteins are confined within this compartment thanks to the KDEL retention signal displayed in their C-terminal region. This retention signal is recognized by a battery of membrane receptors deployed over post-ER compartments, mostly over cis-Golgi, that retrieve escaped ER-resident proteins via retrograde transport[895,896]. The ER is an industrious and logistic platform for protein production and transport through the secretory pathway, that must be quite regulated to function properly[325]. Under cellular stress conditions, as it occurs during malignant transformation, high protein synthesis demand may saturate ER folding and transport capacity, interfering with these processes and causing ER stress. This situation may be even further aggravated in cells with a

highly secretory phenotype, like in MM cells[195]. As a consequence, ER chaperones are upregulated to cope with the increasing protein folding demand and to help mitigate ER stress. Hence, if these pathways are disrupted or overwhelmed, chaperones may accumulate in the cytosol within endosomal vesicles saturating KDEL retention system[325]. Hence, the non-bound ER protein fraction may escape retrograde transport and eventually reach cell membrane or extracellular destinations[325]. In fact, it has been shown that KDEL retention system cannot follow the pace and is not coordinatedly upregulated at the same level to face ER stress conditions[897]. Additionally, since CRT has been physiologically implicated in several cytosolic and nuclear processes, it may exist a route to direct and generate cytosolic CRT. Unfolded and misfolded proteins are retrotranslocated into the cytoplasm following the ubiquitin-proteasome pathway. However, Afshar and coworkers showed that neither ubiquitin nor proteasome activity were essential to CRT retrotranslocation, suggesting a possible alternative mechanism distinct from unfolded/misfolded proteins[869]. It is still controversial whether this cytosolic CRT is the source for membrane-bound or even extracellular CRT. At this respect, the post-translational modification of chaperones could also play a role to modulate their subcellular localization and functions. To enter the anterograde secretory pathway, proteins must be in a glycosylated form. Panretakis and colleagues generated a glycosylated form of CRT that was able to enter and complete the anterograde secretory pathway[255]. Furthermore, a glycosylated variant of CRT has been detected in HL60 myeloid cell line[898]. Arginylated isoforms of CRT have also been found in the cell surface or in the cytosol associated with stress granules[899,900].

Interestingly, mutations on KDEL region could also cause CRT escape from the ER-retention system and reach the plasma membrane or the extracellular space. In fact, CRT mutants in KDEL region are found in approximately 30% of myeloproliferative neoplasms (MPNs)[901,902]. *CALR* mutations associated with MPNs are composed of small insertions or deletions in exon 9 of the *CALR* gene. This creates a new C-terminus that causes the removal of the KDEL ER retention signal, which consequently favours CRT protein mislocalization outside of the ER[734,901,902]. For instance, mutant CRT has been found to accumulate on the cell surface and can also be secreted to the extracellular space[903–905]. *CALR* gene has also been detected frequently mutated, especially in exon 9, in many solid cancers according to COSMIC and cBioPortal databases[734]. Quite recently, it was shown that released mutated CRT forms subverted anticancer immunosurveillance[734]. In particular, this negative immunomodulatory effect was mediated by blunting the recognition and phagocytosis of dying or stressed cancer cells by DCs[734]. This was shown by using several *in vitro* and *in vivo* systems. Thus in MPNs, as well as in solid tumours, mutated CRT could harbour dual functions endowing cancer cells with both oncogenic features and immunosuppressive abilities[734].

Despite these negative effects of mutated CRT on anticancer immunosurveillance, it has been reported that T cells from MPN patients or healthy individuals, can display potent and frequent T cell responses towards CRT neo-

epitopes[906,907]. In fact, isolated T cells from MPN patients harbouring mutated CRT were able to kill autologous CALR-mutant cells[908]. Furthermore, T cells from healthy individuals displayed stronger *ex vivo* responses to several CALR- neo-epitopes[909]. In fact, it was shown that CALR neo-antigen specific T cells share characteristics of memory T cells[909]. Furthermore, a recent Danish population-based study determined that the prevalence of *CALR* mutations in the general population is 0.16%[910]. Given the data presented above, at first it may seem tricky or hard to reconcile the immunosuppressive effects of secreted mutated CRT and the T cell responses found in healthy individuals and MPN patients. Nonetheless, whereas the former respond to the adjuvanticity character of the anticancer immune response, the latter is more concerned with the antigenic component of immunosurveillance. It is possible that in healthy individuals appearance of antigenic *CALR* mutations, could induce T cell responses and mediate clearance of *CALR*-mutant cells during the editing phase of immunosurveillance cycle[906]. However, when cancer cells escape the editing phase and generate an overt disease, secreted mutant CRT could contribute to create an immunosuppressive microenvironment favouring tumour progression. In fact, T cell responses from healthy individuals were stronger than those elicited by MPN patients[906]. Furthermore, not all MPN patients displayed an anti-mutated-CRT T cell response. Specially patients with advanced disease exhibited reduced responses compared to patients suffering other non-advanced forms of MPN[907].

In the specific case of MM, apparently no mutations in *CALR* gene were found according with COSMIC and cBioPortal databases. Nonetheless, lack of mutations in *CALR* gene does not completely rule out neither its overexpression, nor its relocalization to plasma membrane or even to the extracellular space. In MM, two major karyotypic events are thought to be early drivers of plasma cell transformation[854,911]. One of them encompasses the occurrence of translocations involving *IGH* locus[854]. The other is hyperdiploidy (HRD), a state defined by cells bearing between 48 and 74 chromosomes, found in roughly 50% of individuals with plasma cell dyscrasias (MGUS, SMM or MM) [392]. Hyperdiploidy is characterized by multiple chromosomal gains, especially involving odd-numbered chromosomes (3, 5, 7, 9, 11, 15, 19 and/or 21)[392]. It has been shown that translocations are unevenly distributed between HRD and non-HRD patients, with a higher proportion of the translocations affecting non-HRD patients. However, recent evidences suggest that both genomic alterations (HRD and translocations) can coexist in mixed subclones[854]. *CALR* locus is in 19p13.13, therefore it is quite possible that gains in HRD involving chromosome 19 may account for overexpression of CRT protein. Moreover, copy number variants (CNVs) are also a common event in MM[912]. CNVs involving gains of chromosome 19 have been shown to have an average frequency of about 40%[392]. Moreover, total CRT has been found to be upregulated in MM samples, but not in MGUS or control samples measured by flow cytometry or RT-PCR methods[913]. Additionally, in RNA-seq studies also revealed that *CALR* gene was within the top 50 genes highly expressed in MM patients[914]. Interestingly *EIF2A* and other UPR-related markers were also up-regulated in MM patients and were associated with disease

progression[915]. For example, in AML or NSCLC samples, neoplasms that have been found to express elevated and heterogeneous ecto-CRT in basal conditions, only 7 out of 2132 AML samples, were found to be mutated in *CALR* gene, whereas no mutations in NSCLC samples. This indicates that *CALR* mutations are not driving CRT exposure in these types of tumours, which may be similar to what is probably occurring in MM. Furthermore, it would also be interesting to evaluate the relationship between ecto-CRT expression in cancer cells and the anti-myeloma immunosurveillance in MM patients. For instance, in NSCLC and AML patients, increased basal ecto-CRT levels was associated with improved immunosurveillance and superior relapse-free and overall survival[286,916]. Thereby, we aimed to investigate these elements in our patient's samples. In the following section we will address these topics more deeply.

In summary, the diverse and apparent contradictory roles of CRT on the Immune System and the final outcome they produce may depend on different factors, including: protein mutations and polymorphisms, the CRT binding partners, the regions of the protein implicated and the post-translational modifications that CRT may undergo and the subcellular localization[874].

To conclude, here we have shown for the first time that myeloma cells from BM samples isolated from patients with plasma cell dyscrasias, display elevated levels of ecto-CRT on their surface. Moreover, data suggest that ecto-CRT levels seems to increase with disease progression. This observation together with the fact that CRT exposure is chemotherapy-independent, and that patients with an altered cytogenetic signature display increased levels of ecto-CRT, may point towards malignant transformation as the instigator of this molecular event.

4.5.3.2. CRT & BM Microenvironment.

As mentioned before, increased CRT exposure or expression whether chemotherapy-driven or rather, derived from the oncological transformation process, could hold a predictive value in cancer patients. Depending on the cancer cell type, this DAMP has been found to be associated with an improved anticancer immunesurveillance and consequently with an improved patient's outcome[284]. In this work, we sought to investigate the relationship that may exist between CRT exposure and the BM microenvironment in BM samples from patients with plasma cell disorders. Henceforth, we evaluated the infiltration of different immune populations, as well as the expression of immune markers involved in anticancer immune responses, like the PD-L1/PD-1 axis, to determine the immune tonus of affected individuals. To interrogate the connection between ecto-CRT and the BM immune landscape, we segregated patients in two groups (CRT^{hi} and CRT^{lo}) based on the expression of this DAMP in the surface of $CD38^{+}$ cells. The stratification cut-off or threshold was the corresponding ecto-CRT median value from the total sample population. Therefore, those patients that had increased ecto-CRT

levels compared to the median value were categorized as CRT^{hi}, while those patients that exhibited an ecto-CRT expression level equal or inferior to the median value were deemed as CRT^{lo}.

Results presented in **Figure 4.61** exhibit that BM **NK** frequencies were significantly increased in patients with an elevated surface expression of CRT. Regarding the **T cell repertoire**, CRT^{hi} patients significantly exhibited lower total $CD4^+CD3^+$ T cells in the BM compared to CRT^{lo} samples. In contrast, no significant differences in total $CD8^+CD3^+$ T cell counts were found in the BM between patients displaying high or low levels of ecto-CRT. Nonetheless, a slight tendency towards superior total $CD8^+CD3^+$ T cell frequencies could be noticed in CRT^{hi} cohort. Regarding the total number of $CD3^+$ T lymphocytes, a strong tendency towards lower total BM $CD3^+$ cells, that did not reached statistical significance ($p=0.07$), was encountered in patients with increased levels of surface-CRT. Additionally, similar to the total frequency of $CD4^+$ T cell population, the proportion of $CD4^+$ cells within $CD3^+$ subset were significantly reduced in patients with increased ecto-CRT levels. In the case of $CD8^+$ T lymphocytes, the percentage of these cells relative to $CD3^+$ cells were increased in CRT^{hi} group. Total frequencies of different **DCs** subsets were also analysed. Data manifest that both $CD123^+$HLA-DR^+ plasmacytoid (pDCs) and $CD11c^+$HLA-DR^+ myeloid (mDCs) DCs subpopulations, were found to be increased in patients with elevated ecto-CRT expression levels. At first, with data presented so far, patients exhibiting elevated surface expression of CRT correlate with an improved anticancer immunosurveillance. This is indicated by the increased infiltration of NK cells, $CD8^+$ T cells and DCs, possibly reminiscent of a T_H1 anticancer immune response. However, the circumstances described above, won't ensue as easy as initially conceived.

Additionally, two immunosuppressive markers, **Treg** frequencies and **PD-1/PD-L1** expression, were also assessed (**Figure 4.62**). Intriguingly, in sharp contrast to presumed expectations, CRT^{hi} patients displayed a significant superior BM Tregs infiltration compared to patients with lower CRT surface expression. As regards to PD-L1 expression, $CD38^+$ plasma cells from CRT^{hi} patients significantly exhibited increased PD-L1 expression compared to CRT^{lo} group. Similarly immune effector cells from patients expressing high levels of ecto-CRT, revealed an increased expression of the exhaustion marker PD-1. Only PD-1 expression on $CD4^+$ T cell subset reached statistical significance when CRT^{hi} vs. CRT^{lo} groups were compared, whereas a non-significant tendency towards superior PD-1 expression in $CD8^+$ T cells and NK cells from CRT^{hi} patients compared to their CRT^{lo} counterparts was manifested. Therefore, data presented herein, denote that patients with augmented CRT expression, would had an impaired immunosurveillance, with accumulation of immunosuppressive populations (Tregs) and also elevated expression of inhibitory checkpoint proteins both in myeloma cells and effector cells.

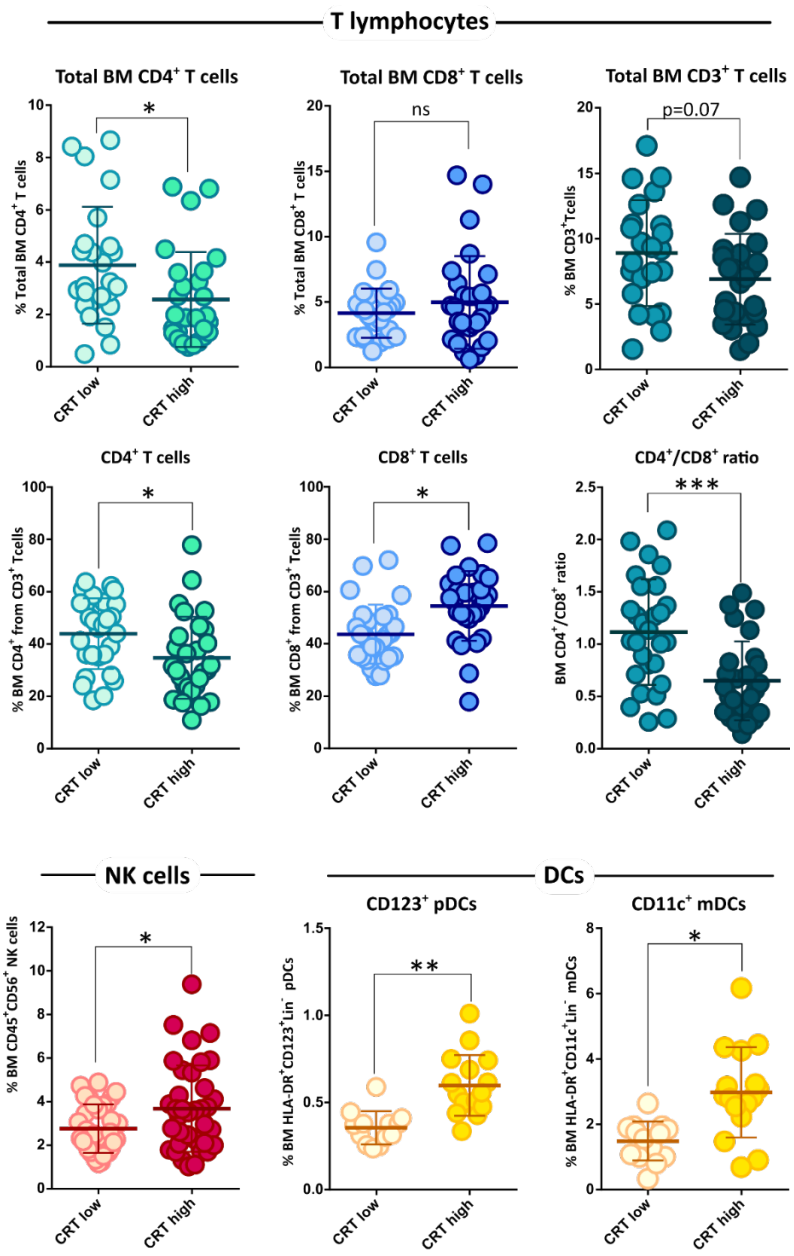

Figure 4.62 | CRT exposure and the BM immune landscape in MM. The relationship between ecto-CRT levels in CD38$^+$ BMMCs isolated from patients with plasma cell dyscrasias and the BM frequencies of different immune populations, or the expression of important immune markers in MM cells was examined. Patients were stratified in two different cohorts based on their median ecto-CRT levels. Individuals with an equal or superior value to the median CRT exposure cut-off of the entire population were deemed CRT^{Hi}, while individuals with an ecto-CRT expression level below the median cut-off were classified under CRT^{Lo} group. BM frequencies of total CD4$^+$CD3$^+$ T cells, total CD8$^+$CD3$^+$ T cells, total CD3$^+$ T lymphocytes, as well as the percentage of CD4$^+$ and CD8$^+$ T cells within CD3$^+$ population and the corresponding CD4$^+$/CD8$^+$ ratios were analysed by flow cytometry in CRT^{Hi} and CRT^{Lo} cohorts. Additionally, BM frequencies from CD56$^+$CD45$^+$ NK cells were determined by flow cytometry in CRT^{Hi} and CRT^{Lo} groups of patients. Plasmacytoid lineage-negative/HLA-DR$^+$/CD123$^+$ DCs (pDCs) as well as myeloid lineage-negative/HLA-DR$^+$/CD11c$^+$ DCs (mDCs) subpopulations were also analysed. Statistical analysis was performed using two-way t test, where *p<0.05, **p<0.01, ***p<0.001, ns, non-significant. Data plotted in the figure represent the frequency of each cell type in each individual. The mean and SD values in each patient cohort are also illustrated.

Data presented above points towards two contrasted findings. First, increased surface CRT expression on patient's myeloma cells correlate with elevated BM infiltration of immune effector cells ($CD8^+$ T cells or NK cells) and DCs. Alone, high density of these two immune subsets within the tumour milieu are indicative of good prognosis in a wide variety of human cancers[286,917,918]. At the same time, we have found that CRT exposure correlates with an immunosuppressive BM microenvironment, with the accumulation of Tregs and the increased expression of the inhibitory PD-1/PD-L1 axis. It is then possible that despite the increased density of the immune BM infiltrate, effector functions may be dampened by the immunosuppressive BM microenvironment, resulting in impaired anticancer immunity. In fact, it has been shown that MGUS progression to more advanced disease states correlated with increased calnexin, CRT and tapasin expression levels[913]. Moreover, MGUS $CD8^+$ T cells were more efficient in targeting autologous transformed plasma cells compared to their MM counterparts. Authors of this study suggested that changes in ER chaperones and antigen processing machinery, may allow transformed plasma cells to evade immunosurveillance more effectively[913]. A closer look into MM-associated BM niche may also point towards the same direction.

MM disease is distinctive for the close bonds that myeloma cells can establish with the BM microenvironment, as well as for the influence that the BM niche could cause to MM pathogenesis[409,432]. Indeed, MM is characterized by a deep immune dysfunction and a robust immunosuppressive phenotype that promotes immune escape and disease progression[409].

It is a well-known and even an assumed fact that MM patients suffer from a general disruption of the **T cell repertoire**[418]. However, despite the quantitative and functional alterations found in the T cell immune profile, clinically, MM patients do not suffer from infections associated with acquired or congenital T-cell deficiencies, like for example fungal or mycobacterial infections[418]. Nonetheless, MM patients hold a 10-fold increased risk for developing certain viral infections like herpes zoster and influenza[418,919]. Early studies reported reduced $CD4^+$ T cell numbers, increased $CD8^+$ T cell frequencies and consequently, low $CD4^+/CD8^+$ T cell ratios in peripheral blood or BM of MM patients[422,920–922]. These results have been validated in subsequent and more recent independent studies[923,924] and has also been associated with patient's survival. In particular, increased baseline $CD4^+$ T cell levels were associated with longer survival rates[422,925,926]. Similarly, marrow-infiltrated $CD4^+$ lymphocytes progressively decreased, while $CD8^+$ T cells gradually increased with advancing disease stages[927]. Additionally, clonal expansion of T cells are also found in MM patients[421,928]. However, despite increased circulating or BM-infiltrating $CD8^+$ T cell pools, that *a priori* might contribute to the anti-myeloma immune response, these cells are usually found to be functionally impaired. Whether MM-associated T cells are exhausted[832,842,843,929,930] or rather in a senescent state[837,838] is still a matter of debate. Current literature could not clearly state whether or not exhaustion and immunosenescence are two functionally and

mechanistically distinct phenotypes that can even coexist in the tumour bed or whether these two states can be functionally reversed[839,931,932]. Several studies have shown increased expression of inhibitory checkpoint proteins like PD-1, TIM-3, LAG-3 and TIGIT in the surface of T cells ($CD4^+$ or $CD8^+$) in peripheral blood or BM of MM patients[502,834,836,842,843,930,933]. Moreover, BM T cells have been shown to be severely more impaired that their peripheral blood counterparts[837,843,934]. In fact, some authors even manifested that exhausted BM $CD8^+$ T cells were hardly responsive to PD-1 blockade alone[930]. These cells downregulate CD28 costimulatory molecule, upregulate CD57 (indicating low proliferative capacity) and exhibit increased PD-1 expression[832]. Moreover, patients bearing T cells with this exhausted or senescent phenotype at baseline or after therapy, are the ones with more advance disease stage[838,934], MRD-positivity[929] or with more odds to relapse after ASCT[832,933].

Regarding the **NK** cell subset, several pieces of evidence indicate that NK cell population is increased both in peripheral blood and BM of MM patients when compared to healthy individuals[923,935–937]. Nonetheless, despite the increased NK trafficking or influx, the phenotype and functionality of these cells may be defective. Downregulation of activating receptors such as NKG2D, NKp30 or DNAM-1 (CD226)[938–941], together with the overexpression of inhibitory molecules like PD-1[942], has been found in NK cells from MM patients, potentially contributing to dampen NK effector functions and anti-myeloma activities. On the contrary, early studies reported discordant NK cell composition manifesting no changes[943,944] or even a decrease[945] in NK cell frequencies in peripheral blood of MM patients.

Frequencies and functions of **DCs** in MM disease still remains a disputed topic. As professional APCs, DCs present self- and non-self antigens to T lymphocytes in order to induce immune tolerance or alternatively, reactive adaptive immune responses. DCs have been reported to participate in normal plasma cell differentiation and survival[946,947]. Under pathologic conditions, pDCs numbers have been shown to be augmented in the BM of MM patients, as well as to foster MM proliferation, survival, chemotaxis and drug resistance[438]. Moreover, studies also manifested that mDCs and pDCs in peripheral blood or BM from MM patients are functionally defective. In particular it has been shown that DCs from MM patients retain impaired antigen presenting functions, decreased expression of maturation markers and a decreased ability to induce T cell proliferation[438,948,949]. Patrizia Leone and coworkers also showed that mDCs and pDCs accumulate in BM during MGUS to MM progression and can contribute to myeloma cell protection against $CD8^+$ T cell-mediated killing[435]. Additionally, it has been found that BM infiltrated DCs can propagate Th17 pool and increase the levels of IL-17 in MM patients, further contributing to myeloma growth and disease progression[950]. pDCs can also contribute to myeloma immune tolerance and to a depressed immune phenotype by inducing Treg development[951]. Conversely, frequencies of both mDCs and pDCs seem to follow another trend in peripheral blood of MM, since several studies reported reduced numbers of both DCs sub-types in MM compared to healthy controls[425,948,949].

Importantly, early studies have shown that increased DC infiltration in the tumour bed, especially if they hold an immature phenotype, correlated with adverse clinical prognosis in a variety of human cancers[952–954]. Conversely, other authors reported that high degree of DC infiltration was associated with improved clinical outcome[286,917,918]. Most probably, these differences may arise from the phenotype and maturation status of these cells, since a proper functional state is critical to generate tolerance or rather adaptive immune responses[415]. In MM, disparities in the clinical significance of DC population have also been encountered. Some authors argue that increased DCs populations may promote disease progression[435], while others revealed an inverse correlation between DCs frequencies and clinical stages. Nonetheless, despite all these confounding reports, many examples in the literature suggest that MM-DCs interplay can negatively impact on MM disease.

Conflicting data have also been reported in the number and functionality of **regulatory T cells** in the context of MM disease. High percentages of functional $CD4^+$ $CD25^+$ $FOXP3^+$ Tregs have been manifested in peripheral blood of MM patients[424,425,427,955,956]. In contrast, some authors manifested reduced peripheral blood Treg frequencies in MM patients compared to healthy controls[957]. Others however, despite finding elevated circulating Treg numbers, they seemed to be dysfunctional[958]. Marrow-residing $CD4^+$ $CD25^+$ $FOXP3^+$ Tregs have also been reported to accumulate in MM patients compared to healthy donors[427,959]. In contrast, some authors report that healthy and myelomatous BM share equivalent numbers of Tregs[960]. Importantly, some authors analysed the clinical significance of Treg population in MM disease. Studies revealed that the median survival rate and time to progression (TTP) of patients with lower Tregs were significantly longer than those with increased Treg numbers[425,427]. However, in a recent study, no clinical correlation between Treg subset and TTP in MGUS or PFS in MM was found, suggesting that although important, Tregs may not be major players in MGUS to MM progression[961]. Perhaps novel high-throughput and high-dimensional techniques like mass cytometry, may provide more clues and better phenotyping criteria to discern discrete immune cell populations that could pose important contributions in the progression through the different disease stages[962]. In fact, in a recent study using these novel tools, a discrete $CD39^-$ Treg subset was able to discriminate between MGUS and newly diagnosed MM patients[962].

Developmental programmes of Treg and Th17 cell subsets are closely intertwined[963]. While upon TCR activation and under TGF-β presence, naïve T cells may derive to express Foxp3 and become Tregs, emergence of IL-6 or IL-21 in conjunction with TGF-β in the T-cell surroundings, abrogates Treg development and shift towards Th17 generation[963]. Although in our study we have not characterized the presence of Th17 cells in MM patients, these T cell subtype has also been revealed to accumulate in the BM and contribute to the immunosuppressive atmosphere generated in the BM in MM disease[964–966]. Furthermore, it has been suggested that the balance of Treg/Th17 subsets may bear more clinical importance than each subset alone in MM disease[965].

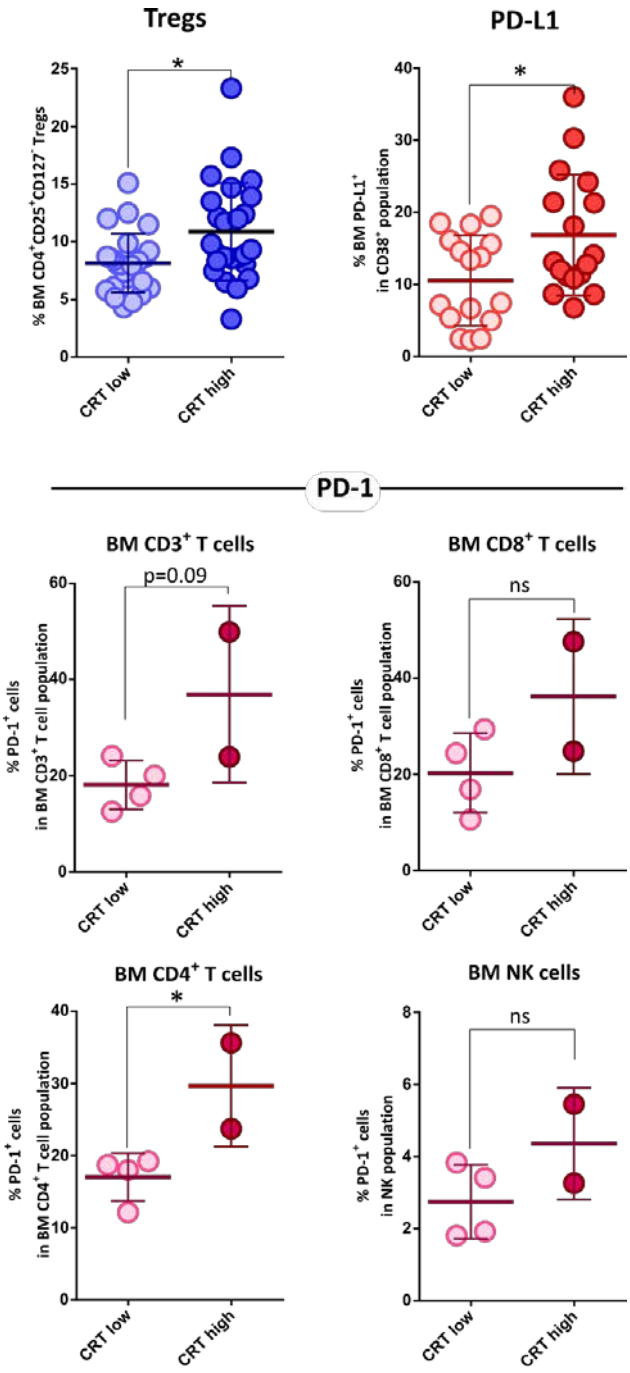

Figure 4.63 | CRT exposure and the BM immune landscape in MM. PD-1/PD-L1 axis and Tregs. The relationship between ecto-CRT levels in CD38$^+$ BMMCs isolated from patients with plasma cell dyscrasias and the BM frequencies of different immune populations, or the expression of important immune markers in MM cells was examined. Patients were stratified in two different cohorts based on their median ecto-CRT levels. Individuals with an equal or superior value to the median CRT exposure cut-off of the entire population were deemed CRT^{Hi}, while individuals with an ecto-CRT expression level below the median cut-off were classified under CRT^{Lo} group. Frequencies of CD4$^+$ CD25$^+$CD127-negative Tregs were also determined in CRT^{Hi} and CRT^{Lo} cohorts. PD-1/PD-L1 axis were also evaluated in BM of CRT^{Hi} and CRT^{Lo} individuals. Expression of PD-L1 was examined in CD38$^+$ BMMCs from affected individuals and PD-L1 levels were compared between CRT^{Hi} and CRT^{Lo} groups. Additionally, PD-1 expression was analysed in the indicated immune subpopulations CD56$^+$CD45$^+$ NK cells, CD3$^+$ T lymphocytes as well as in CD4$^+$CD3$^+$ and CD8$^+$CD3$^+$ T cells. PD-1 levels were then compared in patient's subgroups based on their ecto-CRT expression levels. Statistical analysis was performed using two-tail t test, where *p<0.05, **p<0.01, ***p<0.001, ns, non-significant. Data plotted in the figure represent the frequency of each cell type in each individual. Global Mean and SD in each patient cohort are also illustrated.

As it has been gradually introduced throughout this discussion, PD-1/PD-L1 axis, is also thought to be a major contributor to the MM immunosuppressive profile. As mentioned earlier, MM-associated T cells and NK cells express high levels of inhibitory checkpoint proteins like PD-1. Additionally, MM cells have also been found to express elevated levels for the ligand for this receptor, that is, PD-L1[440,494,502,825,967,968], thereby counteracting and dampening T/NK cell immune activation. For instance, PD-L1 expression on malignant plasma cells is associated with a more aggressive phenotype and with more advanced disease stages[493,969]. Moreover, myeloma cells are not the unique cell type that overexpresses PD-L1. In fact, pDCs or MDSCs have also been found to upregulate PD-L1 levels in MM disease[497,967,968].

Altogether, although some points may remain debatable, the MM immune landscape encompasses the following enactors (**Figure 4.64**):

- Altered and dysfunctional circulating or BM-infiltrating T cell immune profile, with reduced CD4+ T cells, increased CD8 T cells which translates into reduced CD4/CD8 T cell ratios.
- Increased peripheral blood or BM NK cell numbers but with an impaired functionality.
- Elevated BM mDC and pDCs with weakened functions in antigen-presenting and processing capacity.
- Increased Treg frequencies in BM or PB.
- Augmented activity of inhibitory immune checkpoints like PD-1/PD-L1 axis, and possibly others (CTLA-4, TIM-3, LAG-3).
- Elevated immunosuppressive MDSCs and TAMs in the tumour milieu.

As one may figure out from this scenery, MM disease is accompanied by a severe immunosuppressive environment. Intriguingly, some of these factors have been associated with worse clinical outcome and prognosis in MM patients. Therefore, attending at the data presented in this study and the panorama discussed above, it can be suggested that CRT^{hi} patients carry immune features associated with an undermined and subverted immune microenvironment, which could also be translated into a poor clinical outcome. For instance, this assumption also agrees with the fact that CRT^{hi} cohort harboured more cytogenetic abnormalities, some of which have been correlated with worse prognosis[854].

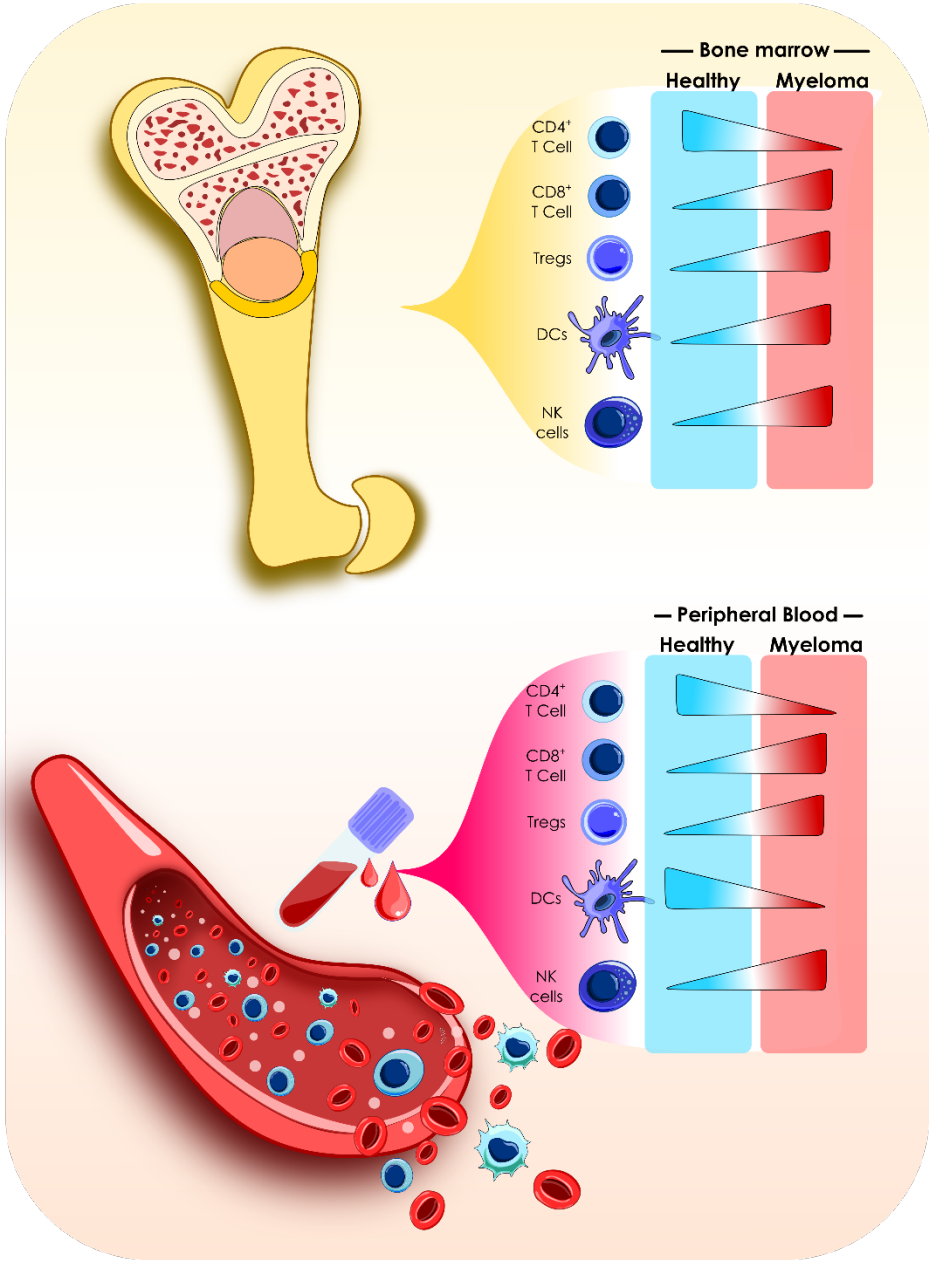

Figure 4.64 | MM immune landscape in BM and peripheral blood. The variation of different immune cells between healthy and myeloma BM and peripheral blood compartments are depicted.

It is enthralling that individuals with higher ecto-CRT expression have more cytogenetic alterations and this subsequently correlated with increased infiltration of effector cells (NK and $CD8^+$ T cells) and DCs, although they may be functionally impaired. Loss of genomic stability is a well-recognized hallmark of cancer in general and especially in MM[970]. Among the different aberrations that emerge as a consequences of this instability, deletions, insertions, inversions, translocations are included[970]. Therefore, cytogenetic alterations may hide a state with increased genomic instability that consequently increase the load of somatic mutations in malignant cells. Supporting this idea there is an emerging concept termed 'transcription-coupled mutagenesis', in which mutations occurred at an increased rate in tumours in which transcriptional

upregulation of genes occurred as a consequence of translocations[970]. Thereby, a link between presence of cytogenetic abnormalities, increased mutational load and consequently enhanced infiltration of immune cells can be established. This is of particular importance since tumour-specific mutations are an estimable source of immunogenic neoantigens. Moreover, neoantigens have the potential to be presented in the context of MHC-I molecules to cytotoxic T cells generating an adaptive antitumour response with the ability to generate memory that tackle cancer relapse.

In solid tumours classically considered highly mutagenic, increased mutational burden and hence neoantigen load, has been associated with increased immune infiltration, improved anticancer immunosurveillance and prolonged survival rates when subjected to checkpoint blockade therapy[402,971,972]. However, this is not the case for MM. Early clinical trials evaluating the use of checkpoint blockade therapy as single-agents were discouraging[496]. In the famous chart depicting pan-cancer somatic mutations and the resultant neoantigens densities, myeloma occupies a median-ranged position, with 1.6 mutations per Mb compared to the 10 mutations per Mb in melanoma or lung cancer[790,831,912]. Nonetheless, it has been shown that mutational load increases with myeloma progression[789,973]. Moreover, it has been recently reported that high somatic mutation densities and neoantigen load correlates with a worse clinical outcome, with reduced PFS in MM patients[789]. At this respect, it is possible that in MM, despite displaying an increased mutational load and a widened neoantigen repertoire, these factors alone (and even with the assistance of checkpoint blockade therapy), might not be sufficient to revert the deep suppressive immune landscape present in this disease. Therefore, although initially primed and instructed, anti-myeloma effector immune responses fail in their mission to confront myeloma disease, underpinning the intricacy of the underlying immunosuppressive networks that give myeloma 'green-light' to escape[831]. Therefore, reverting this immunosuppressive state is of paramount importance.

Finally, it must be mentioned that our data contrast with results presented in other studies in which a positive correlation between CRT exposure or expression and improved anticancer immunosurveillance and immune signatures, usually accompanied by favourable patient's prognosis was found. For example, in NSCLC patients, the level of CRT expression, together with p-eIF2α levels on tumour cells, (measured by immunohistochemistry, IHC) correlated with a dense intratumoral infiltration of mature DCs and effector T cell subsets[286]. These findings were also reproduced at the mRNA expression level, showing that in breast, colorectal and ovarian cancer, *CALR* mRNA expression correlated with the immune infiltrate (CTL and DCs), whereas a negative correlation between these parameters were found in NSCLC patients[287]. Discrepancies between mRNA and protein expression levels in NSCLC studies may arise as a consequence of the lack of reflection of post-transcriptional and post-translational regulatory mechanisms of gene expression in *CALR* mRNA quantification[287]. Similarly, the expression level of CRT was found to be associated with infiltration of T cells in IIIB

stage colon cancer patients[288]. Along similar lines, AML patients in which malignant blast expressed high levels of ecto-CRT regardless of chemotherapy, correlated with the activation of anticancer Th1 immune response[289]. This was translated into elevated circulating tumour-specific $CD4^+$ and $CD8^+$ T cells, as well as increased number of circulating NK cells[289]. Similar conclusions were drawn out by the work from Wemeau *et al.* in AML patients[889]. Additionally, by combining IHC and biomolecular analysis, another study manifested that ovarian cancer patients with elevated expression of CRT strongly correlates with superior density of DC-$LAMP^+$ DCs and $CD20^+$ B cells that result in Th1-polarization and higher cytotoxic functions on effector $CD8^+$ T cells and NK cells[974]. Other studies, however, reported less encouraging results. For example, Aoto *et al.* found no correlations between the number of infiltrating $CD8^+$ T lymphocytes and the expression of CRT or HMGB1 in breast cancer patients[301].

In summary, our data showed that patients with elevated ecto-CRT levels were associated with increased BM infiltration of immune effectors like $CD8^+$ T cells, NK cells and DCs, with the exception of reduced $CD4^+$ T cells. On the other side, CRT^{hi} cohort correlated with expanded immunosuppressive hallmarks like Tregs and PD-1/PD-L1 axis. Together, all these different players delineate a BM immunophenotypic landscape associated with poor clinical outcome and prognosis in the context of MM disease.

4.5.3.3. CRT & Clinical Outcome and Prognosis in MM patients.

To really establish a connection between CRT surface expression and the clinical outcome of patients with plasma cell disorders, we analysed different available clinical prognostic markers in CRT^{hi} and CRT^{lo} patient's cohorts. In particular, we evaluated the relationship between ecto-CRT expression and the number of lines of therapy patients received, the time to progression (TTP) since last treatment, the occurrence of plasmacytomas, the number of exitus during the course of the study, and finally, with the presence of specific cytogenetic abnormalities with a variable range of risk.

As shown in **Figure 4.65**, patients with increased expression of surface-CRT significantly received a higher number of lines of therapy compared to CRT^{lo} cohort. Consequently, CRT^{hi} individuals significantly exhibited a reduced TTP compared to patients displaying low levels of surface-CRT. Furthermore, although it did not reach statistical significance, probably due to the limited number of available clinical data, CRT^{hi} cohort had a higher proportion of *exitus* compared to CRT^{lo} individuals. Development of soft-tissue plasmacytomas is a sign of the presence of clonal plasma cells growing outside the BM that can appear either in newly diagnosed individuals or during disease progression[975,976]. As one would expect, losing BM-dependency is a negative sign and patients bearing extramedullary plasmacytomas, often exhibit poor clinical outcomes[975–977]. The occurrence of extramedullary plasmacytomas were more frequent in patients with higher levels of ecto-CRT. In other words, individuals with presence of

extramedullary plasmacytomas displayed a significant increase of ecto-CRT levels. Finally, as presented before, patients with an altered cytogenetic signature displayed increased levels of ecto-CRT in the surface of malignant plasmablasts. Here, we dissected the different specific cytogenetic abnormalities harboured by these patients and the exposure of CRT that exhibited in each case. As shown, patients with no cytogenetic alteration displayed a lower level of cell surface-CRT. No significant differences were found in ecto-CRT levels between patients bearing a t(11;14) translocation, which is considered to be a neutral prognostic factor[854], with patients with a normal cytogenetic signature. However, the number of data points together with the high dispersion in this group, do not allow to extract clear conclusions. Regarding the high-risk t(4;14) alteration, patients with this cytogenetic abnormality had increased ecto-CRT levels compared to patients with normal cytogenetics. Again, no significant differences were found, probably due to the low number of data points in this condition. Finally, the high-risk cytogenetic abnormalities 1q gain, p53 and t(14;16), all of them associated with an adverse clinical outcome[392,854], showed significant increased levels of surface-CRT compared to the group without any cytogenetic abnormality.

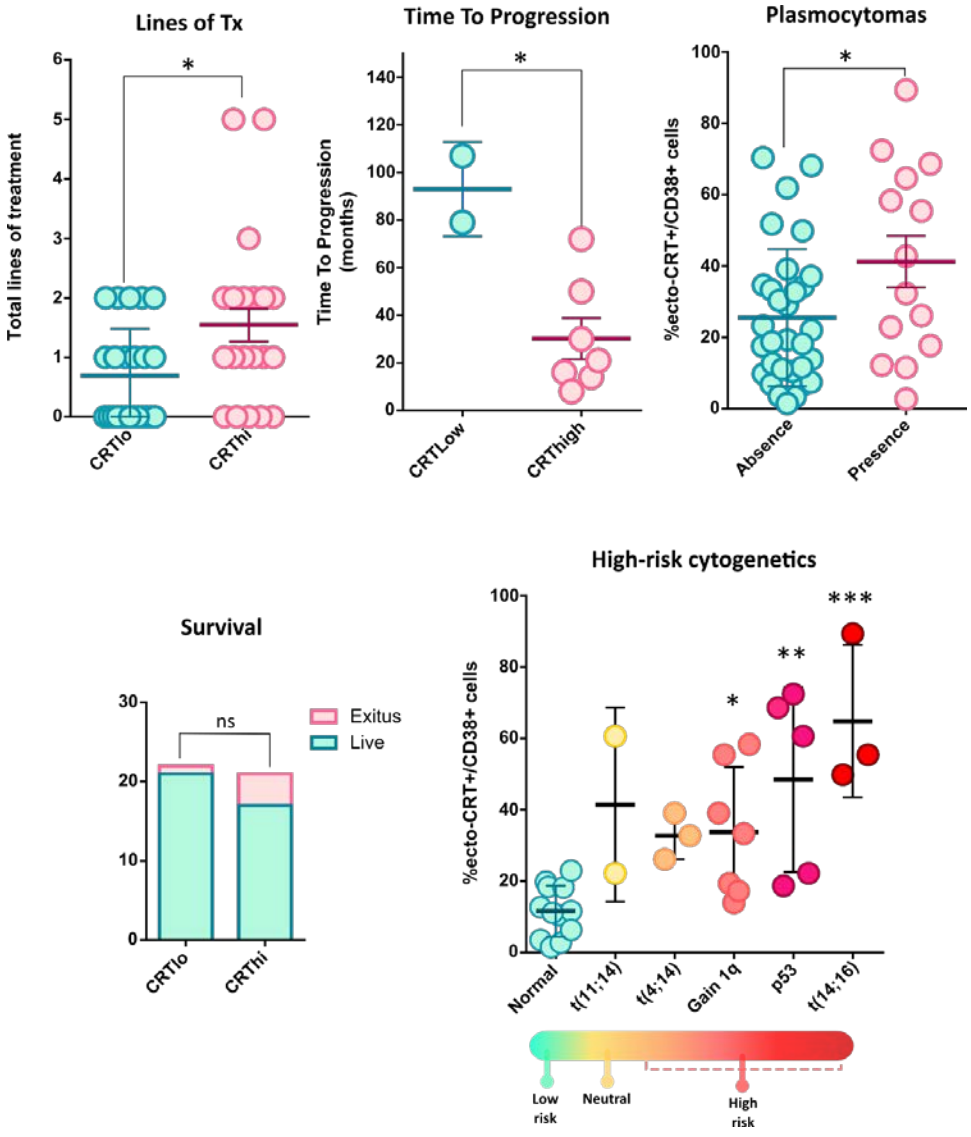

Figure 4.65 | Prognostic potential of CRT exposure on MM clinical outcome. The relationship between ecto-CRT levels in CD38^{+} BMMCs isolated from patients with plasma cell dyscrasias and different clinical markers was examined. Patients were stratified in two different cohorts based on their median ecto-CRT levels. Individuals with an equal or superior value to the median CRT exposure cut-off of the entire population were deemed CRT^{Hi}, while individuals with an ecto-CRT expression level below the median cut-off were classified under CRT^{Lo} group. The number of total lines of therapy patients received, the time to progression (TTP) or in other words, the time that patients take to relapse since last treatment, as well as the occurrence of extramedullary plasmacytomas were compared between CRT^{Hi} and CRT^{Lo} cohorts. Statistical analysis was performed using two-way t test, where *p<0.05, **p<0.01, ***p<0.001, ns, non-significant. Additionally, the proportion of exitus and live patients upon completion of this study were compared between CRT^{Hi} and CRT^{Lo} subgroups. Statistical analysis was performed using Fisher's exact test, where *p<0.05, **p<0.01, ***p<0.001, ns, non-significant. Finally, the relationship between CRT exposure and the presence of different cytogenetic abnormalities with varying degrees of risks were interrogated. In particular ecto-CRT expression was examined in patients with normal cytogenetic signature, patients that harbour neutral-risk t(11;14) abnormalities, and patients with high-risk t(4;14), 1q gain, p53 and t(14;16) cytogenetic abnormalities. Statistical analysis was performed by comparing each of the different groups harbouring cytogenetic abnormalities with the normal group, using one-way ANOVA test, with Tukey post-test where *p<0.05, **p<0.01, ***p<0.001, ns, non-significant.

As mentioned before, accumulating grounds of evidence support the idea that DAMPs may hold prognostic and predictive value for monitoring cancer patients[284,740]. In the previous section, we have seen that the BM microenvironment and the immune landscape established in CRT^{hi} cohort exhibits more immunosuppressive hallmarks that could be translated into advanced disease stages and worse clinical outcome. Here, we directly inspected the clinical significance of ecto-CRT expression and the data presented above point towards the same direction, suggesting that increased levels of cell surface-CRT may be associated with more aggressive clinical features and hence with worse clinical prognosis.

It has been shown that the relationship between CRT levels and clinical outcome in cancer patients strongly relies on the specific tumour type under evaluation. For example, chemotherapy-independent CRT exposure on malignant blasts has been associated with increased circulating frequencies of effector cells and improved relapse-free survival and overall survival in AML patients[889,916]. Likewise, in ovarian cancer patients, CRT exposure regardless of chemotherapy correlated with higher densities of infiltrated immune cells and also improved prognostic assessment on relapse-free survival and overall survival[287,974]. Similar observations can be inferred from studies on NSCLC patients, in which CRT expression also constituted a relevant prognostic biomarker that reflected local immune infiltration and good clinical outcome in two independent cohorts of NSCLC patients[286,287]. Favourable clinical outcomes have been also observed in neuroblastoma, glioblastoma, colorectal and endometrial cancer patients in which cancer cells expressed high levels of CRT[288,292,978,979]. In contrast, in other types of tumours, high expression of CRT may not carry so propitious news as in these previous examples. Indeed, positive immunohistochemical staining of CRT in patient's samples from gastric tumour tissue correlated with more aggressive

clinicopathologic factors and invasiveness and thereby poorer survival rates[293]. In breast cancer patients, CRT overexpression was also associated with post-operative occurrence of distant metastasis[980]. Others, however, reported no significant correlations between clinicopathological parameters and CRT overexpression in infiltrating ductal breast carcinomas[981]. In oral squamous cell carcinoma, high expression of CRT, evaluated by immunohistochemical analysis, correlated with disease stages and reduced term of survival[982]. In addition, increased *CALR* mRNA levels predicted worse clinical outcome in bladder cancer, neuroblastoma and mantle cell lymphoma[295]. Finally, increased CRT expression, analysed by immunohistochemical approaches, in pancreatic cancer tissues was associated with reduced survival rates[983].

Interestingly, there is a marker that has not been assessed in our study and might also contribute to explain the negative relationship between CRT exposure and the clinical outcome in cancer. In particular, it has been reported that CRT exposure is usually accompanied by an enhanced expression of the anti-phagocytic molecule CD47[740]. Thereby, in order to counteract the potent phagocytic signals emanated from stressed high-expressing CRT cancer cells, tumours upregulate anti-phagocytic signals like CD47 in a coordinated manner to prevent becoming an 'appetising meal' to APCs and other phagocytic cells. In this way, anticancer immune responses could be subverted. Increased CD47 expression has been found in a wide variety of human cancers, including AML, esophageal squamous cell carcinoma, mesothelioma, breast, gastric, ovarian cancer, melanoma, NSCLC generally being associated with an aggressive, invasive and metastatic phenotype, adverse prognosis and poor clinical outcome[984–993]. Moreover, potent antitumour activity has been reported in several preclinical solid and haematological cancer models[994,995]. This growing interest and encouraging results has allowed to launch phase I clinical trials investigating different designs of anti-CD47 antibodies[996–998]. In the particular case of MM, several studies have shown that, similar to our findings in the pattern of CRT exposure, CD47 overexpression was directly associated with disease stages (from MGUS to overt MM)[999–1001]. It is tempting to speculate that, as a mechanism to counteract the pro-phagocytic CRT exposure that arise from therapy-driven or oncogenic-induced transformation, myeloma cells overexpress anti-phagocytic molecules like CD47 that may serve as additional immune evasion mechanism. Thereby, this molecule also encompasses a potentially reliable predictor of clinical outcome and survival. This also would explain that increased CRT exposure in MM patients is associated with poorer prognosis. Although to confirm these assumptions both molecules should be tested in patient's samples and proper statistical analysis with clinical data should be performed in different and independent cohorts.

Besides CRT, other cellular markers informing of an ongoing UPR response have also been associated with clinical outcome of cancer patients[740]. For example, variable clinical outcomes have been ascribed to eIF2α phosphorylation in different tumours. While in NSCLC phosphorylated eIF2α has been associated with favourable disease outcome, in breast cancer patients elevated p-eIF2α is correlated with worse

prognosis[81,83,296]. Additionally, high expression of other ER stress proteins like BiP/GRP78 (HSPA5) has negative connotations in diffuse-large B cell lymphomas, gastric, esophageal, ovarian and breast cancer patients, among many others[620,641,1002–1005]. However, lung cancer seems to be an exception and a positive correlation between OS and BiP/GRP78 expression has been found in these cancer patients[297].

Other DAMPs have also been shown to retain predictive potential in cancer patients. For example, as previously noted, ATP is critical in the recruitment of immune cells to initiate the anticancer immune response. Indirect clinical evidence supporting the role of ATP in cancer patients is beginning to emerge. For example, a specific polymorphism of P2X7 receptors that compromise its function, has been correlated with worse clinical outcome in breast[86] and thyroid cancer patients[1006], as well as an increased risk of developing B-CLL[1007]. In contrast, the same P2X7 receptor polymorphism, had no effects on clinical prognostic markers or survival in MM patients[1008]. However, evaluation of the expression of autophagic-related proteins Beclin 1 and LC3, assessed by IHC, revealed that increased expression of these markers in MM samples were associated with superior patient's survival rates[1009]. Additionally, a prognostic evaluation model based on expression signatures of different autophagy-related genes was able to predict the clinical outcome of patients bearing MM disease[1010]. However, whether the role of autophagy in the clinical impact of MM patients is related to its DAMP-trafficking functions or rather to its functions in recycling and degradation pathways, requires further comprehension.

In summary, our data seem to indicate that increased ecto-CRT exposure is associated with poor prognosis in MM disease, since individuals with augmented expression of ecto-CRT significantly exhibit lower time to progression rates, increased chances of developing extramedullary plasmacytomas, are heavily-pretreated and harbour a high-risk cytogenetic signature.

GENERAL DISCUSSION

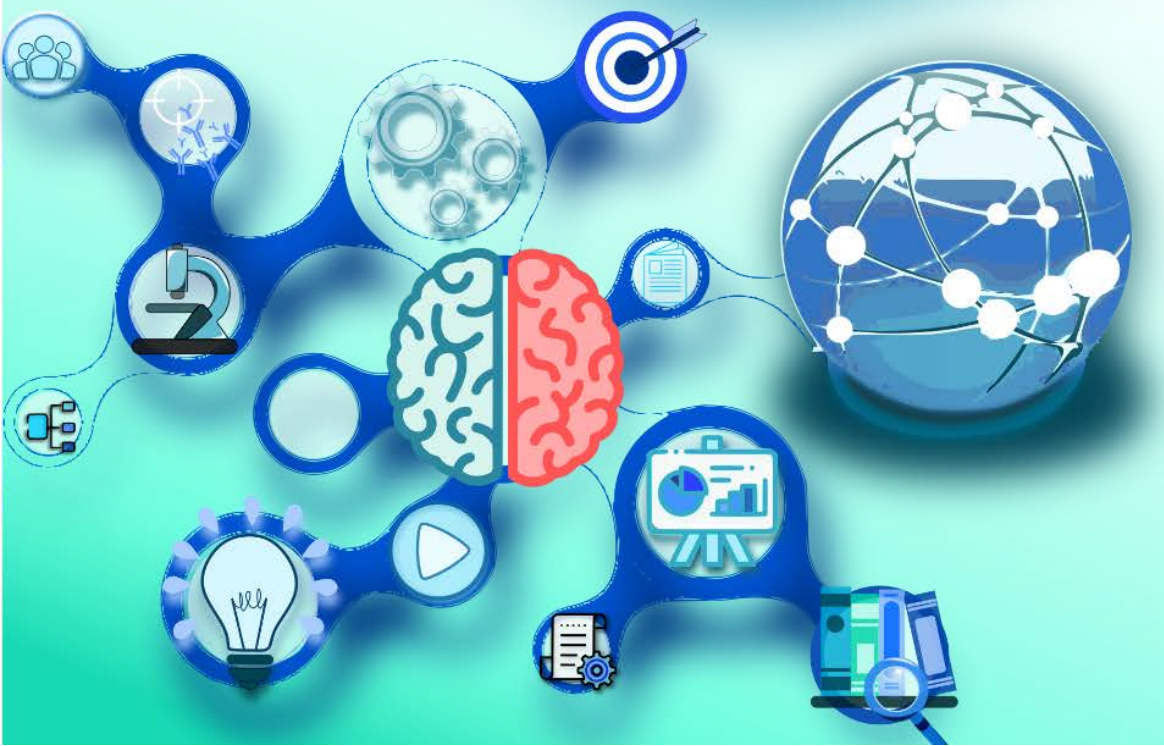

5. GENERAL DISCUSSION.

In cancer research, the study of the molecular cell death mechanisms triggered by chemotherapeutics is paramount not only to understand its inherent mechanisms of action, but also to devise optimized and improved novel therapeutic approaches to tackle relapse. Furthermore, over recent years immunotherapy has burst into the clinic providing optimism for cancer patients. Indeed, immunological responses are thought to underlie the long-term effects of conventional or targeted-therapies. Thereby, when dealing with a complex, heterogeneous and multifaceted disease like cancer, a combined and intertwined examination of these two aspects is of utmost relevance. Nowadays, current anticancer treatments are able to fight cancer and induce cell death through different cellular mechanisms like apoptosis, necroptosis, ICD and mitotic catastrophe, among others. In this work we aimed to study not only the different cell death mechanisms that could potentially contribute to cell death exerted by current and novel antitumoral drugs, but also to explore the immunogenic nature underlying these types of cell demise.

First, the contribution of mitotic catastrophe in the induction of cell death exerted by antimitotic agents and the cell death mechanisms when combined with BH3-mimetics were investigated. As shown, treatment with antimitotic agents alone provoked important hallmarks of mitotic catastrophe, such as multinucleation and micronucleation, which were preceded, in some cases, by a robust mitotic arrest. Nonetheless, cell death upon mitotic inhibition alone did not render a prominent apoptotic response. All these observations were also evidenced in cell fate profiles from cells treated with the different antimitotic drugs alone. Moreover, as witnessed throughout this study and also foreseen by Gascoigne & Taylor[62], inter- and intra-line divergence of cell behaviours in response to the different antimitotic treatments emphasize the complexity of cell fates and cell responses to antimitotic drugs, which hinders finding easy conclusions.

Although mitotic catastrophe could drive cells through different cell death pathways, like apoptosis or necrosis[55], it is generally accepted that a great majority of instances of cell demise show hallmarks of apoptosis in response to antimitotic drugs[63,92]. More specifically, previous reports indicate that cell death induced by mitotic catastrophe, is essentially Bax- and Bak-dependent and proceed through the intrinsic apoptotic and caspase-dependent cell death pathway[549,592–595]. Our results also provide evidences in the same direction since cell death exerted by these drug combinations has been found to be manifestly caspase- and Bax/Bak-dependent. Nonetheless, drug resistance development to classical chemotherapeutics like MTAs[92] and the initial failure of novel antimitotic agents that target mitotic kinases and motor proteins in clinical trials[96], urge to devise new therapeutic approaches that confront these problems.

The competitive networks model declares that cell fate in response to anomalous mitosis is determined by the finely-tuned balance between cell death signals and the mechanisms that control mitotic exit[62,63]. For these reasons, a good therapeutic strategy to tilt the cell fate equilibrium in favour of cell death and upgrade the efficacy of antimitotic drugs, would demand accelerating or increasing the intensity of death signals during mitosis. At this respect, Bcl-2 family of proteins are key regulators of apoptotic cell death pathways and have been shown to be pivotal in cell fate decisions and to confer protection under prolonged mitotic arrest[73,547]. For that reason, BH3-mimetics stand as good therapeutic candidates by targeting anti-apoptotic proteins, neutralising their pro-survival activity and hence tipping the balance towards cell death[12,542]. Therefore, in an attempt to help shedding more light and scrutinising the regulatory interface between mitotic checkpoints and cell death mechanisms during mitotic catastrophe, we aimed to study the role of this critical and at the same time versatile Bcl-2 family of proteins in the regulation of cell fate upon mitotic arrest.

As presented in this work, our results revealed a strong cell death potentiation effect when combining antimitotic agents with the BH3-mimetic ABT-737, especially in A549 and MIA PaCa-2 cell lines. Indeed, literature supports that ABT-737 effectively sensitises multiple cancer cell models to taxanes[544–547], as well as in xenograft models[548]. Probably, the observed increased antitumour efficacy of ABT-737-based combinations compared to that exerted by ABT-199 may be explained by the broader range of inhibitory targets that ABT-737 can handle[12,542]. Although assessing the relative contribution of a given pro-survival member is complicated by the functional overlap that exists between the different proteins, decrypting the relative value of Bcl-2 family members to cell fate is pivotal from a mechanistic and therapeutic point of view. In general, although a particular addiction to a specific anti-apoptotic protein may emerge in some situations, generally, cancer cells could counterbalance this deficiency with other pro-survival members. Several laboratories have struggled to discern the particular participation of each Bcl-2 family member in cell death upon mitotic blockade, but no general consensus has been met so far. While some studies support Mcl-1 as a molecular timer that determines cell survival during mitosis[563–565], others back up for a specific Bcl-X_L addiction[70,72,73,543,549,566–568], or even involve minor secondary members like Bcl-W in cell death during mitotic arrest[569]. However, at least under our experimental settings, the different anti-apoptotic members seem to hold a cooperative and cumulative protection effect. While inhibition of Bcl-2 with ABT-199 slightly potentiated cell death, simultaneous repression of Bcl-2 and Bcl-X_L (and Bcl-W) with ABT-737, had an additive potentiation effect to that observed by ABT-199, but a dramatic effect over antimitotic drugs alone. In the particular case of MIA PaCa-2 cells that hold low basal Bcl-X_L levels, Bcl-X_L overexpression did not completely prevent cell demise but instead, delayed it upon antimitotic and BH3 mimetic drug combination.

Another interesting remark we came across is that compounds that instigated a sustained mitotic blockade, like docetaxel and vincristine, were usually more cytotoxic

than those in which mitotic arrest was only transient, like barasertib. This also correlates with the increased mitotic cell death rates revealed in cell fate profiles, which escalated with those antimitotic agents that provoked a longer mitotic arrest. On that circumstances, a persistent mitotic delay would elicit post-translation modifications that would alter Bcl-2 family functionality like reducing Mcl-1 stability and blunting Bcl-2 and Bcl-X_L anti-apoptotic activities through phosphorylation[55,73,92,547,549]. Indeed, we showed that Bcl-2 and Bcl-X_L became highly phosphorylated in presence of mitotic blockers such as docetaxel and vincristine, but not with barasertib, a mitotic driver. Hence, this might explain the special vulnerability of cells treated with MTAs to ABT-737 administration. Under circumstances in which anti-apoptotic Bcl-2 family function was abrogated, adding a BH3 mimetic further contributed to incline the balance to pro-death signals and ultimately instigated cell demise with more intensity. In addition, during MTA treatment, probably the observed accumulation of mitotic proteins (MAD2, BUB1, BUBR1 and CycB1) observed in A549 cells is indicative of a robust and active SAC signalling. In fact, this accumulation of MAD2, BUB1 and BUBR1 in mitosis-arrested cells has also been reported by others[587]. BUBR1 is one of the mitotic proteins been proposed to sense mitotic damage and engage apoptosis[573,582,588,589]. Then it is possible that BUBR1 accumulation in docetaxel and vincristine treated cells could reflect its increased propensity to die either during or after mitosis, compared to barasertib in which BUBR1 levels were severely diminished. Collectively, from the data obtained in this work, the participation of any particular Bcl-2 member in this scenery cannot be dismissed. Probably our data suggest that all these anti-apoptotic proteins may have redundant and cooperative roles in cell fate decisions during aberrant mitosis. Results point to Bcl-X_L to hold a partial or auxiliary role in cell death regulation during mitotic blockade and that other pro-survival members like Bcl-2 and Mcl-1 among others, could collaboratively take part in cell death modulation by mitotic catastrophe. Nonetheless, this might depend on the specific drug and cell line under evaluation.

One enthralling topic that still remains obscure is whether mitotic timing influences cell fate upon mitotic arrest. Data from time-lapse experiments suggested that the time cells spent blocked in mitosis could determine cell fate during aberrant mitosis. For instance, cell fate profiles revealed that mitotic cell death rates considerably escalated with those antimitotic agents that provoked a longer mitotic arrest, like with the MTAs. Although it has never gained scientific unanimity, the duration of mitotic arrest has been proposed to influence and dictate cell fate[55]. According to the 'competing network' model, the dynamic interplay occurring in response to mitotic arrest, time stands out as a crucial factor impacting cell fate decisions. This has important repercussions since strategies aiming to accelerate or strengthen cell death cues, or by targeting and delaying mitotic exit, the balance could be shifted towards cell death, avoiding potentially unstable and malignant cells to escape. In our experimental settings, results also appear to drift in that direction. Thus, the longer the time cells spend in mitosis, the more pro-apoptotic signals will probably accumulate and as a consequence, cells will die during mitosis rather than slip out and undergo a post-mitotic cell fate. In

this line, we evidenced that survival-prone population spent less time in mitosis. It is consistent to think that cells that manage to survive, spent less time in mitosis, impeding cell death signals to accumulate, and hence escape from dying in mitosis and thrive. Additionally, our data illustrated that addition of ABT-737 to microtubule poisons seemed to accelerate mitotic cell death, while only vincristine+ABT-737 combination precipitated post-mitotic cell death. This acceleration of cell demise is also supported by independent studies showing that administration of BH3 mimetics accelerated apoptosis during mitotic arrest induced by different antimitotic agents[543,568]. However, other authors did not observed this effect, arguing that there may exist additional drug-intrinsic mechanisms that could affect the final outcome[543].

In addition to these cell death mechanisms operating principally on MTAs, the molecular cell death machinery and pathways that govern upon barasertib and ABT-737 concurrent treatment seemed to follow a different molecular path. Aurora B, as part of the CPC, localizes at the kinetochores and later in the mid-zone to regulate chromosome-spindle interactions and SAC signalling to ensure the proper segregation of the chromosomes and cytokinsesis[54]. Interestingly, upon aurora B inhibition, cells did not spend much time halted in mitosis and rapidly 'bypassed' SAC signalling, egressing mitosis and conducting cells through abnormal mitosis. Thus, cells reached G1 phase of the next cycle with overt nuclear morphological alterations. Reduction of MAD2 or BUBR1 levels in A549 cells upon barasertib treatment led to premature mitotic exit giving rise to tetraploid cells with gross nuclear alterations (polyploidy) and chromosome instability[571–573]. Moreover, as indicated earlier aurora B inhibition alone did not promote cell death at the incubation times evaluated so far. In fact, we detected that cells could remain in this state for long periods of time without activating cell death. Indeed, results showed that A549 and HCT-166 cells when treated with aurora B kianse inhibitor, exhibited increased SA β-gal activity as well as morphological hallmarks of cell senescence. Noteworthy, similar to what occurs in barasertib-treated cells, MAD2 and BUBR1 silencing prompted a senescence-like phenotype in several models[574–576]. Given the crucial function of Aurora B in SAC signalling, commanding the recruitment of downstream SAC constituents[53], it seems feasible that upon barasertib treatment, the protein levels and localization of BUBR1, BUB1 and MAD2 at kinetochores were severely impaired[579]. This in turn would trigger cell senescence by upregulating p53-p21 pathway[575,577,578]. Several studies have reported a direct cross-talk between mitotic kinases (Aurora kinases, Mps1, BUB1, BUBR1, Plk1) and p53 function and activity[580,581]. Whether, cell senescence is directly provoked by Aurora B inhibition through p53 stabilization, or rather it is a MAD2 and BUBR1 depletion side-effect, will require further clarification. Noteworthy, when ABT-737 was administered to barasertib-treated cells in a delayed fashion, once the senescent phenotype had been developed, the BH3-mimetic effectively sensitized cancer cells and rescued them from cell senescence and redirected them back to the path of cell demise. ABT-737 senolytic properties pharmacologically targeting and removing senescent cells have been previously demonstrated in two independent *in vivo* models of senescence[558,559]. In this way, making use of this molecular

mechanism, chemotherapeutic removal of senescent cancer cells from premalignant lesions, therapy resistance driven by senescence, or for example, therapies that induce mitotic catastrophe and cell senescence may be benefited by this senolytic therapeutic strategy.

Finally, activation of cell-intrinsic oncosuppressive mechanisms upon mitotic catastrophe is not the only way antimitotic agents could dispose of cancer cells. Indeed, hyperploid cancer cells have been shown to be intrinsically immunogenic by constitutively activating ER stress pathways, with the ensuing exposure of immunogenic signals such as CRT[81,82]. Our results also showed that both A549 and MIA PaCa-2 cells exhibited increased surface expression of CRT with all tested drug regimens. In other studies treatment with vinca alkaloids or taxanes also resulted in *in vitro* DAMP signalling and these drug regimens were reported to effectively vaccinated mice against a subsequent tumour rechallenge[81,82]. Collectively, these studies underpinned the existence of an anticancer immunosurveillance system that selects and eliminates cells with increased cell ploidy, which harbour more potential to become malignant and tumorigenic.

When exploring mitosis and cell cycle deregulation in different cancer models, these processes are also a well-recognised molecular insignia in MM hematologic neoplasms. Deregulation of important cell cycle family genes or disruption of the mitotic apparatus is frequently detected and thought to play an important role in myelomagenesis[597]. In fact, therapeutic targeting of molecules implicated in these processes are currently under clinical development in MM. Additionally, MM survival and resistance is also crucially influenced by Bcl-2 family[598,599]. Therefore using BH3 mimetics concurrently with mitosis targeting therapies could be envisioned as a good strategy to improve anti-myeloma therapy. Nonetheless, our results showed no cell death potentiation when the different antimitotic agents were combined with ABT-737, excepting U266 cells under some conditions. Probably, the best *in vitro* response corresponded to an additive effect between these two types of drugs. This clearly juxtaposes with our results obtained in solid cancer cell models. Perhaps, other mechanisms may govern MM cell death and make myeloma cells less addicted to Bcl-2 family upon antimitotic therapy. To date, clinical trials investigating novel antimitotic in combination with other therapies have only shown partial responses or disease stabilization. Thereby, although targeting the mitotic apparatus may still hold some promise in MM, given these discouraging results, we decided to proceed with a different rationale in our pursuit to deal with myeloma disease.

At this respect, in the scientific community, ER stress is becoming increasingly acclaimed for being a potential and powerful therapeutic target against many solid and haematological cancers[188]. In fact, the malignant transformation process impinges a prominent level of cellular stress, which of course, also reaches and strikes on cellular proteostasis. In the particular case of MM, the general stressful environment created during carcinogenesis, is further exacerbated given the intrinsic nature of plasma cells.

The industrious ability of plasma and myeloma cells to manufacture vast amounts of immunoglobulins makes these cells critically dependent on the survival arm of the UPR. Nevertheless, although myeloma cells trust in the UPR molecular framework to prosper, at the same time, this makes them more addicted and extremely vulnerable to ER stress-associated cell death[196–198]. This peculiarity finds the sense in the distinguished clinical efficacy that proteasome inhibitors (PIs) have shown in the treatment of MM[199,200]. Nonetheless, despite the certified clinical efficacy of these drugs, PI-based resistance is still recurrent and comprises many recidivism cases. Thereby, this situation claims for novel therapeutic schemes to be devised to tackle relapse. Since ER stress seems to be considered the 'Achilles heel' of MM, in the present work we aimed to explore new PI-based combinatorial strategies that severely diminish myeloma cell survival, and to inspect the cell death mechanisms and working components under these molecular processes.

In this regard, autophagy is a recycling cellular system that dispose of undesired cellular proteins and may help 'succouring' ERAD and UPS systems in conditions of staggering ER stress. In fact, under ER stress conditions, the ER pull the cellular alarms and emit signals to trigger autophagy in order to provide assistance to re-establish cellular homeostasis. In the particular case of MM, autophagy has been reported to act as a molecular protecting 'armour' against the detrimental consequences of ER stress derived from the malignant transformation process or from the MM highly secretory phenotype[158]. Additionally, autophagy could also be utilized by myeloma cells to acquire resistance against drug-mediated effects, including PIs[158]. Proteasome inhibition, has also been shown to instigate autophagic responses in different cancer cell models, including MM[603,720–723]. In fact, antioxidant-, chaperone- and autophagy-related genes have been found to be overexpressed correlating with poor prognosis in MM patients[718]. Therefore, targeting the proteasome and autophagy concurrently could be conceived as a promising therapeutic approach against MM. For instance, the ability of chloroquine to strongly potentiate myeloma cell death induced by carfilzomib *in vitro* and *in vivo* was previously demonstrated by our group[238]. During this work, similar cell death intensification has been observed in the different human and murine cell lines tested. Moreover, the improved ability of CLQ and carfilzomib co-administration to unleash cell demise has also been corroborated in an ample collection of isolated primary BM samples from MM patients. Although the full molecular mechanism has not been clarified yet, our results are supported by data from independent groups which showed that autophagy inhibition through CLQ or other autophagic inhibitors can sensitize cancer cells to PIs (including carfilzomib) and also other types of chemotherapeutics[603–605,725–727]. This is not out of polemic since some authors manifested antagonistic responses between bortezomib and CLQ treatment[603]. All this preclinical work urged the scientific community to launch clinical trials evaluating this promising chemotherapeutic scheme. Phase I and a small phase II clinical trials evaluating bortezomib+HCLQ and CLQ in bortezomib and cyclophosphamide regimens respectively, showed the feasibility of this approach and revealed probably a modest

response with conflicting results concerning the efficacy of this approach in overcoming PI-resistance in RRMM patients [181,858,859].

Similarly to CLQ, we have also observed that the VCP/p97 inhibitor, DBeQ, markedly enhanced cell death induced by carfilzomib both in MM cell lines and in isolated primary myeloma cells. Noteworthy, DBeQ cell death sensitization was not so pronounced as that seen with CLQ combinations. Although there is no reported information about carfilzomib and DBeQ combinations, other authors have also reported enhanced cytotoxic power upon dual inhibition of p97/VCP and the proteasome with bortezomib[202,606]. Presumably, the enhanced potentiation effect observed with DBeQ may derive from non-ERAD off-target effects like autophagy[607,608], since combinations with the more specific CB-5083 inhibitor rendered worse responses. In fact, inhibition of p97/VCP with DBeQ or siRNAs-mediated knock-down, has been reported to impair autophagosome maturation[203,607]. Furthermore, proteasome and p97 molecular pathways, although they share some features and molecular components, they show a considerable degree of non-redundancy, creating a window to use these combinations to overcome PI-based resistance.

Importantly, deciphering the resistance mechanisms cancer cells may take advantage of, is critical not only to devise novel therapeutic designs that counteract tumour recurrence but also to provide knowledge of how to select those patients that can benefit from a specific therapeutic strategy. So far, no biomarkers of sensitivity or resistance to chemotherapeutics have been successfully applied in clinical decision making[848]. To further expand our understanding into this subject, we aimed to shed lights on whether the *ex vivo* drug response provoked by carfilzomib and the respective drug combinations with CLQ or DBeQ in primary myeloma cells, was dependent on different clinical or *ex vivo* drug-sensitivity criteria. Our data showed that although primary myeloma cells were sensitive to *ex vivo* carfilzomib treatment alone, some patients failed to respond to this drug. However, no major significant differences were found in the presence of cytogenetic aberrations presented by myeloma patients, nor in the line of therapies patients received, that may anticipate *ex vivo* carfilzomib-based drug-resistance or sensitivity. Nonetheless, individuals bearing cytogenetic abnormalities tended to exhibit augmented *ex vivo* sensitivity to carfilzomib. Similarly, although differences were deemed statistically non-significant, carfilzomib-sensitive individuals displayed a higher number of lines of therapy. As regards to carfilzomib-based combinations with CLQ and DBeQ, our data showed that CLQ or DBeQ can potentiate cell death elicited by carfilzomib-based treatment *ex vivo* even in patients bearing cytogenetic abnormalities, or individuals classified as PI-resistant. This implies that patients with this malignant phenotype could also be benefited by CLQ and DBeQ carfilzomib-based combination regimens. Furthermore, although it was also just a trend, when MM patients were profiled attending at the number of lines of therapy they had received, drug response to *ex vivo* combinatory treatment and cell death rates, escalated with the number of therapies received. Corroborating these observations, individuals

categorized as responders to carfilzomib-CLQ drug combination displayed a higher mean number of total lines of therapies.

Firstly, one would presume that patients presenting an altered cytogenetic signature, giving its augmented malignant phenotype, would exhibit an increased resistance to therapy. However, this assumption could be reformulated in a different way. It has been proposed that myeloma cells with altered cytogenetics, and possibly with a more aggressive phenotype, can take advantage more feverishly of cellular signalling pathways that ultimately require the UPS functioning in immaculate conditions[390]. These cells would then become 'hooked' on the UPS and related cellular pathways, explaining the increased vulnerability to *ex vivo* drug-treatment displayed by cytogenetic aberrant myeloma cells and heavily-treated patients. In fact, it has been reported that clinical efficacy of PI-based therapies when combined with other therapeutic approaches, seem to be especially evident in high-risk MM patients[848–851]. Nonetheless, it should be remarked that these tendencies were deemed non-significant and hence the actual impact of these observations should be taken with prudence. One simple explanation for these weak differences is that *ex vivo* therapy-responses were not related to the cytogenetic signature presented by affected individuals or to the inherent drug-resistance that myeloma cells may exhibit. More than likely, patient's responsiveness to therapy may rely on multiple intrinsic and extrinsic factors that would impact on the final outcome. Nonetheless, it is important to stand out that carfilzomib and CLQ or DBeQ combinations provoked cytotoxic responses even in MM samples showing *ex vivo* resistance to carfilzomib treatment alone. These results may open the possibility to overcome PI-resistance with such combinatory regimens. In line with this, HCLQ or a novel VCP/p97 inhibitor (like DBeQ), have been shown to re-sensitize previously adapted PI-resistant MM cells[602,606]. Although we have not come with clear-cut solutions, perhaps, more novel profiling methods like GEP, RNA-seq signatures or high-throughput *ex vivo* drug-sensitivity testing, will provide better clustering and stratification criteria, and would probably have more potential to find accurate correlations with therapy responses[849,855,856]. More investigations are required to be able to delineate patients clusters that may benefit from a given therapeutic scheme, improving clinical decision making and therapy success[390].

In this work we have also tried to characterise and dissect *in vitro* the molecular pathways that instigate cell death signalling under these conditions. One interesting fact that was also detected in previous work from our group is that CLQ shows predilection for carfilzomib rather for bortezomib in terms of cell death potentiation[238]. Analogous results were obtained by Baranowska *et al.*, showing also a preferential potentiation effect on carfilzomib- rather than bortezomib-induced cell death when combined with hidroxichloroquine in MM cell lines[602]. The molecular mechanism by which cell death amplification upon the aforementioned PI-based combinations is materialised, remains still obscure. Some studies have reported autophagy-independent mechanisms for CLQ sensitization[173,180,728]. Therefore, to unravel this conundrum, here, we have inspected the

molecular players and pathways involved in order to characterise the cell death mechanism exerted by these drug combinations.

During this study we have observed that drug combinations not only potentiated, but also accelerated cell demise. The fact that in presence of CLQ or DBeQ, carfilzomib-based cell death kinetics notably increased, could be interpreted as a rapid accumulation of cell death signals that trigger the apoptotic cascade. In line with this, we have also shown that treatment with carfilzomib and its combination with CLQ or DBeQ increased the expression of several UPR markers (especially XBP1s, BiP, CHOP and in a lesser extent p-eIF2α), indicating the activation of an ER stress response. Nonetheless the observed ER stress response was strongly time-dependent and substantially varied between the different MM cell lines. Furthermore, we also observed that treatment with carfilzomib-based combinations with CLQ and DBeQ were more effective in increasing $O_2^{\bullet -}$ levels in MM cell lines. Although we cannot rule out the ER as an early source of ROS, our data preferentially point to the mitochondria, and particularly to the caspase-dependent cleavage of electron transfer chain subunits, as the major source of ROS in our experimental settings. In fact, several studies have reported that PI-based therapy stimulates ROS overproduction in different cancer cell models and is probably responsible for bortezomib-induced apoptosis in MM[650,658–660]. However this conundrum will probably require more investigation. Since we found evidences of activation of PERK and IRE1α, we also tried to inspect the relative participation of this two UPR branches in cell demise by using chemical inhibitors. At this regard our results showed that PERK inhibition enhanced cell death exerted by carfilzomib-based combinations in most of the cell lines, suggesting that PERK might have a protective, rather a pro-death signalling role against acute ER stress induction. Meanwhile, little or no protective effect were observed when IRE1 RNase activity was inhibited with 4μ8C indicating that this branch may hold a minor role in ER stress-induced cell death. Intensity and duration of stress signals are important parameters that determine cellular responses and cell fate. Cells react to these ER stress insults with two distinct temporally segregated UPR waves[114]. How and why the cell engages a given molecular programme or switches from one to another, still requires further comprehension. As a first course of action, the three UPR branches (PERK, IRE1α and ATF6) activate adaptive and repair mechanisms to re-establish ER homeostasis and promote survival[115]. Thus, by inhibiting PERK under ER stress situations we may also be dampening the primary adaptive and pro-survival response, magnifying ER stress burden and proteotoxic stress that would dramatically precipitate cell demise. In fact, inhibiting or genetically targeting some of these PERK downstream pro-survival targets, has been shown to enhance PI-based cytotoxicity[650].

The induction of the master regulator of the UPR, BiP, is fundamental to maintain ER-associated functions and protect cells from proteotoxic insults. BiP prevents the accumulation of unfolded/misfolded proteins, ROS generation and stabilizes mitochondrial function[137]. Furthermore, under more pathological conditions,

BiP/GRP78 has been found to be upregulated in several human tumours and to contribute in several aspects of cancer progression and therapy resistance (including to PI-based therapy)[213,619–624]. Interestingly our data also revealed that U266 and MOPC315.BM cells, two manifestly drug-resistant MM cell lines, displayed elevated BiP expression in basal conditions and when challenged with carfilzomib-based drug combinations, these cells did not substantially increase BiP expression. In sharp contrast, drug-sensitive MM.1S and NCI-H929 cells exhibited low levels of BiP in control conditions and, as part of the ER stress adaptive response[114,115], treatment with either carfilzomib-based combinatory treatments dramatically enhanced BiP expression. We then hypothesized that the observed increased basal BiP levels could be behind this drug-resistance. Cells armoured with more BiP molecules would have an increased capacity to deal with ER stress and alleviate it[645], possibly increasing the threshold required to shift from the adaptive UPR signalling to the pro-death UPR pathway. However, BiP depletion did not sensitize cancer cells to chemotherapeutic drugs. Our results clearly differ from that reported in the literature in which targeting BiP by siRNA-mediated silencing, sensitized cancer cells to a diverse collection of drugs (including bortezomib) in different cancer cell models[620,641–645]. Alternatively, other chaperones like Hsp90 or Hsp70 related proteins, could also be upregulated under ER stress conditions and could assist by alleviating proteotoxic stress and balance BiP shortage.

Despite the existence of several studies in the literature that support the involvement of both PERK and IRE1α arms in ER stress-induced cell death, in our experimental model, the establishment of a well-defined connection between UPR players and cell death executioners would probably require further clarification. In UPR signalling, although IRE1α-XBP1 axis is mainly pro-survival, IRE1α can also turn on apoptotic pathways, probably, through its ability to activate stress kinases (JNK, p38 and MAPK) that subsequently targets anti-apoptotic and pro-apoptotic Bcl-2 family members through phosphorylation[98,113,115,116,119–121]. Another main mechanism of ER stress-induced cell death is thought to be mediated by PERK/p-eIF2α/ATF4/CHOP axis[114,630,631]. Although the mechanism of CHOP-induced apoptosis is not fully clarified, some studies suggest that it would probably involve downregulation of anti-apoptotic members (Bcl-2 and Mcl-1), while upregulating proapoptotic ones (Bim or PUMA)[98,115,121,126,129,632,633]. Both PERK and IRE1α downstream signalling can mediate opposing effects on cell fate, either survival or cell death. The final cellular outcome is thought to be greatly influenced by the type, the intensity of stress signals and the amplitude of the ER stress response[113,114,640]. In our experimental model we have observed upregulation of markers related to both PERK and IRE1 arms with upregulation of both pro-apoptotic (CHOP) and pro-survival (BiP or XBP1s) markers. It is difficult to unravel the individual contribution of these factors to the final cell fate and also to observe the switch from adaptive to pro-death responses that occurs during ER stress response. Perhaps, more clarity can be drawn out from situations of 'physiological' stress rather than under pharmacological-induced ones. Probably, the acute and irreversible effects derived from drug-based ER stress may abruptly and inevitably push

cells to cell demise. In such situation, adaptive and pro-apoptotic ER stress responses would probably concur in time complicating its analysis[114].

As shown, Bcl-2 family occupies a leading position in ER stress-mediated responses. Our data showed that while the expression levels of some members remained unchanged (Bcl-2), others manifested a transient early accumulation that was dissipated over time (Mcl-1, Bim, PUMA). Whether this expression pattern is a side effect of proteasome inhibition or rather derived from UPR signalling cannot be circumvented with our current data. Some pieces of evidence point to BH3-only proteins like Bim, PUMA or NOXA as important modulators of ER stress-induced cell death[13,121,140,714–716]. Our data showed that despite Bim is upregulated upon ER stress, CRISPR Bim KO cells only offered a partial cell death protection induced by the drug treatment. Hence, this would suggest that although Bim may partially contribute to cell death instigated by PI-based combinations, its deficiency seems to be redundantly replaced by additional BH3-only members or even caspase-8, that can trigger cell death upon drug treatment as defended by some authors[714,1011]. For instance, we also showed that drug treatment was also able to induce an initial accumulation of BH3-only proteins PUMA and in a lesser extent NOXA.

The precise molecular mechanism responsible for ER stress-induced cell death is still unknown. The contribution of both, the cell death receptor and the intrinsic mitochondrial apoptotic pathway, have been evidenced by independent laboratories[108,198,200,238,705,714]. Our results showed that cell death exerted by carfilzomib-based combinations elicited a critical dependency on caspases in the majority of cell lines tested. The relative contribution of each member of the caspase family varied with the different MM cell lines. Caspase-3 as a critical executioner caspase, was the one with more importance in triggering cell death in our experimental settings. The initiator caspase-9 reflected a moderate contribution in cell death, since its inhibition only offered a partial protection suggesting the existence of a bypass that could connect with executioner caspases without involving apoptosome formation. Interestingly, this occurs mainly in cell lines were caspase-8 dependency was more pronounced (U266 and MOPC315.BM cells). Indeed, in these two cell lines, caspase-8 inhibition greatly reduced cell death rates to the levels seen with pan-caspase or caspase-3 inhibitors. Although caspase-8 follows the extrinsic death receptor pathway, it has been manifested that persistent ER stress could also induce caspase-8 mediated cell death[116]. In this scenario, diverse ER stress insults (including PI-based treatment) resulted in UPR-dependent upregulation of DR4 and DR5 receptors and cell death[116,122,609,613–615], although previous work from our group refuted these findings[132]. However, this mechanism is not out of polemic[130,705], since different groups have reported potential mechanisms by which persistent ER stress can induce caspase-8 mediated cell death in absence of death ligands. These mechanisms may entail the formation of an autophagosome-associated platforms. Alternatively, it may also involve the promiscuous binding of DR5 molecules to hydrophobic unfolded/misfolded proteins accumulating during ER stress, favouring

intracellular clustering of DR5 receptors at the ERGIC, thus triggering cell death[116,609–612,638,710,711].

We have witnessed that Bcl-2 family expression pattern is modified under the ER stress conditions evoked by carfilzomib and its drug combinations, possibly inclining the balance towards pro-death signalling. But, to ultimately instigate cell death, this process requires mitochondrial outer membrane permeabilization (MOMP) induced by Bax/Bak oligomerization. Our data have demonstrated the capacity of PI-based therapies, as well as its combination with CLQ or DBeQ to induce cell death upon Bax/Bak deficiency. This is important because lack of expression of these pro-apoptotic mediators are behind the resistance mechanisms harboured by tumour cells[618] and may highlight the promising potential that these strategies could have in patients with acquired apoptotic cell death resistance. Several reports support the contribution of Bax and Bak in ER stress-induced cell death[116,137,698–701]. Conversely, other studies revealed alternative Bax/Bak independent mechanisms, probably including Bax/Bak independent mitochondrial pore formation (mPTP), calcium overload or necroptotic-like cell death pathways, by which cells can succumb to ER stressors[653,702,703]. As regards to necroptosis, our results using necroptotic inhibitors claim for a minor contribution of necroptosis even when caspase action is abrogated[617]. One interesting and alternative explanation for the observed Bax/Bak-independent cell death, may point to caspase-8 and DR4/DR5 as key players in this scenery[609,638]. In fact, the addiction of some of the tested cell lines to caspase-8 action for cell death induction reinforces this idea. It is appealing to theorise that the Bax/Bak-independent cell death induction observed under PI-based treatment could be attributed to DR5 and caspase-8 contribution to cell demise.

It is a well-recognised fact that upon ER stress, autophagy could be activated as a backup mechanism to cope with staggering ER stress including upon proteasome inhibition[109,165,166,603,719–723]. Work form our group previously manifested that carfilzomib treatment was capable to induce autophagy in MM cells in a moderate fashion[238]. However, the observed autophagic flux was not complete probably because the processing of some autophagic components requires an intact proteasome to occur[724]. However, the data presented here from ATG5-deficient cells suggest that autophagy inhibition do not contribute, or at least, may not be the unique cause for the sensitization that CLQ brings about. Indeed, some studies reporting that CLQ sensitized cancer cells to PIs, claimed for autophagy-independent mechanisms, as it apparently occurs in our model[173,180,728]. On our quest, searching for alternative and/or off-target effects of CLQ, we came across with the ability of CLQ to modulate at some degree proteasome activity. Indeed, our data revealed that CLQ administration further diminished proteasome activity, already reduced by the effect of PIs. Intriguingly, CLQ effect was more powerful in abrogating proteasome activity in combination with carfilzomib than under bortezomib treatment. Spranger *et al.* showed that CLQ was able to restrain the enzymatic activity of the proteasome in a non-competitive manner by reversibly binding to the proteasome near to the active site[729,730]. Interestingly, simultaneous binding of a

PI and CLQ to the proteasome was indeed sterically possible[729,730]. These observations along with data presented here, further strengthen the idea that CLQ may operate as an allosteric modulator on PI-based therapy[729,730]. It is possible that through a mechanism not clarified yet, CLQ alter the steric configuration of the proteasome active site in such a manner that facilitates the accessibility of carfilzomib to the catalytic site. Probably, the chemical structure and the irreversibility nature of carfilzomib plays an important role in this mechanism. This would allow for a more intense inhibition of the proteasome when CLQ is combined with carfilzomib compared to reversible PIs like bortezomib or ixazomib, correlating with the increased cell death rates.

Over the last years, the achievements of immunotherapy in clinical oncology has clearly positioned this type of approach in a leading position in cancer treatment. Moreover, the idea that the long-term effects of classical or targeted chemotherapeutics came from the ability to foster anticancer immunosurveillance, has probably transformed the research therapeutic panoramic in oncoimmunology. The introduction of "immunogenic cell death" (ICD) concept has undoubtedly contributed to this new conception[216,230,731]. But perhaps the first question that one should ask when working towards developing antimyeloma immune responses is: Are myeloma cells immunogenic? Considering the whole picture, the immunogenicity of cell death and the ensuing *in vivo* anticancer immune response may involve the following enactors: Antigenicity—Tumour Type; Adjuvanticity & Inflammation—DAMP Signalling; and Genetic & Environmental cues—Host and the TME (see **Figure 5.1**).

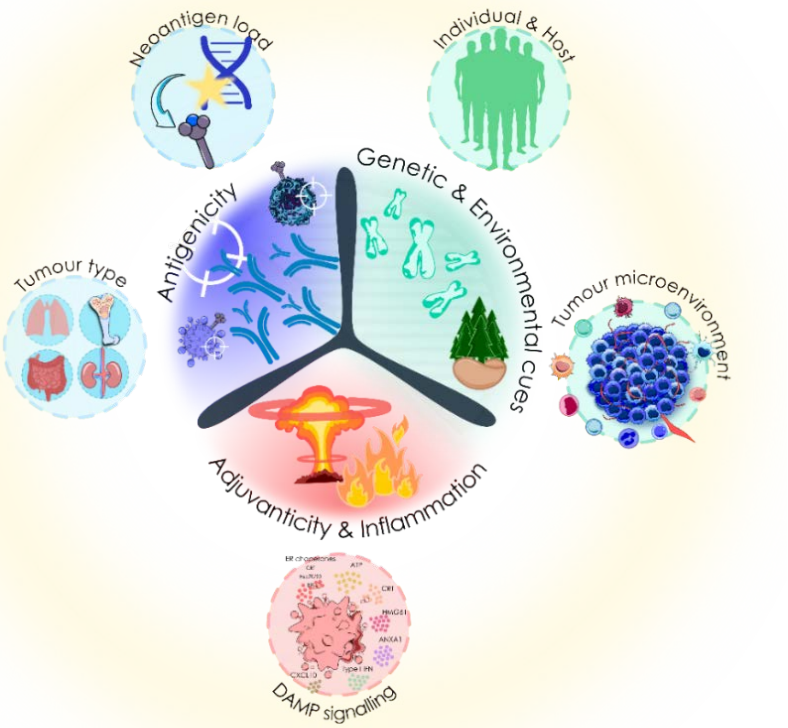

Figure 5.1 | Different players involved in anticancer immune responses. The different factors that can have an impact over anticancer immune responses such as antigenicity, adjuvanticity and the genetic and environmental cues are illustrated.

Starting with the **antigenicity** level, it exist an enormous variation regarding the mutational burden held by each of the different tumour types[789,790]. Cancer types with an increased mutational load like melanoma and lung cancer, show better responses to immunotherapeutic approaches like checkpoint blockade therapy. With regard to MM disease, although this type of neoplasm carry an important amount of cytogenetic abnormalities bears a low to intermediate neoantigen load[789]. Nonetheless, patients exhibiting a high mutational and neoantigen burden were associated with worse PFS rates when subjected current standards of care[789]. Nevertheless several examples supporting the existence of an antigen-specific antimyeloma immune response have been manifested: Graft versus myeloma effect after allo-HSCT, donor lymphocyte infusions[463], neoantigen-directed immunotherapy[791], among others. In fact, myeloma-specific T cells can be isolated from BM of MM patients and can also be identified even in early disease stages[474,777,793]. Moreover, various neoantigen vaccine trials are currently under development[792]. In murine models, efficacy of adoptive transfer of idiotype-specific T cells has been demonstrated in 5TGM1 and MOPC315 myeloma models[540,794]. Additionally, prophylactic vaccination with secreted M315 myeloma paraprotein provided immune protection against a subsequent tumour rechallenge[763,795]. However, when leading with immunization aspects, tolerance and immune reactivity are two faces possibly kept apart by a thin string. Noteworthy, tolerance towards M-protein can be developed when immunization dose exceeded a given threshold has been reported in MOPC315 model[763,800–802]. In fact, since we immunized mice with a relative high amount of whole-tumour cell formulations, this tolerance and T cell exhaustion/anergy response could have also developed under our experimental conditions.

With the exception of the experimental models in Balb/c mice previously indicated here, human MM idiotypes are usually poorly immunogenic. Low bioinformatics scores have been shown on most T-cell interaction-HLA modules[418]. In the clinical setting several vaccination strategies have been tried out, such as DC vaccines, vaccination with MM cells supplemented with adjuvants and vaccination with myeloma-derived proteins. Idiotypic vaccination has not translated into overall therapeutic responses despite the apparent presence of idiotype-specific reactive T cells [418]. Indeed, as our data showed, at least some degree of immune infiltration was also observed even in vaccination formulations that did not offered a substantial protection. Many other myeloma-associated T-cell epitopes have been postulated (eg, MUC1, HM1.24, NY-ESO1, XBP1, HTERT, and RHAMM-R3)[418]. Still, results are far from being successful. Thus far, clinical trials have only granted the practicability and safety of these kind of approaches and only the best patient's outcomes obtained were disease stabilization[463,777,805]. Still, there are many technical and experimental complexities that should be addressed and refined when developing a successful vaccination protocol[763]. Nonetheless, whereas immunization *per se* has not met a dramatic success, the role in antigen-specific chimeric antigen receptor T cells directed at some of these epitopes is under evaluation and may show therapeutic promise[418].

When attending the **adjuvanticity** aspect of regulated cell death programmes, DAMP generation is of utmost importance[731]. During the course of cell demise, different factors such as, the type of cell death, the ICD-inducing agent and the interplay between various cellular stress signalling pathways, have been shown to influence the quantity and type of danger signals emitted[241]. In this matter, ER stress responses, the UPR (especially the PERK-mediated arm) and ROS generation appeared to be leading figures in ICD[225,255,303]. Drugs used in our work can effectively evoke ER stress responses in MM cells, and particularly upregulate markers associated with ICD such as PERK activation and eIF2α phosphorylation. Moreover, here we have evidenced the ability of carfilzomib and the respective drug combinations with CLQ and DBeQ to expose several DAMPs (CRT, Hsp70 and BiP molecular chaperones) to the plasma membrane of MM cells *in vitro*. Therefore, at first these chemotherapeutic regimens seem to be good candidates to potentially be considered *bona-fide* ICD inducers with the presumed ability to empower prophylactic anticancer immune responses *in vivo*[526]. Besides their roles in protein folding, calcium binding and sensing stress signals, chaperones can also acquire novel immunomodulatory properties when ectopically exposed in the outer cell surface or released to the extracellular milieu[230245]. Some chaperones, can function as 'eat-me signals' when externalized to the outer leaflet of the plasma membrane in apoptotic cells, stimulating the uptake of dead-cells and its derived antigens by APCs, favouring their activation and maturation[739]. When released extracellularly, these chaperones can also operate as cytokines or 'chaperokines' stimulating secretion of pro-inflammatory (or even anti-inflammatory mediators), upregulation of adhesion and co-stimulatory molecules on APCs, hence affecting polarization and phenotypic maturation of phagocytic cells[227,317,746,747,753,754]. Moreover, chaperones can also contribute to cancer antigenicity by facilitating cross-presentation process by forming complexes with antigenic peptides[253,254]. Perhaps since these molecular chaperones (CRT, Hsp70 and Hsp90) share some binding partners in APCs[219,247,741], these molecules can contribute to the immunogenicity of dying cancer cells in a partially redundant, yet not identical manner[740].

Nonetheless the whole picture may not appear so simplistic. Several factors can influence and impact CRT-receptor interactions, the downstream signalling pathways stimulated and the final immunomodulatory cellular outcome[739]. For example, the different molecular partners that CRT can interact with, the regions of the protein involved in the interactions, CRT mutations and polymorphisms, the subcellular localization of CRT and also the different and varied post-translational modifications that CRT can be subjected to, all of these elements have been shown to influence CRT-mediated final cellular outcome[739]. In fact, quite recently, it has been reported that a truncated form of CRT was able to escape ER retention system and was released to the extracellular medium, inhibiting the phagocytosis of dying cancer cells by DCs and suppressing chemoimmunotherapeutic driven anticancer immune responses[734]. Independent laboratories have also manifested the ability of soluble CRT to promote

both pro-inflammatory and anti-inflammatory reactions on phagocytes by affecting its activation and polarization state[256,739].

Although in many instances, CRT exposure usually correlates with cell death immunogenicity, CRT expression on its own is not sufficient, since ICD is a multistep process that strongly relies on other danger signals to effectively mount anticancer immune response[286]. Several independent studies have shown that at least, two or three additional danger signals are also required to give rise to an active *in vivo* immune response. These are ATP, HMGB1 and type I IFNs. Depletion or abrogation of the molecular pathways associated with the emission of any of these different signals, prevented the immunogenicity of cell death and *in vivo* immunesurveillance[216,806]. Along with these conventional danger signals, additional influential DAMPs, like Annexin A1, and others, have been shown to take part in ICD[216], being in some context required to instigate a genuine anticancer immune response. But why accidental release of constitutive intracellular DAMPs (ATP, HMGB1), like during accidental necrosis[731], does not elicit *in vivo* immune responses[232,233], but when released in an inducible manner bring about potent anticancer immune responses? This may illustrate that other type of cues should be provided to drive *bona fide* ICD[731]. Perhaps the differentiation between constitutive and inducible DAMPs (cDAMPs and iDAMPs respectively) may provide more clues[731]. iDAMPs encompass a diverse collection of molecules with pro-inflammatory connotations, that are not present in healthy cells but are induced upon stressful or cell death conditions (type I IFNs, IL-6, IL-1, TNF-α)[731,807]. Indeed, **inflammation** has been acknowledged as another decisive element for the success of ICD[731]. Nevertheless, it should be pointed out that some DAMPs (Prostaglandin E2, adenosine, etc) emitted during cell death, may exhibit immunosuppressive properties contributing to immune tolerance[216,241]. This is something that could be left unnoticed and could negatively impact on antitumour immune reactions. In essence, DAMP signalling and trafficking are regarded to be plastic processes and therefore, the mechanisms involved are stimulus and context dependent. Therefore, when addressing these topics the analysis of every ICD inducer, cancer model or experimental setting, should attend and include the whole scenario[264].

One of the important outcomes of danger signalling is the functional activation of DCs. All these danger signals could be sensed by APCs, stimulate phagocytic uptake of cancer-derived antigens, APCs phenotypic maturation and chemotactic attraction[148]. For instance our data reflect that the DAMP signalling signature evoked by the drugs used in our study, have the immunogenic capacity to properly instigate maturation of DCs when confronted with MM drug-treated cells. Probably, DCs maturation may be influenced by the type and spatiotemporal consecution of danger/stress signals that will characterise the level of costimulation provided by DCs and hence the subsequent outcome of anticancer immune responses.

Unravelling the molecular mechanisms that endow dying or stress cells with immunogenic features is paramount to improve the therapeutic potential of current or

novel therapies. The role of ER stress and ROS generation in the immunogenicity of cell death has been widely contrasted by several independent laboratories and not only in the context of ICD but also in other molecular scenarios like infections. Probably, the relative importance of ER stress in ICD is also underscored by the classification of ICD inducers (type I and type II), depending on whether its primary target is the ER or ER stress is merely a secondary effect[225,227]. Thus, since these two types of ICD inducers aim to distinct targets, it seems reasonable to think that the quality and amount, as well as the mechanisms involved in the emission of danger signals would diverge[225,227,257,316,317]. In other words the therapeutic agent used to elicit ICD really matters. In ICD-derived emission of danger signal(s), PERK-mediated arm of the UPR has been acknowledged as a major player[210,225,307]. Its contribution could arise from its UPR-related function[255], but also through its ability to modulate the proximal secretory pathway[257], or through more novel cellular functions related to actin cytoskeleton dynamics and formation of ER-plasma membrane contact sites[210,225,308,309]. Interestingly, although the three branches of the UPR (PERK, IRE1α and ATF6) can be fostered by cardiac glycoside treatment[84], abrogation of PERK, but not IRE1α and ATF6 pathways, through genetic maneuvers, significantly diminished the immunogenicity of stressed cancer cells[255,257]. However, although it seems that ER stress is involved in this process and can restore ICD of reported non-ICD inducers, inducing an ER stress response alone is not sufficient to trigger CRT translocation or *in vivo* immune responses[223,307]. Another important aspect in ICD-mediated danger signal trafficking is the generation of ROS. Quenching chemotherapy-induced ROS with antioxidants and ROS scavengers, abolished CRT exposure[225,232,255]. In our work, we can establish an association between the ER stress response, ROS production and the emission of danger signals prompted by the drugs used in our model. However, we cannot ascertain that danger signalling is a direct consequence of drug-induced ER stress since we have not established a causal relationship at this regard.

The role of autophagy in DAMP signalling is also a matter of debate. Discrepancies have been found regarding the implication of autophagy in CRT translocation during ICD. It has been proposed that since the autophagy machinery is able to remove oxidized proteins and organelles[265,324], this process would relieve the saturated ER retention system that occur during ER stress conditions, thereby decreasing CRT exposure and the ensuing immune responses[243,325]. However, while in some scenarios, like in Hyp-PDT treatment, seems to follow this model[265,323,324], in chemotherapy-induced CRT, autophagy did not alter CRT exposure at all[759]. It should be highlighted that when examining the role of autophagy in DAMP signalling most of these studies targeted early or intermediary mediators of autophagy. This could be of importance since the different steps of the autophagic flux may play different roles in CRT exposure. Recently, one study showed that targeting autophagy at early stages diminished CRT translocation, whereas inhibition of autophagy at later stages with CLQ or other drugs like bafilomycin A1 incremented ecto-CRT levels[760]. This latter study is in consonance with our data since depletion of ATG5 which impairs early autophagy stages,

reduced CRT translocation, whereas inhibition of autophagy with CLQ potentiated ecto-CRT exposure. Hence, CRT exposure may rely on the autophagic inhibitor used and hence the autophagic phase being targeted. Moreover, our results may suggest that CRT trafficking is not controlled, at least significantly, by autophagy.

As shown, all our *in vitro* results supported the idea that the drug treatments used so far instigated ICD in MM cells. However, our results from *in vivo* vaccination experiments revealed that prophylactic vaccination with MM-treated cells did not offer important immune protection against a posterior rechallenge with living MM cells of the same type. Mice vaccinated with MM cells treated with carfilzomib or the combination of carfilzomib and CLQ, did not exhibited any survival advantage or delay in disease progression. A hint of responsiveness could probably be observed when analysing immune infiltration and tumour burden in target organs *ex vivo*, even in vaccination formulations that did not evoked an overall response. Only when mice were vaccinated with a formulation containing MM cell death corpses treated with the combination of carflizomib-CLQ and the caspase inhibitor z-VAD-fmk, a small protection against disease development was evidenced. Clearly, our *in vivo* results do not support the data observed *in vitro*, indicating that other factors may also influence the immunogenicity of cell death and the generation of anticancer immune responses *in vivo*. In this respect, the host and the microenvironment are important elements that should not be overlooked in the context of ICD.

As regards to the host in which tumour develops and in which ICD and anticancer immune responses take place, discussing *in vivo* cancer models is of relevance. These models are certainly invaluable tools, but we should also know their limitations and conclusions should be extracted with care. In particular, in the study of ICD inducers and the effect of chemotherapy on anticancer immune responses, most studies have explored these aspects on transplanted syngeneic murine cancer cell lines. A major limitation of tumour cell line transplantation models is that they do not fully recapitulate *de novo* tumour formation with the co-evolving tumour-host interactions and the presence of an immunosuppressive microenvironment. Clearly, the genetic profile and hence their antigenic repertoire between transplanted cell lines and endogenously arising tumours models is different[816]. This is interesting because some authors showed no significant contribution of the adaptive immune system in the anticancer response exerted by ICD inducers in these type of models[781,816]. Spontaneously arising tumour models are subjected to constant immunoediting by murine Immune System, which better reproduces the real difficulties encountered in human cancer disease with the co-evolving interplay between the tumour and the host Immune System[817,818]. These conditions may also be recapitulated in MM mouse models like the MOPC315.BM model utilized in this work[526] or in the 5T33MM model. Although we have found some degree of immune infiltration in the different tumour niches, differences were weak and non-significant in the majority of the cases. The increased immune infiltration of tumour areas could be interpreted as the ability of immune cells to recognize the tumour.

However, apparently this response was not sufficient enough to delay disease progression. It seems probable, in the MOPC315.BM model, during the selection of myeloma cells with predilection for the BM, that a selection towards immune-evasive cells had also occurred. In contrast, pioneering work from De Beck and colleagues using the 5T33MM model, clearly showed evidences of eliciting ICD-derived antitumour responses *in vivo*, using chemotherapeutics like bortezomib, melphalan, mitoxantrone, among others[819]. However, authors emphasized the complications in achieving efficient immunizations in MM models compared to results observed in solid tumours[219,819].

As shown, emission of DAMPs alone might not be enough to prompt active anticancer immune responses. Indeed, it is considered equally decisive the underlying mechanisms involved in reception, transmission and response by immune cells to these danger signals. Probably one good example could be illustrated by the fact that individuals with severe immunodeficiency or genetically predisposed to be unable to detect danger signals (mutations in TLR4, MyD88, P2RX7, among others) are less responsive to some therapeutic modalities. When facing a complex and adaptive disease such as cancer, additional aspects such as the immunosuppressive nature of cancer should be considered. In particular, MM is characterized by a general immune dysfunction that could hamper immunosurveillance and the efficacy of immunotherapeutic approaches[463,763,812]. Although these immunosuppressive factors have not been assessed *in vivo*, during the course of MM disease, we did observed most of these features in MM patients with high expression of ecto-CRT which indeed were also associated with poor clinical markers. Furthermore, MOPC315.BM model has been shown to compromise important hematopoietic organs like the spleen and BM that may account for the reduced immune response observed in vaccinated mice[813–815]. For that reason, although it may exist an initial antitumour response at early disease stages, MM cells can sabotage the available hematopoietic compartments once disease is established subverting anticancer immunosurveillance.

One important question arising in the field concerns the functions performed by caspases in cell death immunogenicity. Caspases have been revealed as essential players on how cell death is conceived by the Immune System[731,808]. Accumulating evidence points to caspases as modulators of signals emanating from dying cells, hence impacting on the ensuing immune responses[809]. However, this topic is proving to be challenging and no complete answers and easy conclusions can be drawn out from it yet[731]. While early studies on CRT trafficking showed that caspases were required for anthracycline-driven immunogenicity[230,255], additionally, alternative pathways in which caspases were not required for the immunogenicity of death were also demonstrated[257]. *In vitro*, our data showed that depending on the cell line, caspases can pose both positive and negative influences on DAMP signalling. Quite recently, using immunocompetent syngeneic murine models, abrogation of caspase-3 activity genetically or by chemical inhibitors (z-VAD-fmk), was shown to improve type I IFN secretion improving systemic immune responses[276,808]. This effect emanated from the delayed break-down experienced by

caspase-deficient cells, allowing for the accumulation immunogenic signals that promote the ensuing immune responses[276,279]. Additional immunosuppressive functions of caspases have also been reported in other contexts[757,810,811]. Intriguingly our *in vivo* vaccination experiments showed that only when mice were immunized with cells treated with formulations containing z-VAD-fmk, disease progression was succinctly delayed. It is possible that by a yet unknown mechanism, caspases may hinder ectopic CRT translocation under these conditions. For instance, these *in vivo* results agree with our previous finding that z-VAD-fmk also increased the exposure of CRT in MOPC315.BM cells *in vitro*, possibly reflecting its increased immunogenic potential. Perhaps, one possible explanation is that z-VAD-fmk could favour the accumulation of immunostimulatory signals, agumenting its immunogenic potential by preventing cell dismantling, as described by other authors[276,279]. Resolving the dualistic behaviour of caspases on cancer cell immunogenicity, will certainly require further enlightment and inclusion of all the different participants of cell death and immunogenic reactions[731].

In cancer management, a strategy that would depend only on the instigation of ICD, would be probably insufficient to activate the Immune System if the tumour microenvironment is not permissive enough like in MM. One of the reasons behind the MM immune dysfunction is mediated by the upregulation of inhibitory checkpoint proteins like PD-1/PD-L1 axis. Indeed we observed that MOPC315.BM cells expressed high amounts of PD-L1 at basal levels. It seems feasible that the absence of immune protection evidenced when mice were immunized with MM corpses treated with presumably 'immunogenic' chemotherapy, may be a consequence of the ability of MOPC315.BM cells to elude immunesurveillance through PD-1/PD-L1 axis. Thereby, targeting PD-1/PD-L1 axis could be envisaged as a good approach to generate an active induction of ICD and turn the immune-hostile MM microenvironment into an immune-friendly place. However, our data revealed that checkpoint blockade therapy alone or in combination with vaccination formulations, did not significantly extend mice survival at all. From these data we could infer that PD-1/PD-L1 axis may not be implicated in the immune evasion prompted by MM cells, and that may not be responsible for the succint immune protection elicited by vaccine formulations. We cannot rule out the possibility that in our model other treatment schemes might have elicited a potent anti-myeloma activity. Current literature offers a myriad of potentially "valid" checkpoint blockade therapeutic regimens, that differ in several aspects of protocol details. In fact, one study showed that only when checkpoint blockade was administered at the right moment with an optimized schedule, therapeutic response was achieved[829]. For this reason, it is of utmost importance to identify the right therapeutic window in each case, to apply checkpoint blockade therapy and effectively reinvigorate myeloma-specific T cell clones[823,830]. Furthermore, initially Balb/c mice count on a complete and functionally bioactive Immune System, and thereby they should not present exhausted features, hence displaying low PD-1 levels. However, despite these technical issues, others have successfully observed *in vivo* therapeutic responses with this type of immunotherapy both in monotherapy or in combination with different anti-myeloma therapies

(allogeneic-HSCT, IMiDs, radiation therapy, DC-myeloma fusion vaccines, etc)[440,502,822,824,825,827]. Nonetheless, some studies support our observations reporting no repercussions over myeloma disease progression by blocking PD-1 or CTLA-4 in Vk*MYC MM mouse model[828].

It is noteworthy to highlight that in human MM disease, checkpoint blockade in monotherapy also failed to yield clinically objective responses[463,830]. Besides PD-1/PD-L1 pathway, a wide panel of immune checkpoint inhibitors exists and may also have potential roles in myeloma immune evasion (CTLA-4, LAG-3, TIM-3, GITR, TIGIT)[831–836]. This great and versatile variety of co-signalling molecules held by T cells, APCs or tumour cells is thought to be context-dependent and be partially overlapping and redundant. Moreover, it is possible that compensatory mechanisms upon administration of PD-1 blocking antibodies, could emerge and upregulate alternative immune checkpoints, as it has been reported in other cancers[497]. In fact, currently some combinatory regimens of immune checkpoint inhibitors are already being explored in MM patients[497].

Last but not least, gut microbiome and antibiotic usage have been shown to impact the efficacy of checkpoint blockade therapy in several solid tumours. In fact one study showed that mice from different animal care providers, displayed complete different responses to checkpoint blockade therapy. Thereby, gut microbiome could represent a missing piece that may provide further coherence to this conundrum and may also explain the lack of efficacy of checkpoint blockade in our model.

Intense basic research work ‘at the bench’ have helped to consolidate DAMP signalling and ICD as important players in anticancer immune responses. However, some questions remain unresolved especially when translating it to the ‘bed’ in the clinical practice, such as: the real repercussion of these molecular processes in the clinic or whether current chemotherapeutic regimens (doses and schedules) are able to trigger ICD in cancer patients. More importantly, *in vitro* and preclinical data, assume that DAMP exposure only occurs as a consequence of chemotherapy itself. However, this do not fully take into account the possibility that DAMP exposure could also occur in absence of therapy, or neither its implications in malignant transformation or in anticancer immune responses[284]. In fact, depending on the cancer type, DAMPs exposure, could operate as positive or negative prognostic factors in cancer patients. An increasing body of knowledge is consolidating the idea that DAMPs and ICD-related molecular processes, may serve as a productive source of prognostic biomarkers to be unveiled in cancer patients[284].

Here we have shown for the first time that myeloma cells from BM samples isolated from patients with plasma cell dyscrasias, displayed elevated levels of ecto-CRT on their surface. Moreover, although a great interindividual variability was observed, our data suggest that ecto-CRT levels seems to increase with disease progression from control BM to MGUS, smoldering and to overt MM. This finding along with the fact that

patients with an altered cytogenetic signature displayed increased levels of ecto-CRT and that CRT exposure apparently is not influenced by chemotherapy, may point towards malignant transformation as the instigator of the expression of this DAMP. Many studies have revealed that depending on the cancer cell type CRT expression is upregulated in tumour tissue playing an active role in tumorigenesis, associating CRT overexpression with cancer evolution, enhanced invasive capacity, cancer aggressiveness and poor clinical outcome[284,733,868,884–888]. Many types of neoplastic tissue exhibit increased expression of CRT compared to normal tissue, both in haematological (AML, ALL, CML and NHL) and solid malignancies (glioblastoma, bladder, ovarian, breast, prostate, pancreatic, gastric, colorectal, melanoma and esophageal squamous cell carcinoma, among others)[293,295,860–867]. As our data seemed to indicate, during malignant transformation increased CRT expression or exposure, could be provoked as a side effect of cellular stress. For instance, as we have seen in MM disease, AML[289,889] and NSCLC[286] patients exhibited increased levels of CRT in the surface of cancer cells in absence of chemotherapy. It has been hypothesized that cancer cells may undergo some sort of chemotherapy-independent cellular stress that drives DAMP trafficking. Presumably, the origin of this cellular stress may come from the cell's own path through malignant transformation, which already infringes an important load in several cellular systems, including proteostasis[289]. This could also explain the robust correlation found between CRT and expression of other genes related to ER stress responses[289].

At first, the idea of finding an ER-resident protein like CRT in other cellular localizations was a something hard to assimilate. Indeed, the mechanisms of cellular relocalization of CRT have been a matter of intense research, especially in the therapy-driven scenario. Still we don't know why and how CRT is relocalized to the plasma membrane during the malignant transformation process or whether the mechanism driving CRT trafficking is the same as the one operating during therapy driven-ICD. In this regard, one potential mechanism occurring during malignant transformation may involve saturation of ER folding, transport capacity and KDEL-mediated ER retention system, allowing ER-resident proteins to leak out from ER imprinsonment[325,895,896]. This situation may be even further exacerbated in cells with a highly secretory phenotype, like in MM cells[195]. Post-translational modification of chaperones could also play a role in modulating their subcellular localization and functions[255,898–900]. Interestingly, CRT leakage from the ER-retention system could also be caused by mutations on KDEL region, as is the case for myeloproliferative neoplasms (MPNs), allowing CRT to reach the plasma membrane or the extracellular space[901–905]. *CALR* gene has also been detected frequently mutated, in many solid cancers according to COSMIC and cBioPortal databases[734]. In fact, quite recently, it was shown that this type of mutated and released form of CRT undermined anticancer immunosurveillance by blunting the recognition and phagocytosis of dying or stressed cancer cells by DCs[734734]. In MM, apparently there are no reported associated mutations in *CALR* gene according with different databases. Nonetheless, absence of *CALR* mutations does not completely exclude neither its overexpression, nor its ectopic relocalization. In fact MM is associated with other

karyotypic events that could drive CRT overexpression like in HRD or CNVs involved in gains of chromosome 19 (locus of *CALR*)[392,912]. Indeed, total CRT levels were found upregulated in MM samples, but not in MGUS or control samples measured by flow cytometry, RT-PCR methods or RNA-seq studies[913,914].

Whether chemotherapy-driven or rather, arising from the oncological transformation process, the relevance of determining CRT exposure or expression is that it could be applicable to provide prognostic value in cancer patients. Current literature shows that depending on the cancer cell type, this DAMP could be associated with an improved anticancer immunesurveillance and consequently with an improved patient's outcome or alternatively with a more aggressive phenotype and advance disease stage[284]. In line with this, our data showed that patients with elevated ecto-CRT levels were associated with a more dysfunctional and pathological BM microenvironment. Data revealed that patients with increased ecto-CRT exhibited an altered BM-infiltrating T cell immune profile, with reduced CD4/CD8 T cell ratios derived from reduced $CD4^+$ T cells and increased $CD8^+$ T cells, increased BM NK cells, mDC, pDCs and Treg frequencies. Additionally, CRT^{hi} cohort also showed augmented activity of inhibitory immune checkpoints like PD-1/PD-L1 axis. MM disease is emblematic for the close ties established between myeloma cells and the BM microenvironment and for the impact that the BM niche could pose to MM disease[409,432]. Indeed, MM is distinctive for the profound immune impairment and the solid immunosuppressive phenotype that promotes immune evasion and disease progression[409]. In fact, the immunophenotypic landscape depicted during this work actually bears close resemblance with the BM microenvironment usually found in advanced-stage MM patients displaying worse survival rates[418,425,427,438,440,493,935,938–942,969]. Altogether, it can be suggested that CRT^{hi} patients hold immune traits that delineate a BM immunophenotipic landscape associated with a weakened and compromised immune microenvironment, which could also be translated into a poor clinical outcome in the context of MM disease.

Nonetheless, it is intriguing that individuals with increased ecto-CRT levels also carry more cytogenetic alterations and this subsequently correlates with a higher degree of infiltration of immune effector cells (NK, $CD8^+$ T cells and DCs), despite its functional status may not be completely operative. It is possible that these cytogenetic defects may hide a genomically unstable state that consequently increases the number of somatic mutations and neoantigen repertoire in malignant cells[970]. In solid tumours with high mutational burden and hence neoantigen load, these factors have been correlated with an increased immune infiltration, improved anticancer immunosurveillance and extended survival upon checkpoint blockade therapy[402,971,972]. However, this has not been the case for MM[496,790,831,912]. Despite MM cells bear intermediate mutational burden, somatic mutation densities and neoantigen repertoire escalates with myeloma progression and correlates with a worse clinical outcome in MM patients[789789,973]. It is possible that in MM, these factors alone (and even with the assistance of checkpoint blockade therapy), might not be sufficient to revert the deep suppressive immune

landscape present in this disease. Therefore, although initially educated and trained to fight myeloma, effector immune responses may eventually miss in their assignment to cope with myeloma disease. This emphasizes the complexity of the underlying immunosuppressive networks that allow myeloma cells license to slip away[831]. For this reason, rehabilitating this immunosuppressive condition is of supreme relevance.

Accordingly, data from our clinical assessment seem to indicate that increased ecto-CRT exposure is associated with poor prognosis in MM disease. Individuals with augmented expression of ecto-CRT significantly exhibited lower time to progression rates, increased chances of developing extramedullary plasmacytomas, are heavily pre-treated and harbour a high-risk cytogenetic signature[854]. The interconnection between CRT levels and clinical prognosis in cancer patients critically depends on the specific tumour type being analysed. Favourable clinical prognosis has been observed in patients expressing high levels of CRT in glioblastoma, colorectal and endometrial cancer, which includes tumour types with chemotherapy-independent CRT exposure (AML, ovarian or NSCLC)[286–288,292,889,916,974,978,979]. In contrast, in other types of tumours (gastric, oral squamous cell carcinoma, bladder cancer, neuroblastoma, pancreatic cancer and mantle cell lymphoma), high expression of CRT has been associated with more aggressive clinicopathological factors, invasiveness and postoperative occurrence of distant metastasis, thereby supporting poorer survival rates[293,295,980,982,983]. Probably, the negative relationship between CRT exposure and the clinical outcome in cancer could be explained by the fact that CRT exposure is usually accompanied by an enhanced expression of the anti-phagocytic molecule CD47[740]. Thereby, in order to neutralise the potent phagocytic signals radiating from stressed CRT-expressing cancer cells, tumours concomitantly can overexpress anti-phagocytic signals like CD47 to avoid becoming a ‘succulent bite’ to phagocytic cells sabotaging anticancer immune responses. Increased CD47 expression has been found in a wide variety of human cancers, generally being associated with an aggressive, invasive and metastatic phenotype, adverse prognosis and poor clinical outcome[984–993]. In fact, some of these tumour types are those also found to express higher levels of CRT and which correlated with worse prognosis. In the particular case of MM, similar to what occurs with CRT, several studies have shown that CD47 overexpression was directly associated with disease stages (from MGUS to overt MM)[999–1001]. It is tempting to theorise that, as a mechanism to prevent the pro-phagocytic effects of CRT exposure, myeloma cells upregulate anti-phagocytic molecules like CD47 that may serve as additional immune evasion mechanism. Thereby, this molecule could also comprise a potentially reliable predictor of clinical disease status or outcome.

Finally, apart from CRT, accumulating grounds of evidence support the idea that other DAMPs or molecules involved in UPR and autophagy, may hold prognostic and predictive value for monitoring cancer patients[81,83,284,296,740,1009,1010]. However, the relationship between these prognostic biomarkers with the tumour microenvironment and patient’s outcome requires further comprehension and clinical validation[284].

CONCLUSIONS

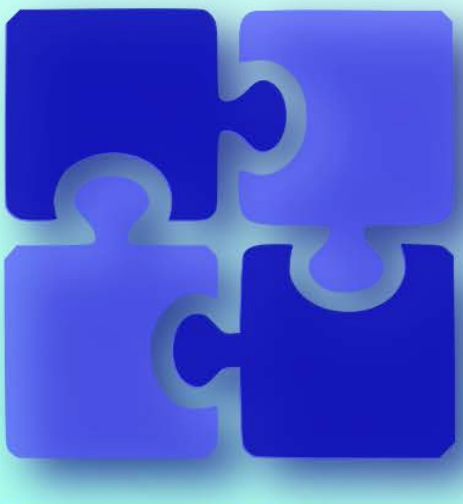

6. CONCLUSIONS

The results obtained in this work allow us to reach the following conclusions:

1. Although antimitotic drugs alone showed few to moderate cytotoxic activity, the proliferative capacity of cells was abrogated and they exhibited main morphological characteristics of mitotic catastrophe.

2. Combination of the BH3 mimetic ABT-737 with antimitotic drugs showed enhanced cytotoxic potential when compared with either drugs alone in adherent cancer cell lines, especially in A549 and MIA PaCa-2 cells. Moreover, cell death was shown to be caspase and Bax/Bak-dependent and data pointed to a redundant role of Bax and Bak in cell death under these conditions in adherent cancer cell lines.

3. Upon treatment with Aurore kinase B inhibitor barasertib, A549 and HCT-116 cells acquired a senescent phenotype and addition of ABT-737 led to cell demise in a caspase-dependent way.

4. When treated with antimitotic agents as well as ABT-737, A549 and MIA PaCa-2 cells, the survival-prone subpopulation spent less time in mitosis. These cells did not accumulate productive death signals during mitosis, thus escaping and surviving. Furthermore, co-administration of ABT-737 and MTAs, accelerated death in mitosis while only vincristine and ABT-737 combination hastened post-mitotic cell death.

5. MAD2, BUB1 and BUBR1 depletion in A549 cells treated with barasertib correlated with their early mitotic exit. On the other hand, mitotic checkpoint protein accumulation under MTA treatment could imply an intense SAC signalling.

6. Anti-apoptotic Bcl-2 family members may play redundant and cooperative roles in cell fate decisions upon mitotic arrest. Bcl-X_L might have an auxiliary role in cell death regulation during mitotic arrest and other pro-survival members like Bcl-2 and Mcl-1 could be engaged and collaborate in cell death modulation in adherent cancer cell lines.

7. Chloroquine and DBeQ but not CB-5083, strongly potentiated carfilzomib-induced cell death in MM cell lines and $CD38^+$ BMMCs isolated from MM patients. In contrast, bortezomib-based drug combinations with CLQ and DBeQ were less effective in enhancing cell demise.

8. The essential role of caspases in cell death exerted by carfilzomib-based combinations with CLQ or DBeQ was dependent on the specific MM cell line. While cell death in NCI-H929 cells was not blocked by caspase inhibition, cell demise was strongly prevented upon caspase inhibition in MM.1S, U266 and MOPC315.BM cells.

9. Necroptosis seems to play a minor role in cell death induced by carfilzomib-based combinations with CLQ or DBeQ since its inhibition with Nec-1 and NSA when caspases were blocked, did not produce significant changes in cell death rates.

10. Treatment of MM cells with carfilzomib combined with either CLQ or DBeQ, augmented the expression of several UPR markers related to both PERK and IRE1α arms, suggesting the activation of an ER stress response.

11. Reducing BIP expression by using siRNAs did not increase cell death triggered by PI-based combination with CLQ or DBeQ in MM.1S and U266 cells, suggesting that BIP do not determines sensitivity to cell death induced by proteasome inhibitors and its combinations.

12. Treatment of U266, MM.1S and MOPC315.BM MM cells with carfilzomib and the combinations with CLQ and DBeQ, can elevate $O2^{\bullet-}$ levels, while co-treatment with pan-caspase inhibitors prevented ROS generation (excepting in NCI-H929 cells).

13. Carflizomib-based single and combinatory treatment induced an early accumulation of BH3-only proteins PUMA, Bim and in a lesser extent NOXA that may counterbalance Mcl-1 initial accumulation and trigger cell death.

14. Proteasome inhibitor (PI)-based combinations instigated cell death in MM.1S Bax/Bak DKO cell line, suggesting that alternative cell death mechanisms may be activated upon Bax/Bak deficiency.

15. Bim seems to mediate in part cell death induced by PI-based drug combinations, since Bim depletion in U266 cells provided an incomplete protection, suggesting that additional BH3-only proteins may be also involved in triggering cell demise.

16. Autophagy seemed not to be the unique mechanism responsible for the cell death potentiation effect exerted by PI-based CLQ combinations. Cell death was still enhanced, although in a lesser extent, in ATG5-defective cells when subjected to PI-based combinations.

17. Chloroquine combination potentiated carfilzomib-induced proteasome inhibition more efficiently than bortezomib-induced inhibition which may explain the observed cell death differences between these two combinatorial drug schemes in MM cells.

18. MM cell lines treated *in vitro* with carfilzomib-CLQ and DBeQ combinations increased cell-surface exposure of ER chaperones (CRT, Hsp70 and BiP) and increased maturation markers on mo-DCs, which suggest that these drug treatments may potentially be ICD inducers.

19. The role of caspases in CRT exposure upon PI-based combinatory treatment is uncertain. Depending on the MM cell line evaluated, caspase inhibition enhanced exposure in MM.1S and MOPC315.BM cells but reduced exposure of this DAMP in NCI-H929 cells.

20. CRT exposure may depend on the targeted autophagic phase under evaluation. When autophagy was inhibited in early phases through ATG5 silencing, CRT exposure was partially compromised, whereas when authopagic flux was inhibited in the terminal phases with CLQ, CRT exposure was strongly potentiated. Nonetheless, the potentiation effect of CLQ over CRT exposure may be autophagy-independent.

21. Subcutaneous vaccination with dead MM cells previously treated *in vitro* with carfilzomib and CLQ did not offered significant immune protection against induced myeloma development by using an orthotopic MOPC315.BM mouse model.

22. Subcutaneous vaccination with dead by *in vitro* treatment with a combination of carfilzomib, CLQ and z-VAD-fmk showed a small survival advantage and slight delay in disease progression, possibly pointing for a immunosuppressive mechanism exerted by caspases in the immunogenicity of cell death.

23. Analysis of immune cell infiltration in BM, spleen and EMTs *ex vivo* may indicate the begining of an anti-myeloma immune response even in vaccination protocols that did not give rise to a net protection.

24. Although MOPC315.BM cells showed a high expression of PD-L1 *in vitro*, combination of vaccination with killed MM cells (carfilzomib+CLQ+zVAD) and anti-PD1 did not improve prophylactic protection offered by the vaccination approach alone.

25. Patients bearing cytogenetic abnormalities or individuals classified as PI-resistant to *ex vivo* treatment, could also be benefited by the cell death potentiation exerted by carfilzomib-based combinations with CLQ or DBeQ.

26. $CD38^{+}$ MM cells isolated from the BM of patients with plasma cell dyscrasias showed elevated levels of ecto-CRT that could be associated with disease progression and cytogenetic abnormalities

27. CRT^{hi} patients display an altered BM microenvironment, showing reduced CD4/CD8 T cell ratios with increased numbers of CD8 and reduced CD4 T cells, increased NK cell numbers, elevated DCs (pDCs and mDCs) and Treg frequencies, and increased expression of PD-1/PD-L1 markers.

28. CRT^{hi} patients may be associated poor prognosis since individuals with elevated ecto-CRT levels exhibited lower time to progression rates, increased chances of developing extramedullary plasmacytomas, are heavily pre-treated and display a high-risk cytogenetic signature.

BIBLIOGRAPHY

7. BIBLIOGRAPHY

1. Di Lonardo, A., Nasi, S. & Pulciani, S. Cancer: we should not forget the past. *J. Cancer* **6**, 29–39 (2015).
2. Hajdu, S. I. A note from history: landmarks in history of cancer, part 1. *Cancer* **117**, 1097–1102 (2011).
3. Boveri, T. Zur frage der entstehung maligner tumoren. (1914).
4. Weinberg, R. A. (Robert A. *The biology of cancer*.
5. Hanahan, D. & Weinberg, R. A. Hallmarks of cancer: the next generation. *Cell* **144**, 646–674 (2011).
6. Kerr, J. F., Wyllie, A. H. & Currie, A. R. Apoptosis: a basic biological phenomenon with wide-ranging implications in tissue kinetics. *Br. J. Cancer* **26**, 239–257 (1972).
7. Renehan, A. G., Booth, C. & Potten, C. S. What is apoptosis, and why is it important? *BMJ* **322**, 1536–1538 (2001).
8. Galluzzi, L., Vitale, I., Aaronson, S. A., Abrams, J. M., Adam, D., Agostinis, P., *et al.* Molecular mechanisms of cell death: Recommendations of the Nomenclature Committee on Cell Death 2018. *Cell Death Differ.* **25**, 486–541 (2018).
9. Shalini, S., Dorstyn, L., Dawar, S. & Kumar, S. Old, new and emerging functions of caspases. *Cell Death Differ.* **22**, 526–539 (2015).
10. Boatright, K. M., Renatus, M., Scott, F. L., Sperandio, S., Shin, H., Pedersen, I. M., *et al.* A unified model for apical caspase activation. *Mol. Cell* **11**, 529–541 (2003).
11. Rupinder, S. K., Gurpreet, A. K. & Manjeet, S. Cell suicide and caspases. *Vascul. Pharmacol.* **46**, 383–393 (2007).
12. Czabotar, P. E., Lessene, G., Strasser, A. & Adams, J. M. Control of apoptosis by the BCL-2 protein family: implications for physiology and therapy. *Nat. Rev. Mol. Cell Biol.* **15**, 49–63 (2014).
13. Pihán, P., Carreras-Sureda, A. & Hetz, C. BCL-2 family: Integrating stress responses at the ER to control cell demise. *Cell Death Differ.* **24**, 1478–1487 (2017).
14. Cory, S. & Adams, J. M. The Bcl2 family: regulators of the cellular life-or-death switch. *Nat. Rev. Cancer* **2**, 647–656 (2002).
15. Shamas-Din, A., Brahmbhatt, H., Leber, B. & Andrews, D. W. BH3-only proteins: Orchestrators of apoptosis. *Biochim. Biophys. Acta - Mol. Cell Res.* **1813**, 508–520 (2011).
16. Letai, A., Bassik, M. C., Walensky, L. D., Sorcinelli, M. D., Weiler, S. & Korsmeyer, S. J. Distinct BH3 domains either sensitize or activate mitochondrial apoptosis, serving as prototype cancer therapeutics. *Cancer Cell* **2**, 183–192 (2002).
17. Willis, S. N., Fletcher, J. I., Kaufmann, T., van Delft, M. F., Chen, L., Czabotar, P. E., *et al.* Apoptosis initiated when BH3 ligands engage multiple Bcl-2 homologs, not Bax or Bak. *Science* **315**, 856–859 (2007).
18. Brunelle, J. K. & Letai, A. Control of mitochondrial apoptosis by the Bcl-2 family. *J. Cell Sci.* **122**, 437–441 (2009).
19. Vela, L., Gonzalo, O., Naval, J. & Marzo, I. Direct Interaction of Bax and Bak Proteins with Bcl-2 Homology Domain 3 (BH3)-only Proteins in Living Cells Revealed by Fluorescence Complementation. *J. Biol. Chem.* **288**, 4935–4946 (2013).
20. Galluzzi, L., Kepp, O., Trojel-Hansen, C. & Kroemer, G. Mitochondrial control of cellular life, stress, and death. *Circ. Res.* **111**, 1198–1207 (2012).
21. Khan, K. H., Blanco-Codesido, M. & Molife, L. R. Cancer therapeutics: Targeting the apoptotic

pathway. *Crit. Rev. Oncol. Hematol.* **90**, 200–219 (2014).

22. Singh, R., Letai, A. & Sarosiek, K. Regulation of apoptosis in health and disease: the balancing act of BCL-2 family proteins. *Nat. Rev. Mol. Cell Biol.* **20**, 175–193 (2019).

23. Bock, F. J. & Tait, S. W. G. Mitochondria as multifaceted regulators of cell death. *Nat. Rev. Mol. Cell Biol.* (2019). doi:10.1038/s41580-019-0173-8

24. Locksley, R. M., Killeen, N. & Lenardo, M. J. The TNF and TNF receptor superfamilies: integrating mammalian biology. *Cell* **104**, 487–501 (2001).

25. Martinez-Lostao, L., Marzo, I., Anel, A. & Naval, J. Targeting the Apo2L/TRAIL system for the therapy of autoimmune diseases and cancer. *Biochem. Pharmacol.* **83**, 1475–1483 (2012).

26. Wang, K., Yin, X. M., Chao, D. T., Milliman, C. L. & Korsmeyer, S. J. BID: a novel BH3 domain-only death agonist. *Genes Dev.* **10**, 2859–2869 (1996).

27. Mariño, G., Niso-Santano, M., Baehrecke, E. H. & Kroemer, G. Self-consumption: the interplay of autophagy and apoptosis. *Nat. Rev. Mol. Cell Biol.* **15**, 81 (2014).

28. Golstein, P. & Kroemer, G. Cell death by necrosis: towards a molecular definition. *Trends Biochem. Sci.* **32**, 37–43 (2007).

29. Pasparakis, M. & Vandenabeele, P. Necroptosis and its role in inflammation. *Nature* **517**, 311–320 (2015).

30. Galluzzi, L., Kepp, O., Krautwald, S., Kroemer, G. & Linkermann, A. Molecular mechanisms of regulated necrosis. *Semin. Cell Dev. Biol.* **35**, 24–32 (2014).

31. Dhuriya, Y. K. & Sharma, D. Necroptosis: A regulated inflammatory mode of cell death. *J. Neuroinflammation* **15**, 1–9 (2018).

32. Conrad, M., Angeli, J. P. F., Vandenabeele, P. & Stockwell, B. R. Regulated necrosis: disease relevance and therapeutic opportunities. *Nat. Rev. Drug Discov.* **15**, 348–366 (2016).

33. Weinlich, R., Oberst, A., Beere, H. M. & Green, D. R. Necroptosis in development, inflammation and disease. *Nat. Rev. Mol. Cell Biol.* **18**, 127 (2016).

34. Ruan, W., Lim, H. H. & Surana, U. Mapping Mitotic Death: Functional Integration of Mitochondria, Spindle Assembly Checkpoint and Apoptosis. *Front. Cell Dev. Biol.* **6**, 1–9 (2019).

35. Cai, Z. & Liu, Q. Cell cycle regulation in treatment of breast cancer. *Adv. Exp. Med. Biol.* **1026**, 251–270 (2017).

36. Pack, L. R., Daigh, L. H. & Meyer, T. Putting the brakes on the cell cycle: mechanisms of cellular growth arrest. *Curr. Opin. Cell Biol.* **60**, 106–113 (2019).

37. Poon, R. Y. C. Cell Cycle Control: A System of Interlinking Oscillators. *Methods Mol. Biol.* **1342**, 3–19 (2016).

38. Barnum, K. J. & O'Connell, M. J. Cell cycle regulation by checkpoints. *Methods Mol. Biol.* **1170**, 29–40 (2014).

39. Wenzel, E. S. & Singh, A. T. K. K. Cell-cycle checkpoints and aneuploidy on the path to cancer. *In Vivo (Brooklyn).* **32**, 1–5 (2018).

40. Malumbres, M. & Barbacid, M. Mammalian cyclin-dependent kinases. *Trends Biochem. Sci.* **30**, 630–41 (2005).

41. Blagosklonny, M. V. Mitotic arrest and cell fate: why and how mitotic inhibition of transcription drives mutually exclusive events. *Cell Cycle* **6**, 70–4 (2007).

42. Le Breton, M., Cormier, P., Bellé, R., Mulner-Lorillon, O. & Morales, J. Translational control during mitosis. *Biochimie* **87**, 805–11 (2005).

43. Vicente, J. J. & Wordeman, L. Mitosis, microtubule dynamics and the evolution of kinesins. *Exp. Cell Res.* **334**, 61–69 (2015).

44. Lischetti, T. & Nilsson, J. Regulation of mitotic progression by the spindle assembly checkpoint.

Mol. Cell. Oncol. **2**, e970484 (2015).

45. Foley, E. a & Kapoor, T. M. Microtubule attachment and spindle assembly checkpoint signalling at the kinetochore. *Nat. Rev. Mol. Cell Biol.* **14**, 25–37 (2013).

46. Pines, J. Mitosis: A matter of getting rid of the right protein at the right time. *Trends Cell Biol.* **16**, 55–63 (2006).

47. Mc Gee, M. M., Gee, M. M. M. & Mc Gee, M. M. Targeting the Mitotic Catastrophe Signaling Pathway in Cancer. *Mediators Inflamm.* **2015**, 146282 (2015).

48. Musacchio, A. The Molecular Biology of Spindle Assembly Checkpoint Signaling Dynamics. *Curr. Biol.* **25**, R1002–R1018 (2015).

49. Lara-Gonzalez, P., Westhorpe, F. G. & Taylor, S. S. The Spindle Assembly Checkpoint. *Curr. Biol.* **22**, R966–R980 (2012).

50. Sacristan, C. & Kops, G. J. P. L. P. L. Joined at the hip: kinetochores, microtubules, and spindle assembly checkpoint signaling. *Trends Cell Biol.* **25**, 21–8 (2015).

51. Sivakumar, S. & Gorbsky, G. J. Spatiotemporal regulation of the anaphase-promoting complex in mitosis. *Nat. Rev. Mol. Cell Biol.* **16**, 82–94 (2015).

52. Penna, L. S., Henriques, J. A. P. J. A. P. & Bonatto, D. Anti-mitotic agents: Are they emerging molecules for cancer treatment? *Pharmacol. Ther.* **173**, 67–82 (2017).

53. Krenn, V. & Musacchio, A. The Aurora B Kinase in Chromosome Bi-Orientation and Spindle Checkpoint Signaling. *Front. Oncol.* **5**, 225 (2015).

54. Lampson, M. A. & Cheeseman, I. M. Sensing centromere tension: Aurora B and the regulation of kinetochore function. *Trends Cell Biol.* **21**, 133–140 (2011).

55. Vitale, I., Galluzzi, L., Castedo, M. & Kroemer, G. Mitotic catastrophe: a mechanism for avoiding genomic instability. *Nat. Rev. Mol. Cell Biol.* **12**, 385–392 (2011).

56. Manic, G., Corradi, F., Sistigu, A., Siteni, S. & Vitale, I. Molecular Regulation of the Spindle Assembly Checkpoint by Kinases and Phosphatases. *Int. Rev. Cell Mol. Biol.* **328**, 105–161 (2017).

57. Galluzzi, L., Vitale, I., Abrams, J. M., Alnemri, E. S., Baehrecke, E. H., Blagosklonny, M. V, *et al.* Molecular definitions of cell death subroutines: recommendations of the Nomenclature Committee on Cell Death 2012. *Cell Death Differ.* **19**, 107–120 (2012).

58. Castedo, M., Perfettini, J.-L., Roumier, T., Valent, A., Raslova, H., Yakushijin, K., *et al.* Mitotic catastrophe constitutes a special case of apoptosis whose suppression entails aneuploidy. *Oncogene* **23**, 4362–70 (2004).

59. Dawar, S., Lim, Y., Puccini, J., White, M., Thomas, P., Bouchier-Hayes, L., *et al.* Caspase-2-mediated cell death is required for deleting aneuploid cells. *Oncogene* **36**, 2704–2714 (2017).

60. Vakifahmetoglu, H., Olsson, M., Tamm, C., Heidari, N., Orrenius, S. & Zhivotovsky, B. DNA damage induces two distinct modes of cell death in ovarian carcinomas. *Cell Death Differ.* **15**, 555–66 (2008).

61. Krumschnabel, G., Sohm, B., Bock, F., Manzl, C. & Villunger, A. The enigma of caspase-2: the laymen's view. *Cell Death Differ.* **16**, 195–207 (2009).

62. Gascoigne, K. E. & Taylor, S. S. Cancer cells display profound intra- and interline variation following prolonged exposure to antimitotic drugs. *Cancer Cell* **14**, 111–22 (2008).

63. Topham, C. H. & Taylor, S. S. Mitosis and apoptosis: how is the balance set? *Curr. Opin. Cell Biol.* **25**, 780–5 (2013).

64. Brito, D. a. & Rieder, C. L. Mitotic checkpoint slippage in humans occurs via cyclin B destruction in the presence of an active checkpoint. *Curr. Biol.* **16**, 1194–1200 (2006).

65. Sakurikar, N., Eichhorn, J. M. & Chambers, T. C. Cyclin-dependent kinase-1 (Cdk1)/cyclin B1 dictates cell fate after mitotic arrest via phosphoregulation of antiapoptotic Bcl-2 proteins. *J. Biol. Chem.* **287**, 39193–39204 (2012).

66. Huang, H.-C. C., Shi, J., Orth, J. D. & Mitchison, T. J. Evidence that mitotic exit is a better cancer therapeutic target than spindle assembly. *Cancer Cell* **16**, 347–358 (2009).

67. Lee, K., Kenny, A. E. & Rieder, C. L. Caspase activity is not required for the mitotic checkpoint or mitotic slippage in human cells. *Mol. Biol. Cell* **22**, 2470–2479 (2011).

68. Huang, H.-C., Mitchison, T. J. & Shi, J. Stochastic competition between mechanistically independent slippage and death pathways determines cell fate during mitotic arrest. *PLoS One* **5**, e15724 (2010).

69. Eichhorn, J. M., Sakurikar, N., Alford, S. E., Chu, R. & Chambers, T. C. Critical role of anti-apoptotic Bcl-2 protein phosphorylation in mitotic death. *Cell Death Dis.* **4**, e834 (2013).

70. Colin, D. J., Hain, K. O., Allan, L. A. & Clarke, P. R. Cellular responses to a prolonged delay in mitosis are determined by a DNA damage response controlled by Bcl-2 family proteins. *Open Biol.* **5**, 140156 (2015).

71. Harley, M. E., Allan, L. A., Sanderson, H. S. & Clarke, P. R. Phosphorylation of Mcl-1 by CDK1-cyclin B1 initiates its Cdc20-dependent destruction during mitotic arrest. *EMBO J.* **29**, 2407–20 (2010).

72. Basu, A. & Haldar, S. Identification of a novel Bcl-xL phosphorylation site regulating the sensitivity of taxol- or 2-methoxyestradiol-induced apoptosis. *FEBS Lett.* **538**, 41–47 (2003).

73. Barillé-Nion, S., Bah, N., Véquaud, E. & Juin, P. Regulation of cancer cell survival by BCL2 family members upon prolonged mitotic arrest: opportunities for anticancer therapy. *Anticancer Res.* **32**, 4225–33 (2012).

74. Fhearraigh, S. Mac, Mc Gee, M. M., Mac Fhearraigh, S. & Mc Gee, M. M. Cyclin B1 interacts with the BH3-only protein Bim and mediates its phosphorylation by Cdk1 during mitosis. *Cell Cycle* **10**, 3886–3896 (2011).

75. Han, C. R., Jun, D. Y., Lee, J. Y. & Kim, Y. H. Prometaphase arrest-dependent phosphorylation of Bcl-2 and Bim reduces the association of Bcl-2 with Bak or Bim, provoking Bak activation and mitochondrial apoptosis in nocodazole-treated Jurkat T cells. *Apoptosis* **19**, 224–240 (2014).

76. Gilley, R., Lochhead, P. A., Balmanno, K., Oxley, D., Clark, J. & Cook, S. J. CDK1, not ERK1/2 or ERK5, is required for mitotic phosphorylation of BIMEL. *Cell. Signal.* **24**, 170–180 (2012).

77. Ganem, N. J., Storchova, Z. & Pellman, D. Tetraploidy, aneuploidy and cancer. *Curr. Opin. Genet. Dev.* **17**, 157–62 (2007).

78. Davoli, T. & de Lange, T. The causes and consequences of polyploidy in normal development and cancer. *Annu. Rev. Cell Dev. Biol.* **27**, 585–610 (2011).

79. Storchova, Z. & Pellman, D. From polyploidy to aneuploidy, genome instability and cancer. *Nat. Rev. Mol. Cell Biol.* **5**, 45–54 (2004).

80. Seelige, R., Searles, S. & Bui, J. D. Mechanisms regulating immune surveillance of cellular stress in cancer. *Cell. Mol. Life Sci.* **75**, 225–240 (2018).

81. Senovilla, L., Vitale, I., Martins, I., Tailler, M., Pailleret, C., Michaud, M., *et al.* An immunosurveillance mechanism controls cancer cell ploidy. *Science (80-.).* **337**, 1678–1684 (2012).

82. Senovilla, L., Vitale, I., Martins, I., Kepp, O., Galluzzi, L., Zitvogel, L., *et al.* An anticancer therapy-elicited immunosurveillance system that eliminates tetraploid cells. *OncoImmunology* (2013).

83. Bezu, L., Sauvat, A., Humeau, J., Gomes-da-Silva, L. C., Iribarren, K., Forveille, S., *et al.* eIF2α phosphorylation is pathognomonic for immunogenic cell death. *Cell Death Differ.* 1–19 (2018). doi:10.1038/s41418-017-0044-9

84. Menger, L., Vacchelli, E., Adjemian, S., Martins, I., Ma, Y., Shen, S., *et al.* Cardiac glycosides exert anticancer effects by inducing immunogenic cell death. *Sci. Transl. Med.* **4**, 143ra99 (2012).

85. Sukkurwala, A. Q., Adjemian, S., Senovilla, L., Michaud, M., Spaggiari, S., Vacchelli, E., *et al.* Screening of novel immunogenic cell death inducers within the NCI mechanistic diversity set.

Oncoimmunology **3**, (2014).

86. Ghiringhelli, F. F., Apetoh, L., Tesniere, A., Aymeric, L., Ma, Y., Ortiz, C., *et al.* Activation of the NLRP3 inflammasome in dendritic cells induces IL-1B-dependent adaptive immunity against tumors. *Nat. Med.* **15**, 1170–1178 (2009).

87. Michaud, M., Martins, I., Sukkurwala, A. Q., Adjemian, S., Ma, Y., Pellegatti, P., *et al.* Autophagy-Dependent Anticancer Immune Responses Induced by Chemotherapeutic Agents in Mice. *Science (80-.).* **334**, 1573 LP – 1577 (2011).

88. Apetoh, L., Ghiringhelli, F., Tesniere, A., Obeid, M., Ortiz, C., Criollo, A., *et al.* Toll-like receptor 4-dependent contribution of the immune system to anticancer chemotherapy and radiotherapy. *Nat. Med.* **13**, 1050–1059 (2007).

89. Galluzzi, L., Senovilla, L., Zitvogel, L. & Kroemer, G. The secret ally: immunostimulation by anticancer drugs. *Nat. Rev. Drug Discov.* **11**, 215–233 (2012).

90. Olziersky, A.-M. & Labidi-Galy, S. I. Clinical Development of Anti-mitotic Drugs in Cancer. *Adv. Exp. Med. Biol.* **1002**, 125–152 (2017).

91. Denisenko, T. V., Sorokina, I. V., Gogvadze, V. & Zhivotovsky, B. Mitotic catastrophe and cancer drug resistance: A link that must to be broken. *Drug Resist. Updat.* **24**, 1–12 (2016).

92. Henriques, A. C., Ribeiro, D., Pedrosa, J., Sarmento, B., Silva, P. M. A. P. M. A. & Bousbaa, H. Mitosis inhibitors in anticancer therapy: When blocking the exit becomes a solution. *Cancer Lett.* **440–441**, 64–81 (2019).

93. Van Vuuren, R. J., Visagie, M. H., Theron, A. E. & Joubert, A. M. Antimitotic drugs in the treatment of cancer. *Cancer Chemother. Pharmacol.* **76**, 1101–1112 (2015).

94. Magnaghi-Jaulin, L., Eot-Houllier, G. G., Gallaud, E. & Giet, R. R. Aurora a protein kinase: To the centrosome and beyond. *Biomolecules* **9**, (2019).

95. Liewer, S. & Huddleston, A. Alisertib: a review of pharmacokinetics, efficacy and toxicity in patients with hematologic malignancies and solid tumors. *Expert Opin. Investig. Drugs* **27**, 105–112 (2018).

96. Marzo, I. & Naval, J. Antimitotic drugs in cancer chemotherapy: Promises and pitfalls. *Biochem. Pharmacol.* **86**, 703–710 (2013).

97. Gutteridge, R. E. A., Ndiaye, M. A., Liu, X. & Ahmad, N. Plk1 Inhibitors in Cancer Therapy: From Laboratory to Clinics. *Mol. Cancer Ther.* **15**, 1427–1435 (2016).

98. Almanza, A., Carlesso, A., Chintha, C., Creedican, S., Doultsinos, D., Leuzzi, B., *et al.* Endoplasmic Reticulum Stress signalling - from basic mechanisms to clinical applications. *FEBS J.* (2018). doi:10.1111/febs.14608

99. Moon, H. W., Han, H. G. & Jeon, Y. J. Protein Quality Control in the Endoplasmic Reticulum and Cancer. *Int. J. Mol. Sci.* **19**, 3020 (2018).

100. Meusser, B., Hirsch, C., Jarosch, E. & Sommer, T. ERAD: The long road to destruction. *Nat. Cell Biol.* **7**, 766–772 (2005).

101. Wu, X. & Rapoport, T. A. Mechanistic insights into ER-associated protein degradation. *Curr. Opin. Cell Biol.* **53**, 22–28 (2018).

102. Wang, M., Law, M. E., Castellano, R. K. & Law, B. K. The unfolded protein response as a target for anticancer therapeutics. *Crit. Rev. Oncol. Hematol.* **127**, 66–79 (2018).

103. Ruggiano, A., Foresti, O. & Carvalho, P. ER-associated degradation: Protein quality control and beyond. *J. Cell Biol.* **204**, 869–879 (2014).

104. Stach, L. & Freemont, P. S. The AAA+ ATPase p97, a cellular multitool. *Biochem. J.* **474**, 2953–2976 (2017).

105. Meyer, H. & Weihl, C. C. The VCP/p97 system at a glance: Connecting cellular function to disease pathogenesis. *J. Cell Sci.* **127**, 3877–3883 (2014).

106. Miller, J. M. & Enemark, E. J. Fundamental Characteristics of AAA+ Protein Family Structure and Function. *Archaea* **2016**, 9294307 (2016).

107. Kwon, Y. T. & Ciechanover, A. The Ubiquitin Code in the Ubiquitin-Proteasome System and Autophagy. *Trends Biochem. Sci.* **42**, 873–886 (2017).

108. Manasanch, E. E. & Orlowski, R. Z. Proteasome inhibitors in cancer therapy. *Nat. Rev. Clin. Oncol.* **14**, 417–433 (2017).

109. Albornoz, N., Bustamante, H., Soza, A. & Burgos, P. Cellular Responses to Proteasome Inhibition: Molecular Mechanisms and Beyond. *Int. J. Mol. Sci.* **20**, 3379 (2019).

110. Thibaudeau, T. A. & Smith, D. M. A Practical Review of Proteasome Pharmacology. *Pharmacol. Rev.* **71**, 170–197 (2019).

111. Coll-mart, B., Coll-Martinez, B., Crosas, B. & Coll-mart, B. How the 26S Proteasome Degrades Ubiquitinated Proteins in the Cell. *Biomolecules* **9**, 1–14 (2019).

112. Dufey, E., Hetz, C., Chevet, E., Urra, H., Avril, T., Dufey, E., *et al.* Endoplasmic Reticulum Stress and the Hallmarks of Cancer. *Trends in Cancer* **2**, 252–262 (2016).

113. Sano, R. & Reed, J. C. ER stress-induced cell death mechanisms. *Biochim. Biophys. Acta - Mol. Cell Res.* **1833**, 3460–3470 (2013).

114. Hetz, C. The unfolded protein response: Controlling cell fate decisions under ER stress and beyond. *Nat. Rev. Mol. Cell Biol.* **13**, 89–102 (2012).

115. Hetz, C. & Papa, F. R. The Unfolded Protein Response and Cell Fate Control. *Mol. Cell* **69**, 169–181 (2018).

116. Iurlaro, R. & Muñoz-Pinedo, C. Cell death induced by endoplasmic reticulum stress. *FEBS J.* **283**, 2640–2652 (2016).

117. Corazzari, M., Gagliardi, M., Fimia, G. M. & Piacentini, M. Endoplasmic Reticulum Stress, Unfolded Protein Response, and Cancer Cell Fate. *Front. Oncol.* **7**, 1–11 (2017).

118. Todd, D. J., Lee, A. H. & Glimcher, L. H. The endoplasmic reticulum stress response in immunity and autoimmunity. *Nat. Rev. Immunol.* **8**, 663–674 (2008).

119. Deng, X., Xiao, L., Lang, W., Gao, F., Ruvolo, P. & May, W. S. Novel Role for JNK as a Stress-activated Bcl2 Kinase. *J. Biol. Chem.* **276**, 23681–23688 (2001).

120. Lei, K. & Davis, R. J. JNK phosphorylation of Bim-related members of the Bcl2 family induces Bax-dependent apoptosis. *Proc. Natl. Acad. Sci.* **100**, 2432–2437 (2003).

121. Puthalakath, H., O'Reilly, L. A., Gunn, P., Lee, L., Kelly, P. N., Huntington, N. D., *et al.* ER stress triggers apoptosis by activating BH3-only protein Bim. *Cell* **129**, 1337–1349 (2007).

122. Yamaguchi, H. & Wang, H.-G. G. CHOP is involved in endoplasmic reticulum stress-induced apoptosis by enhancing DR5 expression in human carcinoma cells. *J. Biol. Chem.* **279**, 45495–45502 (2004).

123. Novoa, I., Zeng, H., Harding, H. P. & Ron, D. Feedback inhibition of the unfolded protein response by GADD34-mediated dephosphorylation of eIF2alpha. *J. Cell Biol.* **153**, 1011–1022 (2001).

124. Cazanave, S. C., Elmi, N. A., Akazawa, Y., Bronk, S. F., Mott, J. L. & Gores, G. J. CHOP and AP-1 cooperatively mediate PUMA expression during lipoapoptosis. *Am. J. Physiol. Gastrointest. Liver Physiol.* **299**, G236-43 (2010).

125. Armstrong, J. L., Flockhart, R., Veal, G. J., Lovat, P. E. & Redfern, C. P. F. F. Regulation of endoplasmic reticulum stress-induced cell death by ATF4 in neuroectodermal tumor cells. *J. Biol. Chem.* **285**, 6091–6100 (2010).

126. McCullough, K. D., Martindale, J. L., Klotz, L.-O. O., Aw, T.-Y. Y. & Holbrook, N. J. Gadd153 sensitizes cells to endoplasmic reticulum stress by down-regulating Bcl2 and perturbing the cellular redox state. *Mol. Cell. Biol.* **21**, 1249–1259 (2001).

127. Marciniak, S. J., Yun, C. Y., Oyadomari, S., Novoa, I., Zhang, Y., Jungreis, R., *et al.* CHOP induces death by promoting protein synthesis and oxidation in the stressed endoplasmic reticulum. *Genes Dev.* **18**, 3066–3077 (2004).

128. Harding, H. P., Zhang, Y., Zeng, H., Novoa, I., Lu, P. D., Calfon, M., *et al.* An Integrated Stress Response Regulates Amino Acid Metabolism and Resistance to Oxidative Stress National Institute of Environmental Health Sciences. *Mol. Cell* **11**, 619–633 (2003).

129. Gomez-Bougie, P., Halliez, M., Moreau, P., Pellat-Deceunynck, C. & Amiot, M. Repression of Mcl-1 and disruption of the Mcl-1/Bak interaction in myeloma cells couple ER stress to mitochondrial apoptosis. *Cancer Lett.* **383**, 204–211 (2016).

130. Iurlaro, R., Puschel, F., Leon-Annicchiarico, C. L., O'Connor, H., Martin, S. J., Palou-Gramon, D., *et al.* Glucose Deprivation Induces ATF4-Mediated Apoptosis through TRAIL Death Receptors. *Mol. Cell. Biol.* **37**, (2017).

131. Hiramatsu, N., Chiang, W. C., Kurt, T. D., Sigurdson, C. J. & Lin, J. H. Multiple Mechanisms of Unfolded Protein Response-Induced Cell Death. *Am. J. Pathol.* **185**, 1800–1808 (2015).

132. Balsas, P., Lopez-Royuela, N., Galan-Malo, P., Anel, A., Marzo, I. & Naval, J. Cooperation between Apo2L/TRAIL and bortezomib in multiple myeloma apoptosis. *Biochem. Pharmacol.* **77**, 804–812 (2009).

133. Li, J., Lee, B. & Lee, A. S. Endoplasmic reticulum stress-induced apoptosis: multiple pathways and activation of p53-up-regulated modulator of apoptosis (PUMA) and NOXA by p53. *J. Biol. Chem.* **281**, 7260–7270 (2006).

134. Lin, W. C., Chuang, Y. C., Chang, Y. S., Lai, M. D., Teng, Y. N., Su, I. J., *et al.* Endoplasmic reticulum stress stimulates p53 expression through NF-κB activation. *PLoS One* **7**, (2012).

135. Sovolyova, N., Healy, S., Samali, A. & Logue, S. E. Stressed to death - Mechanisms of ER stress-induced cell death. *Biol. Chem.* **395**, 1–13 (2014).

136. Ren, D., Tu, H.-C., Kim, H., Wang, G. X., Bean, G. R., Takeuchi, O., *et al.* BID, BIM, and PUMA are essential for activation of the BAX- and BAK-dependent cell death program. *Science* **330**, 1390–1393 (2010).

137. Rao, R. V., Ellerby, H. M. & Bredesen, D. E. Coupling endoplasmic reticulum stress to the cell death program. *Cell Death Differ.* **11**, 372–380 (2004).

138. Bhat, T. A., Chaudhary, A. K., Kumar, S., O'Malley, J., Inigo, J. R., Kumar, R., *et al.* Endoplasmic reticulum-mediated unfolded protein response and mitochondrial apoptosis in cancer. *Biochim. Biophys. acta. Rev. cancer* **1867**, 58–66 (2017).

139. Hetz, C., C., H., P., B., J., F., A.-H., L., M.C., B., *et al.* Proapoptotic BAX and BAK Modulate the Unfolded Protein Response by a Direct Interaction with IRE1 . *Science (80-.).* **312**, 572–576 (2006).

140. Rodriguez, D., Rojas-Rivera, D. & Hetz, C. Integrating stress signals at the endoplasmic reticulum: The BCL-2 protein family rheostat. *Biochim. Biophys. Acta - Mol. Cell Res.* **1813**, 564–574 (2011).

141. Lisbona, F., Rojas-Rivera, D., Thielen, P., Zamorano, S., Todd, D., Martinon, F., *et al.* BAX Inhibitor-1 Is a Negative Regulator of the ER Stress Sensor IRE1α. *Mol. Cell* **33**, 679–691 (2009).

142. Klee, M., Pallauf, K., Alcalá, S., Fleischer, A. & Pimentel-Muños, F. X. Mitochondrial apoptosis induced by BH3-only molecules in the exclusive presence of endoplasmic reticular Bak. *EMBO J.* **28**, 1757–1768 (2009).

143. Wang, X., Olberding, K. E., White, C. & Li, C. Bcl-2 proteins regulate ER membrane permeability to luminal proteins during ER stress-induced apoptosis. *Cell Death Differ.* **18**, 38–47 (2011).

144. Kanekura, K., Ma, X., Murphy, J. T., Zhu, L. J., Diwan, A. & Urano, F. IRE1 prevents endoplasmic reticulum membrane permeabilization and cell death under pathological conditions. *Sci. Signal.* **8**, ra62 (2015).

145. Chong, S. J. F., Marchi, S., Petroni, G., Kroemer, G., Galluzzi, L. & Pervaiz, S. Noncanonical Cell

Fate Regulation by Bcl-2 Proteins. *Trends Cell Biol.* 1–19 (2020). doi:10.1016/j.tcb.2020.03.004

146. Szegezdi, E., Logue, S. E., Gorman, A. M. & Samali, A. Mediators of endoplasmic reticulum stress-induced apoptosis. *EMBO Rep.* **7**, 880–885 (2006).

147. Russo, M. & Russo, G. L. Autophagy inducers in cancer. *Biochem. Pharmacol.* 0–1 (2018). doi:10.1016/j.bcp.2018.02.007

148. Galluzzi, L., Pietrocola, F., Pedro, J. M. B., Ravi, K., Maiuri, M. C., Martin, S. J., *et al.* Autophagy in malignant transformation and cancer progression. **34**, 856–880 (2015).

149. Liang, X. H., Jackson, S., Seaman, M., Brown, K., Kempkes, B., Hibshoosh, H., *et al.* Induction of autophagy and inhibition of tumorigenesis by beclin 1. *Nature* **402**, 672–676 (1999).

150. Takahashi, Y., Hori, T., Cooper, T. K., Liao, J., Desai, N., Serfass, J. M., *et al.* Bif-1 haploinsufficiency promotes chromosomal instability and accelerates Myc-driven lymphomagenesis via suppression of mitophagy. *Blood* **121**, 1622–1632 (2013).

151. Mathew, R., Karp, C. M., Beaudoin, B., Vuong, N., Chen, G., Chen, H.-Y., *et al.* Autophagy suppresses tumorigenesis through elimination of p62. *Cell* **137**, 1062–1075 (2009).

152. Green, D. R., Galluzzi, L. & Kroemer, G. Mitochondria and the autophagy-inflammation-cell death axis in organismal aging. *Science* **333**, 1109–1112 (2011).

153. Zitvogel, L., Kepp, O., Galluzzi, L. & Kroemer, G. Inflammasomes in carcinogenesis and anticancer immune responses. *Nat. Immunol.* **13**, 343–351 (2012).

154. Pietrocola, F., Bravo-San Pedro, J. M., Galluzzi, L. & Kroemer, G. Autophagy in natural and therapy-driven anticancer immunosurveillance. *Autophagy* **13**, 2163–2170 (2017).

155. Lazova, R., Camp, R. L., Klump, V., Siddiqui, S. F., Amaravadi, R. K. & Pawelek, J. M. Punctate LC3B expression is a common feature of solid tumors and associated with proliferation, metastasis, and poor outcome. *Clin. Cancer Res.* **18**, 370–379 (2012).

156. Yun, Z., Zhichao, J., Hao, Y., Ou, J., Ran, Y., Wen, D., *et al.* Targeting autophagy in multiple myeloma. *Leuk. Res.* **59**, 97–104 (2017).

157. Galluzzi, L., Baehrecke, E. H., Ballabio, A., Boya, P., Bravo-San Pedro, J. M., Cecconi, F., *et al.* Molecular definitions of autophagy and related processes. *EMBO J.* **36**, 1811–1836 (2017).

158. Desantis, V., Saltarella, I., Lamanuzzi, A., Mariggiò, M. A., Racanelli, V., Vacca, A., *et al.* Autophagy: A New Mechanism of Prosurvival and Drug Resistance in Multiple Myeloma. *Transl. Oncol.* **11**, 1350–1357 (2018).

159. Yu, L., Chen, Y. & Tooze, S. A. Autophagy pathway: Cellular and molecular mechanisms. *Autophagy* **14**, 207–215 (2018).

160. Marinkovi, M., Matilda, Š., Buljuba, M., Novak, I., Marinkovic, M., Sprung, M., *et al.* Autophagy Modulation in Cancer: Current Knowledge on Action and Therapy. *Oxid. Med. Cell. Longev.* **2018**, 8023821 (2018).

161. Onorati, A. V., Dyczynski, M., Ojha, R. & Amaravadi, R. K. Targeting autophagy in cancer. *Cancer* **124**, 3307–3318 (2018).

162. Pérez-Hernández, M., Arias, A., Martínez-García, D., Pérez-Tomás, R., Quesada, R. & Soto-Cerrato, V. Targeting Autophagy for Cancer Treatment and Tumor Chemosensitization. *Cancers (Basel).* **11**, 1599 (2019).

163. Høyer-Hansen, M. & Jäättelä, M. Connecting endoplasmic reticulum stress to autophagy by unfolded protein response and calcium. *Cell Death Differ.* **14**, 1576–1582 (2007).

164. Corazzari, M., Rapino, F., Ciccosanti, F., Giglio, P., Antonioli, M., Conti, B., *et al.* Oncogenic BRAF induces chronic ER stress condition resulting in increased basal autophagy and apoptotic resistance of cutaneous melanoma. *Cell Death Differ.* **22**, 946–958 (2015).

165. Velasco, G., Verfaillie, T., Salazar, M. & Agostinis, P. Linking ER stress to autophagy: Potential implications for cancer therapy. *Int. J. Cell Biol.* **2010**, (2010).

166. Lin, Y., Jiang, M., Chen, W., Zhao, T. & Wei, Y. Cancer and ER stress: Mutual crosstalk between autophagy, oxidative stress and inflammatory response. *Biomed. Pharmacother.* **118**, 109249 (2019).

167. Eisenberg-Lerner, A., Bialik, S., Simon, H.-U. & Kimchi, A. Life and death partners: apoptosis, autophagy and the cross-talk between them. *Cell Death Differ.* **16**, 966–975 (2009).

168. Maiuri, M. C., Zalckvar, E., Kimchi, A. & Kroemer, G. Self-eating and self-killing: crosstalk between autophagy and apoptosis. *Nat. Rev. Mol. Cell Biol.* **8**, 741–752 (2007).

169. Galluzzi, L., Bravo-San Pedro, J. M., Levine, B., Green, D. R. & Kroemer, G. Pharmacological modulation of autophagy: therapeutic potential and persisting obstacles. *Nat. Rev. Drug Discov.* **16**, 487 (2017).

170. Thorburn, A. Autophagy and disease. *J. Biol. Chem.* **293**, 5425–5430 (2018).

171. Levy, J. M. M., Towers, C. G. & Thorburn, A. Targeting autophagy in cancer. *Nat. Rev. Cancer* **17**, 528–542 (2017).

172. Guo, J. Y., Chen, H.-Y., Mathew, R., Fan, J., Strohecker, A. M., Karsli-Uzunbas, G., *et al.* Activated Ras requires autophagy to maintain oxidative metabolism and tumorigenesis. *Genes Dev.* **25**, 460–470 (2011).

173. Eng, C. H., Wang, Z., Tkach, D., Toral-Barza, L., Ugwonali, S., Liu, S., *et al.* Macroautophagy is dispensable for growth of KRAS mutant tumors and chloroquine efficacy. *Proc. Natl. Acad. Sci.* **113**, 182 LP – 187 (2016).

174. Towers, C. G. & Thorburn, A. Therapeutic Targeting of Autophagy. *EBioMedicine* **14**, 15–23 (2016).

175. Kinsey, C. G., Camolotto, S. A., Boespflug, A. M., Guillen, K. P., Foth, M., Truong, A., *et al.* Protective autophagy elicited by RAF→MEK→ERK inhibition suggests a treatment strategy for RAS-driven cancers. *Nat. Med.* **25**, 620–627 (2019).

176. Bryant, K. L., Stalnecker, C. A., Zeitouni, D., Klomp, J. E., Peng, S., Tikunov, A. P., *et al.* Combination of ERK and autophagy inhibition as a treatment approach for pancreatic cancer. *Nat. Med.* **25**, 628–640 (2019).

177. Ding, W.-X., Ni, H.-M., Gao, W., Hou, Y.-F., Melan, M. A., Chen, X., *et al.* Differential effects of endoplasmic reticulum stress-induced autophagy on cell survival. *J. Biol. Chem.* **282**, 4702–4710 (2007).

178. Cunha, L. D., Yang, M., Carter, R., Guy, C., Harris, L., Crawford, J. C., *et al.* LC3-Associated Phagocytosis in Myeloid Cells Promotes Tumor Immune Tolerance. *Cell* **175**, 429-441.e16 (2018).

179. Bishop, E. & Bradshaw, T. D. Autophagy modulation: a prudent approach in cancer treatment? *Cancer Chemother. Pharmacol.* **82**, 913–922 (2018).

180. Maycotte, P., Aryal, S., Cummings, C. T., Thorburn, J., Morgan, M. J., Thorburn, A., *et al.* Chloroquine sensitizes breast cancer cells to chemotherapy independent of autophagy. *Autophagy* **8**, 200–212 (2012).

181. Vogl, D. T., Stadtmauer, E. A., Tan, K.-S., Heitjan, D. F., Davis, L. E., Pontiggia, L., *et al.* Combined autophagy and proteasome inhibition: a phase 1 trial of hydroxychloroquine and bortezomib in patients with relapsed/refractory myeloma. *Autophagy* **10**, 1380–1390 (2014).

182. Marciniak, S. J. Endoplasmic reticulum stress: a key player in human disease. *FEBS J.* **286**, 228–231 (2019).

183. Riha, R., Gupta-Saraf, P., Bhanja, P., Badkul, S. & Saha, S. Stressed Out - Therapeutic Implications of ER Stress Related Cancer Research. *Oncomedicine* **2**, 156–167 (2017).

184. Mohamed, E., Cao, Y. & Rodriguez, P. C. Endoplasmic reticulum stress regulates tumor growth and anti-tumor immunity: a promising opportunity for cancer immunotherapy. *Cancer Immunol. Immunother.* **66**, 1069–1078 (2017).

185. Mahadevan, N. R., Rodvold, J., Sepulveda, H., Rossi, S., Drew, A. F. & Zanetti, M. Transmission of

endoplasmic reticulum stress and pro-inflammation from tumor cells to myeloid cells. *Proc. Natl. Acad. Sci. U. S. A.* **108**, 6561–6566 (2011).

186. De Sanctis, F., Solito, S., Ugel, S., Molon, B., Bronte, V. & Marigo, I. MDSCs in cancer: Conceiving new prognostic and therapeutic targets. *Biochim. Biophys. Acta - Rev. Cancer* **1865**, 35–48 (2016).

187. Cubillos-Ruiz, J. R., Mohamed, E. & Rodriguez, P. C. Unfolding anti-tumor immunity: ER stress responses sculpt tolerogenic myeloid cells in cancer. *J. Immunother. Cancer* **5**, 1–10 (2017).

188. Hetz, C., Chevet, E. & Harding, H. P. Targeting the unfolded protein response in disease. *Nat. Rev. Drug Discov.* **12**, 703–719 (2013).

189. Reimold, A. M., Iwakoshi, N. N., Manis, J., Vallabhajosyula, P., Szomolanyi-Tsuda, E., Gravallese, E. M., *et al.* Plasma cell differentiation requires the transcription factor XBP-1. *Nature* **412**, 300 (2001).

190. Iwakoshi, N. N., Lee, A. H., Vallabhajosyula, P., Otipoby, K. L., Rajewsky, K. & Glimcher, L. H. Plasma cell differentiation and the unfolded protein response intersect at the transcription factor XBP-I. *Nat. Immunol.* **4**, 321–329 (2003).

191. Nakamura, M., Gotoh, T., Okuno, Y., Tatetsu, H., Sonoki, T., Uneda, S., *et al.* Activation of the endoplasmic reticulum stress pathway is associated with survival of myeloma cells. *Leuk. Lymphoma* **47**, 531–539 (2006).

192. Chapman, M. A., Lawrence, M. S., Keats, J. J., Cibulskis, K., Sougnez, C., Schinzel, A. C., *et al.* Initial genome sequencing and analysis of multiple myeloma. *Nature* **471**, 467–472 (2011).

193. Bagratuni, T., Wu, P., Gonzalez de Castro, D., Davenport, E. L., Dickens, N. J., Walker, B. A., *et al.* XBP1s levels are implicated in the biology and outcome of myeloma mediating different clinical outcomes to thalidomide-based treatments. *Blood* **116**, 250–253 (2010).

194. Carrasco, D. R., Sukhdeo, K., Protopopova, M., Sinha, R., Enos, M., Carrasco, D. E. E., *et al.* The Differentiation and Stress Response Factor XBP-1 Drives Multiple Myeloma Pathogenesis. *Cancer Cell* **11**, 349–360 (2007).

195. Nikesitch, N., Lee, J. M., Ling, S. & Roberts, T. L. Endoplasmic reticulum stress in the development of multiple myeloma and drug resistance. *Clin. Transl. Immunol.* **7**, e1007 (2018).

196. Ling, S. C. W., Lau, E. K. K., Al-Shabeeb, A., Nikolic, A., Catalano, A., Iland, H., *et al.* Response of myeloma to the proteasome inhibitor bortezomib is correlated with the unfolded protein response regulator XBP-1. *Haematologica* **97**, 64–72 (2012).

197. Obeng, E. A., Carlson, L. M., Gutman, D. M., Harrington, W. J. J., Lee, K. P., Boise, L. H., *et al.* Proteasome inhibitors induce a terminal unfolded protein response in multiple myeloma cells. *Blood* **107**, 4907–4917 (2006).

198. Gandolfi, S., Laubach, J. P., Hideshima, T., Chauhan, D., Anderson, K. C. & Richardson, P. G. The proteasome and proteasome inhibitors in multiple myeloma. *Cancer Metastasis Rev.* **36**, 561–584 (2017).

199. Leleu, X., Martin, T. G., Einsele, H., Lyons, R. M., Durie, B. G. M., Iskander, K. S., *et al.* Role of Proteasome Inhibitors in Relapsed and/or Refractory Multiple Myeloma. *Clin. Lymphoma, Myeloma Leuk.* (2018). doi:10.1016/j.clml.2018.08.016

200. Scalzulli, E., Grammatico, S., Vozella, F. & Petrucci, M. T. Proteasome inhibitors for the treatment of multiple myeloma. *Expert Opin. Pharmacother.* **19**, 375–386 (2018).

201. Robak, P., Drozdz, I., Szemraj, J. & Robak, T. Drug resistance in multiple myeloma. *Cancer Treat. Rev.* **70**, 199–208 (2018).

202. Auner, H. W., Moody, A. M., Ward, T. H., Kraus, M., Milan, E., May, P., *et al.* Combined Inhibition of p97 and the Proteasome Causes Lethal Disruption of the Secretory Apparatus in Multiple Myeloma Cells. *PLoS One* **8**, 1–11 (2013).

203. Chou, T. F., Brown, S. J., Minond, D., Nordin, B. E., Li, K., Jones, A. C., *et al.* Reversible inhibitor of

p97, DBeQ, impairs both ubiquitin-dependent and autophagic protein clearance pathways. *Proc. Natl. Acad. Sci. U. S. A.* **108**, 4834–4839 (2011).

204. Zhou, H.-J., Wang, J., Yao, B., Wong, S., Djakovic, S., Kumar, B., *et al.* Discovery of a First-in-Class, Potent, Selective, and Orally Bioavailable Inhibitor of the p97 AAA ATPase (CB-5083). *J. Med. Chem.* **58**, 9480–9497 (2015).

205. Le Moigne, R., Aftab, B. T., Djakovic, S., Dhimolea, E., Valle, E., Murnane, M., *et al.* The p97 inhibitor CB-5083 is a unique disrupter of protein homeostasis in models of Multiple Myeloma. *Mol. Cancer Ther.* molcanther.0233.2017 (2017). doi:10.1158/1535-7163.MCT-17-0233

206. Mimura, N., Fulciniti, M., Gorgun, G., Tai, Y., Cirstea, D., Santo, L., *et al.* Blockade of XBP1 splicing by inhibition of IRE1a is a promising therapeutic option in multiple myeloma Naoya. *Blood* **119**, 5772–5782 (2012).

207. Papandreou, I., Denko, N. C., Olson, M., Van Melckebeke, H., Lust, S., Tam, A., *et al.* Identification of an Ire1alpha endonuclease specific inhibitor with cytotoxic activity against human multiple myeloma. *Blood* **117**, 1311–1314 (2011).

208. Hoi, W., Li, H., Grant, S. W., Heerding, D. A., Minthorn, E. & Mencken, T. Supporting Information Discovery of GSK2656157 : An Optimized PERK Inhibitor Selected for Preclinical Development. 4–8 (2013).

209. Atkins, C., Liu, Q., Minthorn, E., Zhang, S. Y., Figueroa, D. J., Moss, K., *et al.* Characterization of a novel PERK kinase inhibitor with antitumor and antiangiogenic activity. *Cancer Res.* **73**, 1993–2002 (2013).

210. van Vliet, A. R., Martin, S., Garg, A. D. & Agostinis, P. The PERKs of damage-associated molecular patterns mediating cancer immunogenicity: From sensor to the plasma membrane and beyond. *Semin. Cancer Biol.* **33**, 74–85 (2015).

211. Gonzalez-Teuber, V., Albert-Gasco, H., Auyeung, V. C., Papa, F. R., Mallucci, G. R. & Hetz, C. Small Molecules to Improve ER Proteostasis in Disease. *Trends Pharmacol. Sci.* 1–12 (2019). doi:10.1016/j.tips.2019.07.003

212. Neckers, L. & Workman, P. Hsp90 molecular chaperone inhibitors: are we there yet? *Clin. Cancer Res.* **18**, 64–76 (2012).

213. Pyrko, P., Schonthal, A. H., Hofman, F. M., Chen, T. C. & Lee, A. S. The unfolded protein response regulator GRP78/BiP as a novel target for increasing chemosensitivity in malignant gliomas. *Cancer Res.* **67**, 9809–9816 (2007).

214. Poon, I. K. H., Lucas, C. D., Rossi, A. G. & Ravichandran, K. S. Apoptotic cell clearance: Basic biology and therapeutic potential. *Nat. Rev. Immunol.* **14**, 166–180 (2014).

215. Yatim, N., Jusforgues-Saklani, H., Orozco, S., Schulz, O., Barreira da Silva, R., Reis e Sousa, C., *et al.* RIPK1 and NF-κB signaling in dying cells determines cross-priming of CD8+ T cells. *Science (80-.).* **350**, 328 LP – 334 (2015).

216. Galluzzi, L., Buqué, A., Kepp, O., Zitvogel, L. & Kroemer, G. Immunogenic cell death in cancer and infectious disease. *Nat. Rev. Immunol.* **17**, 97–111 (2017).

217. Steller, Y. F. and H. Live to die another way: modes of pprogrammed cell death and the signals emanating drom dying cells. *Nat. Rev. Mol. Cell Biol.* **6**, 1–14 (2015).

218. Matzinger, P. The danger model: a renewed sense of self. *Science* **296**, 301–305 (2002).

219. Obeid, M., Tesniere, A., Ghiringhelli, F., Fimia, G. M., Apetoh, L., Perfettini, J.-L., *et al.* Calreticulin exposure dictates the immunogenicity of cancer cell death. *Nat. Med.* **13**, 54–61 (2007).

220. Garg, A. D., More, S., Rufo, N., Mece, O., Sassano, M. L., Agostinis, P., *et al.* Trial watch: Immunogenic cell death induction by anticancer chemotherapeutics. *Oncoimmunology* **6**, (2017).

221. Golden, E. B., Pellicciotta, I., Demaria, S., Barcellos-Hoff, M. H. & Formenti, S. C. The convergence of radiation and immunogenic cell death signaling pathways. *Front. Oncol.* **2**, 88 (2012).

222. Adkins, I., Fucikova, J., Garg, A. D., Agostinis, P. & Špíšek, R. Physical modalities inducing immunogenic tumor cell death for cancer immunotherapy. *Oncoimmunology* **3**, e968434 (2014).

223. Martins, I., Kepp, O., Schlemmer, F., Adjemian, S., Tailler, M., Shen, S., *et al.* Restoration of the immunogenicity of cisplatin-induced cancer cell death by endoplasmic reticulum stress. *Oncogene* **30**, 1147–1158 (2011).

224. Dudek-Perić, A. M., Ferreira, G. B., Muchowicz, A., Wouters, J., Prada, N., Martin, S., *et al.* Antitumor immunity triggered by melphalan is potentiated by melanoma cell surface-associated calreticulin. *Cancer Res.* **75**, 1603–1614 (2015).

225. Rufo, N., Garg, A. D. & Agostinis, P. The Unfolded Protein Response in Immunogenic Cell Death and Cancer Immunotherapy. *Trends in Cancer* **3**, 643–658 (2017).

226. Berghe, T. Vanden, Vanlangenakker, N., Parthoens, E., Deckers, W., Devos, M., Festjens, N., *et al.* Necroptosis, necrosis and secondary necrosis converge on similar cellular disintegration features. *Cell Death Differ.* **17**, 922 (2009).

227. Krysko, D. V., Garg, A. D., Kaczmarek, A., Krysko, O., Agostinis, P. & Vandenabeele, P. Immunogenic cell death and DAMPs in cancer therapy. *Nat. Rev. Cancer* **12**, 860–875 (2012).

228. Garg, A. D., Dudek-Peric, A. M., Romano, E. & Agostinis, P. Immunogenic cell death. *Int. J. Dev. Biol.* **59**, 131–140 (2015).

229. Kroemer, G., Galluzzi, L., Kepp, O. & Zitvogel, L. Immunogenic Cell Death in Cancer Therapy ICD: immunogenic cell death. *Annu. Rev. Immunol* **31**, 51–72 (2013).

230. Casares, N., Pequignot, M. O., Tesniere, A., Ghiringhelli, F. F., Roux, S. S., Chaput, N., *et al.* Caspase-dependent immunogenicity of doxorubicin-induced tumor cell death. *J. Exp. Med.* **202**, 1691–1701 (2005).

231. Chen, D. S. & Mellman, I. Oncology meets immunology: The cancer-immunity cycle. *Immunity* **39**, 1–10 (2013).

232. Aaes, T. L., Kaczmarek, A., Delvaeye, T., De Craene, B., De Koker, S., Heyndrickx, L., *et al.* Vaccination with Necroptotic Cancer Cells Induces Efficient Anti-tumor Immunity. *Cell Rep.* **15**, 274–287 (2016).

233. Yang, H., Ma, Y., Chen, G., Zhou, H., Yamazaki, T., Klein, C., *et al.* Contribution of RIP3 and MLKL to immunogenic cell death signaling in cancer chemotherapy. *Oncoimmunology* **5**, 1–13 (2016).

234. Schiavoni, G., Sistigu, A., Valentini, M., Mattei, F., Sestili, P., Spadaro, F., *et al.* Cyclophosphamide Synergizes with Type I Interferons through Systemic Dendritic Cell Reactivation and Induction of Immunogenic Tumor Apoptosis. **71**, 768–779 (2011).

235. Tesniere, A., Schlemmer, F., Boige, V., Kepp, O., Martins, I., Ghiringhelli, F., *et al.* Immunogenic death of colon cancer cells treated with oxaliplatin. *Oncogene* **29**, 482–491 (2009).

236. Minotti, G., Menna, P., Salvatorelli, E., Cairo, G. & Gianni, L. Anthracyclines : Molecular Advances and Pharmacologic Developments in Antitumor Activity and Cardiotoxicity. *Pharmacol. Rev.* **56**, 185–229 (2004).

237. Merin, N. & Kelly, K. Clinical Use of Proteasome Inhibitors in the Treatment of Multiple Myeloma. *Pharmaceuticals* **8**, 1–20 (2014).

238. Jarauta, V., Jaime, P., Gonzalo, O., de Miguel, D., Ramírez-Labrada, A., Martínez-Lostao, L., *et al.* Inhibition of autophagy with chloroquine potentiates carfilzomib-induced apoptosis in myeloma cells in vitro and in vivo. *Cancer Lett.* **382**, 1–10 (2016).

239. Bezu, L., Gomes-de-Silva, L. C., Dewitte, H., Breckpot, K., Fucikova, J., Spisek, R., *et al.* Combinatorial strategies for the induction of immunogenic cell death. *Front. Immunol.* **6**, 187 (2015).

240. Medzhitov, R. & Janeway, C. A. J. Decoding the patterns of self and nonself by the innate immune system. *Science* **296**, 298–300 (2002).

241. Agostinis, P. Cell death and immunity in cancer : From danger signals to mimicry of pathogen

defense responses. **280**, 126–148 (2017).

242. Matzinger, P. Tolerance, Danger, and the Extended Family. *Annu. Rev. Immunol.* **12**, 991–1045 (1994).

243. Johnson, S., Michalak, M., Opas, M. & Eggleton, P. The ins and outs of calreticulin: From the ER lumen to the extracellular space. *Trends Cell Biol.* **11**, 122–129 (2001).

244. Michalak, M., Groenendyk, J., Szabo, E., Gold, L. I. & Opas, M. Calreticulin, a multi-process calcium-buffering chaperone of the endoplasmic reticulum. *Biochem. J.* **417**, 651 LP – 666 (2009).

245. Gardai, S. J., Mcphillips, K. A., Frasch, S. C., Janssen, W. J., Starefeldt, A., Murphy-ullrich, J. E., *et al.* Cell-Surface Calreticulin Initiates Clearance of Viable or Apoptotic Cells through trans - Activation of LRP on the Phagocyte. **123**, 321–334 (2005).

246. Pawaria, S. & Binder, R. J. CD91-dependent programming of T-helper cell responses following heat shock protein immunization. *Nat. Commun.* **2**, 511–521 (2011).

247. Spisek, R., Charalambous, A., Mazumder, A., Vesole H., D., Jagannath Sundar & Dhodapkar V., M. Bortezomib enhances dendritic cell (DC)–mediated induction of immunity to human myeloma via exposure of cell surface heat shock protein 90 on dying tumor cells: therapeutic implications. *Blood* **109**, 4839–4845 (2007).

248. Lin, T. J., Lin, H. T., Chang, W. T., Pradeep Mitapalli, S., Hsiao, P. W., Yin, S. Y., *et al.* Shikonin-enhanced cell immunogenicity of tumor vaccine is mediated by the differential effects of DAMP components. *Mol. Cancer* **14**, 1–13 (2015).

249. Pei, Q., Pan, J., Zhu, H., Ding, X., Liu, W., Lv, Y., *et al.* Gemcitabine-treated pancreatic cancer cell medium induces the specific CTL antitumor activity by stimulating the maturation of dendritic cells. *Int. Immunopharmacol.* **19**, 10–16 (2014).

250. Song, S., Zhou, F., Chen, W. R. & Xing, D. PDT-induced HSP70 externalization up-regulates NO production via TLR2 signal pathway in macrophages. *FEBS Lett.* **587**, 128–135 (2013).

251. Liu, T.-T., Wu, Y. & Niu, T. Human DKK1 and human HSP70 fusion DNA vaccine induces an effective anti-tumor efficacy in murine multiple myeloma. *Oncotarget* **9**, 178–191 (2018).

252. Tamura, Y., Hirohashi, Y., Kutomi, G., Nakanishi, K., Kamiguchi, K., Torigoe, T., *et al.* Tumor-Produced Secreted Form of Binding of Immunoglobulin Protein Elicits Antigen-Specific Tumor Immunity. *J. Immunol.* **186**, 4325–4330 (2011).

253. Feng, H., Zeng, Y., Whitesell, L. & Katsanis, E. Stressed apoptotic tumor cells express heat shock proteins and elicit tumor-specific immunity. *Blood* **97**, 3505–3512 (2001).

254. Feng, H., Zeng, Y., Graner, M. W., Likhacheva, A. & Katsanis, E. Exogenous stress proteins enhance the immunogenicity of apoptotic tumor cells and stimulate antitumor immunity. *Blood* **101**, 245–252 (2003).

255. Panaretakis, T., Kepp, O., Brockmeier, U., Tesniere, A., Bjorklund, A.-C. C., Chapman, D. C., *et al.* Mechanisms of pre-apoptotic calreticulin exposure in immunogenic cell death. *EMBO J.* **28**, 578–90 (2009).

256. Osman, R., Tacnet-Delorme, P., Kleman, J.-P. P., Millet, A. & Frachet, P. Calreticulin Release at an Early Stage of Death Modulates the Clearance by Macrophages of Apoptotic Cells. *Front. Immunol.* **8**, 1034 (2017).

257. Garg, A. D., Krysko, D. V, Verfaillie, T., Kaczmarek, A., Ferreira, G. B., Marysael, T., *et al.* A novel pathway combining calreticulin exposure and ATP secretion in immunogenic cancer cell death. *EMBO J.* **31**, 1062–1079 (2012).

258. Païdassi, H., Tacnet-Delorme, P., Verneret, M., Gaboriaud, C., Houen, G., Duus, K., *et al.* Investigations on the c1q-calreticulin-phosphatidylserine interactions yield new insights into apoptotic cell recognition. *J. Mol. Biol.* **408**, 277–290 (2011).

259. Wijeyesakere, S. J., Bedi, S. K., Huynh, D. & Raghavan, M. The C-Terminal Acidic Region of

Calreticulin Mediates Phosphatidylserine Binding and Apoptotic Cell Phagocytosis. *J. Immunol.* **196**, 3896 LP – 3909 (2016).

260. Tarr, J. M., Young, P. J., Morse, R., Shaw, D. J., Haigh, R., Petrov, P. G., *et al.* A Mechanism of Release of Calreticulin from Cells During Apoptosis. *J. Mol. Biol.* **401**, 799–812 (2010).

261. Elliott, M. R., Chekeni, F. B., Trampont, P. C., Lazarowski, E. R., Kadl, A., Walk, S. F., *et al.* Nucleotides released by apoptotic cells act as a find-me signal to promote phagocytic clearance. *Nature* **461**, 282 (2009).

262. Ma, Y., Aymeric, L., Locher, C., Mattarollo, S. R., Delahaye, N. F., Pereira, P., *et al.* Contribution of IL-17–producing γδ T cells to the efficacy of anticancer chemotherapy. *J. Exp. Med.* **208**, 491–503 (2011).

263. Martins, I., Wang, Y., Michaud, M., Ma, Y., Sukkurwala, A. Q., Shen, S., *et al.* Molecular mechanisms of ATP secretion during immunogenic cell death. *Cell Death Differ.* **21**, 79–91 (2014).

264. Garg, A. D., Martin, S., Golab, J. & Agostinis, P. Danger signalling during cancer cell death: Origins, plasticity and regulation. *Cell Death Differ.* **21**, 26–38 (2014).

265. Garg, A. D., Dudek, A. M., Ferreira, G. B., Verfaillie, T., Vandenabeele, P., Krysko, D. V., *et al.* ROS-induced autophagy in cancer cells assists in evasion from determinants of immunogenic cell death. *Autophagy* **9**, 1292–1307 (2013).

266. Garg, A. D., Nowis, D., Golab, J., Vandenabeele, P., Krysko, D. V. & Agostinis, P. Immunogenic cell death , DAMPs and anticancer therapeutics : An emerging amalgamation. *BBA - Rev. Cancer* **1805**, 53–71 (2010).

267. Müller, S., Ronfani, L. & Bianchi, M. E. Regulated expression and subcellular localization of HMGB1, a chromatin protein with a cytokine function. *J. Intern. Med.* **255**, 332–343 (2004).

268. Scaffidi, P., Misteli, T. & Bianchi, M. E. Release of chromatin protein HMGB1 by necrotic cells triggers inflammation. *Nature* **418**, 191–195 (2002).

269. Sims, G. P., Rowe, D. C., Rietdijk, S. T., Herbst, R. & Coyle, A. J. HMGB1 and RAGE in Inflammation and Cancer. *Annu. Rev. Immunol.* **28**, 367–388 (2010).

270. Saenz, R., Futalan, D., Leutenez, L., Eekhout, F., Fecteau, J. F., Sundelius, S., *et al.* TLR4-dependent activation of dendritic cells by an HMGB1-derived peptide adjuvant. *J. Transl. Med.* **12**, 1–11 (2014).

271. Bell, C. W., Jiang, W., Reich, C. F. 3rd & Pisetsky, D. S. The extracellular release of HMGB1 during apoptotic cell death. *Am. J. Physiol. Cell Physiol.* **291**, C1318-25 (2006).

272. Venereau, E., Casalgrandi, M., Schiraldi, M., Antoine, D. J., Cattaneo, A., De Marchis, F., *et al.* Mutually exclusive redox forms of HMGB1 promote cell recruitment or proinflammatory cytokine release. *J. Exp. Med.* **209**, 1519–1528 (2012).

273. Yang, H., Lundbäck, P., Ottosson, L., Erlandsson-Harris, H., Venereau, E., Bianchi, M. E., *et al.* Redox modification of cysteine residues regulates the cytokine activity of high mobility group box-1 (HMGB1). *Mol. Med.* **18**, 250–259 (2012).

274. Jube, S., Rivera, Z. S., Bianchi, M. E., Powers, A., Wang, E., Pagano, I., *et al.* Cancer cell secretion of the DAMP protein HMGB1 supports progression in malignant mesothelioma. *Cancer Res.* **72**, 3290–3301 (2012).

275. Palumbo, R., Sampaolesi, M., De Marchis, F., Tonlorenzi, R., Colombetti, S., Mondino, A., *et al.* Extracellular HMGB1, a signal of tissue damage, induces mesoangioblast migration and proliferation. *J. Cell Biol.* **164**, 441 LP – 449 (2004).

276. Rodriguez-Ruiz, M. E., Buqué, A., Hensler, M., Chen, J., Bloy, N., Petroni, G., *et al.* Apoptotic caspases inhibit abscopal responses to radiation and identify a new prognostic biomarker for breast cancer patients. *Oncoimmunology* **8**, (2019).

277. White, M. J., McArthur, K., Metcalf, D., Lane, R. M., Cambier, J. C., Herold, M. J., *et al.* Apoptotic

caspases suppress mtDNA-induced STING-mediated type I IFN production. *Cell* **159**, 1549–1562 (2014).

278. Rongvaux, A., Jackson, R., Harman, C. C. D., Li, T., West, A. P., de Zoete, M. R., *et al.* Apoptotic caspases prevent the induction of type I interferons by mitochondrial DNA. *Cell* **159**, 1563–1577 (2014).

279. Kesavardhana, S. Spotlight Targeting Apoptosis Inhibition to Activate Antitumor Immunity. *Trends Immunol.* 10–12 (2019). doi:10.1016/j.it.2019.11.002

280. Sistigu, A., Yamazaki, T., Vacchelli, E., Chaba, K., Enot, D. P., Adam, J., *et al.* Cancer cell-autonomous contribution of type I interferon signaling to the efficacy of chemotherapy. *Nat. Med.* **20**, 1301–1309 (2014).

281. Vacchelli, E., Ma, Y., Baracco, E. E., Sistigu, A., Enot, D. P., Pietrocola, F., *et al.* Chemotherapy-induced antitumor immunity requires formyl peptide receptor 1. *Science* **350**, 972–978 (2015).

282. Vacchelli, E., Enot, D. P., Pietrocola, F., Zitvogel, L. & Kroemer, G. Impact of Pattern Recognition Receptors on the Prognosis of Breast Cancer Patients Undergoing Adjuvant Chemotherapy. *Cancer Res.* **76**, 3122–3126 (2016).

283. Ghiringhelli, F., Apetoh, L., Tesniere, A., Aymeric, L., Ma, Y., Ortiz, C., *et al.* Activation of the NLRP3 inflammasome in dendritic cells induces IL-1beta-dependent adaptive immunity against tumors. *Nat. Med.* **15**, 1170–1178 (2009).

284. Fucikova, J., Kasikova, L., Truxova, I., Laco, J., Skapa, P., Ryska, A., *et al.* Relevance of the chaperone-like protein calreticulin for the biological behavior and clinical outcome of cancer. *Immunol. Lett.* **193**, 25–34 (2018).

285. Garg, A. D., De Ruysscher, D. & Agostinis, P. Immunological metagene signatures derived from immunogenic cancer cell death associate with improved survival of patients with lung, breast or ovarian malignancies: A large-scale meta-analysis. *Oncoimmunology* **5**, 1–17 (2016).

286. Fucikova, J., Becht, E., Iribarren, K., Goc, J., Remark, R., Damotte, D., *et al.* Calreticulin expression in human non-small cell lung cancers correlates with increased accumulation of antitumor immune cells and favorable prognosis. *Cancer Res.* **76**, 1–12 (2016).

287. Stoll, G., Iribarren, K., Michels, J., Leary, A., Zitvogel, L., Cremer, I., *et al.* Calreticulin expression: Interaction with the immune infiltrate and impact on survival in patients with ovarian and non-small cell lung cancer. *Oncoimmunology* **5**, 1–8 (2016).

288. Peng, R. Q., Chen, Y. B., Ding, Y., Zhang, R., Zhang, X., Yu, X. J., *et al.* Expression of calreticulin is associated with infiltration of T-cells in stage III B colon cancer. *World J. Gastroenterol.* **16**, 2428–2434 (2010).

289. Fucikova, J., Truxova, I., Hensler, M., Becht, E., Kasikova, L., Moserova, I., *et al.* Calreticulin exposure by malignant blasts correlates with robust anticancer immunity and improved clinical outcome in AML patients. *Blood* **128**, 3113–3124 (2016).

290. Garg, A. D., Elsen, S., Krysko, D. V., Vandenabeele, P., de Witte, P. & Agostinis, P. Resistance to anticancer vaccination effect is controlled by a cancer cell-autonomous phenotype that disrupts immunogenic phagocytic removal. *Oncotarget* **6**, 26841–26860 (2015).

291. Zappasodi, R., Pupa, S. M., Ghedini, G. C., Bongarzone, I., Magni, M., Cabras, A. D., *et al.* Improved clinical outcome in indolent B-cell lymphoma patients vaccinated with autologous tumor cells experiencing immunogenic death. *Cancer Res.* **70**, 9062–9072 (2010).

292. Xu, Q., Chen, C., Chen, G., Chen, W., Zhou, D. & Xie, Y. Significance of calreticulin as a prognostic factor in endometrial cancer. *Oncol. Lett.* **15**, 8999–9008 (2018).

293. Chen, C.-N., Chang, C.-C., Su, T.-E., Hsu, W.-M., Jeng, Y.-M., Ho, M.-C., *et al.* Identification of calreticulin as a prognosis marker and angiogenic regulator in human gastric cancer. *Ann. Surg. Oncol.* **16**, 524–533 (2009).

294. Sheng, W., Chen, C., Dong, M., Zhou, J., Liu, Q., Dong, Q., *et al.* Overexpression of calreticulin contributes to the development and progression of pancreatic cancer. *J. Cell. Physiol.* **229**, 887–

897 (2014).

295. Chao, M. P., Chao, M. P., Jaiswal, S., Weissman-tsukamoto, R., Alizadeh, A. A., Park, C. Y., *et al.* Calreticulin Is the Dominant Pro-Phagocytic Signal on Multiple Human Cancers and Is Counterbalanced by CD47. *Sci. Transl. Med.* **2**, (2010).

296. He, Y., Correa, A. M., Raso, M. G., Hofstetter, W. L., Fang, B., Behrens, C., *et al.* The role of PKR/eIF2α signaling pathway in prognosis of Non-Small cell lung cancer. *PLoS One* **6**, (2011).

297. Uramoto, H., Sugio, K., Oyama, T., Nakata, S., Ono, K., Yoshimastu, T., *et al.* Expression of endoplasmic reticulum molecular chaperone Grp78 in human lung cancer and its clinical significance. *Lung Cancer* **49**, 55–62 (2005).

298. Montico, B., Nigro, A., Casolaro, V. & Dal Col, J. Immunogenic apoptosis as a novel tool for anticancer vaccine development. *Int. J. Mol. Sci.* **19**, (2018).

299. Rapoport, B. L. & Anderson, R. Realizing the Clinical Potential of Immunogenic Cell Death in Cancer Chemotherapy and Radiotherapy. *Int. J. Mol. Sci.* **20**, 959 (2019).

300. Ladoire, S., Enot, D., Andre, F., Zitvogel, L. & Kroemer, G. Immunogenic cell death-related biomarkers: Impact on the survival of breast cancer patients after adjuvant chemotherapy. *Oncoimmunology* **5**, 1–3 (2016).

301. Aoto, K., Mimura, K., Okayama, H., Saito, M., Chida, S., Noda, M., *et al.* Immunogenic tumor cell death induced by chemotherapy in patients with breast cancer and esophageal squamous cell carcinoma. *Oncol. Rep.* **39**, 151–159 (2018).

302. Galluzzi, L., Buqué, A., Kepp, O., Zitvogel, L. & Kroemer, G. Immunological Effects of Conventional Chemotherapy and Targeted Anticancer Agents. *Cancer Cell* **28**, 690–714 (2015).

303. Tesniere, A., Panaretakis, T., Kepp, O., Apetoh, L., Ghiringhelli, F., Zitvogel, L., *et al.* Molecular characteristics of immunogenic cancer cell death. *Cell Death Differ.* **15**, 3–12 (2008).

304. Madeo, F., Durchschlag, M., Kepp, O., Panaretakis, T., Zitvogel, L., Fröhlich, K. U., *et al.* Phylogenetic conservation of the preapoptotic calreticulin exposure pathway from yeast to mammals. *Cell Cycle* **8**, 639–642 (2009).

305. Park, B.-J., Lee, D.-G., Yu, J.-R., Jung, S., Choi, K., Lee, J., *et al. Calreticulin, a Calcium-binding Molecular Chaperone, Is Required for Stress Response and Fertility in Caenorhabditis elegans*. *Molecular Biology of the Cell* **12**, (2001).

306. Wu, H., Ng, B. S. H. & Thibault, G. Endoplasmic reticulum stress response in yeast and humans. *Biosci. Rep.* **34**, 321–330 (2014).

307. Kepp, O., Menger, L., Vacchelli, E., Locher, C., Adjemian, S., Yamazaki, T., *et al.* Crosstalk between ER stress and immunogenic cell death. *Cytokine Growth Factor Rev.* **24**, 311–318 (2013).

308. van Vliet, A. R., Giordano, F., Gerlo, S., Segura, I., Van Eygen, S., Molenberghs, G., *et al.* The ER Stress Sensor PERK Coordinates ER-Plasma Membrane Contact Site Formation through Interaction with Filamin-A and F-Actin Remodeling. *Mol. Cell* **65**, 885-899.e6 (2017).

309. van Vliet, A. R. & Agostinis, P. When under pressure, get closer: PERKing up membrane contact sites during ER stress. *Biochem. Soc. Trans.* **44**, 499–504 (2016).

310. Peters, L. R. & Raghavan, M. Endoplasmic Reticulum Calcium Depletion Impacts Chaperone Secretion, Innate Immunity, and Phagocytic Uptake of Cells. *J. Immunol.* **187**, 919–931 (2011).

311. Ye, T., Jiang, K., Wei, L., Barr, M. P., Xu, Q., Zhang, G., *et al.* Oncolytic Newcastle disease virus induces autophagy-dependent immunogenic cell death in lung cancer cells. *Am. J. Cancer Res.* **8**, 1514–1527 (2018).

312. van Vloten, J. P., Workenhe, S. T., Wootton, S. K., Mossman, K. L. & Bridle, B. W. Critical Interactions between Immunogenic Cancer Cell Death, Oncolytic Viruses, and the Immune System Define the Rational Design of Combination Immunotherapies. *J. Immunol.* **200**, 450–458 (2018).

313. Wong, D. Y. Q., Ong, W. W. F. & Ang, W. H. Induction of immunogenic cell death by chemotherapeutic platinum complexes. *Angew. Chem. Int. Ed. Engl.* **54**, 6483–6487 (2015).

314. Verfaillie, T., Garg, A. D. & Agostinis, P. Targeting ER stress induced apoptosis and inflammation in cancer. *Cancer Lett.* **332**, 249–264 (2013).

315. Lipchick BC, Fink, EE, Nikiforov, M. Oxidative Stress and Proteasome Inhibitors in Multiple Myeloma. *Pharmacol Res* **105**, 210–215 (2016).

316. Garg, A. D., Krysko, D. V, Vandenabeele, P. & Agostinis, P. The emergence of phox-ER stress induced immunogenic apoptosis. *Oncoimmunology* **1**, 786–788 (2012).

317. Garg, A. D., Krysko, D. V, Vandenabeele, P. & Agostinis, P. Hypericin-based photodynamic therapy induces surface exposure of damage-associated molecular patterns like HSP70 and calreticulin. *Cancer Immunol. Immunother.* **61**, 215–221 (2012).

318. Parker, K. H., Beury, D. W. & Ostrand-Rosenberg, S. Myeloid-Derived Suppressor Cells: Critical Cells Driving Immune Suppression in the Tumor Microenvironment. *Adv. Cancer Res.* **128**, 95–139 (2015).

319. Colegio, O. R., Chu, N., Szabo, A. L., Chu, T., Rhebergen, A. M., Jairam, V., *et al.* Functional polarization of tumour-associated macrophages by tumour-derived lactic acid. *Nature* **513**, 559–563 (2014).

320. Mahadevan, N. R., Anufreichik, V., Rodvold, J. J., Chiu, K. T., Sepulveda, H. & Zanetti, M. Cell-Extrinsic Effects of Tumor ER Stress Imprint Myeloid Dendritic Cells and Impair CD8 + T Cell Priming. **7**, (2012).

321. Lee, B.-R. R., Chang, S.-Y. Y., Hong, E.-H. H., Kwon, B.-E. E., Kim, H. M., Kim, Y.-J. J., *et al.* Elevated endoplasmic reticulum stress reinforced immunosuppression in the tumor microenvironment via myeloid-derived suppressor cells. *Oncotarget* **5**, 12331–12345 (2014).

322. Michallet, A. S., Mondiere, P., Taillardet, M., Leverrier, Y., Genestier, L. & Defrance, T. Compromising the unfolded protein response induces autophagy-mediated cell death in multiple myeloma cells. *PLoS One* **6**, 1–12 (2011).

323. Dewaele, M., Martinet, W., Rubio, N., Verfaillie, T., de Witte, P. A., Piette, J., *et al.* Autophagy pathways activated in response to PDT contribute to cell resistance against ROS damage. *J. Cell. Mol. Med.* **15**, 1402–1414 (2011).

324. Rubio, N., Coupienne, I., Di Valentin, E., Heirman, I., Grooten, J., Piette, J., *et al.* Spatiotemporal autophagic degradation of oxidatively damaged organelles after photodynamic stress is amplified by mitochondrial reactive oxygen species. *Autophagy* **8**, 1312–1324 (2012).

325. Wiersma, V. R., Michalak, M., Abdullah, T. M., Bremer, E. & Eggleton, P. Mechanisms of Translocation of ER Chaperones to the Cell Surface and Immunomodulatory Roles in Cancer and Autoimmunity. *Front. Oncol.* **5**, 1–14 (2015).

326. Martin, S., Dudek-Perić, A. M., Maes, H., Garg, A. D., Gabrysiak, M., Demirsoy, S., *et al.* Concurrent MEK and autophagy inhibition is required to restore cell death associated danger-signalling in Vemurafenib-resistant melanoma cells. *Biochem. Pharmacol.* **93**, 290–304 (2015).

327. McKnight, N. C., Zhong, Y., Wold, M. S., Gong, S., Phillips, G. R., Dou, Z., *et al.* Beclin 1 Is Required for Neuron Viability and Regulates Endosome Pathways via the UVRAG-VPS34 Complex. *PLoS Genet.* **10**, 1–18 (2014).

328. Kim, H. J., Zhong, Q., Sheng, Z.-H., Yoshimori, T., Liang, C. & Jung, J. U. Beclin-1-interacting autophagy protein Atg14L targets the SNARE-associated protein Snapin to coordinate endocytic trafficking. *J. Cell Sci.* **125**, 4740–4750 (2012).

329. Hyttinen, J. M. T., Niittykoski, M., Salminen, A. & Kaarniranta, K. Maturation of autophagosomes and endosomes: A key role for Rab7. *Biochim. Biophys. Acta - Mol. Cell Res.* **1833**, 503–510 (2013).

330. Nars, M. S. & Kaneno, R. Immunomodulatory effects of low dose chemotherapy and perspectives of its combination with immunotherapy. *Int. J. Cancer* **132**, 2471–2478 (2013).

331. Kersten, K., Salvagno, C. & de Visser, K. E. Exploiting the Immunomodulatory Properties of Chemotherapeutic Drugs to Improve the Success of Cancer Immunotherapy. *Front. Immunol.* **6**, 516 (2015).

332. Wu, J. & Waxman, D. J. Immunogenic chemotherapy: Dose and schedule dependence and combination with immunotherapy. *Cancer Lett.* **419**, 210–221 (2018).

333. Chen, Y. L., Chang, M. C. & Cheng, W. F. Metronomic chemotherapy and immunotherapy in cancer treatment. *Cancer Lett.* **400**, 282–292 (2017).

334. Tsao, S. Y. The role of metronomic chemotherapy in the era of cancer immunotherapy: an oncologist's perspective. *Curr. Oncol.* **26**, e422–e424 (2019).

335. Bracci, L., Schiavoni, G., Sistigu, A. & Belardelli, F. Immune-based mechanisms of cytotoxic chemotherapy: implications for the design of novel and rationale-based combined treatments against cancer. *Cell Death Differ.* **21**, 15–25 (2014).

336. Carter, C. R. D., Horgan, K., Mounsey, K., Foster, R. E., Verma, R., Smalle, N., *et al.* Lymphocyte depletion and repopulation after chemotherapy for primary breast cancer. *Breast Cancer Res.* **18**, 10 (2016).

337. Fagnoni, F. F., Lozza, L., Zibera, C., Zambelli, A., Ponchio, L., Gibelli, N., *et al.* T-cell dynamics after high-dose chemotherapy in adults: elucidation of the elusive CD8+ subset reveals multiple homeostatic T-cell compartments with distinct implications for immune competence. *Immunology* **106**, 27–37 (2002).

338. Barrett, A. J. & Savani, B. N. Does chemotherapy modify the immune surveillance of hematological malignancies? *Leukemia* **23**, 53–58 (2009).

339. Kim, S. Y., Lee, H., Han, M.-S., Shim, H., Eom, H.-S., Park, B., *et al.* Post-Transplantation Natural Killer Cell Count: A Predictor of Acute Graft-Versus-Host Disease and Survival Outcomes After Allogeneic Hematopoietic Stem Cell Transplantation. *Clin. Lymphoma, Myeloma Leuk.* **16**, 527-535.e2 (2016).

340. de Koning, C., Langenhorst, J., van Kesteren, C., Lindemans, C. A., Huitema, A. D. R., Nierkens, S., *et al.* Innate Immune Recovery Predicts CD4(+) T Cell Reconstitution after Hematopoietic Cell Transplantation. *Biol. Blood Marrow Transplant.* **25**, 819–826 (2019).

341. Snowden, J. A. & Hill, G. R. Conditioning regimens for autologous haematopoietic stem cell transplantation - can natural killer cell therapy help? *British journal of haematology* **177**, 341–342 (2017).

342. Roberto, A., Di Vito, C., Zaghi, E., Mazza, E. M. C., Capucetti, A., Calvi, M., *et al.* The early expansion of anergic NKG2A(pos)/CD56(dim)/CD16(neg) natural killer represents a therapeutic target in haploidentical hematopoietic stem cell transplantation. *Haematologica* **103**, 1390–1402 (2018).

343. Vulpis, E., Stabile, H., Soriani, A., Fionda, C., Petrucci, M. T., Mariggio', E., *et al.* Key Role of the CD56(low)CD16(low) Natural Killer Cell Subset in the Recognition and Killing of Multiple Myeloma Cells. *Cancers (Basel).* **10**, (2018).

344. Jacobs, B., Tognarelli, S., Poller, K., Bader, P., Mackensen, A. & Ullrich, E. NK Cell Subgroups, Phenotype, and Functions After Autologous Stem Cell Transplantation. *Front. Immunol.* **6**, 583 (2015).

345. Dulphy, N., Haas, P., Busson, M., Belhadj, S., Peffault de Latour, R., Robin, M., *et al.* An unusual CD56(bright) CD16(low) NK cell subset dominates the early posttransplant period following HLA-matched hematopoietic stem cell transplantation. *J. Immunol.* **181**, 2227–2237 (2008).

346. Skerget, M., Skopec, B., Zontar, D. & Cernelc, P. Mobilization with cyclophosphamide reduces the number of lymphocyte subpopulations in the leukapheresis product and delays their reconstitution after autologous hematopoietic stem cell transplantation in patients with multiple myeloma. *Radiol. Oncol.* **50**, 402–408 (2016).

347. Russo, A., Oliveira, G., Berglund, S., Greco, R., Gambacorta, V., Cieri, N., *et al.* NK cell recovery

after haploidentical HSCT with posttransplant cyclophosphamide: Dynamics and clinical implications. *Blood* **131**, 247–262 (2018).

348. Valtola, J., Silvennoinen, R., Ropponen, A., Siitonen, T., Saily, M., Sankelo, M., *et al.* Blood graft cellular composition and posttransplant outcomes in myeloma patients mobilized with or without low-dose cyclophosphamide: a randomized comparison. *Transfusion* **56**, 1394–1401 (2016).

349. Valtola, J., Silvennoinen, R., Ropponen, A., Siitonen, T., Saily, M., Sankelo, M., *et al.* Blood graft composition and post-transplant recovery in myeloma patients mobilized with plerixafor: a prospective multicenter study. *Leuk. Lymphoma* **60**, 453–461 (2019).

350. Talebian, L., Wu, J. Y., Fischer, D. A., Hill, J. M., Szczepiorkowski, Z. M., Ernstoff, M. S., *et al.* Novel mobilization strategies to enhance autologous immune effector cells in multiple myeloma. *Front. Biosci. (Elite Ed).* **3**, 1500–1508 (2011).

351. Rey, J. J., Fauriat, C., Kochbati, E. E., Orlanducci, F., Charbonnier, A., D'Incan, E., *et al.* Kinetics of Cytotoxic Lymphocytes Reconstitution after Induction Chemotherapy in Elderly AML Patients Reveals Progressive Recovery of Normal Phenotypic and Functional Features in NK Cells. *Front. Immunol.* **8**, 64 (2017).

352. Wijayahadi, N., Haron, M. R., Stanslas, J. & Yusuf, Z. Changes in cellular immunity during chemotherapy for primary breast cancer with anthracycline regimens. *J. Chemother.* **19**, 716–723 (2007).

353. Mackall, C. L., Fleisher, T. A., Brown, M. R., Andrich, M. P., Chen, C. C., Feuerstein, I. M., *et al.* Distinctions between CD8+ and CD4+ T-cell regenerative pathways result in prolonged T-cell subset imbalance after intensive chemotherapy. *Blood* **89**, 3700–3707 (1997).

354. Ferrandina, G., Pierelli, L., Perillo, A., Rutella, S., Ludovisi, M., Leone, G., *et al.* Lymphocyte recovery in advanced ovarian cancer patients after high-dose chemotherapy and peripheral blood stem cell plus growth factor support: Clinical implications. *Clin. Cancer Res.* **9**, 195–200 (2003).

355. Sportès, C., McCarthy, N. J., Hakim, F., Steinberg, S. M., Liewehr, D. J., Weng, D., *et al.* Establishing a platform for immunotherapy: Clinical outcome and study of immune reconstitution after high-dose chemotherapy with progenitor cell support in breast cancer patients. *Biol. Blood Marrow Transplant.* **11**, 472–483 (2005).

356. Lutsiak, M. E. C., Semnani, R. T., De Pascalis, R., Kashmiri, S. V. S., Schlom, J. & Sabzevari, H. Inhibition of CD4(+)25+ T regulatory cell function implicated in enhanced immune response by low-dose cyclophosphamide. *Blood* **105**, 2862–2868 (2005).

357. Ghiringhelli, F., Menard, C., Puig, P. E., Ladoire, S., Roux, S., Martin, F., *et al.* Metronomic cyclophosphamide regimen selectively depletes CD4+CD25+ regulatory T cells and restores T and NK effector functions in end stage cancer patients. *Cancer Immunol. Immunother.* **56**, 641–648 (2007).

358. Ge, Y., Domschke, C., Stoiber, N., Schott, S., Heil, J., Rom, J., *et al.* Metronomic cyclophosphamide treatment in metastasized breast cancer patients: immunological effects and clinical outcome. *Cancer Immunol. Immunother.* **61**, 353–362 (2012).

359. Shevchenko, I., Karakhanova, S., Soltek, S., Link, J., Bayry, J., Werner, J., *et al.* Low-dose gemcitabine depletes regulatory T cells and improves survival in the orthotopic Panc02 model of pancreatic cancer. *Int. J. cancer* **133**, 98–107 (2013).

360. Rettig, L., Seidenberg, S., Parvanova, I., Samaras, P., Curioni, A., Knuth, A., *et al.* Gemcitabine depletes regulatory T-cells in human and mice and enhances triggering of vaccine-specific cytotoxic T-cells. *Int. J. cancer* **129**, 832–838 (2011).

361. Kodumudi, K. N., Woan, K., Gilvary, D. L., Sahakian, E., Wei, S. & Djeu, J. Y. A novel chemoimmunomodulating property of docetaxel: suppression of myeloid-derived suppressor cells in tumor bearers. *Clin. Cancer Res.* **16**, 4583–4594 (2010).

362. Alizadeh, D., Trad, M., Hanke, N. T., Larmonier, C. B., Janikashvili, N., Bonnotte, B., *et al.* Doxorubicin eliminates myeloid-derived suppressor cells and enhances the efficacy of adoptive T-cell transfer in breast cancer. *Cancer Res.* **74**, 104–118 (2014).

363. Liechtenstein, T., Perez-Janices, N., Gato, M., Caliendo, F., Kochan, G., Blanco-Luquin, I., *et al.* A highly efficient tumor-infiltrating MDSC differentiation system for discovery of anti-neoplastic targets, which circumvents the need for tumor establishment in mice. *Oncotarget* **5**, 7843–7857 (2014).

364. Diaz-Montero, C. M., Salem, M. L., Nishimura, M. I., Garrett-Mayer, E., Cole, D. J. & Montero, A. J. Increased circulating myeloid-derived suppressor cells correlate with clinical cancer stage, metastatic tumor burden, and doxorubicin-cyclophosphamide chemotherapy. *Cancer Immunol. Immunother.* **58**, 49–59 (2009).

365. Ding, Z.-C., Lu, X., Yu, M., Lemos, H., Huang, L., Chandler, P., *et al.* Immunosuppressive Myeloid Cells Induced by Chemotherapy Attenuate Antitumor CD4+ T-Cell Responses through the PD-1–PD-L1 Axis. *Cancer Res.* **74**, 3441 LP – 3453 (2014).

366. Khallouf, H., Marten, A., Serba, S., Teichgraber, V., Buchler, M. W., Jager, D., *et al.* 5-Fluorouracil and interferon-alpha immunochemotherapy enhances immunogenicity of murine pancreatic cancer through upregulation of NKG2D ligands and MHC class I. *J. Immunother.* **35**, 245–253 (2012).

367. Chang, C.-L., Hsu, Y.-T., Wu, C.-C., Lai, Y.-Z., Wang, C., Yang, Y.-C., *et al.* Dose-Dense Chemotherapy Improves Mechanisms of Antitumor Immune Response. *Cancer Res.* **73**, 119 LP – 127 (2013).

368. Tsuchikawa, T., Md, M. M., Yamamura, Y., Shichinohe, T., Hirano, S. & Kondo, S. The immunological impact of neoadjuvant chemotherapy on the tumor microenvironment of esophageal squamous cell carcinoma. *Ann. Surg. Oncol.* **19**, 1713–1719 (2012).

369. Roselli, M., Cereda, V., di Bari, M. G., Formica, V., Spila, A., Jochems, C., *et al.* Effects of conventional therapeutic interventions on the number and function of regulatory T cells. *Oncoimmunology* **2**, e27025 (2013).

370. Rusakiewicz, S., Semeraro, M., Sarabi, M., Desbois, M., Locher, C., Mendez, R., *et al.* Immune Infiltrates Are Prognostic Factors in Localized Gastrointestinal Stromal Tumors. *Cancer Res.* **73**, 3499 LP – 3510 (2013).

371. Lagrue, K., Carisey, A., Morgan, D. J., Chopra, R. & Davis, D. M. Lenalidomide augments actin remodeling and lowers NK-cell activation thresholds. *Blood* **126**, 50–60 (2015).

372. Davies, F. E., Raje, N., Hideshima, T., Lentzsch, S., Young, G., Tai, Y. T., *et al.* Thalidomide and immunomodulatory derivatives augment natural killer cell cytotoxicity in multiple myeloma. *Blood* **98**, 210–216 (2001).

373. Carlsten, M., Namazi, A., Reger, R., Levy, E., Berg, M., St Hilaire, C., *et al.* Bortezomib sensitizes multiple myeloma to NK cells via ER-stress-induced suppression of HLA-E and upregulation of DR5. *Oncoimmunology* **8**, e1534664 (2019).

374. Niu, C., Jin, H., Li, M., Zhu, S., Zhou, L., Jin, F., *et al.* Low-dose bortezomib increases the expression of NKG2D and DNAM-1 ligands and enhances induced NK and gammadelta T cell-mediated lysis in multiple myeloma. *Oncotarget* **8**, 5954–5964 (2017).

375. Lee, Y. S., Heo, W., Nam, J., Jeung, Y. H. & Bae, J. The combination of ionizing radiation and proteasomal inhibition by bortezomib enhances the expression of NKG2D ligands in multiple myeloma cells. *J. Radiat. Res.* **59**, 245–252 (2018).

376. Besson, L., Charrier, E., Karlin, L., Allatif, O., Marcais, A., Rouzaire, P., *et al.* One-Year Follow-Up of Natural Killer Cell Activity in Multiple Myeloma Patients Treated With Adjuvant Lenalidomide Therapy. *Front. Immunol.* **9**, 704 (2018).

377. Erridge, C. Endogenous ligands of TLR2 and TLR4: agonists or assistants? *J. Leukoc. Biol.* **87**, 989–999 (2010).

378. Smith, J. A., Harris, R. A. & Smith, J. A. Regulation of Cytokine Production by the Unfolded Protein Response; Implications for Infection and Autoimmunity. *Front. Immunol.* **9**, 422 (2018).

379. Lerner, A. G., Upton, J.-P., Praveen, P. V. K., Ghosh, R., Nakagawa, Y., Igbaria, A., *et al.* IRE1α induces thioredoxin-interacting protein to activate the NLRP3 inflammasome and promote programmed cell death under irremediable ER stress. *Cell Metab.* **16**, 250–264 (2012).

380. Liu, Y.-P., Zeng, L., Tian, A., Bomkamp, A., Rivera, D., Gutman, D., *et al.* Endoplasmic reticulum stress regulates the innate immunity critical transcription factor IRF3. *J. Immunol.* **189**, 4630–4639 (2012).

381. Hayden, M. S. & Ghosh, S. Shared principles in NF-kappaB signaling. *Cell* **132**, 344–362 (2008).

382. Hiscott, J. Triggering the innate antiviral response through IRF-3 activation. *J. Biol. Chem.* **282**, 15325–15329 (2007).

383. Reverendo, M., Mendes, A., Argüello, R. J., Gatti, E. & Pierre, P. At the crossway of ER-stress and proinflammatory responses. *FEBS J.* **286**, 297–310 (2019).

384. Bruns, A. M. & Horvath, C. M. Antiviral RNA recognition and assembly by RLR family innate immune sensors. *Cytokine Growth Factor Rev.* **25**, 507–512 (2014).

385. Garg, A. D., Vandenberk, L., Fang, S., Fasche, T., Van Eygen, S., Maes, J., *et al.* Pathogen response-like recruitment and activation of neutrophils by sterile immunogenic dying cells drives neutrophil-mediated residual cell killing. *Cell Death Differ.* **24**, 832–843 (2017).

386. Bray, F., Ferlay, J., Soerjomataram, I., Siegel, R. L., Torre, L. A. & Jemal, A. Global cancer statistics 2018: GLOBOCAN estimates of incidence and mortality worldwide for 36 cancers in 185 countries. *CA. Cancer J. Clin.* (2018). doi:10.3322/caac.21492

387. Mateos, M.-V. & Landgren, O. MGUS and Smoldering Multiple Myeloma: Diagnosis and Epidemiology. *Cancer Treat. Res.* **169**, 3–12 (2016).

388. van Nieuwenhuijzen, N., Spaan, I., Raymakers, R. & Peperzak, V. From MGUS to multiple myeloma, a paradigm for clonal evolution of premalignant cells. *Cancer Res.* **78**, 2449–2456 (2018).

389. Pawlyn, C. & Morgan, G. J. Evolutionary biology of high-risk multiple myeloma. *Nat. Rev. Cancer* **17**, 543–556 (2017).

390. Harding, T., Baughn, L., Kumar, S. & Van Ness, B. The future of myeloma precision medicine: integrating the compendium of known drug resistance mechanisms with emerging tumor profiling technologies. *Leukemia* 15–19 (2019). doi:10.1038/s41375-018-0362-z

391. Kumar, S. K., Rajkumar, V., Kyle, R. A., van Duin, M., Sonneveld, P., Mateos, M.-V., *et al.* Multiple myeloma. *Nat. Rev. Dis. Prim.* **3**, 17046 (2017).

392. Manier, S., Salem, K. Z., Park, J., Landau, D. A., Getz, G. & Ghobrial, I. M. Genomic complexity of multiple myeloma and its clinical implications. *Nat. Rev. Clin. Oncol.* **14**, 100–113 (2017).

393. Jovanovic, K. K., Roche-Lestienne, C., Ghobrial, I. M., Facon, T., Quesnel, B. & Manier, S. Targeting MYC in multiple myeloma. *Leukemia* **32**, 1295–1306 (2018).

394. Thomsen, H., Chattopadhyay, S., Weinhold, N., Vodicka, P., Vodickova, L., Hoffmann, P., *et al.* Genome-wide association study of monoclonal gammopathy of unknown significance (MGUS): comparison with multiple myeloma. *Leukemia* (2019). doi:10.1038/s41375-019-0396-x

395. Bustoros, M., Mouhieddine, T. H., Detappe, A. & Ghobrial, I. M. Established and Novel Prognostic Biomarkers in Multiple Myeloma. *Am. Soc. Clin. Oncol. Educ. B.* **37**, 548–560 (2017).

396. Ziogas, D. C., Dimopoulos, M. A. & Kastritis, E. Prognostic factors for multiple myeloma in the era of novel therapies. *Expert Rev. Hematol.* **11**, 863–879 (2018).

397. Levin, A., Hari, P. & Dhakal, B. Novel biomarkers in multiple myeloma. *Transl. Res.* **201**, 49–59 (2018).

398. Larsen, J. T., Kumar, S. K., Dispenzieri, A., Kyle, R. A., Katzmann, J. A. & Rajkumar, S. V. Serum free light chain ratio as a biomarker for high-risk smoldering multiple myeloma. *Leukemia* **27**, 941–946 (2013).

399. Manier, S., Park, J., Capelletti, M., Bustoros, M., Freeman, S. S., Ha, G., *et al.* Whole-exome sequencing of cell-free DNA and circulating tumor cells in multiple myeloma. *Nat. Commun.* **9**, 1691 (2018).

400. Gonsalves, W. I., Rajkumar, S. V, Gupta, V., Morice, W. G., Timm, M. M., Singh, P. P., *et al.* Quantification of clonal circulating plasma cells in newly diagnosed multiple myeloma: implications for redefining high-risk myeloma. *Leukemia* **28**, 2060–2065 (2014).

401. Snyder, A., Makarov, V., Merghoub, T., Yuan, J., Zaretsky, J. M., Desrichard, A., *et al.* Genetic basis for clinical response to CTLA-4 blockade in melanoma. *N. Engl. J. Med.* **371**, 2189–2199 (2014).

402. Rizvi, N. A., Hellmann, M. D., Snyder, A., Kvistborg, P., Makarov, V., Havel, J. J., *et al.* Cancer immunology. Mutational landscape determines sensitivity to PD-1 blockade in non-small cell lung cancer. *Science* **348**, 124–128 (2015).

403. Lee, V., Murphy, A., Le, D. T. & Diaz Jr, L. A. Mismatch Repair Deficiency and Response to Immune Checkpoint Blockade. *Oncologist* **21**, 1200–1211 (2016).

404. Tokito, T., Azuma, K., Kawahara, A., Ishii, H., Yamada, K., Matsuo, N., *et al.* Predictive relevance of PD-L1 expression combined with CD8+ TIL density in stage III non-small cell lung cancer patients receiving concurrent chemoradiotherapy. *Eur. J. Cancer* **55**, 7–14 (2016).

405. Thomas, N. E., Busam, K. J., From, L., Kricker, A., Armstrong, B. K., Anton-Culver, H., *et al.* Tumor-infiltrating lymphocyte grade in primary melanomas is independently associated with melanoma-specific survival in the population-based genes, environment and melanoma study. *J. Clin. Oncol.* **31**, 4252–4259 (2013).

406. Atanackovic, D. & Luetkens, T. Biomarkers for checkpoint inhibition in hematologic malignancies. *Semin. Cancer Biol.* **52**, 198–206 (2018).

407. Huang, S.-Y., Lin, H.-H., Lin, C.-W., Li, C.-C., Yao, M., Tang, J.-L., *et al.* Soluble PD-L1: A biomarker to predict progression of autologous transplantation in patients with multiple myeloma. *Oncotarget* **7**, 62490–62502 (2016).

408. Guillerey, C., Nakamura, K., Vuckovic, S., Hill, G. R. & Smyth, M. J. Immune responses in multiple myeloma: Role of the natural immune surveillance and potential of immunotherapies. *Cell. Mol. Life Sci.* **73**, 1569–1589 (2016).

409. Ghobrial, I. M., Detappe, A., Anderson, K. C. & Steensma, D. P. The bone-marrow niche in MDS and MGUS: Implications for AML and MM. *Nat. Rev. Clin. Oncol.* **15**, 219–233 (2018).

410. Mahindra, A., Hideshima, T. & Anderson, K. C. Multiple myeloma: Biology of the disease. *Blood Rev.* **24**, S5–S11 (2010).

411. Mondello, P., Cuzzocrea, S., Navarra, M. & Mian, M. Bone marrow micro-environment is a crucial player for myelomagenesis and disease progression. *Oncotarget* **8**, 20394–20409 (2017).

412. Wang, J., Hendrix, A., Hernot, S., Lemaire, M., Bruyne, E. De, Valckenborgh, E. Van, *et al.* Bone marrow stromal cell – derived exosomes as communicators in drug resistance in multiple myeloma cells. *Blood J.* **124 (4)**, 555–567 (2014).

413. Giallongo, C., Tibullo, D., Parrinello, N. L., Cava, P. La, Rosa, M. Di, Bramanti, V., *et al.* Granulocyte-like myeloid derived suppressor cells (G-MDSC) are increased in multiple myeloma and are driven by dysfunctional mesenchymal stem cells (MSC). *Oncotarget* **7**, 85764–85775 (2016).

414. Malek, E., de Lima, M., Letterio, J. J., Kim, B. G., Finke, J. H., Driscoll, J. J., *et al.* Myeloid-derived suppressor cells: The green light for myeloma immune escape. *Blood Rev.* **30**, 341–348 (2016).

415. Kawano, Y., Moschetta, M., Manier, S., Glavey, S., Gorgun, G. T., Roccaro, A. M., *et al.* Targeting the bone marrow microenvironment in multiple myeloma. *Immunol. Rev.* **263**, 160–172 (2014).

416. Feyler, S., Selby, P. J. & Cook, G. Regulating the regulators in cancer-immunosuppression in multiple myeloma (MM). *Blood Rev.* **27**, 155–164 (2013).

417. Rawstron, A. C., Davies, F. E., Owkn, R. G., English, A., Pratt, G., Child, J. A., *et al.* B-lymphocyte suppression in multiple myeloma is a reversible phenomenon specific to normal B-cell progenitors and plasma cell precursors. *Br. J. Haematol.* **100**, 176–183 (1998).

418. Joshua, D., Suen, H., Brown, R., Bryant, C., Ho, P. J., Hart, D., *et al.* The T Cell in Myeloma. *Clin. Lymphoma. Myeloma Leuk.* **16**, 537–542 (2016).

419. Braga, W. M. T., da Silva, B. R., de Carvalho, A. C., Maekawa, Y. H., Bortoluzzo, A. B., Rizzatti, E. G., *et al.* FOXP3 and CTLA4 overexpression in multiple myeloma bone marrow as a sign of accumulation of $CD4^+$ T regulatory cells. *Cancer Immunol. Immunother.* **63**, 1189–1197 (2014).

420. Chen, J., Ye, Y., Liu, P., Yu, W., Wei, F., Li, H., *et al.* Suppression of T cells by myeloid-derived suppressor cells in cancer. *Hum. Immunol.* **78**, 113–119 (2017).

421. Péres-Andres, M., Almeida, J., Martin-Ayuso, M., Moro, M. J., Martin-Nuñez, G., Galende, J., *et al.* Characterization of bone marrow T cells in monoclonal gammopathy of undetermined significance, multiple myeloma, and plasma cell leukemia demonstrates increased infiltration by cytotoxic/Th1 T cells demonstrating a squed TCR-Vbeta repertoire. *Cancer* **106**, 1296–1305 (2006).

422. San Miguel, J. F., Gonzalez, M., Gascon, A., Moro, M. J., Hernandez, J. M., Ortega, F., *et al.* Lymphoid subsets and prognostic factors in multiple myeloma. Cooperative Group for the Study of Monoclonal Gammopathies. *Br. J. Haematol.* **80**, 305–309 (1992).

423. Bryant, C., Suen, H., Brown, R., Yang, S., Favaloro, J., Aklilu, E., *et al.* Long-term survival in multiple myeloma is associated with a distinct immunological profile, which includes proliferative cytotoxic T-cell clones and a favourable Treg/Th17 balance. *Blood Cancer J.* **3**, e148 (2013).

424. Beyer, M., Kochanek, M., Giese, T., Endl, E., Weihrauch, M. R., Knolle, P. A., *et al.* In vivo peripheral expansion of naive CD4+CD25high FoxP3+ regulatory T cells in patients with multiple myeloma. *Blood* **107**, 3940–3949 (2006).

425. Giannopoulos, K., Kaminska, W., Hus, I. & Dmoszynska, A. The frequency of T regulatory cells modulates the survival of multiple myeloma patients: Detailed characterisation of immune status in multiple myeloma. *Br. J. Cancer* **106**, 546–552 (2012).

426. Feng, P., Yan, R., Dai, X., Xie, X., Wen, H. & Yang, S. The alteration and clinical significance of Th1/Th2/Th17/Treg cells in patients with multiple myeloma. *Inflammation* **38**, 705–709 (2015).

427. Muthu Raja, K. R., Rihova, L., Zahradova, L., Klincova, M., Penka, M. & Hajek, R. Increased T Regulatory Cells Are Associated with Adverse Clinical Features and Predict Progression in Multiple Myeloma. *PLoS One* **7**, e47077 (2012).

428. Dosani, T., Carlsten, M., Maric, I. & Landgren, O. The cellular immune system in myelomagenesis: NK cells and T cells in the development of myeloma [corrected] and their uses in immunotherapies. *Blood Cancer J.* **5**, e306 (2015).

429. Gabrilovich, D. I. & Nagaraj, S. Myeloid-derived suppressor cells as regulators of the immune system. **9**, (2009).

430. Lee, S. J. & Borrello, I. Role of the Immune Response in Disease Progression and Therapy in Multiple Myeloma. *Cancer Treat. Res.* **169**, 207–225 (2016).

431. Garcia-Sanz, R., Gonzalez, M., Orfao, A., Moro, M. J., Hernandez, J. M., Borrego, D., *et al.* Analysis of natural killer-associated antigens in peripheral blood and bone marrow of multiple myeloma patients and prognostic implications. *Br. J. Haematol.* **93**, 81–88 (1996).

432. Bianchi, G. & Munshi, N. C. Pathogenesis beyond the cancer clone(s) in multiple myeloma. *Blood* **125**, 3049–3058 (2015).

433. Fu, C. & Jiang, A. Dendritic Cells and CD8 T Cell Immunity in Tumor Microenvironment. **9**, 1–11 (2018).

434. Pasiarski, M., Grywalska, E., Kosmaczewska, A., Góźdź, S., Steckiewicz, P., Garus, B., *et al.* Assessment of peripheral blood and bone marrow T, NK, NKT and dendritic cells in patients with multiple myeloma. *Postepy Hig. Med. Dosw. (Online)* **69**, 1435–1442 (2015).

435. Leone, P., Berardi, S., Frassanito, M. A., Ria, R., De Re, V., Cicco, S., *et al.* Dendritic cells accumulate in the bone marrow of myeloma patients where they protect tumor plasma cells from CD8+ T-cell killing. *Blood* **126**, 1443–1451 (2015).

436. Pasiarski, M., Grywalska, E., Kosmaczewska, A., Gozdz, S. & Rolinski, J. The frequency of myeloid and lymphoid dendritic cells in multiple myeloma patients is inversely correlated with disease progression. *Postepy Hig. Med. Dosw.* **67**, 926–932 (2013).

437. Brown, R. D., Pope, B., Murray, A., Esdale, W., Sze, D. M., Gibson, J., *et al.* Dendritic cells from patients with myeloma are numerically normal but functionally defective as they fail to up-regulate CD80 (B7-1) expression after huCD40LT stimulation because of inhibition by transforming growth factor-beta 1 and interleukin-10. **98**, 2992–2999 (2018).

438. Chauhan, D., Singh, A. V, Brahmandam, M., Carrasco, R., Bandi, M., Hideshima, T., *et al.* Functional interaction of plasmacytoid dendritic cells with multiple myeloma cells: a therapeutic target. *Cancer Cell* **16**, 309–323 (2009).

439. Jung, S.-H. H., Lee, H.-J. J., Vo, M.-C. C., Kim, H.-J. J. & Lee, J.-J. J. Immunotherapy for the treatment of multiple myeloma. *Crit. Rev. Oncol. Hematol.* **111**, 87–93 (2017).

440. Paiva, B., Azpilikueta, A., Puig, N., Ocio, E. M., Sharma, R., Oyajobi, B. O., *et al.* PD-L1/PD-1 presence in the tumor microenvironment and activity of PD-1 blockade in multiple myeloma. *Leukemia* **29**, 2110 (2015).

441. Committee, on behalf of the E. G., Moreau, P., Einsele, H., Zweegman, S., Facon, T., Goldschmidt, H., *et al.* Multiple myeloma: ESMO Clinical Practice Guidelines for diagnosis, treatment and follow-up†. *Ann. Oncol.* **28**, iv52–iv61 (2017).

442. Abramson, H. N. The Multiple Myeloma Drug Pipeline—2018: A Review of Small Molecules and Their Therapeutic Targets. *Clin. Lymphoma, Myeloma Leuk.* **18**, 611–627 (2018).

443. Esma, F., Salvini, M., Troia, R., Boccadoro, M., Larocca, A. & Pautasso, C. Melphalan hydrochloride for the treatment of multiple myeloma. *Expert Opin. Pharmacother.* **18**, 1127–1136 (2017).

444. Kfir-Erenfeld, S. & Yefenof, E. Non-genomic events determining the sensitivity of hemopoietic malignancies to glucocorticoid-induced apoptosis. *Cancer Immunol. Immunother.* **63**, 37–43 (2014).

445. Hideshima, T., Chauhan, D., Schlossman, R., Richardson, P. & Anderson, K. C. The role of tumor necrosis factor alpha in the pathophysiology of human multiple myeloma: therapeutic applications. *Oncogene* **20**, 4519–4527 (2001).

446. Gupta, D., Treon, S. P., Shima, Y., Hideshima, T., Podar, K., Tai, Y. T., *et al.* Adherence of multiple myeloma cells to bone marrow stromal cells upregulates vascular endothelial growth factor secretion: therapeutic applications. *Leukemia* **15**, 1950–1961 (2001).

447. Quach, H., Ritchie, D., Stewart, A. K., Neeson, P., Harrison, S., Smyth, M. J., *et al.* Mechanism of action of immunomodulatory drugs (IMiDS) in multiple myeloma. *Leukemia* **24**, 22–32 (2010).

448. Wu, L., Adams, M., Carter, T., Chen, R., Muller, G., Stirling, D., *et al.* lenalidomide enhances natural killer cell and monocyte-mediated antibody-dependent cellular cytotoxicity of rituximab-treated CD20+ tumor cells. *Clin. Cancer Res.* **14**, 4650–4657 (2008).

449. Hayashi, T., Hideshima, T., Akiyama, M., Podar, K., Yasui, H., Raje, N., *et al.* Molecular mechanisms whereby immunomodulatory drugs activate natural killer cells: clinical application. *Br. J. Haematol.* **128**, 192–203 (2005).

450. Ito, T., Ando, H., Suzuki, T., Ogura, T., Hotta, K., Imamura, Y., *et al.* Identification of a primary target of thalidomide teratogenicity. *Science* **327**, 1345–1350 (2010).

451. Holstein, S. A. & McCarthy, P. L. Immunomodulatory Drugs in Multiple Myeloma: Mechanisms of

Action and Clinical Experience. *Drugs* **77**, 505–520 (2017).

452. Hideshima, T., Ikeda, H., Chauhan, D., Okawa, Y., Raje, N., Podar, K., *et al.* Bortezomib induces canonical nuclear factor-kappaB activation in multiple myeloma cells. *Blood* **114**, 1046–1052 (2009).

453. Hideshima, T., Richardson, P., Chauhan, D., Palombella, V. J., Elliott, P. J., Adams, J., *et al.* The proteasome inhibitor PS-341 inhibits growth, induces apoptosis, and overcomes drug resistance in human multiple myeloma cells. *Cancer Res.* **61**, 3071–3076 (2001).

454. Gomez-Bougie, P., Wuilleme-Toumi, S., Menoret, E., Trichet, V., Robillard, N., Philippe, M., *et al.* Noxa up-regulation and Mcl-1 cleavage are associated to apoptosis induction by bortezomib in multiple myeloma. *Cancer Res.* **67**, 5418–5424 (2007).

455. Hideshima, T., Mitsiades, C., Akiyama, M., Hayashi, T., Chauhan, D., Richardson, P., *et al.* Molecular mechanisms mediating antimyeloma activity of proteasome inhibitor PS-341. *Blood* **101**, 1530–1534 (2003).

456. Lub, S., Maes, K., Menu, E., De Bruyne, E., Vanderkerken, K. & Van Valckenborgh, E. Novel strategies to target the ubiquitin proteasome system in multiple myeloma. *Oncotarget* **7**, 6521–6537 (2016).

457. Dimopoulos, M. A., Moreau, P., Palumbo, A., Joshua, D., Pour, L., Hajek, R., *et al.* Carfilzomib and dexamethasone versus bortezomib and dexamethasone for patients with relapsed or refractory multiple myeloma (ENDEAVOR): a randomised, phase 3, open-label, multicentre study. *Lancet. Oncol.* **17**, 27–38 (2016).

458. Kuhn, D. J., Chen, Q., Voorhees, P. M., Strader, J. S., Shenk, K. D., Sun, C. M., *et al.* Potent activity of carfilzomib, a novel, irreversible inhibitor of the ubiquitin-proteasome pathway, against preclinical models of multiple myeloma. *Blood* **110**, 3281–3290 (2007).

459. Imai, Y., Hirano, M., Kobayashi, M., Futami, M. & Tojo, A. HDAC Inhibitors Exert Anti-Myeloma Effects through Multiple Modes of Action. *Cancers (Basel).* **11**, 475 (2019).

460. Imai, Y., Maru, Y. & Tanaka, J. Action mechanisms of histone deacetylase inhibitors in the treatment of hematological malignancies. *Cancer Sci.* **107**, 1543–1549 (2016).

461. Ladetto, M., Ferrero, S., Drandi, D., Festuccia, M., Patriarca, F., Mordini, N., *et al.* Prospective molecular monitoring of minimal residual disease after non-myeloablative allografting in newly diagnosed multiple myeloma. *Leukemia* **30**, 1211–1214 (2016).

462. Paiva, B., Mateos, M. V. M. V., Sanchez-Abarca, L. I., Puig, N., Vidriales, M. B. M.-B., López-Corral, L., *et al.* Immune status of high-risk smoldering multiple myeloma patients and its therapeutic modulation under lendex: A longitudinal analysis. *Blood* **127**, 1151–1162 (2016).

463. Rodríguez-Otero, P., Paiva, B., Engelhardt, M., Prósper, F. & San Miguel, J. F. Is immunotherapy here to stay in multiple myeloma? *Haematologica* **102**, 423–432 (2017).

464. Lokhorst, H. M., Plesner, T., Laubach, J. P., Nahi, H., Gimsing, P., Hansson, M., *et al.* Targeting CD38 with Daratumumab Monotherapy in Multiple Myeloma. *N. Engl. J. Med.* **373**, 1207–1219 (2015).

465. Lonial, S., Weiss, B. M., Usmani, S. Z., Singhal, S., Chari, A., Bahlis, N. J., *et al.* Daratumumab monotherapy in patients with treatment-refractory multiple myeloma (SIRIUS): an open-label, randomised, phase 2 trial. *Lancet* **387**, 1551–1560 (2016).

466. van de Donk, N. W. C. J. & Usmani, S. Z. CD38 Antibodies in Multiple Myeloma: Mechanisms of Action and Modes of Resistance. *Front. Immunol.* **9**, 1–12 (2018).

467. van der Veer, M. S., de Weers, M., van Kessel, B., Bakker, J. M., Wittebol, S., Parren, P. W. H. I., *et al.* Towards effective immunotherapy of myeloma: enhanced elimination of myeloma cells by combination of lenalidomide with the human CD38 monoclonal antibody daratumumab. *Haematologica* **96**, 284–290 (2011).

468. Lonial, S., Dimopoulos, M., Palumbo, A., White, D., Grosicki, S., Spicka, I., *et al.* Elotuzumab Therapy for Relapsed or Refractory Multiple Myeloma. *N. Engl. J. Med.* **373**, 621–631 (2015).

469. Fedele, P. L., Willis, S. N., Liao, Y., Low, M. S., Rautela, J., Segal, D. H., *et al.* IMiDs prime myeloma cells for daratumumab-mediated cytotoxicity through loss of Ikaros and Aiolos. *Blood* **132**, 2166 LP – 2178 (2018).

470. Gavriatopoulou, M., Kastritis, E., Ntanasis-Stathopoulos, I., Fotiou, D., Roussou, M., Migkou, M., *et al.* The addition of IMiDs for patients with daratumumab-refractory multiple myeloma can overcome refractoriness to both agents. *Blood* **131**, 464 LP – 467 (2018).

471. Blair, H. A. Daratumumab: A Review in Relapsed and/or Refractory Multiple Myeloma. *Drugs* **77**, 2013–2024 (2017).

472. Trudel, S., Lendvai, N., Popat, R., Voorhees, P. M., Reeves, B., Libby, E. N., *et al.* Targeting B-cell maturation antigen with GSK2857916 antibody–drug conjugate in relapsed or refractory multiple myeloma (BMA117159): a dose escalation and expansion phase 1 trial. *Lancet Oncol.* **19**, 1641–1653 (2018).

473. Cho, S.-F., Anderson, K. C. & Tai, Y.-T. Targeting B Cell Maturation Antigen (BCMA) in Multiple Myeloma: Potential Uses of BCMA-Based Immunotherapy. *Front. Immunol.* **9**, (2018).

474. Noonan, K. A., Huff, C. A., Davis, J., Lemas, M. V., Fiorino, S., Bitzan, J., *et al.* Adoptive transfer of activated marrow-infiltrating lymphocytes induces measurable antitumor immunity in the bone marrow in multiple myeloma. *Sci. Transl. Med.* **7**, (2015).

475. Cohen, A. D. CAR T Cells and Other Cellular Therapies for MultipleMyeloma: 2018 Update. *Am Soc Clin Oncol Educ B.* e6–e15 (2018). doi:10.1200/EDBK_200889

476. Linette, G. P., Stadtmauer, E. A., Maus, M. V, Rapoport, A. P., Levine, B. L., Emery, L., *et al.* Cardiovascular toxicity and titin cross-reactivity of affinity-enhanced T cells in myeloma and melanoma. *Blood* **122**, 863–871 (2013).

477. Rapoport, A. P., Stadtmauer, E. A., Binder-Scholl, G. K., Goloubeva, O., Vogl, D. T., Lacey, S. F., *et al.* NY-ESO-1-specific TCR-engineered T cells mediate sustained antigen-specific antitumor effects in myeloma. *Nat. Med.* **21**, 914–921 (2015).

478. Maude, S. L., Laetsch, T. W., Buechner, J., Rives, S., Boyer, M., Bittencourt, H., *et al.* Tisagenlecleucel in Children and Young Adults with B-Cell Lymphoblastic Leukemia. *N. Engl. J. Med.* **378**, 439–448 (2018).

479. Porter, D. L., Hwang, W.-T., Frey, N. V, Lacey, S. F., Shaw, P. A., Loren, A. W., *et al.* Chimeric antigen receptor T cells persist and induce sustained remissions in relapsed refractory chronic lymphocytic leukemia. *Sci. Transl. Med.* **7**, 303ra139 (2015).

480. Castella, M., Fernández de Larrea, C. & Martín-Antonio, B. Immunotherapy: A Novel Era of Promising Treatments for Multiple Myeloma. *Int. J. Mol. Sci.* **19**, 3613 (2018).

481. Fionda, C., Stabile, H., Molfetta, R., Soriani, A., Bernardini, G., Zingoni, A., *et al.* Translating the anti-myeloma activity of Natural Killer cells into clinical application. *Cancer Treat. Rev.* **70**, 255–264 (2018).

482. Wang, X., Walter, M., Urak, R., Weng, L., Huynh, C., Lim, L., *et al.* Lenalidomide Enhances the Function of CS1 Chimeric Antigen Receptor–Redirected T Cells Against Multiple Myeloma. *Clin. Cancer Res.* **24**, 106 LP – 119 (2018).

483. Chang, S. K., Hou, J., Chen, G. G., Yu, D. D., Wu, H. Q., Xie, Y. S., *et al.* Carfilzomib combined with ex vivo-expanded patient autologous natural killer cells for myeloma immunotherapy. *Neoplasma* **65**, 720–729 (2018).

484. Sanchez-Martinez, D., Allende-Vega, N., Orecchioni, S., Talarico, G., Cornillon, A., Vo, D.-N. N., *et al.* Expansion of allogeneic NK cells with efficient antibody-dependent cell cytotoxicity against multiple tumors. *Theranostics* **8**, 3856–3869 (2018).

485. Villalba, M., Alexia, C., Bellin-Robert, A., Fayd'herbe de Maudave, A. & Gitenay, D. Non-Genetically Improving the Natural Cytotoxicity of Natural Killer (NK) Cells. *Front. Immunol.* **10**, 1–10 (2020).

486. Robert, C., Thomas, L., Bondarenko, I., O'Day, S., Weber, J., Garbe, C., *et al.* Ipilimumab plus

Dacarbazine for Previously Untreated Metastatic Melanoma. *N. Engl. J. Med.* **364**, 2517–2526 (2011).

487. Sharma, P. & Allison, J. P. The future of immune checkpoint therapy. *Science (80-.).* **348**, 56 LP – 61 (2015).

488. Cogdill, A. P., Andrews, M. C. & Wargo, J. A. Hallmarks of response to immune checkpoint blockade. *Br. J. Cancer* **117**, 1–7 (2017).

489. Mu, C.-Y. Y., Huang, J.-A. A., Chen, Y., Chen, C. & Zhang, X.-G. G. High expression of PD-L1 in lung cancer may contribute to poor prognosis and tumor cells immune escape through suppressing tumor infiltrating dendritic cells maturation. *Med. Oncol.* **28**, 682–688 (2011).

490. Ghebeh, H., Mohammed, S., Al-Omair, A., Qattan, A., Lehe, C., Al-Qudaihi, G., *et al.* The B7-H1 (PD-L1) T Lymphocyte-Inhibitory Molecule Is Expressed in Breast Cancer Patients with Infiltrating Ductal Carcinoma: Correlation with Important High-Risk Prognostic Factors. *Neoplasia* **8**, 190–198 (2006).

491. Zhang, Y., Huang, S., Gong, D., Qin, Y. & Shen, Q. Programmed death-1 upregulation is correlated with dysfunction of tumor-infiltrating CD8+ T lymphocytes in human non-small cell lung cancer. *Cell. Mol. Immunol.* **7**, 389–395 (2010).

492. Fourcade, J., Sun, Z., Benallaoua, M., Guillaume, P., Luescher, I. F., Sander, C., *et al.* Upregulation of Tim-3 and PD-1 expression is associated with tumor antigen-specific CD8+ T cell dysfunction in melanoma patients. *J. Exp. Med.* **207**, 2175–2186 (2010).

493. Tamura, H., Ishibashi, M., Yamashita, T., Tanosaki, S., Okuyama, N., Kondo, A., *et al.* Marrow stromal cells induce B7-H1 expression on myeloma cells, generating aggressive characteristics in multiple myeloma. *Leukemia* **27**, 464–472 (2013).

494. Liu, J., Hamrouni, A., Wolowiec, D., Coiteux, V. V., Kuliczkowski, K., Hetuin, D., *et al.* Plasma cells from multiple myeloma patients express B7-H1 (PD-L1) and increase expression after stimulation with IFN-γ and TLR ligands via a MyD88-, TRAF6-, and MEK-dependent pathway. *Blood* **110**, 296–304 (2007).

495. Yousef, S., Marvin, J., Steinbach, M., Langemo, A., Kovacsovics, T., Binder, M., *et al.* Immunomodulatory molecule PD-L1 is expressed on malignant plasma cells and myeloma-propagating pre-plasma cells in the bone marrow of multiple myeloma patients. *Blood Cancer J.* **5**, e285 (2015).

496. Lesokhin, A. M., Ansell, S. M., Armand, P., Scott, E. C., Halwani, A., Gutierrez, M., *et al.* Nivolumab in Patients With Relapsed or Refractory Hematologic Malignancy: Preliminary Results of a Phase Ib Study. *J. Clin. Oncol.* **34**, 2698–2704 (2016).

497. Paul, B., Kang, S., Zheng, Z. & Kang, Y. The challenges of checkpoint inhibition in the treatment of multiple myeloma. *Cell. Immunol.* **334**, 87–98 (2018).

498. Pfirschke, C., Engblom, C., Rickelt, S., Cortez-Retamozo, V., Garris, C., Pucci, F., *et al.* Immunogenic Chemotherapy Sensitizes Tumors to Checkpoint Blockade Therapy. *Immunity* **44**, 343–354 (2016).

499. Varpe, S. S., Juvekar, A. R., Bidikar, M. P. & Juvekar, P. R. Evaluation of anti-inflammatory activity of Typha angustifolia pollen grains extracts in experimental animals. *Indian J. Pharmacol.* **44**, 788–791 (2012).

500. Mathew, M., Enzler, T., Shu, C. A. & Rizvi, N. A. Combining chemotherapy with PD-1 blockade in NSCLC. *Pharmacol. Ther.* **186**, 130–137 (2018).

501. Amin, A., Plimack, E. R., Infante, J. R., Ernstoff, M. S., Rini, B. I., McDermott, D. F., *et al.* Nivolumab (anti-PD-1; BMS-936558, ONO-4538) in combination with sunitinib or pazopanib in patients (pts) with metastatic renal cell carcinoma (mRCC). *J. Clin. Oncol.* **32**, 5010 (2014).

502. Görgün, G., Samur, M. K., Cowens, K. B., Paula, S., Bianchi, G., Anderson, J. E., *et al.* Lenalidomide Enhances Immune Checkpoint Blockade-Induced Immune Response in Multiple Myeloma. *Clin. Cancer Res.* **21**, 4607–4618 (2015).

503. Wilson, L., Cohen, A. D., Weiss, B. M., Vogl, D. T., Garfall, A. L., Capozzi, D. L., *et al.* Pembrolizumab in Combination with Pomalidomide and Dexamethasone (PEMBRO/POM/DEX) for Pomalidomide Exposed Relapsed or Refractory Multiple Myeloma. *Blood* **128**, 2119 LP – 2119 (2016).

504. Badros, A., Hyjek, E., Ma, N., Lesokhin, A., Dogan, A., Rapoport, A. P., *et al.* Pembrolizumab, pomalidomide, and low-dose dexamethasone for relapsed/refractory multiple myeloma. *Blood* **130**, 1189–1197 (2017).

505. Malavasi, F., Sheng Guo, Z., Decker, W. K., Dhodapkar, M. V, Bailur, K. J., Costa, F., *et al.* Citation: Checkpoint Inhibition in Myeloma: Opportunities and Challenges. *Front. Immunol. | www.frontiersin.org* **9**, 2204 (2018).

506. Mukherji, B., Chakraborty, N. G., Yamasaki, S., Okino, T., Yamase, H., Sporn, J. R., *et al.* Induction of antigen-specific cytolytic T cells in situ in human melanoma by immunization with synthetic peptide-pulsed autologous antigen presenting cells. *Proc. Natl. Acad. Sci. U. S. A.* **92**, 8078–8082 (1995).

507. Cao, J., Zhang, X., Liu, J., Li, D., Li, J., Liu, Y., *et al.* Clinical Efficacy of Tumor Antigen-Pulsed DC Treatment for High-Grade Glioma Patients : Evidence from a. **9**, (2014).

508. Anguille, S., Smits, E. L., Lion, E., van Tendeloo, V. F. & Berneman, Z. N. Clinical use of dendritic cells for cancer therapy. *Lancet Oncol.* **15**, e257–e267 (2014).

509. Nakai, N., Hartmann, G., Kishimoto, S. & Katoh, N. Dendritic cell vaccination in human melanoma : relationships between clinical effects and vaccine parameters. 607–619 (2010). doi:10.1111/j.1755-148X.2010.00736.x

510. Kantoff, P. W., Higano, C. S., Shore, N. D., Berger, E. R., Small, E. J., Penson, D. F., *et al.* Sipuleucel-T Immunotherapy for Castration-Resistant Prostate Cancer. *N. Engl. J. Med.* **363**, 411–422 (2010).

511. Rosenblatt, J., Vasir, B., Uhl, L., Blotta, S., MacNamara, C., Somaiya, P., *et al.* Vaccination with dendritic cell/tumor fusion cells results in cellular and humoral antitumor immune responses in patients with multiple myeloma. *Blood* **117**, 393 LP – 402 (2011).

512. Rosenblatt, J., Avivi, I., Vasir, B., Uhl, L., Munshi, N. C., Katz, T., *et al.* Vaccination with dendritic cell/tumor fusions following autologous stem cell transplant induces immunologic and clinical responses in multiple myeloma patients. *Clin. Cancer Res.* **19**, 3640–3648 (2013).

513. Vandenberk, L., Belmans, J., Van Woensel, M., Riva, M. & Van Gool, S. W. Exploiting the Immunogenic Potential of Cancer Cells for Improved Dendritic Cell Vaccines. *Front. Immunol.* **6**, 663 (2015).

514. Chung, C. Role of Immunotherapy in Targeting the Bone Marrow Microenvironment in Multiple Myeloma: An Evolving Therapeutic Strategy. *Pharmacotherapy* **37**, 129–143 (2017).

515. Goldszmid, R. S., Idoyaga, J., Bravo, A. I., Steinman, R., Mordoh, J. & Wainstok, R. Dendritic Cells Charged with Apoptotic Tumor Cells Induce Long-Lived Protective CD4+ and CD8+ T Cell Immunity against B16 Melanoma. *J. Immunol.* **171**, 5940–5947 (2003).

516. Strome, S. E., Voss, S., Wilcox, R., Wakefield, T. L., Tamada, K., Flies, D., *et al.* Strategies for antigen loading of dendritic cells to enhance the antitumor immune response. *Cancer Res.* **62**, 1884–1889 (2002).

517. Brusa, D., Garetto, S., Chiorino, G., Scatolini, M., Migliore, E., Camussi, G., *et al.* Post-apoptotic tumors are more palatable to dendritic cells and enhance their antigen cross-presentation activity. *Vaccine* **26**, 6422–6432 (2008).

518. Donnelly, O. G., Errington-Mais, F., Steele, L., Hadac, E., Jennings, V., Scott, K., *et al.* Measles virus causes immunogenic cell death in human melanoma. *Gene Ther.* **20**, 7 (2011).

519. Mikyšková, R., Štěpánek, I., Indrová, M., Bieblová, J., Šímová, J., Truxová, I., *et al.* Dendritic cells pulsed with tumor cells killed by high hydrostatic pressure induce strong immune responses and display therapeutic effects both in murine TC-1 and TRAMP-C2 tumors when combined with

docetaxel chemotherapy. *Int. J. Oncol.* **48**, 953–964 (2016).

520. Adkins, I., Sadilkova, L., Hradilova, N., Tomala, J., Kovar, M. & Spisek, R. Severe, but not mild heat-shock treatment induces immunogenic cell death in cancer cells. *Oncoimmunology* **6**, 1–13 (2017).

521. Sanovic, R., Verwanger, T., Hartl, A. & Krammer, B. Low dose hypericin-PDT induces complete tumor regression in BALB/c mice bearing CT26 colon carcinoma. *Photodiagnosis Photodyn. Ther.* **8**, 291–296 (2011).

522. Jung, N. C., Kim, H. J., Kang, M. S., Lee, J. H., Song, J. Y., Seo, H. G., *et al.* Photodynamic therapy-mediated DC immunotherapy is highly effective for the inhibition of established solid tumors. *Cancer Lett.* **324**, 58–65 (2012).

523. Garg, A. D., Vandenberk, L., Koks, C., Verschuere, T., Boon, L., Van Gool, S. W., *et al.* Dendritic cell vaccines based on immunogenic cell death elicit danger signals and T cell-driven rejection of high-grade glioma. *Sci. Transl. Med.* **8**, 1–16 (2016).

524. Cho, D. Y., Yang, W. K., Lee, H. C., Hsu, D. M., Lin, H. L., Lin, S. Z., *et al.* Adjuvant immunotherapy with whole-cell lysate dendritic cells vaccine for glioblastoma multiforme: A phase II clinical trial. *World Neurosurg.* **77**, 736–744 (2012).

525. Henry, J. Y., Labarthe, M.-C., Meyer, B., Dasgupta, P., Dalgleish, A. G. & Galustian, C. Enhanced cross-priming of naive CD8+ T cells by dendritic cells treated by the IMiDs(R) immunomodulatory compounds lenalidomide and pomalidomide. *Immunology* **139**, 377–385 (2013).

526. Hofgaard, P. O., Jodal, H. C., Bommert, K., Huard, B., Caers, J., Carlsen, H., *et al.* A Novel Mouse Model for Multiple Myeloma (MOPC315.BM) That Allows Noninvasive Spatiotemporal Detection of Osteolytic Disease. *PLoS One* **7**, (2012).

527. Posch, W., Lass-Flörl, C. & Wilflingseder, D. Generation of Human Monocyte-derived Dendritic Cells from Whole Blood. *J. Vis. Exp.* 2–7 (2016). doi:10.3791/54968

528. Figueroa, G., Parira, T., Laverde, A., Casteleiro, G., El-Mabhouh, A., Nair, M., *et al.* Characterization of Human Monocyte-derived Dendritic Cells by Imaging Flow Cytometry: A Comparison between Two Monocyte Isolation Protocols. *J. Vis. Exp.* 1–9 (2016). doi:10.3791/54296

529. Martins, I., Tesniere, A., Kepp, O., Michaud, M., Schlemmer, F., Senovilla, L., *et al.* Chemotherapy induces ATP release from tumor cells. *Cell Cycle* **8**, 3723–3728 (2009).

530. Forveille, S., Humeau, J., Sauvat, A., Bezu, L., Kroemer, G. & Kepp, O. Quinacrine-mediated detection of intracellular ATP. *Methods Enzymol.* **629**, 103–113 (2019).

531. Seminario-Vidal, L., Lazarowski, E. R. & Okada, S. F. Assessment of extracellular ATP concentrations. *Methods Mol. Biol.* **574**, 25–36 (2009).

532. Logue, S. E., Elgendy, M. & Martin, S. J. Expression, purification and use of recombinant annexin V for the detection of apoptotic cells. *Nat. Protoc.* **4**, 1383–1395 (2009).

533. Rello-Varona, S., Kepp, O., Vitale, I., Michaud, M., Senovilla, L., Jemaà, M., *et al.* An automated fluorescence videomicroscopy assay for the detection of mitotic catastrophe. *Cell Death Dis.* **1**, e25 (2010).

534. Kepp, O., Galluzzi, L., Lipinski, M., Yuan, J. & Kroemer, G. Cell death assays for drug discovery. *Nat. Rev. Drug Discov.* **10**, 221–37 (2011).

535. Hatakeyama, S., Yamamoto, H. & Ohyama, C. Tumor formation assays. *Methods Enzymol.* **479**, 397–411 (2010).

536. Ishino, Y., Shinagawa, H., Makino, K., Amemura, M. & Nakata, A. Nucleotide sequence of the iap gene, responsible for alkaline phosphatase isozyme conversion in Escherichia coli, and identification of the gene product. *J. Bacteriol.* **169**, 5429–5433 (1987).

537. Mojica, F. J., Díez-Villaseñor, C., Soria, E. & Juez, G. Biological significance of a family of regularly spaced repeats in the genomes of Archaea, Bacteria and mitochondria. *Mol. Microbiol.* **36**, 244–

246 (2000).

538. Ran, F. A., Hsu, P. D., Wright, J., Agarwala, V., Scott, D. A. & Zhang, F. Genome engineering using the CRISPR-Cas9 system. *Nat. Protoc.* **8**, 2281–308 (2013).

539. Doudna, J. A. & Charpentier, E. Genome editing. The new frontier of genome engineering with CRISPR-Cas9. *Science* **346**, 1258096 (2014).

540. Lauritzsen, G. F., Weiss, S., Dembic, Z. & Bogen, B. Naive idiotype-specific CD4+ T cells and immunosurveillance of B-cell tumors. *Proc. Natl. Acad. Sci. U. S. A.* **91**, 5700–5704 (1994).

541. Castedo, M., Perfettini, J.-L., Roumier, T., Andreau, K., Medema, R. & Kroemer, G. Cell death by mitotic catastrophe: a molecular definition. *Oncogene* **23**, 2825–37 (2004).

542. Opydo-Chanek, M. M., Gonzalo, O. & Marzo, I. Multifaceted anticancer activity of BH3 mimetics: Current evidence and future prospects. *Biochem. Pharmacol.* **136**, 12–23 (2017).

543. Bennett, A., Sloss, O., Topham, C., Nelson, L., Tighe, A. & Taylor, S. S. Inhibition of Bcl-xL sensitizes cells to mitotic blockers, but not mitotic drivers. *Open Biol.* **6**, (2016).

544. Lieber, J., Eicher, C., Wenz, J., Kirchner, B., Warmann, S. W., Fuchs, J., *et al.* The BH3 mimetic ABT-737 increases treatment efficiency of paclitaxel against hepatoblastoma. *BMC Cancer* **11**, 362 (2011).

545. Panayotopoulou, E. G., Muller, A.-K., Borries, M., Busch, H., Hu, G., Lev, S., *et al.* Targeting of apoptotic pathways by SMAC or BH3 mimetics distinctly sensitizes paclitaxel-resistant triple negative breast cancer cells. *Oncotarget* **8**, 45088–45104 (2017).

546. Parrondo, R., de Las Pozas, A., Reiner, T. & Perez-Stable, C. ABT-737, a small molecule Bcl-2/Bcl-xL antagonist, increases antimitoticmediated apoptosis in human prostate cancer cells. *PeerJ* **2013**, 1–22 (2013).

547. Whitaker, R. H. & Placzek, W. J. Regulating the BCL2 Family to Improve Sensitivity to Microtubule Targeting Agents. *Cells* **8**, 346 (2019).

548. Oakes, S. R., Vaillant, F., Lim, E., Lee, L., Breslin, K., Feleppa, F., *et al.* Sensitization of BCL-2-expressing breast tumors to chemotherapy by the BH3 mimetic ABT-737. *Proc. Natl. Acad. Sci. U. S. A.* **109**, 2766–2771 (2012).

549. Bah, N., Maillet, L., Ryan, J., Dubreil, S., Gautier, F., Letai, A., *et al.* Bcl-xL controls a switch between cell death modes during mitotic arrest. *Cell Death Dis.* **5**, e1291 (2014).

550. Haschka, M. D., Soratroi, C., Kirschnek, S., Häcker, G., Hilbe, R., Geley, S., *et al.* The NOXA-MCL1-BIM axis defines lifespan on extended mitotic arrest. *Nat. Commun.* **6**, 1–13 (2015).

551. López-Otín, C., Blasco, M. A., Partridge, L., Serrano, M. & Kroemer, G. The Hallmarks of Aging. *Cell* **153**, 1194–1217 (2013).

552. Noren Hooten, N. & Evans, M. K. Techniques to Induce and Quantify Cellular Senescence. *J. Vis. Exp.* **2017**, 10.3791/55533 (2017).

553. Munoz-Espin, D., Serrano, M., Muñoz-Espín, D. & Serrano, M. Cellular senescence: from physiology to pathology. *Nat. Rev. Mol. Cell Biol.* **15**, 482–496 (2014).

554. He, S. & Sharpless, N. E. Senescence in Health and Disease. *Cell* **169**, 1000–1011 (2017).

555. Lasry, A. & Ben-Neriah, Y. Senescence-associated inflammatory responses: Aging and cancer perspectives. *Trends Immunol.* **36**, 217–228 (2015).

556. Sikora, E., Bielak-Zmijewska, A. & Mosieniak, G. Targeting normal and cancer senescent cells as a strategy of senotherapy. *Ageing Res. Rev.* **55**, 100941 (2019).

557. Wang, Q., Wu, P. C., Dong, D. Z., Ivanova, I., Chu, E., Zeliadt, S., *et al.* Polyploidy road to therapy-induced cellular senescence and escape. *Int. J. cancer* **132**, 1505–1515 (2013).

558. Ovadya, Y. & Krizhanovsky, V. Senescent cell death brings hopes to life. *Cell Cycle* **16**, 9–10 (2017).

559. Yosef, R., Pilpel, N., Tokarsky-Amiel, R., Biran, A., Ovadya, Y., Cohen, S., *et al.* Directed elimination of senescent cells by inhibition of BCL-W and BCL-XL. *Nat. Commun.* **7**, 11190 (2016).

560. Ben-David, U., Siranosian, B., Ha, G., Tang, H., Oren, Y., Hinohara, K., *et al.* Genetic and transcriptional evolution alters cancer cell line drug response. *Nature* **560**, 325–330 (2018).

561. Bekier, M. E., Fischbach, R., Lee, J. & Taylor, W. R. Length of mitotic arrest induced by microtubule-stabilizing drugs determines cell death after mitotic exit. *Mol. Cancer Ther.* **8**, 1646–1654 (2009).

562. Topham, C., Tighe, A., Ly, P., Bennett, A., Sloss, O., Nelson, L., *et al.* MYC Is a Major Determinant of Mitotic Cell Fate. *Cancer Cell* **28**, 129–140 (2015).

563. Sloss, O., Topham, C., Diez, M. & Taylor, S. Mcl-1 dynamics influence mitotic slippage and death in mitosis. *Oncotarget* **7**, 5176–5192 (2016).

564. Allan, L. A., Skowyra, A., Rogers, K. I., Zeller, D. D., Clarke, P. R. & Allan, L. A. Atypical APC/C-dependent degradation of Mcl-1 provides an apoptotic timer during mitotic arrest. *EMBO J.* **37**, 1–15 (2018).

565. Clarke, P. R. Timed degradation of Mcl-1 controls mitotic cell death. *Mol. Cell. Oncol.* **5**, 1–3 (2018).

566. Kueh, H. Y., Zhu, Y. & Shi, J. A simplified Bcl-2 network model reveals quantitative determinants of cell-to-cell variation in sensitivity to anti-mitotic chemotherapeutics. *Sci. Rep.* **6**, 36585 (2016).

567. Tan, N., Malek, M., Zha, J., Yue, P., Kassees, R., Berry, L., *et al.* Navitoclax enhances the efficacy of taxanes in non-small cell lung cancer models. *Clin. Cancer Res.* **17**, 1394–404 (2011).

568. Shi, J., Zhou, Y., Huang, H. & Mitchison, T. J. Navitoclax (ABT-263) Accelerates Apoptosis during Drug- Induced Mitotic Arrest by Antagonizing Bcl-xL. **71**, 4518–4527 (2011).

569. Huang, S., Tang, R. & Poon, R. Y. C. BCL-W is a regulator of microtubule inhibitor-induced mitotic cell death. *Oncotarget* **7**, 38718–38730 (2016).

570. Vanoosthuyse, V. & Hardwick, K. G. The complexity of Bub1 regulation--phosphorylation, phosphorylation, phosphorylation. *Cell Cycle* **2**, 118–119 (2003).

571. Michel, L., Diaz-Rodriguez, E., Narayan, G., Hernando, E., Murty, V. V. V. S. & Benezra, R. Complete loss of the tumor suppressor MAD2 causes premature cyclin B degradation and mitotic failure in human somatic cells. *Proc. Natl. Acad. Sci. U. S. A.* **101**, 4459–4464 (2004).

572. Kops, G. J. P. L., Foltz, D. R. & Cleveland, D. W. Lethality to human cancer cells through massive chromosome loss by inhibition of the mitotic checkpoint. *Proc. Natl. Acad. Sci. U. S. A.* **101**, 8699–8704 (2004).

573. Shin, H. J., Baek, K. H., Jeon, A. H., Park, M. T., Lee, S. J., Kang, C. M., *et al.* Dual roles of human BubR1, a mitotic checkpoint kinase, in the monitoring of chromosomal instability. *Cancer Cell* **4**, 483–497 (2003).

574. Jim, B., Bargiela-Iparraguirre, J., Prado-Marchal, L., Pajuelo-Lozano, N., Jimenez, B., Perona, R., *et al.* Mad2 and BubR1 modulates tumourigenesis and paclitaxel response in MKN45 gastric cancer cells. *Cell Cycle* **13**, 3590–3601 (2014).

575. Lentini, L., Barra, V., Schillaci, T. & Di Leonardo, A. MAD2 depletion triggers premature cellular senescence in human primary fibroblasts by activating a p53 pathway preventing aneuploid cells propagation. *J. Cell. Physiol.* **227**, 3324–3332 (2012).

576. Lentini, L., Piscitello, D. D., Veneziano, L., Di Leonardo, A. & Leonardo, A. Di. Simultaneous reduction of MAD2 and BUBR1 expression induces mitotic spindle alterations associated with p53 dependent cell cycle arrest and death. *Cell Biol. Int.* **38**, 933–941 (2014).

577. Yun, M., Han, Y.-H., Yoon, S. H., Kim, H. Y., Kim, B.-Y., Ju, Y., *et al.* p31comet Induces cellular senescence through p21 accumulation and Mad2 disruption. *Mol. Cancer Res.* **7**, 371–382 (2009).

578. Kim, H., Cho, J. H., Quan, H. & Kim, J. Down-regulation of Aurora B kinase induces cellular

senescence in human fibroblasts and endothelial cells through a p53-dependent pathway. *FEBS Lett.* **585**, 3569–3576 (2011).

579. Morrow, C. J., Tighe, A., Johnson, V. L., Scott, M. I. F., Ditchfield, C. & Taylor, S. S. Bub1 and aurora B cooperate to maintain BubR1-mediated inhibition of APC/CCdc20. *J. Cell Sci.* **118**, 3639–3652 (2005).

580. Sasai, K., Treekitkarnmongkol, W., Kai, K., Katayama, H. & Sen, S. Functional Significance of Aurora Kinases–p53 Protein Family Interactions in Cancer. *Front. Oncol.* **6**, (2016).

581. Ha, G.-H. & Breuer, E. Y. Mitotic Kinases and p53 Signaling. *Biochem. Res. Int.* **2012**, 195903 (2012).

582. Phosphorylation, S. B., Ha, G., Baek, K., Kim, H., Jeong, S., Kim, C., *et al.* p53 activation in response to mitotic spindle damage requires signaling via BubR1-mediated phosphorylation. *Cancer Res.* **67**, 7155–7164 (2007).

583. Suematsu, T., Li, Y., Kojima, H., Nakajima, K., Oshimura, M. & Inoue, T. Deacetylation of the mitotic checkpoint protein BubR1 at lysine 250 by SIRT2 and subsequent effects on BubR1 degradation during the prometaphase/anaphase transition. *Biochem. Biophys. Res. Commun.* **453**, 588–594 (2014).

584. Sisinni, L., Maddalena, F., Condelli, V., Pannone, G., Simeon, V., Li Bergolis, V., *et al.* TRAP1 controls cell cycle G2-M transition through the regulation of CDK1 and MAD2 expression/ubiquitination. *J. Pathol.* **243**, 123–134 (2017).

585. Sitry-shevah, D., Kaisari, S., Teichner, A., Miniowitz-shemtov, S. & Hershko, A. Role of ubiquitylation of components of mitotic checkpoint complex in their dissociation from anaphase-promoting complex/cyclosome. *Proc. Natl. Acad. Sci. U. S. A.* **115**, 1777–1782 (2018).

586. Andonegui-elguera, M. A., Cáceres-gutiérrez, R. E., Luna-maldonado, F., López-saavedra, A., Díaz-chávez, J., Cisneros-soberanis, F., *et al.* BUB1 and SURVIVIN proteins are not degraded after a prolonged mitosis and accumulate in the nuclei of. *Nat. Publ. Gr.* (2016). doi:10.1038/cddiscovery.2016.79

587. Masawang, K., Pedro, M., Cidade, H., Reis, R. M., Neves, M. P., Corrêa, A. G., *et al.* Evaluation of 2',4'-dihydroxy-3,4,5-trimethoxychalcone as antimitotic agent that induces mitotic catastrophe in MCF-7 breast cancer cells. *Toxicol. Lett.* **229**, 393–401 (2014).

588. Fu, Y., Ye, D., Chen, H., Lu, W., Ye, F. & Xie, X. Weakened spindle checkpoint with reduced BubR1 expression in paclitaxel-resistant ovarian carcinoma cell line SKOV3-TR30. *Gynecol. Oncol.* **105**, 66–73 (2007).

589. Kita, K., Imai, Y., Asaka, N., Suzuki, T. & Ochi, T. BubR1 Is Essential for Thio-Dimethylarsinic Acid-Induced Spindle Assembly Checkpoint and Mitotic Cell Death for Preventing the Accumulation of Abnormal Cells. *Biol. Pharm. Bull.* **42**, 1089–1097 (2019).

590. Jeganathan, K., Malureanu, L., Baker, D. J., Abraham, S. C., Deursen, J. M. Van & van Deursen, J. M. Bub1 mediates cell death in response to chromosome missegregation and acts to suppress spontaneous tumorigenesis. *J. Cell Biol.* **179**, 255–267 (2007).

591. Andonegui-Elguera, M. A., Caceres-Gutierrez, R. E., Luna-Maldonado, F., Lopez-Saavedra, A., Diaz-Chavez, J., Cisneros-Soberanis, F., *et al.* BUB1 and SURVIVIN proteins are not degraded after a prolonged mitosis and accumulate in the nuclei of HCT116 cells. *Cell death Discov.* **2**, 16079 (2016).

592. Upreti, M., Chu, R., Galitovskaya, E., Smart, S. K. & Chambers, T. C. Key role for Bak activation and Bak-Bax interaction in the apoptotic response to vinblastine. *Mol. Cancer Ther.* **7**, 2224–2232 (2008).

593. Li, M., Jung, A., Ganswindt, U., Marini, P., Friedl, A., Daniel, P. T., *et al.* Aurora kinase inhibitor ZM447439 induces apoptosis via mitochondrial pathways. *Biochem. Pharmacol.* **79**, 122–129 (2010).

594. Levesley, J., Steele, L., Bruning-Richardson, A., Davison, A., Zhou, J., Ding, C., *et al.* Selective BCL-

XL inhibition promotes apoptosis in combination with MLN8237 in medulloblastoma and pediatric glioblastoma cells. *Neuro. Oncol.* **20**, 203–214 (2018).

595. Flores, M. L., Castilla, C., Avila, R., Ruiz-Borrego, M., Saez, C. & Japon, M. A. Paclitaxel sensitivity of breast cancer cells requires efficient mitotic arrest and disruption of Bcl-xL/Bak interaction. *Breast Cancer Res. Treat.* **133**, 917–928 (2012).

596. Taguchi, T., Kato, Y., Baba, Y., Nishimura, G., Tanigaki, Y., Horiuchi, C., *et al.* Protein levels of p21, p27, cyclin E and Bax predict sensitivity to cisplatin and paclitaxel in head and neck squamous cell carcinomas. *Oncol. Rep.* **11**, 421–426 (2004).

597. Maes, A., Menu, E., Veirman, K. De, Maes, K., Vand Erkerken, K., de Bruyne, E., *et al.* The therapeutic potential of cell cycle targeting in multiple myeloma. *Oncotarget* **8**, 90501–90520 (2017).

598. Gong, J.-N., Khong, T., Segal, D., Yao, Y., Riffkin, C. D., Garnier, J.-M., *et al.* Hierarchy for targeting pro-survival BCL2 family proteins in multiple myeloma: pivotal role of MCL1. *Blood* **128**, 1834–1844 (2016).

599. Bodet, L., Gomez-Bougie, P., Touzeau, C., Dousset, C., Descamps, G., Maiga, S., *et al.* ABT-737 is highly effective against molecular subgroups of multiple myeloma. *Blood* **118**, 3901–3910 (2011).

600. Touzeau, C., Maciag, P., Amiot, M. & Moreau, P. Targeting Bcl-2 for the treatment of multiple myeloma. *Leukemia* **32**, 1899–1907 (2018).

601. Harousseau, J.-L., Attal, M., Avet-Loiseau, H., Marit, G., Caillot, D., Mohty, M., *et al.* Bortezomib plus dexamethasone is superior to vincristine plus doxorubicin plus dexamethasone as induction treatment prior to autologous stem-cell transplantation in newly diagnosed multiple myeloma: results of the IFM 2005-01 phase III trial. *J. Clin. Oncol.* **28**, 4621–4629 (2010).

602. Baranowska, K., Misund, K., Starheim, K. K., Holien, T., Johansson, I., Darvekar, S., *et al.* Hydroxychloroquine potentiates carfilzomib toxicity towards myeloma cells. *Oncotarget* **7**, 70845–70856 (2016).

603. Hoang, B., Benavides, A., Shi, Y., Frost, P. & Lichtenstein, A. Effect of autophagy on multiple myeloma cell viability. *Mol. Cancer Ther.* **8**, 1974–1984 (2009).

604. Moriya, S., Che, X.-F., Komatsu, S., Abe, A., Kawaguchi, T., Gotoh, A., *et al.* Macrolide antibiotics block autophagy flux and sensitize to bortezomib via endoplasmic reticulum stress-mediated CHOP induction in myeloma cells. *Int. J. Oncol.* **42**, 1541–1550 (2013).

605. Kawaguchi, T., Miyazawa, K., Moriya, S., Ohtomo, T., Che, X.-F., Naito, M., *et al.* Combined treatment with bortezomib plus bafilomycin A1 enhances the cytocidal effect and induces endoplasmic reticulum stress in U266 myeloma cells: crosstalk among proteasome, autophagy-lysosome and ER stress. *Int. J. Oncol.* **38**, 643–654 (2011).

606. Nishimura, N., Radwan, M. O., Amano, M., Endo, S., Fujii, E., Hayashi, H., *et al.* Novel p97/VCP inhibitor induces ER stress and apoptosis in both bortezomib sensitive and resistant multiple myeloma cells. *Cancer Sci.* 1–13 (2019). doi:10.1111/cas.14154

607. Tresse, E., Salomons, F. A., Vesa, J., Bott, L. C., Kimonis, V., Yao, T.-P., *et al.* VCP/p97 is essential for maturation of ubiquitin-containing autophagosomes and this function is impaired by mutations that cause IBMPFD. *Autophagy* **6**, 217–227 (2010).

608. Ju, J.-S., Fuentealba, R. A., Miller, S. E., Jackson, E., Piwnica-Worms, D., Baloh, R. H., *et al.* Valosin-containing protein (VCP) is required for autophagy and is disrupted in VCP disease. *J. Cell Biol.* **187**, 875–888 (2009).

609. Lu, M., Lawrence, D. A., Marsters, S., Acosta-Alvear, D., Kimmig, P., Mendez, A. S., *et al.* Opposing unfolded-protein-response signals converge on death receptor 5 to control apoptosis. *Science* **345**, 98–101 (2014).

610. Estornes, Y., Aguileta, M. A., Dubuisson, C., De Keyser, J., Goossens, V., Kersse, K., *et al.* RIPK1 promotes death receptor-independent caspase-8-mediated apoptosis under unresolved ER

stress conditions. *Cell Death Dis.* **5**, e1555–e1555 (2014).

611. Deegan, S., Saveljeva, S., Logue, S. E., Pakos-Zebrucka, K., Gupta, S., Vandenabeele, P., *et al.* Deficiency in the mitochondrial apoptotic pathway reveals the toxic potential of autophagy under ER stress conditions. *Autophagy* **10**, 1921–1936 (2014).

612. Tomar, D., Prajapati, P., Sripada, L., Singh, K., Singh, R., Singh, A. K., *et al.* TRIM13 regulates caspase-8 ubiquitination, translocation to autophagosomes and activation during ER stress induced cell death. *Biochim. Biophys. Acta* **1833**, 3134–3144 (2013).

613. Liu, X., Yue, P., Chen, S., Hu, L., Lonial, S., Khuri, F. R., *et al.* The proteasome inhibitor PS-341 (bortezomib) up-regulates DR5 expression leading to induction of apoptosis and enhancement of TRAIL-induced apoptosis despite up-regulation of c-FLIP and survivin expression in human NSCLC cells. *Cancer Res.* **67**, 4981–4988 (2007).

614. Bui, H. T. T., Le, N. H., Le, Q. A., Kim, S. E., Lee, S. & Kang, D. Synergistic apoptosis of human gastric cancer cells by bortezomib and TRAIL. *Int. J. Med. Sci.* **16**, 1412–1423 (2019).

615. Han, B., Yao, W., Oh, Y.-T., Tong, J.-S., Li, S., Deng, J., *et al.* The novel proteasome inhibitor carfilzomib activates and enhances extrinsic apoptosis involving stabilization of death receptor 5. *Oncotarget* **6**, 17532–17542 (2015).

616. Sun, L., Wang, H., Wang, Z., He, S., Chen, S., Liao, D., *et al.* Mixed lineage kinase domain-like protein mediates necrosis signaling downstream of RIP3 kinase. *Cell* **148**, 213–227 (2012).

617. Ali, M. & Mocarski, E. S. Proteasome inhibition blocks necroptosis by attenuating death complex aggregation. *Cell Death Dis.* **9**, 346 (2018).

618. Garg, A. D., Maes, H., van Vliet, A. R. & Agostinis, P. Targeting the hallmarks of cancer with therapy-induced endoplasmic reticulum (ER) stress. *Mol. Cell. Oncol.* **2**, 1–20 (2015).

619. Casas, C. GRP78 at the Centre of the Stage in Cancer and Neuroprotection. *Front. Neurosci.* **11**, 177 (2017).

620. Lee, A. S. GRP78 induction in cancer: therapeutic and prognostic implications. *Cancer Res.* **67**, 3496–3499 (2007).

621. Kern, J., Untergasser, G., Zenzmaier, C., Sarg, B., Gastl, G., Gunsilius, E., *et al.* GRP-78 secreted by tumor cells blocks the antiangiogenic activity of bortezomib. *Blood* **114**, 3960–3967 (2009).

622. Roller, C. & Maddalo, D. The Molecular Chaperone GRP78/BiP in the Development of Chemoresistance: Mechanism and Possible Treatment. *Front. Pharmacol.* **4**, 10 (2013).

623. Virrey, J. J., Dong, D., Stiles, C., Patterson, J. B., Pen, L., Ni, M., *et al.* Stress chaperone GRP78/BiP confers chemoresistance to tumor-associated endothelial cells. *Mol. Cancer Res.* **6**, 1268–1275 (2008).

624. Tsutsumi, S., Namba, T., Tanaka, K. I., Arai, Y., Ishihara, T., Aburaya, M., *et al.* Celecoxib upregulates endoplasmic reticulum chaperones that inhibit celecoxib-induced apoptosis in human gastric cells. *Oncogene* **25**, 1018–1029 (2006).

625. Kimmig, P., Diaz, M., Zheng, J., Williams, C. C., Lang, A., Aragón, T., *et al.* The unfolded protein response in fission yeast modulates stability of select mRNAs to maintain protein homeostasis. *Elife* **1**, e00048–e00048 (2012).

626. Salaroglio, I. C., Panada, E., Moiso, E., Buondonno, I., Provero, P., Rubinstein, M., *et al.* PERK induces resistance to cell death elicited by endoplasmic reticulum stress and chemotherapy. *Mol. Cancer* **16**, 1–13 (2017).

627. McConkey, D. J. The integrated stress response and proteotoxicity in cancer therapy. *Biochem. Biophys. Res. Commun.* **482**, 450–453 (2017).

628. Schewe, D. M. & Aguirre-Ghiso, J. A. Inhibition of eIF2α Dephosphorylation maximizes bortezomib efficiency and eliminates quiescent multiple myeloma cells surviving proteasome inhibitor therapy. *Cancer Res.* **69**, 1545–1552 (2009).

629. Novoa, I., Zhang, Y., Zeng, H., Jungreis, R., Harding, H. P. & Ron, D. Stress-induced gene

expression requires programmed recovery from translational repression. *EMBO J.* **22**, 1180–1187 (2003).

630. Siwecka, N., Rozpędek, W., Pytel, D., Wawrzynkiewicz, A., Dziki, A., Dziki, Ł., *et al.* Dual role of Endoplasmic Reticulum Stress-Mediated Unfolded Protein Response Signaling Pathway in Carcinogenesis. *Int. J. Mol. Sci.* **20**, 4354 (2019).

631. Karagöz, G. E., Aragón, T. & Acosta-Alvear, D. Recent advances in signal integration mechanisms in the unfolded protein response. *F1000Research* **8**, F1000 Faculty Rev-1840 (2019).

632. Urra, H., Dufey, E., Lisbona, F., Rojas-Rivera, D. & Hetz, C. When ER stress reaches a dead end. *Biochim. Biophys. Acta - Mol. Cell Res.* **1833**, 3507–3517 (2013).

633. White-Gilbertson, S., Hua, Y. & Liu, B. The role of endoplasmic reticulum stress in maintaining and targeting multiple myeloma: A double-edged sword of adaptation and apoptosis. *Front. Genet.* **4**, 1–8 (2013).

634. Han, J., Back, S. H., Hur, J., Lin, Y. H., Gildersleeve, R., Shan, J., *et al.* ER-stress-induced transcriptional regulation increases protein synthesis leading to cell death. *Nat. Cell Biol.* **15**, 481–490 (2013).

635. Soriano, G. P., Besse, L., Li, N., Kraus, M., Besse, A., Meeuwenoord, N., *et al.* Proteasome inhibitor-adapted myeloma cells are largely independent from proteasome activity and show complex proteomic changes, in particular in redox and energy metabolism. *Leukemia* **30**, 2198–2207 (2016).

636. Leung-Hagesteijn, C., Erdmann, N., Cheung, G., Keats, J. J., Stewart, A. K., Reece, D. E., *et al.* Xbp1s-Negative Tumor B Cells and Pre-Plasmablasts Mediate Therapeutic Proteasome Inhibitor Resistance in Multiple Myeloma. *Cancer Cell* **24**, 289–304 (2013).

637. Lin, J. H., Li, H., Yasumura, D., Cohen, H. R., Zhang, C., Panning, B., *et al.* IRE1 signaling affects cell fate during the unfolded protein response. *Science* **318**, 944–949 (2007).

638. Chang, T.-K. K., Lawrence, D. A., Lu, M., Tan, J., Harnoss, J. M., Marsters, S. A., *et al.* Coordination between Two Branches of the Unfolded Protein Response Determines Apoptotic Cell Fate. *Mol. Cell* **71**, 629-636.e5 (2018).

639. Lee, A.-H., Iwakoshi, N. N., Anderson, K. C. & Glimcher, L. H. Proteasome inhibitors disrupt the unfolded protein response in myeloma cells. *Proc. Natl. Acad. Sci. U. S. A.* **100**, 9946–51 (2003).

640. DuRose, J. B., Tam, A. B. & Niwa, M. Intrinsic capacities of molecular sensors of the unfolded protein response to sense alternate forms of endoplasmic reticulum stress. *Mol. Biol. Cell* **17**, 3095–3107 (2006).

641. Mozos, A., Roué, G. G., López-Guillermo, A., Jares, P., Campo, E., Colomer, D., *et al.* The expression of the endoplasmic reticulum stress sensor BiP/GRP78 predicts response to chemotherapy and determines the efficacy of proteasome inhibitors in diffuse large b-cell lymphoma. *Am. J. Pathol.* **179**, 2601–2610 (2011).

642. Cerezo, M., Benhida, R. & Rocchi, S. Targeting BIP to induce Endoplasmic Reticulum stress and cancer cell death. *Oncoscience* **3**, 306–307 (2016).

643. Mhaidat, N. M., Alzoubi, K. H., Khabour, O. F., Banihani, M. N., Al-Balas, Q. A. & Swaidan, S. GRP78 regulates sensitivity of human colorectal cancer cells to DNA targeting agents. *Cytotechnology* **68**, 459–467 (2016).

644. Yun, S., Han, Y.-S., Lee, J. H., Kim, S. & Lee, S. H. Enhanced Susceptibility to 5-Fluorouracil in Human Colon Cancer Cells by Silencing of GRP78. *Anticancer Res.* **37**, 2975–2984 (2017).

645. Abdel Malek, M. A. Y., Jagannathan, S., Malek, E., Sayed, D. M., Elgammal, S. A., Abd El-Azeem, H. G., *et al.* Molecular chaperone GRP78 enhances aggresome delivery to autophagosomes to promote drug resistance in multiple myeloma. *Oncotarget* **6**, 3098–3110 (2015).

646. Axten, J. M., Medina, J. R., Feng, Y., Shu, A., Romeril, S. P., Grant, S. W., *et al.* Discovery of 7-methyl-5-(1-{[3-(trifluoromethyl)phenyl]acetyl}-2,3-dihydro-1H-indol-5-yl)-7H-pyrrolo[2,3-d]pyrimidin-4-amine (GSK2606414), a potent and selective first-in-class inhibitor of protein

kinase R (PKR)-like endoplasmic reticulum kinase (PERK). *J. Med. Chem.* **55**, 7193–7207 (2012).

647. Cross, B. C. S., Bond, P. J., Sadowski, P. G., Jha, B. K., Zak, J., Goodman, J. M., *et al.* The molecular basis for selective inhibition of unconventional mRNA splicing by an IRE1-binding small molecule. *Proc. Natl. Acad. Sci. U. S. A.* **109**, E869–E878 (2012).

648. Sporn, M. B. & Liby, K. T. NRF2 and cancer: the good, the bad and the importance of context. *Nat. Rev. Cancer* **12**, 564–571 (2012).

649. Jaramillo, M. C. & Zhang, D. D. The emerging role of the Nrf2-Keap1 signaling pathway in cancer. *Genes Dev.* **27**, 2179–2191 (2013).

650. Li, X., Liang, M., Jiang, J., He, R., Wang, M., Guo, X., *et al.* Combined inhibition of autophagy and Nrf2 signaling augments bortezomib-induced apoptosis by increasing ROS production and ER stress in pancreatic cancer cells. *Int. J. Biol. Sci.* **14**, 1291–1305 (2018).

651. Kovac, S., Angelova, P. R., Holmström, K. M., Zhang, Y., Dinkova-Kostova, A. T. & Abramov, A. Y. Nrf2 regulates ROS production by mitochondria and NADPH oxidase. *Biochim. Biophys. Acta* **1850**, 794–801 (2015).

652. Ma, Q. Role of nrf2 in oxidative stress and toxicity. *Annu. Rev. Pharmacol. Toxicol.* **53**, 401–426 (2013).

653. Janssen, K., Horn, S., Niemann, M. T., Daniel, P. T., Schulze-Osthoff, K. & Fischer, U. Inhibition of the ER Ca2+ pump forces multidrug-resistant cells deficient in Bak and Bax into necrosis. *J. Cell Sci.* **122**, 4481–4491 (2009).

654. Mimura, N., Fulciniti, M., Gorgun, G., Tai, Y.-T., Cirstea, D., Santo, L., *et al.* Blockade of XBP1 splicing by inhibition of IRE1α is a promising therapeutic option in multiple myeloma. *Blood* **119**, 5772–5781 (2012).

655. Rojas-Rivera, D., Delvaeye, T., Roelandt, R., Nerinckx, W., Augustyns, K., Vandenabeele, P., *et al.* When PERK inhibitors turn out to be new potent RIPK1 inhibitors: Critical issues on the specificity and use of GSK2606414 and GSK2656157. *Cell Death Differ.* **24**, 1100–1110 (2017).

656. Nogueira, V. & Hay, N. Molecular pathways: reactive oxygen species homeostasis in cancer cells and implications for cancer therapy. *Clin. Cancer Res.* **19**, 4309–4314 (2013).

657. Dikalov, S. I. & Harrison, D. G. Methods for detection of mitochondrial and cellular reactive oxygen species. *Antioxid. Redox Signal.* **20**, 372–382 (2014).

658. Gao, M., Chen, G., Wang, H., Xie, B., Hu, L., Kong, Y., *et al.* Therapeutic potential and functional interaction of carfilzomib and vorinostat in T-cell leukemia/lymphoma. *Oncotarget* **7**, 29102–29115 (2016).

659. Pérez-Galán, P., Roué, G., Villamor, N., Montserrat, E., Campo, E. & Colomer, D. The proteasome inhibitor bortezomib induces apoptosis in mantle-cell lymphoma through generation of ROS and Noxa activation independent of p53 status. *Blood* **107**, 257–264 (2006).

660. Ri, M. Endoplasmic-reticulum stress pathway-associated mechanisms of action of proteasome inhibitors in multiple myeloma. *Int. J. Hematol.* **104**, 273–280 (2016).

661. Schuiki, I., Zhang, L. & Volchuk, A. Endoplasmic reticulum redox state is not perturbed by pharmacological or pathological endoplasmic reticulum stress in live pancreatic β-cells. *PLoS One* **7**, e48626–e48626 (2012).

662. Cao, S. S. & Kaufman, R. J. Endoplasmic reticulum stress and oxidative stress in cell fate decision and human disease. *Antioxid. Redox Signal.* **21**, 396–413 (2014).

663. Zeeshan, H. M. A., Lee, G. H., Kim, H.-R. & Chae, H.-J. Endoplasmic Reticulum Stress and Associated ROS. *Int. J. Mol. Sci.* **17**, 327 (2016).

664. Murphy, M. P. How mitochondria produce reactive oxygen species. *Biochem. J.* **417**, 1–13 (2009).

665. Bhandary, B., Marahatta, A., Kim, H.-R. & Chae, H.-J. An involvement of oxidative stress in endoplasmic reticulum stress and its associated diseases. *Int. J. Mol. Sci.* **14**, 434–456 (2012).

666. Redza-Dutordoir, M. & Averill-Bates, D. A. Activation of apoptosis signalling pathways by reactive oxygen species. *Biochim. Biophys. Acta* **1863**, 2977–2992 (2016).

667. Yazdani, M. Concerns in the application of fluorescent probes DCDHF-DA, DHR 123 and DHE to measure reactive oxygen species in vitro. *Toxicol. In Vitro* **30**, 578–582 (2015).

668. Gomez-Bougie, P., Oliver, L., Le Gouill, S., Bataille, R. & Amiot, M. Melphalan-induced apoptosis in multiple myeloma cells is associated with a cleavage of Mcl-1 and Bim and a decrease in the Mcl-1/Bim complex. *Oncogene* **24**, 8076–8079 (2005).

669. Gomez-Bougie, P., Bataille, R. & Amiot, M. The imbalance between Bim and Mcl-1 expression controls the survival of human myeloma cells. *Eur. J. Immunol.* **34**, 3156–3164 (2004).

670. Iglesias-Serret, D., Piqué, M., Gil, J., Pons, G. & López, J. M. Transcriptional and translational control of Mcl-1 during apoptosis. *Arch. Biochem. Biophys.* **417**, 141–152 (2003).

671. Mojsa, B., Lassot, I. & Desagher, S. Mcl-1 ubiquitination: unique regulation of an essential survival protein. *Cells* **3**, 418–437 (2014).

672. Slomp, A. & Peperzak, V. Role and Regulation of Pro-survival BCL-2 Proteins in Multiple Myeloma. *Front. Oncol.* **8**, 533 (2018).

673. Herrant, M., Jacquel, A., Marchetti, S., Belhacène, N., Colosetti, P., Luciano, F., *et al.* Cleavage of Mcl-1 by caspases impaired its ability to counteract Bim-induced apoptosis. *Oncogene* **23**, 7863–7873 (2004).

674. Zang, Y., Thomas, S. M., Chan, E. T., Kirk, C. J., Freilino, M. L., DeLancey, H. M., *et al.* The next generation proteasome inhibitors carfilzomib and oprozomib activate prosurvival autophagy via induction of the unfolded protein response and ATF4. *Autophagy* **8**, 1873–1874 (2012).

675. Nencioni, A., Hua, F., Dillon, C., Yokoo, R., Scheiermann, C., Cardone, M., *et al.* Evidence for a protective role of Mcl-1 in proteasome inhibitor-induced apoptosis. *Blood* **105**, 3255–3262 (2005).

676. Qin, J.-Z., Ziffra, J., Stennett, L., Bodner, B., Bonish, B. K., Chaturvedi, V., *et al.* Proteasome inhibitors trigger NOXA-mediated apoptosis in melanoma and myeloma cells. *Cancer Res.* **65**, 6282–6293 (2005).

677. Podar, K., Gouill, S. L., Zhang, J., Opferman, J. T., Zorn, E., Tai, Y.-T., *et al.* A pivotal role for Mcl-1 in Bortezomib-induced apoptosis. *Oncogene* **27**, 721–731 (2008).

678. Allagnat, F., Cunha, D., Moore, F., Vanderwinden, J. M., Eizirik, D. L. & Cardozo, A. K. Mcl-1 downregulation by pro-inflammatory cytokines and palmitate is an early event contributing to β-cell apoptosis. *Cell Death Differ.* **18**, 328–337 (2011).

679. Hadji, A., Clybouw, C., Auffredou, M.-T., Alexia, C., Poalas, K., Burlion, A., *et al.* Caspase-3 triggers a TPCK-sensitive protease pathway leading to degradation of the BH3-only protein puma. *Apoptosis* **15**, 1529–1539 (2010).

680. Fricker, M., O'Prey, J., Tolkovsky, A. M. & Ryan, K. M. Phosphorylation of Puma modulates its apoptotic function by regulating protein stability. *Cell Death Dis.* **1**, e59–e59 (2010).

681. Reimertz, C., Kögel, D., Rami, A., Chittenden, T. & Prehn, J. H. M. Gene expression during ER stress-induced apoptosis in neurons: induction of the BH3-only protein Bbc3/PUMA and activation of the mitochondrial apoptosis pathway. *J. Cell Biol.* **162**, 587–597 (2003).

682. Jiang, C. C., Lucas, K., Avery-Kiejda, K. A., Wade, M., deBock, C. E., Thorne, R. F., *et al.* Up-regulation of Mcl-1 is critical for survival of human melanoma cells upon endoplasmic reticulum stress. *Cancer Res.* **68**, 6708–6717 (2008).

683. Concannon, C. G., Koehler, B. F., Reimertz, C., Murphy, B. M., Bonner, C., Thurow, N., *et al.* Apoptosis induced by proteasome inhibition in cancer cells: predominant role of the p53/PUMA pathway. *Oncogene* **26**, 1681–1692 (2007).

684. Shukla, S., Saxena, S., Singh, B. K. & Kakkar, P. BH3-only protein BIM: An emerging target in chemotherapy. *Eur. J. Cell Biol.* **96**, 728–738 (2017).

685. Sionov, R. V., Vlahopoulos, S. A. & Granot, Z. Regulation of Bim in Health and Disease. *Oncotarget* **6**, 23058–23134 (2015).

686. Puthalakath, H., Huang, D. C., O'Reilly, L. A., King, S. M. & Strasser, A. The proapoptotic activity of the Bcl-2 family member Bim is regulated by interaction with the dynein motor complex. *Mol. Cell* **3**, 287–296 (1999).

687. Akiyama, T., Dass, C. R. & Choong, P. F. M. Bim-targeted cancer therapy: a link between drug action and underlying molecular changes. *Mol. Cancer Ther.* **8**, 3173–3180 (2009).

688. Callus, B. A., Moujallad, D. M., Silke, J., Gerl, R., Jabbour, A. M., Ekert, P. G., *et al.* Triggering of apoptosis by Puma is determined by the threshold set by prosurvival Bcl-2 family proteins. *J. Mol. Biol.* **384**, 313–323 (2008).

689. Fennell, D. A., Chacko, A. & Mutti, L. BCL-2 family regulation by the 20S proteasome inhibitor bortezomib. *Oncogene* **27**, 1189–1197 (2008).

690. Baou, M., Kohlhaas, S. L., Butterworth, M., Vogler, M., Dinsdale, D., Walewska, R., *et al.* Role of NOXA and its ubiquitination in proteasome inhibitor-induced apoptosis in chronic lymphocytic leukemia cells. *Haematologica* **95**, 1510–1518 (2010).

691. Craxton, A., Butterworth, M., Harper, N., Fairall, L., Schwabe, J., Ciechanover, A., *et al.* NOXA, a sensor of proteasome integrity, is degraded by 26S proteasomes by an ubiquitin-independent pathway that is blocked by MCL-1. *Cell Death Differ.* **19**, 1424–1434 (2012).

692. Pang, X., Zhang, J., Lopez, H., Wang, Y., Li, W., O'Neill, K. L., *et al.* The carboxyl-terminal tail of Noxa protein regulates the stability of Noxa and Mcl-1. *J. Biol. Chem.* **289**, 17802–17811 (2014).

693. Scorrano, L., Oakes, S. A., Opferman, J. T., Cheng, E. H., Sorcinelli, M. D., Pozzan, T., *et al.* BAX and BAK regulation of endoplasmic reticulum Ca2+: a control point for apoptosis. *Science* **300**, 135–139 (2003).

694. Zong, W.-X., Li, C., Hatzivassiliou, G., Lindsten, T., Yu, Q.-C., Yuan, J., *et al.* Bax and Bak can localize to the endoplasmic reticulum to initiate apoptosis. *J. Cell Biol.* **162**, 59–69 (2003).

695. Mathai, J. P., Germain, M. & Shore, G. C. BH3-only BIK regulates BAX,BAK-dependent release of Ca2+ from endoplasmic reticulum stores and mitochondrial apoptosis during stress-induced cell death. *J. Biol. Chem.* **280**, 23829–23836 (2005).

696. Nutt, L. K., Chandra, J., Pataer, A., Fang, B., Roth, J. A., Swisher, S. G., *et al.* Bax-mediated Ca2+ mobilization promotes cytochrome c release during apoptosis. *J. Biol. Chem.* **277**, 20301–20308 (2002).

697. Nutt, L. K., Pataer, A., Pahler, J., Fang, B., Roth, J., McConkey, D. J., *et al.* Bax and Bak promote apoptosis by modulating endoplasmic reticular and mitochondrial Ca2+ stores. *J. Biol. Chem.* **277**, 9219–9225 (2002).

698. Wei, M. C., Zong, W. X., Cheng, E. H., Lindsten, T., Panoutsakopoulou, V., Ross, A. J., *et al.* Proapoptotic BAX and BAK: a requisite gateway to mitochondrial dysfunction and death. *Science* **292**, 727–730 (2001).

699. Pan, J.-A., Ullman, E., Dou, Z. & Zong, W.-X. Inhibition of protein degradation induces apoptosis through a microtubule-associated protein 1 light chain 3-mediated activation of caspase-8 at intracellular membranes. *Mol. Cell. Biol.* **31**, 3158–3170 (2011).

700. Busacca, S., Chacko, A. D., Klabatsa, A., Arthur, K., Sheaff, M., Barbone, D., *et al.* BAK and NOXA are critical determinants of mitochondrial apoptosis induced by bortezomib in mesothelioma. *PLoS One* **8**, e65489–e65489 (2013).

701. Laussmann, M. A., Passante, E., Düssmann, H., Rauen, J. A., Würstle, M. L., Delgado, M. E., *et al.* Proteasome inhibition can induce an autophagy-dependent apical activation of caspase-8. *Cell Death Differ.* **18**, 1584–1597 (2011).

702. Ullman, E., Fan, Y., Stawowczyk, M., Chen, H.-M., Yue, Z. & Zong, W.-X. Autophagy promotes necrosis in apoptosis-deficient cells in response to ER stress. *Cell Death Differ.* **15**, 422–425 (2008).

703. Lomonosova, E., Ryerse, J. & Chinnadurai, G. BAX/BAK-independent mitoptosis during cell death induced by proteasome inhibition? *Mol. Cancer Res.* **7**, 1268–1284 (2009).

704. Zamorano, S., Rojas-Rivera, D., Lisbona, F., Parra, V., Court, F. A., Villegas, R., *et al.* A BAX/BAK and cyclophilin D-independent intrinsic apoptosis pathway. *PLoS One* **7**, e37782–e37782 (2012).

705. Glab, J. A., Doerflinger, M., Nedeva, C., Jose, I., Mbogo, G. W., Paton, J. C., *et al.* DR5 and caspase-8 are dispensable in ER stress-induced apoptosis. *Cell Death Differ.* **24**, 944–950 (2017).

706. Walczak, H., Degli-Esposti, M. A., Johnson, R. S., Smolak, P. J., Waugh, J. Y., Boiani, N., *et al.* TRAIL-R2: a novel apoptosis-mediating receptor for TRAIL. *EMBO J.* **16**, 5386–5397 (1997).

707. Hymowitz, S. G., Christinger, H. W., Fuh, G., Ultsch, M., O'Connell, M., Kelley, R. F., *et al.* Triggering cell death: the crystal structure of Apo2L/TRAIL in a complex with death receptor 5. *Mol. Cell* **4**, 563–571 (1999).

708. Muzio, M., Stockwell, B. R., Stennicke, H. R., Salvesen, G. S. & Dixit, V. M. An induced proximity model for caspase-8 activation. *J. Biol. Chem.* **273**, 2926–2930 (1998).

709. Dickens, L. S., Boyd, R. S., Jukes-Jones, R., Hughes, M. A., Robinson, G. L., Fairall, L., *et al.* A death effector domain chain DISC model reveals a crucial role for caspase-8 chain assembly in mediating apoptotic cell death. *Mol. Cell* **47**, 291–305 (2012).

710. Lam, M., Marsters, S. A., Ashkenazi, A. & Walter, P. Misfolded proteins bind and activate death receptor 5 to trigger apoptosis during unresolved endoplasmic reticulum stress. *Elife* **9**, e52291 (2020).

711. Lam, M., Lawrence, D. A., Ashkenazi, A. & Walter, P. Confirming a critical role for death receptor 5 and caspase-8 in apoptosis induction by endoplasmic reticulum stress. *Cell Death Differ.* **25**, 1530–1531 (2018).

712. Hübner, A., Barrett, T., Flavell, R. A. & Davis, R. J. Multisite phosphorylation regulates Bim stability and apoptotic activity. *Mol. Cell* **30**, 415–425 (2008).

713. Ley, R., Balmanno, K., Hadfield, K., Weston, C. & Cook, S. J. Activation of the ERK1/2 signaling pathway promotes phosphorylation and proteasome-dependent degradation of the BH3-only protein, Bim. *J. Biol. Chem.* **278**, 18811–18816 (2003).

714. Muñoz-Pinedo, C. & López-Rivas, A. A role for caspase-8 and TRAIL-R2/DR5 in ER-stress-induced apoptosis. *Cell Death Differ.* **25**, 226 (2017).

715. Ramírez-Peinado, S., Alcázar-Limones, F., Lagares-Tena, L., El Mjiyad, N., Caro-Maldonado, A., Tirado, O. M., *et al.* 2-Deoxyglucose induces Noxa-dependent apoptosis in alveolar rhabdomyosarcoma. *Cancer Res.* **71**, 6796–6806 (2011).

716. Caro-Maldonado, A., Tait, S. W. G., Ramírez-Peinado, S., Ricci, J. E., Fabregat, I., Green, D. R., *et al.* Glucose deprivation induces an atypical form of apoptosis mediated by caspase-8 in Bax-, Bak-deficient cells. *Cell Death Differ.* **17**, 1335–1344 (2010).

717. Jaganathan, S., Malek, E., Vallabhapurapu, S., Vallabhapurapu, S. & Driscoll, J. J. Bortezomib induces AMPK-dependent autophagosome formation uncoupled from apoptosis in drug resistant cells. *Oncotarget* **5**, 12358–12370 (2014).

718. Papanagnou, E.-D., Terpos, E., Kastritis, E., Papassideri, I. S., Tsitsilonis, O. E., Dimopoulos, M. A., *et al.* Molecular responses to therapeutic proteasome inhibitors in multiple myeloma patients are donor-, cell type- and drug-dependent. *Oncotarget* **9**, 17797–17809 (2018).

719. Bustamante, H. A., González, A. E., Cerda-Troncoso, C., Shaughnessy, R., Otth, C., Soza, A., *et al.* Interplay Between the Autophagy-Lysosomal Pathway and the Ubiquitin-Proteasome System: A Target for Therapeutic Development in Alzheimer's Disease. *Front. Cell. Neurosci.* **12**, 126 (2018).

720. Bao, W., Gu, Y., Ta, L., Wang, K. & Xu, Z. Induction of autophagy by the MG-132 proteasome inhibitor is associated with endoplasmic reticulum stress in MCF-7 cells. *Mol. Med. Rep.* **13**, 796–804 (2016).

721. Lan, D., Wang, W., Zhuang, J. & Zhao, Z. Proteasome inhibitor-induced autophagy in PC12 cells

overexpressing A53T mutant α-synuclein. *Mol. Med. Rep.* **11**, 1655–1660 (2015).

722. Zhu, K., Dunner, K., McConkey, D. J., Dunner Jr, K. & McConkey, D. J. Proteasome inhibitors activate autophagy as a cytoprotective response in human prostate cancer cells. *Oncogene* **29**, 451–462 (2010).

723. Milani, M., Rzymski, T., Mellor, H. R., Pike, L., Bottini, A., Generali, D., *et al.* The role of ATF4 stabilization and autophagy in resistance of breast cancer cells treated with Bortezomib. *Cancer Res.* **69**, 4415–4423 (2009).

724. Wojcik, S. Crosstalk between autophagy and proteasome protein degradation systems: Possible implications for cancer therapy. *Folia Histochem. Cytobiol.* **51**, 249–264 (2013).

725. Hui, B., Shi, Y.-H., Ding, Z.-B., Zhou, J., Gu, C.-Y., Peng, Y.-F., *et al.* Proteasome inhibitor interacts synergistically with autophagy inhibitor to suppress proliferation and induce apoptosis in hepatocellular carcinoma. *Cancer* **118**, 5560–5571 (2012).

726. Yao, F., Wang, G., Wei, W., Tu, Y., Tong, H. & Sun, S. An autophagy inhibitor enhances the inhibition of cell proliferation induced by a proteasome inhibitor in MCF-7 cells. *Mol. Med. Rep.* **5**, 84–88 (2012).

727. Carew, J. S., Medina, E. C., Esquivel 2nd, J. A., Mahalingam, D., Swords, R., Kelly, K., *et al.* Autophagy inhibition enhances vorinostat-induced apoptosis via ubiquitinated protein accumulation. *J. Cell. Mol. Med.* **14**, 2448–2459 (2010).

728. Maes, H., Kuchnio, A., Peric, A., Moens, S., Nys, K., De Bock, K., *et al.* Tumor vessel normalization by chloroquine independent of autophagy. *Cancer Cell* **26**, 190–206 (2014).

729. Ruschak, A. M., Slassi, M., Kay, L. E. & Schimmer, A. D. Novel Proteasome Inhibitors to Overcome Bortezomib Resistance. *JNCI J. Natl. Cancer Inst.* **103**, 1007–1017 (2011).

730. Sprangers, R., Li, X., Mao, X., Rubinstein, J. L., Schimmer, A. D. & Kay, L. E. TROSY-based NMR evidence for a novel class of 20S proteasome inhibitors. *Biochemistry* **47**, 6727–6734 (2008).

731. Legrand, A. J., Konstantinou, M., Goode, E. F. & Meier, P. Review The Diversification of Cell Death and Immunity : Memento Mori. 1–11 (2019).

732. Henson, P. M. Cell Removal: Efferocytosis. *Annu. Rev. Cell Dev. Biol.* **33**, 127–144 (2017).

733. Venkateswaran, K., Verma, A., Bhatt, A. N., Shrivastava, A., Manda, K., Raj, H. G., *et al.* Emerging Roles of Calreticulin in Cancer: Implications for Therapy. *Curr. Protein Pept. Sci.* **19**, 344–357 (2018).

734. Liu, P., Zhao, L., Loos, F., Marty, C., Xie, W., Martins, I., *et al.* Immunosuppression by Mutated Calreticulin Released from Malignant Cells. *Mol. Cell* S1097-2765(19)30833–0 (2019). doi:10.1016/j.molcel.2019.11.004

735. Imai, M., Araki, M. & Komatsu, N. Somatic mutations of calreticulin in myeloproliferative neoplasms. *Int. J. Hematol.* **105**, 743–747 (2017).

736. Nangalia, J., Massie, C. E., Baxter, E. J., Nice, F. L., Gundem, G., Wedge, D. C., *et al.* Somatic CALR mutations in myeloproliferative neoplasms with nonmutated JAK2. *N. Engl. J. Med.* **369**, 2391–2405 (2013).

737. Grinfeld, J., Nangalia, J., Baxter, E. J., Wedge, D. C., Angelopoulos, N., Cantrill, R., *et al.* Classification and Personalized Prognosis in Myeloproliferative Neoplasms. *N. Engl. J. Med.* **379**, 1416–1430 (2018).

738. How, J., Hobbs, G. & Mullally, A. Mutant calreticulin in myeloproliferative neoplasms. *Blood* blood.2019000622 (2019). doi:10.1182/blood.2019000622

739. Schcolnik-Cabrera, A., Oldak, B., Juárez, M., Cruz-Rivera, M., Flisser, A. & Mendlovic, F. Calreticulin in phagocytosis and cancer: opposite roles in immune response outcomes. *Apoptosis* **0**, 0 (2019).

740. Fucikova, J., Moserova, I., Urbanova, L., Bezu, L., Kepp, O., Cremer, I., *et al.* Prognostic and Predictive Value of DAMPs and DAMP-Associated Processes in Cancer . *Front. Immunol.* **6**, 402

(2015).

741. Basu, S., Binder, R. J., Ramalingam, T. & Srivastava, P. K. CD91 is a common receptor for heat shock proteins gp96, hsp90, hsp70, and calreticulin. *Immunity* **14**, 303–313 (2001).

742. Di Blasio, S., Wortel, I. M. N., van Bladel, D. A. G., de Vries, L. E., Duiveman-de Boer, T., Worah, K., *et al.* Human CD1c(+) DCs are critical cellular mediators of immune responses induced by immunogenic cell death. *Oncoimmunology* **5**, e1192739–e1192739 (2016).

743. Multhoff, G., Botzler, C., Jennen, L., Schmidt, J., Ellwart, J. & Issels, R. Heat shock protein 72 on tumor cells: a recognition structure for natural killer cells. *J. Immunol.* **158**, 4341–4350 (1997).

744. Vulpis, E., Cecere, F., Molfetta, R., Soriani, A., Fionda, C., Peruzzi, G., *et al.* Genotoxic stress modulates the release of exosomes from multiple myeloma cells capable of activating NK cell cytokine production: Role of HSP70/TLR2/NF-kB axis. *Oncoimmunology* **6**, 1–15 (2017).

745. Asea, A. Chaperokine-induced signal transduction pathways. *Exerc. Immunol. Rev.* **9**, 25–33 (2003).

746. Calderwood, S. K., Mambula, S. S., Gray Jr, P. J. & Theriault, J. R. Extracellular heat shock proteins in cell signaling. *FEBS Lett.* **581**, 3689–3694 (2007).

747. Calderwood, S. K., Theriault, J., Gray, P. J. & Gong, J. Cell surface receptors for molecular chaperones. *Methods* **43**, 199–206 (2007).

748. Radons, J. & Multhoff, G. Immunostimulatory functions of membrane-bound and exported heat shock protein 70. *Exerc. Immunol. Rev.* **11**, 17–33 (2005).

749. Tsai, Y.-L., Ha, D. P., Zhao, H., Carlos, A. J., Wei, S., Pun, T. K., *et al.* Endoplasmic reticulum stress activates SRC, relocating chaperones to the cell surface where GRP78/CD109 blocks TGF-β signaling. *Proc. Natl. Acad. Sci. U. S. A.* **115**, E4245–E4254 (2018).

750. Arap, M. A., Lahdenranta, J., Mintz, P. J., Hajitou, A., Sarkis, A. S., Arap, W., *et al.* Cell surface expression of the stress response chaperone GRP78 enables tumor targeting by circulating ligands. *Cancer Cell* **6**, 275–284 (2004).

751. Gonzalez-Gronow, M., Selim, M. A., Papalas, J. & Pizzo, S. V. GRP78: a multifunctional receptor on the cell surface. *Antioxid. Redox Signal.* **11**, 2299–2306 (2009).

752. Zhang, Y., Liu, R., Ni, M., Gill, P. & Lee, A. S. Cell surface relocalization of the endoplasmic reticulum chaperone and unfolded protein response regulator GRP78/BiP. *J. Biol. Chem.* **285**, 15065–15075 (2010).

753. Graner, M. W., Lillehei, K. O. & Katsanis, E. Endoplasmic reticulum chaperones and their roles in the immunogenicity of cancer vaccines. *Front. Oncol.* **4**, 379 (2015).

754. Asea, A. Heat shock proteins and toll-like receptors. *Handb. Exp. Pharmacol.* 111–127 (2008). doi:10.1007/978-3-540-72167-3_6

755. Kepp, O., Senovilla, L., Vitale, I., Vacchelli, E., Adjemian, S., Agostinis, P., *et al.* Consensus guidelines for the detection of immunogenic cell death. *Oncoimmunology* **3**, e955691–e955691 (2014).

756. Zitvogel, L., Kepp, O., Senovilla, L., Menger, L., Chaput, N. & Kroemer, G. Immunogenic tumor cell death for optimal anticancer therapy: The calreticulin exposure pathway. *Clin. Cancer Res.* **16**, 3100–3104 (2010).

757. Werthmöller, N., Frey, B., Wunderlich, R., Fietkau, R. & Gaipl, U. S. Modulation of radiochemoimmunotherapy-induced B16 melanoma cell death by the pan-caspase inhibitor zVAD-fmk induces anti-tumor immunity in a HMGB1-, nucleotide- and T-cell-dependent manner. *Cell Death Dis.* **6**, e1761–e1761 (2015).

758. Ferraro-Peyret, C., Quemeneur, L., Flacher, M., Revillard, J.-P. & Genestier, L. Caspase-independent phosphatidylserine exposure during apoptosis of primary T lymphocytes. *J. Immunol.* **169**, 4805–4810 (2002).

759. Bloy, N., Garcia, P., Laumont, C. M., Pitt, J. M., Sistigu, A., Stoll, G., *et al.* Immunogenic stress and

death of cancer cells: Contribution of antigenicity vs adjuvanticity to immunosurveillance. *Immunol. Rev.* **280**, 165–174 (2017).

760. Li, D.-D., Xie, B., Wu, X.-J., Li, J.-J., Ding, Y., Wen, X.-Z., *et al.* Late-stage inhibition of autophagy enhances calreticulin surface exposure. *Oncotarget* **7**, 80842–80854 (2016).

761. Martin, K., Schreiner, J. & Zippelius, A. Modulation of APC Function and Anti-Tumor Immunity by Anti-Cancer Drugs. *Front. Immunol.* **6**, 501 (2015).

762. Zitvogel, L., Pitt, J. M., Daillère, R., Smyth, M. J. & Kroemer, G. Mouse models in oncoimmunology. *Nat. Rev. Cancer* **16**, 759–773 (2016).

763. Binsfeld, M., Fostier, K., Muller, J., Baron, F., Schots, R., Beguin, Y., *et al.* Cellular immunotherapy in multiple myeloma: Lessons from preclinical models. *Biochim. Biophys. Acta - Rev. Cancer* **1846**, 392–404 (2014).

764. Tassone, P., Neri, P., Burger, R., Di Martino, M. T., Leone, E., Amodio, N., *et al.* Mouse models as a translational platform for the development of new therapeutic agents in multiple myeloma. *Curr. Cancer Drug Targets* **12**, 814–822 (2012).

765. Sanchez, E., Chen, H. & Berenson, J. R. In vivo models of multiple myeloma (MM). *Biochem. Pharmacol.* **89**, 313–320 (2014).

766. Paton-Hough, J., Chantry, A. D. & Lawson, M. A. A review of current murine models of multiple myeloma used to assess the efficacy of therapeutic agents on tumour growth and bone disease. *Bone* **77**, 57–68 (2015).

767. Maes, K., Boeckx, B., Vlummens, P., De Veirman, K., Menu, E., Vanderkerken, K., *et al.* The genetic landscape of 5T models for multiple myeloma. *Sci. Rep.* **8**, 15030 (2018).

768. Libouban, H. The use of animal models in multiple myeloma. *Morphologie* **99**, 63–72 (2015).

769. Vanderkerken, K., Asosingh, K., Croucher, P. & Van Camp, B. Multiple myeloma biology: lessons from the 5TMM models. *Immunol. Rev.* **194**, 196–206 (2003).

770. Asosingh, K., Radl, J., Van Riet, I., Van Camp, B. & Vanderkerken, K. The 5TMM series: a useful in vivo mouse model of human multiple myeloma. *Hematol. J. Off. J. Eur. Haematol. Assoc.* **1**, 351–356 (2000).

771. Oyajobi, B. O., Muñoz, S., Kakonen, R., Williams, P. J., Gupta, A., Wideman, C. L., *et al.* Detection of myeloma in skeleton of mice by whole-body optical fluorescence imaging. *Mol. Cancer Ther.* **6**, 1701–1708 (2007).

772. Garrett, I. R., Dallas, S., Radl, J. & Mundy, G. R. A murine model of human myeloma bone disease. *Bone* **20**, 515–520 (1997).

773. Rossi, M., Botta, C., Arbitrio, M., Grembiale, R. D., Tagliaferri, P. & Tassone, P. Mouse models of multiple myeloma: technologic platforms and perspectives. *Oncotarget* **9**, 20119–20133 (2018).

774. Anderson, P. N. & Potter, M. Induction of plasma cell tumours in BALB-c mice with 2,6,10,14-tetramethylpentadecane (pristane). *Nature* **222**, 994–995 (1969).

775. Kobayashi, H., Potter, M. & Dunn, T. B. Bone Lesions Produced by Transplanted Plasma-Cell Tumors in BALB/c Mice. *JNCI J. Natl. Cancer Inst.* **28**, 649–677 (1962).

776. POTTER, M., FAHEY, J. L. & PILGRIM, H. I. Abnormal serum protein and bone destruction in transmissible mouse plasma cell neoplasm (multiple myeloma). *Proc. Soc. Exp. Biol. Med.* **94**, 327–333 (1957).

777. Garfall, A. L. & Stadtmauer, E. A. Cellular and vaccine immunotherapy for multiple myeloma. *Hematol. Am. Soc. Hematol. Educ. Progr.* **2016**, 521–527 (2016).

778. Riedel, S. S., Mottok, A., Brede, C., Bäuerlein, C. A., Jordán Garrote, A. L., Ritz, M., *et al.* Non-Invasive Imaging Provides Spatiotemporal Information on Disease Progression and Response to Therapy in a Murine Model of Multiple Myeloma. *PLoS One* **7**, (2012).

779. Cesta, M. F. Normal Structure, Function, and Histology of the Spleen. *Toxicol. Pathol.* **34**, 455–

465 (2006).

780. Mosely, S. I. S., Prime, J. E., Sainson, R. C. A., Koopmann, J., Wang, D. Y. Q., Greenawalt, D. M., *et al.* Rational Selection of Syngeneic Preclinical Tumor Models for Immunotherapeutic Drug Discovery. 29–42 (2017). doi:10.1158/2326-6066.CIR-16-0114

781. Medicine, N., Ciampricotti, M., Hau, C.-S., Doornebal, C. W., Jonkers, J. & de Visser, K. E. Chemotherapy response of spontaneous mammary tumors is independent of the adaptive immune system. *Nat. Med.* **18**, 344–6; author reply 346 (2012).

782. Lyons, S. K. Imaging mouse models of cancer. *Cancer J. (United States)* **21**, 152–164 (2015).

783. Humeau, J., Lévesque, S., Kroemer, G. & Pol, J. G. Gold Standard Assessment of Immunogenic Cell Death in Oncological Mouse Models. *Methods Mol. Biol.* **1884**, 297–315 (2019).

784. Podar, K., Richardson, P. G., Hideshima, T., Chauhan, D. & Anderson, K. C. The malignant clone and the bone-marrow environment. *Best Pract. Res. Clin. Haematol.* **20**, 597–612 (2007).

785. Jaime-Sánchez, P., Catalán, E., Uranga-Murillo, I., Aguiló, N., Santiago, L., M Lanuza, P., *et al.* Antigen-specific primed cytotoxic T cells eliminate tumour cells in vivo and prevent tumour development, regardless of the presence of anti-apoptotic mutations conferring drug resistance. *Cell Death Differ.* **25**, 1536–1548 (2018).

786. Baklaushev, V. P., Kilpeläinen, A., Petkov, S., Abakumov, M. A., Grinenko, N. F., Yusubalieva, G. M., *et al.* Luciferase Expression Allows Bioluminescence Imaging But Imposes Limitations on the Orthotopic Mouse (4T1) Model of Breast Cancer. *Sci. Rep.* **7**, 7715 (2017).

787. Clark, A. J., Safaee, M., Oh, T., Ivan, M. E., Parimi, V., Hashizume, R., *et al.* Stable luciferase expression does not alter immunologic or in vivo growth properties of GL261 murine glioma cells. *J. Transl. Med.* **12**, 345 (2014).

788. Liao, J. B., Ovenell, K. J., Curtis, E. E. M., Cecil, D. L., Koehnlein, M. R., Rastetter, L. R., *et al.* Preservation of tumor-host immune interactions with luciferase-tagged imaging in a murine model of ovarian cancer. *J. Immunother. Cancer* **3**, 16 (2015).

789. Miller, A., Asmann, Y., Cattaneo, L., Braggio, E., Keats, J., Auclair, D., *et al.* High somatic mutation and neoantigen burden are correlated with decreased progression-free survival in multiple myeloma. *Blood Cancer J.* **7**, e612–e612 (2017).

790. Lawrence, M. S., Stojanov, P., Polak, P., Kryukov, G. V, Cibulskis, K., Sivachenko, A., *et al.* Mutational heterogeneity in cancer and the search for new cancer-associated genes. *Nature* **499**, 214–218 (2013).

791. Perumal, D., Imai, N., Laganà, A., Finnigan, J., Melnekoff, D., Leshchenko, V. V, *et al.* Mutation-derived Neoantigen-specific T-cell Responses in Multiple Myeloma. *Clin. Cancer Res.* (2019). doi:10.1158/1078-0432.CCR-19-2309

792. Blazquez, A., Rubinsteyn, A., Kodysh, J., Finnigan, J. P., Marron, T. U., Meseck, M., *et al.* A phase I study of the safety and immunogenicity of a multi-peptide personalized genomic vaccine in the adjuvant treatment of solid tumors and hematological malignancies. *J. Clin. Oncol.* **37**, e14307–e14307 (2019).

793. Noonan, K., Matsui, W., Serafini, P., Carbley, R., Tan, G., Khalili, J., *et al.* Activated marrow-infiltrating lymphocytes effectively target plasma cells and their clonogenic precursors. *Cancer Res.* **65**, 2026–2034 (2005).

794. Hong, S., Qian, J., Yang, J., Li, H., Kwak, L. W. & Yi, Q. Roles of idiotype-specific t cells in myeloma cell growth and survival: Th1 and CTL cells are tumoricidal while Th2 cells promote tumor growth. *Cancer Res.* **68**, 8456–8464 (2008).

795. Lynch, R. G., Graff, R. J., Sirisinha, S., Simms, E. S. & Eisen, H. N. Myeloma proteins as tumor-specific transplantation antigens. *Proc. Natl. Acad. Sci. U. S. A.* **69**, 1540–1544 (1972).

796. Bogen, B. A mouse model for immunotherapy of myeloma. *Hematol. J. Off. J. Eur. Haematol. Assoc.* **3**, 224–229 (2002).

797. Bogen, B., Malissen, B. & Haas, W. Idiotope-specific T cell clones that recognize syngeneic immunoglobulin fragments in the context of class II molecules. *Eur. J. Immunol.* **16**, 1373–1378 (1986).

798. Bogen, B., Gleditsch, L., Weiss, S. & Dembic, Z. Weak positive selection of transgenic T cell receptor-bearing thymocytes: importance of major histocompatibility complex class II, T cell receptor and CD4 surface molecule densities. *Eur. J. Immunol.* **22**, 703–709 (1992).

799. Corthay, A., Lundin, K. U., Lorvik, K. B., Hofgaard, P. O. & Bogen, B. Secretion of tumor-specific antigen by myeloma cells is required for cancer immunosurveillance by CD4+ T cells. *Cancer Res.* **69**, 5901–5907 (2009).

800. Bogen, B. Peripheral T cell tolerance as a tumor escape mechanism: deletion of CD4+ T cells specific for a monoclonal immunoglobulin idiotype secreted by a plasmacytoma. *Eur. J. Immunol.* **26**, 2671–2679 (1996).

801. Lauritzsen, G. F., Hofgaard, P. O., Schenck, K. & Bogen, B. Clonal deletion of thymocytes as a tumor escape mechanism. *Int. J. cancer* **78**, 216–222 (1998).

802. Zeis, M., Frenzke, H., Schmitz, N., Uharek, L. & Steinmann, J. Idiotype protein-pulsed dendritic cells produce strong anti-myeloma effects after syngeneic stem cell transplantation in mice. *Bone Marrow Transplant.* **29**, 213–221 (2002).

803. Kepp, O., Galluzzi, L., Martins, I., Schlemmer, F., Adjemian, S., Michaud, M., *et al.* Molecular determinants of immunogenic cell death elicited by anticancer chemotherapy. *Cancer Metastasis Rev.* **30**, 61–69 (2011).

804. Martins, I., Michaud, M., Sukkurwala, A. Q., Adjemian, S., Ma, Y., Shen, S., *et al.* Premortem autophagy determines the immunogenicity of chemotherapy-induced cancer cell death. *Autophagy* **8**, 413–415 (2012).

805. Franssen, L. E., Mutis, T., Lokhorst, H. M. & Donk, N. W. C. J. Van De. Immunotherapy in myeloma : how far have we come ? 1–19 (2019). doi:10.1177/https

806. Ocadlikova, D., Lecciso, M., Isidori, A., Loscocco, F., Visani, G., Amadori, S., *et al.* Chemotherapy-Induced Tumor Cell Death at the Crossroads Between Immunogenicity and Immunotolerance: Focus on Acute Myeloid Leukemia. *Front. Oncol.* **9**, 1–10 (2019).

807. Martin, S. J. Cell death and inflammation: the case for IL-1 family cytokines as the canonical DAMPs of the immune system. *FEBS J.* **283**, 2599–2615 (2016).

808. Buqué, A., Rodriguez-Ruiz, M. E., Fucikova, J. & Galluzzi, L. Apoptotic caspases cut down the immunogenicity of radiation. *Oncoimmunology* **8**, e1655364–e1655364 (2019).

809. De Martino, M. & Vanpouille-Box, C. Apoptotic Caspases: A Double-Edged Sword in Radiation-Induced Immunogenicity. *Trends Cell Biol.* **29**, 851–853 (2019).

810. Huang, Q., Li, F., Liu, X., Li, W., Shi, W., Liu, F.-F., *et al.* Caspase 3-mediated stimulation of tumor cell repopulation during cancer radiotherapy. *Nat. Med.* **17**, 860–866 (2011).

811. Lauber, K., Bohn, E., Kröber, S. M., Xiao, Y., Blumenthal, S. G., Lindemann, R. K., *et al.* Apoptotic cells induce migration of phagocytes via caspase-3-mediated release of a lipid attraction signal. *Cell* **113**, 717–730 (2003).

812. Swan, D., Lynch, K., Gurney, M. & O'Dwyer, M. Current and emerging immunotherapeutic approaches to the treatment of multiple myeloma. *Ther. Adv. Hematol.* **10**, 2040620719854171 (2019).

813. Di Rosa, F. & Pabst, R. The bone marrow: a nest for migratory memory T cells. *Trends Immunol.* **26**, 360–366 (2005).

814. Di Rosa, F. Maintenance of memory T cells in the bone marrow: survival or homeostatic proliferation? *Nat. Rev. Immunol.* **16**, 271 (2016).

815. Di Rosa, F. & Gebhardt, T. Bone marrow T cells and the integrated functions of recirculating and tissue-resident memory T cells. *Front. Immunol.* **7**, 1–13 (2016).

816. Hernandez, C., Huebener, P. & Schwabe, R. F. Damage-associated molecular patterns in cancer: a double-edged sword. *Oncogene* **35**, 5931–5941 (2016).

817. Teng, M. W. L., Galon, J., Fridman, W. H. & Smyth, M. J. From mice to humans: Developments in cancer immunoediting. *J. Clin. Invest.* **125**, 3338–3346 (2015).

818. Schreiber, R. D., Old, L. J. & Smyth, M. J. Cancer immunoediting: Integrating immunity's roles in cancer suppression and promotion. *Science (80-.).* **331**, 1565–1570 (2011).

819. De Beck, L., Melhaoui, S., De Veirman, K., Menu, E., De Bruyne, E., Vanderkerken, K., *et al.* Epigenetic treatment of multiple myeloma mediates tumor intrinsic and extrinsic immunomodulatory effects. *Oncoimmunology* **7**, 1–13 (2018).

820. Tamura, H. Immunopathogenesis and immunotherapy of multiple myeloma. *Int. J. Hematol.* **107**, 278–285 (2018).

821. Costa, F., Das, R., Kini Bailur, J., Dhodapkar, K. & Dhodapkar, M. V. Checkpoint Inhibition in Myeloma: Opportunities and Challenges. *Front. Immunol.* **9**, 2204 (2018).

822. Kearl, T. J., Jing, W., Gershan, J. A. & Johnson, B. D. Programmed death receptor-1/programmed death receptor ligand-1 blockade after transient lymphodepletion to treat myeloma. *J. Immunol.* **190**, 5620–5628 (2013).

823. Cooke, R. E., Koldej, R. & Ritchie, D. Immunotherapeutics in Multiple Myeloma: How Can Translational Mouse Models Help? *J. Oncol.* **2019**, 2186494 (2019).

824. Iwai, Y., Ishida, M., Tanaka, Y., Okazaki, T., Honjo, T. & Minato, N. Involvement of PD-L1 on tumor cells in the escape from host immune system and tumor immunotherapy by PD-L1 blockade. *Proc. Natl. Acad. Sci. U. S. A.* **99**, 12293–12297 (2002).

825. Hallett, W. H. D., Jing, W., Drobyski, W. R. & Johnson, B. D. Immunosuppressive effects of multiple myeloma are overcome by PD-L1 blockade. *Biol. Blood Marrow Transplant.* **17**, 1133–1145 (2011).

826. Jing, W., Gershan, J. A., Weber, J., Tlomak, D., McOlash, L., Sabatos-Peyton, C., *et al.* Combined immune checkpoint protein blockade and low dose whole body irradiation as immunotherapy for myeloma. *J. Immunother. cancer* **3**, 2 (2015).

827. Rosenblatt, J., Glotzbecker, B., Mills, H., Vasir, B., Tzachanis, D., Levine, J. D., *et al.* PD-1 blockade by CT-011, anti-PD-1 antibody, enhances ex vivo T-cell responses to autologous dendritic cell/myeloma fusion vaccine. *J. Immunother.* **34**, 409–418 (2011).

828. Guillerey, C., Ferrari de Andrade, L., Vuckovic, S., Miles, K., Ngiow, S. F., Yong, M. C. R., *et al.* Immunosurveillance and therapy of multiple myeloma are CD226 dependent. *J. Clin. Invest.* **125**, 2077–2089 (2015).

829. Minnie, S. A., Kuns, R. D., Gartlan, K. H., Zhang, P., Wilkinson, A. N., Samson, L., *et al.* Myeloma escape after stem cell transplantation is a consequence of T-cell exhaustion and is prevented by TIGIT blockade. *Blood* **132**, 1675–1688 (2018).

830. Jelinek, T., Paiva, B. & Hajek, R. Update on PD-1/PD-L1 Inhibitors in Multiple Myeloma. *Front. Immunol.* **9**, 2431 (2018).

831. Asimakopoulos, F. TIGIT checkpoint inhibition for myeloma. *Blood* **132**, 1629–1630 (2018).

832. Chung, D. J., Pronschinske, K. B., Shyer, J. A., Sharma, S., Leung, S., Curran, S. A., *et al.* T-cell Exhaustion in Multiple Myeloma Relapse after Autotransplant: Optimal Timing of Immunotherapy. *Cancer Immunol. Res.* **4**, 61–71 (2016).

833. Lucas, F., Pennell, M., Huang, Y., Benson, D. M., Efebera, Y. A., Chaudhry, M., *et al.* T Cell Transcriptional Profiling and Immunophenotyping Uncover LAG3 as a Potential Significant Target of Immune Modulation in Multiple Myeloma. *Biol. Blood Marrow Transplant.* **26**, 7–15 (2020).

834. Yadav, M., Green, C., Ma, C., Robert, A., Glibicky, A., Nakamura, R., *et al.* Tigit, CD226 and PD-L1/PD-1 Are Highly Expressed By Marrow-Infiltrating T Cells in Patients with Multiple Myeloma. *Blood* **128**, 2102 (2016).

835. Kwon, M., Choi, Y. S., Park, J. & Shin, E.-C. Expression of Immune Checkpoint Receptors in Multiple Myeloma Patients. *J. Immunol.* **198**, 56.1 LP-56.1 (2017).

836. Guillerey, C., Harjunpää, H., Carrié, N., Kassem, S., Teo, T., Miles, K., *et al.* TIGIT immune checkpoint blockade restores CD8(+) T-cell immunity against multiple myeloma. *Blood* **132**, 1689–1694 (2018).

837. Zelle-Rieser, C., Thangavadivel, S., Biedermann, R., Brunner, A., Stoitzner, P., Willenbacher, E., *et al.* T cells in multiple myeloma display features of exhaustion and senescence at the tumor site. *J. Hematol. Oncol.* **9**, 116 (2016).

838. Suen, H., Brown, R., Yang, S., Weatherburn, C., Ho, P. J., Woodland, N., *et al.* Multiple myeloma causes clonal T-cell immunosenescence: identification of potential novel targets for promoting tumour immunity and implications for checkpoint blockade. *Leukemia* **30**, 1716–1724 (2016).

839. Crespo, J., Sun, H., Welling, T. H., Tian, Z. & Zou, W. T cell anergy, exhaustion, senescence, and stemness in the tumor microenvironment. *Curr. Opin. Immunol.* **25**, 214–221 (2013).

840. Wherry, E. J. & Kurachi, M. Molecular and cellular insights into T cell exhaustion. *Nat. Rev. Immunol.* **15**, 486–499 (2015).

841. Suen, H., Brown, R., Yang, S., Ho, P. J., Gibson, J. & Joshua, D. The failure of immune checkpoint blockade in multiple myeloma with PD-1 inhibitors in a phase 1 study. *Leukemia* **29**, 1621–1622 (2015).

842. Sponaas, A.-M., Yang, R., Rustad, E. H., Standal, T., Thoresen, A. S., Dao Vo, C., *et al.* PD1 is expressed on exhausted T cells as well as virus specific memory CD8+ T cells in the bone marrow of myeloma patients. *Oncotarget* **9**, 32024–32035 (2018).

843. Tan, J., Chen, S., Huang, J., Chen, Y., Yang, L., Wang, C., *et al.* Increased exhausted CD8(+) T cells with programmed death-1, T-cell immunoglobulin and mucin-domain-containing-3 phenotype in patients with multiple myeloma. *Asia. Pac. J. Clin. Oncol.* **14**, e266–e274 (2018).

844. Turner, S. J. & Russ, B. E. Can T cells be too exhausted to fight back? *Science* **354**, 1104–1105 (2016).

845. Pauken, K. E., Sammons, M. A., Odorizzi, P. M., Manne, S., Godec, J., Khan, O., *et al.* Epigenetic stability of exhausted T cells limits durability of reinvigoration by PD-1 blockade. *Science* **354**, 1160–1165 (2016).

846. Sen, D. R., Kaminski, J., Barnitz, R. A., Kurachi, M., Gerdemann, U., Yates, K. B., *et al.* The epigenetic landscape of T cell exhaustion. *Science* **354**, 1165–1169 (2016).

847. Groen, K., van de Donk, N., Stege, C., Zweegman, S. & Nijhof, I. S. Carfilzomib for relapsed and refractory multiple myeloma. *Cancer Manag. Res.* **11**, 2663–2675 (2019).

848. Baljevic, M. & Orlowski, R. Z. Pharmacodynamics and pharmacokinetics of proteasome inhibitors for the treatment of multiple myeloma. *Expert Opin. Drug Metab. Toxicol.* **15**, 459–473 (2019).

849. Heckman, C. A., Suvela, M., Eldfors, S., Silvennoinen, R., Yadav, B., Karjalainen, R., *et al.* Identification of precision treatment strategies for relapsed/ refractory multiple myeloma by functional drug sensitivity testing. *Oncotarget* **8**, 56338–56350 (2017).

850. Goldschmidt, H., Neben, K., Bertsch, U., Hielscher, T., van der Holt, B., Hose, D., *et al.* Bortezomib-Based Induction Therapy Followed by Autologous Stem Cell Transplantation and Maintenance Therapy with Bortezomib Improves Outcome In Myeloma Patients with Gain 1q21 and t(4;14) - a Subgroup Analysis of the HOVON-65/GMMG-HD4 Trial. *Blood* **116**, 305 (2010).

851. Rajan, A. M. & Rajkumar, S. V. Interpretation of cytogenetic results in multiple myeloma for clinical practice. *Blood Cancer J.* **5**, 1–7 (2015).

852. Vu, T., Gonsalves, W., Kumar, S., Dispenzieri, A., Lacy, M. Q., Buadi, F., *et al.* Characteristics of exceptional responders to lenalidomide-based therapy in multiple myeloma. *Blood Cancer J.* **5**, e363–e363 (2015).

853. Kumar, S., Kaufman, J. L., Gasparetto, C., Mikhael, J., Vij, R., Pegourie, B., *et al.* Efficacy of

venetoclax as targeted therapy for relapsed/refractory t(11;14) multiple myeloma. *Blood* **130**, 2401–2409 (2017).

854. Saxe, D., Seo, E. J., Bergeron, M. B. & Han, J. Y. Recent advances in cytogenetic characterization of multiple myeloma. *Int. J. Lab. Hematol.* **41**, 5–14 (2019).

855. Mitra, A. K., Harding, T., Mukherjee, U. K., Jang, J. S., Li, Y., HongZheng, R., *et al.* A gene expression signature distinguishes innate response and resistance to proteasome inhibitors in multiple myeloma. *Blood Cancer J.* **7**, e581–e581 (2017).

856. Chapman, M. A., Sive, J., Ambrose, J., Roddie, C., Counsell, N., Lach, A., *et al.* RNA-seq of newly diagnosed patients in the PADIMAC study leads to a bortezomib/lenalidomide decision signature. *Blood* **132**, 2154–2165 (2018).

857. Khin, Z. P., Ribeiro, M. L. C., Jacobson, T., Hazlehurst, L., Perez, L., Baz, R., *et al.* A preclinical assay for chemosensitivity in multiple myeloma. *Cancer Res.* **74**, 56–67 (2014).

858. Ho, M., Patel, A., Hanley, C., Murphy, A., Mcsweeney, T. & Zhang, L. Exploiting autophagy in multiple myeloma. (2019). doi:10.20517/2394-4722.2019.25

859. Montanari, F., Lu, M., Marcus, S., Saran, A., Malankar, A. & Mazumder, A. A Phase II Trial of Chloroquine in Combination with Bortezomib and Cyclophosphamide in Patients with Relapsed and Refractory Multiple Myeloma. *Blood* **124**, 5775 (2014).

860. Bini, L., Magi, B., Marzocchi, B., Arcuri, F., Tripodi, S., Cintorino, M., *et al.* Protein expression profiles in human breast ductal carcinoma and histologically normal tissue. *Electrophoresis* **18**, 2832–2841 (1997).

861. Chahed, K., Kabbage, M., Ehret-Sabatier, L., Lemaitre-Guillier, C., Remadi, S., Hoebeke, J., *et al.* Expression of fibrinogen E-fragment and fibrin E-fragment is inhibited in the human infiltrating ductal carcinoma of the breast: the two-dimensional electrophoresis and MALDI-TOF-mass spectrometry analyses. *Int. J. Oncol.* **27**, 1425–1431 (2005).

862. Kageyama, S., Isono, T., Iwaki, H., Wakabayashi, Y., Okada, Y., Kontani, K., *et al.* Identification by proteomic analysis of calreticulin as a marker for bladder cancer and evaluation of the diagnostic accuracy of its detection in urine. *Clin. Chem.* **50**, 857–866 (2004).

863. Alaiya, A., Roblick, U., Egevad, L., Carlsson, A., Franzén, B., Volz, D., *et al.* Polypeptide expression in prostate hyperplasia and prostate adenocarcinoma. *Anal. Cell. Pathol.* **21**, 1–9 (2000).

864. Hong, S.-H., Misek, D. E., Wang, H., Puravs, E., Giordano, T. J., Greenson, J. K., *et al.* An autoantibody-mediated immune response to calreticulin isoforms in pancreatic cancer. *Cancer Res.* **64**, 5504–5510 (2004).

865. Du, X.-L., Hu, H., Lin, D.-C., Xia, S.-H., Shen, X.-M., Zhang, Y., *et al.* Proteomic profiling of proteins dysregulted in Chinese esophageal squamous cell carcinoma. *J. Mol. Med. (Berl).* **85**, 863–875 (2007).

866. Vougas, K., Gaitanarou, E., Marinos, E., Kittas, C. & Voloudakis-Baltatzis, I. E. Two-dimensional electrophoresis and immunohistochemical study of calreticulin in colorectal adenocarcinoma and mirror biopsies. *J. BUON.* **13**, 101–107 (2008).

867. White, T. K., Zhu, Q. & Tanzer, M. L. Cell surface calreticulin is a putative mannoside lectin which triggers mouse melanoma cell spreading. *J. Biol. Chem.* **270**, 15926–15929 (1995).

868. Zamanian, M., Veerakumarasivam, A., Abdullah, S. & Rosli, R. Calreticulin and cancer. *Pathol. Oncol. Res.* **19**, 149–154 (2013).

869. Afshar, N., Black, B. E. & Paschal, B. M. Retrotranslocation of the chaperone calreticulin from the endoplasmic reticulum lumen to the cytosol. *Mol. Cell. Biol.* **25**, 8844–8853 (2005).

870. Gold, L. I., Eggleton, P., Sweetwyne, M. T., Van Duyn, L. B., Greives, M. R., Naylor, S.-M., *et al.* Calreticulin: non-endoplasmic reticulum functions in physiology and disease. *FASEB J.* **24**, 665–683 (2010).

871. Sadasivan, B., Lehner, P. J., Ortmann, B., Spies, T. & Cresswell, P. Roles for Calreticulin and a

Novel Glycoprotein, Tapasin, in the Interaction of MHC Class I Molecules with TAP. *Immunity* **5**, 103–114 (1996).

872. Arshad, N. & Cresswell, P. Tumor-associated calreticulin variants functionally compromise the peptide loading complex and impair its recruitment of MHC-I. *J. Biol. Chem.* **293**, 9555–9569 (2018).

873. Fu, H., Liu, C., Flutter, B., Tao, H. & Gao, B. Calreticulin maintains the low threshold of peptide required for efficient antigen presentation. *Mol. Immunol.* **46**, 3198–3206 (2009).

874. Raghavan, M., Wijeyesakere, S. J., Peters, L. R. & Del Cid, N. Calreticulin in the immune system: ins and outs. *Trends Immunol.* **34**, 13–21 (2013).

875. Orr, A. W., Pallero, M. A., Xiong, W.-C. & Murphy-Ullrich, J. E. Thrombospondin induces RhoA inactivation through FAK-dependent signaling to stimulate focal adhesion disassembly. *J. Biol. Chem.* **279**, 48983–48992 (2004).

876. Goicoechea, S., Orr, A. W., Pallero, M. A., Eggleton, P. & Murphy-Ullrich, J. E. Thrombospondin mediates focal adhesion disassembly through interactions with cell surface calreticulin. *J. Biol. Chem.* **275**, 36358–36368 (2000).

877. Coppolino, M. G., Woodside, M. J., Demaurex, N., Grinstein, S., St-Arnaud, R. & Dedhar, S. Calreticulin is essential for integrin-mediated calcium signalling and cell adhesion. *Nature* **386**, 843–847 (1997).

878. Fan, X., Yao, Y. & Zhang, Y. Calreticulin promotes proliferation and extracellular matrix expression through Notch pathway in cardiac fibroblasts. *Adv. Clin. Exp. Med.* **27**, 887–892 (2018).

879. Huang, G., Sun, Z., Wu, J., Shui, S., Han, X., Guo, D., *et al.* Calreticulin Promotes Proliferation and Migration But Inhibits Apoptosis in Schwann Cells. *Med. Sci. Monit.* **22**, 4516–4522 (2016).

880. Pallero, M. A., Elzie, C. A., Chen, J., Mosher, D. F. & Murphy-Ullrich, J. E. Thrombospondin 1 binding to calreticulin-LRP1 signals resistance to anoikis. *FASEB J.* **22**, 3968–3979 (2008).

881. Holaska, J. M., Black, B. E., Rastinejad, F. & Paschal, B. M. Ca2+-dependent nuclear export mediated by calreticulin. *Mol. Cell. Biol.* **22**, 6286–6297 (2002).

882. Holaska, J. M., Black, B. E., Love, D. C., Hanover, J. A., Leszyk, J. & Paschal, B. M. Calreticulin Is a receptor for nuclear export. *J. Cell Biol.* **152**, 127–140 (2001).

883. Lee, A. C.-L., Shih, Y.-Y., Zhou, F., Chao, T.-C., Lee, H., Liao, Y.-F., *et al.* Calreticulin regulates MYCN expression to control neuronal differentiation and stemness of neuroblastoma. *J. Mol. Med. (Berl).* **97**, 325–339 (2019).

884. Han, A., Li, C., Zahed, T., Wong, M., Smith, I., Hoedel, K., *et al.* Calreticulin is a Critical Cell Survival Factor in Malignant Neoplasms. *PLoS Biol.* **17**, e3000402–e3000402 (2019).

885. Lu, Y.-C., Weng, W.-C. & Lee, H. Functional roles of calreticulin in cancer biology. *Biomed Res. Int.* **2015**, 526524 (2015).

886. Zamanian, M., Qader Hamadneh, L. A., Veerakumarasivam, A., Abdul Rahman, S., Shohaimi, S. & Rosli, R. Calreticulin mediates an invasive breast cancer phenotype through the transcriptional dysregulation of p53 and MAPK pathways. *Cancer Cell Int.* **16**, 56 (2016).

887. Lwin, Z.-M., Guo, C., Salim, A., Yip, G. W.-C., Chew, F.-T., Nan, J., *et al.* Clinicopathological significance of calreticulin in breast invasive ductal carcinoma. *Mod. Pathol.* **23**, 1559–1566 (2010).

888. Han, Y., Liao, Q., Wang, H., Rao, S., Yi, P., Tang, L., *et al.* High expression of calreticulin indicates poor prognosis and modulates cell migration and invasion via activating Stat3 in nasopharyngeal carcinoma. *J. Cancer* **10**, 5460–5468 (2019).

889. Wemeau, M., Kepp, O., Tesnière, A., Panaretakis, T., Flament, C., De Botton, S., *et al.* Calreticulin exposure on malignant blasts predicts a cellular anticancer immune response in patients with acute myeloid leukemia. *Cell Death Dis.* **1**, 1–9 (2010).

890. Tarr, J. M., Winyard, P. G., Ryan, B., Harries, L. W., Haigh, R., Viner, N., *et al.* Extracellular calreticulin is present in the joints of patients with rheumatoid arthritis and inhibits FasL (CD95L)-mediated apoptosis of T cells. *Arthritis Rheum.* **62**, 2919–2929 (2010).

891. Weber, C. K., Haslbeck, M., Englbrecht, M., Sehnert, B., Mielenz, D., Graef, D., *et al.* Antibodies to the endoplasmic reticulum-resident chaperones calnexin, BiP and Grp94 in patients with rheumatoid arthritis and systemic lupus erythematosus. *Rheumatology (Oxford).* **49**, 2255–2263 (2010).

892. Bodman-Smith, M. D., Fife, M. F., Wythe, H., Corrigal, V. M., Panayi, G. S., Wedderburn, L. R., *et al.* Anti-BiP antibody levels in juvenile idiopathic arthritis (JIA). *Rheumatology* **43**, 1305–1306 (2004).

893. Liu, X., Ji, J., Forsti, A., Sundquist, K., Sundquist, J. & Hemminki, K. Autoimmune disease and subsequent urological cancer. *J. Urol.* **189**, 2262–2268 (2013).

894. Hemminki, K., Liu, X., Försti, A., Ji, J., Sundquist, J. & Sundquist, K. Subsequent leukaemia in autoimmune disease patients. *Br. J. Haematol.* **161**, 677–687 (2013).

895. Murshid, A. & Presley, J. F. ER-to-Golgi transport and cytoskeletal interactions in animal cells. *Cell. Mol. Life Sci.* **61**, 133–145 (2004).

896. Jin, H., Komita, M. & Aoe, T. The Role of BiP Retrieval by the KDEL Receptor in the Early Secretory Pathway and its Effect on Protein Quality Control and Neurodegeneration. *Front. Mol. Neurosci.* **10**, 222 (2017).

897. Llewellyn, D. H., Roderick, H. L. & Rose, S. KDEL receptor expression is not coordinatedly up-regulated with ER stress-induced reticuloplasmin expression in HeLa cells. *Biochem. Biophys. Res. Commun.* **240**, 36–40 (1997).

898. Denning, G., Leidal, K., Holst, V., Iyer, S., Pearson, D., Clark, J., *et al.* Calreticulin Biosynthesis and Processing in Human Myeloid Cells: Demonstration of Signal Peptide Cleavage and N-Glycosylation. *Blood* **90**, 372–381 (1997).

899. Decca, M. B., Carpio, M. A., Bosc, C., Galiano, M. R., Job, D., Andrieux, A., *et al.* Post-translational arginylation of calreticulin: a new isospecies of calreticulin component of stress granules. *J. Biol. Chem.* **282**, 8237–8245 (2007).

900. López Sambrooks, C., Carpio, M. A. & Hallak, M. E. Arginylated calreticulin at plasma membrane increases susceptibility of cells to apoptosis. *J. Biol. Chem.* **287**, 22043–22054 (2012).

901. Araki, M. & Komatsu, N. The role of calreticulin mutations in myeloproliferative neoplasms. *Int. J. Hematol.* **111**, 200–205 (2020).

902. Merlinsky, T. R., Levine, R. L. & Pronier, E. Unfolding the Role of Calreticulin in Myeloproliferative Neoplasm Pathogenesis. *Clin. Cancer Res.* **25**, 2956–2962 (2019).

903. Masubuchi, N., Araki, M., Yang, Y., Hayashi, E., Imai, M., Edahiro, Y., *et al.* Mutant calreticulin interacts with MPL in the secretion pathway for activation on the cell surface. *Leukemia* 10.1038/s41375-019-0564-z (2019). doi:10.1038/s41375-019-0564-z

904. Pecquet, C., Chachoua, I., Roy, A., Balligand, T., Vertenoeil, G., Leroy, E., *et al.* Calreticulin mutants as oncogenic rogue chaperones for TpoR and traffic-defective pathogenic TpoR mutants. *Blood* **133**, 2669–2681 (2019).

905. Han, L., Schubert, C., Köhler, J., Schemionek, M., Isfort, S., Brümmendorf, T. H., *et al.* Calreticulin-mutant proteins induce megakaryocytic signaling to transform hematopoietic cells and undergo accelerated degradation and Golgi-mediated secretion. *J. Hematol. Oncol.* **9**, 45 (2016).

906. Holmström, M. O., Cordua, S., Skov, V., Kjær, L., Pallisgaard, N., Ellervik, C., *et al.* Evidence of immune elimination, immuno-editing and immune escape in patients with hematological cancer. *Cancer Immunol. Immunother.* 10.1007/s00262-019-02473-y (2020). doi:10.1007/s00262-019-02473-y

907. Holmström, M. O., Riley, C. H., Svane, I. M., Hasselbalch, H. C. & Andersen, M. H. The CALR exon 9 mutations are shared neoantigens in patients with CALR mutant chronic myeloproliferative

neoplasms. *Leukemia* **30**, 2413–2416 (2016).

908. Holmström, M. O., Martinenaite, E., Ahmad, S. M., Met, Friese, C., Kjær, L., *et al.* The calreticulin (CALR) exon 9 mutations are promising targets for cancer immune therapy. *Leukemia* **32**, 429–437 (2018).

909. Holmström, M. O., Ahmad, S. M., Klausen, U., Bendtsen, S. K., Martinenaite, E., Riley, C. H., *et al.* High frequencies of circulating memory T cells specific for calreticulin exon 9 mutations in healthy individuals. *Blood Cancer J.* **9**, 8 (2019).

910. Cordua, S., Kjaer, L., Skov, V., Pallisgaard, N., Hasselbalch, H. C. & Ellervik, C. Prevalence and phenotypes of JAK2 V617F and calreticulin mutations in a Danish general population. *Blood* **134**, 469–479 (2019).

911. Bolli, N., Biancon, G., Moarii, M., Gimondi, S., Li, Y., de Philippis, C., *et al.* Analysis of the genomic landscape of multiple myeloma highlights novel prognostic markers and disease subgroups. *Leukemia* 10.1038/leu.2017.344 (2017). doi:10.1038/leu.2017.344

912. Manier, S., Salem, K., Glavey, S. V, Roccaro, A. M. & Ghobrial, I. M. Genomic Aberrations in Multiple Myeloma. *Cancer Treat. Res.* **169**, 23–34 (2016).

913. Racanelli, V., Leone, P., Frassanito, M. A., Brunetti, C., Perosa, F., Ferrone, S., *et al.* Alterations in the antigen processing-presenting machinery of transformed plasma cells are associated with reduced recognition by CD8+ T cells and characterize the progression of MGUS to multiple myeloma. *Blood* **115**, 1185–1193 (2010).

914. Sarıman, M., Abacı, N., Sırma Ekmekçi, S., Çakiris, A., Perçin Paçal, F., Üstek, D., *et al.* Investigation of Gene Expressions of Myeloma Cells in the Bone Marrow of Multiple Myeloma Patients by Transcriptome Analysis. *Balkan Med. J.* **36**, 23–31 (2019).

915. Jang, J. S., Li, Y., Mitra, A. K., Bi, L., Abyzov, A., van Wijnen, A. J., *et al.* Molecular signatures of multiple myeloma progression through single cell RNA-Seq. *Blood Cancer J.* **9**, 2 (2019).

916. Truxova, I., Kasikova, L., Salek, C., Hensler, M., Lysak, D., Holicek, P., *et al.* Calreticulin exposure on malignant blasts correlates with improved natural killer cell-mediated cytotoxicity in acute myeloid leukemia patients. *Haematologica* haematol.2019.223933 (2019). doi:10.3324/haematol.2019.223933

917. Galon, J., Costes, A., Sanchez-Cabo, F., Kirilovsky, A., Mlecnik, B., Lagorce-Pagès, C., *et al.* Type, density, and location of immune cells within human colorectal tumors predict clinical outcome. *Science* **313**, 1960–1964 (2006).

918. Fialová, A., Partlová, S., Sojka, L., Hromádková, H., Brtnický, T., Fučíková, J., *et al.* Dynamics of T-cell infiltration during the course of ovarian cancer: the gradual shift from a Th17 effector cell response to a predominant infiltration by regulatory T-cells. *Int. J. cancer* **132**, 1070–1079 (2013).

919. Blimark, C., Holmberg, E., Mellqvist, U.-H., Landgren, O., Björkholm, M., Hultcrantz, M., *et al.* Multiple myeloma and infections: a population-based study on 9253 multiple myeloma patients. *Haematologica* **100**, 107–113 (2015).

920. Mellstedt, H., Holm, G., Pettersson, D., Björkholm, M., Johansson, B., Lindemalm, C., *et al.* T cells in monoclonal gammopathies. *Scand. J. Haematol.* **29**, 57–64 (1982).

921. Mills, K. H. & Cawley, J. C. Abnormal monoclonal antibody-defined helper/suppressor T-cell subpopulations in multiple myeloma: relationship to treatment and clinical stage. *Br. J. Haematol.* **53**, 271–275 (1983).

922. Willenbacher, W., Willenbacher, E., Zelle-Rieser, C., Biedermann, R., Weger, R., Jöhrer, K., *et al.* Bone marrow microenvironmental CD4 + and CD8 + lymphocyte infiltration patterns define overall- and progression free survival in standard risk multiple myeloma--an analysis from the Austrian Myeloma Registry. *Leuk. Lymphoma* **57**, 1478–1481 (2016).

923. Pessoa de Magalhaes, R. J., Vidriales, M.-B. M.-B., Paiva, B., Fernandez-Gimenez, C., Garcia-Sanz, R., Mateos, M.-V. M.-V., *et al.* Analysis of the immune system of multiple myeloma patients

achieving long-term disease control by multidimensional flow cytometry. *Haematologica* **98**, 79–86 (2013).

924. Koike, M., Sekigawa, I., Okada, M., Matsumoto, M., Iida, N., Hashimoto, H., *et al.* Relationship between CD4(+)/CD8(+) T cell ratio and T cell activation in multiple myeloma: reference to IL-16. *Leuk. Res.* **26**, 705–711 (2002).

925. Kay, N. E., Leong, T., Kyle, R. A., Greipp, P., Billadeau, D., Van Ness, B., *et al.* Circulating blood B cells in multiple myeloma: analysis and relationship to circulating clonal cells and clinical parameters in a cohort of patients entered on the Eastern Cooperative Oncology Group phase III E9486 clinical trial. *Blood* **90**, 340–345 (1997).

926. Kay, N. E., Leong, T., Bone, N., Kyle, R. A., Greipp, P. R., Van Ness, B., *et al.* T-helper phenotypes in the blood of myeloma patients on ECOG phase III trials E9486/E3A93. *Br. J. Haematol.* **100**, 459–463 (1998).

927. Corso, A., Castelli, G., Pagnucco, G., Lazzarino, M., Bellio, L., Klersy, C., *et al.* Bone marrow T-cell subsets in patients with monoclonal gammopathies: correlation with clinical stage and disease status. *Haematologica* **82**, 43–46 (1997).

928. Halapi, E., Werner, A., Wahlström, J., Osterborg, A., Jeddi-Tehrani, M., Yi, Q., *et al.* T cell repertoire in patients with multiple myeloma and monoclonal gammopathy of undetermined significance: Clonal CD8+ T cell expansions are found preferentially in patients with a low tumor burden. *Eur. J. Immunol.* **27**, 2245–2252 (1997).

929. Bhutani, M., Foureau, D., Zhang, Q., Robinson, M., Wynn, A. S., Steuerwald, N. M., *et al.* Peripheral Immunotype Correlates with Minimal Residual Disease Status and Is Modulated by Immunomodulatory Drugs in Multiple Myeloma. *Biol. Blood Marrow Transplant.* **25**, 459–465 (2018).

930. Kwon, M., Kim, C. G., Lee, H., Cho, H., Kim, Y., Lee, E. C., *et al.* PD-1 blockade reinvigorates bone marrow CD8+ T cells from patients with multiple myeloma in the presence of TGF-b inhibitors. *Clin. Cancer Res.* clincanres.0267.2019 (2020). doi:10.1158/1078-0432.CCR-19-0267

931. Akbar, A. N. & Henson, S. M. Are senescence and exhaustion intertwined or unrelated processes that compromise immunity? *Nat. Rev. Immunol.* **11**, 289–295 (2011).

932. Zhao, Y., Shao, Q. & Peng, G. Exhaustion and senescence: two crucial dysfunctional states of T cells in the tumor microenvironment. *Cell. Mol. Immunol.* **17**, 27–35 (2020).

933. Fostier, K., Caers, J., Meuleman, N., Broos, K., Corthals, J., Thielemans, K., *et al.* Impact of lenalidomide maintenance on the immune environment of multiple myeloma patients with low tumor burden after autologous stem cell transplantation. *Oncotarget* **9**, 20476–20489 (2018).

934. Chang, Y., Jiang, Y., Chen, Y., Xing, X., Zhou, Y., Sang, T., *et al.* Bone marrow PD-1 positive T cells reflect tumor mass and prognosis in multiple myeloma. *Int. J. Clin. Exp. Pathol.* **11**, 304–313 (2018).

935. Famularo, G., D'Ambrosio, A., Quintieri, F., Di Giovanni, S., Parzanese, I., Pizzuto, F., *et al.* Natural killer cell frequency and function in patients with monoclonal gammopathies. *J. Clin. Lab. Immunol.* **37**, 99–109 (1992).

936. Sawanobori, M., Suzuki, K., Nakagawa, Y., Inoue, Y., Utsuyama, M. & Hirokawa, K. Natural killer cell frequency and serum cytokine levels in monoclonal gammopathies: correlation of bone marrow granular lymphocytes to prognosis. *Acta Haematol.* **98**, 150–154 (1997).

937. Frassanito, M. A., Silvestris, F., Cafforio, P., Silvestris, N. & Dammacco, F. IgG M-components in active myeloma patients induce a down-regulation of natural killer cell activity. *Int. J. Clin. Lab. Res.* **27**, 48–54 (1997).

938. von Lilienfeld-Toal, M., Frank, S., Leyendecker, C., Feyler, S., Jarmin, S., Morgan, R., *et al.* Reduced immune effector cell NKG2D expression and increased levels of soluble NKG2D ligands in multiple myeloma may not be causally linked. *Cancer Immunol. Immunother.* **59**, 829–839 (2010).

939. Jinushi, M., Vanneman, M., Munshi, N. C., Tai, Y.-T., Prabhala, R. H., Ritz, J., *et al.* MHC class I chain-related protein A antibodies and shedding are associated with the progression of multiple myeloma. *Proc. Natl. Acad. Sci. U. S. A.* **105**, 1285–1290 (2008).

940. El-Sherbiny, Y. M., Meade, J. L., Holmes, T. D., McGonagle, D., Mackie, S. L., Morgan, A. W., *et al.* The requirement for DNAM-1, NKG2D, and NKp46 in the natural killer cell-mediated killing of myeloma cells. *Cancer Res.* **67**, 8444–8449 (2007).

941. Costello, R. T., Boehrer, A., Sanchez, C., Mercier, D., Baier, C., Le Treut, T., *et al.* Differential expression of natural killer cell activating receptors in blood versus bone marrow in patients with monoclonal gammopathy. *Immunology* **139**, 338–341 (2013).

942. Benson Jr, D. M., Bakan, C. E., Mishra, A., Hofmeister, C. C., Efebera, Y., Becknell, B., *et al.* The PD-1/PD-L1 axis modulates the natural killer cell versus multiple myeloma effect: a therapeutic target for CT-011, a novel monoclonal anti-PD-1 antibody. *Blood* **116**, 2286–2294 (2010).

943. De Rossi, G., De Sanctis, G., Bottari, V., Tribalto, M., Lopez, M., Petrucci, M. T., *et al.* Surface markers and cytotoxic activities of lymphocytes in monoclonal gammopathy of undetermined significance and untreated multiple myeloma. Increased phytohemagglutinin-induced cellular cytotoxicity and inverted helper/suppressor cell ratio are features. *Cancer Immunol. Immunother.* **25**, 133–136 (1987).

944. King, M. A. & Radicchi-Mastroianni, M. A. Natural killer cells and CD56+ T cells in the blood of multiple myeloma patients: analysis by 4-colour flow cytometry. *Cytometry* **26**, 121–124 (1996).

945. Tienhaara, A. & Pelliniemi, T. T. Peripheral blood lymphocyte subsets in multiple myeloma and monoclonal gammopathy of undetermined significance. *Clin. Lab. Haematol.* **16**, 213–223 (1994).

946. García de Vinuesa, C., Gulbranson-Judge, A., Khan, M., O'Leary, P., Cascalho, M., Wabl, M., *et al.* Dendritic cells associated with plasmablast survival. *Eur. J. Immunol.* **29**, 3712–3721 (1999).

947. Jego, G., Palucka, A. K., Blanck, J.-P., Chalouni, C., Pascual, V. & Banchereau, J. Plasmacytoid dendritic cells induce plasma cell differentiation through type I interferon and interleukin 6. *Immunity* **19**, 225–234 (2003).

948. Ratta, M., Fagnoni, F., Curti, A., Vescovini, R., Sansoni, P., Oliviero, B., *et al.* Dendritic cells are functionally defective in multiple myeloma: the role of interleukin-6. *Blood* **100**, 230–237 (2002).

949. Brimnes, M. K., Svane, I. M. & Johnsen, H. E. Impaired functionality and phenotypic profile of dendritic cells from patients with multiple myeloma. *Clin. Exp. Immunol.* **144**, 76–84 (2006).

950. Dhodapkar, K. M., Barbuto, S., Matthews, P., Kukreja, A., Mazumder, A., Vesole, D., *et al.* Dendritic cells mediate the induction of polyfunctional human IL17-producing cells (Th17-1 cells) enriched in the bone marrow of patients with myeloma. *Blood* **112**, 2878–2885 (2008).

951. Banerjee, D. K., Dhodapkar, M. V, Matayeva, E., Steinman, R. M. & Dhodapkar, K. M. Expansion of FOXP3high regulatory T cells by human dendritic cells (DCs) in vitro and after injection of cytokine-matured DCs in myeloma patients. *Blood* **108**, 2655–2661 (2006).

952. Treilleux, I., Blay, J.-Y., Bendriss-Vermare, N., Ray-Coquard, I., Bachelot, T., Guastalla, J.-P., *et al.* Dendritic cell infiltration and prognosis of early stage breast cancer. *Clin. Cancer Res.* **10**, 7466–7474 (2004).

953. Sandel, M. H., Dadabayev, A. R., Menon, A. G., Morreau, H., Melief, C. J. M., Offringa, R., *et al.* Prognostic value of tumor-infiltrating dendritic cells in colorectal cancer: role of maturation status and intratumoral localization. *Clin. Cancer Res.* **11**, 2576–2582 (2005).

954. Bell, D., Chomarat, P., Broyles, D., Netto, G., Harb, G. M., Lebecque, S., *et al.* In breast carcinoma tissue, immature dendritic cells reside within the tumor, whereas mature dendritic cells are located in peritumoral areas. *J. Exp. Med.* **190**, 1417–1426 (1999).

955. Beyer, M., Classen, S., Endl, E., Kochanek, M., Weihrauch, M. R., Debey-Pascher, S., *et al.* Comparative approach to define increased regulatory T cells in different cancer subtypes by combined assessment of CD127 and FOXP3. *Clin. Dev. Immunol.* **2011**, 734036 (2011).

956. Feyler, S., von Lilienfeld-Toal, M., Jarmin, S., Marles, L., Rawstron, A., Ashcroft, A. J., *et al.* CD4(+)CD25(+)FoxP3(+) regulatory T cells are increased whilst CD3(+)CD4(-)CD8(-)alphabetaTCR(+) Double Negative T cells are decreased in the peripheral blood of patients with multiple myeloma which correlates with disease burden. *Br. J. Haematol.* **144**, 686–695 (2009).

957. Gupta, R., Ganeshan, P., Hakim, M., Verma, R., Sharma, A. & Kumar, L. Significantly reduced regulatory T cell population in patients with untreated multiple myeloma. *Leuk. Res.* **35**, 874–878 (2011).

958. Prabhala, R. H., Neri, P., Bae, J. E., Tassone, P., Shammas, M. A., Allam, C. K., *et al.* Dysfunctional T regulatory cells in multiple myeloma. *Blood* **107**, 301–304 (2006).

959. Atanackovic, D., Cao, Y., Luetkens, T., Panse, J., Faltz, C., Arfsten, J., *et al.* CD4+CD25+FOXP3+ T regulatory cells reconstitute and accumulate in the bone marrow of patients with multiple myeloma following allogeneic stem cell transplantation. *Haematologica* **93**, 423–430 (2008).

960. Foglietta, M., Castella, B., Mariani, S., Coscia, M., Godio, L., Ferracini, R., *et al.* The bone marrow of myeloma patients is steadily inhabited by a normal-sized pool of functional regulatory T cells irrespectiveof the disease status. *Haematologica* **99**, 1605–1610 (2014).

961. Lad, D., Huang, Q., Hoeppli, R., Garcia, R., Xu, L., Levings, M., *et al.* Evaluating the role of Tregs in the progression of multiple myeloma. *Leuk. Lymphoma* 1–9 (2019). doi:10.1080/10428194.2019.1579324

962. Marsh-Wakefield, F., Kruzins, A., McGuire, H. M., Yang, S., Bryant, C., Fazekas de St Groth, B., *et al.* Mass Cytometry Discovers Two Discrete Subsets of CD39(-)Treg Which Discriminate MGUS From Multiple Myeloma. *Front. Immunol.* **10**, 1596 (2019).

963. Braga, W. M. T., Atanackovic, D. & Colleoni, G. W. B. The role of regulatory T cells and TH17 cells in multiple myeloma. *Clin. Dev. Immunol.* **2012**, 293479 (2012).

964. Noonan, K., Marchionni, L., Anderson, J., Pardoll, D., Roodman, G. D. & Borrello, I. A novel role of IL-17-producing lymphocytes in mediating lytic bone disease in multiple myeloma. *Blood* **116**, 3554–3563 (2010).

965. Favaloro, J., Brown, R., Aklilu, E., Yang, S., Suen, H., Hart, D., *et al.* Myeloma skews regulatory T and pro-inflammatory T helper 17 cell balance in favor of a suppressive state. *Leuk. Lymphoma* **55**, 1090–1098 (2014).

966. Calcinotto, A., Brevi, A., Chesi, M., Ferrarese, R., Garcia Perez, L., Grioni, M., *et al.* Microbiota-driven interleukin-17-producing cells and eosinophils synergize to accelerate multiple myeloma progression. *Nat. Commun.* **9**, 4832 (2018).

967. Ray, A., Das, D. S., Song, Y., Richardson, P., Munshi, N. C., Chauhan, D., *et al.* Targeting PD1-PDL1 immune checkpoint in plasmacytoid dendritic cell interactions with T cells, natural killer cells and multiple myeloma cells. *Leukemia* **29**, 1441–1444 (2015).

968. Sponaas, A.-M., Moharrami, N. N., Feyzi, E., Standal, T., Holth Rustad, E., Waage, A., *et al.* PDL1 Expression on Plasma and Dendritic Cells in Myeloma Bone Marrow Suggests Benefit of Targeted anti PD1-PDL1 Therapy. *PLoS One* **10**, e0139867–e0139867 (2015).

969. Dhodapkar, M. V, Sexton, R., Das, R., Dhodapkar, K. M., Zhang, L., Sundaram, R., *et al.* Prospective analysis of antigen-specific immunity, stem-cell antigens, and immune checkpoints in monoclonal gammopathy. *Blood* **126**, 2475–2478 (2015).

970. Janz, S., Zhan, F., Sun, F., Cheng, Y., Pisano, M., Yang, Y., *et al.* Germline risk contribution to genomic instability in multiple myeloma. *Front. Genet.* **10**, 1–20 (2019).

971. Rajasagi, M., Shukla, S. A., Fritsch, E. F., Keskin, D. B., DeLuca, D., Carmona, E., *et al.* Systematic identification of personal tumor-specific neoantigens in chronic lymphocytic leukemia. *Blood* **124**, 453–462 (2014).

972. Van Allen, E. M., Miao, D., Schilling, B., Shukla, S. A., Blank, C., Zimmer, L., *et al.* Genomic correlates of response to CTLA-4 blockade in metastatic melanoma. *Science* **350**, 207–211 (2015).

973. Gupta, A., Place, M., Goldstein, S., Sarkar, D., Zhou, S., Potamousis, K., *et al.* Single-molecule analysis reveals widespread structural variation in multiple myeloma. *Proc. Natl. Acad. Sci. U. S. A.* **112**, 7689–7694 (2015).

974. Kasikova, L., Hensler, M., Truxova, I., Skapa, P., Laco, J., Belicova, L., *et al.* Calreticulin exposure correlates with robust adaptive antitumor immunity and favorable prognosis in ovarian carcinoma patients. *J. Immunother. cancer* **7**, 312 (2019).

975. Jiménez-Segura, R., Granell, M., Gironella, M., Abella, E., García-Guiñón, A., Oriol, A., *et al.* Pomalidomide-dexamethasone for treatment of soft-tissue plasmacytomas in patients with relapsed / refractory multiple myeloma. *Eur. J. Haematol.* **102**, 389–394 (2019).

976. Usmani, S. Z., Heuck, C., Mitchell, A., Szymonifka, J., Nair, B., Hoering, A., *et al.* Extramedullary disease portends poor prognosis in multiple myeloma and is over-represented in high-risk disease even in the era of novel agents. *Haematologica* **97**, 1761–1767 (2012).

977. Chen, H.-F., Wu, T.-Q., Li, Z.-Y., Shen, H.-S., Tang, J.-Q., Fu, W.-J., *et al.* Extramedullary plasmacytoma in the presence of multiple myeloma: clinical correlates and prognostic relevance. *Onco. Targets. Ther.* **5**, 329–334 (2012).

978. Hsu, W. M., Hsieh, F. J., Jeng, Y. M., Kuo, M. L., Chen, C. N., Lai, D. M., *et al.* Calreticulin expression in neuroblastoma--a novel independent prognostic factor. *Ann. Oncol. Off. J. Eur. Soc. Med. Oncol.* **16**, 314–321 (2005).

979. Muth, C., Rubner, Y., Semrau, S., Rühle, P.-F., Frey, B., Strnad, A., *et al.* Primary glioblastoma multiforme tumors and recurrence : Comparative analysis of the danger signals HMGB1, HSP70, and calreticulin. *Strahlenther. Onkol.* **192**, 146–155 (2016).

980. Erić, A., Juranić, Z., Milovanović, Z., Marković, I., Inić, M., Stanojević-Bakić, N., *et al.* Effects of humoral immunity and calreticulin overexpression on postoperative course in breast cancer. *Pathol. Oncol. Res.* **15**, 89–90 (2009).

981. Kabbage, M., Trimeche, M., Bergaoui, S., Hammann, P., Kuhn, L., Hamrita, B., *et al.* Calreticulin expression in infiltrating ductal breast carcinomas: relationships with disease progression and humoral immune responses. *Tumour Biol.* **34**, 1177–1188 (2013).

982. Harada, K., Takenawa, T., Ferdous, T., Kuramitsu, Y. & Ueyama, Y. Calreticulin is a novel independent prognostic factor for oral squamous cell carcinoma. *Oncol. Lett.* **13**, 4857–4862 (2017).

983. Matsukuma, S., Yoshimura, K., Ueno, T., Oga, A., Inoue, M., Watanabe, Y., *et al.* Calreticulin is highly expressed in pancreatic cancer stem-like cells. *Cancer Sci.* **107**, 1599–1609 (2016).

984. Majeti, R., Chao, M. P., Alizadeh, A. A., Pang, W. W., Jaiswal, S., Gibbs Jr, K. D., *et al.* CD47 is an adverse prognostic factor and therapeutic antibody target on human acute myeloid leukemia stem cells. *Cell* **138**, 286–299 (2009).

985. Suzuki, S., Yokobori, T., Tanaka, N., Sakai, M., Sano, A., Inose, T., *et al.* CD47 expression regulated by the miR-133a tumor suppressor is a novel prognostic marker in esophageal squamous cell carcinoma. *Oncol. Rep.* **28**, 465–472 (2012).

986. Yuan, J., Shi, X., Chen, C., He, H., Liu, L., Wu, J., *et al.* High expression of CD47 in triple negative breast cancer is associated with epithelial-mesenchymal transition and poor prognosis. *Oncol. Lett.* **18**, 3249–3255 (2019).

987. Schürch, C. M., Forster, S., Brühl, F., Yang, S. H., Felley-Bosco, E. & Hewer, E. The 'don't eat me' signal CD47 is a novel diagnostic biomarker and potential therapeutic target for diffuse malignant mesothelioma. *Oncoimmunology* **7**, e1373235–e1373235 (2017).

988. Sudo, T., Takahashi, Y., Sawada, G., Uchi, R., Mimori, K. & Akagi, Y. Significance of CD47 expression in gastric cancer. *Oncol. Lett.* **14**, 801–809 (2017).

989. Li, Y., Lu, S., Xu, Y., Qiu, C., Jin, C., Wang, Y., *et al.* Overexpression of CD47 predicts poor prognosis and promotes cancer cell invasion in high-grade serous ovarian carcinoma. *Am. J. Transl. Res.* **9**, 2901–2910 (2017).

990. Fu, W., Li, J., Zhang, W. & Li, P. High expression of CD47 predicts adverse prognosis in Chinese patients and suppresses immune response in melanoma. *Biomed. Pharmacother.* **93**, 1190–1196 (2017).

991. Barrera, L., Montes-Servín, E., Hernandez-Martinez, J.-M., García-Vicente, M. de L. Á., Montes-Servín, E., Herrera-Martínez, M., *et al.* CD47 overexpression is associated with decreased neutrophil apoptosis/phagocytosis and poor prognosis in non-small-cell lung cancer patients. *Br. J. Cancer* **117**, 385–397 (2017).

992. Zhao, H., Wang, J., Kong, X., Li, E., Liu, Y., Du, X., *et al.* CD47 Promotes Tumor Invasion and Metastasis in Non-small Cell Lung Cancer. *Sci. Rep.* **6**, 29719 (2016).

993. Yoshida, K., Tsujimoto, H., Matsumura, K., Kinoshita, M., Takahata, R., Matsumoto, Y., *et al.* CD47 is an adverse prognostic factor and a therapeutic target in gastric cancer. *Cancer Med.* **4**, 1322–1333 (2015).

994. Liu, J., Wang, L., Zhao, F., Tseng, S., Narayanan, C., Shura, L., *et al.* Pre-Clinical Development of a Humanized Anti-CD47 Antibody with Anti-Cancer Therapeutic Potential. *PLoS One* **10**, e0137345–e0137345 (2015).

995. Iribarren, K., Buque, A., Mondragon, L., Xie, W., Lévesque, S., Pol, J., *et al.* Anticancer effects of anti-CD47 immunotherapy in vivo. *Oncoimmunology* **8**, 1–8 (2019).

996. Russ, A., Hua, A. B., Montfort, W. R., Rahman, B., Riaz, I. Bin, Khalid, M. U., *et al.* Blocking 'don't eat me' signal of CD47-SIRPα in hematological malignancies, an in-depth review. *Blood Rev.* **32**, 480–489 (2018).

997. Advani, R., Flinn, I., Popplewell, L., Forero, A., Bartlett, N. L., Ghosh, N., *et al.* CD47 Blockade by Hu5F9-G4 and Rituximab in Non-Hodgkin's Lymphoma. *N. Engl. J. Med.* **379**, 1711–1721 (2018).

998. Sikic, B. I., Lakhani, N., Patnaik, A., Shah, S. A., Chandana, S. R., Rasco, D., *et al.* First-in-Human, First-in-Class Phase I Trial of the Anti-CD47 Antibody Hu5F9-G4 in Patients With Advanced Cancers. *J. Clin. Oncol.* **37**, 946–953 (2019).

999. Sun, J., Muz, B., Alhallak, K., Markovic, M., Gurley, S., Wang, Z., *et al.* Targeting CD47 as a Novel Immunotherapy for Multiple Myeloma. *Cancers (Basel).* **12**, E305 (2020).

1000. Rendtlew Danielsen, J. M., Knudsen, L. M., Dahl, I. M., Lodahl, M. & Rasmussen, T. Dysregulation of CD47 and the ligands thrombospondin 1 and 2 in multiple myeloma. *Br. J. Haematol.* **138**, 756–760 (2007).

1001. Kim, D., Wang, J., Willingham, S. B., Martin, R., Wernig, G. & Weissman, I. L. Anti-CD47 antibodies promote phagocytosis and inhibit the growth of human myeloma cells. *Leukemia* **26**, 2538–2545 (2012).

1002. Yang, C., Zhang, Z., Zou, Y., Gao, G., Liu, L., Xu, H., *et al.* Expression of glucose-regulated protein 78 as prognostic biomarkers for triple-negative breast cancer. *Histol. Histopathol.* 18185 (2019). doi:10.14670/HH-18-185

1003. Samanta, S., Tamura, S., Dubeau, L., Mhawech-Fauceglia, P., Miyagi, Y., Kato, H., *et al.* Clinicopathological significance of endoplasmic reticulum stress proteins in ovarian carcinoma. *Sci. Rep.* **10**, 2160 (2020).

1004. Langer, R., Feith, M., Siewert, J. R., Wester, H.-J. & Hoefler, H. Expression and clinical significance of glucose regulated proteins GRP78 (BiP) and GRP94 (GP96) in human adenocarcinomas of the esophagus. *BMC Cancer* **8**, 70 (2008).

1005. Zheng, H., Takahashi, H., Li, X., Hara, T., Masuda, S., Guan, Y., *et al.* Overexpression of GRP78 and GRP94 are markers for aggressive behavior and poor prognosis in gastric carcinomas. *Hum. Pathol.* **39**, 1042–1049 (2008).

1006. Dardano, A., Falzoni, S., Caraccio, N., Polini, A., Tognini, S., Solini, A., *et al.* 1513A>C polymorphism in the P2X7 receptor gene in patients with papillary thyroid cancer: correlation with histological variants and clinical parameters. *J. Clin. Endocrinol. Metab.* **94**, 695–698 (2009).

1007. Wiley, J. S., Dao-Ung, L. P., Gu, B. J., Sluyter, R., Shemon, A. N., Li, C., *et al.* A loss-of-function

polymorphic mutation in the cytolytic P2X7 receptor gene and chronic lymphocytic leukaemia: a molecular study. *Lancet (London, England)* **359**, 1114–1119 (2002).

1008. Paneesha, S., Starczynski, J., Pepper, C., Delgado, J., Hooper, L., Fegan, C., *et al.* The P2X7 receptor gene polymorphism 1513 A-->C has no effect on clinical prognostic markers and survival in multiple myeloma. *Leuk. Lymphoma* **47**, 281–284 (2006).

1009. Jung, G., Roh, J., Lee, H., Gil, M., Yoon, D. H., Suh, C., *et al.* Autophagic Markers BECLIN 1 and LC3 are Associated with Prognosis of Multiple Myeloma. *Acta Haematol.* **134**, 17–24 (2015).

1010. Zhu, F.-X., Wang, X.-T., Zeng, H.-Q., Yin, Z.-H. & Ye, Z.-Z. A predicted risk score based on the expression of 16 autophagy-related genes for multiple myeloma survival. *Oncol. Lett.* **18**, 5310–5324 (2019).

1011. Cano-González, A., Mauro-Lizcano, M., Iglesias-Serret, D., Gil, J. & López-Rivas, A. Involvement of both caspase-8 and Noxa-activated pathways in endoplasmic reticulum stress-induced apoptosis in triple-negative breast tumor cells. *Cell Death Dis.* **9**, (2018).